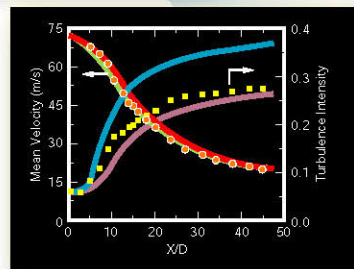
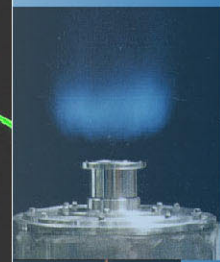
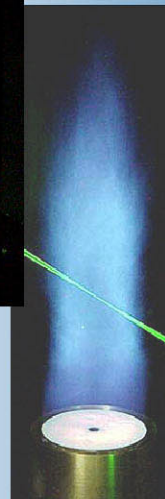
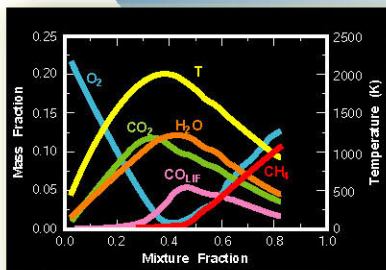
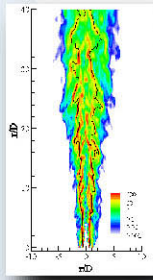
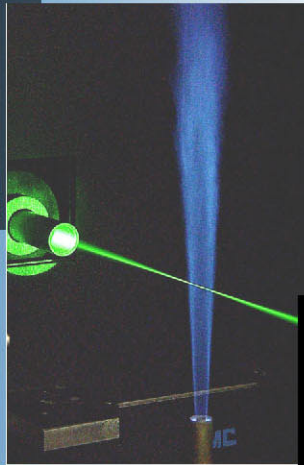


TNF6

18-20 July 2002

Sapporo, Japan



*Sixth International Workshop on
Measurement and Computation of
Turbulent Nonpremixed Flames*

TNF6 Workshop Sponsors

Continuum®



TAKUMA



Sponsorship funds have been used to lower the registration fees for university faculty and students

TNF6 Proceedings – Final PDF Version

Table of Contents

(Sections in **bold** were added or modified after the workshop.)

Summary	5
Preface.....	14
List of Participants	15
Agenda	16
Poster Authors and Titles.....	18
Poster Abstracts	21
Contributed Notes and Vugraphs on TNF6 Focus Topics	91
(included in the order of the agenda)	
Mixing Models Performance in the Calculations of Nonpremixed Piloted Jet Flames (vugraphs) 92	
S. B. Pope	
Contribution on Mixing Models (vugraphs).....	127
R. P. Lindstedt	
Bluff-Body Stabilized Jets and Flames.....	137
P. A. M. Kalt and A. R. Masri	
Swirl Stabilized Jets and Flames.....	159
A. R. Masri and Y. M. Al-Abdeli	
Swirl Stabilized Jet LES (summary and vugraphs).....	172
H. Pitsch	
Modeling of Scalar Dissipation (vugraphs)	184
R. W. Bilger	
Measurement of Scalar Dissipation (vugraphs).....	191
R. S. Barlow, A. N. Karpetis and J. H. Frank	
Predictions of the Mean Scalar Dissipation Rate in the Barlow and Frank Flame D.....	201
S. B. Pope and G. M. Goldin	
Spatial Structure in Sandia Flame D.....	208
A. N. Karpetis and R. S. Barlow	
New Experiments on TNF Flames.....	213
A. Dreizler	
Turbulent Opposed Jet (vugraphs)	217
D. Geyer and A. Dreizler	

TNF6 Proceedings – Final PDF Version

Table of Contents (cont.)

New Measurements on Piloted Flames and Simultaneous Line Raman and Crossed PLIF (vugraphs).....	230
A. N. Karpetis and R. S. Barlow	
Two-Dimensional Reaction-Rate, Mixture Fraction, and Temperature Imaging in Piloted Methane/Air Jet Flames (vugraphs)	243
J. H. Frank, S. A. Kaiser and M. B. Long	
Time Domain Imaging (vugraphs)	262
C. Kaminski	
Measurements and Calculations of Mean Spectral Radiation Intensities Leaving Turbulent Non-Premixed and Partially Premixed Flames	273
Y. Zheng, R. S. Barlow and J. P. Gore	
Measurements Directed at LES Validation (includes vugraphs).....	286
A. Dreizler	
Comparison of Measured and Predicted Scalar Time Series in Flame H3 (vugraphs) ..	297
M. R. Renfro et al.	

SUMMARY

Sixth International Workshop on Measurement and Computation of Turbulent Nonpremixed Flames

18-20 July 2002
Sheraton Sapporo Hotel
Sapporo, Japan

Robert S. Barlow, Stephan B. Pope, Assaad R. Masri, and Joseph C. Oefelein

INTRODUCTION

The series of workshops on Measurement and Computation of Turbulent Nonpremixed Flames (TNF) is intended to facilitate collaboration and information exchange among experimental and computational researchers in the field of turbulent nonpremixed (and partially premixed) combustion. The emphasis is on fundamental issues of turbulence-chemistry interaction, as revealed by comparisons of measured and modeled results for selected flames.

TNF6 was attended by 64 researchers from 12 countries. Thirty-five posters were contributed and abstracts are included in the proceedings. The main agenda for the discussion sessions was divided roughly into four parts:

1. Presentations and discussion on specific submodels (mixing, chemistry, radiation, and scalar dissipation) mainly in the context of piloted jet flames
2. Comparison of measured and modeled results on bluff-body-stabilized and swirl-stabilized jets and flames
3. New experimental work, including new measurements on TNF target flames and experimental techniques directed at LES validation.
4. Proposals, priorities, and planning for future work and TNF7 (Chicago, 2004).

The complete TNF6 Proceedings are available for download in pdf format from the Internet at www.ca.sandia.gov/tdf/Workshop. The pdf file includes materials from the proceedings notebook that was distributed to workshop participants in Sapporo, as well as additional materials (such as vugraph copies) contributed after the workshop. This summary briefly outlines highlights from presentations and discussions on these topics. Comments and conclusions given here are based on the perspectives of the authors and do not necessarily represent consensus opinions of the workshop participants. This summary does not attempt to address all topics discussed at the Workshop.

Results in this and other TNF Workshop proceedings are contributed in the spirit of open scientific collaboration. Some results represent completed work, while others are from work in progress. Readers should keep this in mind when reviewing these materials. It may be inappropriate to quote or reference specific results from these proceedings without first checking with the individual authors for permission and for their latest information on results and references. It should also be noted that several papers relevant to the target flames were presented at the 29th Combustion Symposium, and these papers contain more detailed descriptions and comparisons than are included here.

ACKNOWLEDGMENTS

Local arrangements for TNF6 were expertly coordinated by Yuji Ikeda of Kobe University and Masashi Katsuki of Osaka University. Sponsorship contributions from Continuum Lasers, Dow Chemical, Fluent, GE Aircraft Engines, Nippon Sanso, Seika Corporation, Takuma, and Tokyo Gas are gratefully acknowledged. These contributions were used to reduce the registration fee for university faculty and eliminate the fee for students. Support for R. Barlow's work in coordinating TNF Workshop activities and the web site is provided by Sandia National Laboratories with funding from the US Department of Energy, Office of Basic Energy Sciences.

HIGHLIGHTS OF TECHNICAL DISCUSSIONS

Mixing Models and Piloted Jet Flame Calculations

Parametric evaluation of mixing models for pdf calculations was a major focus topic for this workshop. S. Pope (see full Proceedings) presented comparisons of the properties and results of three mixing models: modified Curl, EMST, and IEM. Highlights are outlined below in the context of the piloted methane flames.

At TNF4 and TNF5 calculations of the Barlow & Frank flames, *D*, *E* and *F* were presented by several groups. But for flame *F*, which exhibits substantial local extinction, there were only four sets of calculations, all using PDF methods. These were from the groups at Berkeley, Cornell, Darmstadt, and Imperial College. At TNF6 further PDF calculations were contributed by the Imperial College and Cornell/Fluent groups, and predictions of extinction/re-ignition in the *D-E-F* flame series was demonstrated using ODT (Echekki et al. poster). From all of these calculations the following conclusions can be drawn, and suggestions made.

- The model calculations have a first order dependence on both the mixing model and chemical mechanism used.
- Increasing the mixing rate (through the constant C_ϕ) decreases the calculated extent of local extinction.
- Calculations in good agreement with the data for flame *F* have been obtained with two approaches:
 1. with the modified Curl model ($C_\phi = 2.3$) and the Lindstedt mechanism (Imperial College)
 2. with the EMST model ($C_\phi = 1.5$) and the augmented reduced mechanism (Cornell University).
- Flame *F*, being close to global extinction, is sensitive to small changes in boundary conditions and model constants. Hence it is more reliable to study the behavior of models as a function of jet velocity (from flame *D* to *E* to *F*), rather than just at one fixed condition.
- All current mixing models have unsatisfactory aspects.
- The fuel used by Barlow & Frank (methane/air in volume ratio 1:3) has a stoichiometric mixture fraction of $\xi_s \approx 0.35$, which makes the flame easier to model than a flame of pure methane ($\xi_s \approx 0.05$). Hence it would be valuable in future experiments to vary the fuel mixture (and hence ξ_s), as well as for modelers to consider the older data, which is available for a range of fuels.
- A systematic study of different mixing models *and* chemistry mechanisms is still needed. To this end, the different mixing models and mechanisms are to be made available on the web.

In addition to the calculations noted above, Lindstedt and Louloudi presented a paper at the 29th Combustion Symposium that is directly relevant to this TNF6 discussion topic. They performed pdf calculations on a series of four piloted methanol flames ($\xi_s = 0.135$) and achieved reasonable agreement with measured trends in local extinction by using the same mixing model parameters as for their methane flame calculations. They also include some discussion of the effects of changing C_ϕ , and note that re-ignition may be more sensitive than extinction.

Chemical Mechanisms

For methane/air flame studies, the principal mechanisms in use by TNF Workshop participants are GRI 2.11, GRI 3.0, Lindstedt's mechanism, and reduced versions of these same mechanisms (with 12 or more steps and 16-20 species, including NO). Differences among these mechanisms are considered small with regard to predictions of major species. However, flames approaching blowoff are recognized as sensitive to small differences in various parameters. Therefore, broad availability of mechanisms will facilitate further parametric studies on the coupled influence of submodels and their parameters on computed results.

Work was begun immediately after TNF6 to make several relevant mechanisms available in Chemkin format. The following reduced mechanisms will be made available for download from the TNF web site:

- Methanol – reduced mechanism from Lindstedt with Chemkin translation by J-Y Chen
- Methane – reduced versions of GRI 2.11 and GRI 3.0 from Chen and coworkers, including ARM2 as used by the Cornell group.
- CO/H₂/N₂ – reduced mechanism from Chen (tested only for the Sandia flame mixture)
- H₂ – 5-step reduced mechanism from Chen (already on the web)

The relative performance of various mechanisms in predicting NO formation in laminar CH₄/air flames was a major topic at TNF5 (Delft 2000). Further direct comparisons are needed and would be facilitated by availability of mechanisms in a common format. However, the tentative conclusion from TNF5 remains that the Lindstedt methane mechanism and GRI 2.11, as well as reduced versions, yield NO results in reasonable agreement with measurements in laminar CH₄/air flames having the same degree of partial premixing as the piloted jet flames (75% air, 25% CH₄).

It appears that the relative performance of mechanisms in predicting NO in methane flames depends on the degree of partial premixing. In the context of future TNF comparisons of NO results in the Sydney bluff-body and swirl flames (CH₄, 1:2 CH₄/air, and 1:1 CH₄/H₂), it would be useful to test various mechanisms against measurements from laminar flames with these same fuel mixtures.

Radiation

The main effect of flame radiation in calculations of the piloted jet flames is to reduce the predicted level of NO; the influence of radiation on major species mass fractions is not significant in the calculations. Therefore, the main question facing TNF participants is whether the recommended radiation model, which assumes the optically thin limit, is adequate for assessment of NO predictions in the target flames. Unfortunately, we have yet to reach a clear conclusion on this because there appear to be contradictions among calculated results for total radiant fraction, which

is the most reliable experimental indicator of the integrated effect of radiation. Values (from past workshops) of the predicted total radiant fraction from piloted flame D range from about 6% to about 12%, even though the radiation model is supposed to be the same and the predicted scalar and velocity fields are similar. The measured radiant fraction is 5.1%, so some calculations suggest the optically thin model is about right, while others suggest that it over predicts radiation by more than a factor of two. Reasons for the differences in the predictions are still unclear, and careful comparisons of model implementations might be useful.

A detailed study of several radiation models applied to flame D was presented on a poster by Coelho et al. Their results suggest that the optically thin model is not accurate for flame D and that a more sophisticated radiation model is needed for agreement with the measured radiant fraction. Unfortunately, the authors were unable to attend the workshop, so this work was not fully discussed. Detailed radiation calculations are computationally expensive, and the consensus among modelers present at TNF6 was to continue using the optically thin model for now.

For calculations that include NO formation, modelers are still encouraged to run both adiabatic and radiative cases to represent upper and lower bounds on the predicted NO levels.

New spectral radiation data are available on several of the TNF jet flames (see the contribution by Zheng et al.). Such data can be used to evaluate the relative importance of absorption of the strong CO₂ band within the flame.

Scalar Dissipation

The scalar dissipation, χ , is an important quantity in most modeling approaches to non-premixed turbulent combustion. The statistics of primary interest are its PDF, its variance, and its conditional mean. In spite of their importance, model predictions of scalar dissipation statistics are seldom reported. It would be profitable now for modelers to pay more attention to scalar dissipation. What do different models imply for scalar-dissipation statistics? How do these compare to the available experimental data?

Overviews of issues relevant to the modeling and measurement of scalar dissipation were presented by R. Bilger and R. Barlow, respectively. The main conclusion from both is that more work is needed. Good progress is being made on the experimental side, as represented by the contributions from Karpetsis & Barlow and Frank et al. Details of both experiments are presented in 29th Combustion Symposium papers. However, we are not yet at the point of fully understanding the limitations and accuracy of these measurements, so it is still premature to conduct quantitative comparisons with models.

Another 29th Symposium paper that is very relevant to this topic is from H. Pitsch and presents a LES/unsteady-flamelet calculation of flame D that achieves improved agreement on CO, H₂, and NO by accounting for the effect of resolved scalar dissipation rate fluctuations. This result suggests that the over prediction of reaction progress in fuel-rich conditions observed in other flamelet-based calculations and in CMC results for flame D may also be corrected by improved modeling of scalar dissipation.

Scalar dissipation is expected to be a major topic for the next workshop. An important issue to be addressed by experimentalists and modelers in collaboration is how best to compare 1D and 2D results from experiments with models representing scalar dissipation in the 3D field. Issues of spatial resolution in the measurements will also require careful attention.

Bluff Body Flow and Flame Comparisons

For the non-reacting case, two submissions were made: an LES calculation from TU Darmstadt (Kempf and Janicka) and a standard RANS(k-e) calculation by McDermott Technology (Sayre). For the reacting case HM1, there were a range of submissions from three groups: Pope's at Cornell using the PDF approach, Lindstedt's at Imperial College using unsteady RANS and PDF, and Roerkaerts' at TU-Delft using RANS (and computing case HM1E instead of HM1). In his PDF calculations, Lindstedt used a 20 species detailed mechanism that included NO. All other calculations assumed either flamelets or equilibrium chemistry.

Generally, calculations are in much better agreement with the measurements and this is a substantial advance made since the last workshop. The LES calculations for the non-reacting cases are very promising and should be extended to the reacting cases. Improved numerical methods used with Pope's PDF approach have resulted in significant improvements, since TNF5. It appears that the discrepancy, which remains between the measurements and the calculations at downstream locations in the jets and flames, may be due to vortex shedding on the outer surface of the bluff-body. Lindstedt's transient calculations support this argument, since they show better agreement at downstream locations. It is worth noting here that vortex shedding was imaged in these flames and reported in 1998 (Masri et al., *Proc. Comb. Inst.* 27:1031-1038, 1998). It is of interest, therefore, to compare approaches based on steady RANS, unsteady RANS (axi-symmetric and 3D) and LES.

While using the fast chemistry assumption (or flamelets) may be adequate to compute the mean temperature and compositional structure in the recirculation zone of flame HM1, calculations further downstream are more likely to require detailed chemical kinetics due to the occurrence of some localized extinction. The computations of Lindstedt, which use 20 species, are adequate for temperature, major species and NO but not for CO and OH, which still show significant deviations. It should be noted that the flame considered here (HM1) does not exhibit large finite-rate chemistry effects. For TNF7, the series HM1, HM2 and HM3 should be target flames, so as to test the models' abilities to represent local extinction and other finite-rate chemistry phenomena. For these flames the comparisons should be expanded beyond spatial profiles to include such things as scatter plots, conditional means, and the burning index for select scalars.

Swirl Flow and Flame Comparisons

It is a natural progression for the TNF program to tackle increasingly complex flows, which are more relevant to practical combustors. The swirl burner, developed at the University of Sydney and introduced in TNF5, provides such a flow, which has the added complexity of swirl and flow recirculation, while maintaining simple boundary conditions. Depending on the swirl number and stream velocities, this flow displays a rich variety of qualitatively different flow patterns. In many cases there appears to be large-scale unsteadiness, including the precession of the jet. A range of swirling jets and flames, for which an extensive database is made available on the web, are now target problems for TNF workshops.

For TNF6, two non-reacting jets and two flames were selected for calculations. The jets (N16S159 and N29S054) have swirl numbers of 0.5 and 1.6 and a jet velocity of 66m/s. The first flame is (SMH1) which uses a mixture of methane-hydrogen (1/1 by vol.), has a swirl number of 0.37, a fuel jet velocity of 140.8m/s and is at 53% of the blow off velocity. The second flame is (SMA2) with a methane-air mixture (1/2 by vol.), a swirl number of 1.59, a fuel jet velocity of 66.3m/s. Flame SMA2 is at 31% of the blow off velocity.

Only a few calculations of these new target cases were presented. The University of Sydney submitted results using full 3D, transient RANS calculations for the non-reacting jets and 2D axisymmetric calculations for the flame. The computed velocities for the non-reacting jets are very close to the measurements for the low swirl number case (N29S054) but deviations are more significant at high swirl numbers (N16S159). The 2D axisymmetric results for the flames are less encouraging implying that full 3D transient calculations are necessary. It should be noted that vortex breakdown and jet precession are computed for the non-reacting cases and these must be verified against experimental data. Pitsch from Stanford performed LES calculations for the high swirl case of the nonreacting flow and showed encouraging results (vugraphs added to the final proceedings).

It is noted that an improved set of boundary conditions is necessary and this will be provided in time for TNF7.

New Experiments on TNF Flames and Experiments Directed at LES Validation

Nearly all comparisons of measured and modeled results for TNF target flames have been based on single point statistics of scalars and velocity. Such comparisons are relatively easy to perform and interpret, and they are expected to remain the primary means for quantitative evaluation of turbulent combustion models. However, it will be necessary to expand comparisons to include quantities that represent the spatial structure and flow dynamics of target flames, such as the bluff-body and swirl flames, which may be strongly affected by large-scale unsteadiness. The definition of procedures and criteria for such comparisons will be an important area for collaboration between experimental and computational researchers.

These two sessions in the TNF6 agenda were intended to: i) raise awareness concerning experimental techniques and types of data that may be useful for future comparisons with models, ii) promote discussion to identify specific data needs of modelers, particularly with regard to LES validation, and iii) promote discussion of specific criteria for comparing measured and modeled results on spatial structure and flame dynamics.

Several new experiments were conducted on various TNF Workshop flames over the past two years, and the majority of these involved imaging techniques or time series measurements of spatial structure or dynamics. New experiments included various measurements in the Darmstadt turbulent opposed jet burner, measurements of scalar dissipation in piloted flame D, combined PIV and multi-frame OH-PLIF imaging in the DLR $\text{CH}_4/\text{H}_2/\text{N}_2$ jet flame, and OH time series measurements in the Darmstadt "H3" hydrogen jet flame. In addition, A. Dreizler presented an overview of techniques and issues related to experimental validation of LES models.

Discussions of specific data needs and criteria for comparison were limited, reflecting the fact that this is new ground. Continued discussion of these issues is strongly encouraged because the high costs of relevant experiments and large-scale calculations will limit our opportunities for meaningful, quantitative comparisons.

State of LES

A significant advance in TNF6 was the presentation of LES calculations of several of the target flames. In order for LES to be a reliable predictive tool, care must be taken (a) to ensure that the grid is sufficiently fine to resolve the bulk of the energy and stress (b) to have an appropriate means to specify time-dependent turbulent inflow conditions, and (c) to model the subgrid turbulence/chemistry interactions.

It is clear from the LES calculations presented that a wide variety of grid resolutions are being employed. This disparity is primarily due to limited computational resources and the long turn-around times required when one uses denser (but preferable) grids. As research progresses, it will become imperative that grid resolution issues be addressed in a systematic way to establish the appropriate performance metrics and better separate numerical errors from modeling errors.

The issue of boundary conditions was also addressed to some degree and will be an issue of high priority in future workshops. LES requires the specification of both mean flow quantities and the higher time evolving moments at respective inflow boundaries. Well-defined pressure conditions must be provided at out-flow boundaries of bounded domains with subsonic flow. This is especially important for recirculating swirl flows in confined geometries. Unbounded domains pose analogous requirements. It will be important in future studies to understand the influence of various boundary condition treatments on interior flow characteristics.

The appropriate specification of boundary conditions is inherently coupled to the specification of grid resolution requirements and the related sensitivities. Ideally, future studies should address both issues simultaneously. Detailed analysis of the accuracy and sensitivities associated with LES subgrid-scale models, particularly those associated with turbulence/chemistry interactions, can only occur after we have a high level of confidence in our ability to simulate the geometrically dominated turbulent fluid dynamic processes associated with the various target flames.

Because combustion occurs at the smallest scales, it will become more and more important to study subgrid turbulence/chemistry interactions with minimal ambiguities associated with both the experiments and companion calculations. To achieve this goal in the systematic manner described above it is imperative that the target flame descriptions include simultaneous velocity-scalar measurements with well documented boundary conditions. Good progress has been made, and it will become more and more important to establish high-fidelity benchmarks that systematically focus on the three key areas outlined above.

Other Topics

While the TNF Workshop is mainly focused on fundamental issues, many participants are separately involved in research more directly related to applications and, in particular, gas turbine combustors. In the interest of promoting collaboration and information exchange in this area of common interest, time was allotted for several people to give brief overviews of research activities related to combustion in gas turbines, including both premixed and nonpremixed combustion. Details are not included in the proceedings, but expanded collaborations in this area are expected.

L. Rahn (see poster abstract) described US DOE supported work to develop network tools for data sharing. One current project that may be directly useful to TNF participants is the development of web-based tools for automatic translation of chemical mechanisms across different formats. This could facilitate parametric comparison of chemical mechanisms in combination with other submodels. Formatting and sharing of large data sets from imaging experiments and from LES calculations is another area of anticipated future need. We will be following progress in both areas.

AREAS FOR FURTHER WORK

During the closing discussion, several areas for further work related to the main target flames were identified and are listed below with the hope that progress can be made in these areas before the next workshop. In addition to these listed topics there is ongoing work by several groups on other TNF target flames and other topics closely related to the workshop objectives. This includes work

on such things as chemical mechanisms for TNF use, radiation modeling, turbulence modeling, development of LES for combustion, measurement and calculation of other TNF flames, and development of experimental methods.

Piloted Jet Flames

- Systematic evaluation of mixing models and chemical mechanisms (in combination), with particular attention to the sensitivity of local extinction and re-ignition to changes in these submodels.
- Further experiments in which parameters are varied (e.g., the fuel composition). There is particular interest in cases with a lower stoichiometric value of the mixture fraction.
- Calculations and evaluation of older Sydney/Sandia data sets with other fuels. There may be greater errors in some species results from these older experiments, but information on local extinction trends should be very useful for the combined evaluation of mixing models and chemical mechanisms.
- Continued experiments on scalar dissipation and related quantities, combined with collaborative work to define appropriate ways of comparing measured and modeled results.

Bluff Body Flames and Swirl Flames

- Examination of turbulence/chemistry interactions in the series of bluff-body flames HM1, HM2, and HM3. Model calculations that achieve good agreement with measured velocity and scalar fields in a complex, recirculating flow and also track the trends of localized extinction and re-ignition would represent a major step forward.
- Measurements of velocity profiles upstream of the burner exit and inside the annulus of the swirl burner were specifically requested by LES modelers because bulk velocities and profiles downstream of the exit are not sufficient for good specification of the model problem.
- More calculations of the Sydney bluff-body swirl burner using LES, PDF, and 3D-transient RANS.
- Examination of large-scale, unsteady motions via LES and/or unsteady RANS.
- Examination of flames of other fuels such as methanol and H₂/CO.
- Consideration of existing data and future needs for experimental results on the spatial structure and dynamics of the bluff-body and swirl cases.

PROPOSALS FOR NEW TNF TARGET FLAMES

TNF Workshop has approached the model validation process by selecting target flames that cover a progression in complexity, with respect to both fluid dynamics and chemical kinetics. This has made it easier to isolate specific submodels and understand their capabilities and limitations. In adding new target flames it is desirable to select cases that test the robustness of specific submodels or include new combustion processes that must be mastered on the way to developing predictive capabilities for practical combustion systems. It is also important to avoid cases that are too far

beyond present modeling capabilities or cannot be characterized with the accuracy and completeness needed for useful comparisons with models.

Three types of flames were proposed. Inclusion of these flames as formal workshop targets will depend upon the level of interest from modelers and upon the quality and completeness of the available measurements.

Lifted Jet Flames

Flame stabilization in a non-uniformly mixed flow is a challenging model problem. Most turbulent burners are operated so that the flame is not in direct contact with hardware (i.e. lifted). The nonpremixed swirl flames being studied at DLR and at Stanford as simple analogues of gas turbine combustors are both lifted. Furthermore, in many of the Sydney Bluff-Body and Swirl cases the reaction zone at the outer edge of the recirculation zone is lifted above the corner of the bluff body. The lifted jet flame is an appropriate starting point for investigation of models that must eventually predict the flame stabilization details of more complicated burners.

Lifted flames have received a lot of attention in the experimental literature. Therefore, existing experimental data on lifted flames should be considered before new experiments are undertaken. There is also a need for some discussion regarding the types of experimental data that will be most useful. Because lifted flames can be sensitive to coflow conditions, the coflow needs to be carefully controlled and characterized. The same is true for all boundary conditions. Experimental parameters, such as coflow velocity and jet velocity, and fuel composition, should be varied in order to test models' abilities to reproduce trends.

Vitiated Coflow Flames

Data for a possible model flame investigated at UC Berkeley by Dibble and Cabra are available (see Cabra et al. poster abstract). The Berkeley flames are lifted flames stabilized in a vitiated coflow. Practical burners use recirculation of combustion products to promote flame stabilization, and the Berkeley burner was designed to examine flame stabilization in combustion products without the complexity of flow recirculation.

Dally at Adelaide has also a possible data set for a range of flames stabilized on a FLOX burner, which has reduced O_2 and elevated temperature in the coflow. (see Dally et al. poster abstract).

Spray Flames

Masri's group at the University of Sydney is developing a data set for spray flames with well-defined boundary conditions and dilute loadings.

ORGANIZATION OF TNF7

Location and Dates – The TNF7 Workshop will be held in the Chicago area near the time of the 30th Combustion Symposium (probably just before).

Target Problems – We can expect TNF7 to include work on piloted, bluff-body, and swirl flames as outlined above in AREAS FOR FUTURE WORK. Additional target flames or focus topics will be added as appropriate, based on research progress and the interests of the organizers and participants.

Sixth International Workshop on Measurement and Computation of Turbulent Nonpremixed Flames

18-20 July 2002, Sapporo, Japan
Editors: R. S. Barlow and H. Pitsch

PREFACE:

The TNF Workshop series facilitates collaboration and information exchange among experimental and computational researchers in the field of turbulent nonpremixed and partially premixed combustion, with current emphasis on fundamental issues of turbulence-chemistry interactions in gaseous, non-sooting flames. The 1st TNF Workshop was held in Naples, Italy in July 1996, before the 26th Combustion Symposium. Its purpose was to select experimental data sets for testing combustion models and establish guidelines for collaborative comparisons of measured and calculated results on these target flames. Subsequent workshops were held in Heppenheim, Germany (1997), Boulder, Colorado (1998), Darmstadt, Germany (1999), and Delft, The Netherlands (2000). Proceedings of TNF3, TNF4, and TNF5 are available on the Internet.

Our overall objectives are to: i) provide an effective framework for comparison of different combustion modeling approaches, ii) identify and correct inconsistencies or gaps in the experimental data sets, iii) establish series of benchmark experiments and calculations that cover a progression in geometric and chemical kinetic complexity, and iv) gain a better understanding of the capabilities and limitations of combustion models and submodels. We emphasize that this is not a competition, but rather a means of identifying areas for potential improvements in a variety of modeling approaches. This collaborative process benefits from contributions by participants having different areas of expertise, including velocity measurements, scalar measurements, turbulence modeling, chemical kinetics, reduced mechanisms, mixing models, radiation, and combustion theory. The process also benefits from the rapid time scale of communication that is afforded by the Internet. Data sets, computational submodels, and results of comparisons are being made available on the web to allow convenient access by all interested researchers. In many cases results are shared before they appear in the open literature.

The TNF Workshop format is intended to promote open discussion of fundamental research issues that are relevant to our overall objectives. All participants are encouraged to be active in these discussions, during the scheduled technical sessions and in small groups at other times.

ACKNOWLEDGEMENTS:

Partial support for the organization of the TNF Workshop series is provided by Sandia National Laboratories with funding from the United States Department of Energy, Office of Basic Energy Sciences.

Sponsorship contributions for Continuum, Dow Chemical, Fluent, GE Aircraft Engines, Nippon Sanso, Seika Corporation, Takuma, and Tokyo Gas are gratefully acknowledged and have been used to reduce the registration fees for university faculty and students.

TNF6 ORGANIZING COMMITTEE: R. S. Barlow, R. W. Bilger, J.-Y. Chen, A. Dreizler, J. P. Gore, Y. Ikeda, J. Janicka, W. P. Jones, M. Katsuki, R. P. Lindstedt, A. R. Masri, J. C. Oefelein, H. Pitsch, S. B. Pope, D. Roekaerts

LOCAL HOST COMMITTEE: Y. Ikeda, M. Katsuki, R. Homma

TNF6 Workshop Participants

Name		Affiliation	Country	Email
Ahn	Chul-Ju, Mr.	Osaka University	Japan	ahncj@mech.eng.osaka-u.ac.jp
Al-Abdeli	Yasir, Mr.	The University of Sydney	Australia	alabdeli@mech.eng.usyd.edu.au
Bai	Xue-Song, Prof.	Lund Institute of Technology	Sweden	Xue-Song.Bai@vok.lth.se
Barlow	Robert S., Dr.	Sandia National Laboratories	US	barlow@ca.sandia.gov
Bilger	Robert W., Prof	The University of Sydney	Australia	bilger@aeromech.usyd.edu.au
Cabra	Ricardo, Mr.	University of California, Berkeley	US	ricardo@me.berkeley.edu
Cha	Chong, Dr.	Stanford University	US	chongcha@stanford.edu
Chen	J.-Y., Prof.	University of California, Berkeley	US	jychen@newton.me.berkeley.edu
Cho	Joho, Mr.	Hanyang University	Korea	ymkim@hanyang.ac.kr
Dally	Bassam, Dr.	Adelaide University	Australia	bassam.dally@adelaide.edu.au
Demiraydin	Läle, Ms.	ETH Zurich	Switzerland	demiraydin@hnt-iet.mavt.ethz.ch
Dibble	Robert, Prof.	UC Berkeley	US	rdibble@me.berkeley.edu
Dinkelacker	Friedrich, Dr	University of Erlangen	Germany	fdi@ltt.uni-erlangen.de
Dreizler	Andreas, Dr.	TU Darmstadt	Germany	dreizler@ekt.tu-darmstadt.de
Frank	Jonathan, Dr.	Sandia National Laboratories	US	jhfrank@sandia.gov
Goldin	Graham, Dr.	Fluent	US	gmg@fluent.com
Gomez	Alessandro, Prof.	Yale University	US	allesandro.gomez@yale.edu
Gore	Jay, Prof.	Purdue University	US	Gore@ecn.purdue.edu
Hasse	Christian	Institut fuer Technische Mechanik, Aachen	Germany	c.hasse.itm.rwth-aachen.de
Homma	Ryoji, Dr	Tokyo Gas	Japan	homma@tokyo-gas.co.jp
Ikeda	Yuji, Prof.	Kobe University	Japan	ikeda@mech.kobe-u.ac.jp
Jeffries	Jay, Dr.	Stanford University	US	jay.jeffries@stanford.edu
Jones	Bill, Prof.	Imperial College	UK	w.jones@ic.ac.uk
Kalt	Peter, Dr.	The University of Sydney	Australia	pkalt@mech.eng.usyd.edu.au
Karpetsis	Adonios, Dr.	Sandia National Laboratories	US	ankarpe@ca.sandia.gov
Katsuki	Masashi, Prof.	Osaka University	Japan	katsuki@mech.eng.osaka-u.ac.jp
Keller	Jay, Dr.	Sandia National Laboratories	US	jokelle@ca.sandia.gov
Kelman	James, Dr.	Cranfield University	UK	j.kelman@cranfield.ac.uk
Kempf	Andreas, Mr.	TU Darmstadt	Germany	akempf@gmx.net
Kerstein	Alan R., Dr.	Sandia National Laboratories	US	arkerst@sandia.gov
Kim	Gunhong, Mr.	Hanyang University	Korea	ymkim@hanyang.ac.kr
Kim	Hoojoong, Mr.	Hanyang University	Korea	hoojoong@korea.com
Kim	Yong-Mo, Prof.	Hanyang University	Korea	ymkim@hanyang.ac.kr
Kronenburg	Andreas, Dr.	Imperial College, London	UK	a.kronenburg@ic.ac.uk
Kurose	Ryoichi, Dr.	Yokosuka Research Laboratory	Japan	kurose@criepi.denken.or.jp
Kyritsis	Dimitrios, Dr.	Yale University	US	dimitrios.kyritsis@yale.edu
Lindstedt	R.P., Prof (Peter)	Imperial College, London	UK	p.lindstedt@ic.ac.uk
Long	Marshall, Prof.	Yale University	US	marshall.long@yale.edu
Masri	Assaad R., Prof.	The University of Sydney	Australia	masri@aeromech.usyd.edu.au
Meier	Wolfgang, Dr.	DLR Stuttgart	Germany	wolfgang.meier@dlr.de
Miller	J. Houston, Prof.	George Washington University	US	houston@gwu.edu
Mizobuchi	Yasuhiro, Dr.	National Aerospace Laboratory of Japan	Japan	mizo@nal.go.jp
Mueller	Christian, Dr.	Abo Akademi University	Finland	cmueller@mail.abo.fi
Muradoglu	Metin, Dr.	Koc University	Turkey	mmuradoglu@ku.edu.tr
Myhrvold	Tore, Mr.	Norwegian University of Science and Technology	Norway	tore.myhrvold@energy.sintef.no
Oefelein	Joseph, Dr.	Sandia National Laboratories	US	oefelei@sandia.gov
Pitsch	Heinz, Dr.	Stanford University	US	H.Pitsch@stanford.edu
Pope	Stephen, Prof.	Cornell University	US	pope@mae.cornell.edu
Rahn	Larry, Dr.	Sandia National Laboratories	US	rahn@sandia.gov
Renfro	Michael W., Dr.	Purdue University	US	renfro@ecn.purdue.edu
Roekaerts	Dirk, Prof.	Delft University of Technology	Netherlands	dirkr@ws.tn.tudelft.nl
Sayre	Alan, Prof.	MTI	US	ansayre@mcdermott.com
Schulz	Christof, Dr.	University of Heidelberg	Germany	christof.schulz@pci.uni-heidelberg.de
Shinjo	Junji, Dr.	National Aerospace Laboratory of Japan	Japan	shinjou@nal.go.jp
Smith	Nigel, Dr.	Defence Science & Technology Organisation	Australia	nigel.smith@defence.gov.au
Takeno	Tadao, Prof.	Meijo University	Japan	takeno@ccmfs.meijo-u.ac.jp
Tang	Qing, Mr.	Cornell University	US	qtang@mae.cornell.edu
Trouillet	Philippe, Dr.	Stanford University	US	trou@navier.stanford.edu
Vagelopoulos	Christina, Dr.	Sandia National Laboratories	US	cmvangel@ca.sandia.gov
Weydahl	Torleif, Dr.	SINTEF Energy Research	Norway	Torleif.Weydahl@energy.sintef.no
Williams	Forman A., Prof.	University of California, San Diego	US	faw@mae.ucsd.edu
Zimmer	Laurent, Dr.	Kobe University	Japan	zimmer@ms-5.mech.kobe-u.c.ac.jp

TNF6 – Agenda

Sheraton Sapporo, 18-20 July 2002

(Times may be adjusted to accommodate discussion.)

Thursday July 18, 2002

- 4:00 – 6:00 Registration and Poster Setup
6:00 – 9:00 Welcoming Remarks, Reception, and Poster Session
(Masashi Katsuki, Yuji Ikeda, and Rob Barlow)

Friday July 19, 2002

- 8:00 – 8:15 Overview of the TNF Workshop Process, Summary of TNF5
(Rob Barlow)
- 8:15 – 10:00 Submodel Investigations in Connection with Simple Jet and Piloted Flames:
Mixing (Coordinator: Steve Pope)
Chemistry (Coordinator: Peter Lindstedt)
Turbulence Models (Coordinator: Dirk Roekaerts)
(This session will continue after the break.)
- 10:00 – 10:30 Coffee Break in the Poster Area
- 10:30 – 12:30 Submodels (continued):
Radiation (Coordinators: Jay Gore and Dirk Roekaerts)
- Comparison of Measured and Modeled Results on Bluff-Body and Swirl Flames
(Coordinator: Assaad Masri)
- 12:30 – 1:30 Lunch
- 1:30 – 3:00 Measurement and Modeling of Scalar Dissipation
(Coordinators: Bob Bilger and Rob Barlow)
New Experiments on TNF Flames
(Coordinator: Andreas Dreizler)
- 3:00 – 3:30 Coffee Break in the Poster Area
- 3:30 – 5:00 Measurements Directed at LES Validation (Spatial Structure and Dynamics)
(Coordinator: Andreas Dreizler)
Progress, Problems, and Future Directions for LES of TNF Workshop Flames
(Coordinators: Bill Jones and Heinz Pitsch)
- 5:00 – 6:30 Informal Poster Session
- 6:30 Dinner

TNF6 – Agenda (continued)
Sheraton Sapporo, 18-20 July 2002
(Times may be adjusted to accommodate discussion.)

Saturday July 20, 2002

- 8:30 – 10:00 Continued Discussion on Day-1 Topics (as needed)
Modeling and Measurement of Mixed-Mode Combustion (re-ignition, lifted flames, edge flames, lifted regions of the bluff body and swirl flames, etc.)
(Coordinator: J-Y Chen)
- 10:00 – 10:30 Coffee Break in the Poster Area
- 10:30 – 12:30 Opportunities for Collaboration on Problems Related to Gas Turbine Combustion
(Coordinator: Rob Barlow)
Data Sharing Technologies
(Discussion Leader: Larry Rahn)
Proposals and Priorities for Future TNF Comparisons
(Discussion Leader: Assaad Masri)
- 12:30 – 1:30 Lunch (Working lunch for Organizing Committee)
- 1:30 – 2:30 Summary Discussion and Planning for the next Workshop
(Discussion Leader: Steve Pope)
- 2:30 – 3:30 Remove Posters, Free Discussion Time
- 3:30 Depart for Excursion to the Sapporo Beer Brewery

Abstracts

1. Ahn, C.-J., Kitajima, A., Akamatsu, F., Katsuki, M.:
The Effect of O₂ Concentration and Temperature on Turbulent Flame Structure
2. Bessler, W. G., Schulz, C., Lee, T., Shin, S.-I., Jeffries, J. B., Hanson, R. K.:
Quantitative Temperature Imaging Using NO-LIF in Flames at Elevated Pressures (1-60 bar)
3. Cabra, R., Chen, J. Y., Dibble, R. W., Karpetis, A. N., Barlow, R. S.:
Simultaneous Laser Raman-Rayleigh-LIF Measurements of a Lifted Turbulent CH₄/Air Jet Flame in a Vitiated Coflow
4. Cao, R., Liu, K., Tang, Q., Pope, S. B., Caughey, D. A.:
Joint PDF Calculations of the Piloted Methane/Air Jet Flames
5. Cha, C.:
 $\sigma^2 \approx 5$ for the Sandia Piloted Jet Flames (Analysis and Implications of the Intermittency of Bilger's Scalar Dissipation Rate)
6. Coelho, P. J., Teerling, O. J., Roekaerts, D.:
Spectral Radiative Effects and Turbulence-Radiation-Interaction in Sandia Flame D
7. Dally, B. B., Karpetis, A. N., Barlow, R. S.:
Turbulent Nonpremixed Jet Flames at Reduced Temperature
8. Demiraydin, L., Gass, J., Poulidakos, D.:
Numerical Simulation of a Piloted Methane/Air Jet Flame Using the Coupled TLFM/PDF Model
9. Dreizler, A., Janicka, J.:
Measurements Directed at LES Validation
10. Echehki, T., Kerstein, A. R., Chen, J. Y.:
One-Dimensional Turbulence Simulation of Extinction and Re-ignition Predictions in Piloted Methane-Air Jet Diffusion Flames
11. Frank, J. H., Kaiser, S. A., Long, M. B.:
Two-Dimensional Measurements of Reaction-Rate, Mixture Fraction, and Temperature in Turbulent Methane/Air Jet Flames
12. Geyer, D., Dreizler, A., Nauert, A., Omar, S., Janicka, J.:
A Comprehensive Characterization of a Turbulent Opposed-Jet by 1D-Raman/Rayleigh, 2D-LIF and LDV

13. Hassel, E. , Nocke, J. , Leder, A. , Brede, M. , Meier, W., Keck, O.:
Proposal of New Kind of Burner for Pure Hydrocarbon Flames with Minimal Soot, Ros-
tocker Ring Burner (RRB)
14. Hoffmann, A., Zimmermann, F., Schulz, C.:
Instantaneous Three-Dimensional Visualization of Concentration Distributions and Gra-
dients in Turbulent Processes with a Single Laser
15. Karpetsis, A. N., Barlow, R. S.:
New Measurements on Piloted Flames and Simultaneous Line Raman and Crossed PLIF
16. Kelman, J. B.:
The Role of Partially Premixed Flames in Industrial Processes
17. Kempf, A., Sadiki, A., Janicka, J.:
Large Eddy Simulation of Turbulent Jet Flames: A Comparison
18. Kempf, A., Sadiki, A., Janicka, J.:
Large Eddy Simulation of a Turbulent Opposed Jet: The Darmstadt Configuration
19. Kim, H. J., Kim, Y. M.:
Prediction of Flame Liftoff and Structure in Non-Premixed Turbulent Jet Flames
20. Kim, G. H., Cho, J. H., Kim, Y. M., Kang, S. M.:
Transient Flamelet Analysis for Detailed Structure and NO_x Formation Characteristics of
 H_2/CO Bluff-Body Flames
21. Klein, M., Kempf, A., Janicka, J.:
Generating Turbulent Inflow Conditions for Combustion LES
22. Krasinsky, D., Roekaerts, D., Naud, B., Nieuwstadt, F.:
LES Results of the Bluff-Body Stabilized Flow
23. Li, G., Naud, B., Roekaerts, D.:
Sensitivity to model constants, boundary conditions and grid in a Simulation of a Bluff-
Body Flame with the Reynolds Stress Model
24. Liu, K., Muradoglu, M., Tang, Q., Pope, S. B., Caughey, D. A.:
JPDF/ARM Calculations of Bluff-Body Stabilized Flames
25. Meier, W., Weigand, P., Keck, O., Duan, X., Lehmann, B., Stricker, W., Aigner, M.:
Experimental Analysis of Swirling Flames in a Gas Turbine Model Combustor
26. Merci, B., Roekaerts, D., Dick, E.:
Influence of Computational Aspects on Results for Flame D
27. Mizobuchi, Y., Shinjo, J., Tachibana, S., Ogawa, S., Takeno, T.:
Effects of Turbulence on Flame Chemistry

28. Muradoglu, M., Liu, K., Pope, S. B.:
PDF Modeling of a Bluff-Body Stabilized Turbulent Flame
29. Oefelein, J. C., Schefer, R. W.:
Modeling and Validation of Lean Premixed Combustion For Ultra-Low Emission Gas Turbine Combustors
30. Pitsch, H., Trouillet, P., Pierce, C. D., Tribbett, E., Sipperley, C. M., Edwards, C. F., Bowman, C. T.:
A Joint Experimental/Large-Eddy Simulation Study of a Model Gas Turbine Combustor
31. Pope, S. B., Goldin, G. M.:
Composition PDF Calculations of Piloted-Jet Non-Premixed Turbulent Flames
32. Rahn, L., Yang, C., Pancerella, C., Hewson, J., Koegler, W., Leahy, D., Lee, M., Nichols, J., Didier, B., Windus, T., Myers, J., Schuchardt, K., Stephan, E., Wagner, A., Ruscic, B., Minkoff, M., Liming, L., von Laszewski, G., Bittner, S., Moran, B., Pitz, W., Montoya, D., Allison, T., Green, W., Frenklach, M.:
Collaboratory for Multi-scale Chemical Sciences (CMCS): Data Format Standards and Data Sharing Technologies
33. Ren, Z., Pope, S. B.:
Investigation of Turbulent Mixing Models
34. Renfro, M. W., Chaturvedy, A., King, G. B., Laurendeau, N. M., Kempf, A., Dreizler, A., Sadiki, A., Janicka, J.:
Comparison of Measured and Predicted Scalar Time Scales in Flame H3
35. Vagelopoulos, C. M., Frank, J. H.:
Flame-Vortex Interactions in Partially Premixed CH₄/Air Flames

The Effect of O₂ Concentration and Temperature on Turbulent Flame Structure

CHUL-JU AHN*, AKIO KITAJIMA**, FUMITERU AKAMATSU*, MASASHI KATSUKI*

* Department of Mechanical Engineering
Osaka University

2-1 Yamada-oka, Suita, Osaka 565-0871, Japan

** Research Institute for Energy Utilization, AIST

16-1, Onogawa, Tsukuba, Ibaraki 305-8569, Japan

E-mail: ahncj@mech.eng.osaka-u.ac.jp

Introduction

One of the important dimensionless parameter in understanding the turbulent premixed flame structure is Ka number, classically interpreted as criterion between the flamelet regime and distributed reaction zone. Recently, Ka is newly interpreted as criterion between thin reaction zone and flamelet regime by Peters *et al.* ⁽¹⁾ In order to discuss the transition of flame structure by the variation of chemical time in high temperature, OH-LIPF measurements were carried out under various O₂ concentration in high temperature condition, and flame classification was carried out on the basis of Ka number.

Experimental Apparatus

The burner consists of three parts for preheating, mixing of hot-air and fuel and observing of the flame. [Fig. 1] An electric heater and H₂ diffusion flame were used for preheating of oxidizer stream containing various O₂ concentration. Fuel nozzle has 12 holes with the diameter of 0.5mm for rapid mixing of fuel into the oxidizer stream to create premixed reactants.

The reactant stream ejected from the burner impinges on the center of a deep cylindrical dish having inner diameter of 38mm, 30mm in depth. Flame is formed in the space between the burner and the dish, and the reflected burned gas flows back surrounding the burner preventing the entrainment of cool ambient air. The flow configuration creates the similar condition of mild combustion in furnaces.

Results and Discussion

Flame feature and lean flammable limit

Figure 2 shows the direct photograph of typical flames for methane. Equivalence ratio is calculated on O₂ concentration in reactant stream. The sum of Q_{Air} and Q_{N_2} was fixed as 60L/min. Supplied H₂ and O₂ for preheating is regarded to be converted into H₂O. Final O₂ concentration was estimated as the mole fraction in Q_T ($Q_{Air}+Q_{N_2}+Q_{H_2O}$: 65L/min). With decreasing O₂ concentration, flame is broadened and combustion noise is decreased. Figure 3 shows the lean flammable limit of mixture for CH₄ and city gas.

Flammable limit is expanded to low O₂ concentration with the increase in temperature of reactants, and flam-

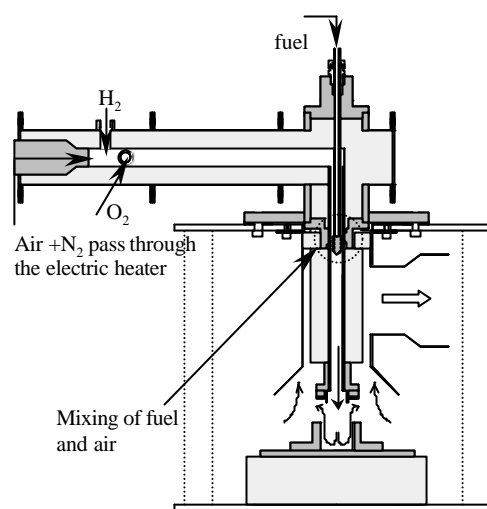


Fig. 1 Configuration of the burner

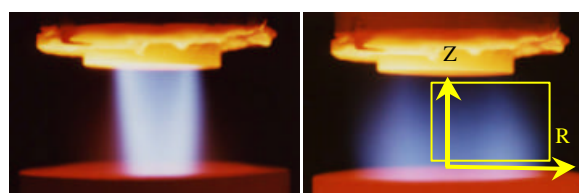


Fig. 2 Direct Photograph of typical flames.

Left: T_u 1173K, O₂ 19.4%, $\phi = 0.6$

Right: T_u 1173K, O₂ 7.4%, $\phi = 1.0$

Rectangular box: OH-LIPF image region

27mm(width) \times 18mm(height)

mable limit of city gas is wider than that of CH₄. Autoignition occurs in case of high temperature (1173K) and high O₂ concentration when city gas was used. Figure 4 shows the calculated laminar burning velocity [S_L] for CH₄ flame.

Flame classification

Experimental conditions and relevant parameters are shown in Table 1. Turbulent properties were measured by one-dimensional LDV, S_L was calculated by PREMIX with GRI-Mech3.0.

Typical instantaneous OH-LIPF images are shown in Fig. 5. F3 flames have steep OH gradient and Ka numbers near unity. F2-19.4% and F2-13.0% flame still have steep OH gradient and Ka numbers over unity. F2-13.0% flame shows frequent local extinction. OH

intensity is distributed in flame region in the F2-7.4% flame. Same tendency can be observed in F1-19.4% flame. It never shows flamelet-like features and Ka number is not so large. This implies the criterion between flamelet regime and broken reaction zones (or well-stirred reactor regime) can be changed by varying chemical property of mixture.

Flame feature in low O_2 concentration resembles flameless oxidation⁽²⁾ in HPAC⁽³⁾(Highly Preheated Air Combustion). Flameless oxidation can be interpreted as well-stirred reaction regime represented by smaller turbulent time compared with chemical time.

References

1. Mansour, M. N., Peters, N., Chen, Y.C., Proc. of the Combustion Institute, Vol. 27, 767-773, 1998.
2. Plessing, T., Peters, N., Wüning, J. G., Proc. of the Combustion Institute, Vol. 27, 3197-3104, 1998.
3. Katsuki, M., Hasegawa, T., Proc. of the Combustion Institute, Vol. 27, 3135-3146, 1998.

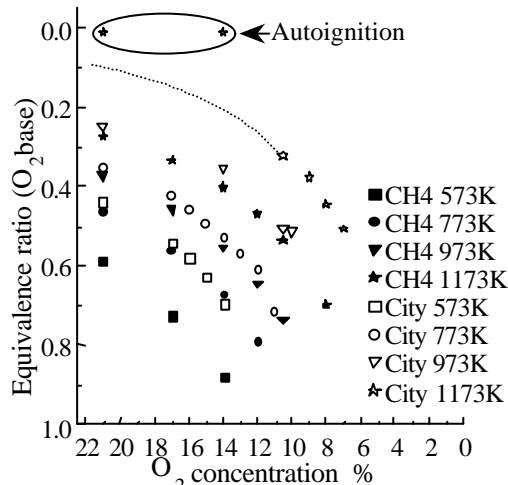


Fig. 3 Flammable limit for CH_4 and city gas

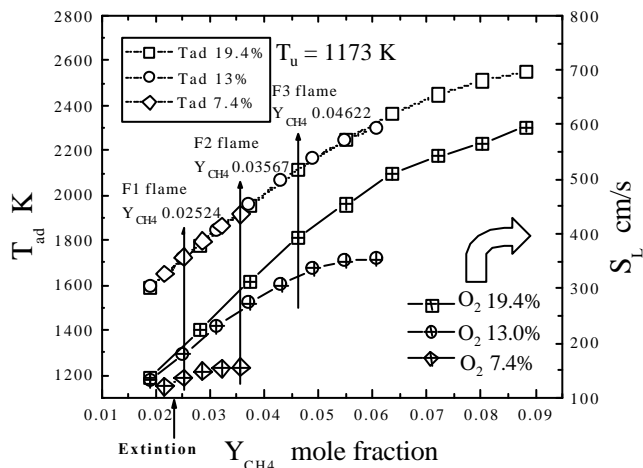


Fig. 4 S_L and adiabatic flame temperature (T_{ad})

Table 1

T^0 is temperature at maximum temperature gradient.

$T_u = 1173K$ in all conditions. $\delta_F = (\lambda C_p)_T^0 / (\rho S_L)_u$

Flame name	Q_{CH_4} L/min	δ_F μm	T^0 K	T_{ad} K	$Ka = (\delta_F / \eta)^2$
F3 19.4%	3.15	74	1551	2112	0.85
F3 13.0%	3.15	90	1549	2118	1.27
F2 19.4%	2.40	95	1528	1923	1.42
F2 13.0%	2.40	109	1519	1927	1.85
F2 7.4%	2.404	183	1507	1917	5.20
F1 19.4%	1.683	141	1441	1719	3.08

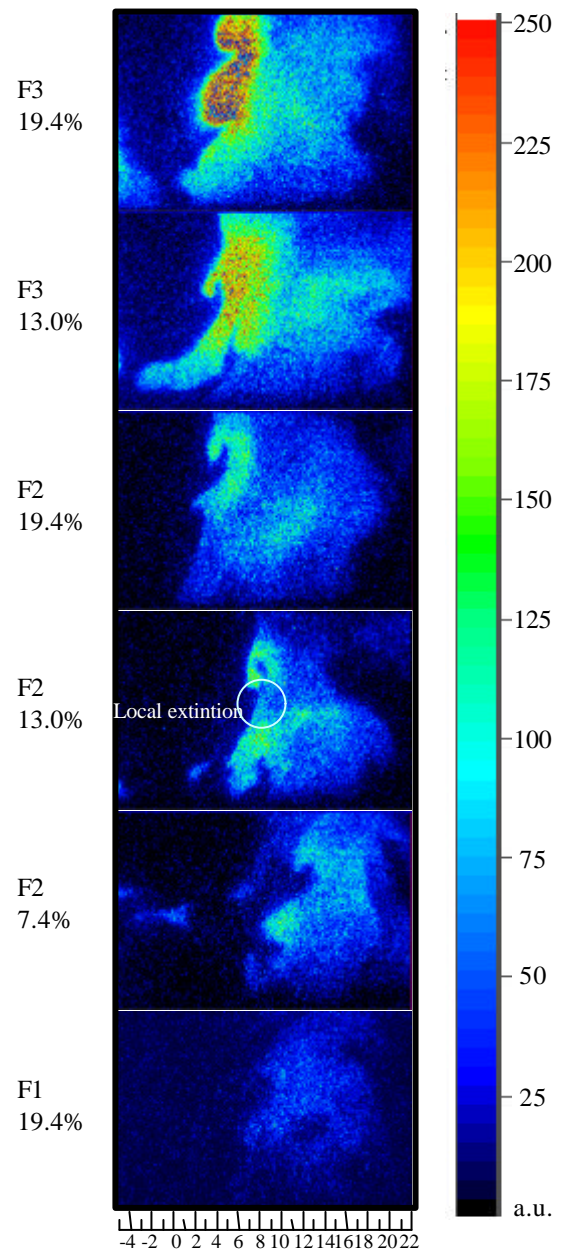


Fig. 5 Instantaneous OH-PLIF images. $T_u = 1173K$

Quantitative Temperature Imaging using NO-LIF in Flames at Elevated Pressures (1-60 bar)

W. G. Bessler², C. Schulz², T. Lee¹, D.-I. Shin¹, J. B. Jeffries¹, R. K. Hanson¹

¹Mechanical Engineering Department, Stanford University, Stanford CA 94305

²Physikalisch-Chemisches Institut, Heidelberg University,

Im Neuenheimer Feld 253, 69120 Heidelberg

Jay.Jeffries@Stanford.edu

Christof.Schulz@urz.uni-heidelberg.de

A novel technique for temperature imaging in laminar, steady flames is presented using multi-line LIF in the A-X(0,0) band of nitric oxide (NO). Example measurements from premixed methane/air flames are shown in figure 1 for pressures between 1 and 40 bar; results from flames with pressures as high as 60 bar will be shown in the poster. The technique yields temperatures with high accuracy even in high-pressure environments without the requirement of external calibration. This premixed steady flame provides an understandable test-bed for our development of high-pressure diagnostics. The current goal is to develop an understanding of the sources and magnitudes of the errors in concentration and temperature determined from NO LIF in high-pressure environments. We have already published work discussing the errors in high-pressure NO LIF and evaluated the optimum choice for high pressure concentration measurements of NO free from oxygen interference.[1,2]

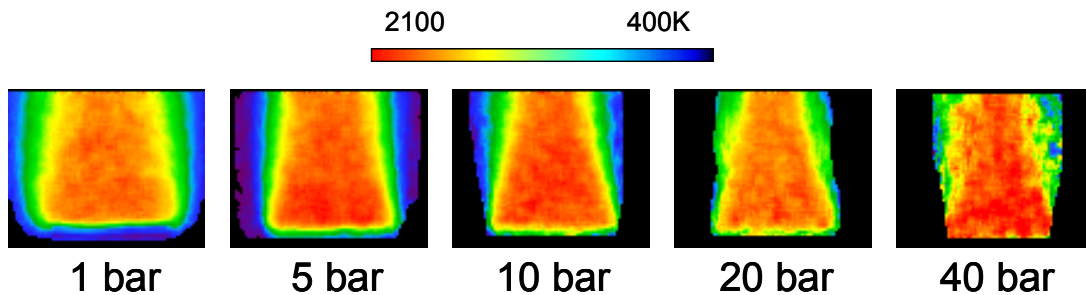


Figure 1: NO LIF using A-X (0,0) band excitation and (0,2) band detection in a slightly fuel rich methane/air premixed flame

Planar temperatures are usually based on the ratio of population in two ground states of an atom or molecule, probed via laser-induced fluorescence imaging [3-5]. Only few techniques, however, have been used in high-pressure flames [6,7], and they suffer from low signal-to-noise ratios, high background sensitivity, and the requirement of external calibration. Multi-line-LIF-measurements, on the other hand, can provide accurate quantitative temperature information, but to date only point measurements [6,8] have been demonstrated. We combine these approaches by performing planar LIF excitation scans of NO over a long spectral range (ca. 1 nm). This allows the probing of a large

number of rotational transitions with a wide range of ground state energies. The temperature of simulated spectra is fitted to the experimental scans for each pixel of the 2D images, yielding the absolute temperature distribution of the flame. This approach provides the high quality temperature field needed to provide a test environment to validate single shot strategies for use in high-pressure turbulent systems.

LIF techniques applied at elevated pressures are often complicated by collisional broadening of the investigated transitions. We assess these effects in detailed spectroscopic simulations used for the temperature fit. This approach enables application in atmospheric pressure flames (where NO transitions form distinct excitation peaks) as well as high-pressure flames (where structure is lost due to pressure broadening). The spectroscopy of the NO molecule is known well enough to describe high-pressure quenching and line-broadening effects, and simulated spectra are found to agree very well with the experimental data. The fitting procedure also accounts for broadband background signals e.g. due to soot incandescence or PAH-LIF, making the technique applicable in different types of flames.

The measured temperature fields of the investigated flames are used to quantify our PLIF images of natural NO concentrations between 1 and 60 bar.[2] Here, temperature information is needed to interpret the NO-LIF signal and to correct for laser and signal attenuation due to UV light absorption. The technique thus serves as a temperature reference system for steady laminar flames, laying the ground work for future work to develop and test two-line techniques for single-shot measurements.

- [1] W. Bessler, C. Schulz, T. Lee, J. B. Jeffries, and Ronald K. Hanson, "Strategies for laser-induced fluorescence detection of nitric oxide in high-pressure flames: I. A-X (0,0) excitation," *Applied Optics*, (2002) in press.
- [2] W.G. Bessler, C. Schulz, T. Lee, D.-I. Shin, M. Hofmann, J.B. Jeffries, J. Wolfrum, and R.K. Hanson, "Quantitative NO-LIF Imaging in High-pressure Flames," *Appl. Phys. B*, submitted, May, 2002.
- [3] M. Tamura, J. Luque, J.E. Harrington, P.A. Berg, G.P. Smith, J.B. Jeffries, D.R. Crosley, *Appl. Phys. B* 66, 503-510 (1998).
- [4] W. G. Bessler, F. Hildenbrand, C. Schulz, *Appl. Opt.* 40, 748-756 (2001).
- [5] B. K. McMillin, J. L. Palmer, R. K. Hanson, *Appl. Opt.* 32, 7532-7545 (1993).
- [6] B. Atakan, J. Heinze, U.E. Meier, *Appl. Phys. B*64, 585-591 (1997).
- [7] C. F. Kaminski, J. Engström, M. Aldén, *Proc. Combust. Inst.* 27, 85-93 (1998).
- [8] A.O. Vydrov, J. Heinze, M. Dillmann, U.E. Meier, W. Stricker, *Appl. Phys. B*61, 409-414 (1995).

Simultaneous Laser Raman-Rayleigh-LIF Measurements of a Lifted Turbulent CH₄/Air Jet Flame in a Vitiated Coflow

R. Cabra[†], J.Y. Chen, and R.W. Dibble

Department of Mechanical Engineering, University of California at Berkeley

A.N. Karpetis and R.S. Barlow

Combustion Research Facility, Sandia National Laboratories

SUMMARY

An experimental investigation is presented of a lifted turbulent CH₄/Air jet flame in a coflow of hot, vitiated gases (Fig. 1). The vitiated coflow burner emulates the coupling of turbulent mixing and chemical kinetics exemplary of the reacting flow in the recirculation region of advanced combustors. The coannular jet configuration simplifies numerical investigations of this coupled problem by removing the complexity of recirculating flow. Additionally, the open configuration makes this burner amenable to experimental investigation with optical diagnostics. Scalar measurements are reported for a lifted turbulent jet flame of CH₄/Air (Re=28,000, H/d=35) in a coflow of hot combustion products from a lean H₂/Air flame (T=1,350K, X_{O₂}=0.12). The combination of Rayleigh scattering, Raman scattering, and laser-induced fluorescence is used to obtain simultaneous measurements of temperature and concentrations of O₂, CH₄, H₂, H₂O, N₂, CO₂, CO, OH, and NO. The data attest to the success of the experimental design in providing a uniform vitiated coflow throughout the entire test region.

BURNER CONFIGURATION

Experiments were conducted on a lifted turbulent jet flame in a vitiated coflow. The combustor consists of a central CH₄/Air turbulent jet (X_{CH₄}=0.33, Re=28,000) with a coaxial flow of hot combustion products from a lean premixed H₂/Air flame (V=4.7m/s, X_{O₂}=0.12, T=1,350K). The combustor is an adaptation of the design by Chen et al. [1]. The central jet exit diameter is d=4.57mm and the coflow flame is stabilized on a perforated disk with 87% blockage and an outer diameter of 210mm. The central jet extends 70mm above the surface of the perforated disk. For the conditions listed in Table 1, the observed lift-off height was H/d=35.

RESULTS

The radial profiles of Favre averaged temperature at z/d=1, 15, 30, 40, 50 and 70 (Fig. 2) attest to the success of the experimental design. The measured mean temperature in the coflow at z/d=1 is uniform (2% RMS), indicating a uniform, well-mixed coflow flame. Also, the far-field (coflow) temperature measurements are uniform in the axial direction; thus, the integrity of the coflow is maintained over the entire test region. The radial species profiles also exhibit the same well-defined boundary conditions. The flame can therefore be modeled as a jet flame issuing into an infinite vitiated coflow.

The flame evolution through the stabilization region is characterized by the scatter plots shown in Fig. 3. Also plotted are solutions from single strain laminar opposed flow flame computations. These solution curves visually provide the extrema from the fully attached equilibrium to highly strained lifted flame conditions. Computations were executed with the following conditions: unstrained equilibrium/fast-chemistry (solid red), strain rate of a=100s⁻¹ (solid blue), strain rate of a=5,000s⁻¹ with a modified rich-side boundary condition (dashed blue), mixing without reaction (dashed red) and stoichiometric mixture fraction (dotted black). The modified rich-side boundary condition (f₁=0.4, T₁=900K) for the a=5,000s⁻¹ calculation accounts for the mixing of fuel and oxidizer between the nozzle exit and the flame base. All calculations are conducted with equal molecular and thermal diffusivities. Corresponding calculations with differential diffusion poorly fit the data, suggesting a greater relative importance of turbulent mixing.

Observed in the scatter plots is a definite transition from a mixing condition (z/d=30) to vigorous combustion (z/d=70). There is a bimodal distribution between the mixing and combustion conditions at the intermediate axial locations (z/d=40 & 50); this is in contrast to research conducted on a lifted H₂/N₂ flame with vitiated coflow [2] where the majority of scatter data was distributed over the entire region between the mixing and reacting conditions. This clear bimodal distribution suggests a thinner reaction zone than that seen in the H₂/N₂ flame.

REFERENCES

1. Chen, Y.G., Peters, N., Schneemann, G.A., Wruck, N., Renz, U., & Mansour, M.S., *Combust. Flame* 107:223 (1996)
2. Cabra, R., Myhrvold, T., Chen, J.Y., Dibble, R.W., Karpetis, A.N., & Barlow R.S., *Proc. 29th Comb. Inst* (accepted) Publication:1A03 (2002)

[†] Corresponding Author: Ricardo Cabra (ricardo@me.berkeley.edu)

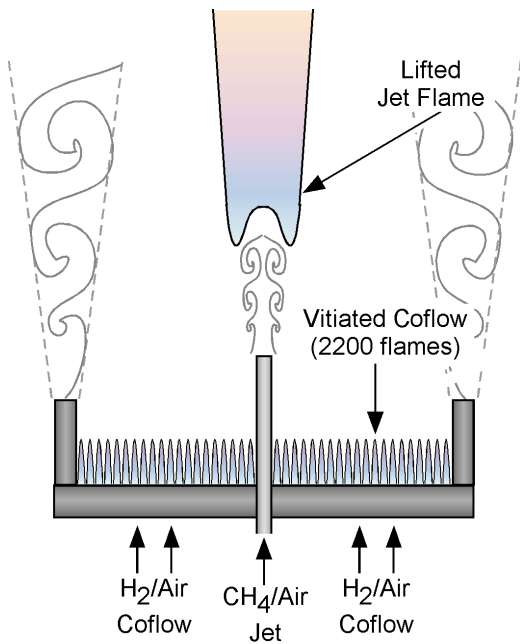


Figure 1: Lifted turbulent jet flame in a vitiated coflow

Table 1: Experiment Conditions

Central Jet		Coflow	
T (K)	320	T (K)	1,350
V (m/s)	100	V (m/s)	4.7
Re	28,000	Re	20,260
X_{CH_4}	0.33	X_{O_2}	0.12
d (mm)	4.57	D (mm)	210

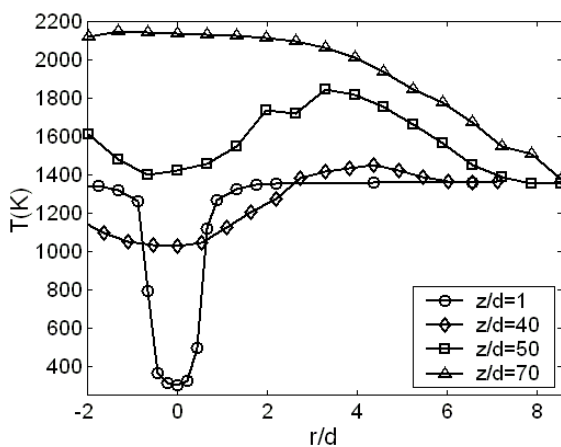
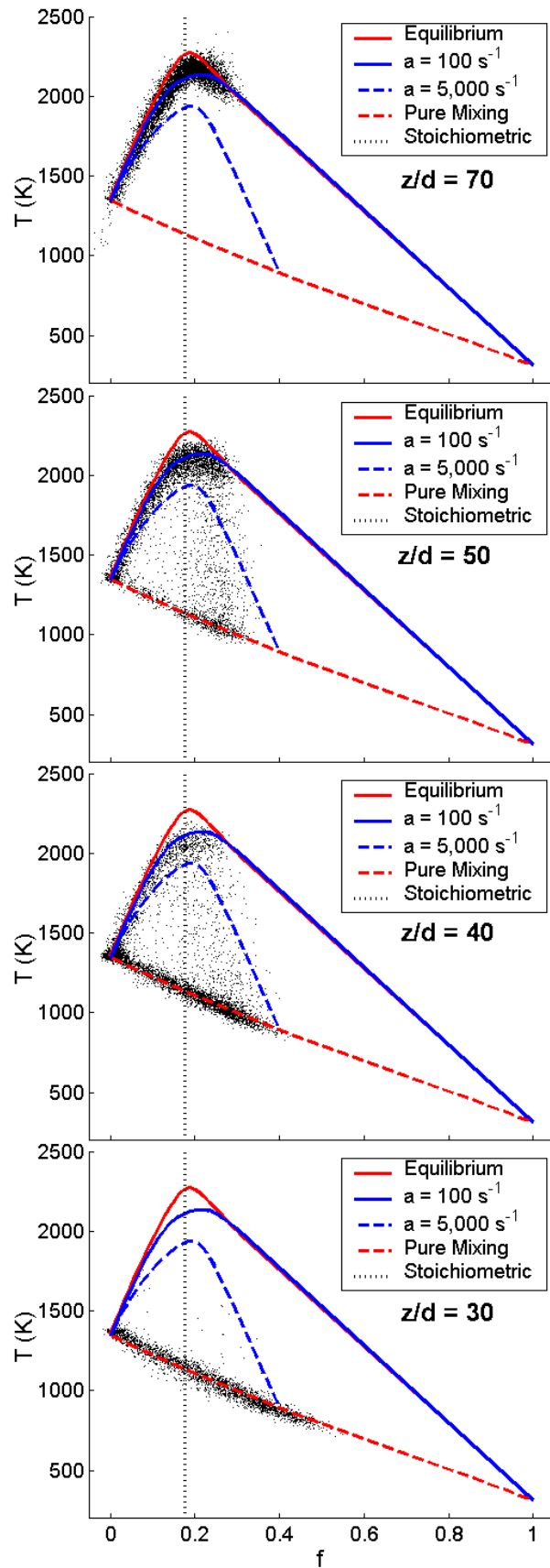


Figure 2: Radial profiles of temperature

Figure 3 (right column): Flame evolution trough the stabilization region. Plotted with laminar opposed flow flame model results; **solid-red:** unstrained fast-chemistry, **solid-blue:** $a=100s^{-1}$ strain rate, **dash-blue:** $a=5,000s^{-1}$, modified rich-side boundary conditions ($f_1=0.4$), **dash-red:** no-reaction/mixing solution, **dot-black:** stoichiometric mixture fraction.



Joint PDF Calculations of the Piloted Methane/Air Jet Flames

R. Cao †, K. Liu, Q. Tang, S. B. Pope and D. A. Caughey

Sibley School of Mechanical & Aerospace Engineering
Cornell University, Ithaca, NY 14853

E-mail: † renfeng@mae.cornell.edu

ABSTRACT

In application to turbulent reactive flows, probability density function (PDF) methods have the advantage of providing full information on the turbulent fluctuations, and hence of avoiding the closure associated with non-linear chemical reactions.

The PDF method has been successfully used to calculate a series of piloted-jet non-premixed flames of methane/air (Flames D, E, and F of Barlow and Frank [1]) by Xu & Pope [7] and Tang, Xu & Pope [6]. Their calculation results clearly demonstrate the ability of PDF methods to account accurately for strong turbulent-combustion interactions such as local extinction and re-ignition.

In their study, a self-contained joint velocity-composition-turbulence-frequency PDF method is used. The modelled PDF equation is solved by a particle/mesh method implemented in the code *PDF2DV*. Improvement in the numerical accuracy and computational efficiency of the algorithm employed are desirable so that calculations can be made for the downstream portion of the flames.

Some progress has been recently made in this direction by the development of the consistent hybrid method [3]. The hybrid method solves the modelled transport equation for the joint PDF of velocity, turbulence frequency, and compositions for turbulent flows. A finite volume (FV) method is used to solve the mean conservation equations for mass, momentum, energy and the mean equation of state; and a particle method is used to solve the modelled PDF equation.

The content in the poster is a comprehensive investigation of the performance of HYB2D in the calculation of piloted methane/air jet flames. A new version of ISAT-CK [4] is coupled with the HYB2D to perform the reaction calculations, with the reaction mechanisms (denoted by ARM2) being a 19 species (including NO), and a 15-step augmented reduced mechanism (ARM1) derived from GRI-Mech 2.11 and 1.2, respectively for methane oxidation [5].

First, the same stochastic model of turbulence frequency and the Euclidean minimum spanning tree (EMST) mixing model is used to repeat the Tang, Xu & Pope [6] calculations to identify any differences between the calculations of PDF2DV and HYB2D.

Next, calculations with the Modified Curl (MC) model and the IEM model are performed to investigate their performance relative to EMST.

Finally, calculations with other available chemical mechanisms are performed to investigate their performance relative to ARM2.

References

- [1] Barlow, R. S. and J. H. Frank, "Effects of turbulence on species mass fractions in methane/air jet flames", *Proc. Combust. Inst.*, 27, 1087-1095, 1998
- [2] Lindstedt R. P., S. A. Louloudi, and E. M. Vaos, "Joint Scalar Probability Density Function Modeling of Pollutant Formation in Piloted Turbulent Jet Diffusion Flames with Comprehensive Chemistry", *Proc. Combust. Inst.*, 28, 149-156, 2000
- [3] Muradoglu, M., S. B. Pope, and D. A. Caughey, "The hybrid method for the PDF equations of turbulent reactive flows: consistency conditions and correction algorithms", *J. Comp. Phys.*, 172, 841-878, 2001
- [4] Pope, S. B., "Computationally efficient implementation of combustion chemistry using *in situ* adaptive tabulation", *Combust. Theory Modelling*, 1, 41-63, 1997
- [5] Sung, C.J., C.K. Law, and J. Y. Chen "An Augmented Reduced Mechanism for Methane Oxidation with Comprehensive Global Parametric Validation", *Proc. Combust. Inst.*, 27, 285-304, 1998
- [6] Tang, Q., J. Xu and S. B. Pope, "PDF Calculations of Local Extinction and NO Production in Piloted-jet Turbulent Methane/Air Flames" *Proc. Combust. Inst.*, 28, 133-139, 2000
- [7] Xu, J. and S. B. Pope, "PDF Calculations of Turbulent Non-premixed Flames with Local Extinction ", *Combust. Flame*, 123, 281-307, 2000

$\sigma^2 \approx 5$ for the Sandia piloted jet flames (Analysis and implications of the intermittency of Bilger's scalar dissipation rate)

Chong M. Cha¹

*Center for Turbulence Research
Stanford University, Stanford, CA 94305-3030, USA*

The amazing detail of the experimental data from the piloted methane/air flames allow sophisticated modeling studies to be performed analogous to studies generally performed using high fidelity DNS. Here, an important parameter characterizing the intermittency of the scalar dissipation rate of Bilger's mixture fraction, ξ , is estimated from the available single-shot data of temperature and mixture fraction. In the poster, the modeling implications are discussed and applied to develop new modeling strategies within a conditional moment closure framework.

The importance of the scalar dissipation rate, $\chi \equiv 2D(\nabla\xi)^2$, in nonpremixed turbulent combustion was first pointed out by Bilger [1]. For order unity Schmidt number, the insights into the small-scale structure of turbulence made by Oboukhov and Kolmogorov [2] are applicable to a passive scalar field. Then, for sufficiently high Reynolds numbers, the dissipation rate of Bilger's mixture fraction follows a lognormal distribution:

$$p_\chi(X) = \frac{1}{X\sigma\sqrt{2\pi}} \exp\left[-\frac{(\log\frac{X}{\langle\chi\rangle} + \frac{\sigma^2}{2})^2}{2\sigma^2}\right], \quad (1)$$

where σ^2 is the variance of $\log\chi$. DNS upto moderate Reynolds numbers [3] and laboratory experiments [4] suggest σ is approximately constant for high Reynolds numbers. Here, I estimate σ for piloted flame D. Due to the universality of σ , the estimate is valid for all the turbulent jets at higher or comparable Reynolds numbers.

Define the reduced temperature as $\theta \equiv (T - T_{Ox})/(T_f - T_{Ox})$, where $T_f = 2,234$ K is the adiabatic flame temperature of the piloted jet flames and $T_{Ox} = 300$ K. Assume stable burning and approximate the temperature outside the reaction zone in mixture fraction phase space using a linear profile in ξ . Then, on the lean side ($0 < \xi < \xi_{st}$), $\theta(\xi; \chi) \xi_{st} = \theta_{st}(\chi_{st}) \xi$ with $\theta(0) = 0$. Taking θ_{st} as a random variable, due to the fluctuations of χ_{st} , the n -th conditional moment of θ can be determined by the n -th moment at the ξ_{st} boundary, *i.e.*, $\langle\theta^n|\eta\rangle \xi_{st}^2 = \langle\theta_{st}^n\rangle \eta^n$. Assuming the scaling $\theta_{st} \sim \chi_{st}^\beta$ yields

$$\frac{\langle\theta'^2|\eta\rangle^{1/2}}{\langle\theta|\eta\rangle} = [\exp(\beta^2\sigma^2) - 1]^{1/2} \quad (2)$$

upon integration over the presumed lognormal pdf of χ_{st} for the special case $n = 2$. (This equation is readily generalized for any n or covariances!) The experimental data, shown in Fig. 1, corroborates the approximate validity of the assumptions made and yields an estimate of the lhs of Eq. 2, defined as m .

To approximate β in the presumed scaling $\theta_{st} \sim \chi_{st}^\beta$, stochastic simulations of the flamelet equations are performed following the Monte Carlo flamelet equations:

$$\frac{\partial Y_j}{\partial t} = \frac{1}{2}\chi_{st}F\frac{\partial^2 Y_j}{\partial \xi^2} + \frac{\dot{w}_j}{\rho} \quad \text{for } j = 1, \dots, N_s + 1 \quad (3a)$$

$$d\chi_{st} = -\chi_{st} \left(\log\frac{\chi_{st}}{\langle\chi_{st}\rangle} + \frac{\sigma^2}{2} \right) \frac{dt}{T_L} + \chi_{st} \sqrt{\frac{2\sigma^2}{T_L}} \circ dW, \quad (3b)$$

where $F(\xi)$ is taken from counterflow, $T_L \sim L/u'$ is the integral timescale, and W is the standard Wiener process. Equation (3) is simulated at a fixed axial location from the jet nozzle. Numerous simulations are performed corresponding to various axial locations. The standard scalings for $L \sim x$ and $u' \approx 0.2\langle u \rangle \sim 1/x$ estimate T_L away from the reference position taken at $x/D = 1$, where the velocity scale is given by the bulk jet nozzle velocity (50 m/s). The nozzle diameter is $D = 7.2$ mm. Closure is obtained from the reference value of $\langle\chi_{st}\rangle \approx 10 \text{ sec}^{-1}$ at $x/D = 30$ taken from LES simulations of the same flame [5] and using the

¹E-mail: chongcha@stanford.edu, Tel: 650-725-6635, Fax: 650-725-3525

centerline scaling $\sim 1/x^4$. Full methane chemistry is described by GRI v2.11. The results, shown in Fig. 2, show a linear dependence of $\log \theta_{st}$ on $\log \chi_{st}$ (not shown) and can readily be used to calculate β . Under stable burning, β depends mainly on $\langle \chi_{st} \rangle$.

With m from the experimental data (Fig. 1) and β from the Monte Carlo simulations (Fig. 2), the desired estimate for σ^2 follows from Eq. (2). Results are summarized in Table 1. The average value from the estimates at the four different axial locations yields an estimate of $\sigma^2 \approx 5.0$.

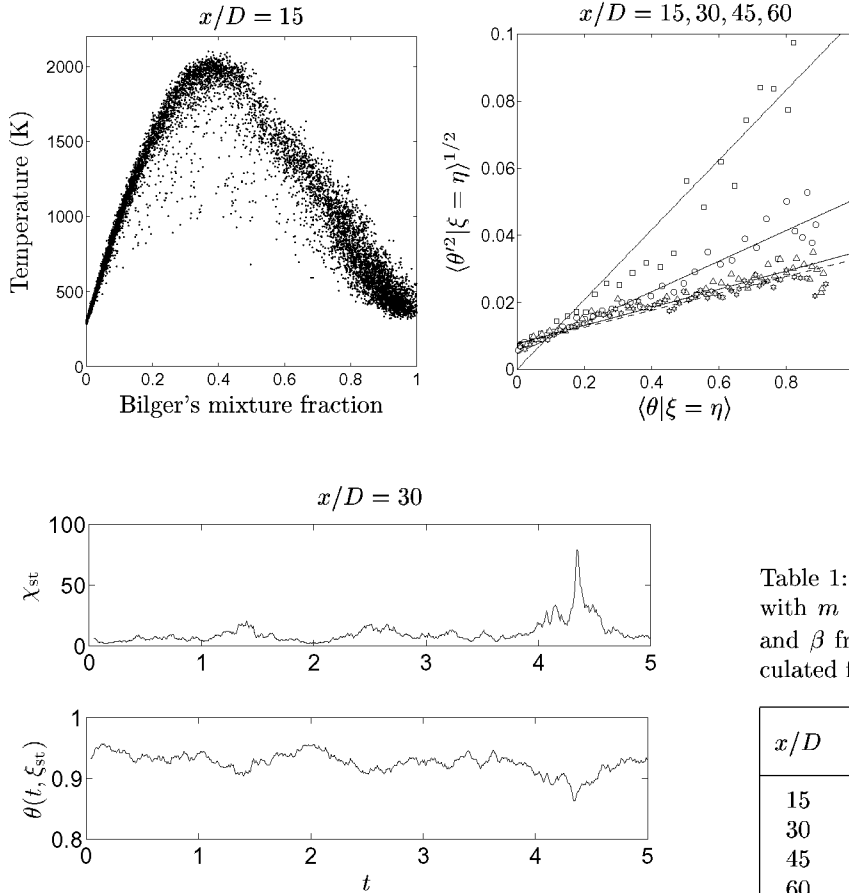


Figure 1: $m \equiv \langle \theta'^2 | \eta \rangle^{1/2} / \langle \theta | \eta \rangle$ calculation. Conditionally averaged data from flame D (symbols) and least-squares curve-fit (lines) on the lean size and at various axial locations from the jet nozzle.

Table 1: Estimates of σ^2 from Eq. (2) with $m \equiv \langle \theta'^2 | \eta \rangle^{1/2} / \langle \theta | \eta \rangle$ from Fig. 1 and β from the scaling $\theta_{st} \sim \chi_{st}^\beta$, calculated from simulations of Eq. (3).

x/D	m	β	σ^2
15	0.1038	-0.0395	6.8686
30	0.0456	-0.0254	3.2197
45	0.0270	-0.0121	4.9774
60	0.0251	-0.0113	4.9323

Figure 2: β calculation. Monte Carlo flamelet results showing response of reduced temperature and NO mass fractions to the stochastic variations of χ_{st} .

References

- [1] R. W. Bilger. *Combust. Sci. and Tech.*, 13:155–170, 1976.
- [2] A. S. Monin and A. M. Yaglom. *Statistical Fluid Mechanics* (Vol. 2). MIT Press, 1971.
- [3] P. K. Yeung and S. B. Pope. *J. Fluid Mech.*, 207:531–586, 1989.
- [4] E. Effelsberg and N. Peters. *Proc. Combust. Inst.*, 22:693–700, 1988.
- [5] H. Pitsch and H. Steiner. *Proc. Combust. Inst.*, 28:41–49, 2000.

Spectral radiative effects and turbulence-radiation-interaction in Sandia Flame D

P. J. Coelho*, O. J. Teerling* and D. Roekaerts**

*Instituto Superior Técnico, Mechanical Engineering Department
Av. Rovisco Pais, 1049-001 Lisboa, Portugal
E-mail: coelho@navier.ist.utl.pt

**Delft University of Technology, Thermal and Fluids Sciences,
P.O. Box 5046, 2600 GA Delft, The Netherlands
Also at: Shell Research and Technology Centre, Amsterdam
E-mail: dirkr@ws.tn.tudelft.nl

A nonluminous piloted turbulent jet diffusion flame (Sandia Flame D [1]) is numerically simulated using a Reynolds stress second-order closure, the steady laminar flamelet model, and different approaches for radiative transfer. The result of the commonly used optically thin approximation is compared with the solution of the radiative transfer equation (RTE) obtained using the discrete ordinates method (DOM). Calculations assuming a Planck mean absorption coefficient are compared with computations performed using the spectral line-based weighted-sum-of-grey-gases model (SLW). The interaction between turbulence and radiation (TRI) is simulated, and its influence on the predicted results is investigated.

The calculations are carried out for six different radiative heat transfer models.

1. Excluding radiative heat transfer (Adiabatic flame)
2. Optically thin flame (No RTE), partial TRI, Planck mean.
3. RTE (DOM), partial TRI, Planck mean
4. RTE (DOM), complete TRI, Planck mean
5. RTE (DOM), partial TRI, spectral model (SLW)
6. RTE (DOM), complete TRI, spectral model (SLW)

In the optically thin model, the source term of the enthalpy equation is calculated from

$$\overline{\nabla \cdot \mathbf{q}} = 4 \kappa \sigma \left(\overline{T^4} - T_\infty^4 \right) \quad (1)$$

where κ is the emission/absorption coefficient and T_∞ is the background temperature. (The RTE is not solved.). The absorption coefficient depends on composition and temperature but not on wavelength (grey medium). It is calculated as recommended on the website of the TNF workshop [1] and described in [2], i.e., using the curve fits for the Planck mean absorption coefficients of H_2O , CO_2 , CO and CH_4 . The optically thin model (1) contains an inaccurate and ad hoc term referring to the background temperature, but this term is so small that it can be neglected. On the contrary the RTE describes the absorption of radiation as function of local conditions. (Scattering can be neglected.) It has been found that the model for κ is of larger impact on the predictions than the difference between RTE and optically thin treatment at fixed κ [3].

The difference between “partial TRI” and “complete TRI” here concerns the evaluation of the mean emissive source term, proportional to $\overline{\kappa T^4}$. “Partial TRI” refers to the case were this is

approximated as $\overline{\kappa T^4}$, with κ calculated using the local mean temperatures and mean species concentrations. Because $\overline{T^4}$ rather than \bar{T}^4 is used, the influence of turbulent fluctuations of mixture fraction on radiative transfer is taken into account. However, the TRI is not fully accounted for, because the turbulent fluctuations are ignored in the calculation of the mean absorption coefficient, and the correlation between the absorption coefficient and the blackbody emissive power is neglected. This is the most common approach in flame radiation calculations. “Complete TRI” here denotes the case where $\overline{\kappa I_b}$ is calculated using the presumed PDF. In an even more detailed treatment also spatial correlations and temporal-spatial correlations would also have to be considered.

The SLW model, is an improved version of the spectral weighted-sum-of-grey-gases model, which has emerged in the last decade as a promising alternative model able to provide high accuracy at moderate computational cost, and compatible with any solution method of the RTE. References to the literature and detailed explanations on models and numerical methods are given in Refs. [4,5].

Using the six different radiative transfer models, fields of mean species mass fractions and mean temperature have been obtained. Axial and radial profiles are included in the poster presentation. It is found that the difference between the temperatures calculated with radiation and those computed for adiabatic conditions do not exceed 150 K, no matter the radiation model employed.

The optically thin approach overpredicts the radiation loss by a factor of 2.6, i.e., it estimates the radiant fraction X_R , defined as the ratio of the total radiative heat loss to the power released in combustion, to be 13.6 % rather than 5.1 % found experimentally. By construction more accurate results are generated if radiative transfer is calculated using the complete RTE. However, if the medium is treated as grey, using the Planck mean absorption coefficient, then X_R is still much too large compared with the experimental data, namely 11.4% in case 3, and 12.1% in case 4. Using an accurate spectral model brings a more significant improvement. In case 5, X_R is marginally underestimated (5.0 %), in case 6, it is slightly overpredicted (5.3 %). Such an overprediction is consistent with the observed overprediction of temperature and absorbing species concentration. Therefore, it is concluded that the DOM with the gas radiative properties computed using the SLW model and accounting for the TRI provides an accurate description of radiative transfer in this flame.

Acknowledgements

This work was financially supported by the European Commission in the framework of the TMR Network Contract No. ERBFMRX-CT98-0224 (RADIARE), and by the PRAXIS XXI Programme of the Portuguese Ministry of Science and Technology under contract PRAXIS/P/EME/12034/1998.

References

1. <http://www.ca.sandia.gov/tdf/Workshop.html>
2. Barlow, R.S., Karpets, A.N., Frank, J.H. and Chen, J.-Y., *Combust. Flame* 127 (2001) 2102-2118
3. Mbiock, A., Teerling, O.J., Roekaerts, D, and Merci, B., submitted for publication
4. Coelho, P.J., Teerling, O.J., Ströhle, J. and Quintino, T., in proceedings *6th Int. Conf. On Technologies and Combustion for a Clean Environment*, Oporto, 9-12 July, 2001
5. Coelho, P.J., Teerling, O.J. and Roekaerts, D., submitted for publication

Turbulent Nonpremixed Jet Flames at Reduced Temperature

Bassam B. Dally

bassam.dally@adelaide.edu.au

Department of Mechanical Engineering
Adelaide University, South Australia, 5005 AUSTRALIA

Adonios N. Karpetis and Robert S. Barlow

Combustion Research Facility
Sandia National Laboratories, Livermore, CA, USA

The motivation of this work is to generate detailed information on the structure of turbulent nonpremixed flames stabilizing at reduced temperature. The approach to establish such flame is similar to the vitiation principle. Such conditions can be found in many reacting flows applying any sort of recirculation which in turn brings back hot products upstream which helps preheat the reactants and provide a continuous source of ignition. In many cases such recirculation of hot products dilute the incoming reactants while maintaining the temperature at moderate levels. The axisymmetric bluff-body flames are a good example of such flows where the recirculation zone structure and temperature depend on the extent or strength of the recirculation vortex [1].

Another application of this work is MILD combustion. MILD (Moderate and Intense Low Oxygen Dilution) Combustion or a variation over that known as Flameless Oxidation (FLOX[®]) is a newly developed and implemented technique to achieve very low emission of pollutants and to improve thermal efficiency of combustion systems [2-4]. MILD Combustion takes place at reduced temperature in the range of 1100-1500K, and is characterized by a flat thermal field and minor temperature fluctuations. It is also called Flameless because at optimised conditions the oxidation proceeds with no visible or audible flame. The main principle of operation for this technique lies in the concept of exhaust gas and heat recirculation. The heat from the exhaust gases is used to raise the temperature of the oxidant stream and the exhaust gases are used to dilute the oxidant stream in order to reduce the oxygen concentration and maintain low temperature in the combustion zone.

In this abstract we report on an experimental burner, technique used and data available.

Jet in Hot Coflow Burner Assembly

The burner used in this study is referred to as Jet in Hot Coflow (JHC). Figure 1 shows a cross section of the JHC burner design. It consists of an insulated and cooled central jet (ID=4.25mm) and an annulus (ID=82mm) with a secondary burner mounted upstream of the exit plane. The secondary burner provides hot combustion products which are mixed with air and nitrogen via two side inlets at the bottom of the annulus to control the O₂ levels in the mixture. The cold mixture of air and nitrogen also assists in cooling the secondary burner. The burner can operate at a wide range of coflow temperatures and O₂ levels. The burner allows easy optical access to measure initial and boundary conditions at the exit plane. The outer annulus is insulated using ceramic straps to minimize heat loss to the surroundings. The hot coflow stream is wide enough to sustain the same conditions close to the reaction zone for the full length of laminar flames. For turbulent flames some mixing with fresh air from the surroundings starts to have an effect at ~100 mm above the jet exit plane. The burner was mounted on a wind tunnel which provided room temperature air at the same velocity as the hot coflow. The hot co-flow in the annulus and the tunnel air had a fixed velocity of 3.2 m/s in all experiments.

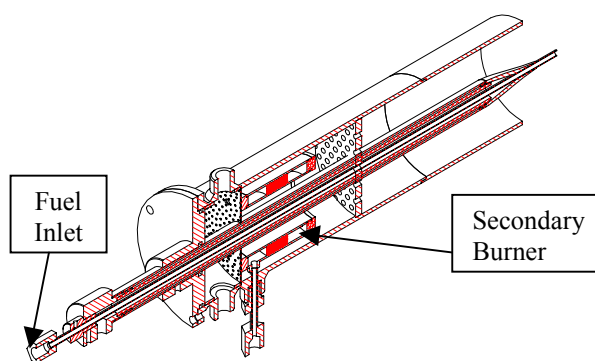


Figure 1 Sketch of Jet in a Hot Coflow Burner

Experimental Technique

Experiments were conducted at the Combustion Research Facility at Sandia National Laboratories, Livermore California. The Single-Point Raman-Rayleigh-LIF technique was used in this study. This technique is well developed, providing quantitative, spatially and temporally resolved measurement of temperature, concentration of major species CH₄, H₂, H₂O, CO₂, N₂ and O₂ and minor species, NO, CO and OH. These scalars were

measured instantaneously and simultaneously using this technique. This setup was described in numerous publications e.g. [5-6] and will not be described here due to lack of space.

A mixture of H₂ and CH₄, equal in volume, was used as the fuel in the central jet. The same fuel mixture was also used in the secondary burner and the products were mixed with N₂ and air to control the oxygen concentration in the annulus. The temperature of the mixture in the annulus was fixed at ~1300K for all experiments. For low jet Reynolds number flames the fuel mixture in the jet was heated slightly despite the insulation and cooling of the central jet. Table 1 shows the different operating conditions of the cases studied. The mass fraction of CO₂ and H₂O was kept constant while the mass fraction of O₂ and N₂ was changed.

Fuel Jet (CH ₄ /H ₂)			Oxidant Coflow				
Case	Re	T(K)	T(K)	YO ₂ %	YN ₂ %	YH ₂ O %	YCO ₂ %
HM2O3	4741	315	1300	3	85	6.5	5.5
HM3O3	9482	305	1300	3	85	6.5	5.5
HM3O6	9482	305	1300	6	82	6.5	5.5
HM3O9	9482	305	1300	9	79	6.5	5.5
HM4O3	18964	292	1300	3	85	6.5	5.5

Results and Discussion

Figure 2 shows radial profiles of mean temperature and mass fractions of CO for flames HM2, HM3 and HM4 with 3% oxygen level in the coflow at different axial locations above the jet exit.

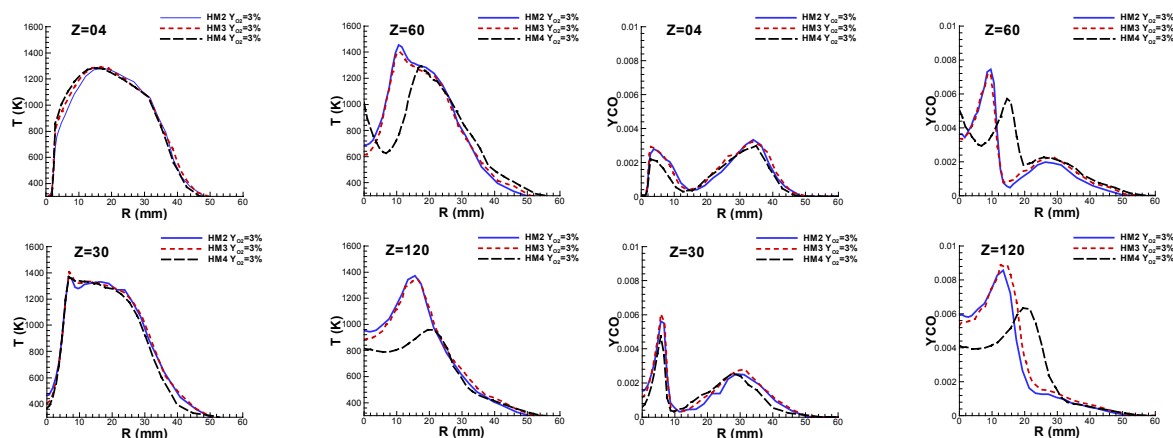


Figure 2 Radial profiles of mean temperature and CO mass fractions at different axial locations

The temperature profiles show very little reaction at $z=4$ mm and slight increase in temperature for all flames at location $z=30$ mm. At locations $z=60$ mm and 120mm the third stream have substantial effects on the flame structure for flame HM4 which has the highest Reynolds number. A small residual of CO can be seen in the coflow up to location $z=60$ mm. The amount of CO produces by the flame at these conditions is very small when compared to standard fuel in air flames. The effect of the mixing by the third stream is also apparent in the CO profiles. This data can be made available on the web once it appeared in the literature.

Acknowledgments

Dr Dally acknowledges the support of the Australian Research Council and the United States Department of Energy, Office of Basic Energy Sciences, Division of Chemical Sciences.

References

- [1] Dally, B.B., Masri, A.R. Barlow, R.S, and Fiechtner, G.J., *Combust. Flame*, vol 114/1-2, pp.119-148, 1998
- [2] Katsuki, M. and Hasegawa, T., *Twenty-Seventh Symposium (International) on Combustion*, Combustion Institute, Pittsburgh, PA, 1998, vol. 2, pp. 3135-3146
- [3] Wünnig, J.A. and Wünnig, J.G., *Progress in Energy and Combustion Science*, Vol. 23, pp. 81-94, 1997
- [4] Plessing, T. Peters, N. and Wünnig, J.G., *Twenty-Seventh Symposium (International) on Combustion*, Combustion Institute, Pittsburgh, PA, 1998, vol. 2, pp. 3197-3204.
- [5] Dally, B.B., Masri, A.R. Barlow, R.S, Fiechtner, G.J. and Fletcher, D.F., *Twenty-Sixth Symposium (International) on Combustion*, Combustion Institute, Pittsburgh, PA, 1996, vol 2, pp. 2191-2197.
- [6] Masri, A.R., Barlow, R.S. and Dibble, R., *Prog. Energy Combust. Sci.*, vol. 22, 307-362, 1996

Numerical Simulation of a Piloted Methane/Air jet flame using the coupled TLFM/PDF Model

L. Demiraydin, J. Gass, D. Poulidakos
 Laboratory of Thermodynamics in Emerging Technologies
 ETH-ZENTRUM, CH-8092 Zurich Switzerland
 e-mail:demiraydin@lnt.iet.mavt.ethz.ch

The PDF transport equation models [1] and the steady laminar flamelet models [2] are the two of the most recent and commonly used nonpremixed turbulent combustion models. Both of these models handle turbulence statistically and the scalar statistics in these models is performed by solving the joint probability density function (PDF) transport equation or by defining presumed probability density function (PDF) shapes, respectively. The solution of the PDF transport equation model can be achieved with Monte Carlo simulations. The model has the advantage of a closed chemical source term, although it has the disadvantage of the modeled molecular mixing term. As a result, there is a tight statistical correlation between the chemistry and the molecular transport, which limits the applicability regime of the PDF transport equation model. Additionally, due to the high dimensionality of the problem, the model can be computationally demanding. The flamelet models are based on the presumed PDFs, which have free parameters that are obtained from the governing equations of those parameters. There is a strong chemistry and molecular transport interaction in the flamelet models but the flamelet models are only valid in the flamelet regime. Lately, the applicability regime of the flamelet models are extended by including the unsteadiness effects, e.g. unsteady flamelet model [3], transient laminar flamelet model [4].

The aim of this work is to introduce a new coupled model, by combining the PDF transport equation model and the transient laminar flamelet model. The new model is termed the coupled Transient Laminar Flamelet /Probability Density Function (TLFM/PDF) model and aims to combine the advantages of the existing models and avoid the disadvantages of them. The flow chart of the model is represented in Figure 1. The coupled TLFM/PDF model calculates the mixture fraction with the PDF transport equation by using the Monte Carlo method.

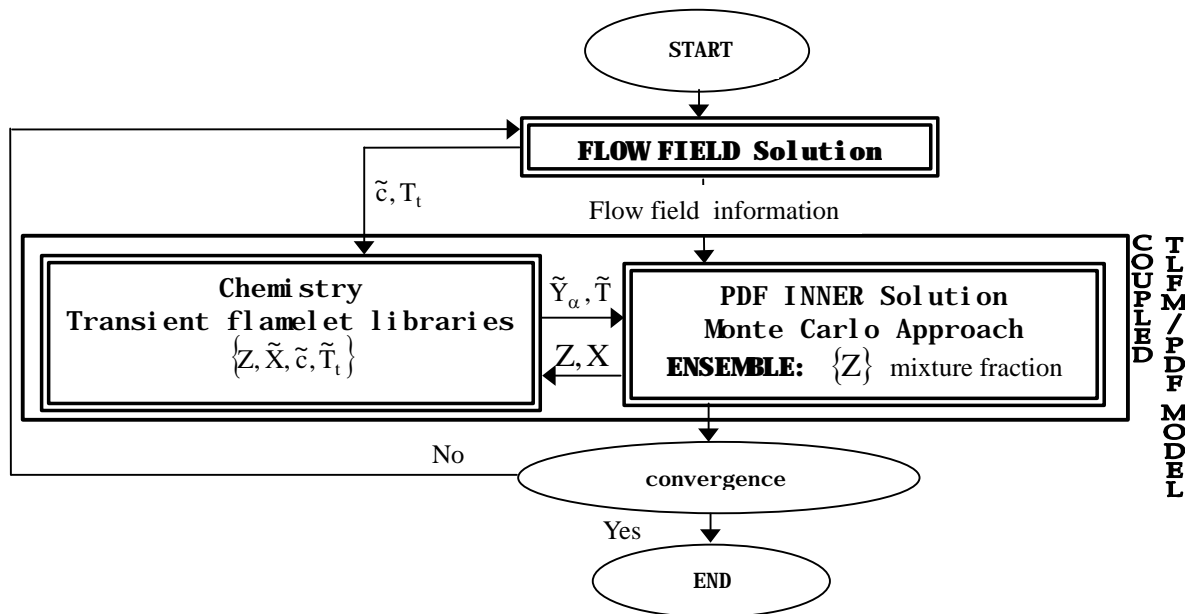


Figure 1: Schematic representation of the Coupled TLFM/PDF Model

The scalar dissipation rate, which represents the highly strained flame sheets in the flow field, is determined by calculating the variance of the mixture fraction. The chemical source term of the PDF transport equation is solved by using the transient laminar flamelet model (TLFM) which is introduced in [4]. The mass fraction of species Y_α and the temperature T are read from the tabulated flamelet libraries, which are generated for four variables. These

variables are the mixture fraction Z , the scalar dissipation rate X , the reaction progress variable c and the turbulent time scale T_t . The model captures the extinction and re-ignition due to the introduced parameter, reaction progress variable. The reaction progress variable is suggested mostly in premixed combustion modeling and helps to define the partially premixed structures, which appears in the turbulent nonpremixed flame which can locally be extinguished and can be re-ignited later in the flame. The turbulent time scale defines the dynamic behaviour of combustion. As a conclusion, in the coupled TLFM/PDF model, the PDF shapes are deterministic. There is a wider regime applicability compared to the PDF model and the steady laminar flamelet model. The chemistry-mixing interaction is better compared to the PDF transport equation model. The partially premixing can be captured.

The results are validated with the experimental work of Barlow et.al. [5] for piloted jet flames. The chosen configuration introduces the local extinction and the re-ignition phenomena, thus, it is a good test case to investigate the statistical reliability of the existing and proposed models. In Figure 2, the results for the PDF transport equation model with a 4 step-reduced mechanism [6] and the coupled TLFM/PDF model are compared with the experimental data at axial direction along the centerline. The results of the coupled TLFM/PDF model present a better agreement for the quantities which are mentioned.

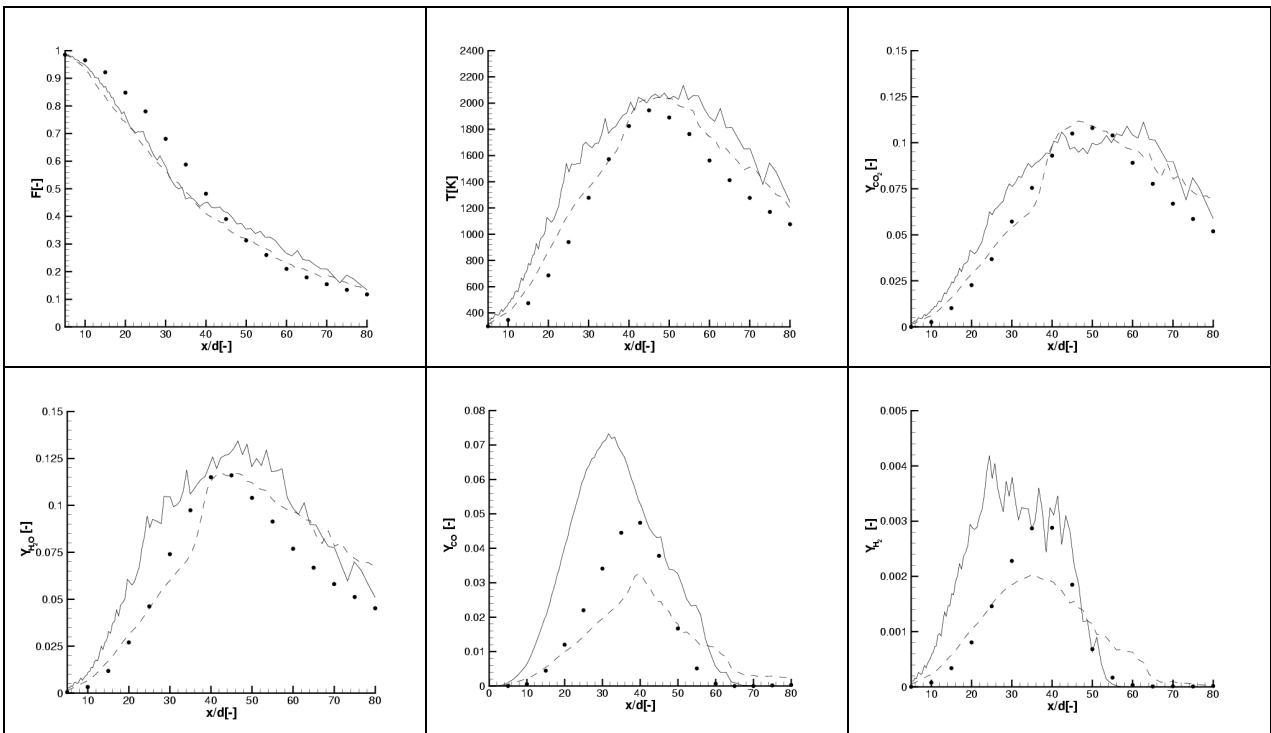


Figure 2: Axial profiles along the centerline. (—) PDF Transport Computation with 4-step reduced mechanism, (---) Coupled TLFM/PDF Computation, (·) Experimental data

REFERENCES

- [1] Peters, N., *Prog. Energy Combust. Sci.*, 10:319, (1984).
- [2] Pitsch, H., Chen, M., and Peters, N., *Twenty-Seventh Symposium (International) on Combustion, The Combustion Institute, Pittsburgh*, 1998, p. 1057.
- [3] Pope, S.B., *Prog. Energy Combust. Sci.*, 11:119, (1985).
- [4] Ferreira, J.C., *Prog. in Comp. Fluid Dynamics*, 1:29, (2001).
- [5] Barlow, R.S. (1988). <http://www.ca.sandia.gov/tdf/Workshop.html>.
- [6] Peters, N., Kee, R.J., *Combust. Flame*, 68:17, (1987).

Measurements directed at LES validation

A. Dreizler, J. Janicka

FG Energie- und Kraftwerkstechnik, TU Darmstadt, Petersenstrasse 30, Germany

dreizler@ekt.tu-darmstadt.de

Introduction

Recently, large eddy simulation (LES) has emerged to be a very promising technique to predict turbulent reacting flows. Within the LES approach, turbulent motion is separated into small and large scales. This separation is achieved by spatially filtering the conservation equations. The filter size is larger than the Kolmogorov scale and therefore sub-filter scales have to be modeled. As a consequence, experimental data is required to assist the development and validation of LES models.

In contrast to the traditional Reynolds averaged Navier Stokes (RANS) assumption, LES has the potential to describe transient flows. Accordingly, the experimental requirements rise. While single-point statistics (mean values and higher moments) of the velocity vector, species concentrations, and temperature are sufficient to test the RANS simulation performance, for LES validation, in addition, spatially and temporally correlated information is essential.

In a first step, the task “LES validation” can be split into two subtasks: (1) *a priori* test of sub-model assumptions, and (2) *a posteriori* analysis of the simulation. The first subtask is addressed to measure quantities determined by a sub-model that are not resolved by the spatial filter. Inherently, this requires experimental approaches using spatially a high resolution much finer than the LES filter size. At the current stage, however, it is under debate if a priori testing is of significance. The second subtask is to measure quantities that are predicted by LES. In this way models are evaluated after their implementation in a simulation. To be useful, this second task needs very detailed information on the inflow boundaries.

Similar to a discussion forum for non-reactive LES ¹, this contribution is intended to trigger a discussion identifying the most promising diagnostics and experiments for combustor LES. Exemplary, some experimental approaches are discussed.

General aspects

As stated before, LES needs the same experimental data as necessary for RANS validation but in addition spatially and temporally correlated information. It is essential that temporal and especially spatial resolution applied in the experiments are well documented. It is desirable to experimentally achieve a spatial resolution as high as possible. Taking laser Doppler velocimetry (LDV) as an example, this technique – as a commonly used laser diagnostic method – exhibits an extension of the measurement volume in beam direction in the order of 0.5 to 1 mm – a range similar to most recent and future LES approaches. Consequently, efforts to reduce measurement volumes in laser diagnostics are of high importance. In addition, an increase of repetition rates is desirable for some common laser diagnostics to deduce reliable temporal gradients and auto-correlations from highly resolved time series.

Inflow boundaries

In addition to single-point statistics regarding the inflow velocity vector and – for more complex geometries than jets – parameters such as unmixedness of fuel and oxidizer, temporally resolved information at a single-point (time series) as well as multi-point velocity measurements are important. From single-point time-series measurements, a temporal auto-correlation can be deduced. Subsequently, temporal time scale and power spectrum can be obtained by integration and Fourier transformation, respectively. In the spatial domain, similar information can be obtained by two- or multi-point correlation measurements. For these tasks, in general, highly repetitive techniques with small measurement volumes are needed. On the poster an example will be given using two-point LDV to measure both temporal auto- and spatial cross-correlations.

As LES requires temporally resolved inflow boundaries, in principal time series recorded simultaneously at various locations might be used to feed the simulation directly. However, it seems to be more practical to deduce these temporally and spatially resolved inflow boundaries from correlation information such as integral length scales using an inflow generator ². Alternatively, the LES inflow boundary can be set upstream of the burner mouth, but for model validation purposes this approach is, in general, computationally expensive.

A posteriori analysis

As for the inflow boundaries, time series of single-point measurements and spatial multi-point investigations are valuable. Most important, these techniques should be developed and applied on the flow field and on the mixture fraction as the most important scalar in non-premixed flames. Applying random mode sampling and a slot correlation technique on LDV, for the flow field already a promising technique exists. For scalars, however, high repetitive LIF for radical-time series measurement has been developed³ but might be extended to high repetitive mixture fraction determination. Alternatively, *cw* Rayleigh scattering could be used to temporally track the density. From time series of velocities, in addition to temporal auto-correlation, time scales, and power spectra as mentioned before, time derivatives applied on velocity measurements can be used to deduce acceleration as exemplified in⁴.

Supplementary to these quantities, the measurements of cross-correlations are important. While using LDV cross-correlations of the form $u'_i u'_j$ can be measured, but only some approaches exist to determine $u'_i f'$ that requires the simultaneous measurement of a mixture fraction (or a different scalar) and at least one velocity component⁵.

Similar to the time domain, spatial correlation measurements are of high importance for LES validation to achieve, i.e., integral length scales. This is especially important when Taylor's hypothesis is not valid. In analogy to time derivatives, space derivatives are especially valuable. Taking the mixture fraction as an example, its space derivative can be used to determine the scalar dissipation rate. For this purpose 1D line Raman measurements⁶ show very promising potential.

A priori tests of sub-models

For low Reynolds-numbers direct numerical simulation (DNS) is most commonly used to develop and test sub-models. In general, it is difficult to achieve representative boundary conditions and computational prohibitive to apply high Re-numbers important for technical combustion. Therefore, effort is needed to experimentally perform a priori tests of sub-models. This task is difficult due to the high spatial resolution required. If, for example, the sub-grid variance of the mixture fraction determined by a sub-model is to be tested, at a single time the mixture fraction has to be measured at various spatial locations. Most promising for this kind of task are 2D techniques such as particle imaging velocimetry (PIV), planar Rayleigh or planar laser-induced fluorescence (PLIF) to measure flow- and scalar-field properties, respectively. Compared to approaches commonly used, the spatial resolution has to be improved by an order of magnitude. No principal difficulties are expected but problems might occur with respect to appropriate particle densities seeded to the flow for PIV or a relatively low signal-to-noise ratio for PLIF applications.

Conclusions

For LES sub-model development few selected but very detailed measurements are required. It might be useful to evaluate a test case by DNS and experimental methods for a variety of Re-numbers. By this means the reliability of extrapolation of model assumptions obtained by DNS to high Re-numbers might be checked. For a posteriori analysis, more and different configurations have to be characterised, including a detailed investigation of the inflow boundaries of each test case. In total, this approach should help to identify and characterise the applicability of LES models and to build up confidence what type of turbulent flame can be predicted by the respective set of models.

Generally speaking, dedicated laser based methods exist to determine the information required but efforts are needed to improve the spatial resolution of multi-point techniques and the repetition rate of single-point techniques to obtain correlated information both in space and time. In addition, combination of methods is essential to simultaneously measure properties of the flow- and scalar field.

¹ Adrian, R. J., Meneveau, C., Moser, R. D., Riley, J.: "Final Report on "Turbulence Measurements for LES" Workshop." (1999).

² Klein, M., Sadiki, A., Janicka, J.: "A Digital Filter Based Generation of Inflow Data for Spatially Developing Direct Numerical or Large Eddy Simulations." submitted for publication (2002).

³ Renfro, M., Guttenfelder, W. A., King, G. B., Laurendeau, N. M.: "Scalar Time-Series Measurements in Turbulent CH₄/H₂/N₂ Nonpremixed Flames: OH.", *Combust. Flame* 123, 389 (2000).

⁴ Nobach, H., Schneider, C., Dreizler, A., Janicka, J., Tropea, C.: "Laser-Doppler-Messungen von Teilchenbeschleunigungen und der Dissipationsrate in einem runden Freistrah." to be presented at GALA (2002).

⁵ Dibble, R. W., Hartmann, V., Schefer, R. W., Kollmann, W.: "Conditional sampling of velocity and scalars in turbulent flames using simultaneous LDV-Raman scattering." *Exp. in Fluids* 5, 103 – 113 (1987).

⁶ Geyer, D., Dreizler, A., Janicka, J.: "A Comprehensive Characterization of a Turbulent Opposed Jet Burner by 1D-Raman/Rayleigh, 2D-LIF and LDV." *TNF* 6 (2002).

One-Dimensional Turbulence Simulation of Extinction and Re-ignition Predictions in Piloted Methane-Air Jet Diffusion Flames

Tarek Echekki

Department of Mechanical and Aerospace Engineering

North Carolina State University

Raleigh, NC 27695-7910

(+1) 919 515 5238 - fax: (+1) 919 515 7968 - e-mail: techekk@eos.ncsu.edu

Alan R. Kerstein

Sandia National Laboratories

Livermore, CA 94551-0969

and

J.Y. Chen

Department of Mechanical Engineering, UC Berkeley

Berkeley, CA 94720-1740

Simulations of extinction and re-ignition phenomena in turbulent piloted methane-air jet diffusion flames (Sandia flames D, E and F) are performed using the One-Dimensional Turbulence (ODT) model [1]. The calculations of temporally and spatially resolved thermochemical scalars on a 1D domain include a 12-step chemistry model for methane-air [2]. Mixture averaged transport models are implemented using the CHEMKIN libraries. The ODT model formulation is based on a deterministic integration of unsteady reaction-diffusion equations (for species, temperature and the streamwise velocity) and stochastic implementation of turbulent advection through stirring events (“triplet maps”) applied to the streamwise velocity and thermochemical scalar profiles on a 1D domain. The 1D domain corresponds to a radial direction (transverse to the mean flow). The temporal evolution of these 1D profiles is interpreted as a downstream evolution using a bulk velocity based on the jet momentum. The rate distribution of stirring events is governed by the local strain (i.e. the resolved streamwise velocity on the 1D domain). The model has two parameters, which govern the rate distribution of stirring events and the evolution of the large scales. The parameters are adopted from recent validations of hydrogen-air simulations with experiment [3].

The jet inlet velocity species profiles (for the fuel, co-flow air and pilot streams) are consistent with recommendations provided with the experimental data. Conditional statistics of thermochemical scalars at various downstream distances are obtained from multiple realizations of ODT solutions, which differ by the sequence of random numbers used to implement stirring events.

One important objective of the present simulations is to investigate ODT’s ability to predict extinction and re-ignition. Both phenomena present important challenges for state-of-the-art models in turbulent combustion. Figure 1 shows conditional PDF’s of the mass fraction of CO at $x/d = 7.5, 15, 30$ and 45 for a range of the mixture fraction between 0.43 and 0.53 based on both experiment (Sandia D, E and F) and corresponding ODT computations. Experiment and computations show clear distinctions between conditional PDF’s for the various flames and at downstream distances indicating the presence of extinction and re-ignition as the Reynolds number increases. Near the jet inlet (at x/d of 7.5 and 15), the conditional PDF’s peaks shift toward zero, especially for flame F, indicating the presence of extinction. Bi-modal shapes of the conditional PDF’s at $x/d = 30$ for flame F indicate the presence of both extinguished and re-igniting flames. The results show that the computations yield more extinction for the lower Reynolds flames, D and E than the experiment. Further downstream, the shift of the conditional PDF’s towards a single peak mark the completion of the re-ignition process. The exact downstream locations marking the onsets of extinction and re-ignition are not well predicted by ODT. This is attributed to the interpretation of the temporal evolution of 1D ODT profiles as downstream evolutions. Nonetheless, the ODT model is able to predict extinction and re-ignition in jet diffusion flames using the same model parameters adopted for other flames [3,4]. Moreover, conditional PDF’s of products and intermediate species (OH, H₂, CO₂ and H₂O) and

temperature show essentially similar trends to Fig. 1, further indicating the presence of extinction and re-ignition.

1. Kerstein, A.R., *J. Fluid Mech.*, Vol. 392, pp. 277-334 (1999).
2. <http://www.princeton.edu/~cklaw/kinetics/12-step>.
3. Echehki, T., Kerstein, A.R., Chen, J.Y., and Dreeben, T.D., *Combust. Flame*, Vol. 125, pp. 1083-1105 (2001).
4. Hewson, J.C. and Kerstein, A.R., *Combust. Theory Model.*, Vol. 5, pp. 669-697 (2001).

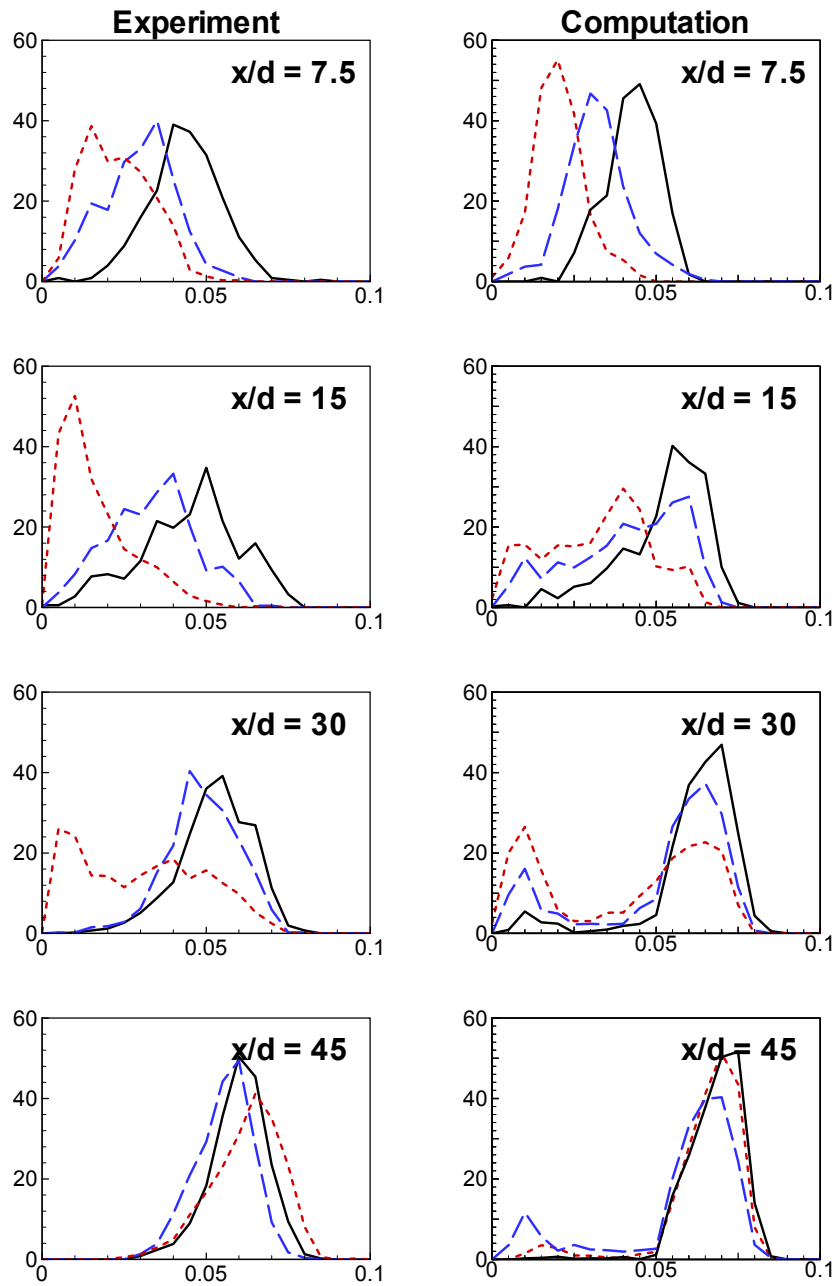


Figure 1. Conditional PDF's of Mass Fraction of CO at $x/d = 7.5, 15, 30$ and 45 for a mixture fraction interval between 0.43 and 0.5 and flames D (—), E (---) and F (-.-).

**TWO-DIMENSIONAL MEASUREMENTS OF REACTION-RATE,
MIXTURE FRACTION, AND TEMPERATURE
IN TURBULENT METHANE/AIR JET FLAMES**

JONATHAN H. FRANK*

*Combustion Research Facility
Sandia National Laboratories
Livermore, CA 94551, USA*

SEBASTIAN A. KAISER AND MARSHALL B. LONG

*Department of Mechanical Engineering
Yale University
New Haven, CT 06520, USA*

*Corresponding Author: Jonathan H. Frank
email: jhfrank@ca.sandia.gov

ABSTRACT

Instantaneous two-dimensional measurements of reaction-rate, mixture fraction, ξ , and temperature are demonstrated in turbulent partially premixed methane/air jet flames [1]. The forward reaction-rate of the reaction $\text{CO} + \text{OH} \Rightarrow \text{CO}_2 + \text{H}$ is measured by simultaneous OH laser-induced fluorescence (LIF) and two-photon CO LIF. The product of the two LIF signals is shown to be proportional to the reaction-rate. Temperature and fuel concentration are measured using polarized and depolarized Rayleigh scattering [2]. A three-scalar technique for determining mixture fraction is investigated using a combination of polarized Rayleigh scattering, fuel concentration, and CO LIF. Measurements of these three quantities are coupled with previous detailed multiscalar point measurements [3] to obtain the most probable value of mixture fraction at each point in the imaged plane. This technique offers improvements over two-scalar methods. Previous efforts have focused on a two-scalar approach that combines Rayleigh scattering and fuel concentration measurements. A fundamental difficulty with this approach is that it is not very sensitive near stoichiometric conditions where the fuel signal disappears and the Rayleigh signal does not vary greatly as a function of mixture fraction. Methods for obtaining fuel concentration have included laser-induced fluorescence of fuel tracers [4,5], Raman scattering from fuel [4-7], and difference Rayleigh scattering [2]. The most promising of these techniques is the difference Rayleigh scattering, which is used in the present experiments.

A primary objective for developing these imaging diagnostics is to provide measurements of fundamental quantities that are needed to accurately model interactions between turbulent

flows and flames. Examples of simultaneous reaction-rate, mixture fraction, and temperature imaging are shown for turbulent partially premixed jet flames, which are target flames for the TNF Workshop. Multi-dimensional measurements of mixture fraction are needed to determine scalar dissipation rates, χ , where $\chi = 2D\nabla\xi\cdot\nabla\xi$. The mixture fraction images are used to determine the radial and axial components of scalar dissipation rate (see Fig. 1).

References

1. Frank, J. H., Kaiser, S. A., and Long, M. B., *Proc. Combust. Inst.*, 29 (2002), to appear.
2. Fielding, J., Frank, J. H., Kaiser, S. A., and Long, M. B., *Proc. Combust. Inst.*, 29 (2002), to appear.
3. Barlow, R. S., and Frank, J. H., *Proc. Combust. Inst.*, 27:1087-1095 (1998).
4. Frank, J. H., Lyons, K. M., Marran, D. F., Long, M. B., Stårner, S. H., and Bilger, R. W., *Proc. Combust. Inst.*, 25:1159-1166 (1994).
5. Long, M. B., Frank, J. H., Lyons, K. M., Marran, D. F., and Stårner, S. H., *Int. J. Phys. Chem.* 97:1555 (1993).
6. Stårner, S. H., Bilger, R. W., Lyons, K. M., Frank, J. H., Long, and M. B., *Combust. Flame* 99:347 (1994).
7. Kelman, J. B. and Masri, A. R., *Comb. Sci. Technol.* 129:17-55 (1997).

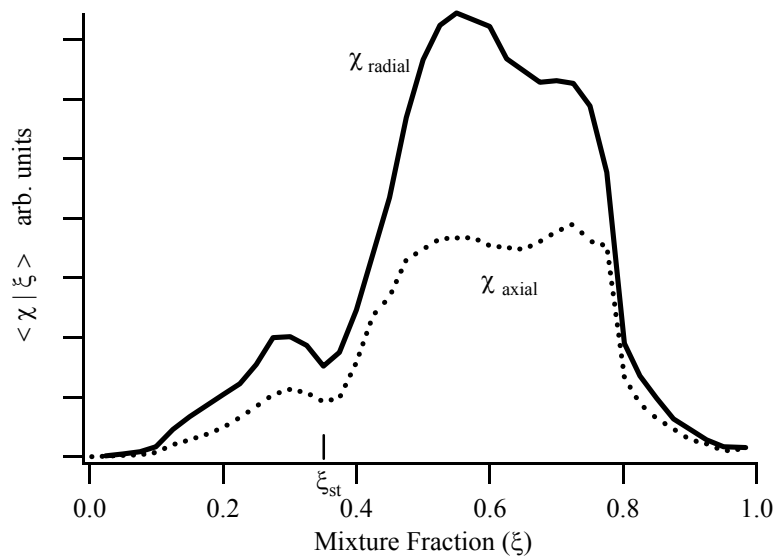


Fig. 1. Measurements of conditional mean scalar dissipation rates in a turbulent CH₄/Air (1/3 by vol.) jet flame of Re = 22,400 (Flame D of the TNF Workshop).

A COMPREHENSIVE CHARACTERIZATION OF A TURBULENT OPPOSED-JET BY 1D-RAMAN/RAYLEIGH, 2D-LIF AND LDV

DIRK GEYER¹, ANDREAS DREIZLER, ANDREAS NAUERT, SUNIL OMAR and
JOHANNES JANICKA

*Fachgebiet Energie und Kraftwerkstechnik, Technische Universität Darmstadt
64287 Darmstadt, Germany*

A turbulent opposed-jet was investigated with different laser diagnostic methods in order to provide comprehensive information about its non-reacting and reacting flow field in terms of species concentrations, gradients of concentrations, velocities and, for reacting flows, flame thickness parameters. The turbulent-opposed jet was designed with special emphasis on optical access for laser diagnostics and it was developed in connection with the TNF workshop as a cooperation project including mainly EKT and Sandia as contributors.

The series of experiments was motivated by the search for a flame which is simple but different from the well known jet flames, and thereby provides a challenge for mixing models. Due to the rotational symmetry and the limited extensions of the flow field the turbulent opposed jet is also very well suited to explore chemistry-turbulence interaction by using either advanced chemical models or more sophisticated modeling of the turbulent flow like LES or even DNS.

Flows issuing from two contoured jet nozzles, which oppose each other and are vertically aligned, are impinging with equal momentum in a horizontal stagnation plane. Each jet has an exit diameter of $D=30$ mm and is surrounded by a concentric ring with a diameter of 60 mm for the nitrogen co-flow. For all experiments the nozzles were $H=30$ mm separated, resulting in a ratio of $H/D = 1.0$. Turbulence is enhanced by perforated plates 50 mm upstream of the nozzle exit. Characteristically for the flow facility is that single shot 1-D measurements of main species concentrations and temperatures take place along a line intersecting the stagnation plane approximately perpendicular, which allows the determination of gradients of these quantities across this zone. Optical access along the centerline of the burner is provided by laser-windows, a more detailed description of the opposed-jet can be found elsewhere¹.

Partially premixed methane with two different equivalence ratios ($\phi = 2.0$ and $\phi = 3.18$) was used as fuel. The Reynolds numbers, based on the bulk velocity at the nozzle exit and the nozzle diameter, were 5000, 6650, 7200 for the lower and 3300, 5000, 6650 for the higher equivalence ratio, where the highest Reynolds number for the respective equivalence ratio corresponds to the extinction limit of the flame. Naturally, a flame with a higher degree of premixing extinguishes at higher Reynolds numbers. Measurements of non-reacting flows were conducted for the same Reynolds numbers by Raman scattering and LDV in order to provide insight into the mixing process and allow a comparison with the reacting cases.

Information on major species concentrations as well as their gradients were obtained by single-shot 1D-Raman/Rayleigh scattering. The experimental setup consists of a frequency doubled Nd:YAG laser (900 mJ), a two leg pulse-stretcher and a 16 bit ICCD for planar imaging of the Rayleigh scattering. Raman scattering is sampled by a custom-designed achromatic lens with high f-number and excellent imaging properties onto the slit of a spectrograph and recorded by the means of a second, highly sensitive Gen IV ICCD. The spatial resolution of the system is $0.35 \times 0.38 \times 0.11$ mm for the reacting flow, where the

¹ Corresponding Authors : geyer@hrz2.hrz.tu-darmstadt.de or dreizler@hrz2.hrz.tu-darmstadt.de

resolution perpendicular to the averaged orientation of the stagnation plane is 0.35 mm, thereby matching the Batchelor length scales. For non-reacting flow experiments the resolution was 0.30x0.30x0.11 mm.

Data evaluation of the Raman signal is based, in contrast to more commonly used schemes, on a full spectral fit of the measured spectra to spectra libraries. These temperature-dependent libraries are computed by using theoretical scattering models for all diatomic and triatomic species. Only the methane library is build from calibrations in heated gas flows and laminar opposed jet flames, since no sufficient theoretical description for Raman scattering of methane exists. For a full spectral fit only one reference point at a known temperature and concentration must be measured for each species. This is of particular advantage in the investigated opposed-jet configuration where commonly employed calibration burners can not be used because of the vertical laser beam guidance.

Results from a configuration with a Reynolds number of 6650 and an equivalence ratio $\phi = 2.0$ are shown in figure 1. The turbulence intensity at nozzle exit is about 10 % and increases drastically in around the stagnation plane, not only caused by the decrease of the mean velocity but also by a 3-fold increase of the fluctuations. A comparison of the scalar dissipation rate in centerline-direction of the same non-reacting and reacting flow is presented in figure 2. Scalar dissipation rates for the reacting case are more than a magnitude higher as a result of the increased diffusivities, whereas the steepest gradients of the mixture fraction are smoothed at elevated temperatures. Similar as in jet flamesⁱⁱ a local minima is found for the scalar dissipation at stoichiometric mixture fraction and the maximum at slightly rich conditions.

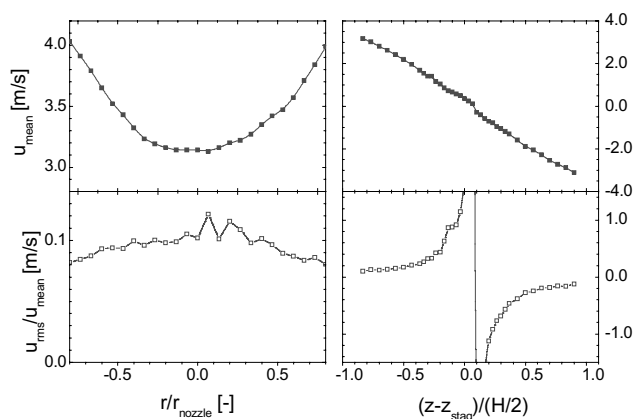


Figure 1 : Axial velocity profile at nozzle exit (left side) and along centerline (right side) for $Re=6650$, $\phi = 2.0$. Upper part shows mean velocity, lower part normalized rms. velocity.

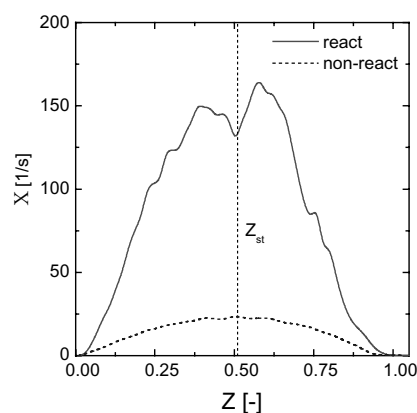


Figure 2 : Scalar dissipation rate in centerline direction non-reacting and reacting case for same configuration

Additionally, a series of single point Raman/Rayleigh/LIF measurements was performed in the TDF Lab, Sandia Nat. Labs on an identical copy of the EKT opposed-jet-burner, which provide not only major but also minor species concentrations.

The quantitative data described above are rounded off by an extensive series of qualitative 2D OH-LIF images of the reaction zone. These images reveal information on flame thickness, flame surface density and flame wrinkling and thereby provide insight into the flame structure.

ⁱ Proceedings of the TNF 5 Workshop, <http://ca.sandia.gov/tdf/Workshop>.

ⁱⁱ Karpetis, A.N. and Barlow, R.S., to appear in *Proc. Comb. Inst.* 29 (2002).

Proposal of new kind of burner for pure hydrocarbon flames with minimal soot, Rostocker Ring Burner (RRB)

E. Hassel, J. Nocke, University of Rostock, Germany, Institute of Thermodynamics,
corresponding author: egon.hassel@mbst.uni-rostock.de

A. Leder, M. Brede, University of Rostock, Germany, Institute of Fluid Mechanics
Meier, W.; Keck, O.; German Aerospace Research Institution, DLR, Stuttgart, Germany

Introduction:

To improve models for simulation of hydrocarbon diffusion flames measurement data are necessary for validation. There is a long tradition in constructing and building burners that will create flames which can be both, simulated and measured. From these both methods result a number of different requirements for the final design of burner and flames to be investigated. One critical aspect is local soot and PAH concentration within the flames due to the fact, that spectroscopic measurement techniques, like Raman or LIF, which are used for concentration determination, are strongly hampered by soot or PAHs within the measurement volume. Most of the flames used so far have tried to overcome this problem with more or less success and with more or less disadvantages on other aspects as they tried to make a trade-off. We have developed a new kind of burner, which will overcome some problems and which we propose as a new test case burner. It creates swirling turbulent diffusion hydrocarbon flames. So far we used methane as fuel. The burner and flames show the following advantages and disadvantages. Advantages: a) pure hydrocarbon flames; b) recirculation strengths can be adjusted easily; c) simple construction: e.g. no cooling required, easy to operate, cheap, simple to copy; d) well defined boundary conditions for CFD; e) (nearly) no soot: so far we could not detect soot with LIF methods; f) excellent optical access for all laser diagnostic techniques; g) no contact of the (visible) flame to surfaces: that means no flame quenching, no catalytic effects and no steep gradients of quantities near surfaces (reduces CFD spatial resolution requirements near walls, no wall turbulence model necessary). Disadvantages: a) three dimensional problem for CFD; b) maybe partial premixed combustion; c) different geometric length scales: small at fuel exits (diameter < 0.6 mm), large for global flame (flame diameter about 60 mm,): maybe problem for CFD, d) fuel inlet condition at small fuel inlet pipes might not be fully turbulent for some interesting conditions. What we have done so far: a) build several burners and made visual investigations with home video equipment of influence of geometrical parameters (like angle and number of fuel inlet pipes) on flame appearance and flow conditions, b) made 3D-LDV measurements of one cold condition with special focus on fuel inlet condition, data are available, c) made some OH- and CH-2D-LIF experiments, d) took some time averaged Raman spectra with high spectral resolution in order to look for soot or PAHs, that is to study spectra quality, e) currently we are doing full 3D simulations with commercial CFD code FIRE, that is work in progress. More info about this work can be found under http://priapos.fms.uni-rostock.de/text/tmd_vbfltt.htm.

Figure 1 shows a sketch of the burner. Fuel is streaming through the tangential inlet pipes, goes into the ring with about 80 mm diameter, and flows through the small pipes with a diameter of about 0.6 mm with an angle of 45 degrees to the radius and 45 degrees to the vertical with a tangential velocity component to the main axis. The burner is placed within a channel that provides the combustion air with a low air velocity of about 0.5 m/s. For LDV air and fuel is seeded with particles.

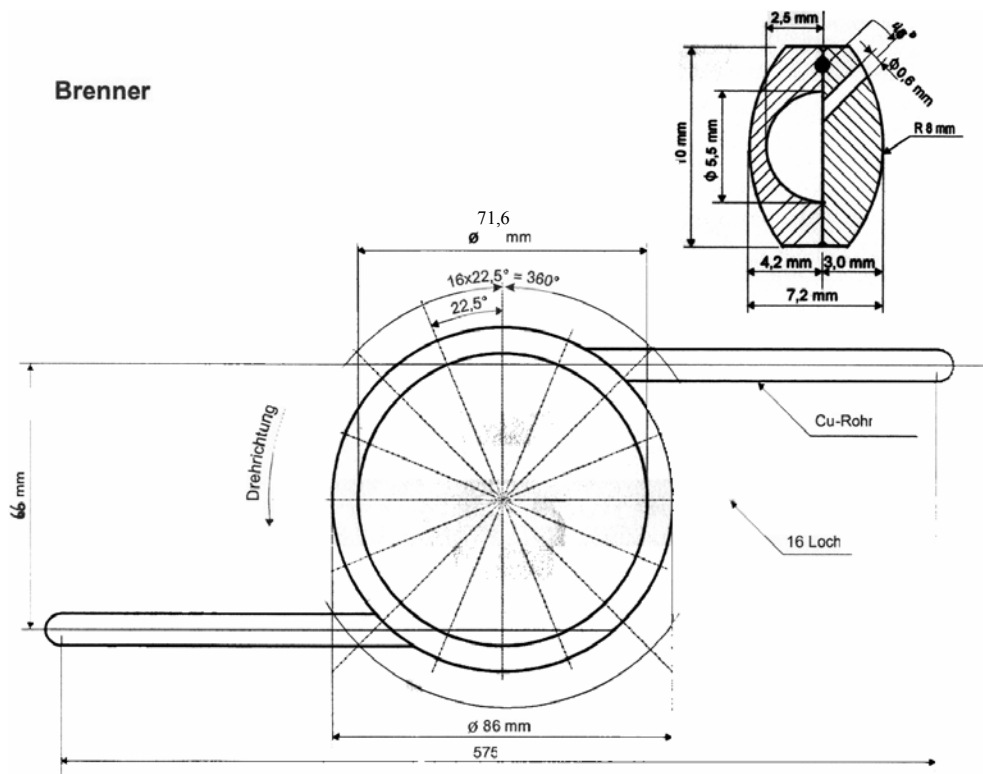


Figure 2 shows one example of the flame, seen from side, the flame is clearly detached from the burner.

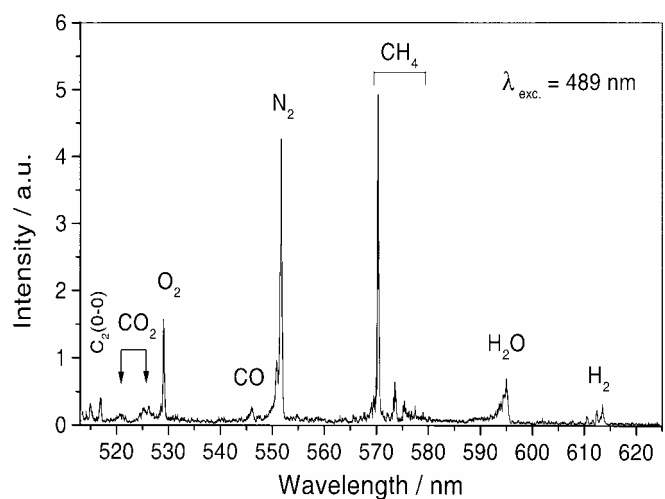


Figure 3 shows a time averaged Raman spectrum with high spectral resolution. Because it is time averaged, there is fuel and oxygen to be seen simultaneously, but no soot or PAH influence.

Instantaneous three-dimensional visualization of concentration distributions and gradients in turbulent processes with a single laser

A. Hoffmann, F. Zimmermann, C. Schulz

PCI, Universität Heidelberg

Im Neuenheimer Feld 253, 69120 Heidelberg, Germany

(Email: axel.hoffmann@pci.uni-heidelberg.de, frank.zimmermann@pci.uni-heidelberg.de)

Techniques for observing instantaneous three-dimensional gradients in turbulent flows are of major interest for obtaining insight into the spatial structures of turbulent flows and for measuring concentration gradients. We present a new laser-based technique for the measurement of instantaneous three-dimensional species concentration distributions and gradients in turbulent combustion and flows.

The laser beam from a single laser is formed into two crossed light sheets that illuminate the area of interest, as shown in figure 1. By means of a special optical set up the signal light from both planes can be detected with a single camera via a mirror arrangement. Using a spherical mirror, no refractive optical elements have to be introduced. In this set up the signal from both planes is measured simultaneously. With this method, the additional integrated signal of the respective perpendicular light sheet must be corrected for by image post processing to regain the information in the cutting line [1]. This procedure can be avoided with two-camera detection, each camera observing one plane. However, then one of the laser beams must be delayed by approximately 50 ns to enable independent detection.

The 3D-imaging technique can be applied to measuring Mie-scattering, laser induced incandescence (LII) or laser induced fluorescence (LIF) to excite and detect specific molecules and species.

Image post processing enables the reconstruction of a three-dimensional data set from the two crossing planes in close proximity of the cutting line of the two light sheets. This reconstruction is accomplished within a three-dimensional data matrix and can be described as a repeated diffusion process of data out of the measured planes. The original images are hereby treated as regenerating sources by restoring the original pixel values in the image planes after each diffusion step [2].

The three-dimensional data field can then be visualized using standard volume-visualization methods that assign a given intensity value not only a color, but also a transparency value [3]. This visualization of the volumetric data set gives unique insight into instantaneous three-dimensional structures within the turbulent processes. Figure 2 shows the visualization of the three-dimensional distribution of OH-LIF intensity in a small volume element of a lean Bunsen burner flame.

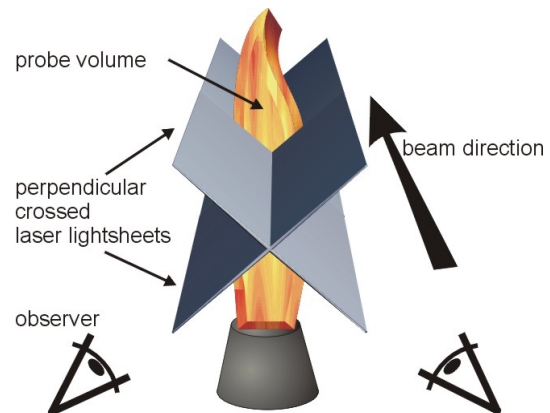


Figure 1: Arrangement of the crossed light sheets in the probe volume

From the volumetric data set three-dimensional gradients can be determined along the intersection line. In contrast, gradients evaluated from two-dimensional images, show a projection on the respective plane only. Analyzing the correlation of local concentration gradients with local (scalar) concentration is of major interest for developing PDF-type (probability density function) simulation approaches in turbulent combustion. Recent experiments show that neglecting the third spatial component leads to significant mistakes in the norm of spatial concentration gradients [1].

We applied this technique to measurements of the hydroxyl laser induced fluorescence (OH-LIF) in a turbulent methane-air Bunsen flame upon A-X(3,0) excitation at 248 nm with a tunable KrF excimer laser. Further measurements address the three-dimensional distribution of toluene-LIF in a turbulent, non-reactive gaseous mixing process seeded with toluene.

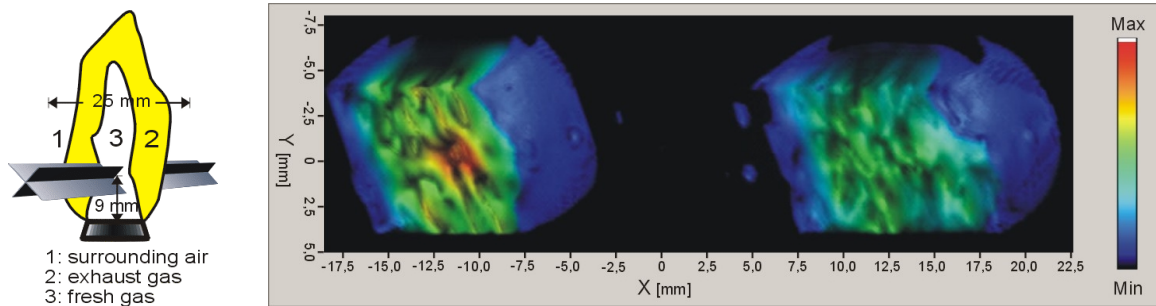


Figure 2: 3D-visualization of OH-LIF in a lean Bunsen burner flame.

- [1] Zimmermann, F., *Entwicklung einer Methode zur in-situ Messung dreidimensionaler Gradienten in turbulenten Flammen und Strömungen*, Diploma theses, University of Heidelberg (2001)
- [2] Scharr, H., *Optimale Operatoren in der Digitalen Bildverarbeitung*, Dissertation, University of Heidelberg (2000)
- [3] Dartu, C., *Visualization of volumetric dataset*, Dissertation, University of Heidelberg (1998)

New measurements on piloted flames and simultaneous line Raman and crossed PLIF

A. N. Karpetis and R. S. Barlow

Combustion Research Facility

Sandia National Laboratories, Livermore, CA 94551-0969, USA

email: ankarpe@ca.sandia.gov, barlow@ca.sandia.gov

Scalar dissipation plays a central role in the theory and modeling of turbulent flames. In the present Symposium we report measurements of the radial component of scalar dissipation in partially premixed CH_4/air jet flames [1]. The experimental system combines line imaging of Raman scattering, Rayleigh scattering, and CO LIF and allows for the measurement of major species, temperature, mixture fraction, and scalar dissipation in one dimension. Such measurements are quite useful for evaluating scalar dissipation models, investigating the influence of high scalar dissipation on reactive species concentrations, and determining the length scales associated with scalar fluctuations in turbulent flames. Such measurements are even more useful if the instantaneous orientation of the reaction zone relative to the 1D scalar measurement is known. Here we describe an experimental system that combines multispectral line imaging with OH PLIF imaging in two intersecting planes. The technique provides measurements of OH mass fraction along the 1D line, and it allows for determination of the local and instantaneous flame orientation and curvature. This, in turn, can be used to estimate scalar dissipation in the flame-normal direction, such that the instantaneous effects of scalar dissipation on compositional structure may be evaluated more accurately and the joint conditional statistics of species mass fractions, mixture fraction, scalar dissipation, flame orientation, and flame curvature may be quantified. The first results, using this 5-camera, combined imaging system in partially premixed CH_4/air jet flames, are presented.

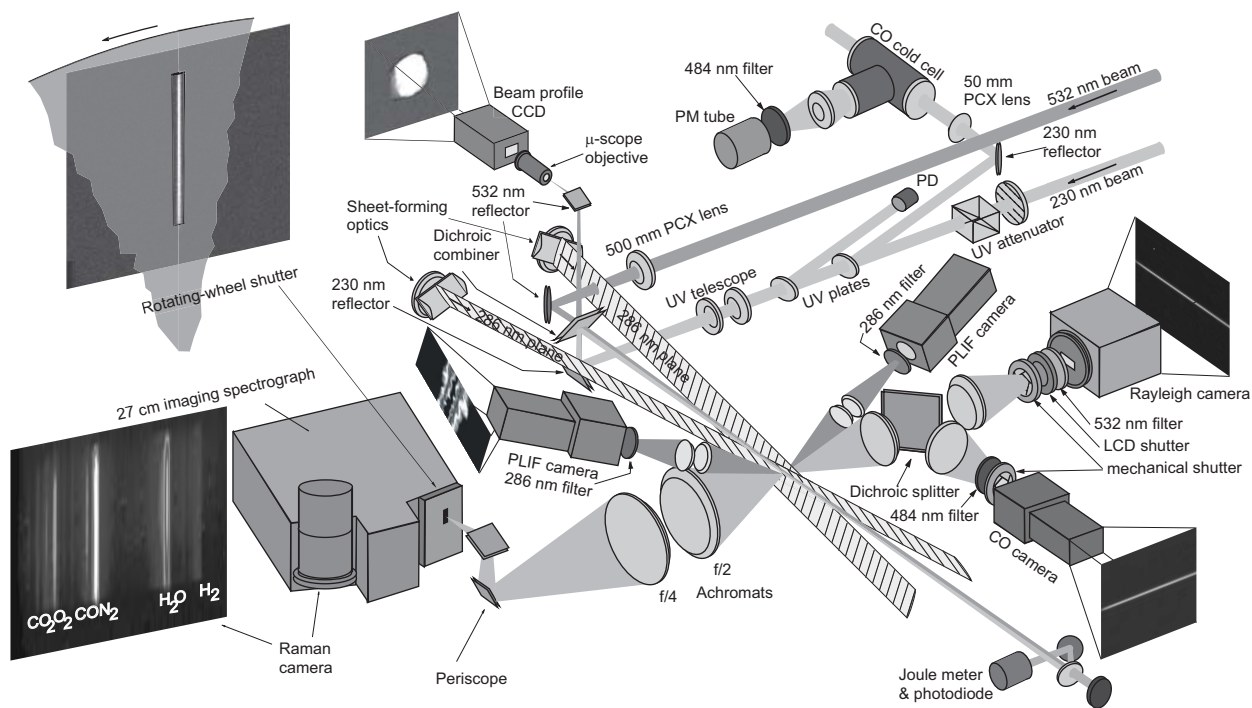


Figure 1: Schematic diagram of the experiment

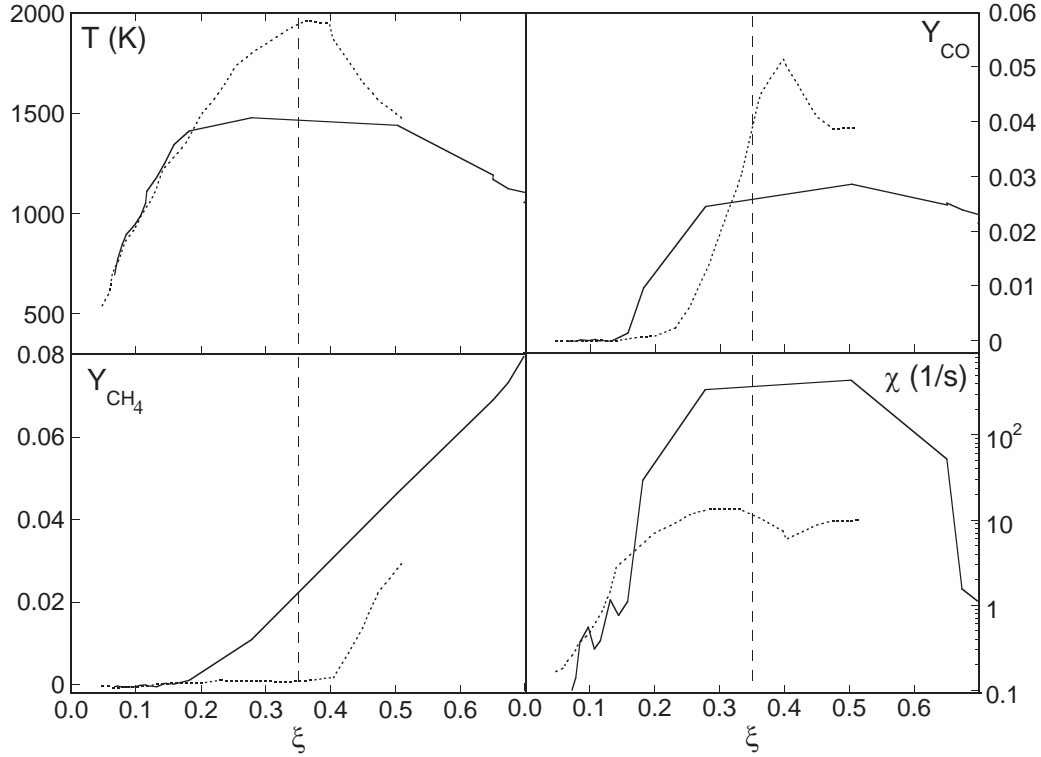


Figure 2: Single-shot profiles of temperature, mass fractions of CO and CH₄, and the 1-D measured scalar dissipation in flame D. Solid/dotted line: low/high values of scalar dissipation at stoichiometry (shown by vertical dashed line).

Single-shot measurements of temperature and the concentrations of all major species were obtained along radial segments in a piloted turbulent CH₄/air jet flame (Sandia flame D). Figure 2 shows two single-shot realizations of flame structure in that flame. The choice of profiles was based on extremes of χ measured near the stoichiometric condition (shown by the vertical dashed line). We show results for temperature and the mass fractions of CH₄ and CO, as well as χ , for a case of very high χ (430 1/s, solid line) and relatively low χ (14 1/s, dotted line). The profiles of Y_{CO} and Y_{CH_4} , plotted vs. mixture fraction, show clear differences in chemical composition between low and high scalar dissipation conditions. High χ causes a significant reduction in both T and Y_{CO} , and there is greater leakage of CO and CH₄ into lean mixtures. The main advantage of line measurements such as these is precisely the capability to condition statistics of temperature and species upon the measured value of χ . While the 1-D, line measurement of χ suffices for conditioning statistics as shown in figure 2, the technique suffers an inherent bias towards smaller values of χ : the measurement registers only the projection of the mixture fraction gradient vector along the laser axis, the magnitude of which can in some cases be smaller than the magnitude of the full mixture fraction gradient vector². Measurement of the local flame curvature can, at the very least, identify these biased cases and potentially produce an estimate of the 3-D scalar dissipation.

[1] Karpetis, A. N., and Barlow, R. S., to appear in *Proc. Comb. Inst.* 29 (2002).

[2] Dahm, W. J. A., and Buch, K. A., *Phys. Fluids A* 1:1290 (1989).

The Role of Partially Premixed Flames in Industrial Processes

James B Kelman
Cranfield University, England
j.kelman@cranfield.ac.uk

While non-premixed flames have drawn a lot of attention from the modelling community in the past, partially premixed flames have gained wider use through industry. This has been the result of emission legislation throughout the world. Although fully premixed flames would be preferred from an emission's point of view, achieving full premixing in industrial process is extremely difficult, and partially premixed flames generally result from the mixing process. The high levels of NO_x that occur in diffusion flames are the reason that industry has turned to premixed regimes. Issues of mixing times in industrial burners mean that although the overall Air Fuel Ratio (AFR) may be designed to reduce NO_x, the non-homogeneous mixing that occurs produces local partial premixing or stratification. While this may be desirable in some cases, such as IC engines, for gas turbines, the partial premixing produces regions of higher heat release, flame speed and pressure fluctuations. This results in, not only higher levels of NO_x, but also in acoustic instabilities which can cause the failure of the turbine combustors. Subsequently, much work needs to be done in establishing the behaviour of PPFs in terms of flame speed, and the coupling of pressure fluctuations and heat release.

The propagation of partially premixed flames is poorly understood, due to the complex coupling between stratification levels, turbulence and heat release. The two main contributors believed to be influencing the heat release in the PPF combustors are fluctuations in the AFR and flame stretch induced by large scale structures in the flow. It has been shown theoretically that AFR fluctuations play a significant role in driving instabilities in combustors, but research so far, has not been able to de-couple the influence of AFR and flame stretch¹. Significant theoretical work has been carried out at Cambridge University but a lack of experimental data in realistic systems hinders validation of the results². The influence of flame stretch, defined by the Karlovitz flame stretch factor, has received significant attention from Abedel-Gayed et al³ over the years. They have related flame speeds to turbulence intensity and stretch, but have not dealt with PPFs, limiting their approach to investigating premixed flames. Experimentally detailing the propagation of the flame front through partially premixed systems is required to complement existing calculations and provide sound understanding of the fundamentals involved.

It is critical to develop burners and experimental programs that can de-couple stretch, heat release and stoichiometry factors and details flame behaviour under isolated conditions. The initial stages of this process are to use an acoustically forced counterflow burner with the opposing streams rich and lean of stoichiometric. Previous work by Harding⁴ has shown that stratified flames are very sensitive to global strain rates and the levels of stratification. The same burner is to be modified so that both streams may be oscillated in phase at up to 10 kHz. This enables strain rate frequency dependence to be investigated in a quasi-steady state system. The effects of dynamic strain rates on the chemistry can then be established. Previous theoretical and experimental work on similar burners, in both diffusion flames and premixed flames have shown that the structural response of the two flame types varies significantly⁵. Additionally, extinction strain rates are increased by higher frequency oscillations. This may have impact on the extinction mechanism in turbulent flames where high vortex shedding strain may be sustainable for short periods. This burner type enables the de-coupling of the

AFR, the heat release and the strain rate, allowing one to controlled while observing the others.

Further work is then needed to look at more complex flows involving re-circulation and swirl effects. This is to be accomplished in a gas turbine type combustor, where acoustic forcing can be used to introduce AFR fluctuations to the flow. Flame speed and heat release are then of interest to look at the stability of the flame and it's susceptibility to acoustic self-excitation.

Diagnostics are obviously needed to quantify many of the effects expected to be seen in these flames and required development. Heat release is a primary concern, and techniques for the measurement of heat release, which are already under development, require refinement for PPFs⁶. A combination of measurement techniques for some, or all of, simultaneous velocimetry, temperature, radicals and stoichiometry, is required to be able to map flame speed with respect to the stratification levels. It is the complexity of attaining all these simultaneously which makes the counterflow geometry attractive. As it provides a quasi-steady state flame, different quantities may be measured separately and remapped. However to examine the more complex interactions involved with re-circulation and turbulence, techniques need to be developed.

In summary, a program of burner design, modelling and experimental work, is being established to build a data base of flame structures, from fundamental flame attributes through to complex geometry flame behaviour. It is hoped that this program will link experiments, kinetics and modelling, and provide a solid foundation to understanding Partially Premixed Flame behaviour.

¹ Lieuwen, T. and Zinn, B.T., Twenty-Seventh Symposium (international) on Combustion, The Combustion Institute, Pittsburgh, (1998) pp. 1809-1816.

² Dowling, A.P., "Thermo-acoustic Instability", presented at the 6th International Conference on Sound and Vibration, Copenhagen, July, 1999.

³ Abdel-Gayed, R.G., Bradley D. and Lawes, M., Proc. R. Soc. Lond. A, 414:389-413, 1987.

⁴ Harding, S. C. "Investigation into mixing and combustion in an optical, lean, premixed, prevaporised combustor", PhD Thesis, Cranfield University, 1996.

⁵ C. J. Sung and C. K. Law, "Structural Sensitivity, Response, and Extinction of Diffusion and Premixed Flames in Oscillating Counterflow", Combustion and Flames, 123:375-388, 2000.

⁶ J. E. Rehm and P. H. Paul, "Reaction Rate Imaging", Twenty-Eighth Symposium (international) on Combustion, The Combustion Institute, Pittsburgh, (2000), pp. 1775-1782.

Large Eddy Simulation of Turbulent Jet Flames: A comparison

A. Kempf, A. Sadiki, J. Janicka
Institute for Energy- and Powerplant Technology
Petersenstr. 30
64287 Darmstadt, Germany
www.tu-darmstadt.de/fb/mb/ekt
akempf@gmx.net

In recent years, many jet-flames have been a target of large eddy simulations. In most cases, simplified flamelet models have been applied. Aim of the present work is to revisit the flames investigated and to recompute them with the latest version of our code. Thus, the flames may be compared and a better assessment of the LES-flamelet approach is achieved.

The first flame in the comparison is the EKT-H3 [1] flame, as already investigated by H. Forkel in 1999 [2]. This flame features a nozzle of 8 mm in diameter that injects fuel at a rate of 34.8 m/s, corresponding to a Reynoldsnumber of 10,000. An air-coflow to stabilize the flame has a velocity of 0.2 m/s. The fuel is a mixture of 50 % vol. of hydrogen and 50 % vol. of nitrogen.

The second test flame is the DLR flame by W. Meier [3]. Its Reynoldsnumber is 15,200, based on a bulk velocity of 42.2 m/s and a nozzle-diameter of 8 mm. The coflow velocity is set to 0.3 m/s. The fuel is a special mixture consisting of 33.2 % vol. of methane, 22.1 % vol. of hydrogen and 44.7 % of nitrogen. The large amount of nitrogen has been chosen to inhibit the formation of soot, which would render laser-diagnostics impossible. The hydrogen component is necessary to stabilize the flame. This flame is well investigated both experimentally and numerically (RANS) [4], while an LES of this flame has been presented in 2001 [5].

As third and last flame, we present the EKT-HD (Highly Diluted) flame [6]. A fuel jet with a bulk-velocity of 36.3 m/s exits from a nozzle of 8 mm in diameter into a coflow of ambient air at 0.2 m/s. This results in a Reynoldsnumber of 16,000, which is close to the experimentally determined blow-off limit of 17,000. Thus, a significant amount of non-equilibrium chemistry will occur. A special fuel mixture has been used to observe finite chemistry with hydrogen fuel: It consists of only 23 % vol. of hydrogen and 77 % vol. of nitrogen. The LES of this flame is presented in depth at the 29th symposium on combustion.

To simulate these flames, we apply the latest version of the LES code that has already been used for previous simulations of this works target-flames. This version of the LES-code is fully conservative for mass and species and does no longer require an under-relaxation for density. A finite volume method is used to solve the incompressible governing equations for mass, momentum and species. In this context, incompressible means that density is no function of pressure but only of the chemical state. All fluxes are discretized by central schemes, only the convective scalar fluxes are computed by a TVD scheme. This is necessary to avoid inac-

ceptable numerical oscillation, a problem hardly known with RANS due to lower gradients. Sub-grid transport is modeled by increasing diffusion with an added turbulent viscosity, which is determined according to the classical Smagorinsky-model [8]. The model constant is determined dynamically by the approach due to Germano [7] et al.

For non-premixed flames, the mixture-fraction formulation may be applied. With the flamelet-theory for non-premixed flames, the chemical state only depends of the mixture-fraction and its scalar rate of dissipation. To determine the mixture-fraction, a conservation equation for $\overline{\rho f}$ is solved. The scalar rate of dissipation is modeled with the square of the mixture-fraction-gradient. To account for subgrid-fluctuations in mixture-fraction, a beta-distribution is assumed; for the scalar rate of dissipation, a dirac-peak was chosen. The sub-grid variance of the mixture fraction is modeled by the variance resolved in the local test-cell.

A comparison of numerical results to experimental data shows that the chosen LES-flamelet approach is suited to simulate the flames investigated.

References

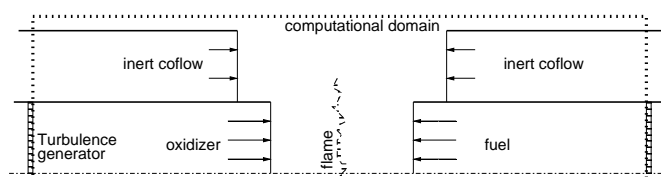
- [1] D.G. Pfuderer, A.A. Neuber, G. Früchtel, E.P. Hassel, J. Janicka, *Turbulence Modulation in Jet Diffusion Flames: Modeling and Experiments*, Combustion and Flame 106: 301-317 (1996)
- [2] H. Forkel, J. Janicka, *Large Eddy Simulation of a Turbulent Hydrogen Diffusion Flame*, 1st Symposium on Turbulent Shear Flow Phenomena (1999)
- [3] W. Meier, R. Barlow, Y.-L. Chen, J.-Y. Chen, *Raman/Rayleigh/LIF Measurements in a Turbulent CH₄/H₂/N₂ Jet Flame: Experimental Techniques and Turbulence Chemistry Interaction*, Combustion and Flame 123, pp. 326-343 (2000)
- [4] H. Pitsch, O. Kunz, J.-Y. Chen, *Rans Modeling of the DLR-flame*, 5th Workshop on Measurement and Computation of Turbulent Non-Premixed Combustion, Delft, Netherlands (2000)
- [5] A. Kempf, C. Schneider, A. Sadiki, J. Janicka, *Large Eddy Simulation of a Highly Turbulent Methane Flame: Application to the DLR Standard Flame*, Proc. 2nd Symposium on Turbulent Shear Flow Phenomena: III, 315-320 (2001)
- [6] M.M. Tacke, S. Linow, S. Geiss, E.P. Hassel, J. Janicka, J.Y. Chen, *Experimental and Numerical Study of a Highly Diluted Turbulent Diffusion Flame Close to Blowout*, Proc. Combust. Inst. 27: 1139-1148 (1998)
- [7] M. Germano, U. Piomelli, P. Moin und W.H. Cabot, *A dynamic subgridscale eddy viscosity model*, Phys. Fluids A, 3, pp. 1760-1765, 1991
- [8] J.S. Smagorinsky, *General circulation experiments with the primitive equations*, 1. The basic experiment, Monthly Weather Rev., 91, pp. 99-164 (1963)

Large Eddy Simulation of a Turbulent Opposed Jet: The Darmstadt Configuration

A. Kempf, A. Sadiki, J. Janicka
Institute for Energy- and Powerplant Technology
Petersenstr. 30
64287 Darmstadt, Germany
www.tu-darmstadt.de/fb/mb/ekt
akempf@gmx.net

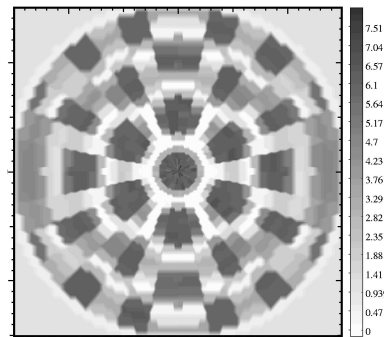
It is widely accepted that LES has a great potential for the simulation of turbulent flames, since all fluctuations are resolved down to the filter-width. LES is very capable to predict mixing, which is the driving mechanism of combustion in non-premixed flames. The aim of the present work is to give LES results for the Turbulent Opposed Jet burner set up by EKT-Darmstadt and currently being investigated by different groups. Counterflow burners are extremely well suited to calibrate, validate and compare different models for mixing and combustion. Applying the RANS approach, counter-flow systems may even be simulated in one spatial dimension only, rendering possible simulations with detailed chemistry.

For this work, an incompressible (Low-Mach assumption) LES-code is applied. Momentum flux is discretized by high-order central schemes, whereas scalar fluxes were described by a TVD scheme to avoid numerical oscillations. The sub-grid fluctuations are modeled according to Smagorinsky [2] with a dynamically [1] determined model-constant. The chemical processes are described based on the mixture fraction formulation, where $f = 0$ in the oxidizer stream and $f = 1.0$ in the fuel stream. The chemical state is then derived from the mixture fraction by using a flamelet table for constant strain. To account for sub-grid fluctuations in mixture-fraction, a beta-distribution has been assumed. The sub-grid variance is then modeled by the variance resolved by the local test-cell. The whole approach is based on the method presented in [3], while due to improvements to the numerical procedure, an underrelaxation in time is no longer necessary.

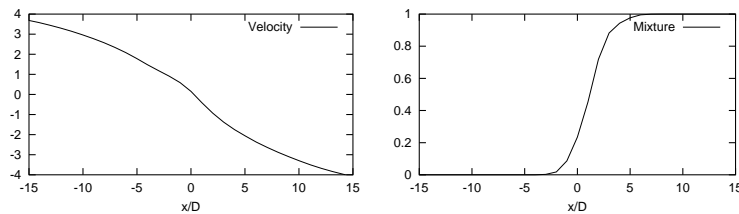


The Opposed Jet Burner consists of two coaxial nozzles (diameter 30 mm) opposed to each other (separated by 30 mm) spending fuel and air respectively. In the pipes feeding the nozzles, at a position of 50 mm upstream of each nozzle, turbulence generating plates were inserted to create a (statistically) reproduceable turbulent state. Surrounding the nozzles, an inert coflow of 60 mm in diameter provides some shielding and inhibits unburnt fuel from igniting in the flue.

The entire setup has been modeled by a cylindrical domain of 130 mm in length and 32 mm in radius. It was first resolved by a grid with $129 \times 32 \times 36$ (≈ 150.000) cells in axial, tangential and radial direction. Then, the grid was refined to $256 \times 32 \times 36$ (≈ 300.000) nodes. The nozzles and the coflow-pipe are located within the computational domain, which is modeled by immersed-boundary conditions. These conditions force the velocities to zero in the cells which are cut by a wall. Since we are mainly interested in the flow along the axis, the errors introduced by this approach are negligible. To describe the flow through the turbulence-generators, the inflow-velocity profile was set to reproduce the flow through that grid.



To give some example-results, the mean axial velocity and the mean mixture fraction along the axis are presented.



References

- [1] M. Germano, U. Piomelli, P. Moin und W.H. Cabot, *A dynamic subgrid-scale eddy viscosity model*, Phys. Fluids A, 3 (1991), 1760-1765
- [2] J.S. Smagorinsky, *General circulation experiments with the primitive equations*, 1. The basic experiment, Monthly Weather Rev., 91 (1963), 99-164
- [3] A. Kempf, H. Forkel, J.-Y. Chen, A. Sadiki, J. Janicka, 2000, *Large Eddy Simulation of a Counterflow Configuration with and without Combustion*, Proc. Combust. Inst. 28: 28-34 (2000)

Prediction of Flame Liftoff and Structure in Non-Premixed Turbulent Jet Flames

Hoo-Joong Kim and Yong-Mo Kim

Department of Mechanical Engineering, Hanyang University, Seoul 133-791, Korea

e-mail : ymkim@hanyang.ac.kr

The flame liftoff characteristics considerably influences the flame stabilization and pollutant formation in practical combustion devices and largely depends on flow configurations, fuel type, heat losses and mixing conditions etc. The lifted non-premixed turbulent jet flames involve many fundamental mechanisms which involve ignition, local extinction, re-ignition, and flame propagation. Since these physical phenomena are strongly coupled and highly nonlinear, explanations of the stabilization mechanism have been quite controversial.

This study is mainly motivated to numerically analyze the detailed flame structure and stabilization mechanism in the lifted non-premixed turbulent jet flames. The present study adopt the turbulent combustion model [1] based on the strained laminar premixed flamelets, which use two parameters such as mixture fraction and reaction progress variable, in order to get closure of turbulence-chemistry interaction. In this model, the laminar heat release rate is obtained at each mixture fraction and reaction progress variable and turbulent mean heat release rate in energy equation is calculated by using the joint PDF of mixture fraction and reaction progress variable. For simplicity, the mixture fraction and reaction progress variable are assumed to be statistically independent each other, the joint PDF is equal to the product of each PDF. The commonly used PDFs for mixture fraction and reaction progress variable is beta function distribution. In order to account the flame straining effect, the distribution of flame straining is assumed to be a quasi-Gaussian PDF [2]. The laminar heat release rate is calculated using one dimensional premix code with chemical kinetics of GRI-Mech 2.11. The validation case includes the measurement of Muniz and Mungal [3] which has the detailed experimental data of liftoff height and velocity fields near flame base for various co-flow air conditions. In their experiment, the fuel of methane (99.0% purity) is injected through the nozzle of 4.8mm diameter and the co-flow velocity ranges from 0 to 1.85m/s. Figure 1 shows that the comparison of liftoff height as a function of jet exit velocity for two different co-flow conditions. The predicted liftoff heights are defined by the onset of heat release rate. Except the jet exit velocity of 16m/s, the predicted liftoff heights reasonably well agree with the experimental data. Figure 2 and Figure 3 present the mean temperature fields for various flow inlet conditions. By increasing the jet exit velocity, the stabilization point is progressively apart from inlet and centerline. Numerical results indicate that the present approach has the predicative capability to realistically represent the essential features of the lifted turbulent jet flames in terms of flame liftoff height and mean flow patterns near flame stabilization point.

References

1. Bradley, D., Gaskell, P. H., and Lau, A. K. C., "A Mixedness-Reactedness Flamelet Model for Turbulent Diffusion Flames," *23rd Symposium (Int.) on Combustion*, Combustion Institute, pp. 685-692, 1990.
2. Abdel-Gayed, R. G, Bradley, D., and Lau, A. K. C., "The Straining of Premixed Turbulent Flames," *22nd Symposium (int.) on Combustion*, Combustion Institute, pp. 731-738, 1988.
3. Muniz, L., and Mungal, G., "Instantaneous Flame-Stabilization Velocities in Lifted-Jet Diffusion Flames," *Combustion and Flame*, Vol. 111, pp. 16-31, 1997.

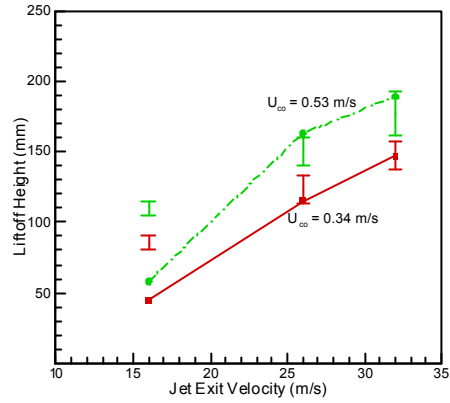


Figure 1. Comparisons of liftoff height for methane lifted jet flame are plotted as a function of jet exit velocity (symbol : prediction, error bar : experiment)

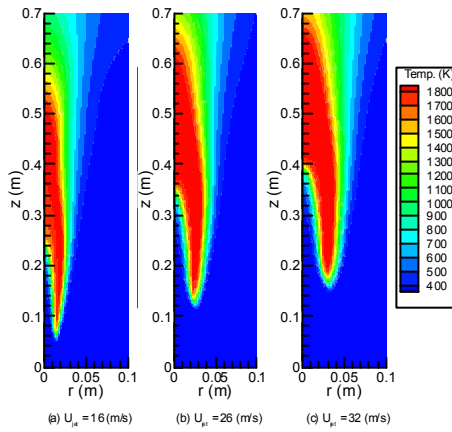


Figure 2 Temperature distributions for various jet exit velocity at co flow air velocity = 0.34 m/s.

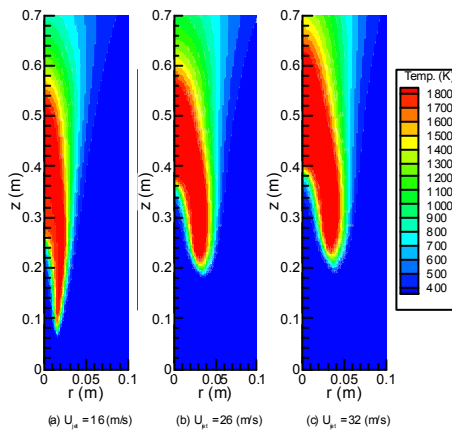


Figure 3 Temperature distributions for various jet exit velocity at co flow air velocity = 0.53 m/s.

Transient Flamelet Analysis for Detailed Structure and NO_x Formation Characteristics of H₂/CO Bluff-body Flames

Gun-Hong Kim, Ji-Ho Cho and Yong-Mo Kim

Department of Mechanical Engineering, Hanyang University, Seoul 133-791, KOREA

Sung-Mo Kang

CLEANCOM Inc., Seoul 133-791, KOREA

e-mail:ymkim@hanyang.ac.kr

The transient model[1] has been applied to predict the flame structure and NO_x formation of the H₂/CO bluff-body stabilized flames for which the detailed experimental data[2] are available. The diameters of bluff-body and fuel jet are 50mm and 3.6mm, respectively. Computations are performed for two jet velocities of 134m/s(HC1 flame) and 321m/s(HC2 flame) which are corresponding to 18 and 43% of the extinction velocity, respectively and the coflow air velocity is set to 40m/s. According to suggestion of TNF Workshop, the model constant $C_{\epsilon 1}$ of the standard k- ϵ turbulence model are modified from 1.44 to 1.60.

The hybrid unstructured grid is used to improve the computational efficiency and grid flexibility in the complex reacting flows. In order to evaluate the prediction capabilities of NO_x emission, calculations are made for the steady flamelet model and the transient flamelet model. The present transient flamelet model adopts the full NO_x chemistry which is able to account for the detailed analysis of NO_x formation mechanisms including prompt and nitrous NO_x formation, and reburn by hydrocarbon radicals[3], while the steady flamelet model employs the only thermal NO mechanism.

In Figure 1, radial profiles of mean and rms mixture fraction are presented at different axial locations. Two flames have the distinctly different mixing characteristics at the recirculation zone. Compared to the standard k- ϵ model, the modified k- ϵ model predicts significantly improved the flow structure and mixing characteristics. However, especially in the outer vortex region of both flames, there exist the large differences between prediction and measurement in terms of the level and uniformity of mean mixture fraction. These discrepancies are relatively pronounced for the HC1 flame and the noticeable deviations are also found in the downstream recirculation zone. At the further downstream regions ($x/D_B > 0.9$), the mixture fraction fields of the two flames become gradually similar and numerical results are reasonably well agreed experimental data. Figure 2 displays the radial profiles of NO mass fraction for two flames. Compared to the steady flamelet model, the present transient flamelet model yields the much better conformity with the measured distribution of NO mass fraction. However, the overall NO levels predicted by two flamelet models are considerably different from the measured ones at 4 axial stations. Especially in the upstream vortex region of HC1 flames, the NO mass fraction is substantially underestimated. These discrepancies are directly tied with the deviated mixture fraction field which is attributed mainly to the defect of the k- ϵ turbulence model to represent the mixing field of turbulent recirculating flows. Another potential error could be partly related to the limitation of the present turbulent combustion model to deal with the relatively thick flame zone and the partially premixed flame region encountered in the complex turbulent reacting flows.

References

- [1] Pitsch, H., Barths, H., and Peters, N., "Three-Dimensional Modeling of NO_x and Soot Formation in DI-Diesel Engines Using Detailed Chemistry Based on the Interactive Flamelet Approach", SAE paper 962057, 1996.
- [2] Dally, B. B., Masri, A. R., Barlow, R. S. and Fiechtner, G. J., "Instantaneous and Mean Compositional Structure of Bluff-Body Stabilized Nonpremixed Flames", *Combustion and Flame*, Vol.114, pp.119-149, 1998.
- [3] Hewson, J.C., "Pollutant Emissions from Nonpremixed Hydrocarbon Flames", PhD Thesis, University of California, San Diego, 1997.

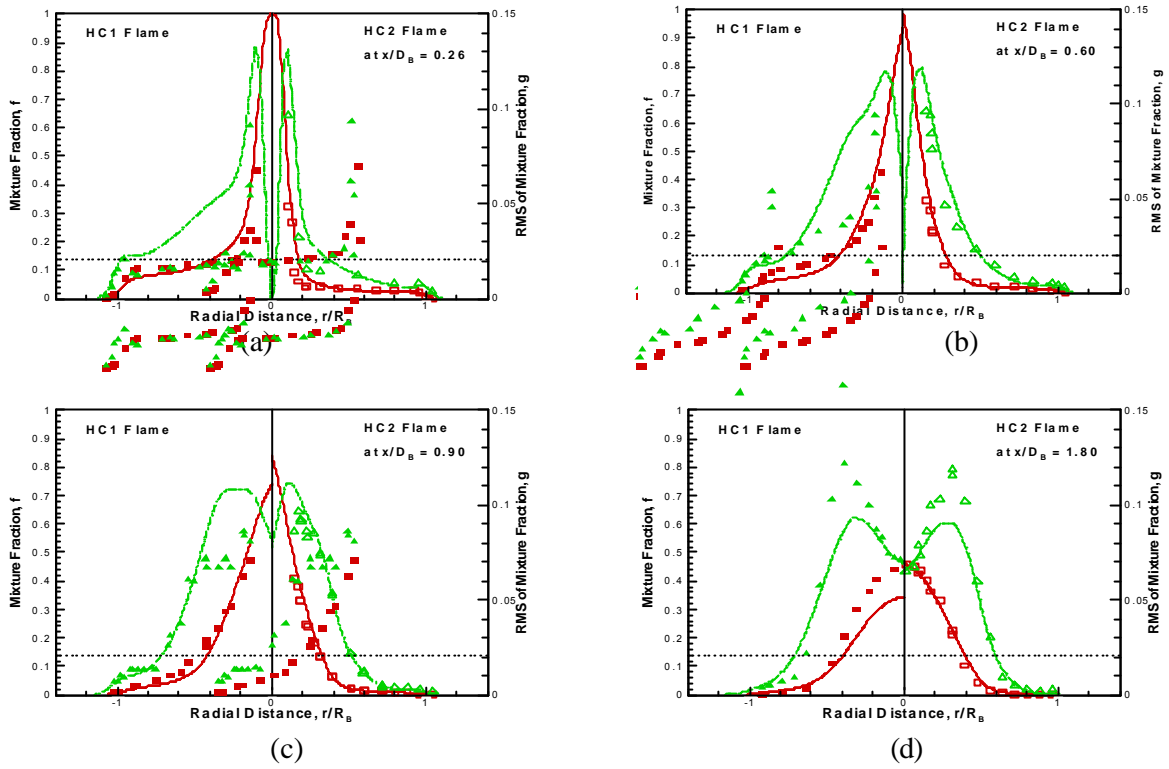


Fig 1. Radial profiles of mean (solid lines, squares) and rms (dashdot lines, triangles) of mixture fraction

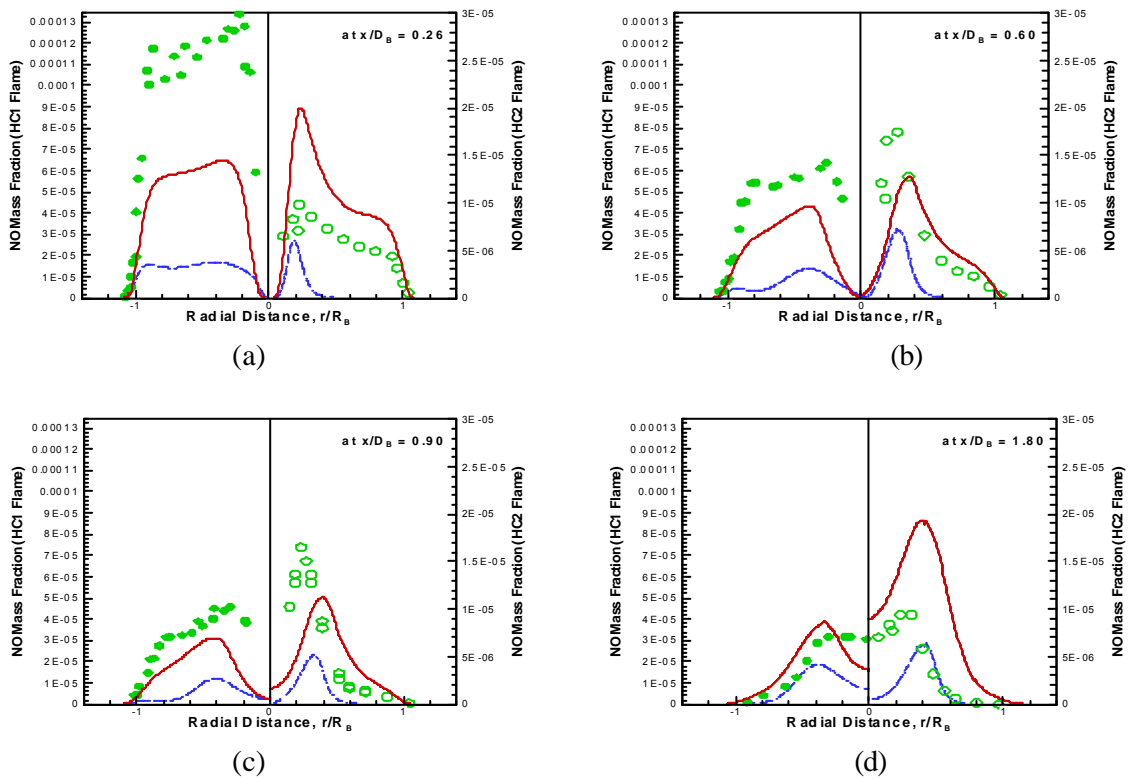


Fig 2. Radial profiles of mean mass fractions of NO; transient flamelet model (solid lines), steady flamelet model (dashdot lines), and experimental data (symbols)

Generating Turbulent Inflow conditions for Combustion LES

Markus Klein, Andreas Kempf, Johannes Janicka

Institute for Energy- and Powerplant Technology
Darmstadt Technical University
Petersenstr. 30
64287 Darmstadt, Germany

kleinm@hrzpub.tu-darmstadt.de
akempf@gmx.net

In recent years, more and more research groups focus on Direct Numerical Simulation (DNS) and Large Eddy Simulation (LES) to predict turbulent reacting flows. This promises a more comprehensive description of turbulent transport of momentum, energy and species. With LES/DNS, many classical problems of solving the Reynolds-averaged Navier-Stokes-Equations do not appear. However, setting accurate inflow-conditions becomes much more complicated with LES/DNS, unless the turbulent structures are entirely generated within the computational domain. In most cases, (unknown) turbulent structures will enter the domain and greatly influence the results of the simulations [1]. In contrast to RANS, it is not sufficient to set the first moments on the inflow. Instead, the velocity field on the inflow-plane must be modified in time to generate real turbulent structures, which yield the Reynolds-Stress-Tensor.

In this work, we will present a new approach to generate these fluctuating inflow conditions.

To model the turbulent structures entering the flow-field, a pseudo-turbulent velocity field is created. This field needs to have the same first and second moments, spectra or length and time-scales as the real flow. A moving slice of this field is copied to the inflow plane for each time step, setting appropriate fluctuating inflow-conditions.

Let us sketch the creation of the turbulent velocity field. First, a three dimensional fluctuating signal \mathcal{U}_i for $i = 1, 2, 3$ is created, corresponding to a prescribed spectrum or length-scale. Then, this signal is applied to construct the pseudo-turbulent velocity field u_i according to a procedure described below.

There are two distinct ways to generate the signal \mathcal{U}_i . The first one is to use inverse Fast-Fourier-Transformation (i-FFT) to map the spectrum to a signal (see [2]). However, i-FFT in three dimensions is complicated, inflexible and requires the turbulent spectrum to be known.

A more elegant method for signal-generation is filtering a noisy signal. This three dimensional field of random numbers does not have a turbulent spectrum or length-scale yet. However, by convolution with an appropriate filter, all modes can be filtered to result in the fluctuating field \mathcal{U}_i with an almost turbulent spectrum and the proper length-scale. Assuming that the two-point auto-correlation function is a Gauss-curve, a relation between the filter-coefficients and the length-scale was deduced.

We now have a simple tool to create a scalar field of fluctuations in three dimensions which only requires the proper length-scale as input. In contrast to the i-FFT approach, one may apply variable length-scales, for example to approximate walls.

Finally, we generate a turbulent velocity field from the scalar fields. First, the scalar fields \mathcal{U}_i are conditioned to a mean value of $\overline{\mathcal{U}_i} = 0$, and to cross-correlations of $\overline{\mathcal{U}_i \mathcal{U}_j} = \delta_{ij}$.

Then, the velocity field is constructed from the given Reynolds-Stress-Tensor R_{ij} according to the relation $u_i = \overline{u}_i + a_{ij} \mathcal{U}_j$. The coefficients of the tensor a_{ij} can be computed by a simple explicit relation by Lund et al. [3].

$$\begin{aligned} a_{11} &= \sqrt{R_{11}} & a_{12} &= 0 & a_{13} &= 0 \\ a_{21} &= \frac{R_{21}}{a_{11}} & a_{22} &= \sqrt{R_{22} - a_{21}^2} & a_{23} &= 0 \\ a_{31} &= \frac{R_{31}}{a_{11}} & a_{32} &= \frac{R_{32} - a_{21}a_{31}}{a_{22}} & a_{33} &= \sqrt{R_{33} - a_{31}^2 - a_{32}^2} \end{aligned}$$

Finally, we have a pseudo turbulent velocity field u_i which may be used to extract slices as inflow data for LES/DNS. It must be stressed that the three-dimensional pseudo-turbulent velocity field neither satisfies momentum-conservation nor continuity. It is only based on statistics, not on conservation properties. However, it generates some turbulence-like structures which are a great improvement over classical inflow-conditions like noise or laminar inflow.

Bibliography

1. M. Klein, A. Sadiki and J. Janicka. *Influence of the boundary conditions on the direct numerical simulation of a plane turbulent jet*. 2nd International Symposium on Turbulent Shear Flow Phenomena, Vol. I, pp. 401-406, Stockholm, Sweden, 2001
2. S. Lee, S.K. Lele, P. Moin, *Simulation of spatially evolving compressible turbulence and the application of Taylors hypothesis*. Physics of Fluids, A4, 1521-1530, 1992
3. T.S. Lund, X. Wu, D. Squires, *Generation of Turbulent Inflow Data for Spatially-Developing Boundary Layer Simulations*, Journal of Computational Physics, 140, 233-258, 1998
4. A. Kempf, M. Klein, R. Bauer, A. Sadiki, J. Janicka, *Towards the Generation of Turbulent Inflow conditions for Comustion LES*, Ninth International Conference on Combustion, Sorrento 2002, Paper No. 076, p. 27
5. M. Klein, A. Sadiki, J. Janicka, *A Digital Filter Based Generation of Inflow Data for Spatially Developing Direct Numerical or Large Eddy Simulations*, submitted to Journal of Computational Physics (2002). For preprints, contact kleinm@hrzpub.tu-darmstadt.de

LES RESULTS OF THE BLUFF-BODY STABILIZED FLOW

D. Krasinsky¹, D. Roekaerts¹, B. Naud¹, F. Nieuwstadt²

¹Thermal and Fluids Sciences Section, Delft University of Technology, The Netherlands
dkr@ws.tn.tudelft.nl, dirkr@ws.tn.tudelft.nl

²Laboratory for Aero and Hydrodynamics, Delft University of Technology, The Netherlands

Numerical simulation of turbulent combustion in the bluff-body stabilized non-premixed flames is seen as a challenging problem that has, on the one hand, a sufficiently high level of complexity to be relevant for industrial users, and, on the other hand, has simple geometry and its Re number is not very large. This problem is the subject of investigation for the TNF Workshop Series [1] and the detailed experimental datasets [2, 3] are available for the validation of numerical results. As it has been generally concluded during the previous Workshop Series, the bluff-body stabilized jet simulations based on the steady-RANS approach have so far been lacking ability to provide a “desirable” level of agreement with experiments on the flowfield and turbulent characteristics, mainly due to essentially oscillating nature of the flow. Therefore the use of Large-Eddy-Simulation (LES) approach has been recommended in this case and is seen as a necessary step towards more adequate modelling of the flowfield dynamics as well as the compositional structure.

To realize the potential of LES for combustion problems, the essentially non-linear effect of chemical reactions should be modelled adequately in the context of LES. For this, the novel LES-FMDF modelling approach based on hybrid Eulerian/Lagrangian description has been recently developed (e.g. in [4]). In this approach the unresolved mixing and reaction phenomena are described by the Filtered Mass Density Function (FMDF) which is essentially the PDF of subgrid-scale scalar variables. The thermochemical scalars are obtained from the solution of the FMDF transport equation via the Lagrangian (Monte Carlo) scheme. This Lagrangian solution is coupled with the pressure-velocity field resolved by LES in Eulerian framework. The primary goals of the ongoing project work are to validate this LES-FMDF technique on the test case of the bluff-body stabilized jet diffusion flame and to assess the applicability of this method in engineering CFD.

As a first step, LES of a non-reacting bluff-body stabilized jet air flow in isothermal incompressible formulation (NRBB case, see [3]) has been performed and some of these results are shown in Fig. 1–3. The LES/DNS parallelized code which has originally been developed for the DNS of turbulent jets by B.J.Boersma et.al. [5] is used for simulation runs on multi-processor PC cluster. The bulk inlet velocity values are equal to 61 m/s for the central jet and 20 m/s for the coflow, thus the Re number based on the bluff-body diameter $D_{bb}=50$ mm and the central jet bulk velocity is estimated as $6 \cdot 10^4$. The inlet velocity profiles taken as the polynomial fits of the experimental data [3] will be used in the next simulations. Statistical averages (in Fig. 1–3) were obtained from the subset of 128 instantaneous samples (taken from the set of 32000 iterations processed after the flow has been developed). A typical $160 \times 100 \times 24$ grid was used, with this the computational domain is about $5.5 D_{bb}$ in length (axial coordinate) and about $2.4 D_{bb}$ in width (i.e. the limit in radial coordinate is $1.2 D_{bb}=60$ mm).

From comparison of the mean axial velocity profile along the centerline with experimental data [3, case NRBB] a tuning of the subgrid-scale Smagorinsky eddy viscosity model has been done, with the choice of Smagorinsky constant as $C_s=0.2$. A comparison of mean $\langle U \rangle$ and r.m.s. V' profiles in radial direction taken at the axial cross-planes of $0.4 D_{bb}$ and $1.2 D_{bb}$ with the measured data [3], presented in Fig.1 and Fig.2, demonstrates a reasonable agreement, though it is not perfect. However for the results further downstreams the disagreement becomes more pronounced. Therefore the results will be improved in the nearest future: by using the realistic inlet velocity profiles (instead of the flat ones); by grid refinement towards the central jet and towards the bluff-body face; by increasing substantially the number of instantaneous samples taken for averaging.

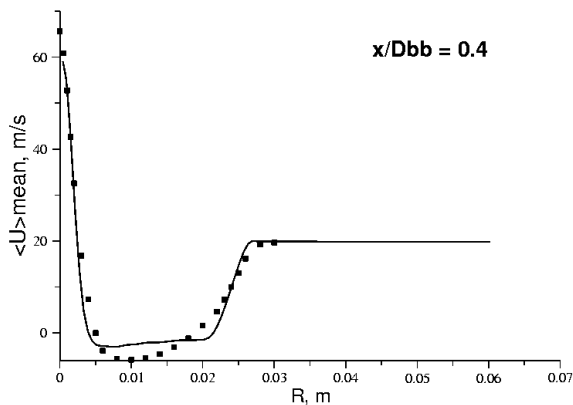


Fig. 1. Axial mean velocity profile vs radial coordinate at $x/D_{bb}=0.4$, m/s

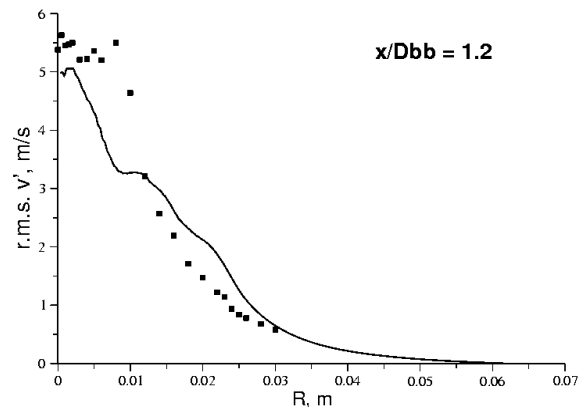


Fig. 2. Radial velocity fluctuations r.m.s. profile vs radial coordinate at $x/D_{bb}=1.2$, m/s

The computed instantaneous flowfield structure observed in LES shows that the central jet behaviour is inherently unstable, with the jet flowing quasi-stationary to and fro through the axis and the jet core length fluctuating. One of phenomena influencing this behaviour is that the tip of the jet undergoes interaction with the backward flow from the recirculation vortex. This observation is in line with a picture in Fig. 3 showing a typical distribution of the velocity fluctuations, with their maximum intensity located at the tip of the central jet.

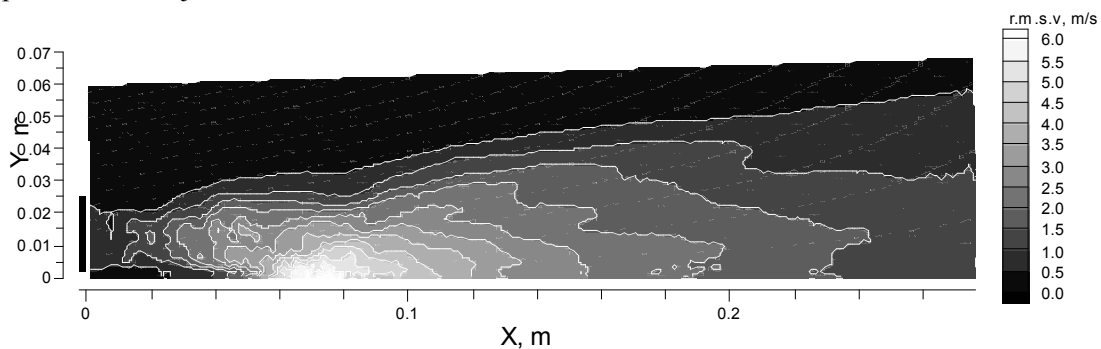


Fig. 3. Grayscale contours of the radial velocity fluctuations r.m.s., m/s

In the ongoing work, the LES-FMDF procedure [4] is under implementation by coupling the present LES/DNS code [5] with an extension of the Lagrangian PDF code developed at the Thermal and Fluids Sciences Section, TU Delft. An extended model of resolved scalar transport will be considered. A reduced chemical model will be used. Further development and fine-tuning of the method will be carried out on the basis of test simulations of the bluff-body stabilized reacting jet.

Acknowledgements. The financial support of this work by the Dutch Technology Foundation STW (project DTN 4852) is gratefully acknowledged.

- [1] <http://www.ca.sandia.gov/tdf/Workshop.html>
- [2] B.B.Dally, A.R.Masri, R.S.Barlow, G.J.Fiechtner Instantaneous and Mean Compositional Structure of Bluff-Body Stabilized Nonpremixed Flames. *Combustion and Flame* 114: 119-148 (1998).
- [3] <http://www.mech.eng.usyd.edu.au/thermofluids/tnf6/tnf6bb.htm>
- [4] F.A.Jaberi, P.J.Colucci, S.James, P.Givi and S.B.Pope Filtered mass density function for large-eddy simulation of turbulent reacting flows. *J.Fluid Mech.*, v.401, pp.85-121 (1999).
- [5] B.J.Boersma, G.Brethouwer, and F.T.M.Nieuwstadt A numerical investigation on the effect of the inflow conditions on the self-similar region of a round jet, *Phys.Fluids*, 10, 899-909 (1998).

The effect of the grid and turbulence model on the simulation of a bluff-body flame with the Reynolds Stress Model

Guoxiu Li, Bertrand Naud, and Dirk Roekaerts
Thermal and Fluids Sciences, Delft University of Technology
P.O.Box 5046, 2600 GA Delft, The Netherlands
E-mail:li@ws.tn.tudelft.nl

A bluff-body flame described in Refs. [1,2] is numerically simulated. The problem is characterized by: the diameter of the central fuel nozzle (3.6 mm), the bluff-body diameter (50 mm), the fuel composition ($\text{CH}_4/\text{H}_2 = 1/1$, by volume) and the bulk velocity (fuel jet 118 m/s, co-flow velocity 40 m/s.) In the resulting flow field, the central fuel jet is separated from the co-flowing air stream, by the hot recirculation zone in the wake of the bluff-body. Results for this type of flame presented at the previous workshop (TNF5 [3]) illustrate that factors influencing the quality of the prediction of the flow fields deserve special attention. This poster reports on a study of such factors in the frame of Reynolds stress second-moment closure combined with equilibrium chemistry and a PDF for the mixture fraction. Both assumed beta PDF and hybrid finite volume / Monte Carlo PDF methods have been used. To model pressure-strain correlation, the Isotropization-of-Production (IP) model ($C_1 = 1.8$, $C_2 = 0.6$) and the Rotta model ($C_1 = 4.15$, $C_2 = 0$) have been used, respectively corresponding to a generalised Langevin model and a simplified Langevin model for particle velocities in the Monte Carlo method. The constant $C_{\epsilon 1}$ in the ϵ -equation is set to the non-standard value 0.6.

A 2D simulation with the symmetry axis as boundary is performed. The width of the solution domain is 750 mm in the axial direction and 150 mm in the radial direction. The grid is stretched in both directions. The inflow boundary conditions are as follows: the mean flow velocity of the co-flow and the profiles of Reynolds stresses uu and vv of the center jet and co-flow are obtained and calculated from the experimental data. The U -velocity in the central jet region, the shear stress uv and the dissipation rate ϵ are calculated according to the formulas provided in [4].

Firstly, a grid refinement study has been performed using the assumed shape PDF and the IP model. Radial profiles of the mean axial velocity are shown in Figure 1. Close to the burner exit, there is a little difference between the results on the different grids, but that there is a strong grid dependence further downstream. The best agreement with experimental data is obtained on the finest grid but grid independence is not demonstrated. Secondly, also using the assumed shape PDF, the predictions of the two Reynolds stress closures on the finest grid are compared. In Figures 2 and 3 it is shown that for mean and rms axial velocity, the difference between the predictions of the two models is rather small. Thirdly the predictions of the hybrid finite volume / Monte Carlo PDF method and the assumed PDF method using equilibrium chemistry were shown to hardly differ from each other provided a consistent choice of Langevin model and RSM model is made. Calculations using detailed chemistry are ongoing.

References

- [1] B.B. Dally, D.F. Fletcher, and A.R.Masri, Flow and mixing fields of turbulent bluff-body jets and flames. *Combust. Theory Modeling* 2(1998) 193-219.
- [2] <http://www.mech.eng.usyd.edu.au/research/energy/resources.html>
- [3] <http://www.ca.sandia.gov/Workshop.html>, Proceedings TNF5
- [4] P. Jenny, S.B. Pope, M. Muradoglu, and D.A.Cauchy, PDF simulations of a bluff-body stabilized flow, *J. Comp. Phys.* 169, 1 (2001)

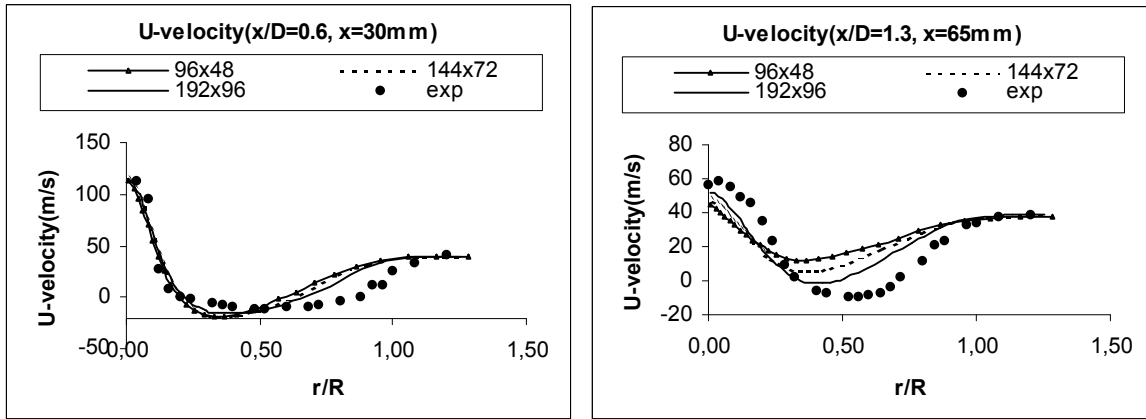


Figure 1 Radial profiles of mean axial velocity U . Comparison of the simulation results with the IP model for three different grids.

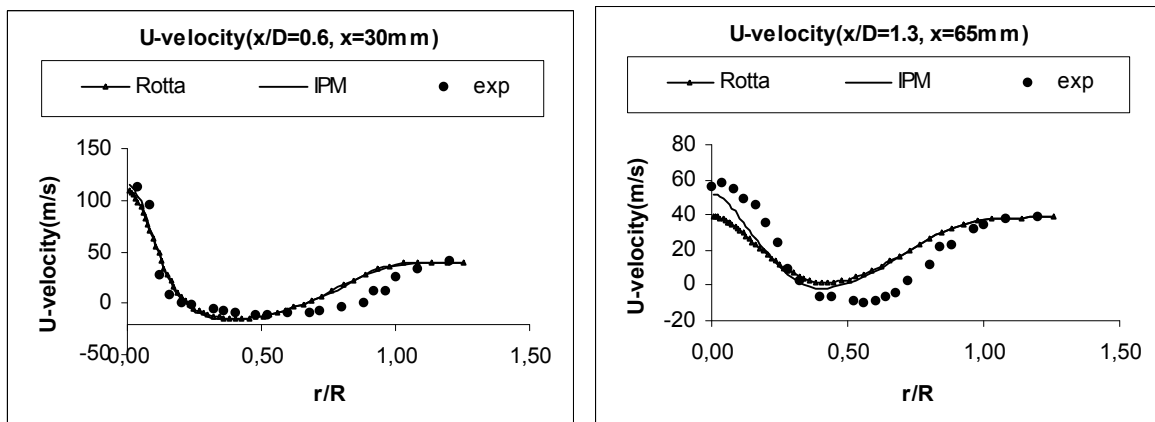


Figure 2 Radial profiles of the mean axial velocity U . Comparison of the simulation results with the Rotta model and with the IP model (192x96 grid)

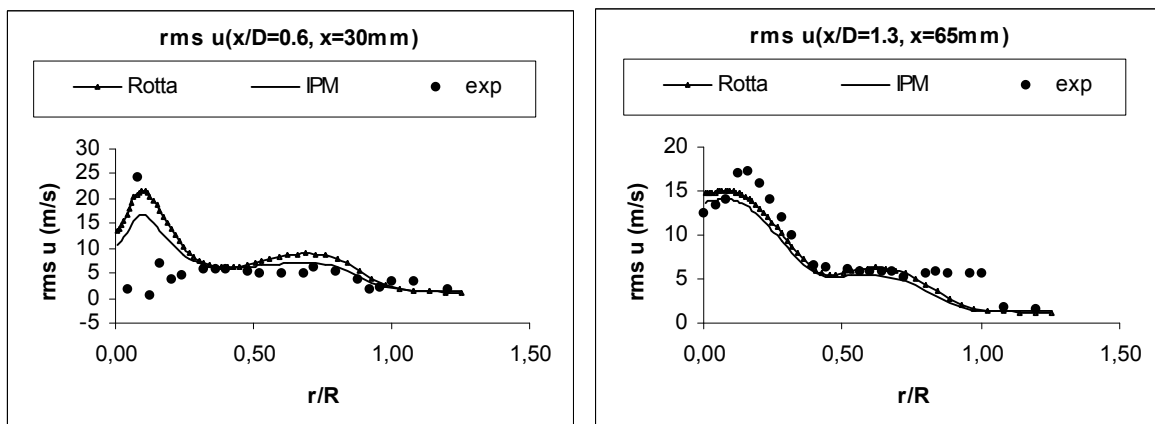


Figure 3 Radial profiles of the rms of axial velocity u . Comparison of the simulation results with the Rotta model and with the IP model (192x96 grid)

Acknowledgements

B. Naud is supported by the Foundation for Fundamental Research on Matter (FOM)

JPDF/ARM Calculations of Bluff-Body Stabilized Flames

Kai Liu

Sibley School of Mechanical and Aerospace Engineering
Cornell University, Ithaca, NY 14853, USA

Email: kl47@cornell.edu

Metin Muradoglu

Department of Mechanical Engineering, Koc Univ. TURKEY

Qing Tang, Stephen B. Pope and David A. Caughey

Sibley School of Mechanical and Aerospace Engineering
Cornell University, Ithaca, NY 14853, USA

ABSTRACT

The probability density function (PDF) method has been demonstrated to be a successful modelling approach for turbulence combustion [7]. The reason is the exact treatment of the chemical reaction terms in the PDF method [5]. The velocity-turbulence frequency-composition Joint PDF (JPDF) method provides the additional advantage that turbulent convection is also in closed form. At the same time, time scale information is provided through modelling the turbulence frequency [6].

Whether a method can be applied to practical computations depends on the efficiency of the numerical algorithm. Recently, a consistent hybrid finite volume (FV)/Monte Carlo particle method has been successfully developed [4]. Compared to the previous stand-alone particle method, the complicated pressure algorithm is avoided and the bias error is small compared with other numerical errors. The benefit of small bias error is that the number of particles per cell can be decreased dramatically and hence numerical efficiency can be improved. One important feature of the present hybrid algorithm is that it is fully consistent at the equation level, and consistency at the numerical level is achieved through correction algorithms [3].

The hybrid FV/particle method has been implemented in the code HYB2D. With simple flamelet chemistry, it has been applied to several non-premixed flames [4, 2]. Generally, the results are in good agreement with corresponding experimental data.

In the present work, we implement detailed chemistry by ISAT with ARM2 and apply the methodology to bluff body stabilized flames, i.e. HM1 etc. Numerical accuracy and sensitivity to inlet boundary conditions are investigated using the simple flamelet chemistry model. The grid size and the number of particles per cell are determined for a 5% error tolerance. Finally, the advanced models of JPDF, namely LIPM for velocity, JPM for turbulence frequency, and EMST for mixing combined with detailed chemistry described by ISAT with ARM2 are applied to HM1 flame. The model constants adopted depend on previous works based on simple flamelet chemistry.

The results will be presented in the poster include a detailed comparison of calculations with the available experimental data [1] on mean and conditional profiles and distributions of major and minor species.

References

- [1] A. R. Masri. <http://www.mesh.eng.usyd.edu.au/research/energy/#data>. The University of Sydney and The combustion Research Facility, Sandia National Laboratories,.
- [2] M. Muradoglu, K. Liu, and S. B. Pope. Pdf modelling of a bluff-body stabilized turbulent flame. *Combust. Flame*, 2002. To be pulished.
- [3] M. Muradoglu, S. B. Pope, and D. A. Caughey. The hybrid method for the pdf equations of turbulent reactive flows: Consistency conditions and correction algorithms. *J. Comput. Phys.*, 172:841, 2001.
- [4] Metin Muradoglu. *A consistent hybrid finite-volume/particle method for the PDF equations of turbulent reactive flows*. PhD thesis, Cornell University, 2000.
- [5] S. B. Pope. PDF methods for turbulent reactive flows. *Prog. Energy Combust. Sci.*, 11:119, 1985.
- [6] S. B. Pope. Lagrangian PDF methods for turbulent flows. *Ann. Rev. Fluid Mech.*, 26:23, 1994.
- [7] J. Xu and S. B. Pope. PDF calculations of turbulent nonpremixed flames with local extinction. *Combust. Flame*, 123:281–307, 2000.

Experimental Analysis of Swirling Flames in a Gas Turbine Model Combustor

W. Meier, P. Weigand, O. Keck, X. Duan, B. Lehmann*, W. Stricker, M. Aigner

Institut für Verbrennungstechnik

*Institut für Antriebstechnik

Deutsches Zentrum für Luft- und Raumfahrt (DLR), Pfaffenwaldring 38, D-70569 Stuttgart

E-mail: wolfgang.meier@dlr.de

A lab-scale gas turbine combustor for confined swirling CH₄/air diffusion flames is presented. Swirling air is injected through a central contoured nozzle (i.d. 15 mm) and an annular nozzle (i.d. 17 mm, o.d. 25 mm, contoured to o.d. 40 mm) and CH₄ is supplied through 72 channels (0.5 mm x 0.5 mm) forming a ring between the air nozzles (see Fig.1). The housing consists of 4 quartz windows (height 117 mm, width 80 mm) allowing almost complete optical access and a top with a central tube as exhaust. Three flames have been chosen as “standard” configurations: one near the lean extinction limit (7.4 kW thermal power, equivalence ratio $\Phi=0.53$), the second as a stable reference case (10 kW, $\Phi=0.73$), and a third with increased thermal power (35 kW, $\Phi=0.75$). The aims of the investigations were a detailed understanding of the flame behavior, especially of instabilities near the lean extinction limit and of thermoacoustic oscillations, and the generation of a data base for the verification of numerical simulations.

The flow field has been characterized by laser Doppler velocimetry yielding mean and rms fluctuations of all 3 velocity components and the Reynolds stress tensor components. The flame structures have been visualized by qualitative planar laser induced fluorescence (PLIF) of OH, CH, and H₂CO. These images characterize the turbulent structures, areas of hot exhaust gas (OH) and fuel rich mixtures (H₂CO), and the shape of the reaction zones and regions of heat release (CH). Finally, the Raman measurements which are currently performed yield the PDFs of temperature, mixture fraction, and major species concentrations and an insight into turbulence-chemistry interaction.

The measurements showed that the flame is stabilized by a strong inner recirculation zone of hot combustion products which reaches down to the nozzle exit and even into the central nozzle for air supply. Mixing is extremely fast: at the lowest position for the Raman measurements ($h=5$ mm above the nozzles) the highest mean CH₄ concentration is 8%. In the near field ($h\leq 20$ mm), the thermochemical state of the flame is dominated by a large variation of reaction progress from non-reacted, via partially reacted to completely reacted. Further downstream, the state of the flame is close to adiabatic equilibrium. Heat loss due to thermal radiation or wall contact seems to be of minor importance. The single-pulse exposures of CH LIF distributions show that the reaction zones are thin vortical structures throughout the flame, whereas the OH and H₂CO distributions are broad. Single-pulse images are dominated by the turbulent fluctuations, but averaged images exhibit a pronounced dependence of the structure on the flame parameters, e.g., the mean CH distributions form a v-shaped conical region with different angles of the cone for the flames investigated.

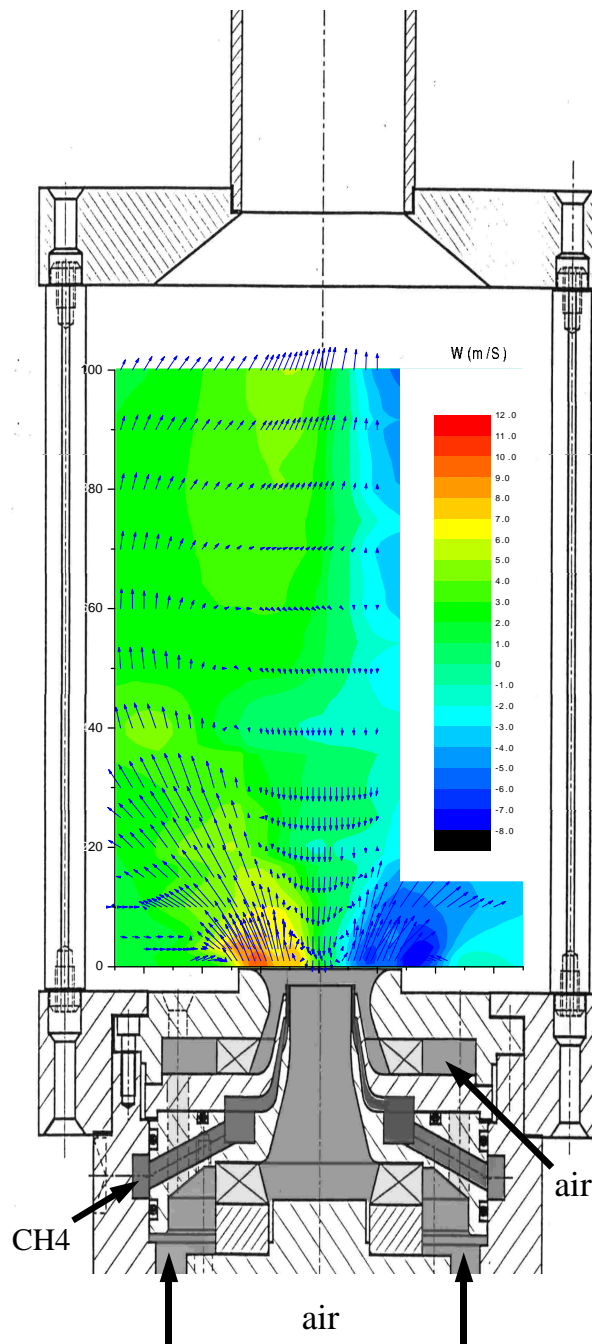


Fig.1: Schematic drawing of the burner and combustion chamber. The mean distribution of the velocities of the reference flame (10 kW) is indicated by the arrows and different shades of grey.

Influence of Computational Aspects on Results for Flame D

Bart Merci^{*,**}, Dirk Roekaerts^{***} and Erik Dick^{*}

^{*} Ghent University, Dept. of Flow, Heat and Combustion Mechs., Belgium. E-mail: Bart.Merci@rug.ac.be

^{**} Postdoctoral Fellow of the Fund for Scientific Research - Flanders (Belgium) (F.W.O.-Vlaanderen)

^{***} Delft University of Technology, Faculty of Applied Sciences, The Netherlands

The influence of computational aspects are quantitatively investigated for 'Sandia Flame D'[1]. The standard $k - \varepsilon$ model is used (with $c_{\varepsilon 2} = 1.8$). For the turbulence-chemistry interaction, a pre-assumed β -PDF is used, with the standard transport equations for the mean mixture fraction and its variance. As chemistry model, a simplified version of the constrained equilibrium model is used.

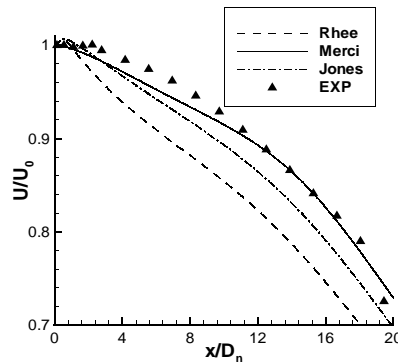
1. Inlet Boundary Conditions

Profiles are imposed from experimental data of Darmstadt University of Technology[2]. The dissipation rate ε , crucial for the flame structure, cannot be measured, so that there is some 'freedom'. It is very important to impose a reasonable inlet ε profile. Two methods are acceptable[3]. In the first method, the measured profiles for the mean velocity components and turbulent kinetic energy are fixed, and the ε transport equation is solved, under the assumption of fully developed flow conditions (axial derivatives set to zero). The additional computation is very fast, since the equation only has to be solved on one grid line. The advantages are that the method can easily be applied to any inlet geometry and that an ε profile is obtained which is consistent with the $k - \varepsilon$ model, applied in the actual simulation. It is very important that **not** both transport equations (for k and ε) are solved (Rhee's method[4]), since otherwise the obtained ε profile is extremely sensitive to details in the velocity profile.

The alternative method is to determine ε from a mixing length, as suggested by Jones[5]: $\varepsilon = \frac{c_{\mu}^{3/4} k^{3/2}}{l_m}$, where the measured profile for k is introduced. The problem is shifted to the determination of the mixing length l_m . In [3], the following expression is obtained:

$$\frac{l_m}{D_h} = (1 - \exp(-2.10^6(y/D_h)^3))(1/15 - (1/2 - y/D_h)^4), \quad (1)$$

where y is the normal distance from the nearest solid boundary and D_h is the hydraulic diameter.



ε on mean axial velocity.

2. Outlet Boundary Conditions

The outlet boundary conditions are straightforward (atmospheric pressure and zero axial derivatives for all other quantities). The axial position of the outlet boundary does not affect the results upstream (not shown).

3. Numerical Scheme

The accuracy of the numerical scheme is very important. Comparisons are made between a first order upwind scheme for the convective fluxes and second order accurate upwinding[6]. When a first order accurate scheme is used for the convective fluxes, the leading order truncation error is equivalent to a viscous term, with 'numerical' viscosity $\mu_{num} = \frac{1}{2}\rho U h$, where h is the grid spacing[7]. In table 1 and fig. 2, its influence is demonstrated.

Model	first order	second order	Exp.
x_{st}/D_n	53.2	49.7	47 ± 2.3

Table 1: Position of stoichiometric conditions at the axis.

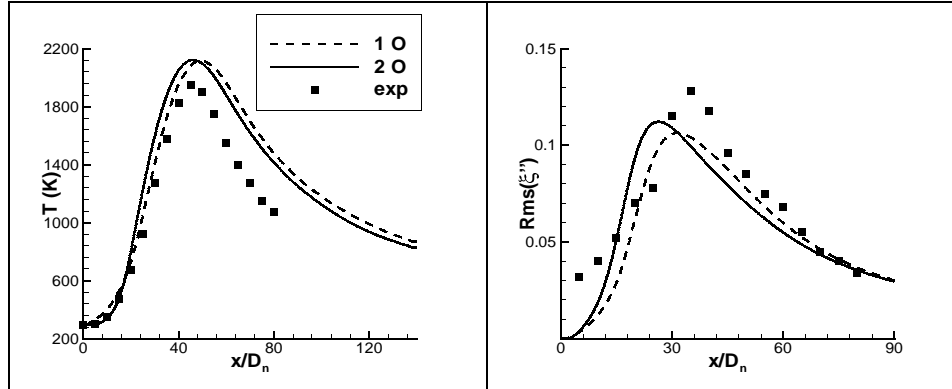


Figure 2: Axial profiles of mean temperature and the rms value of the mixture fraction fluctuations.

4. Grid Refinement

Results have been obtained on a refined grid (225×177 points). In fig. 3 it is illustrated that only the results with the second order accurate scheme are grid independent. This can hardly be seen in the mean velocity (or mixture fraction), so that it is very dangerous to claim grid independence, based on those quantities!

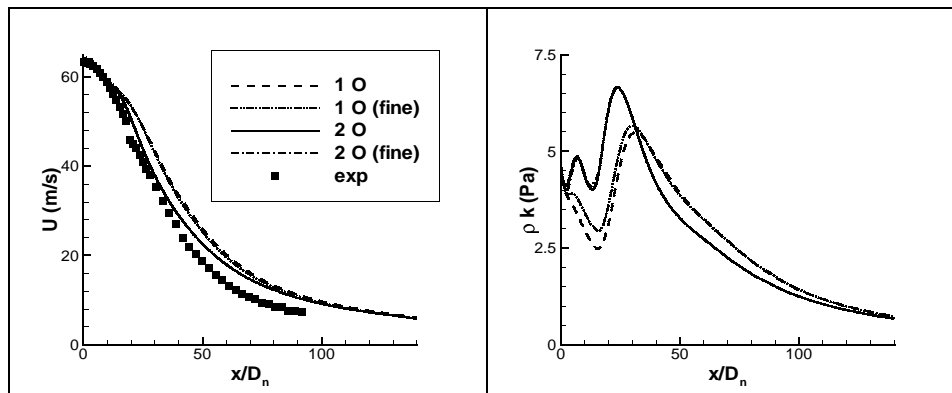


Figure 3: Comparison of axial profiles for the basic grid (113×89 points) and a refined grid (225×177 points).

References

- [1] Barlow, R.S., and Frank, J.H., *Twenty-Seventh Symposium (International) on Combustion*, The Combustion Institute, Pittsburgh, 1998, p. 1087.
- [2] <http://www.ca.sandia.gov/tdf/Workshop/Submodels.html>.
- [3] Merci, B., Dick, E., Vierendeels, J., and De Langhe, C., *Int. J. Num. Methods Heat Fluid Flow* 12(1):65 (2002).
- [4] Rhee, G.H., and Sung, H.J., *AIAA J.*, 38:545 (2000).
- [5] Jones, W.P., in *Turbulent Reacting Flows* (P.A. Libby and F.A. Williams, Eds.), Academic Press, 1994, p. 309.
- [6] Vierendeels, J., Merci, B., and Dick, E., *AIAA J.*, 39(12):2278 (2001).
- [7] Pope, S.B., *Turbulent Flows*, Cambridge University Press, 2000.

Effects of Turbulence on Flame Chemistry

*Yasuhiro Mizobuchi¹, Junji Shinjo¹, Shigeru Tachibana¹, Satoru Ogawa¹ and Tadao Takeno²

¹National Aerospace Laboratory of Japan

²Meijo University

*Email: mizo@nal.go.jp

Lifted flame by turbulent fuel jet is a typical non-premixed flame configuration and the observation of the various complicated flame behaviors in it will lead to finding and understanding of various flame structures. The authors have been simulating a turbulent hydrogen jet lifted flame by DNS approach with detailed kinetics and rigorous transport properties¹. The nozzle diameter is 2mm, the hydrogen jet velocity is 680m/sec and the Reynolds number based on the diameter is 13600². The analysis of the DNS data reveals some interesting features of the lifted flame, and in this study, the turbulence effects on the flame will be mainly discussed.

The analysis based on Flame Index³ shows that the lifted flame consists of three flame elements; leading edge flame, inner rich premixed flame and outer diffusion flame islands as shown in Fig.1. The leading edge flame, which is composed of lean premixed, diffusion and rich premixed flames, has a strongly three-dimensional structure but is rather stable. The outer diffusion flame islands flow slowly downstream outside the turbulent jet, and the behavior is quite calm. The local flame structures in both flames are similar to those of one-dimensional laminar flames. On the other hand, the inner rich premixed flame is vigorously turbulent affected by the strong instability of the hydrogen jet of high Reynolds number.

One of the interesting phenomena observed in the inner rich premixed flame is the deviation of the heat release layer from the hydrogen consumption layer. Figures 2 a) and b) show the instantaneous distributions of hydrogen consumption rate and heat release rate, respectively, in a cutting plane. The deviation is remarkable in the upper half of the figures where the hydrogen consumption layers are rather continuous while the succeeding heat release layers are rather disrupted. When we use detailed kinetics and rigorous transport properties, there can be a displacement between the two layers even in laminar normal flames, because major elementary reactions of hydrogen consumption and heat release are different and the thermal diffusivity and molecular diffusivity are different. Nevertheless, in this inner turbulent premixed flame, the displacement is strongly distributed and modified. Hence, the inner turbulent premixed flame is not a normal flame to which the laminar flamelet concept⁴ can be applied.

Figures 3 b) and c) show the internal structure of the inner premixed flame along the normal vector indicated in a). The profiles of thermochemical quantities and chemical species are quite different from those of normal premixed flame, which tells that the internal chemistry is largely disturbed and modified.

The time scale analysis is conducted to investigate the internal structure modification of the inner turbulent rich premixed flame. In

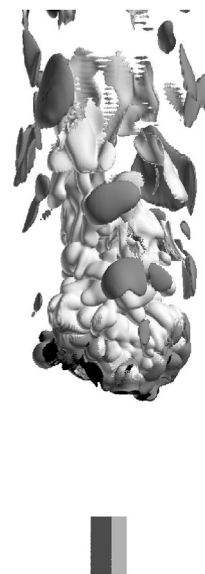


Fig.1 Structure of a hydrogen/air jet lifted flame. Instantaneous iso-surfaces of hydrogen consumption rate at 10^4 mol/m³/sec are drawn. The surface color corresponds to the flame configuration, white: rich premixed flame, black: lean premixed flame, gray: diffusion flame.

the turbulent premixed flames, the time scale of turbulent convection τ_f is small and the Fourier analysis of the mixture fraction time histories shows that τ_f is from 0.02 to 0.05 msec in the region of large deviation. The reaction time scale in the flame can be defined as $\tau_r = \Delta x / S_L$, where Δx is the distance between the peak locations of hydrogen consumption rate and heat release rate in one-dimensional normal premixed flame and S_L is the corresponding laminar burning velocity. This time scale can be estimated from the local mixture fraction in the premixed flame and one-dimensional premixed flame computation. Around the stoichiometric condition τ_r is the smallest and it becomes larger abruptly as the mixture becomes rich or lean. In the regions where the deviation is remarkable, the mixture is very rich and the mixture fraction is from 0.08 to 0.12, which corresponds to τ_r from 0.05 to 0.15 msec. In the large deviation region, the two time scales are of the same order, and that τ_f is smaller than τ_r . Hence, the kinetics in the reaction layers can be easily disturbed by turbulent convection and the deviation is produced.

In vigorously turbulent flames, where the time scales of turbulent convection and combustion reaction are of the same order, the internal flame chemistry is disturbed and modified by the turbulence and the heat release layers are deviated from the fuel consumption layers. The laminar flamelet concept cannot be applied to such turbulent flames.

References

1. Mizobuchi, Y. et al, *IUTAM Symp. on Turbulent Mixing and Combustion*, to be published, 2001.
2. Cheng, T. S. et al, *Combust. Flame*, 91:323-345 (1992).
3. Yamashita, H. et al, *Proc. Combust. Inst.* 26: 27-34 (1996).
4. Peters, N., *Proc. Combust. Inst.* 21:1231-1250 (1986).

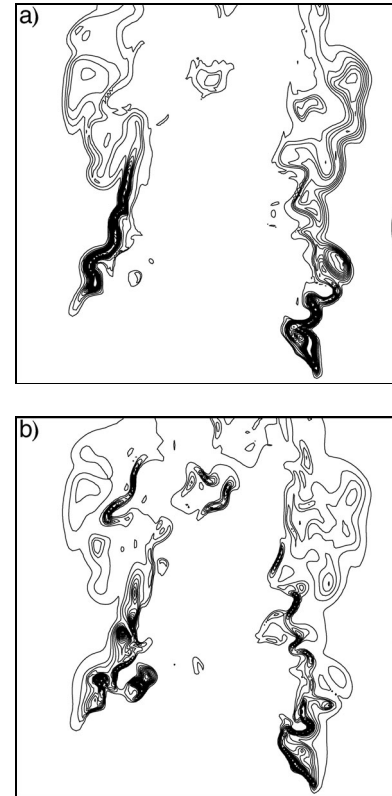


Fig.2 Deviation of heat release layer from hydrogen consumption layer, a): hydrogen consumption rate, b): heat release rate.

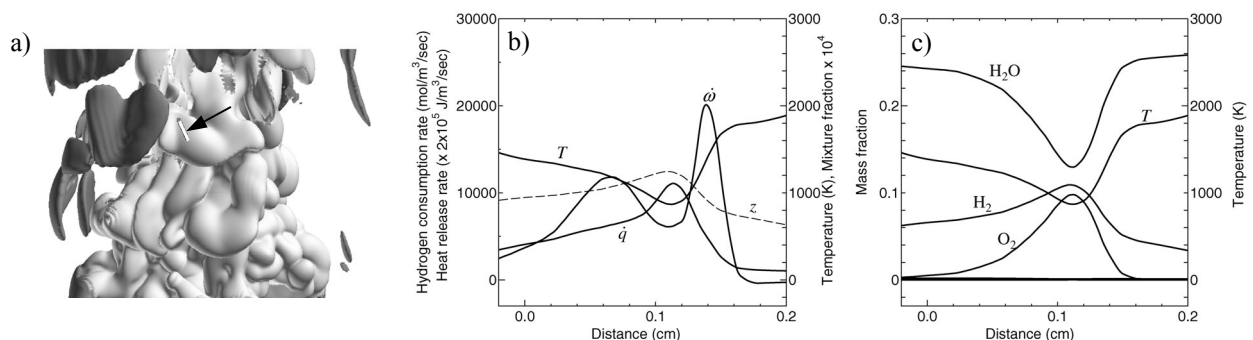


Fig.3 Local structure of an inner turbulent rich premixed flame. The profiles of T : Temperature, z : mixture fraction, $\dot{\omega}$: hydrogen consumption rate, \dot{q} : heat release rate are shown in b), and major chemical species in c), along the normal vector indicated in a). The axis direction is from inside to outside.

PDF Modeling of a Bluff-Body Stabilized Turbulent Flame

M. Muradoglu¹

Department of Mechanical Engineering, Koc Univ., TURKEY

K. Liu² and **S.B. Pope**²

Sibley School of Mechanical and Aerospace Engineering
Cornell University, Ithaca, NY 14853, U.S.A.

The probability density function (PDF) method has proven to be among the most promising approaches for accurate modeling of turbulent reacting flows of practical importance[2, 7]. Compared to conventional turbulence models, the PDF method offers the unique advantages of being able to take into account the important processes of convection and non-linear reaction in closed form[6]. Hence the effects of turbulent fluctuations on chemical reactions are treated exactly, and the gradient diffusion assumption is avoided. Of these advantages, the exact treatment of finite-rate non-linear chemistry makes the PDF method particularly attractive for simulations of complex turbulent reacting flows.

As for any turbulence model, an efficient numerical solution algorithm is of essential importance to apply the PDF method to flow problems of practical interest. Significant progress has been recently made in this direction by the development of the consistent hybrid finite volume (FV)/particle-based Monte Carlo method[3, 4]. The hybrid method combines the best features of the FV and particle-based Monte Carlo methods in order to efficiently solve the PDF model equations. The method is completely consistent at the level of governing equations and the full consistency at the numerical solution level is enforced by using efficient correction algorithms[4]. It has been shown that the consistent hybrid method is computationally more efficient than the best available alternative solution technique by a factor of an order of magnitude or more[4, 2]. The numerical efficiency of the hybrid algorithm is further improved by the recent development of a local time stepping algorithm that has been shown to accelerate the global convergence of the hybrid method as much as by a factor of an order of magnitude depending on grid stretching[5]. Combined with the local time stepping algorithm, the consistent hybrid method thus makes the PDF methodology a feasible design tool for the practical applications in engineering or elsewhere.

The primary purpose of the present work is to demonstrate the performance of the velocity-turbulent frequency-compositions joint PDF method combined with the hybrid FV/particle solution algorithm in predicting the properties of the bluff-body stabilized turbulent flame studied experimentally first by Dally et al.[1] and recently by Kalt and Masri[1]. Besides its practical importance, the bluff-body flame studied here provides an excellent but challenging test case for turbulence and chemistry models as well as for numerical solution algorithms for studying turbulence and chemistry interactions in turbulent recirculating flows due to its simple and well defined initial and boundary conditions, and its ability to maintain the flame stabilization for a wide range of inlet flow conditions with a complex recirculation zone.

The statistical stationarity is shown and the performance of the PDF method is assessed by comparing the mean fields with the available experimental data. The effects of the model constants $C_{\omega 1}$ in the turbulence frequency model and C_{ϕ} in the mixing model on the numerical

¹E-mail: mmuradoglu@ku.edu.tr

²E-mail: {kliu,pope}@mae.cornell.edu

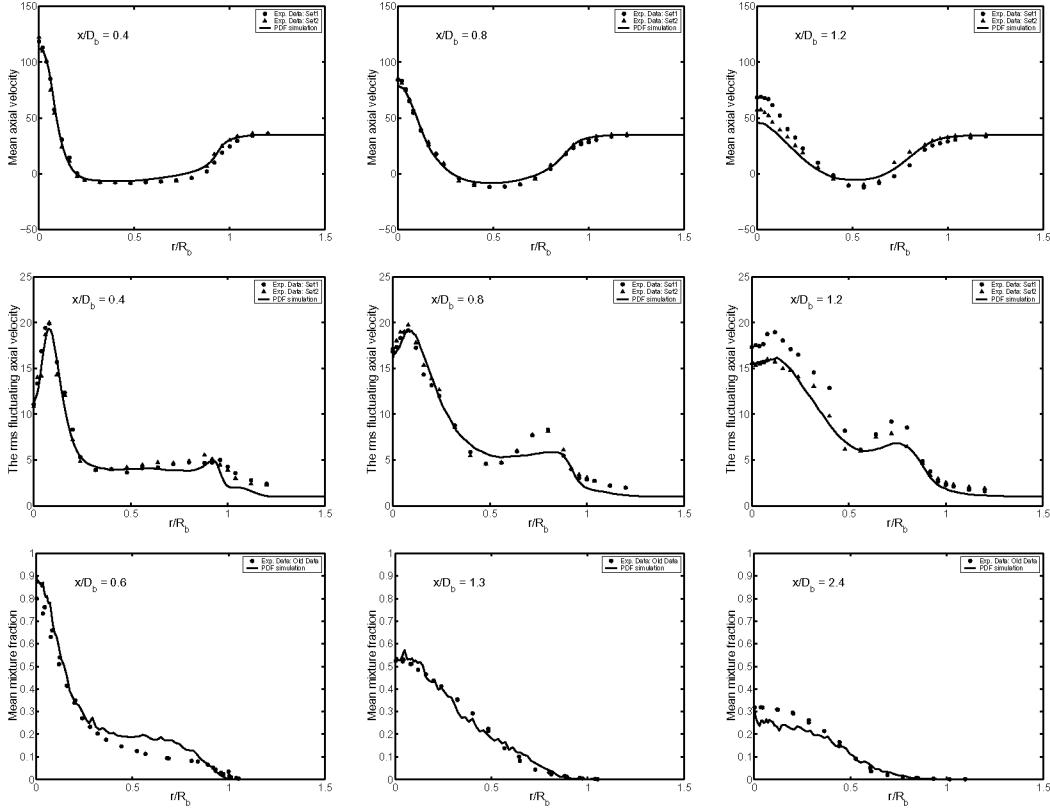


Figure 1: Mean axial velocity (\bar{U}) (top figures) and the rms fluctuating axial velocity (u') (middle figures) profiles at the axial locations $0.4D_b$, $0.8D_b$, $1.2D_b$ and mean mixture fraction ($\bar{\xi}$) (bottom figures) profiles at the axial locations $0.6D_b$, $1.3D_b$, and $2.4D_b$. Symbols denote the experimental data and solid lines denote the PDF simulations. Grid: $176 \times 136, N_{pc} = 50$.

solutions are examined and it is found that all the mean fields are very sensitive to the changes in C_{ω_1} while only the mixture fraction variance seems to be very sensitive to the changes in C_{ϕ} but not the other mean fields. The spatial and bias errors are also examined and it is shown that the hybrid method is second order accurate in space and the bias error is vanishingly small in all the mean fields. The grid size and the number of particles per cell are determined for a 5% error tolerance. The chemistry is described by the simplest possible flamelet/PDF model. Hence the main focus here is on the accurate calculations of the mean flow, turbulence and mixing, which lays the foundation for future work in which the chemistry is described in greater detail.

References

- [1] A.R. Masri. <http://www.mech.eng.usyd.edu.au/research/energy>
- [2] P. Jenny, M. Muradoglu, K. Liu, S.B. Pope, and D.A. Caughey. *J. Comp. Phys.*, 166, (2001).
- [3] M. Muradoglu, P. Jenny, S.B. Pope and D.A. Caughey. *J. Comp. Phys.*, 154, (1999).
- [4] M. Muradoglu, S.B. Pope and D.A. Caughey. *J. Comp. Phys.*, 172(2), (2001).
- [5] M. Muradoglu and S.B. Pope. *AIAA J.*, (in press), (2002).
- [6] S. B. Pope. *Prog. Energy Combust. Sci.*, 11, (1985).
- [7] J. Xu and S. B. Pope. *J. Comput. Phys.*, 10, (1998).

Modeling and Validation of Lean Premixed Combustion For Ultra-Low Emission Gas Turbine Combustors

J. C. Oefelein (*oefelei@sandia.gov*) and R. W. Schefer (*rwsche@sandia.gov*)

Combustion Research Facility
Sandia National Laboratories, Livermore, CA 94551-0960, USA

The Combustion Research Facility (CRF) is currently conducting research in areas related to ultra-lean premixed hydrocarbon combustion and hydrogen-enriched hydrocarbon fuels, with emphasis placed on turbulent swirl-stabilized thermo-chemistry and flow dynamics typically encountered in gas turbine combustors. Research is focused on the development of high-fidelity subgrid-scale models based on the Large Eddy Simulation (LES) technique and the development of appropriate experiments for validation of these models. Major collaborators include the DOE Hydrogen Office and the National Energy Technology Laboratory (NETL). This effort also involves an international collaboration with a consortium of European partners organized through the International Energy Agency (IEA). The joint computational-experimental effort focuses on laboratory-scale geometric and flow environments that match the conditions specified in full-scale gas turbines.

The baseline experimental configuration (shown to the right) is a laboratory-scale swirling-flow dump-combustor that generically emulates the fluid dynamic, thermodynamic, thermo-chemical and transport processes that occur in typical industrial gas-turbine combustors. The flow conditions were selected with two primary objectives. The first was to provide a set of parametric conditions that are representative of those typically encountered in gas turbine combustors. The second was to match these parametric conditions to CRF laboratory facilities. The design has been optimized to provide non-ambiguous boundary conditions required for the validation of high-fidelity LES simulations while making optimal use of the advanced laboratory and diagnostic capabilities developed at CRF. The burner consists of a centerbody with an annular premixed methane-air jet injected through a series of swirl vanes into an expansion chamber. The base fuel, methane, can be enriched with hydrogen. The annular injector is designed to provide an acoustically clean, fully developed turbulent profile at the exit with a uniform equivalence ratio, a uniform flow rate, and diminished wake effects due to the swirler. All wall surfaces are hydraulically smooth and designed to provide no-slip and adiabatic conditions. The nozzle is designed to provide a constant pressure exit boundary condition, with zero axial gradients.

Verification of the experimental configuration is ongoing and directly focused on issues related the validation of LES subgrid-scale models. To assist in the verification process, a series of LES calculations have been performed to corroborate the existence of well-posed boundary conditions and relevant flow characteristics. Because LES requires the specification of both mean flow quantities and the higher time evolving moments, verifying the existence of clean, non-ambiguous boundary conditions is imperative. After establishing the appropriate boundary and operating conditions, attention will focus on validation requirements. Systematic activities will closely follow the extensive amount of past experience in the area of experimental validation of models for turbulent nonpremixed and partially premixed flames under the framework of the International Workshop on Measurement and Computation of Turbulent Nonpremixed Flames.



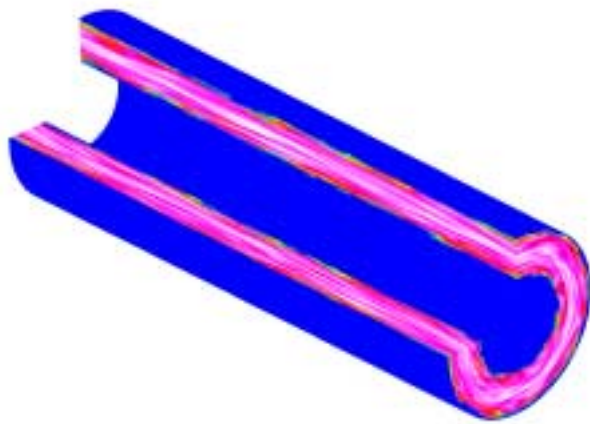
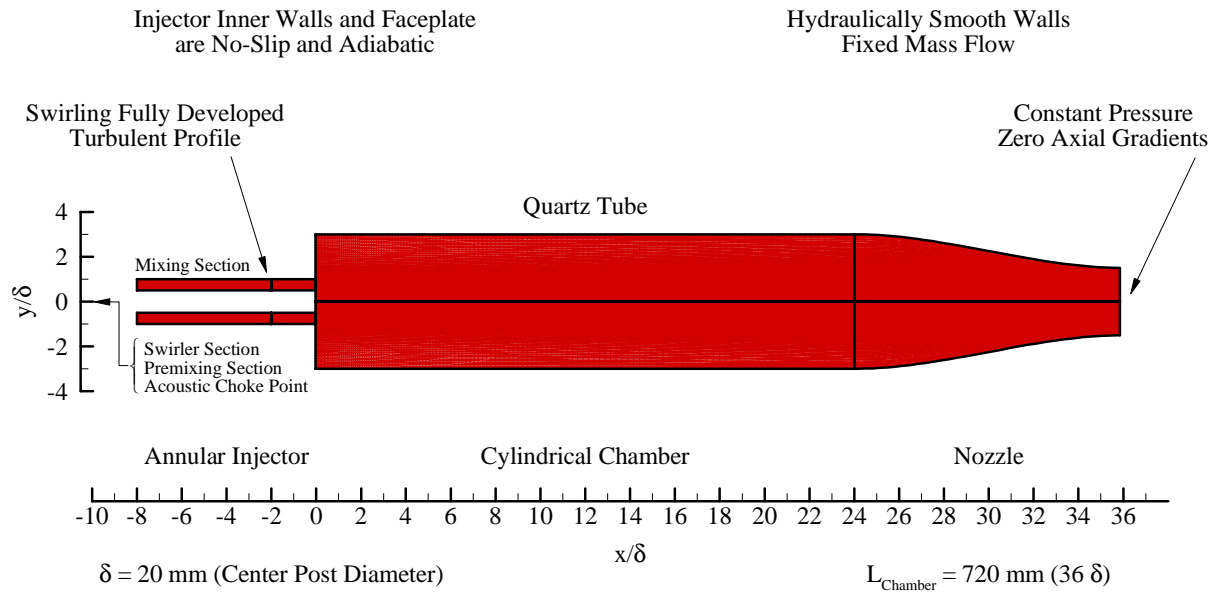
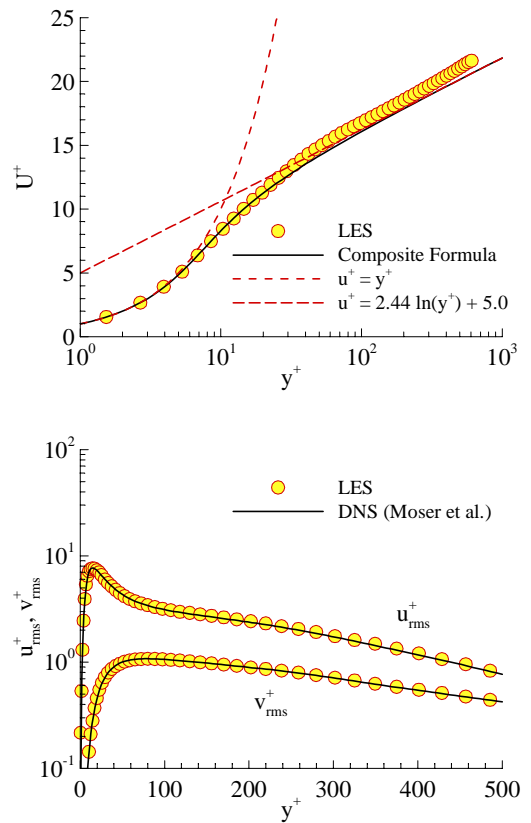


Diagram at top shows key features of the computational domain used for the LES simulations. Figure above shows contours of the magnitude of vorticity inside the swirling annular mixing section obtained using LES. Plots to the right show validated profiles of the mean and rms velocity components inside the section.



A Joint Experimental/Large-Eddy Simulation Study of a Model Gas Turbine Combustor

H. Pitsch*, P. Trouillet, C. D. Pierce
Center for Turbulence Research
Stanford University, Stanford, CA 94305-3030

E. Tribbett, C. M. Sipperley, C. F. Edwards, C. T. Bowman
Department of Mechanical Engineering
Stanford University, Stanford, CA 94305

Our aim is to develop a predictive model applicable in LES of general combustion situations, such as those encountered in gas-turbine combustors. This goal should be achieved by a step-by-step approach from low to high complexity with extensive validation at each level. In the past we have performed LES of a purely premixed and an essentially non-premixed, piloted jet flame. For the non-premixed case, an unsteady flamelet formulation has been developed, which has proven to be very accurate not only for the heat release and major species mass fractions, but also for mass fractions of minor species such as carbon monoxide and NO. For LES of premixed turbulent combustion we have formulated a model based on the level set approach using the G -equation, similar to the Reynolds-averaged model given by Peters.

To account for premixed, non-premixed, and partially premixed combustion situations we intend to use a Combined Conserved Scalar/Level-Set Flamelet Method, composed of the diffusion flamelet model for non-premixed combustion and the level-set method for premixed combustion. In preliminary studies we have already applied this model to LES of a lean, partially premixed combustor and a series of lifted jet diffusion flames.

The purpose of the present study is first to provide an experimental data set of a combustion experiment with the flow complexity resembling that of a gas-turbine combustor, but avoiding the geometric complexity and the uncertainty introduced by the modeling of liquid sprays. The investigated experimental configuration is therefore operated with gaseous fuel, has swirling air intake, and is designed to have a compact combustion region with a flame, which is not attached to the nozzle. The second aim is to use the obtained set of experimental data to perform a validation study of the Combined Scalar/Level-Set Method and assess its applicability to gas-turbine engine combustion.

A swirl-stabilized, methane combustor which produces a compact, lifted flame was developed. Figure 1 is a schematic of the combustor. It is composed of three key sections: the flow development section, the test section, and a tail pipe.

The combustor operating conditions were chosen to provide high-intensity, compacted-but-lifted combustion without significant acoustic excitation. Details of the operating conditions are given in Ref. [1]. A photograph of the flame operating at these conditions is shown in Fig. 1. The same conditions have been used for both the cold flow and the fired experiment. Note that also for the cold flow experiment methane has been used in the fuel tube to ensure the same mass flow rate, momentum flux, and inner tube Reynolds number as in the fired experiment. For the cold flow experiments and the fired case radial velocity profiles obtained by LDV measurements are given at different downstream stations. For the fired case, also temperature data from thermocouple measurements, mass fractions of stable species by gas-chromatographic measurements, and global emissions data are provided.

Instantaneous fields from the simulation of the cold flow and the fired case are shown in Fig. 2. In the cold flow simulation, the indicated contours of zero axial velocity show that a large recirculation region forms in the center of the flow close to the inner nozzle. A second recirculation forms in the corner of the main combustor tube right after the sudden expansion. Downstream of the recirculation zone a vortex core forms, which is promoted by a favorable pressure gradient caused by the contraction. A low pressure region in the core of this vortex leads to a jet-like structure observable in the axial velocity field. This central jet also appears in the experimental data, but is overpredicted by the simulations.

Comparing the results from the fired simulation shown in Fig. 2 to the cold flow simulation, it is observed

*Corresponding author: H.Pitsch@stanford.edu

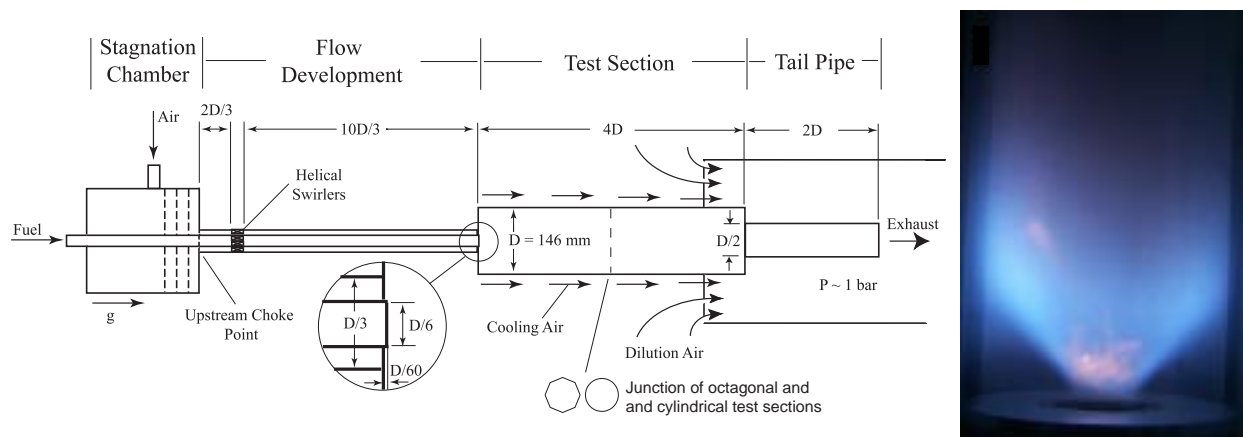


Figure 1: Schematic and photograph of the gas-phase combustor. The flame is highly turbulent and lifted from the fuel entrance plane.

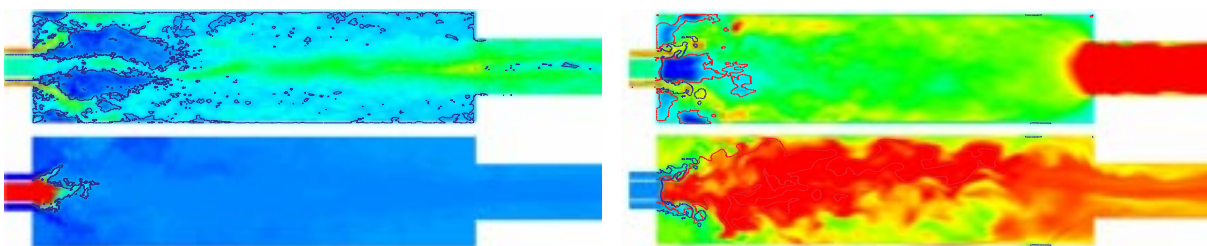


Figure 2: Left: Axial velocity (top) and mixture fraction (bottom) from the cold flow simulation. The blue lines are zero axial velocity and stoichiometric mixture fraction in the velocity and the mixture fraction figure, respectively. Right: Axial velocity (top) and temperature (bottom) from the fired case simulation. Blue lines represent the instantaneous flame surface, red lines are zero axial velocity and stoichiometric mixture fraction in the velocity and the temperature figure, respectively

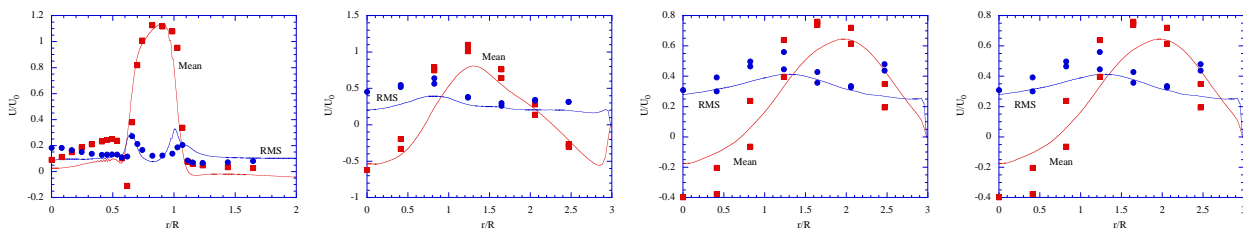


Figure 3: Axial velocities from the fired simulation (lines) compared with experimental data (symbols) at $x/R = 0.08$, $x/R = 1.8$, $x/R = 3.3$, and $x/R = 6.3$ from left to right

that the heat release changes the flow field entirely. The central vortex core, which dominates the flow field in the cold flow has disappeared for the fired case. This also leads to a much more stable swirl cone and central recirculation zone.

An example for a quantitative comparison with experimental data is shown Fig. 3, where axial velocities and velocity fluctuations are shown for the fired case at different downstream locations.

References

- [1] H. Pitsch, P. Trouillet, C. D. Pierce, E. Tribbett, C. M. Sipperley, C. F. Edwards, and C. T. Bowman. A joint experimental/large-eddy simulation study of a model gas turbine combustor. *Western States Section Meeting of the Combustion Institute, 2002, San Diego, CA*, pages WSSCI 02S-59, 2002.

Composition PDF Calculations of Piloted-Jet Non-Premixed Turbulent Flames

Stephen B. Pope
Cornell University
Ithaca, NY 14853, USA
pope@mae.cornell.edu

Graham M. Goldin
Fluent, Inc.
10 Cavendish Court, Lebanon, NH 03766, USA
gmg@fluent.com

The experiments of Barlow & Frank [1] reveal increasing levels of local extinction in piloted nonpremixed jet flames as the jet and pilot stream velocities are increased. PDF computations of these flames have previously been reported by Xu & Pope [2], Tang et al. [3] and Lindstedt et al. [4]. In the present work we investigate the sensitivity of predicted levels of local extinction to the reaction and mixing sub-models.

The calculations are based on the solution of the standard modelled transport equation for the joint PDF of the fluid composition [5]. Two different chemical mechanisms are used: a skeletal C₁ mechanism for methane; and the augmented reduced mechanism (ARM [6]) based as GRI 2.11. And two different mixing models are used, namely, IEM and modified Curl. The results, which include conditional means of major and minor species, demonstrate the sensitivity to the choice of these sub-models.

As an illustration of the results obtained, Fig. 1 shows means conditional on the mixture being stoichiometric against axial distance for Flame D. As may be seen, these statistics reveal differences in the mixing model performance. For temperature and CO₂, the calculations based on the IEM mixing model are generally in better agreement with the experimental data; whereas, for the other quantities shown, the calculations based on the modified Curl mixing model are generally more accurate.

The computations are performed using a new implementation of the distributed-particle composition PDF algorithm [5] in the Fluent code, with reaction implemented through the ISAT algorithm [7]. Results are also given on the computational performance of this scheme.

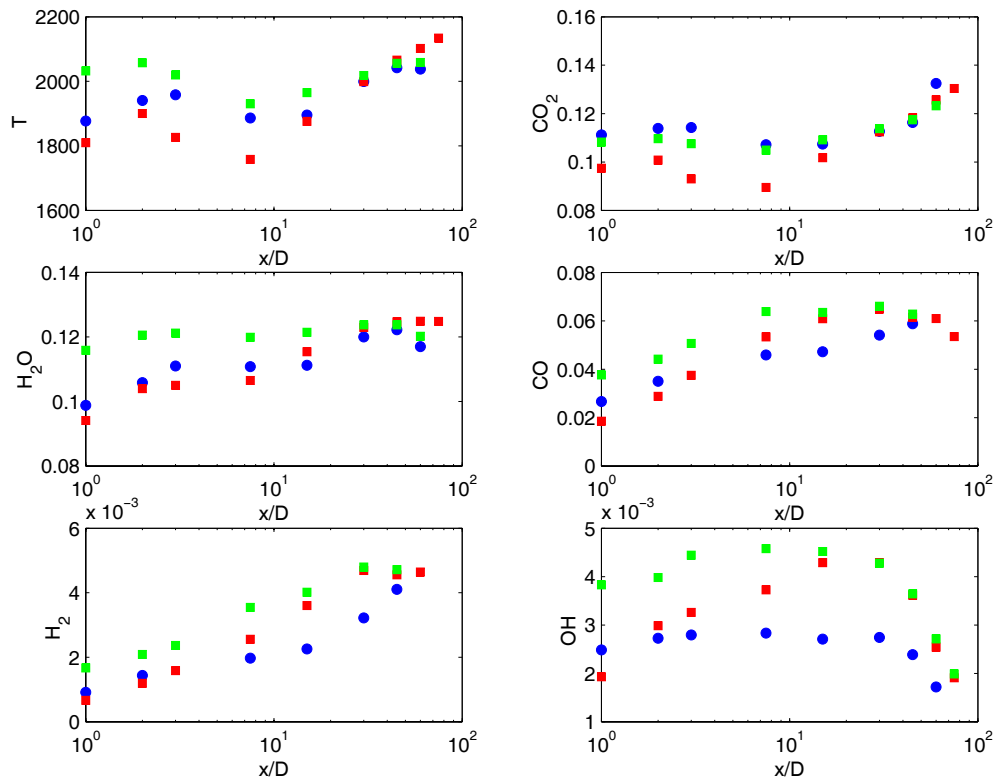


Figure 1: Means conditional on the mixture being stoichiometric in Flame D against axial distance: blue circles, experimental data; green squares, IEM mixing model; red squares, modified Curl mixing model. (The IEM results are generally above the MC results.)

- [1] Barlow, R. S. and Frank, J. H., *Proc. Combust. Inst.* **27**, 1087 (1998)
- [2] Xu, J. and Pope, S. B., *Combust. Flame* **123**, 281 (2000)
- [3] Tang, Q., Xu, J. and Pope, S. B., *Proc. Combust. Inst.* **28**, 133 (2000)
- [4] Lindstedt, R. P. Louloudi, S. A., and Vaos, E.M., *Proc. Combust. Inst.* **28**, 149 (2000)
- [5] Pope, S. B., *Prog. Energy Combust. Sci.* **11**, 119 (1985)
- [6] Sung, C. J., Law, C. K. and Chen, J.-Y., *Proc. Combust. Inst.* **27**, 295 (1998)
- [7] Pope, S. B., *Combust. Theory Modelling*, **1**, 41 (1997)

Collaboratory for Multi-scale Chemical Sciences (CMCS): Data Format Standards and Data Sharing Technologies

L. Rahn, C. Yang, C. Pancerella, J. Hewson, W. Koegler, D. Leahy, M. Lee, Sandia National Laboratories; J. Nichols, B. Didier, T. Windus, J. Myers, K. Schuchardt, E. Stephan, Pacific Northwest National Laboratory; A. Wagner, B. Ruscic, M. Minkoff, L. Liming, G. von Laszewski, S. Bittner, B. Moran, Argonne National Laboratory; W. Pitz, Lawrence Livermore National Laboratory; D. Montoya, Los Alamos National Laboratory; T. Allison, National Institute of Standards and Technology; W. Green, Massachusetts Institute of Technology; M. Frenklach, University of California at Berkeley

rahn@sandia.gov
<http://cmcs.ca.sandia.gov/>

The Collaboratory for Multiscale Chemical Sciences (CMCS) is designed, in part, to serve a growing unmet need for basic researchers: sharing experimental and computational data across application environments, scales, and disciplines. Through reuse of new protocols and standards, including Digital Authoring and Versioning (WebDAV) and Extensible Markup Language (XML), CMCS will be able to provide a significant improvement in data-centric collaboration for scientific researchers. While our project has broad goals to serve the entire chemistry community, our pilot is focusing on the field of combustion chemistry.

“Sharing data” has three major facets, as shown in the Figure 1. The first facet focuses on supplying tools for chemists to simply store and retrieve data from a common repository, minimizing or eliminating barriers associated with custom data formats. A second facet is meeting new, higher standards for the annotation of data, describing exactly how the data came to be, and providing a powerful search interface so that the CMCS visitors can easily find relevant datasets. A third facet is developing powerful visualization tools that take advantage of new data standards. Finally, CMCS will provide a new sort of digital publication forum, providing permanent and unalterable presentation of published datasets and knowledge bases that may be cited elsewhere in the scientific literature.

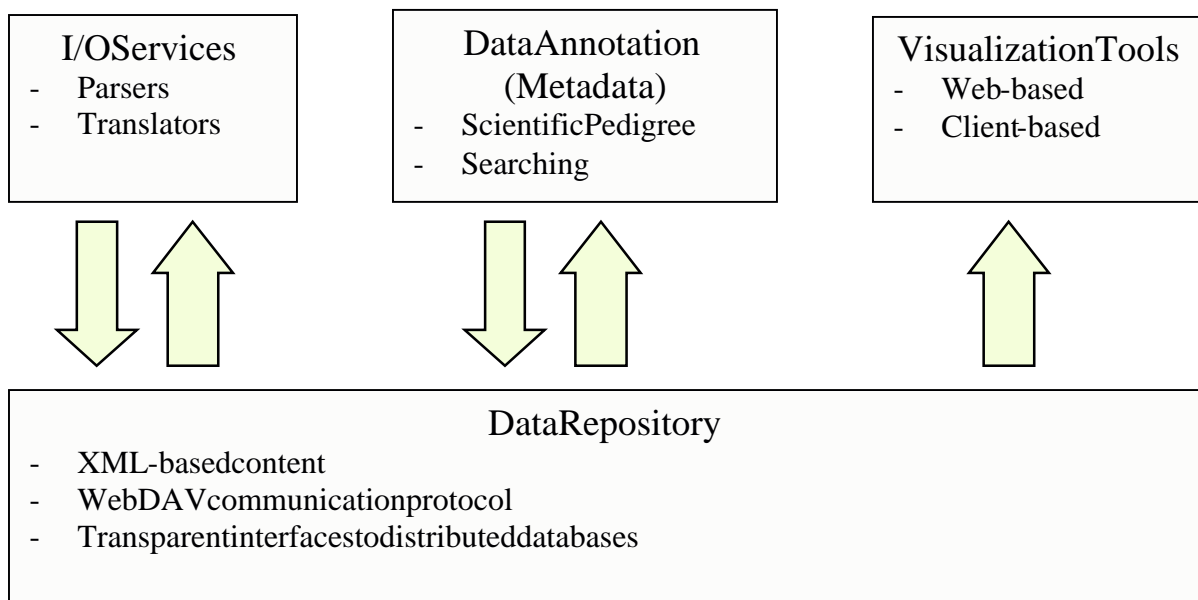
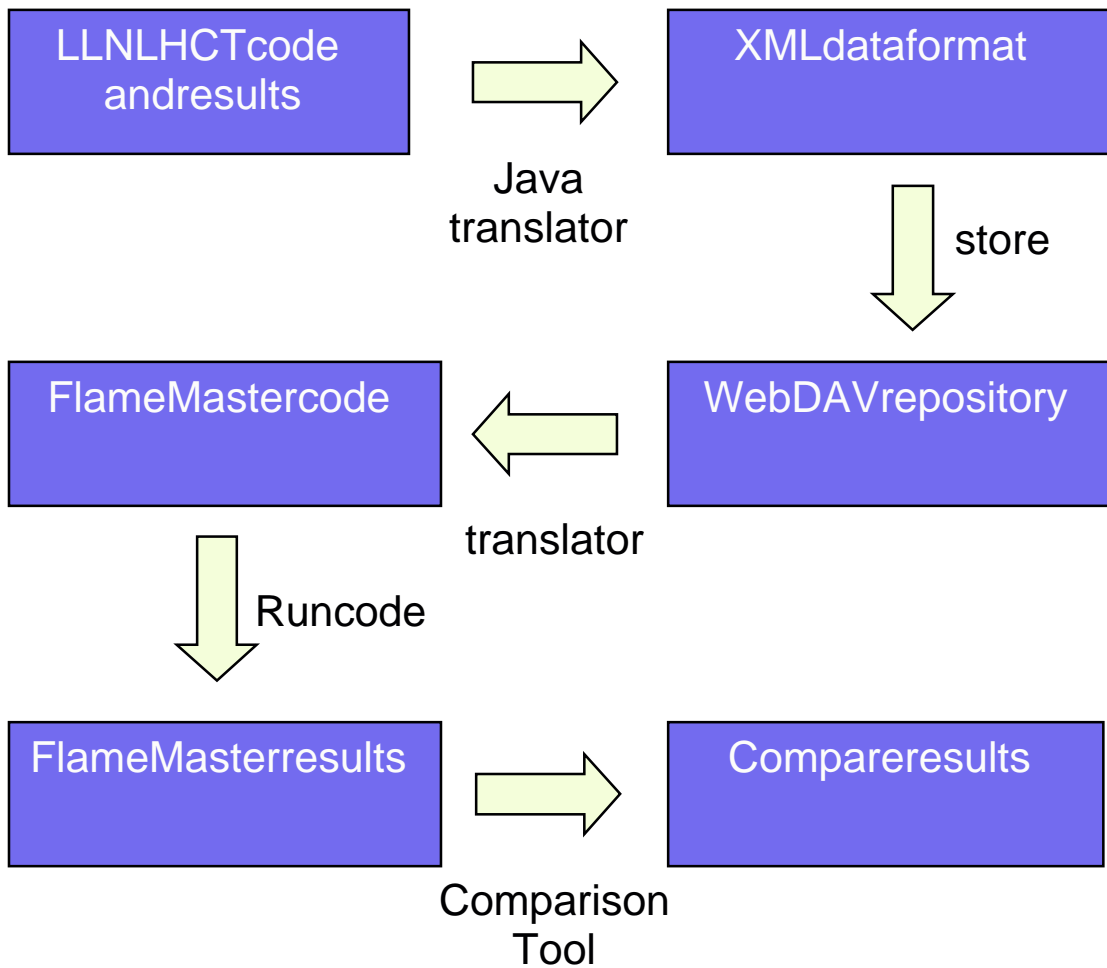


Figure 1. Simple schematic of services using a common chemistry data repository.

In the early stages, the CMCS project's most visible developments are related to the first facet mentioned above: a common data repository with facile tools for I/O and translation. As an example, we are developing tools to translate datasets to and from specific combustion modeling application formats into a common XML-based format. This straightforward effort will make possible to perform calculations with a single combustion mechanism in more than one application environment. Figure 2 shows an example that allows comparison of LLNLHCT results with those from FlameMaster.

With this sort of technology in the hands of combustion researchers, collaboration will scale beyond occasional one-to-one data sharing to a working many-to-many collaboration. When combined with our efforts in annotation, searching, visualization and publishing facilities, we at the CMCS hope to enable much more efficient sharing and leveraging of the new knowledge being generated by basic research.

Figure 2. Example of data comparison via CMCS infrastructure.



Investigation of Turbulent Mixing Models

Zhuyin Ren †, Qing Tang, Stephen B. Pope
Sibley School of Mechanical & Aerospace Engineering
Cornell University, Ithaca, NY 14853, USA

E-mail: † zr26@cornell.edu

ABSTRACT

In modeling turbulent reactive flows based on pdf methods, the change in fluid composition due to convection and reaction is treated exactly, while molecular mixing has to be modeled. Modeling mixing in pdf methods involves prescribing the evolution of stochastic/conditional particles in composition space such that they mimic the change in the composition of a fluid particle due to mixing in a turbulent reactive flow.

Mixing models are essential for pdf methods and previous calculations show sensitivity of piloted flame results to the choice of mixing model. Calculations of flame F performed by different groups, especially at Cornell University [1, 2] and Imperial College[3], demonstrate the sensitivity of extinction results to the choice of the mixing model and constants.

In order to understand the relative performance of different mixing models for non-premixed turbulent reactive flow, this work is concentrating on investigating the performance of three different existing mixing models: the interaction by exchange with the mean (IEM) model[6], the modified Curl's mixing model (MC) [7], and the Euclidean Minimum Spanning Tree (EMST) model[4] in the Partially Stirred Reactor (PaSR).

In the PaSR calculations, there are two inflow streams: the fuel stream (H_2 and N_2 , 1:1 by volume, $T=300K$) and the oxidant stream(N_2 and O_2 , 79:21 by volume, $T=300K$). The detailed mechanism for hydrogen oxidation, which involves 9 species and 19 reactions, is incorporated into the calculation using the *in situ* adaptive tabulation(ISAT) algorithm[5]. The ISAT error tolerance, ε_{tol} , is set to be 1.0×10^{-5} , which guarantees less than 1% tabulation error for all species in our calculation. The initial condition for the calculations is that all particles are in chemical equilibrium: 60% of the particles have stoichiometric mixture fraction ξ_{stoich} ; and the remaining 40% of the particles are uniformly distributed based on mixture fraction.

In the PaSR calculations, there are three time scales: the mixing time τ_{mix} , the residence time τ_{res} and the chemical reaction time τ_c (determined by the fuel we choose), and three important parameters: the number of particles N, the Fuel/Air flow ratio and the particle weights. In our calculations, we investigate the following situations:

1. Fix τ_{res} , investigate IEM/MC/EMST for different τ_{mix}/τ_{res} .
2. Fix τ_{mix}/τ_{res} , investigate IEM/MC/EMST for different τ_{res} .
3. Investigate the dependence of IEM/MC/EMST on the number of particles N.
4. Investigate the dependence of IEM/MC/EMST on particle weights.
5. Investigate IEM/MC/EMST for different Fuel/Air ratio.

Figure 1 shows that the three mixing models lead to substantially different behavior, both qualitatively and quantitatively. The last subplot shows that IEM and MC lead to extinction as τ_{mix} increases, whereas EMST does not.

References

- [1] Xu, J., and Pope, S.B., *Combust. Flame* 123, 281 (2000)
- [2] Tang, Q., Xu, J., and Pope, S.B., *Proc. Combust. Inst.* 28, 133 (2000)
- [3] Lindstedt, R.P., Louloudi, S.A., and Vaos, E.M., *Proc. Combust. Inst.* 28, 149 (2000)
- [4] S. Subramaniam, and S. B. Pope, *Combust. Flame*, 115: 487-514 (1998)
- [5] Pope, S. B., *Combust. Theory Modelling* 1, 41-63 (1997)
- [6] Dopazo, C., *Phys. Fluids A* 18:389(1975)
- [7] Janicka, J., Kolbe, W., and Kollman, W., *J. Nonequilib. Thermodyn* 4:47 (1979)
- [8] Nooren, P.A., Wouters, H.A., Peeters, T.W.J., Roekaerts, D., Mass, U., and Schmidt, D., *Combust. Theory Modelling* 1, 79-96 (1997)

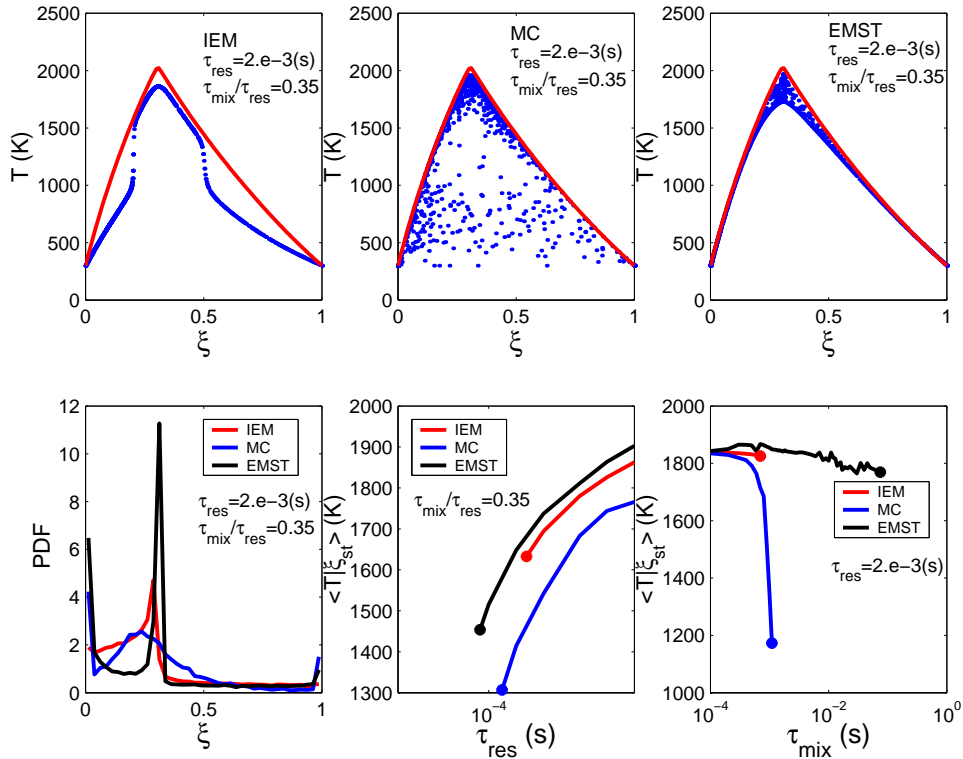


Figure 1: PaSR results obtained with $N=1000$, equal-weight particles. Subplots[1][2][3]: Scatter plots of temperature against mixture fraction for different mixing models (the red line is equilibrium); Subplot[4]: PDF of mixture fraction for different mixing models; Subplot[5][6]: Mean temperature conditional on stoichiometric against mixture fraction for different τ_{res} and τ_{mix} . (In order of increasing temperature, the lines correspond to MC, IEM and EMST.)

Comparison of measured and predicted scalar time scales in flame H3

Michael W. Renfro¹, Amit Chaturvedy, Galen B. King, Normand M. Laurendeau
School of Mechanical Engineering, Purdue University
West Lafayette, IN 47907 USA

Andreas Kempf, Andreas Dreizler², Amsini Sadiki, Johannes Janicka
Technische Universität Darmstadt
Darmstadt, Germany

Measurements of time series have been demonstrated in turbulent flames for velocity, temperature, and some reactive species (including OH). Traditional Reynolds-averaged modeling of turbulence cannot predict the temporal information in these measurements; thus, direct comparisons between the high-bandwidth data and numerical simulations have been limited. Advanced modeling approaches, including large-eddy simulations (LES) and direct numerical simulations (DNS), can predict fluctuation time scales, but the accuracy of these predictions has not been tested. Measurements of OH time-scale statistics and predictions of the same using LES are presented and compared to address this predictive capability of emerging models.

Large-eddy simulations of the H3 hydrogen/nitrogen diffusion flame ($Re=10,000$) burning in a co-flow air stream have been performed with a temporal resolution of less than 5 μs . Details of the flame have been presented by Meier *et al.* (1996), including single-shot Raman scattering measurements. Single-shot Raman scattering with OH and NO laser-induced fluorescence have been reported by Neuber *et al.* (1998), and time-averaged velocity measurements, single-shot Raman and CARS measurements have been reported by Pfuderer *et al.* (1996). None of these measurements recover fluctuation time scales. Measurements of OH concentration time series have been recently made in flame H3 using picosecond time-resolved laser-induced fluorescence (PITLIF). Figure 1 shows an example of the signal quality for these OH measurements. The spatial and temporal resolution is better than 100 μm and 100 μs , respectively. Details of the measurement technique and data processing approach have been presented (Renfro *et al.*, 2000). Hydroxyl statistics were measured at many radial locations for axial height from $x/D=5$ to $x/D=40$, and along the jet centerline for $x/D=20-50$. The time-series were processed to recover the mean, rms, probability density function (PDF), and power spectral density (PSD). The PSD was further processed to determine the integral time scale for OH fluctuations at each point. This integral time scale is the primary focus for comparisons between PITLIF and LES in the present work.

The measured OH PSDs collapse to a single curve when normalized by the integral time scale. This curve has the same shape as measured in $H_2/N_2/CH_4$ diffusion flames under different flow conditions. Some of the normalized measurements are shown in Fig. 2. The integral time scales themselves show significant variation through flame H3. Below the flame tip ($\sim x/D=34$), the time scale are strong functions of radial location, increasing by a factor of at least 2 from high-velocity to low-velocity locations. This trend was discussed by Renfro *et al.* (2002), and the detailed shape of the radial profile was correctly simulated based on simple flamelet fluctuations. The axial variation of integral time scales in flame H3 are shown in Fig. 3. Below the flame tip, the time scales weakly decrease with axial height, but are within 20% of a constant 0.9 ms. Above the flame tip (defined here as peak [OH]), the time scales rapidly increase with x/D , in a manner qualitatively consistent with a non-reacting jet. In this case, the increase in time scale is described by the local decrease in velocity and increase in jet width. However, below the flame tip, the effects of the flame on the growth of the fluctuation rate is significant.

The LES results have been computed applying a mixture fraction formulation and the flamelet assumption, considering variable scalar rates of dissipation in space. The subgrid-variance of the mixture-fraction was modeled by the resolved variance in a test-filter cell, whereas the subgrid-fluctuation of the scalar rate of dissipation is modeled by a Dirac-peak. Scalar rate of dissipation itself is computed based on an approach by Girimaji & Zhou (1996) and de Bruyn Kops *et al.* (1997). The governing equations were solved by a 3d finite volume code based on the low-mach assumption of incompressibility. Since density is assumed to only depend on the chemical state, not on pressure, the timestep is only limited by convection, not by the speed of sound. Time integration is performed by a 3rd order low-storage Runge Kutta scheme, momentum fluxes are modeled by 2nd order central schemes. For species transport, a 2nd order TVD scheme (Charm) has been applied to avoid numerical oscillations. Scalar transport is integrated in a way ensuring conservation of both mass and species. More information on this LES can be found in Kempf *et al.* (2001, 2002). The LES results are sampled to recover predicted time series for mixture fraction, veloc-

¹ renfro@ecn.purdue.edu, ² dreizler@ekt.tu-darmstadt.de

ity, temperature, and OH concentrations. The OH concentrations are processed using the same approach as for the PITLIF measurements. A sample LES time series for OH is shown in Fig. 4, and has similar structure as the measurements. Detailed comparisons of the time-series statistics will be presented.

References

deBruynKops, S.M., Riley, J.J., and Kosaly, G. (1997). Toward large eddy simulations of non-premixed turbulent reactive flows. *Western Section of the Combustion-Institute, Spring Meeting*, Paper No. 97S-051.

Girimaji, S.S. and Zhou, Y. (1996). Analysis and modeling of subgrid scalar mixing using numerical data. *Phys. Fluids A* 8:1224-1236.

Kempf, A., Sadiki, A., and Janicka, J. (2002). Prediction of finite chemistry effects using large eddy simulation, accepted for presentation at 29th Symp. Internat. on Combustion, Sapporo.

Kempf, A., Schneider, C., Sadiki, A., and Janicka, J. (2001). Large eddy simulation of a highly turbulent methane flame: Application to the DLR standard flame. *2nd Symp. Turb. Shear Flow Phenomena: III*, 315.

Meier, W., Prucker, S., Cao, M.-H., and Stricker, W. (1996). Characterization of turbulent H₂/N₂/Air jet diffusion flames by single-pulse spontaneous Raman scattering. *Combust. Sci. Technol.* 118:292-312.

Neuber, A., Krieger, G., Tacke, M., Hassel, E., and Janicka, J. (1998). Finite rate chemistry and NO molefraction in non-premixed turbulent flames. *Combust. Flame* 113:198-211.

Pfuderer, D.G., Neuber, A.A., Früchtel, G., Hassel, E.P., and Janicka, J. (1996). Turbulence modulation in jet diffusion flames: modeling and experiments. *Combust. Flame* 106:301-317.

Renfro, M.W., Gore, J.P., and Laurendeau, N.M. (2002). Scalar time-series simulations for turbulent nonpremixed flames. *Combust. Flame* 129:120-135.

Renfro, M.W., Guttenfelder, W.A., King, G.B., and Laurendeau, N.M. (2000). Scalar time-series measurements in turbulent CH₄/H₂/N₂ nonpremixed flames: OH. *Combust. Flame* 123:389-401.

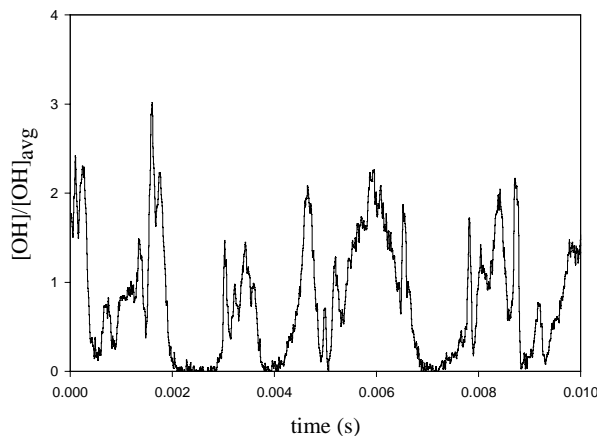


Fig. 1: Typical OH time-series measurements by PITLIF in flame H3.

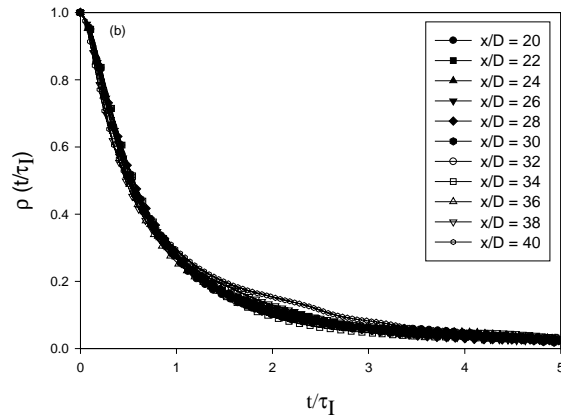


Fig. 2: OH autocorrelation functions normalized by their measured intergral time scales.

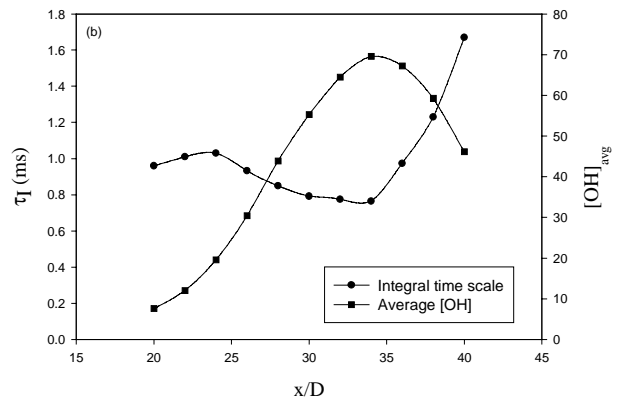


Fig. 3: Measured OH integral time scales along the jet centerline compared to mean OH concentrations.

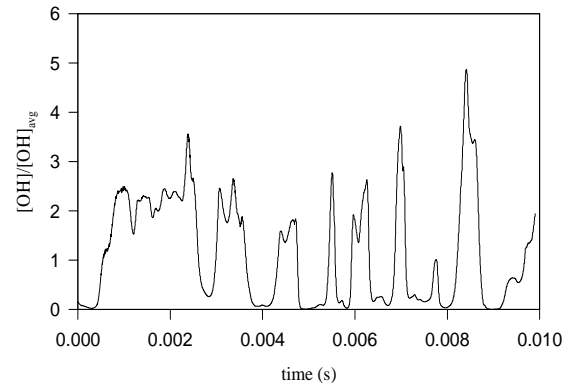


Fig. 4: LES-simulated time series for OH in flame H3.

FLAME-VORTEX INTERACTIONS IN PARTIALLY PREMIXED CH₄/AIR FLAMES

CHRISTINA M. VAGELOPOULOS and JONATHAN H. FRANK*

*Combustion Research Facility
Sandia National Laboratories
Livermore, CA 94551, USA*

*Corresponding Author: Jonathan H. Frank
email: jhfrank@ca.sandia.gov

ABSTRACT

Previous experimental efforts related to the TNF Workshop include studies of partially premixed methane/air flames. The detailed structure of these flames has been studied in steady laminar flames [1], and turbulence-chemistry interactions have been investigated in turbulent jet flames [2]. However, there remains a gap in our understanding of the effects of flow-flame interactions in these flames. To help fill this gap, we are studying experimentally the transient response of a laminar partially premixed CH₄/air flame subject to perturbation by a toroidal vortex ring. The vortex-flame interaction represents a fundamental component of turbulence-flame interactions. Isolated vortex-flame interactions can be studied in a well-controlled and systematic way. Initial results of OH planar laser-induced fluorescence (PLIF) imaging show the temporal evolution of an axisymmetric partially premixed methane/air flame as it is deformed and stretched by the vortex ring. The fuel composition (1/3 CH₄/air by volume) is the same as the Sandia piloted jet flames, which are currently target flames of the TNF Workshop.

The effect of vortex strength was investigated by employing three different vortices. Case I was a weak vortex that did not survive the flame. Case II was a vortex of intermediate strength. Case III was a strong vortex that induced local extinction during its interaction with the flame surface. The temporal evolution and spatial distribution of OH along the vortex contour is discussed for all three cases. PIV is utilized to provide information for the detailed characteristics of the three vortices. The OH distribution appears to depend strongly on the curvature and local distribution of unsteady strain-rate. Figure 1 shows results from Case III in which a flame ring appears later into the interaction (see Frame 4 of Fig. 1).

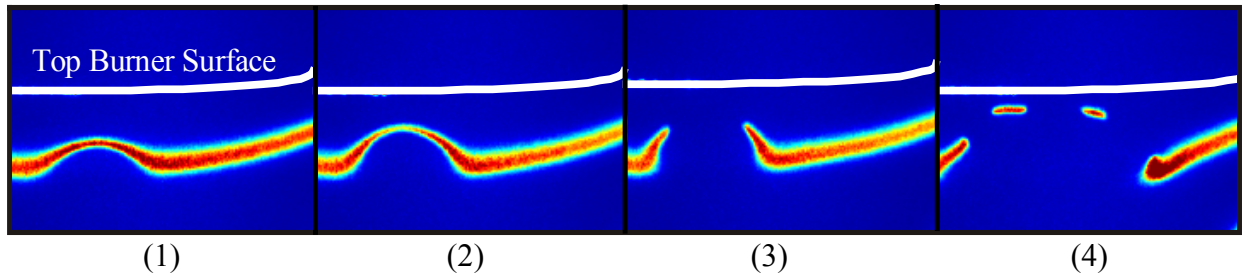


Fig.1 Temporal evolution of OH PLIF signal during the interaction of an axisymmetric partially premixed CH_4 -air flame with a toroidal vortex ring. The images have been corrected for spatial and temporal variations of the laser sheet. The time between consecutive frames is 4 ms. Frame 1 corresponds to a time early in the interaction while the frames 3 and 4 correspond to times at which the vortex ring has partially extinguished the flame surface. The OH signal has a minimum at the centerline of the vortex ring at all times. Extinction is initiated along the centerline, where unsteady stretch is expected to be maximum.

References

1. Barlow, R. S., Karpetis, A. N., Frank, J. H., and Chen, J.-Y., *Combust. Flame*, 127:2102 (2001).
2. Barlow, R. S., and Frank, J. H., *Proc. Combust. Inst.*, 27:1087-1095 (1998).

Contributed Notes and Vugraphs on TNF6 Focus Topics
(included in the order of the agenda)

Mixing Model Performance in the Calculation of Nonpremixed Piloted Jet Flames

Stephen B. Pope
Cornell University

1 Introduction

The Barlow and Frank (1998) series of piloted jet flames (D, E, and F) provides an excellent test for turbulent combustion models which attempt to account for the strong turbulence/chemistry interactions that accompany local extinction and reignition. For Flame D there is little local extinction, and reasonably accurate calculations have been reported (at TNF5 and elsewhere) using several different modelling approaches. But flames E and F provide more of a challenge. The only calculations of these flames at TNF5 were from the groups at Berkeley, Imperial College and Cornell: all of these calculations are based on PDF transport equations.

A conclusion from TNF5 based on these results is “that it is now possible to obtain very good agreement between model and experiment” for the piloted jet flames. But nevertheless, several fundamental questions about the modelling of turbulent mixing remain unanswered.

In the following sections we review the calculations of the Barlow & Frank flames presented at TNF5; describe some more recent results; discuss the physics of mixing models in the context of nonpremixed combustion; and suggest some useful directions for future experiments.

2 Review of TNF5 Calculations

We restrict attention to the only three sets of calculations presented at TNF5 that included Flame F - which is close to global extinction.

The calculation of J.-Y. Chen (Berkeley) are based on the standard modelled transport equation for the composition joint PDF using the modified Curl (MC, Janicka et al. 1977) mixing model (with $C_\phi = 2.0$) and a 13-step augmented reduced mechanism. However, in the Flame F calculations, a flamelet model was used in the upstream region ($0 \leq x/D \leq 7.5$), for otherwise the flame would have extinguished. Hence, the reasonable calculations for $x/D > 30$ notwithstanding, it is clear that the strong turbulence/chemistry interaction in the vital upstream region are not adequately represented by the sub-models employed.

The calculations of Lindstedt et al. (Imperial College, see Lindstedt et al. 2000) are similar to those of Chen: they are based on the modelled transport equation for the joint PDF of composition using the modified Curl mixing model (with $C_\phi = 2.3$) and a different 16- species augmented reduced mechanism. But in contrast to Chen’s calculations, no special treatment is required to yield a burning solution for Flame F.

The calculations of Tang et al. (Cornell – see also Tang et al. 2000 and Xu and Pope 2000) are based on the modelled velocity-frequency-composition joint PDF equation, using the EMST mixing model (Subramaniam and Pope 1998 and a 19-species augmented reduced mechanism. Albeit with a reduced value of the mixing model constant ($C_\phi = 1.5$), these calculations show the correct levels of local extinction in Flames D, E and F as quantified by means conditional on stoichiometric.

3 Recent Calculations

It is clear that — as should be expected — the calculations (especially for Flame F) are sensitive to the choice of both the chemical mechanism and the mixing model, including the value of the model constant. Since different groups use different chemical mechanisms, it is difficult to draw conclusions about the performance of the different mixing models by comparing the results from different groups. There have been two recent sets of calculations, to be presented at TNF6, in which only the mixing model is varied — the chemistry and other sub-models being fixed.

Lindstedt has extended his previous work (which was based on the modified Curl mixing model) by making calculations of Flames D and F with the LMSE mixing model (Dopazo and O’Brien 1974), which is exactly equivalent to the IEM mixing model (Villernaux and Devillon 1972). In addition, the dependence of the modified-Curl results on the model constant C_ϕ has been studied. The results show that Flame F calculated with IEM is burning, whereas all other groups find that Flame F extinguishes when IEM is used in conjunction with their chemical mechanisms. The agreement with experimental data is far superior with modified Curl than with IEM. The modified Curl results for Flame F show that: the flame extinguishes for $C_\phi = 2.2$; about the right amount of local extinction is obtained with $C_\phi = 2.3$; and much less local extinction is obtained for $C_\phi \geq 2.4$. Since in the experiment Flame F is close to global extinction, this observed sensitivity to C_ϕ is quite reasonable. The decrease in the amount of local extinction with increasing values of C_ϕ was also observed by Xu & Pope (2000) for the EMST mixing model.

The successful calculations of Tang et al. at TNF6 raised the question: can similarly good agreement with experimental data be achieved with simpler mixing models (than EMST) and with simpler mechanisms (than the 19-species ARM)? For TNF6, Pope & Goldin have performed a series of composition PDF calculations of Flames D and E in which the sub-models have been varied systematically. For example, Fig. 1 shows means conditional upon the mixture being close to stoichiometric calculated using both the IEM and modified Curl mixing models. (These conditional means are found to be a sensitive discriminant of model behavior.) It may be seen that for $\langle T | \xi_s \rangle$ and $\langle Y_{CO_2} | \xi_s \rangle$ the IEM calculations agree very well

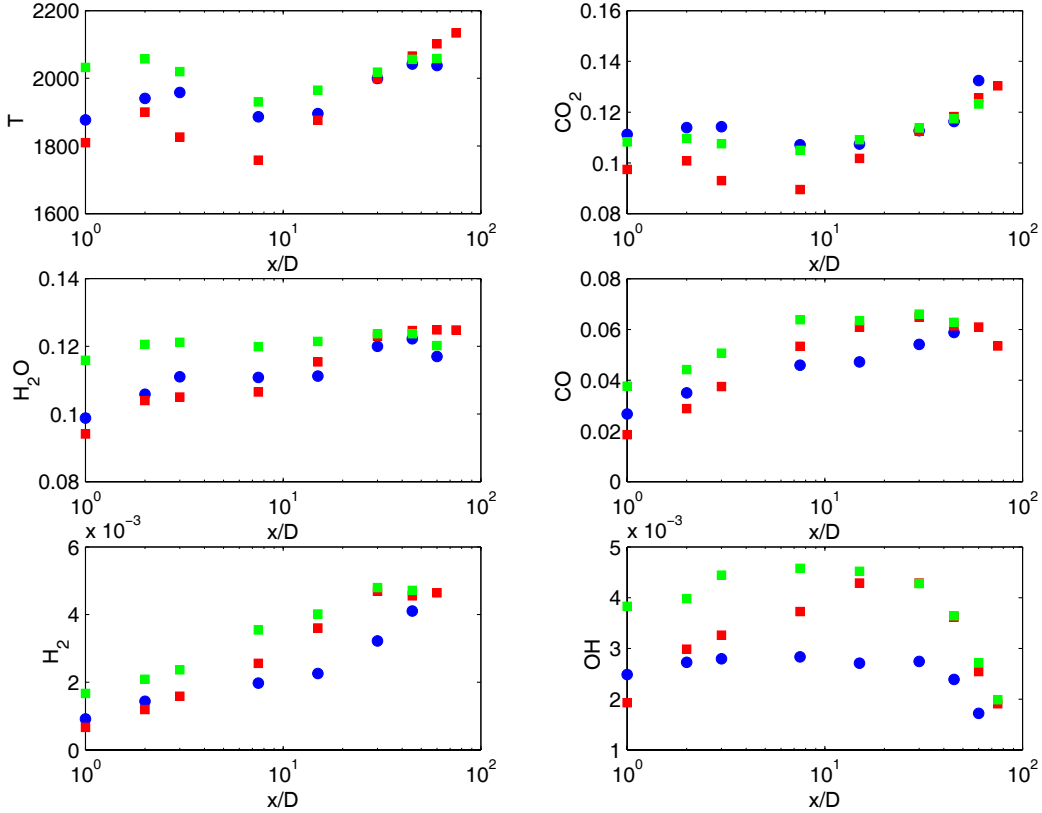


Figure 1: Mean temperature and mass fractions conditional upon the mixture being close to stoichiometric against axial location: blue circles, experimental data; red (lower) squares, MC; and, green (upper) squares IEM. Composition PDF calculations of Pope & Goldin using a skeletal mechanism and $C_\phi = 2.0$.

with the data, whereas the MC calculations are superior for the other species shown. It is particularly noticeable that, at the first four locations, $\langle T | \xi_s \rangle$ is substantially lower for MC than it is for IEM. At the downstream locations ($x/D \geq 7.5$) there is little difference between the calculations based on the two mixing models — in contrast to Lindstedt’s finding. The skeletal mechanism — which contains only C_1 species — yields noticeably poorer agreement for the conditional mean of CO for rich mixtures, which is to be expected.

Barlow & Frank (and others before) have studied experimentally the global extinction in piloted jet flames by varying the jet and pilot velocities. It can also be studied by varying the pilot temperature. With every other parameter fixed, there is a lowest value of the pilot temperature for which the flame burns (i.e., it does not blow off). In Flames D and E, the measured pilot temperature is $T_{pilot} = 1880\text{K}$. A series of calculations was performed in which the the pilot temperature (which is a boundary condition) was successively changed by 50K in order to determine (approximately) the lowest temperature at which the flame

Table 1: The (approximate) lowest value of the pilot temperature, T_{pilot} (K), at which the flame does not extinguish. Calculations using IEM and MC, the skeletal mechanism (SK), and the augmented reduced mechanism (ARM).

	SK/MC	SK/IEM	ARM/IEM
Flame D	1830	1730	2130
Flame E	1930	1880	—

does not blow out. These calculations were performed with: both the IEM and modified Curl (MC) mixing models; for both Flames D and E; and with both the skeletal mechanism (SK) and the augmented reduced mechanism (ARM). The results are summarized in Table 1. At temperatures 50K below those shown in the table, the flames blow off. Hysteresis is not observed: that is, starting from a “just-blown-off” calculation, the flames re-ignite when T_{pilot} is increased by 50K.

It may be seen that there is a strong dependence in the results both on the mixing model and on the chemical mechanism. For the experimental value of $T_{pilot} = 1880\text{K}$, with the skeletal mechanism both mixing models correctly predict the flame to be burning; whereas with ARM it has blown out. For Flame E, the modified Curl calculations have (incorrectly) blown out. Clearly all combinations of mechanisms and mixing models considered here would incorrectly predict extinction for Flame F. This is in contrast to the EMST/ARM Flame F calculations of Xu & Pope (2000) and Tang et al. (2000) which show burning (with the correct amount of local extinction) with $T_{pilot} = 1870\text{K}$.

4 Physical Basis of Mixing Models

In some respects, the success of the PDF model calculations for Flames E and F is surprising, because it is not clear that the mixing models employed contain an adequate representation of the physical processes involved.

Much attention has been paid to the performance of mixing models in the context of inert scalar mixing, and many criteria for successful performance have been established. For non-premixed combustion additional criteria are appropriate. In the “flamelet regime” with little local extinction, the theory is well established (see, e.g., Peters 2000), and flamelet theory and the conditional moment closure (CMC, Klimenko and Bilger 1999) give essentially the same result. The dominant balance is between reaction and mixing, and according to CMC it is:

$$-\frac{1}{2}\langle\chi|\xi\rangle\frac{d^2\langle Y|\xi\rangle}{d\xi^2}\approx S(\xi,\langle Y|\xi\rangle), \quad (1)$$

where ξ is mixture fraction, χ is scalar dissipation, Y is the product mass fraction, and $S(\xi, Y)$ is its chemical rate of creation. In PDF methods the reaction is treated exactly, and mixing takes place at the mean rate $\langle\chi\rangle$. But the dependence of mixing on the curvature of

the conditional mean mass fraction, $d^2\langle Y|\xi\rangle/d\xi^2$ is less obvious. In the flamelet limit, the EMST model (like the mapping closure) converges to a diffusion equation similar to Eq. 1, and hence it implicitly contains this dependence. But the situation for IEM and modified Curl is less clear.

The curvature of $\langle Y|\xi\rangle$ at stoichiometric can be estimated as:

$$\left(\frac{d^2\langle Y|\xi\rangle}{d\xi^2}\right)_{\xi=\xi_s} \approx \frac{-\langle Y|\xi_s\rangle}{\xi_s(1-\xi_s)\Delta\xi_r}, \quad (2)$$

where ξ_s is the stoichiometric mixture fraction and $\Delta\xi_r$ is the width of the reaction zone in mixture-fraction space. The fuel used in the Barlow & Frank flames (1 part methane to 3 parts air) has $\xi_s \approx 0.35$ and $\Delta\xi_r \approx 0.2$. But for natural pure fuels, both ξ_s and $\Delta\xi_r$ are much smaller, and hence $|d^2\langle Y|\xi\rangle/d\xi^2|$ is much larger. It is important, therefore, to determine whether or not the modified Curl and EMST mixing models (with a fixed value of C_ϕ) can accurately predict the degree of local extinction for fuel mixtures with a range of values of ξ_s and $\Delta\xi_r$.

It is also known from theory, experiment and DNS that local extinction is associated with regions of very large scalar dissipation — e.g., values of χ more than 10 times the mean $\langle\chi\rangle$. Since neither the modified Curl model nor the EMST model explicitly models the fluctuations in χ it remains to be explained why these models are capable of describing local extinction quite accurately.

5 Future Experiments

The Barlow & Frank experiments have provided a comprehensive data base for the series of flames, A-F. In these experiments, the only parameter that is varied is the jet velocity (with the pilot velocity being kept in a fixed proportion). It would provide a valuable test of models if other parameters were varied, such as: the methane/air ratio of the fuel used in the jet; and the composition and temperature of the pilot. Measurements at just a few locations (especially at $x/D = 7.5$) would suffice.

References

- Barlow, R. S. and J. H. Frank (1998). Effects of turbulence on species mass fraction in methane/air jet flames. *Proc. Combust. Inst* 27, 1087–1095.
- Dopazo, C. and E. E. O’Brien (1974). An approach to the autoignition of a turbulent mixture. *Acta Astronaut.* 1, 1239–1266.
- Janicka, J., W. Kolbe, and W. Kollmann (1977). Closure of the transport equation for the probability density function of turbulent scalar fields. *J. Non-Equilib. Thermodyn* 4, 47–66.

- Klimenko, A. Y. and R. W. Bilger (1999). Conditional moment closure for turbulent combustion. *Prog. Energy Combust. Sci.* 25, 595–687.
- Lindstedt, R. P., S. A. Louloudi, and E. M. Váos (2000). Joint scalar probability density function modeling of pollutant formation in piloted turbulent jet diffusion flames with comprehensive chemistry. *Proc. Combust. Inst* 28, 149–156.
- Peters, N. (2000). *Turbulent Combustion*. Cambridge University Press.
- Subramaniam, S. and S. B. Pope (1998). A mixing model for turbulent reactive flows based on Euclidean minimum spanning trees. *Combust. Flame* 115, 487–514.
- Tang, Q., J. Xu, and S. B. Pope (2000). Probability density function calculations of local extinction and NO production in piloted-jet turbulent methane/air flames. *Proc. Combust. Inst* 28, 133–139.
- Villiermaux, J. and J. C. Devillon (1972). Représentation de la coalescence et de la re-dispersion des domaines de ségrégation dans un fluide par un modèle d’interaction phénoménologique. In *Proceedings of the 2nd International Symposium on Chemical Reaction Engineering*, New York, pp. 1–13. Elsevier.
- Xu, J. and S. B. Pope (2000). PDF calculations of turbulent nonpremixed flames with local extinction. *Combust. Flame* 123, 281–307.

Discussion on:
Mixing Model Performance
in the Calculation of Nonpremixed
Piloted Jet Flames

Stephen B. Pope
Cornell University

TNF6, Sapporo, Japan

July 18, 2002

Discussion Outline

- Nonpremixed piloted jet flames
- Review of calculations at TNF5
- Review of mixing models
- Calculations for TNF6
 - Lindstedt
 - Pope & Goldin
 - ...
- Physical basis of mixing models
- Conclusions, Questions, Suggestions

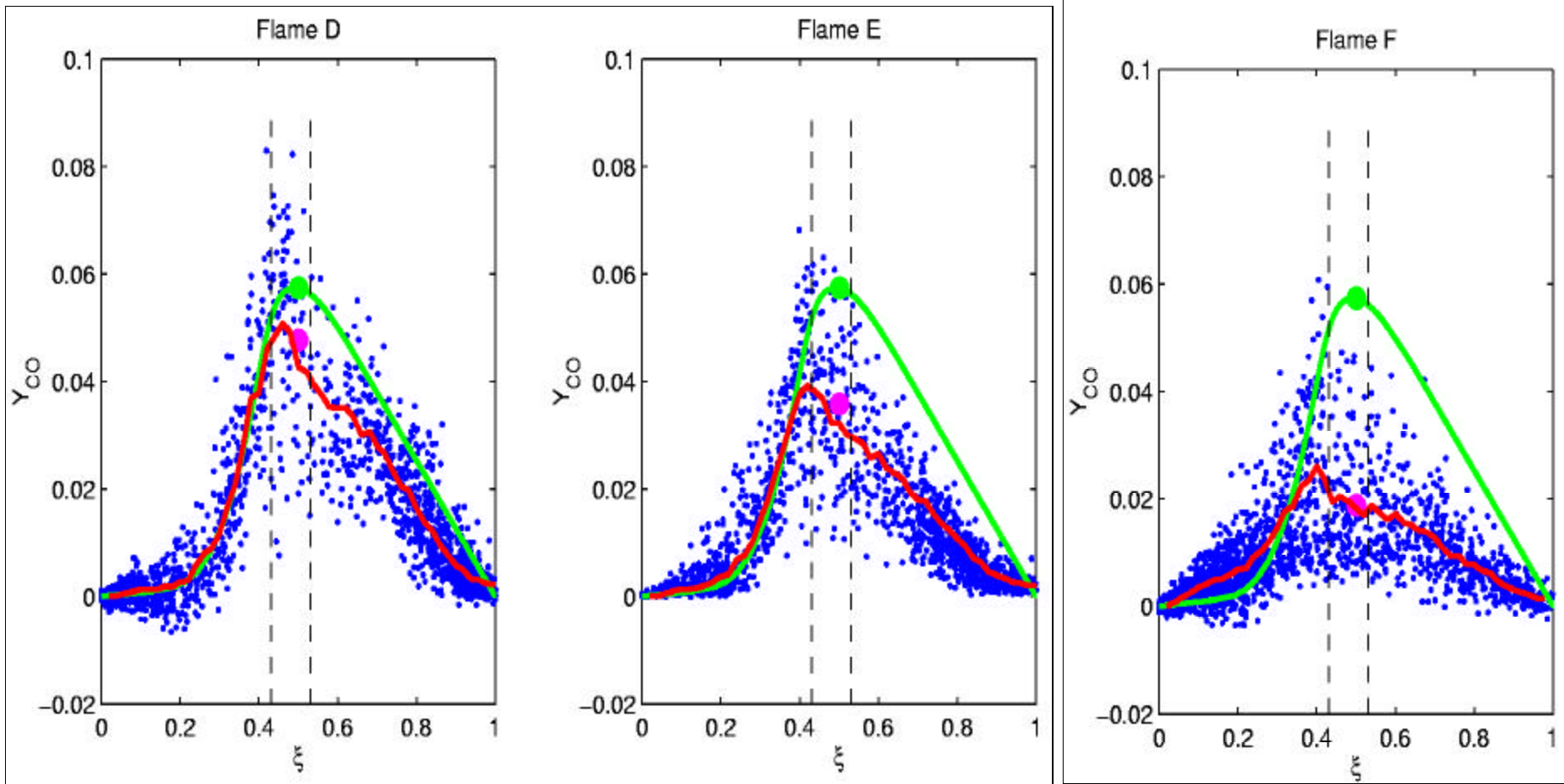
Barlow & Frank Experiment



- Sydney burner
 - Jet: 25% CH₄, 75% air
 - Pilot: $\Phi = 0.77$

Flame	U_{jet} (m/s)	U_{pilot} (m/s)
D	49.6	11.4
E	74.4	17.1
F	99.2	22.8

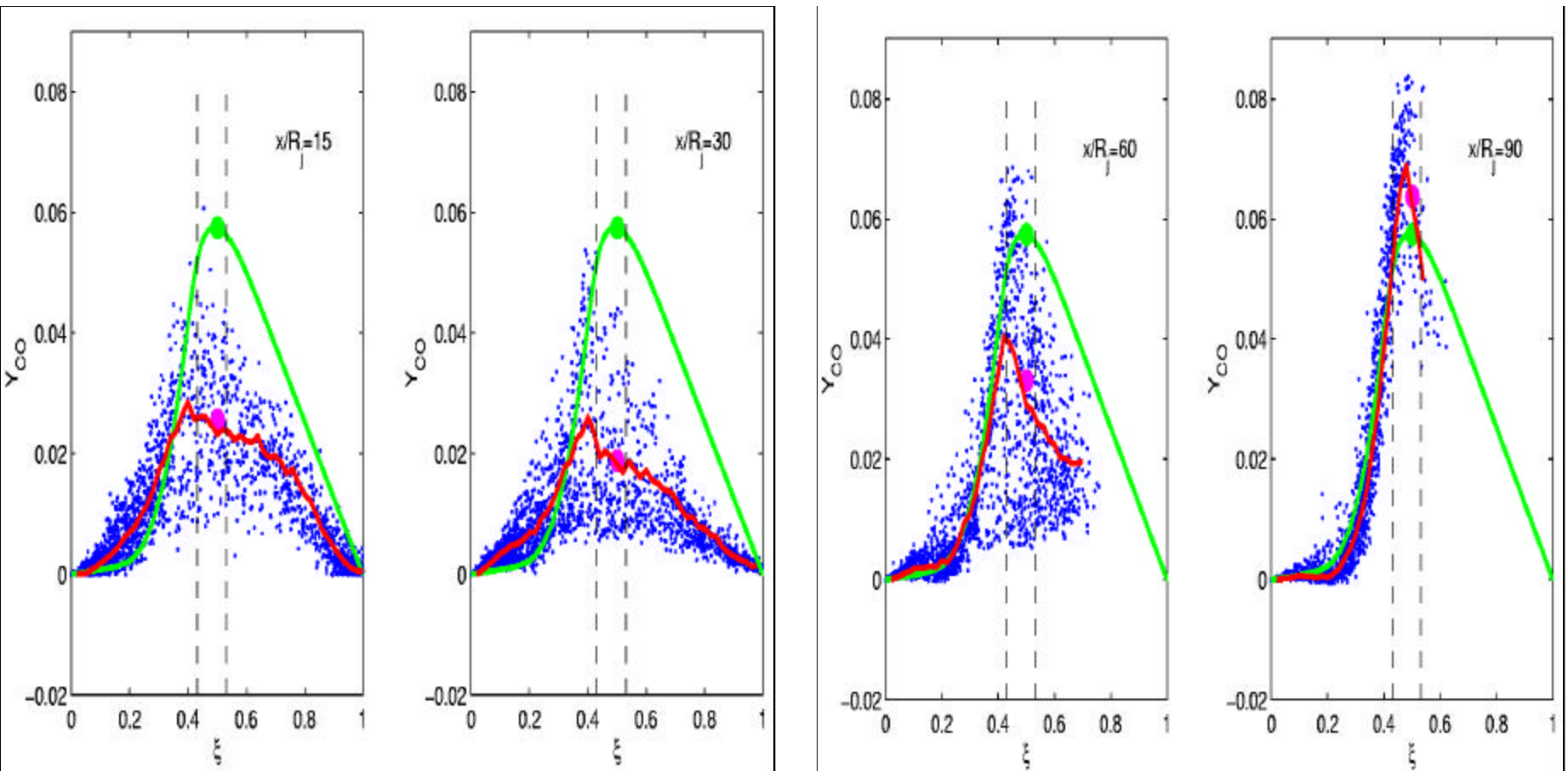
Scatter Plots of CO vs. ξ : Effect of Jet Velocity ($x/D=15$)



Barlow & Frank (1998)

- conditional mean
- laminar flamelet ($a=100s^{-1}$)

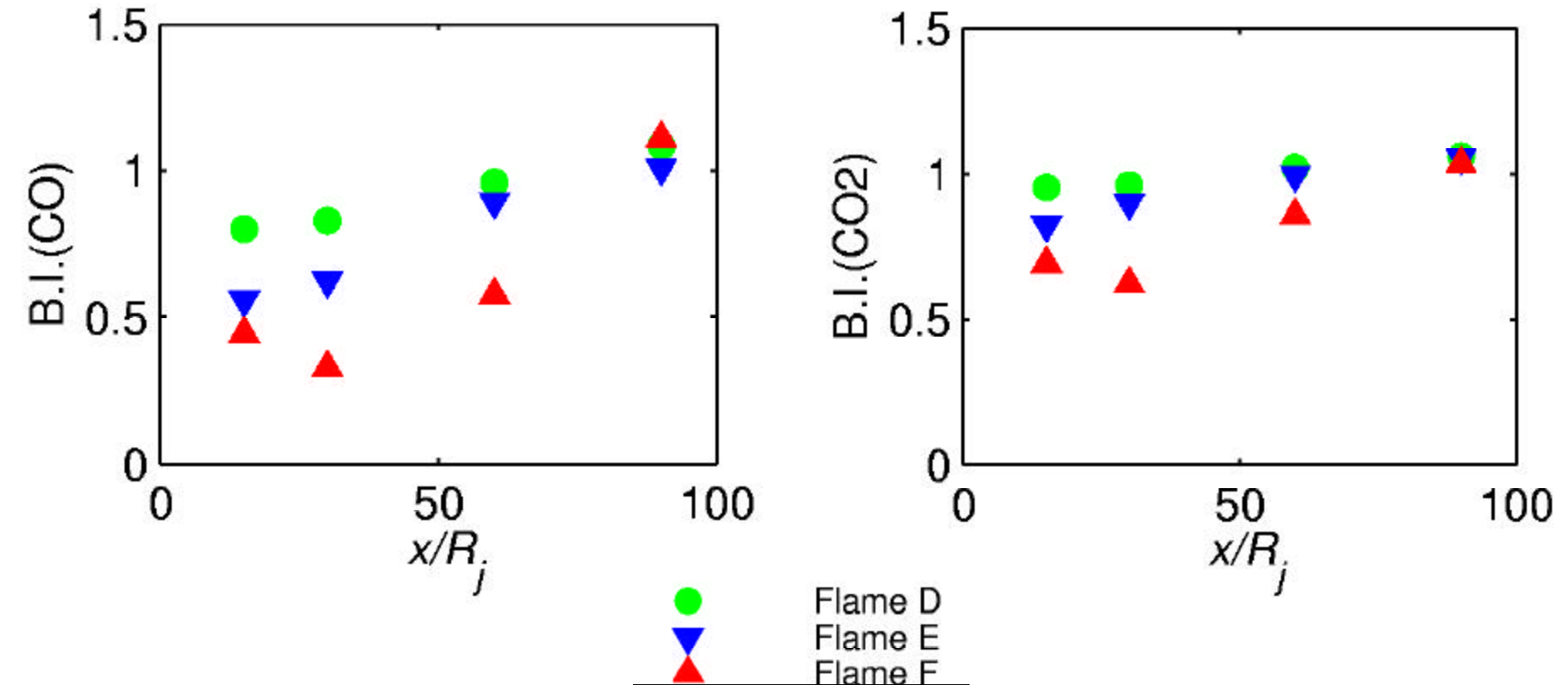
Scatter Plots of CO vs. ξ : Axial Development for Flame F



Barlow & Frank (1998)

- conditional mean
- laminar flamelet ($a=100s^{-1}$)

Burning Index vs. x/R_j : CO and CO₂



Barlow & Frank (1998)

Xu & Pope (2000)

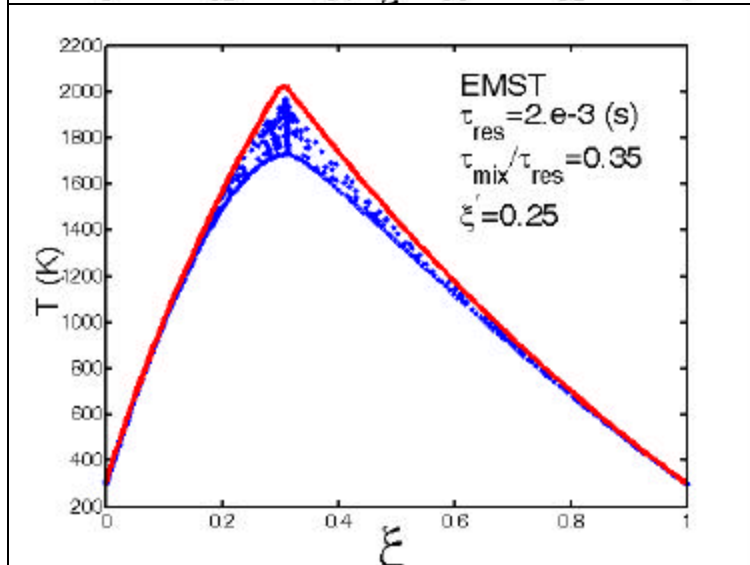
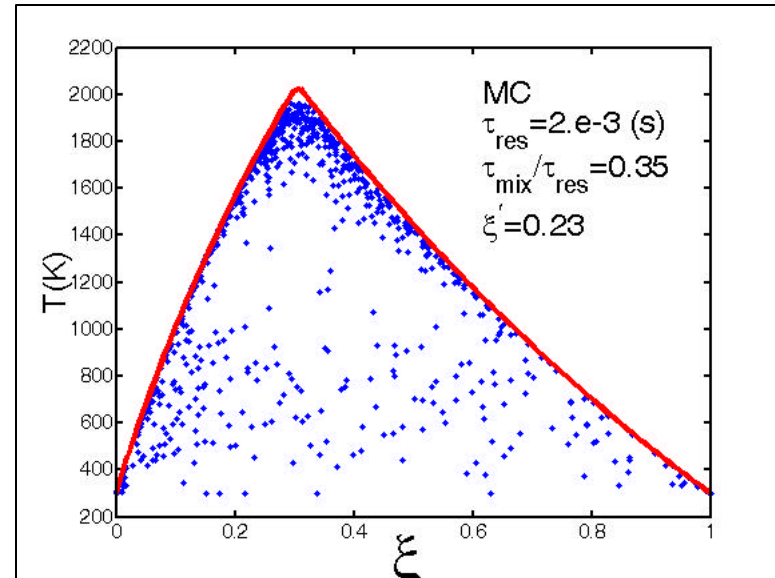
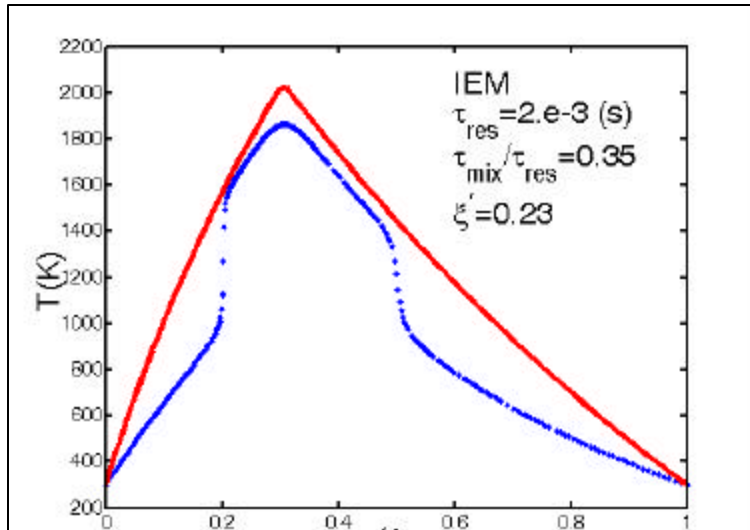
Review of TNF5 Calculations

- Several approaches successful for Flame D
- Flame F calculations:
 - J.-Y. Chen (Berkeley) Comp. PDF, 13-step ARM, modified Curl mixing model (MC)
 - Lindstedt et al. (Imperial), Comp. PDF, 16-species ARM, MC
 - Tang et al. (Cornell) Vel.-Comp. PDF, 16/19-species ARM, EMST mixing model

Mixing Models in PDF Methods

- Following a fluid particle, species mass fractions change due to:
 - Reaction
 - Mixing (molecular diffusion)
- Relevant mixing models
 - IEM/LMSE (Villermaux & Devillon 1972, Dopazo & O'Brien 1974)
 - Modified Curl (MC, Janicka et al. 1977)
 - Euclidean minimum spanning tree (EMST, Subramaniam & Pope 1998)
- Does it make a difference?

Qualitatively Different Behavior of Mixing Models



H_2 /air Pasr test case.
See Ren, Tang & Pope poster

Effect of Mixing

- Decreases scalar variance:

$$\frac{\partial \langle \mathbf{x}'^2 \rangle}{\partial t} \dots = \dots - C_f \frac{\mathbf{e}}{k} \langle \mathbf{x}'^2 \rangle = \dots - \langle \mathbf{c} \rangle$$

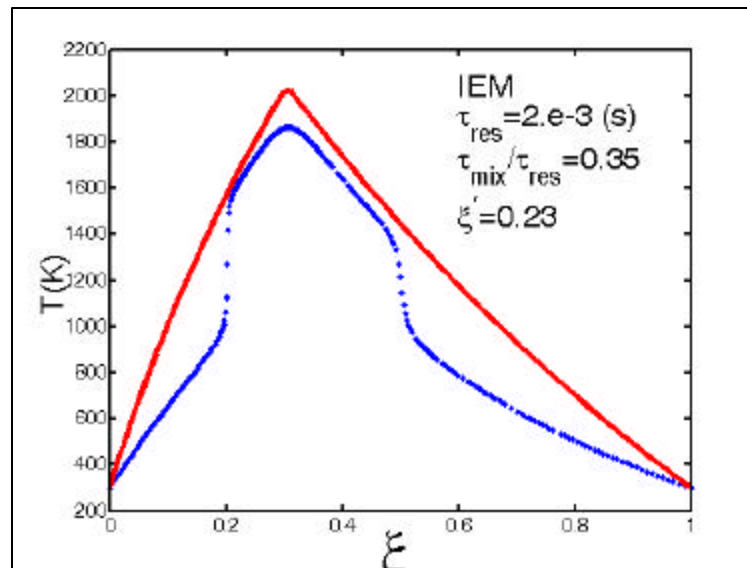
- Affects PDF shape
- Understand in terms of effect on stochastic particle composition

IEM/LMSE

- Particle composition relaxes to the mean:

$$\frac{d\mathbf{f}}{dt} = -\frac{1}{2} C_f \frac{\mathbf{e}}{k} (\mathbf{f} - \langle \mathbf{f} \rangle)$$

- PDF contracts, but its shape does not change

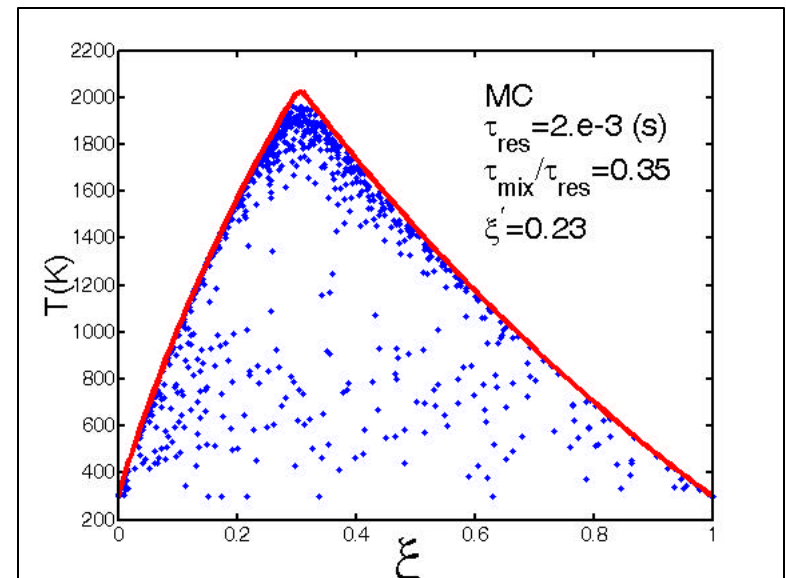


Modified Curl (MC)

- From the ensemble of N particles, pairs of particles (denoted by p and q) are randomly selected at a rate proportional to $NC_f \frac{e}{k}$
- The particles instantly change their composition to:

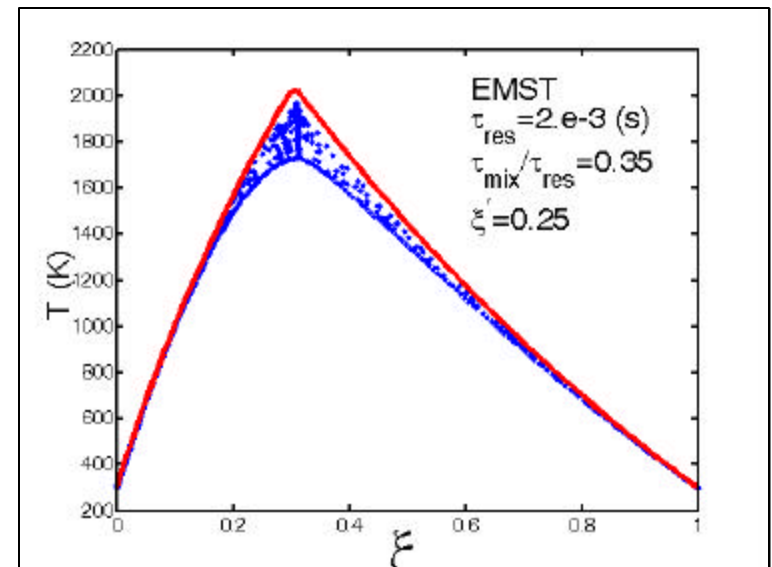
$$\mathbf{f}_{new}^{(p)} = u \mathbf{f}^{(p)} + (1-u) \mathbf{f}^{(q)}$$

where u is random,
uniform in $(0,1)$



Euclidean Minimum Spanning Tree (EMST)

- In the composition space, each particle is connected to one or more neighboring particles by an “edge”, such that the sum of the lengths of the edges is minimized
- The particle composition relaxes towards its neighbors’ composition



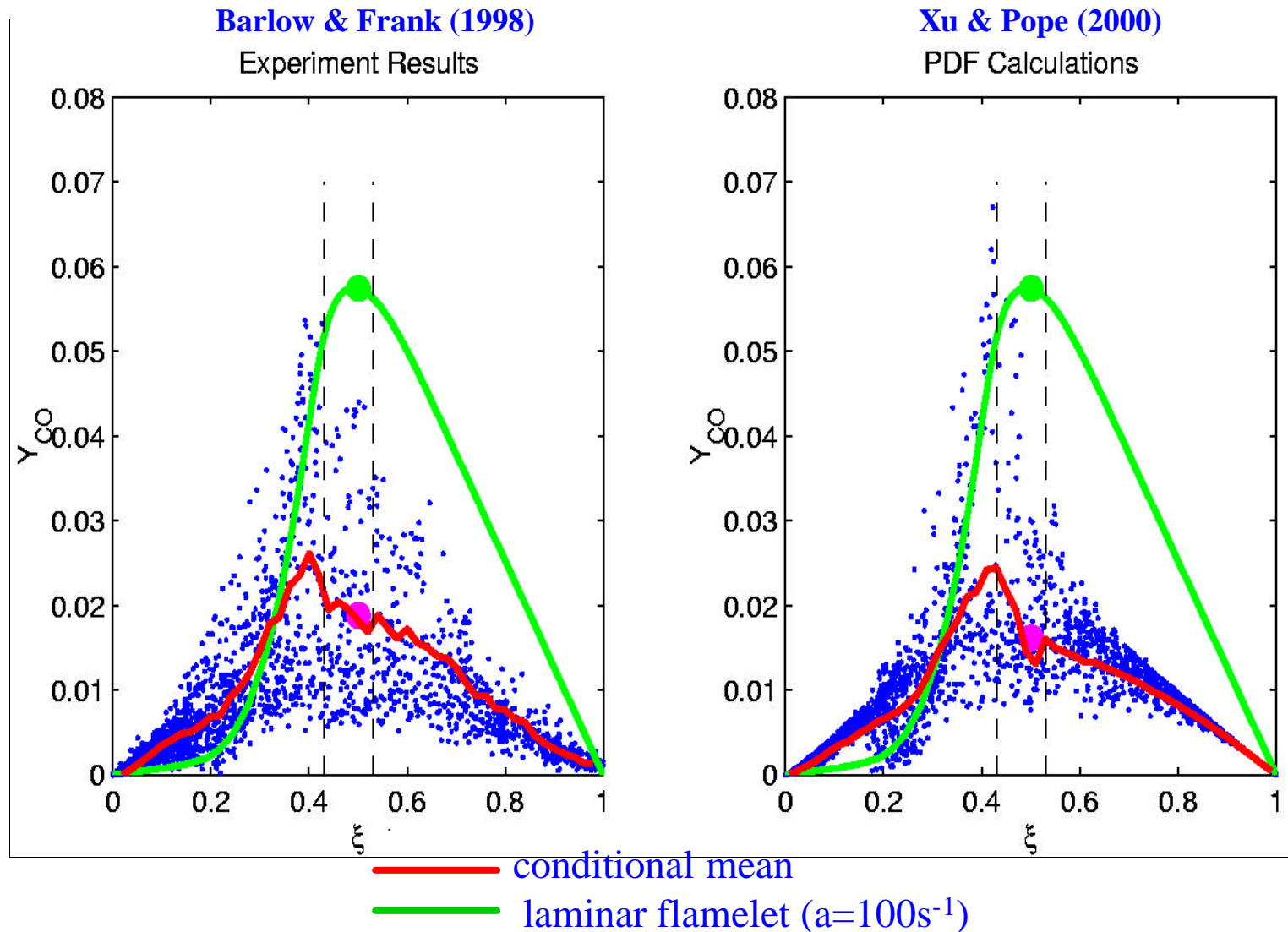
Performance of Mixing Models

	IEM	MC	EMST
Conservation of means	Yes	Yes	Yes
Decay of variances	Yes	Yes	Yes
Boundedness	Yes	Yes	Yes
Linearity and independence	Yes	Yes	No
Relaxation to Gaussian	No	No	No
Numerical convergence	Yes	Yes/No	No
Localness	No	No	Yes
Flamelet limit	No	No	Yes

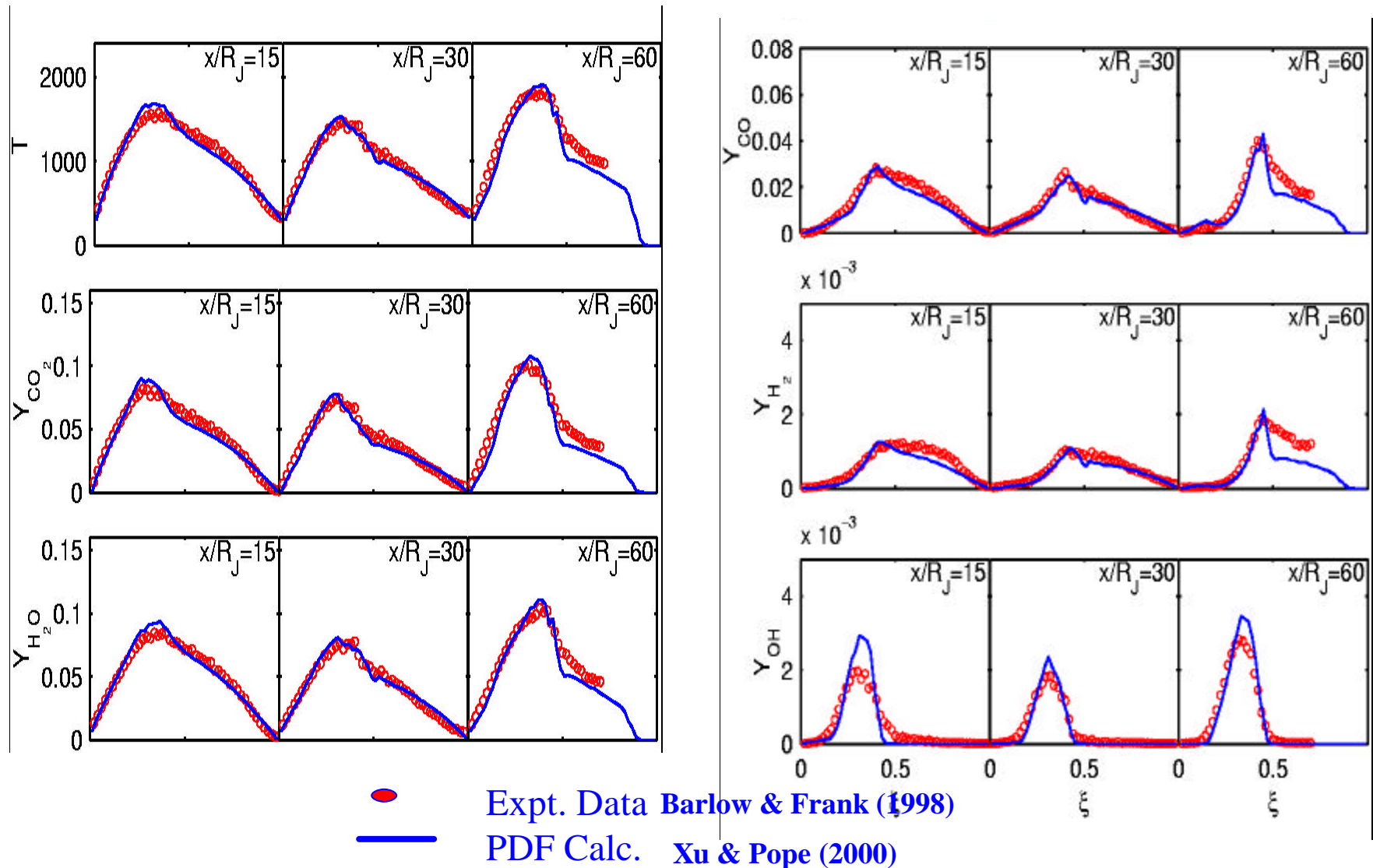
Flame F Calculations from TNF5

- Berkeley, Imperial, Cornell
- Only “good” results shown
- Need to understand each models’ limits and shortcomings
- Example: Tang, Xu & Pope
 - Vel.-Freq-Comp. PDF
 - EMST
 - ARM/ISAT

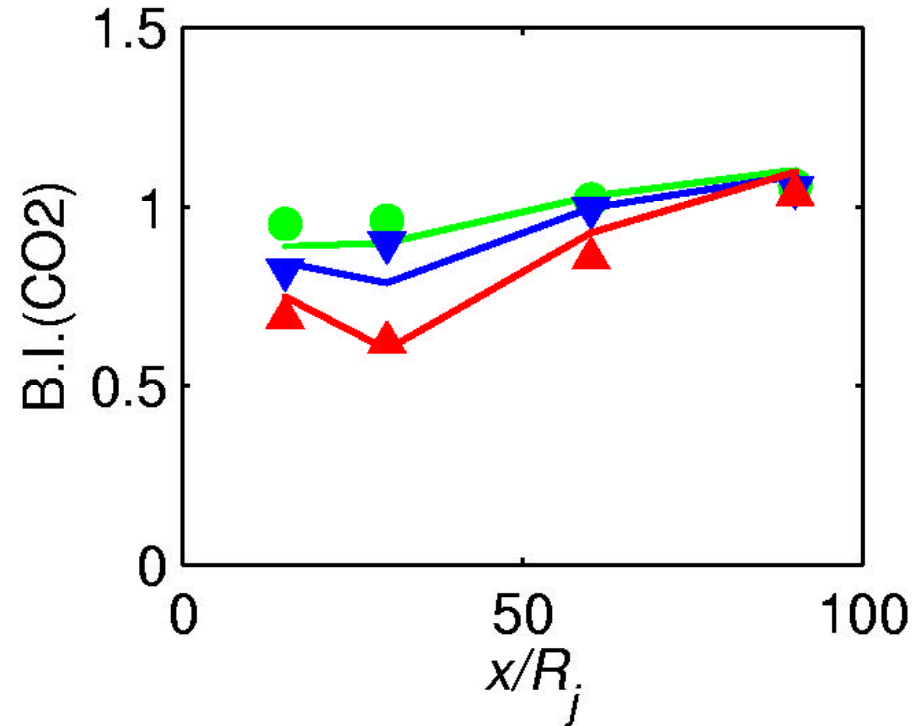
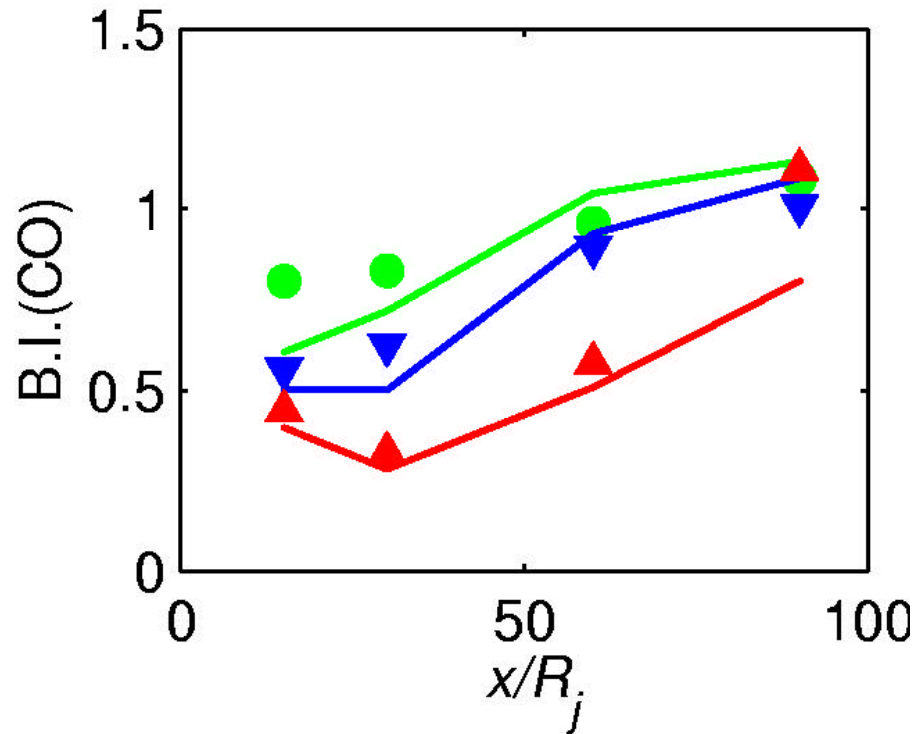
Flame F: Scatter Plots of CO vs. ξ at $x/D = 15$, Expt. and PDF Calc.



Conditional Means in Flame F



Burning Index vs. x/R_j : CO and CO₂



Symbols, Expt. Barlow & Frank (1998)
Lines, PDF Calcs. Xu & Pope (2000)

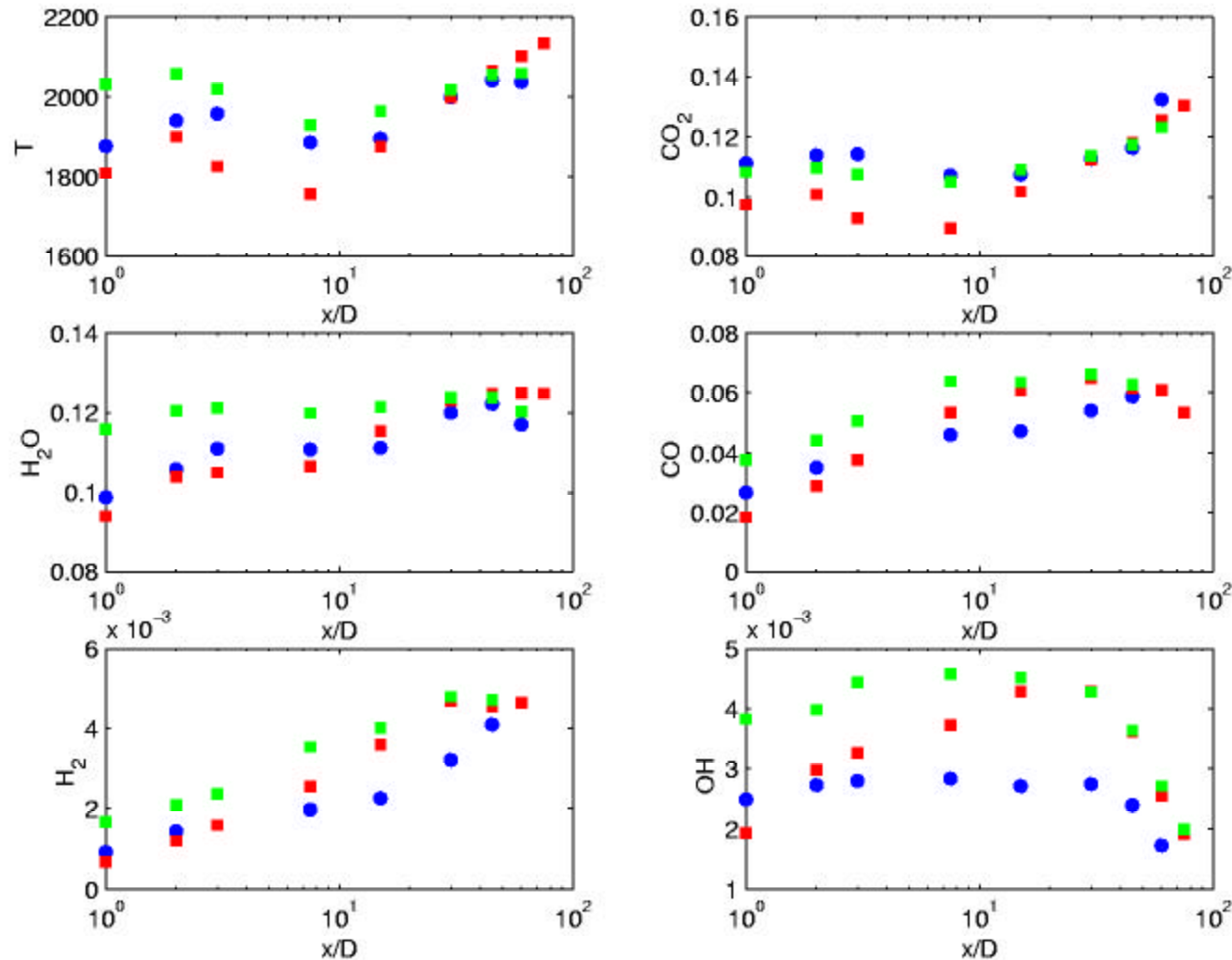
Recent Calculations

- Lindstedt
 - Effect of C_f
 - IEM vs. MC
- Pope & Goldin
 - MC/IEM
 - ARM/skeletal
-

TNF6 Pope & Goldin

- Composition PDF
- Flames D and E
- IEM/MC $C_f = 2.0$
- 16-species C_1 skeletal/ARM

Means Conditional on Stoichiometric in Flame D



Expt. Data

MC

IEM

Minimum Pilot Temperature for Burning Flame

Measured temperature is 1880(K)

	SK/MC	SK/IEM	ARM/IEM
Flame D	1830	1730	2130
Flame E	1930	1880	-

Exit-plane temperature may be 45(K) higher

Physical Basis: Flamelet Limit

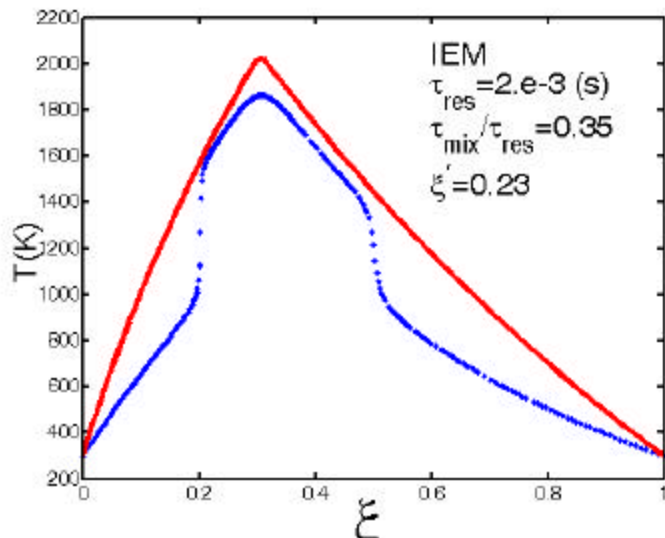
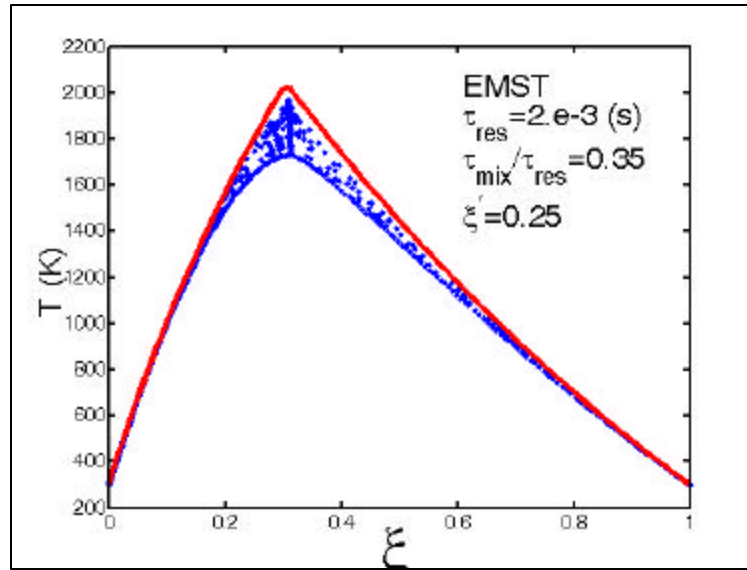
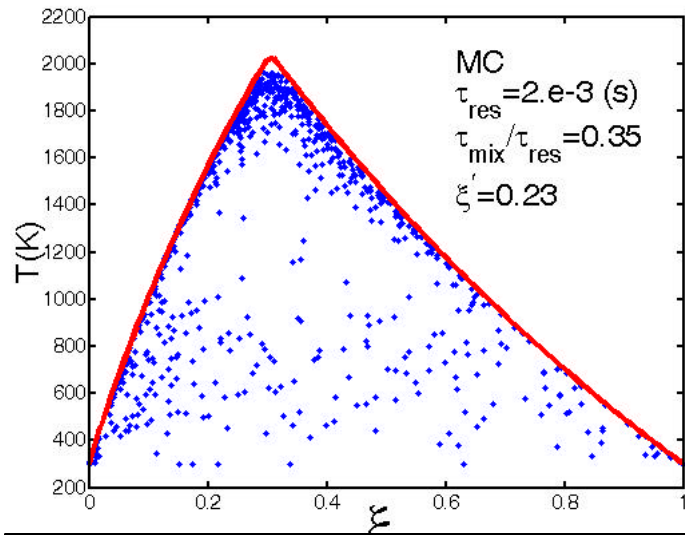
- Flamelet regime, little local extinction
- Dominant balance between reaction and mixing:
e.g., CMC

$$-\frac{1}{2}\langle \mathbf{c} | \mathbf{x} \rangle \frac{d^2 \langle Y | \mathbf{x} \rangle}{d\mathbf{x}^2} \approx S(\mathbf{x}, \langle Y | \mathbf{x} \rangle)$$

$$\left(\frac{d^2 \langle Y | \mathbf{x} \rangle}{d\mathbf{x}^2} \right)_{\mathbf{x}=\mathbf{x}_s} \approx \frac{-\langle Y | \mathbf{x}_s \rangle}{\mathbf{x}_s (1 - \mathbf{x}_s) \Delta \mathbf{x}_R}$$

- Do mixing models contain the correct dependence on \mathbf{x}_s and $\Delta \mathbf{x}_R$?

Qualitatively Different Behavior of Mixing Models



H₂/air Pasr test case.
See Ren, Tang & Pope poster

Comparison of Flame D Fuel and Methane

■ Flame D

$$\mathbf{x}_s = 0.35, \Delta \mathbf{x}_R = 0.2:$$

$$1 / [\mathbf{x}_s (1 - \mathbf{x}_s) \Delta \mathbf{x}_R] = 22$$

■ Methane

$$\mathbf{x}_s = 0.05, \Delta \mathbf{x}_R = 0.03:$$

$$1 / [\mathbf{x}_s (1 - \mathbf{x}_s) \Delta \mathbf{x}_R] = 700$$

Physical Basis: Intermittency of Scalar Dissipation

- Experiments, DNS and theory show that local extinction is associated with regions of very large scalar dissipation, e.g., 10 times the mean
- Existing mixing models do not explicitly represent the distribution of scalar dissipation
- Conditional scalar dissipation in exact PDF equation:

$$\left\langle D \frac{\partial \mathbf{f}_a}{\partial x_i} \frac{\partial \mathbf{f}_b}{\partial x_i} \mid \mathbf{f} = \mathbf{y} \right\rangle$$

Conclusions

- Need to consider “mixing model/chemical mechanism” combination
- Increasing C_f decreases local extinction
- Flame F (close to blow off) is very sensitive to T_{pilot} and C_f
- All current mixing models have unsatisfactory aspects

Questions

- What ingredient in Lindstedt's mechanism delays global extinction?
- Does the special fuel in the Barlow & Frank flames make their modelling relatively easy?
- Is the good performance of MC and EMST maintained in flames with smaller values of the stoichiometric mixture fraction?

Suggestions

■ Future experiments

- ❑ Vary parameters
 - Fuel mixture
 - Pilot composition/temperature
- ❑ Focus on conditional means at $x/D=7.5$ and 15

■ Calculations

- ❑ Continue systematic study of mechanisms and mixing models
- ❑ Make EMST available
- ❑ Make mechanisms available
- ❑ Relate calculations to measured joint composition and composition gradients
- ❑ Develop a satisfactory mixing model!

Contribution on Mixing Models from R. P. Lindstedt

(Notes by R. Barlow)

Nine vugraphs follow, which show variation in computed results for the piloted CH₄/air flames with changes in parameters of the mixing model:

1. Effect of C_ϕ on conditional means in flame F at $x/d=15$
2. Effect of C_ϕ on conditional means in flame F at $x/d=15$
3. Effect of C_ϕ on conditional means in flame F at $x/d=15$

Results show high sensitivity to the value of C_ϕ as the flame approaches extinction. Re-ignition is also highly sensitive to C_ϕ .

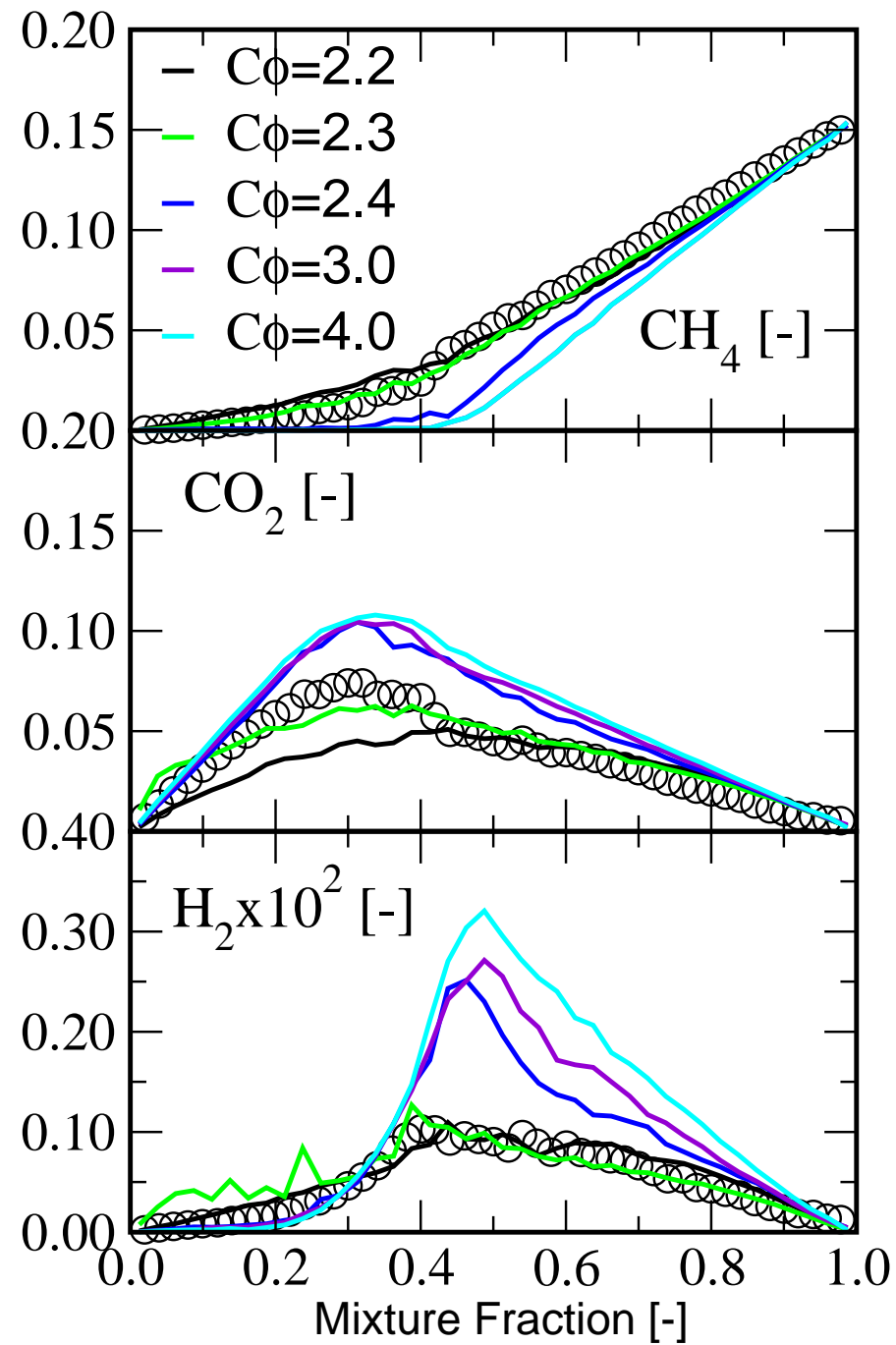
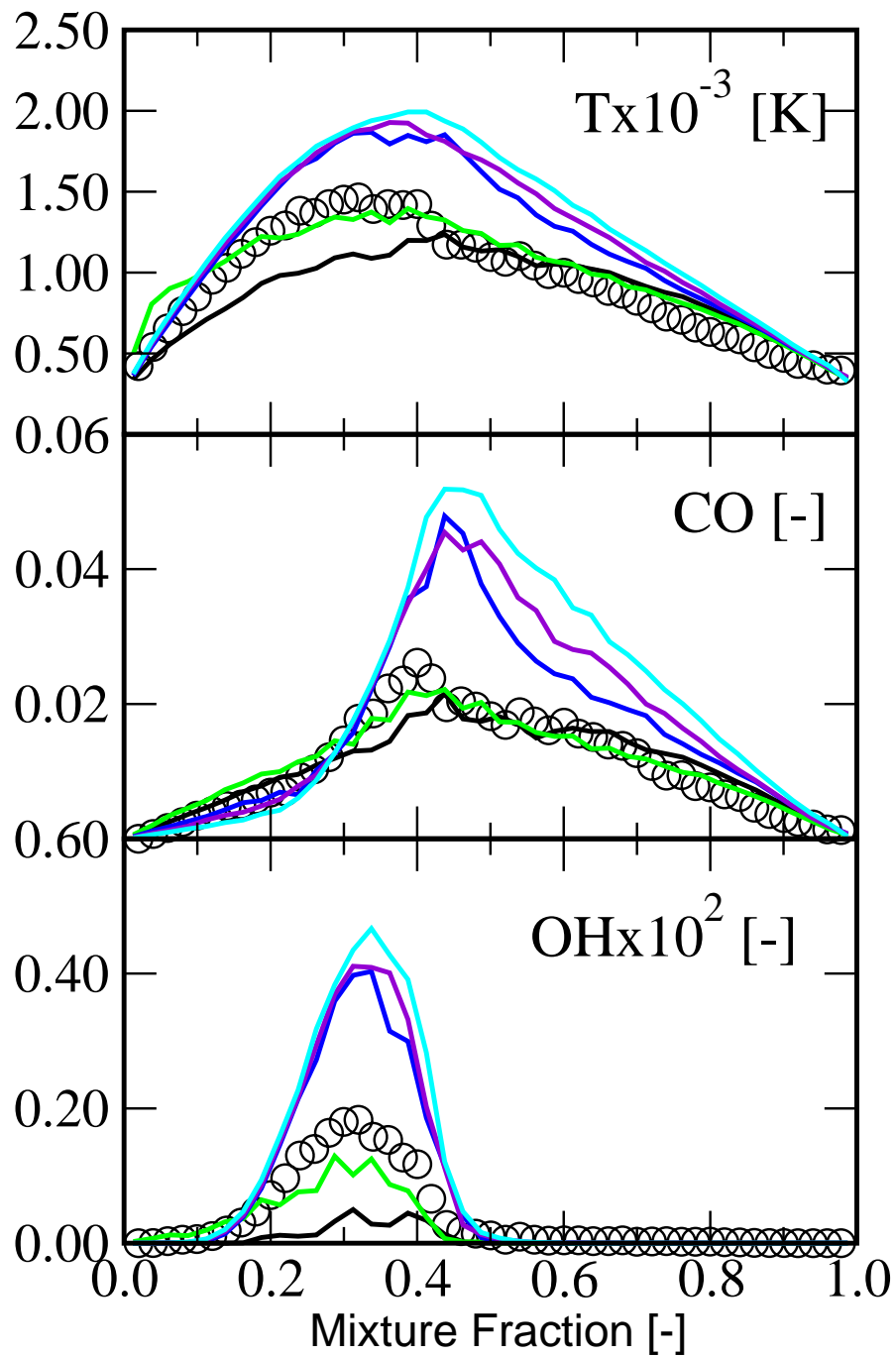
4. Curl vs. LMSE in flame D at $x/d=15$
5. Curl vs. LMSE in flame D at $x/d=30$
6. Curl vs. LMSE in flame D at $x/d=45$

In flame D the differences between results using the Curl and LMSE mixing models are most obvious for the mass fractions of CO and H₂ in fuel rich conditions. Differences decrease with downstream distance and are minor at $x/d=45$.

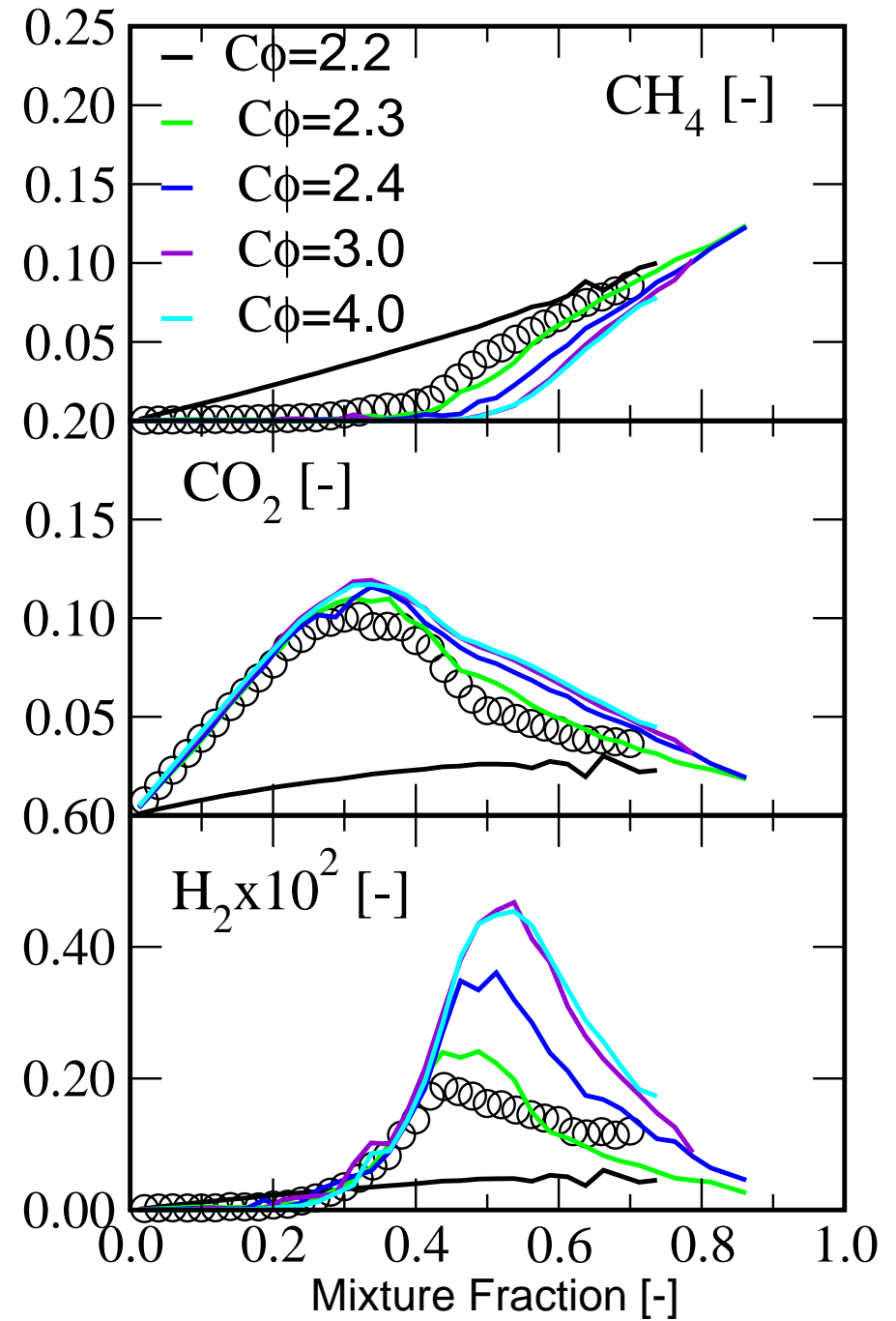
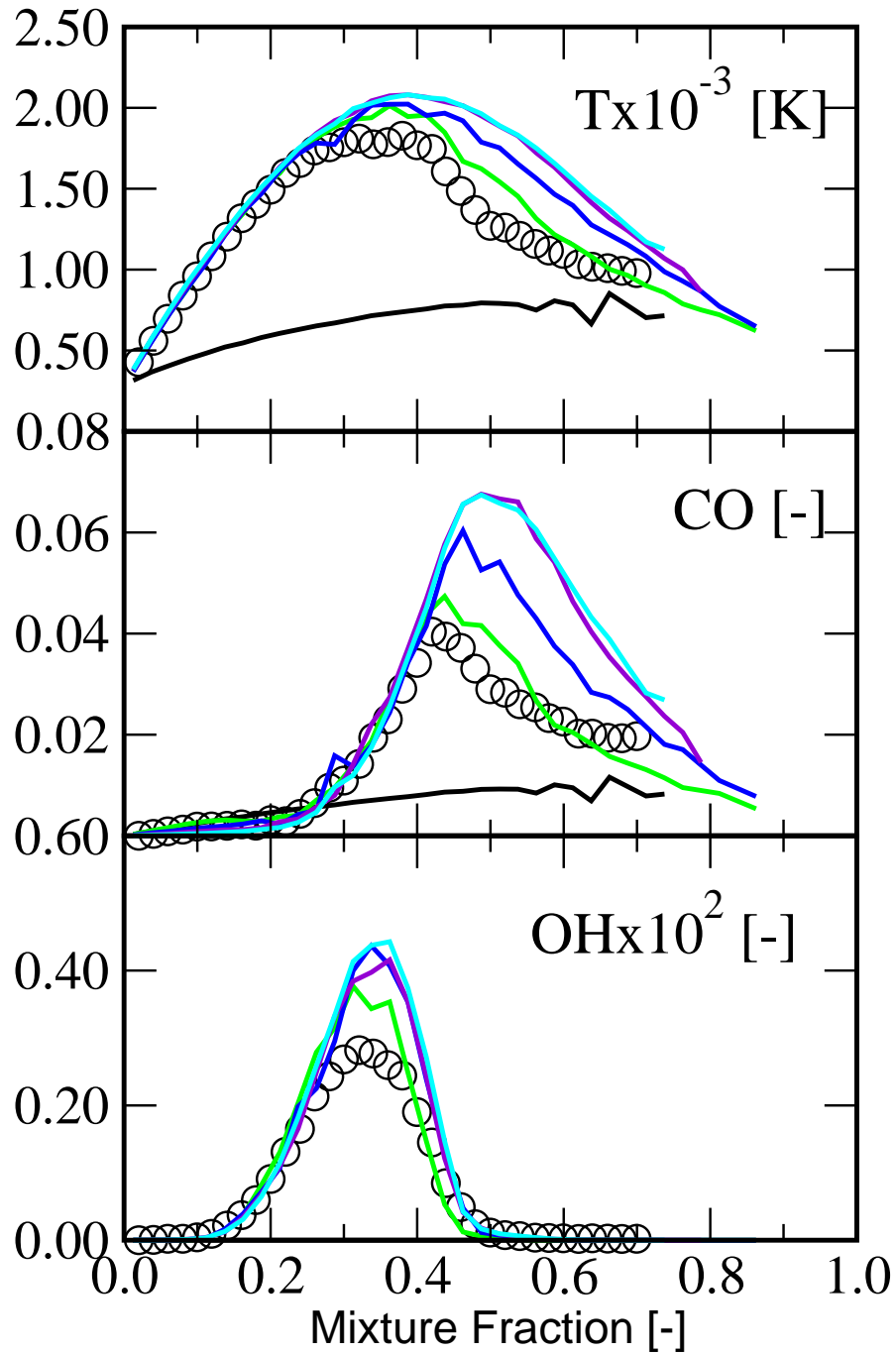
7. Curl vs. LMSE in flame F at $x/d=15$
8. Curl vs. LMSE in flame F at $x/d=30$
9. Curl vs. LMSE in flame F at $x/d=45$

Much greater differences are observed between the Curl and LMSE results for flame F than for flame D.

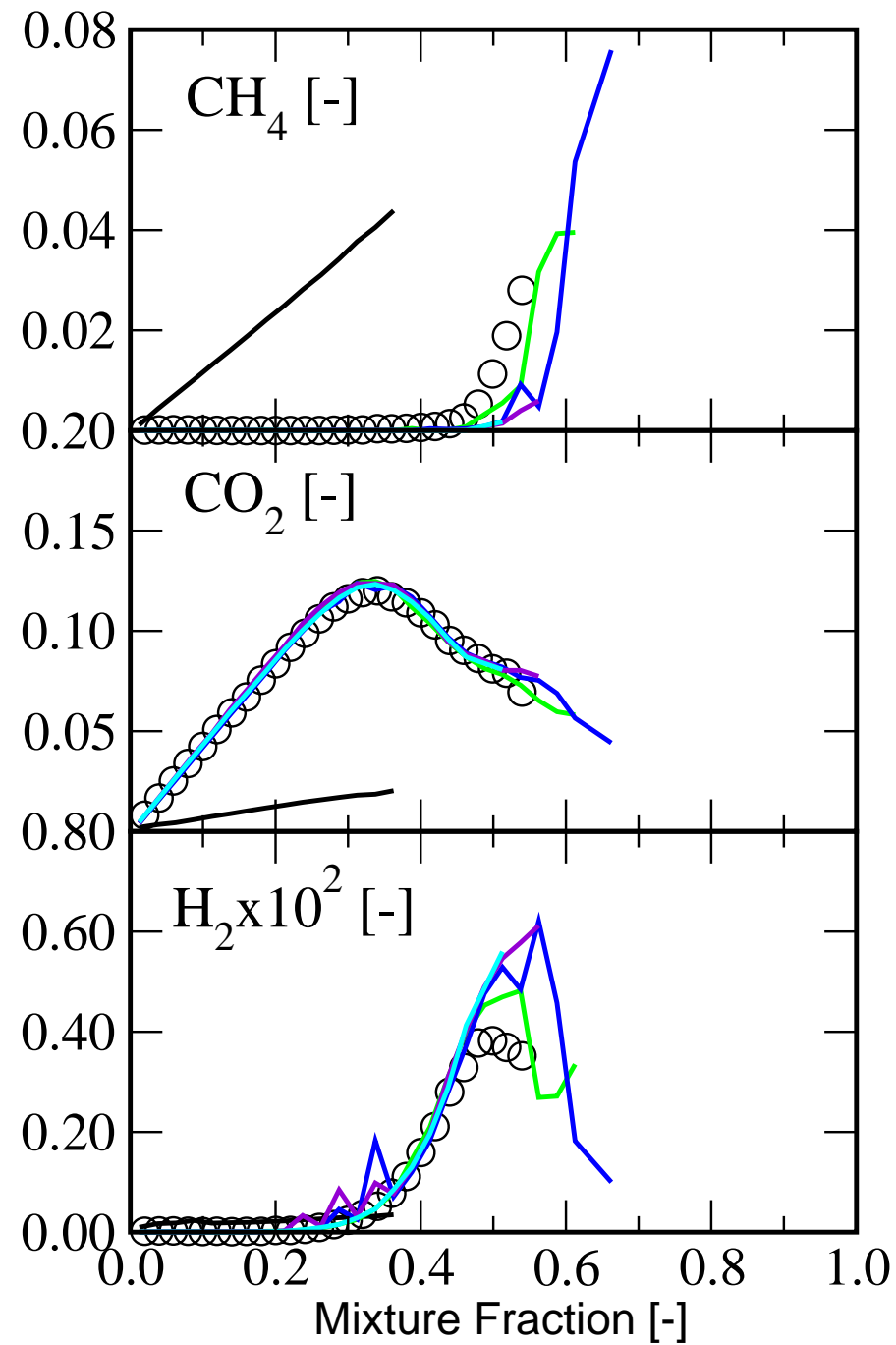
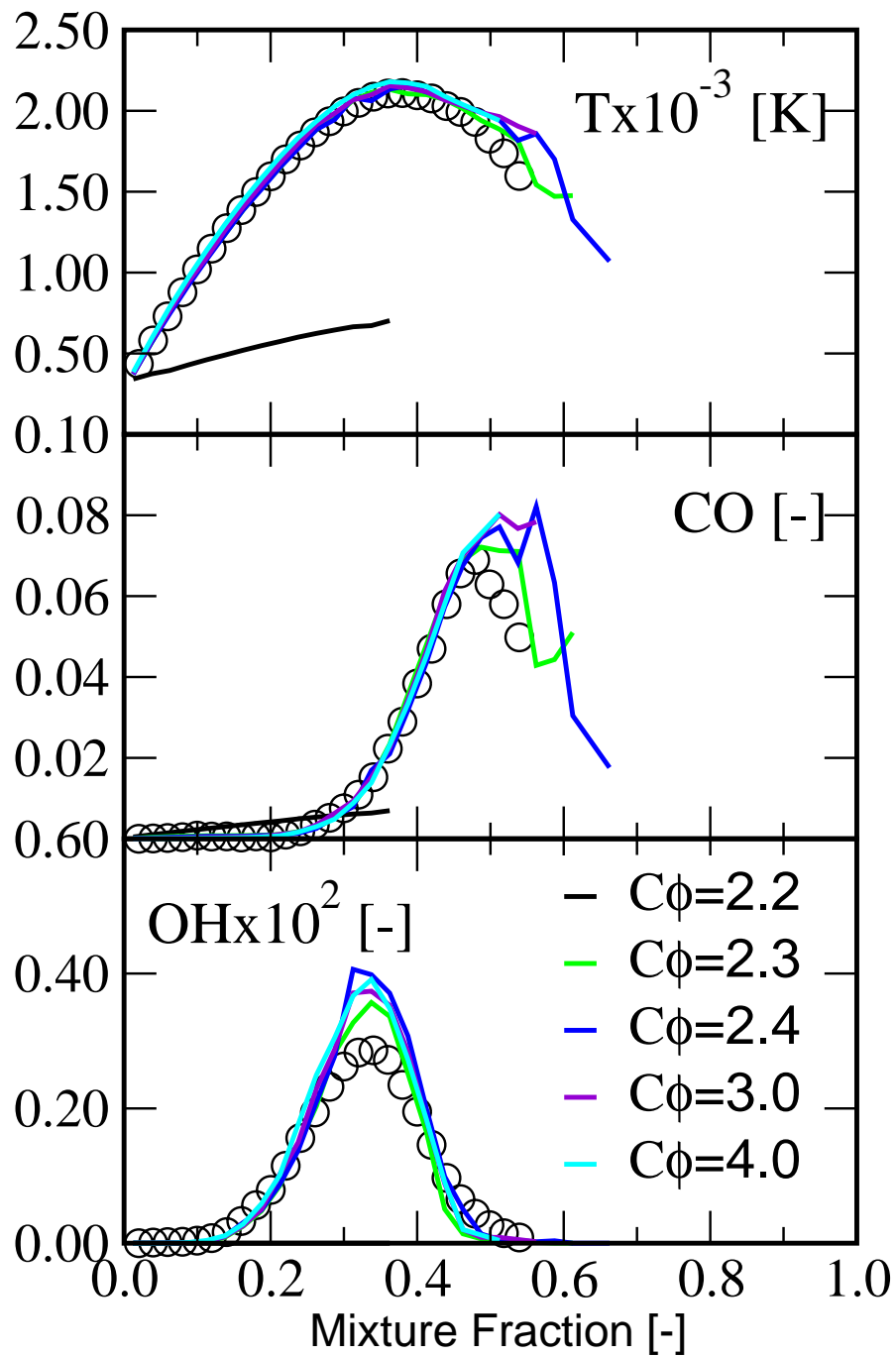
Piloted Flame F: Conditional Averages at $x/D=15$



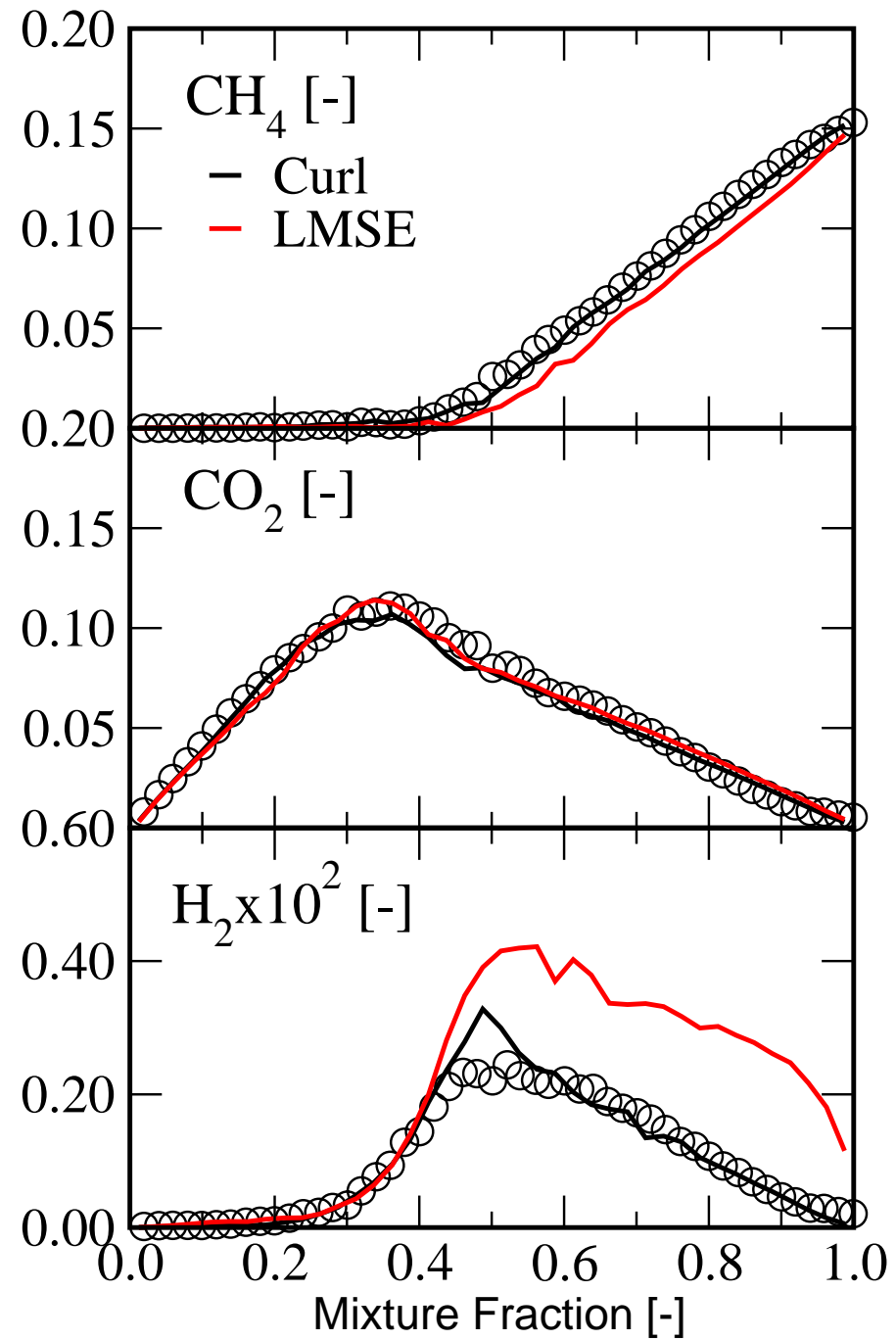
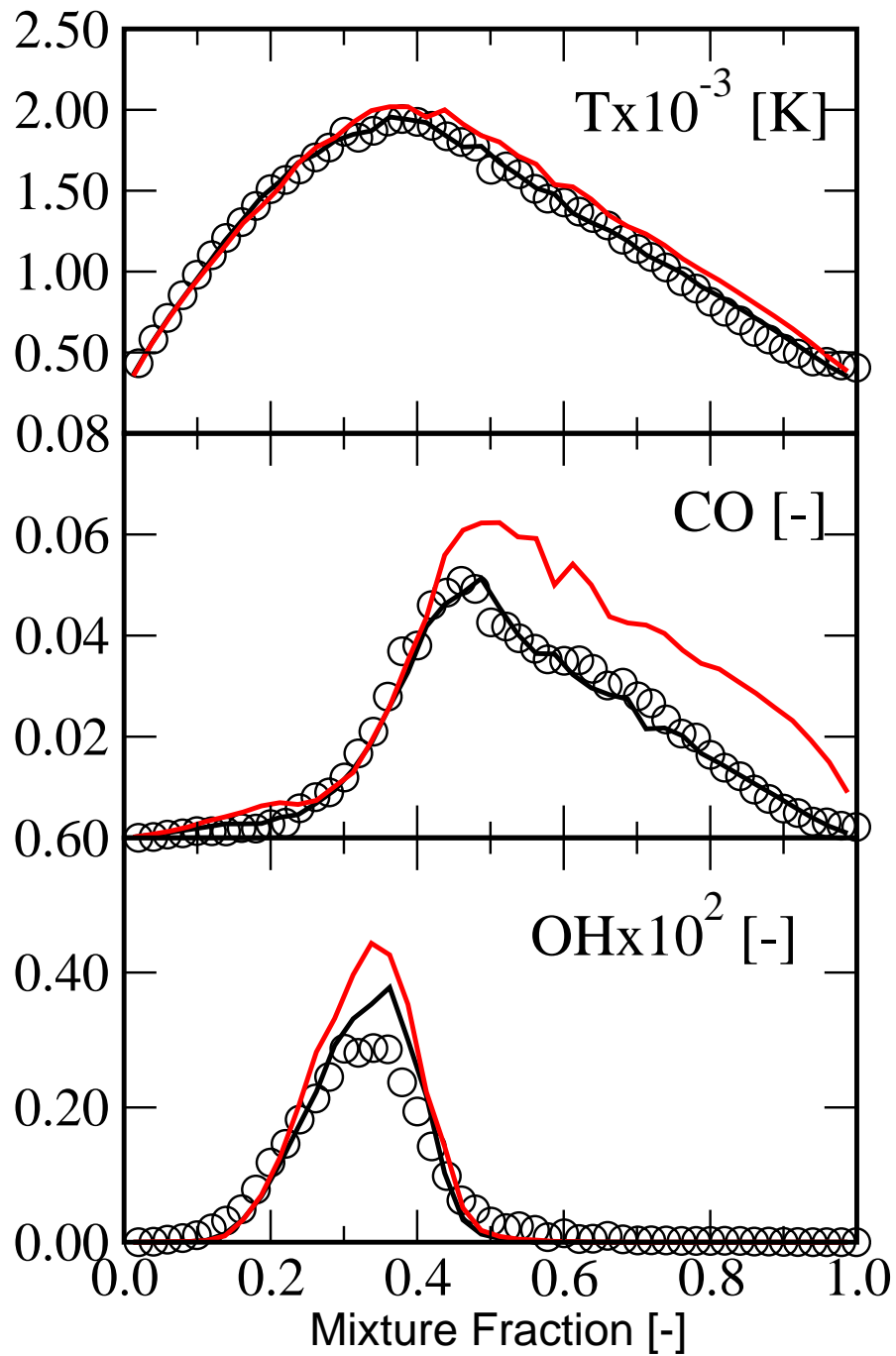
Piloted Flame F: Conditional Averages at $x/D=30$



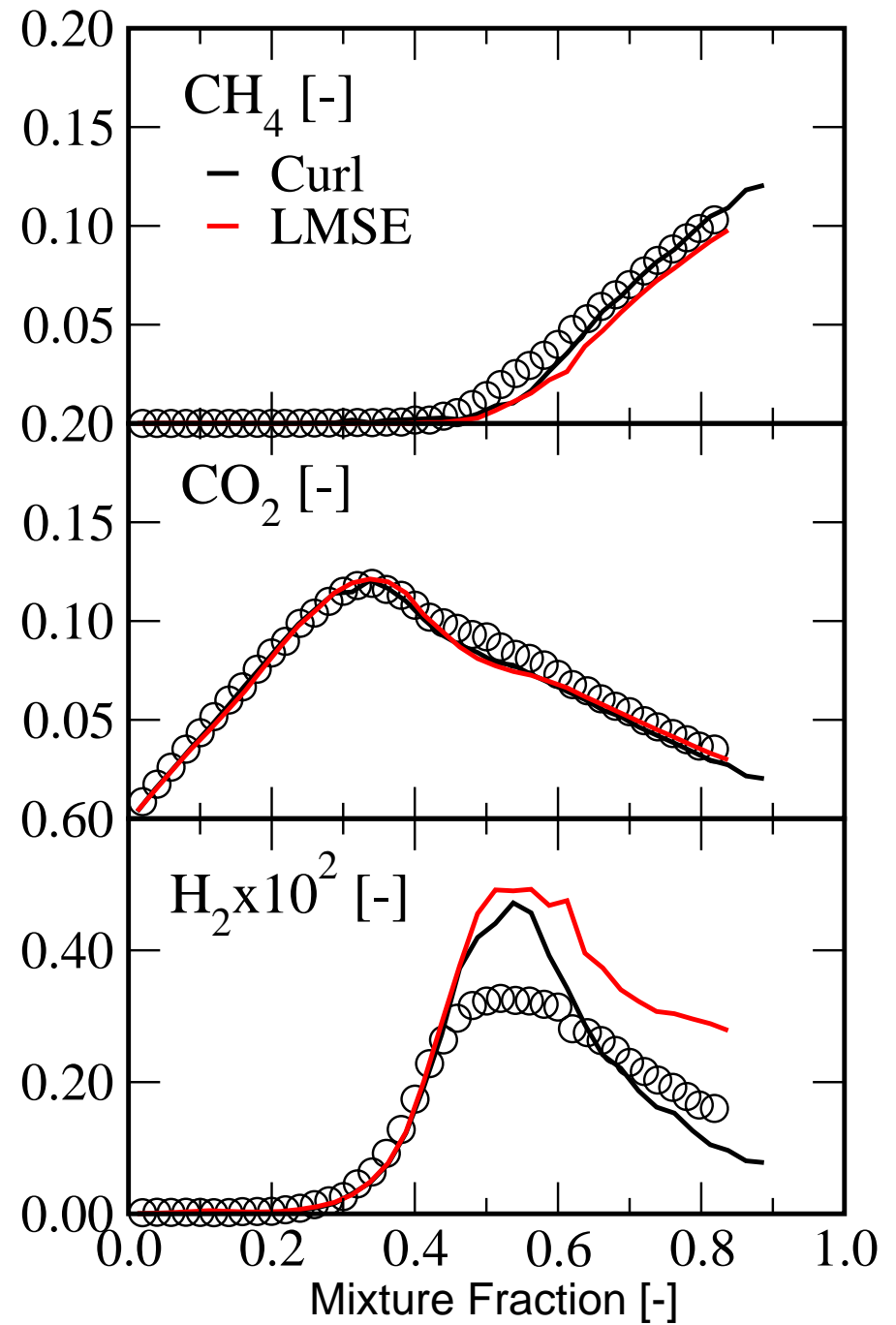
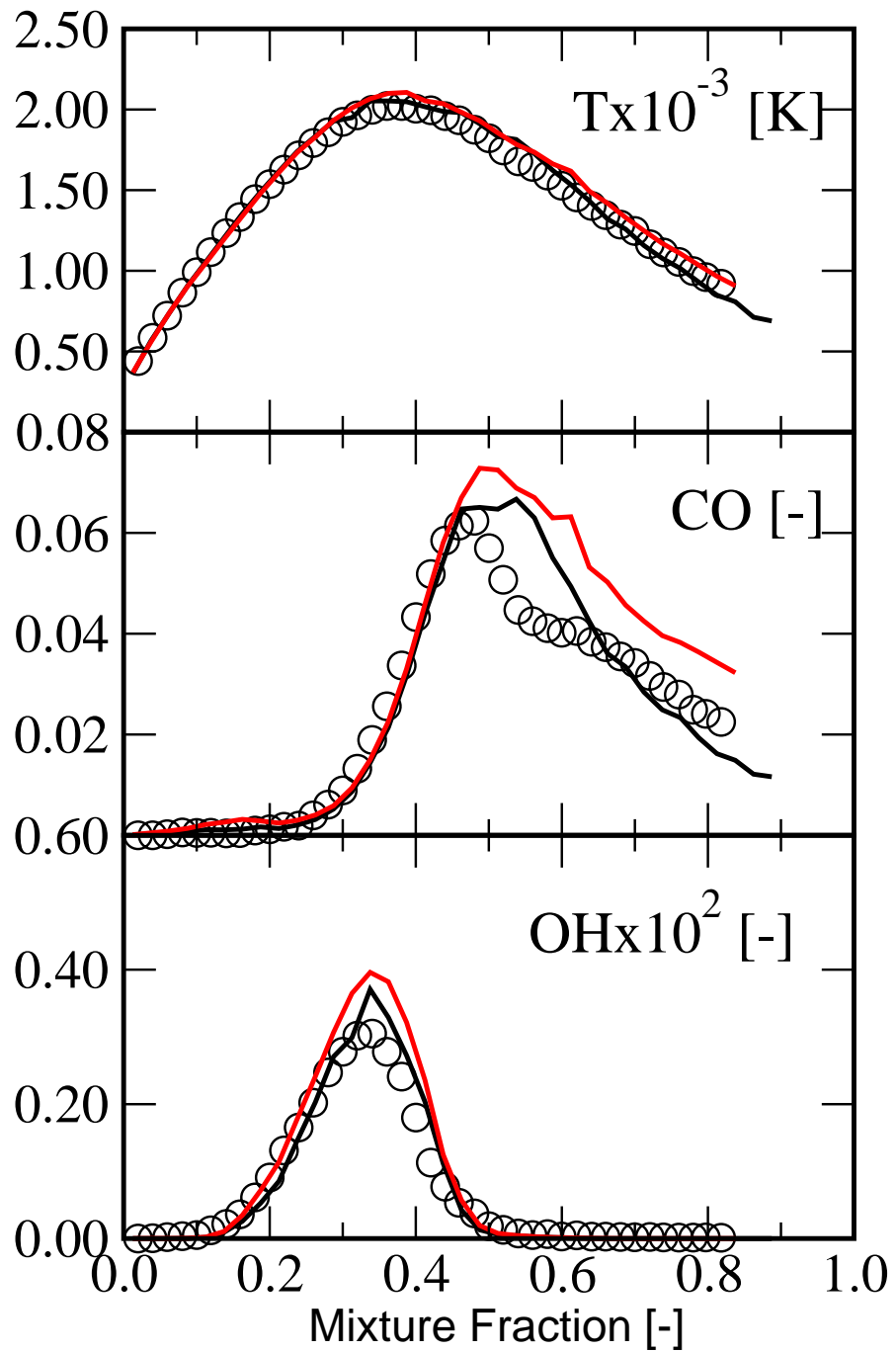
Piloted Flame F: Conditional Averages at $x/D=45$



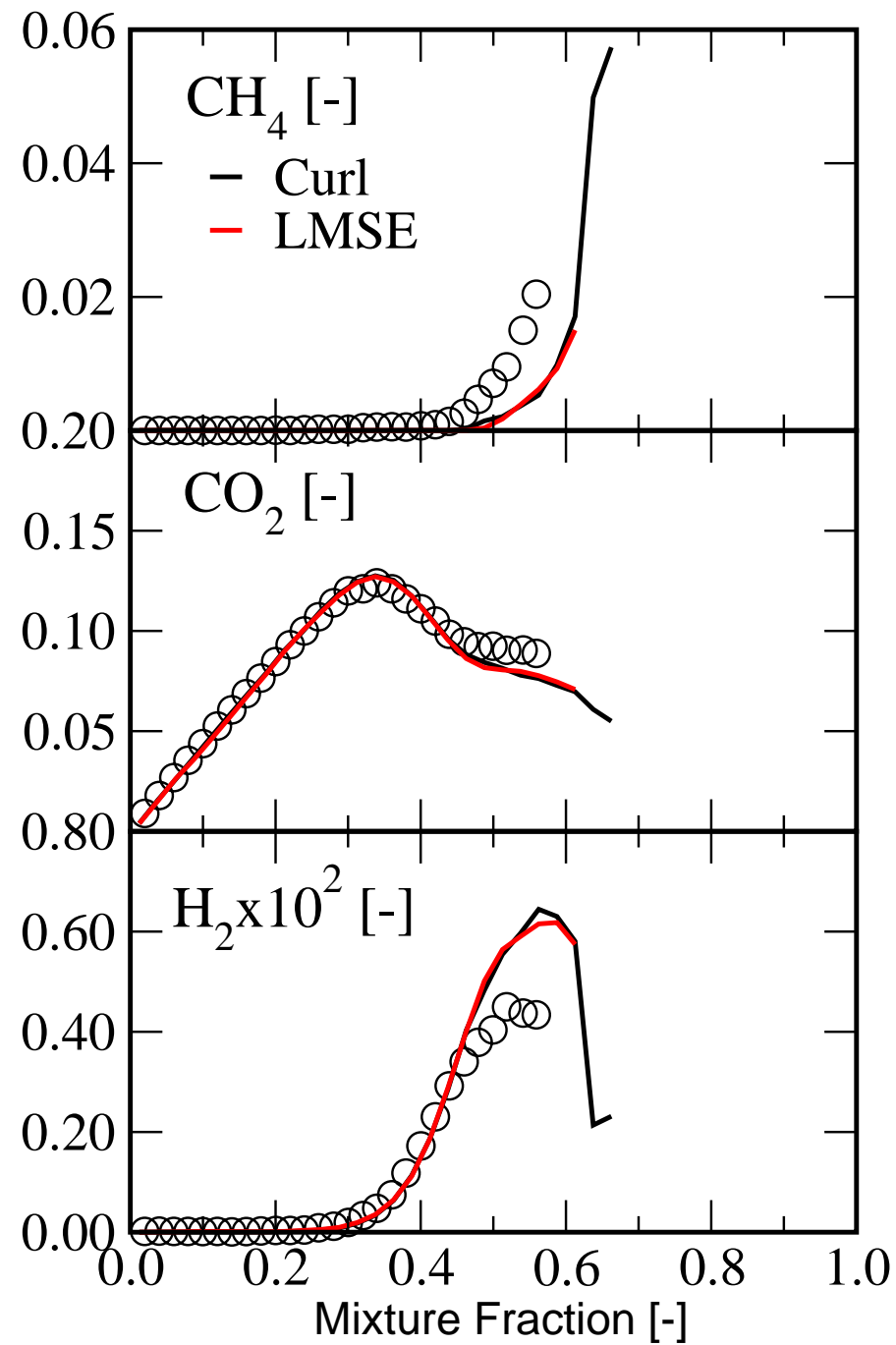
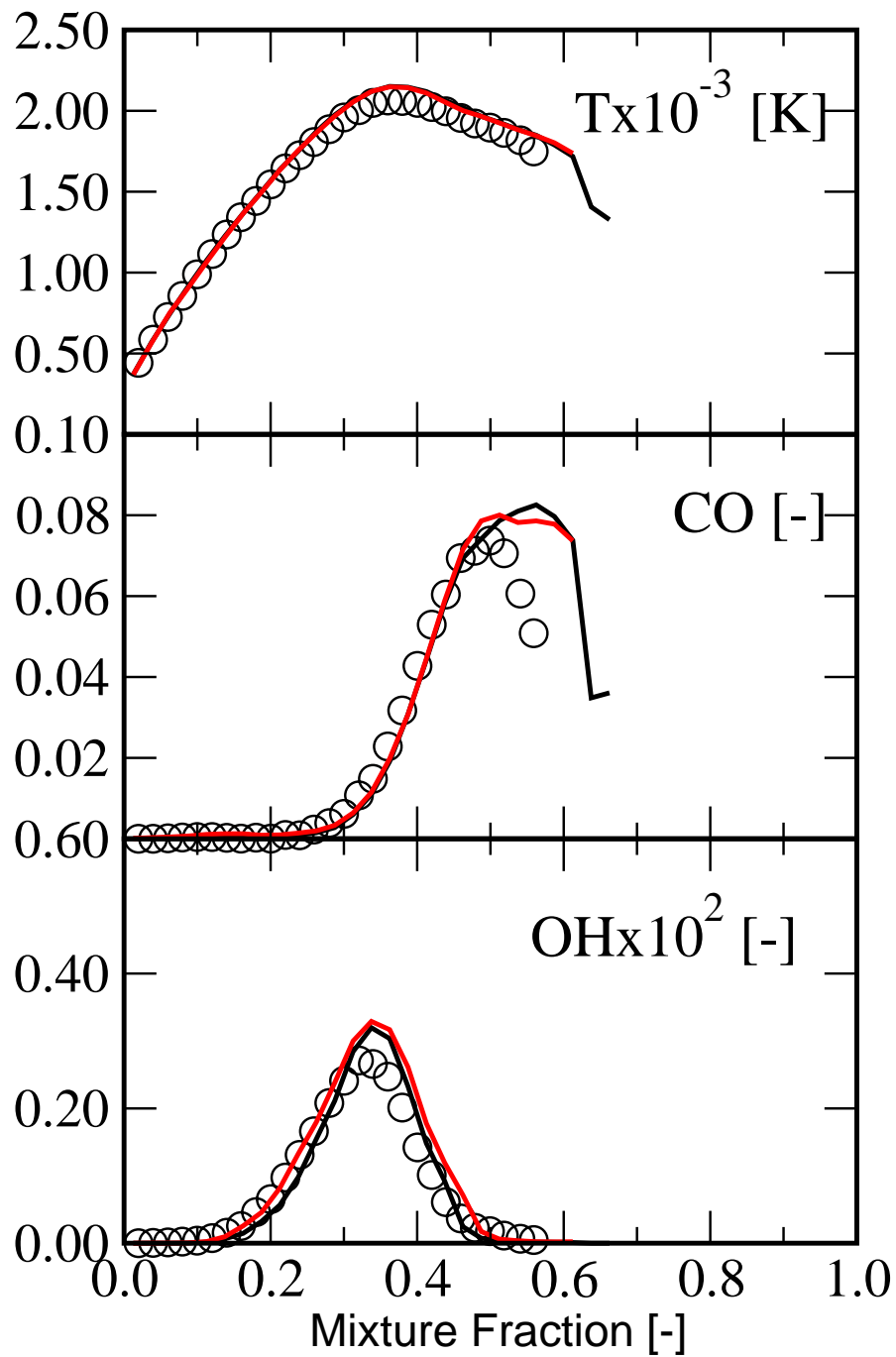
Piloted Flame D: Conditional Averages at $x/D=15$
PRT=1.00 & CSR=1.15



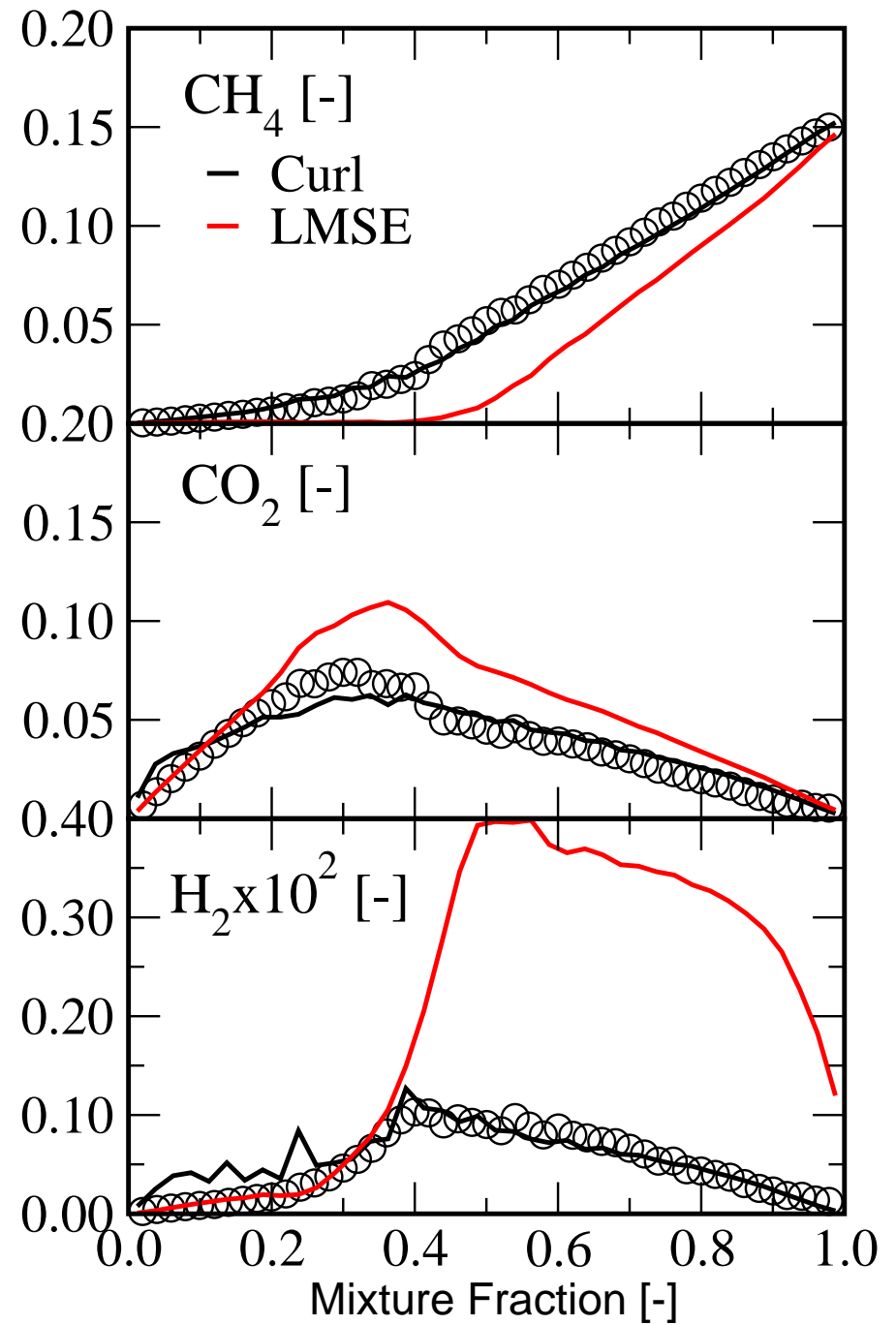
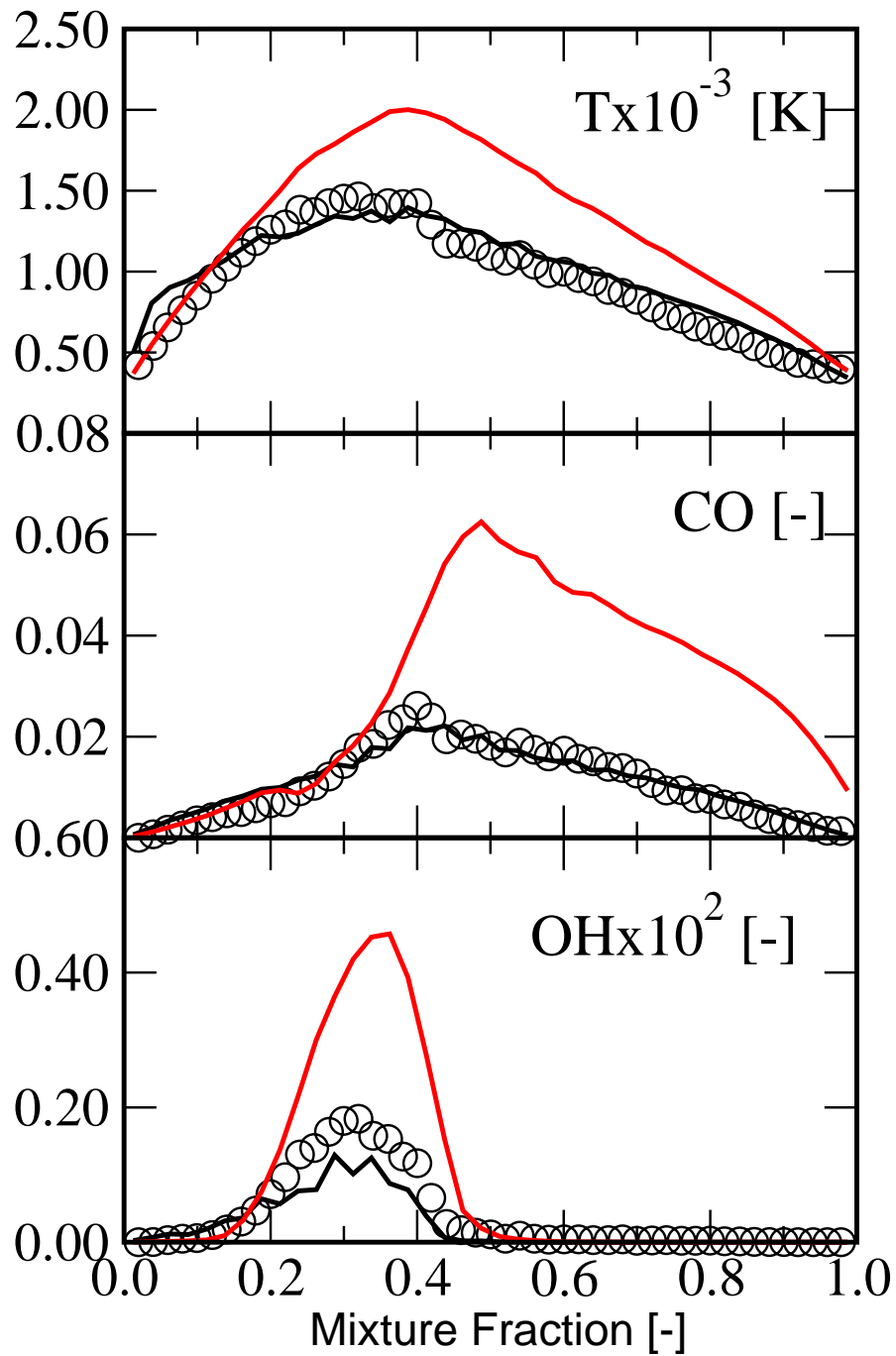
Piloted Flame D: Conditional Averages at $x/D=30$
PRT=1.00 & CSR=1.15



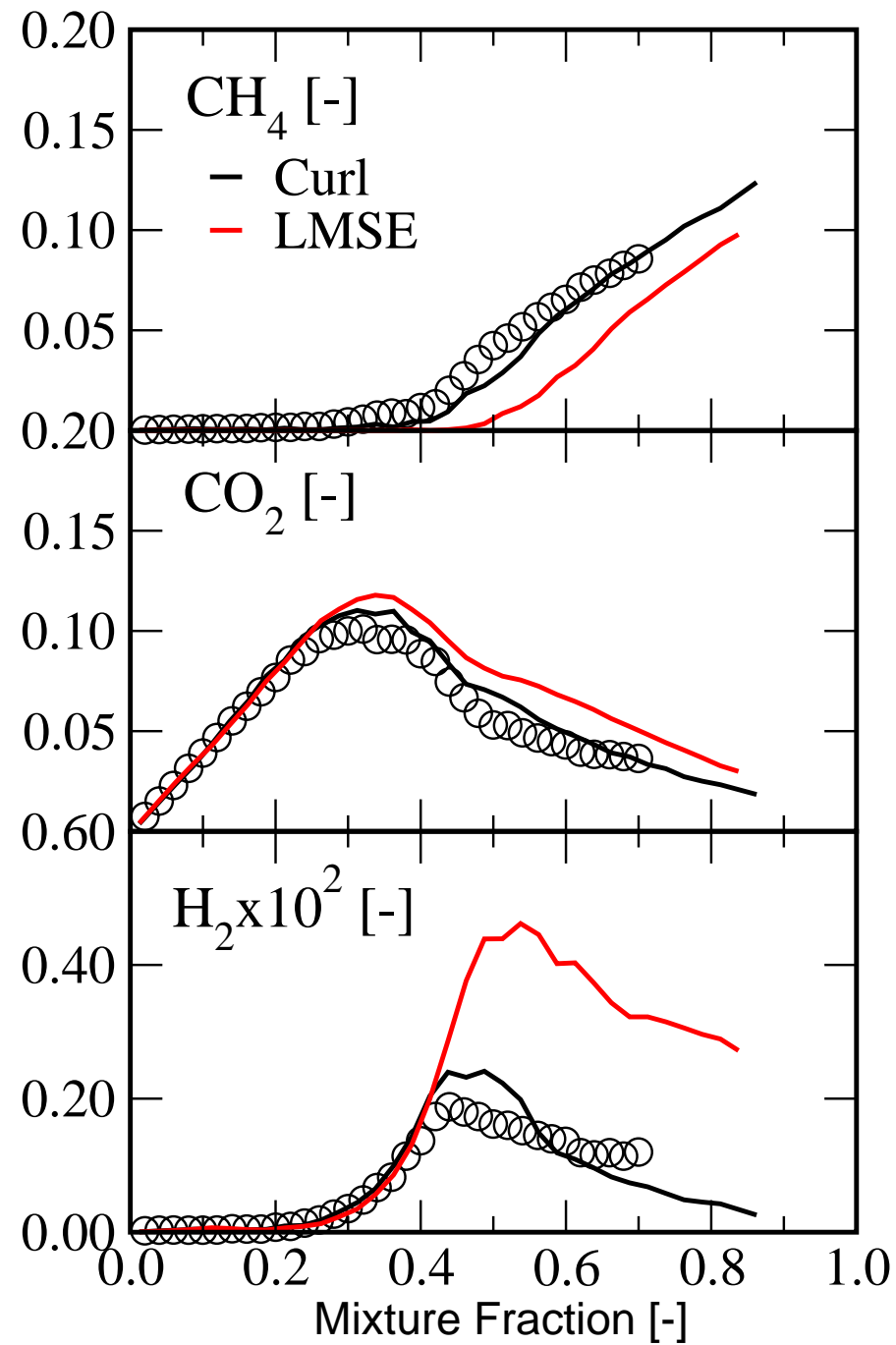
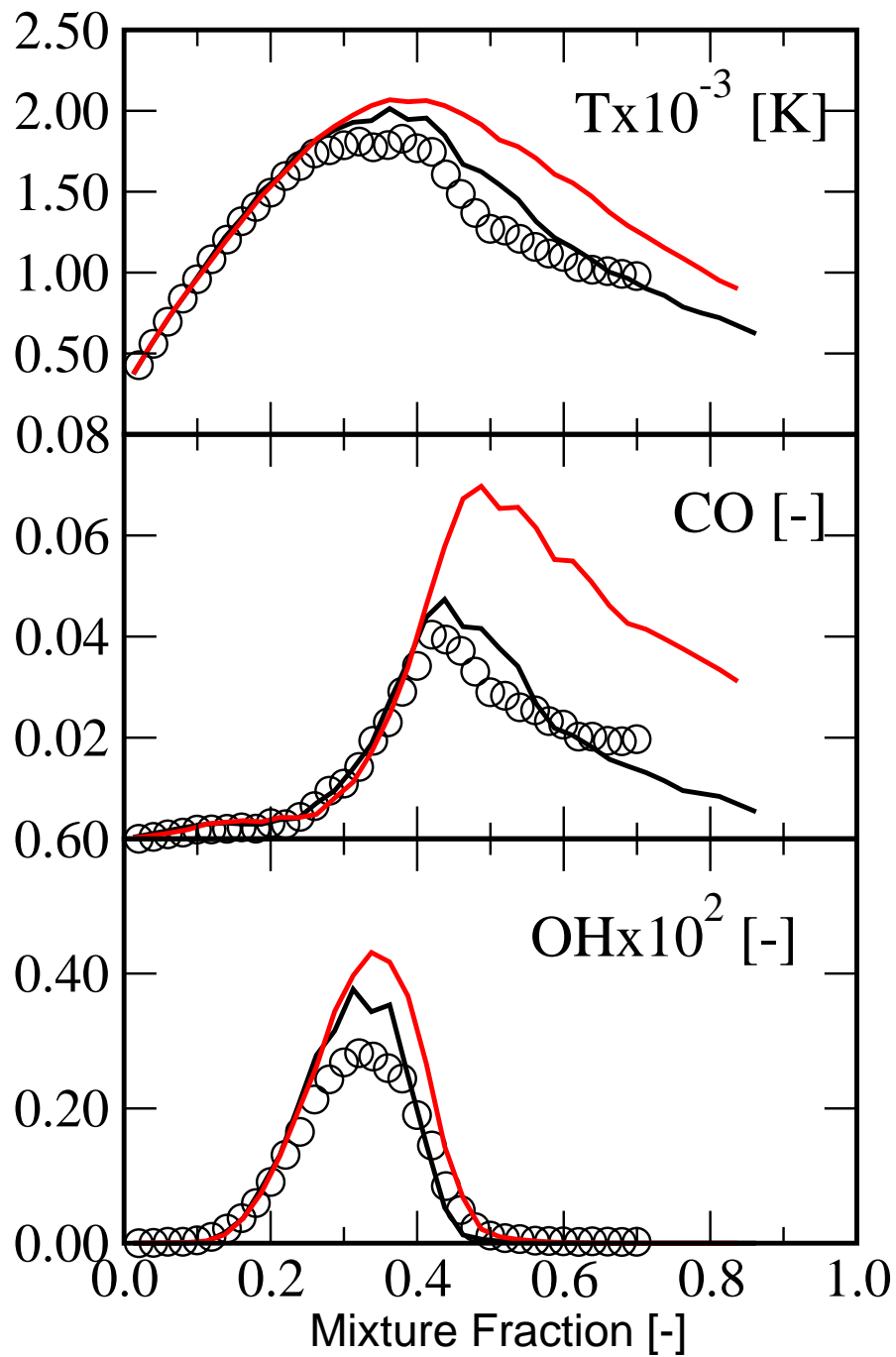
Piloted Flame D: Conditional Averages at $x/D=45$
PRT=1.00 & CSR=1.15



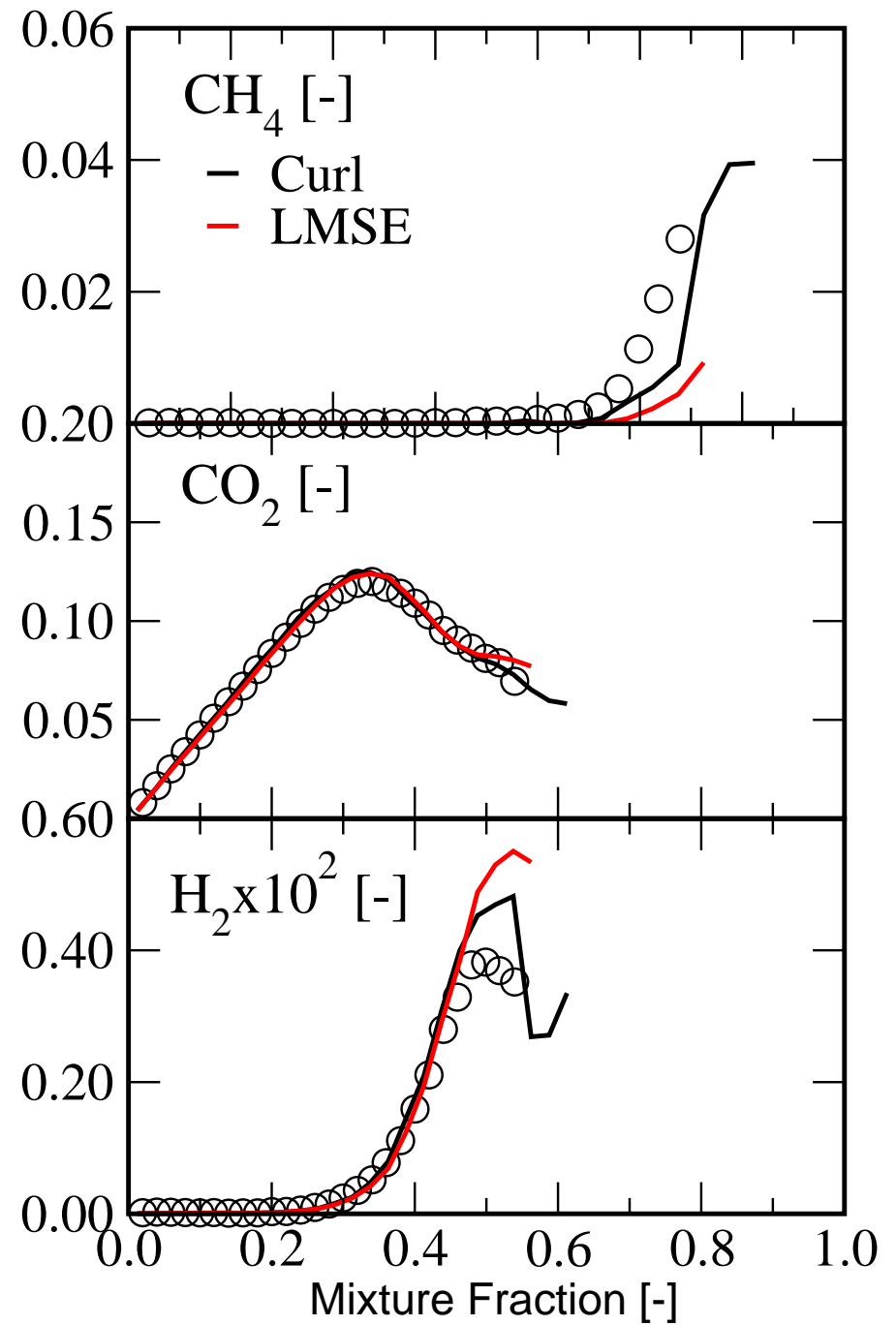
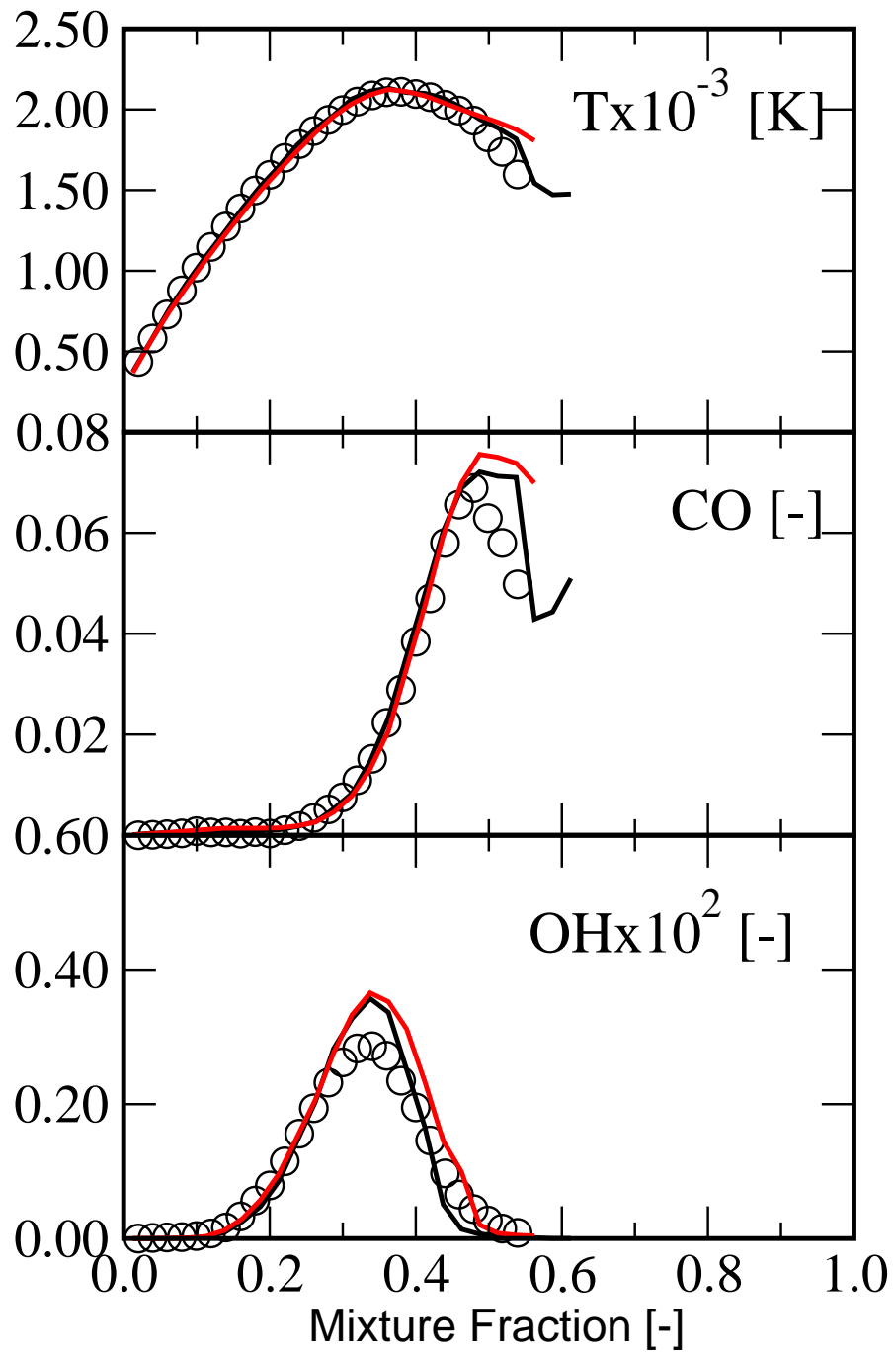
Piloted Flame F: Conditional Averages at $x/D=15$
PRT=1.00 & CSR=1.15



Piloted Flame F: Conditional Averages at $x/D=30$
PRT=1.00 & CSR=1.15



Piloted Flame F: Conditional Averages at $x/D=45$
PRT=1.00 & CSR=1.15



**Sixth international Workshop on Measurement and Computation of
Turbulent Nonpremixed Flames**
Sapporo, Japan July 18-20, 2002

Bluff-Body Stabilised Jets & Flames

Prepared by: **Peter A. M. Kalt and Assaad R. Masri**
School of Aerospace, Mechanical and Mechatronic Engineering
The University of Sydney
N.S.W., Australia

Introduction

The Bluff-body burner has been presented as a target case at previous TNF Workshops. Some new calculations are presented for validation against the experimental velocity and compositional data taken in selected test cases. Both a reacting and a non-reacting case are considered. The data are freely accessible to researchers on the internet [1].

Bluff-Body Burner

The bluff-body stabilised burner is located in a coflowing air stream. The flame is not enclosed. The bulk velocity of the co-flowing air stream, \bar{U}_e , varies depending on the flow case. The fuel jet velocity, \bar{U}_j , also varies. The reacting case uses a mixture of CNG and Hydrogen, whereas the non-reacting case uses air (only). The burner face is made of ceramic. The diameter of the bluff-body is 50mm and the central fuel jet diameter is 3.6mm. The burner assembly is located in a wind tunnel. For compositional measurements taken at the Turbulent Diffusion Flame Laboratory at Sandia's CRF, the wind tunnel dimensions are 305×305mm. For the flowfield measurements using Laser Doppler Velocimetry at Sydney University Heat Laboratory, the wind tunnel dimensions are 130×130mm. Free stream turbulence in the air coflow is around 2%.

Examined Cases - NRBB

Flow Parameters

Jet:	air
Jet Axial Velocity, \bar{U}_j :	61 m/s
Co-Flow Air Velocity, \bar{U}_e :	20 m/s

Submitted Computations for NRBB

Kempf (Darmstadt GER)

Authors: Andreas Kempf
Institution: Technical University of Darmstadt, Germany
Case: NRBB
Method: LES
Constants: Dynamic Procedure for Smagorinsky-Constant
Grid Size: $155 \times 48 \times 32$ (X \times Y \times Z)
Chemistry: None Yet

Sayre (McDermott Tech Inc. USA)

Authors: Alan N. Sayre
Institution: McDermott Technology, Inc. USA
Case: NRBB
Method: Multiple Time Scale $k - \epsilon$
Constants: $C_{ED,1} = 1.44$
 $C_{ED,2} = 1.92$
 $c_{P,1} = 0.21$
 $c_{P,2} = 1.24$
 $c_{P,3} = 1.84$
 $c_{T,1} = 0.29$
 $c_{T,2} = 1.28$
 $c_{T,3} = 1.66$

Examined Cases - HM1E

Flow Parameters

Jet:	CNG/Hydrogen (1:1 by vol.)
Jet Axial Velocity, \bar{U}_j :	108 m/s
Co-Flow Air Velocity, \bar{U}_e :	35 m/s

Submitted Computations for flowfield HM1E

Kuan/Lindstedt (Imperial College UK)

Authors: T.S. Kuan and R.P. Lindstedt
Institution: Imperial College, United Kingdom
Case: HM1 (*approximately equivalent to HM1E*)
Method: Second Moment Closure.
PDF: Presumed β PDF
Grid Size: 124×109 (X \times Y)
Chemistry: Laminar flamelet with diff. diff., $a = 120^{-s}$.
Notes: Results are profiles averaged over a time window of 33 ms.

Liu et al. (Cornell USA)

Authors: Kai Liu, M. Muradoglu, S. B. Pope, and D. A. Caughey
Institution: Cornell University, New York USA
Case: HM1E
Method: Joint PDF Model (SLM-JPM-IEM)
Constants: $c_0 = 2.1$
 $c_{\omega,1} = 0.65$
 $c_{\omega,2} = 0.9$
 $c_3 = 1.0$
 $c_4 = 0.25$
 $c_\phi = 2.0$
PDF: Full PDF
Grid Size: 129×97 (X \times Y)
Chemistry: Laminar flamelet calcs, $a = 100^{-s}$.

Sayre (McDermott Tech Inc. USA)

Authors: Alan N. Sayre
Institution: McDermott Technology, Inc. USA
Case: HM1
Method: Multiple Time Scale $k - \epsilon$
Chemistry: EDC chemistry using 19 step Frenclach reduced mechanism.
Notes: Radiation - weighted sum of grey gases

Muradoglu/Pope(KOC Turkey/Cornell USA)

Authors: Metin Muradoglu and Stephen B. Pope
Institution: KOC University, Turkey/Cornell University, New York USA
Case: HM1E
Method: Joint PDF Model (SLM-JPM-IEM)
Constants: $c_0 = 2.1$
 $c_\omega = 0.6893$
 $c_{\omega,1} = 0.65$
 $c_{\omega,2} = 0.9$
 $c_3 = 1.0$
 $c_4 = 0.25$
 $c_\phi = 2.0$
Grid Size: 176×136 (X×Y)
Chemistry: Laminar flamelet calcs

Li et al. (TUDelft NL)

Authors: Guoxiu Li, Bertrand Naud and Dirk Roekaerts
Institution: Delft University of Technology, Netherlands
Case: HM1E
Method: Reynolds stress model
Constants: $c_1 = 1.8$
 $c_2 = 0.6$
 $c_{1,\epsilon} = 1.65$
 $c_{2,\epsilon} = 1.92$
PDF: Presumed β function
Grid Size: 160×128 (X×Y)
Chemistry: equilibrium (conserved scalar → mixture fraction)

Examined Cases - HM1

Flow Parameters

Jet:	CNG/Hydrogen (1:1 by vol.)
Jet Axial Velocity, \bar{U}_j :	118 m/s
Co-Flow Air Velocity, \bar{U}_e :	40 m/s

Submitted Computations for Compositions HM1

Liu et al. (Cornell USA)

Authors: Kai Liu, M. Muradoglu, S. B. Pope, and D. A. Caughey
Institution: Cornell University, New York USA
Case: HM1
Method: Joint PDF (SLM-JPM-IEM)
Constants: $c_0 = 2.1$
 $c_{\omega,1} = 0.65$
 $c_{\omega,2} = 0.9$
 $c_3 = 1.0$
 $c_4 = 0.25$
 $c_\phi = 2.0$
PDF: Full PDF
Grid Size: 129×97 (X×Y)
Chemistry: Laminar flamelet calcs, $a = 100^{-s}$.

Kuan/Lindstedt (Imperial College UK)¹

Authors: T.S. Kuan and R.P. Lindstedt
Institution: Imperial College, United Kingdom
Case: HM1
Method: Joint Transported PDF/Second Moment Closure.
Grid Size: 124×109 (X×Y)
Chemistry: Lindstedt et al. (2000). 20 species including NO_x .

Kuan/Lindstedt (Imperial College UK)³

Authors: T.S. Kuan and R.P. Lindstedt
Institution: Imperial College, United Kingdom
Case: HM1
Method: Second Moment Closure.
PDF: presumed β PDF
Grid Size: 124×109 (X×Y)
Chemistry: Laminar flamelet with diff. diff., $a = 120^{-s}$.
Notes: Results are profiles averaged over a time window of 38 ms.

Kuan/Lindstedt (Imperial College UK)⁵

Authors: T.S. Kuan and R.P. Lindstedt
Institution: Imperial College, United Kingdom
Case: HM1
Method: Second Moment Closure.
PDF: presumed β PDF
Grid Size: 124×109 (X \times Y)
Chemistry: Laminar flamelet with diff. diff., $a = 120^{-8}$.
Notes: Results are profiles averaged over a time window of 33 ms.

Li et al. (TUDelft NL)

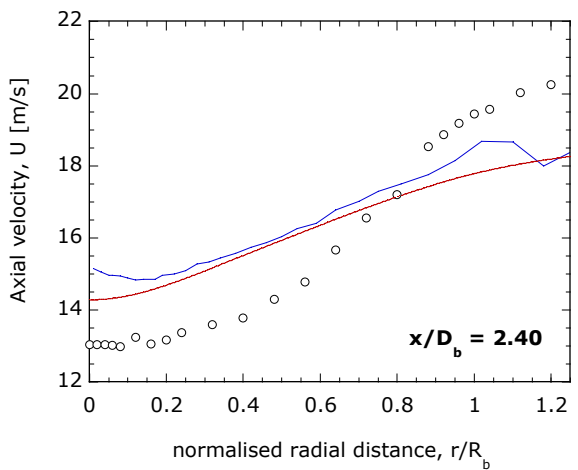
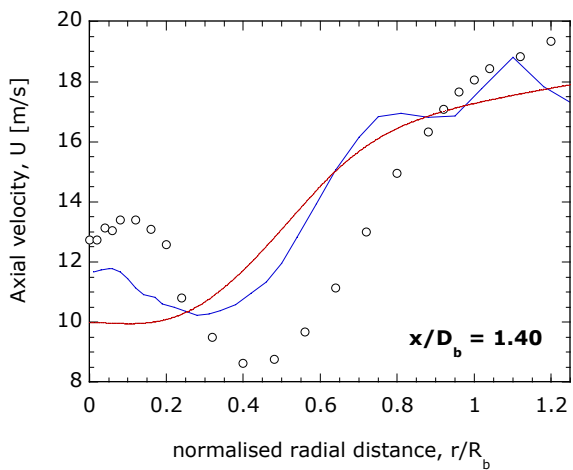
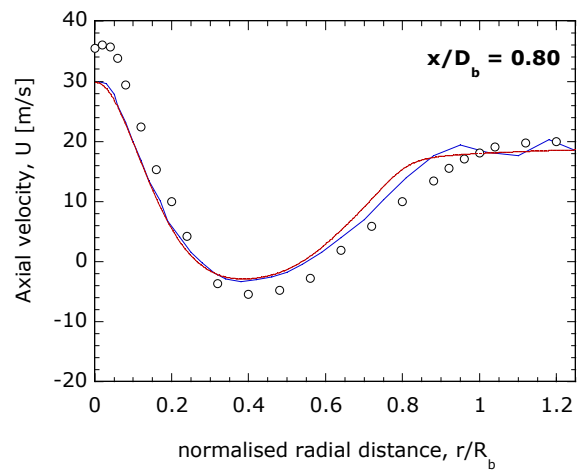
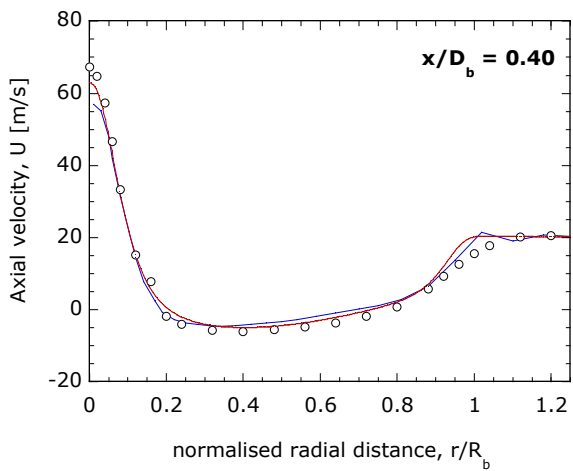
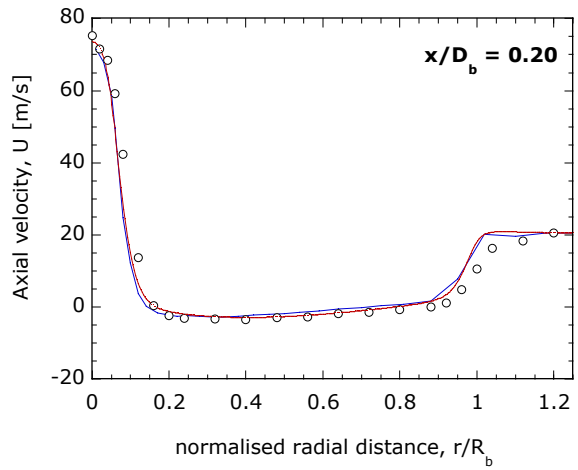
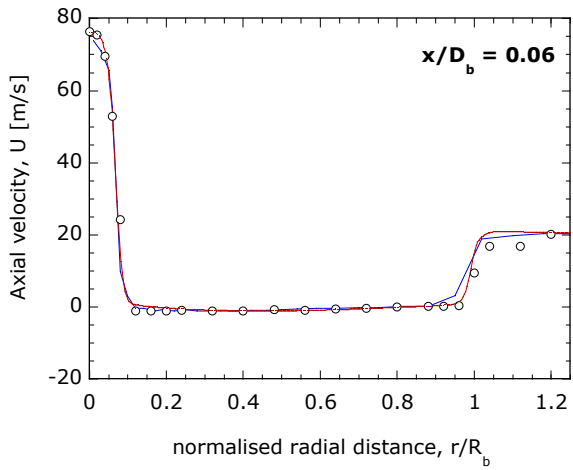
Authors: Guoxiu Li, Bertrand Naud and Dirk Roekaerts
Institution: Delft University of Technology, Netherlands
Case: HM1E (*Warning: Should be HM1 instead*)
Method: Reynold's stress model
Constants: $c_1 = 1.8$
 $c_2 = 0.6$
 $c_{1,\epsilon} = 1.65$
 $c_{2,\epsilon} = 1.92$
PDF: Presumed β function
Grid Size: 160×128 (X \times Y)
Chemistry: equilibrium (conserved scalar \rightarrow mixture fraction)

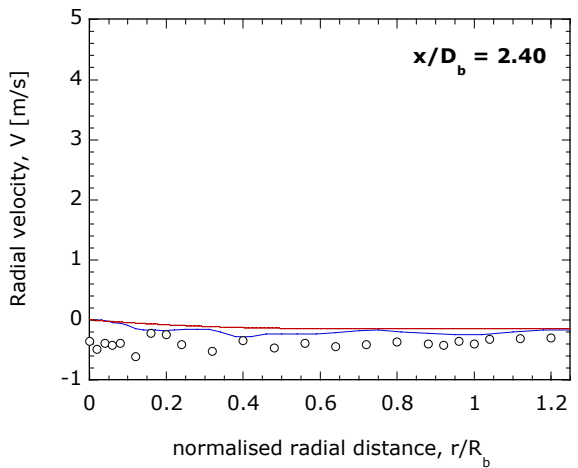
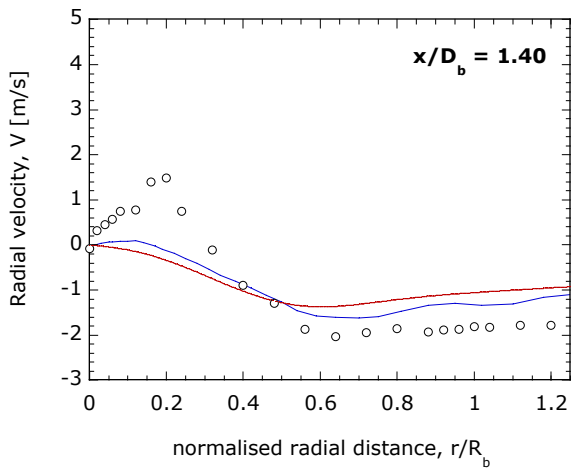
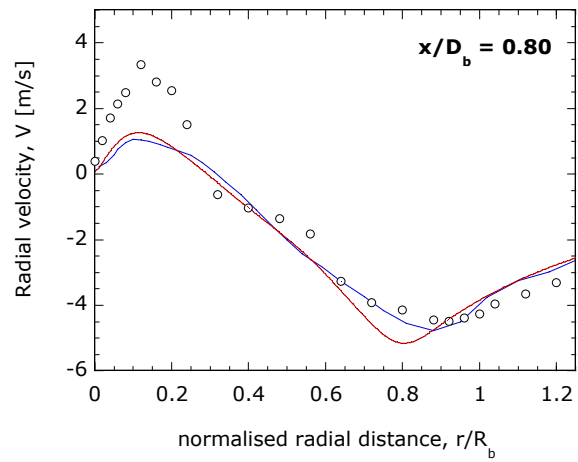
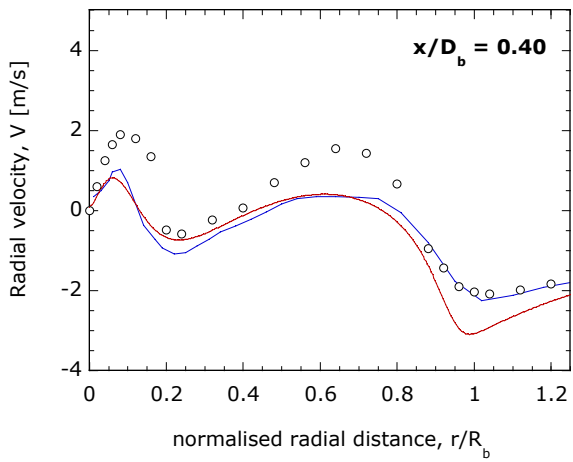
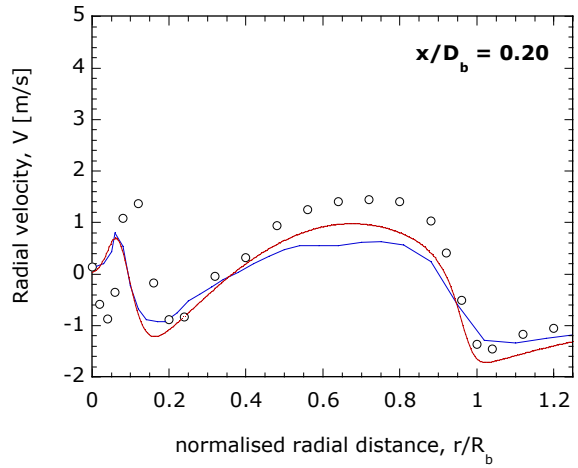
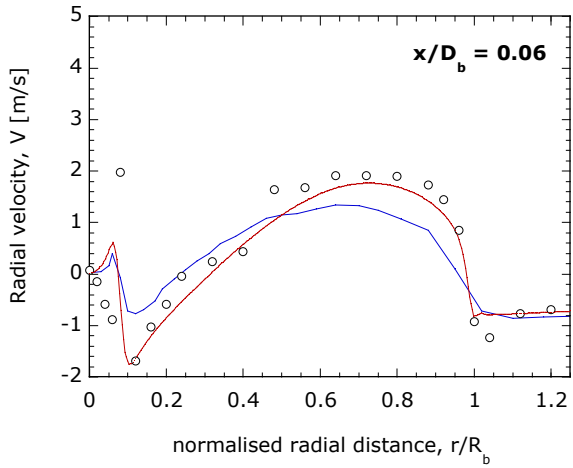
Acknowledgement

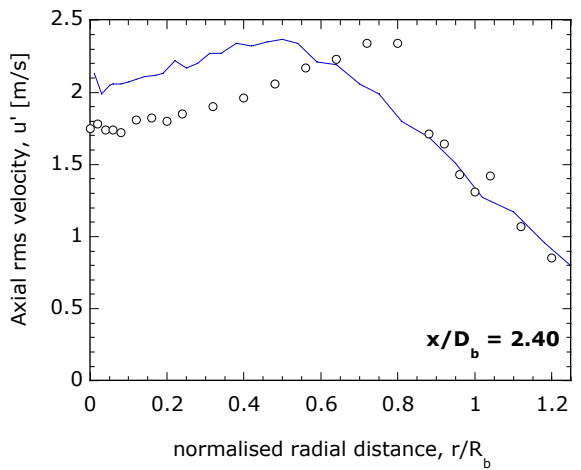
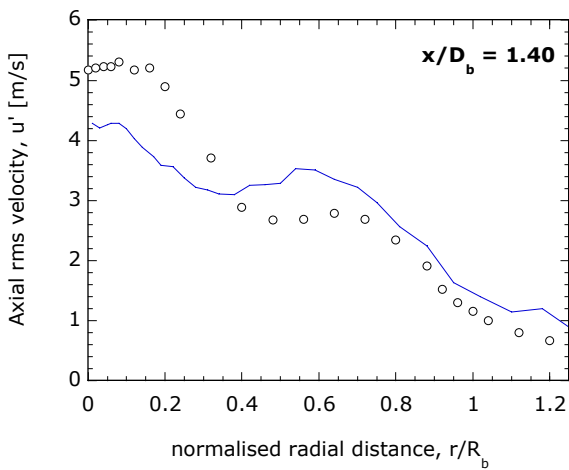
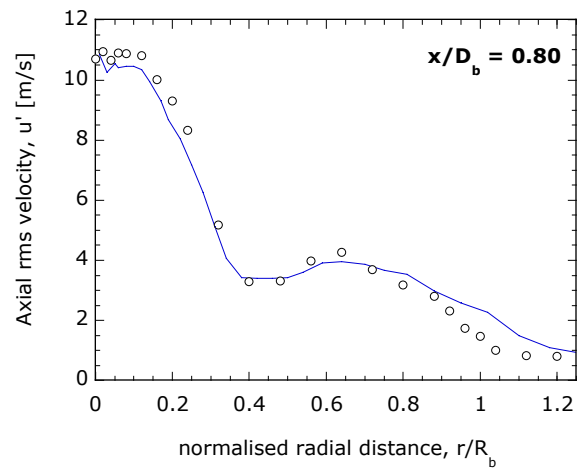
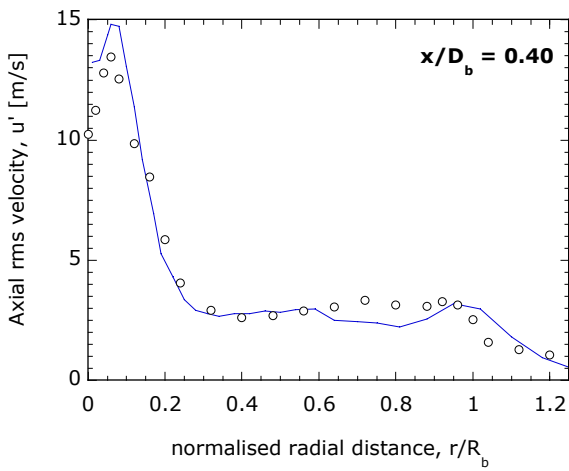
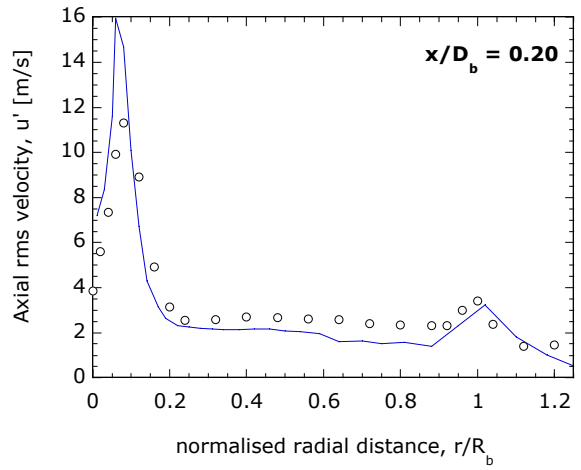
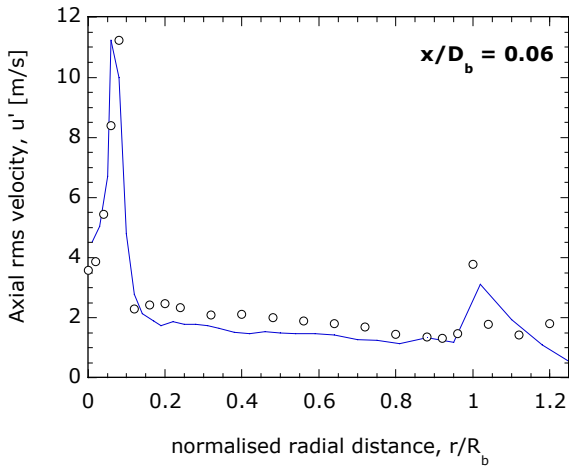
This work is supported by the Australian Research Council and the US Department of Energy, Office of Basic Energy Sciences. Special thanks to all the groups and individuals who have contributed their results for comparison.

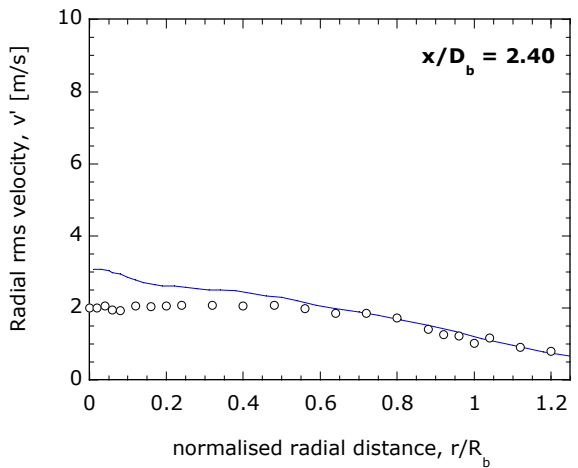
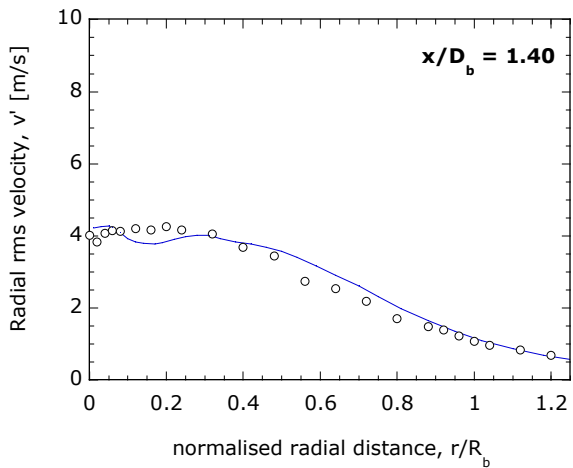
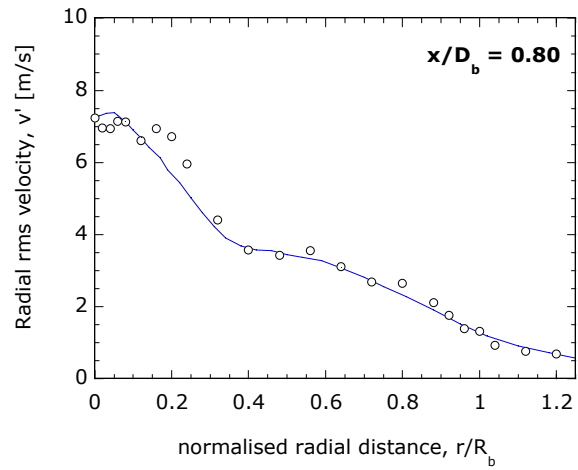
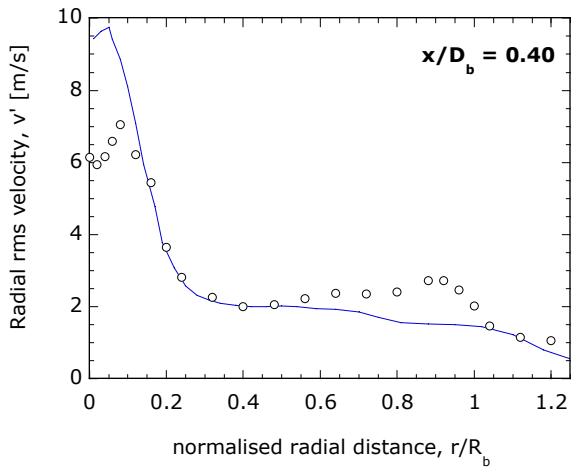
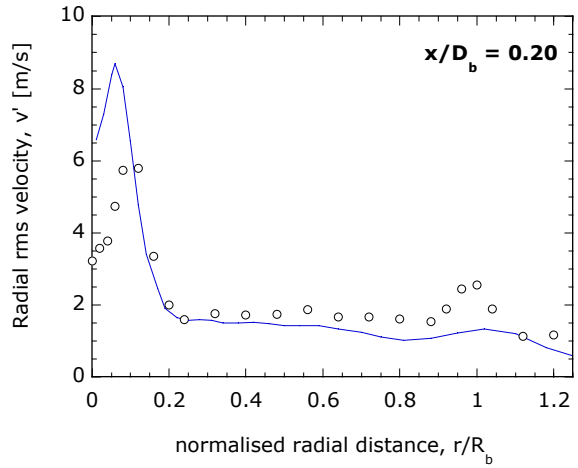
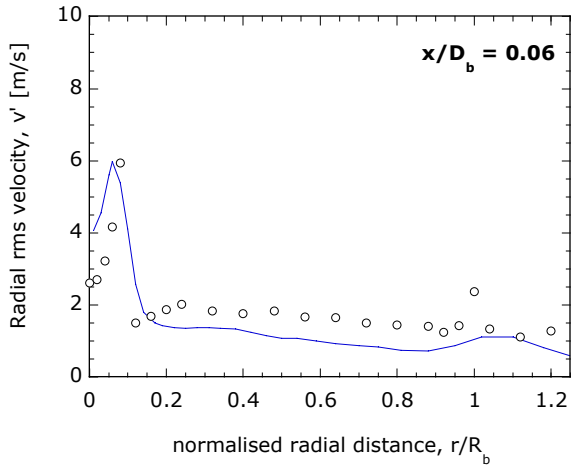
References

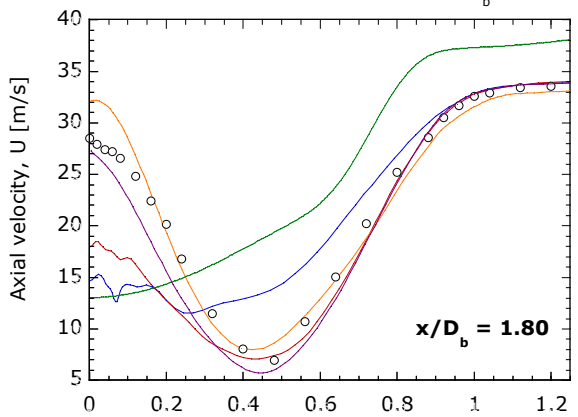
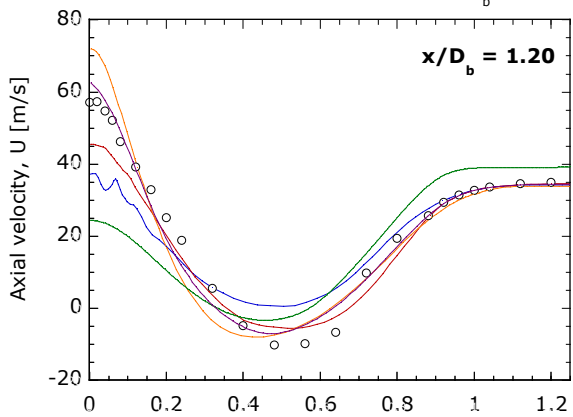
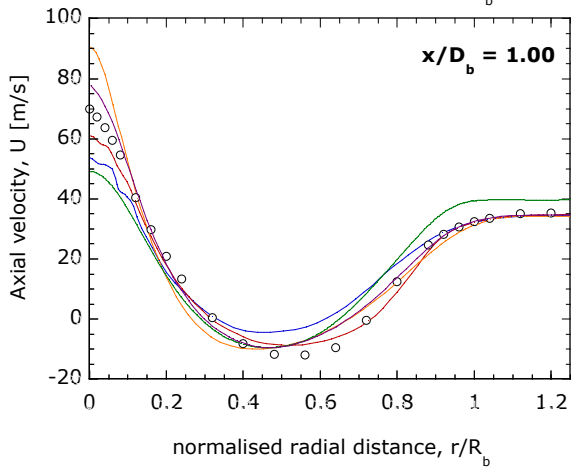
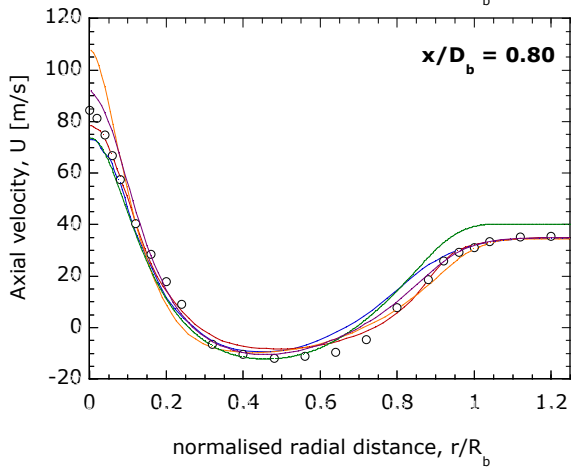
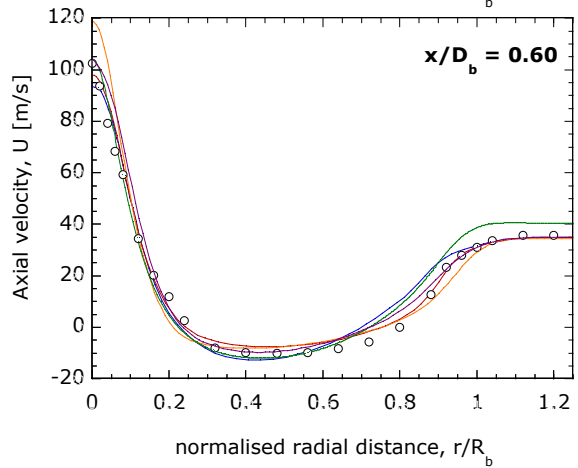
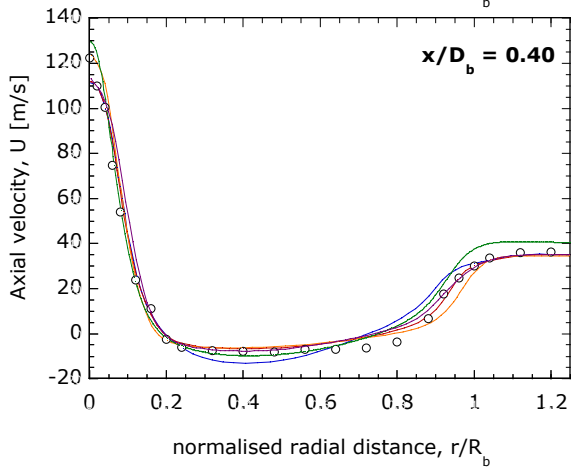
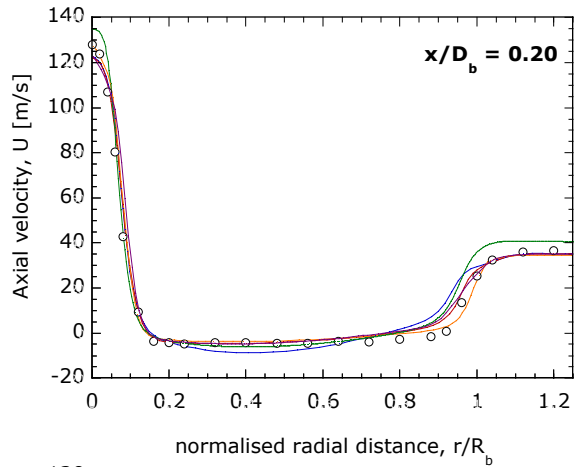
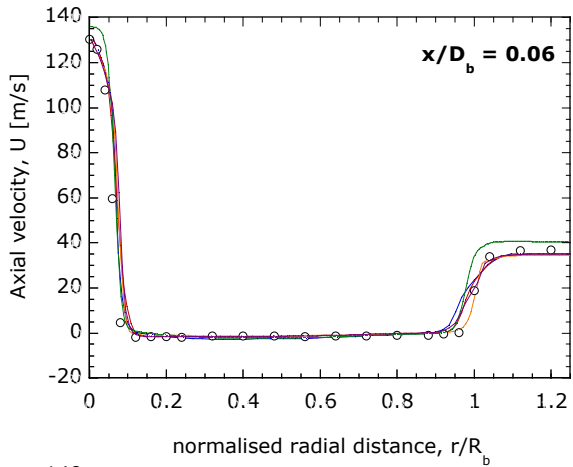
[1] Masri, A.R., <http://www.mech.eng.usyd.edu.au/thermofluids/>

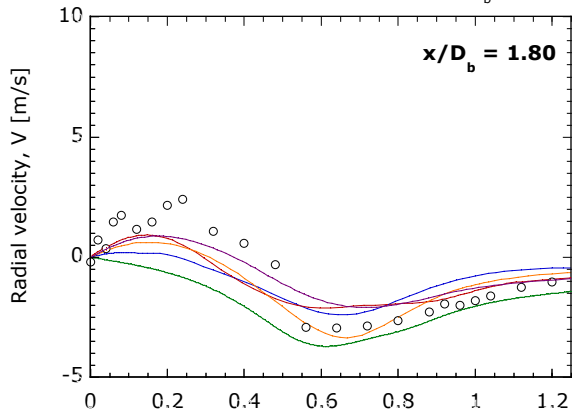
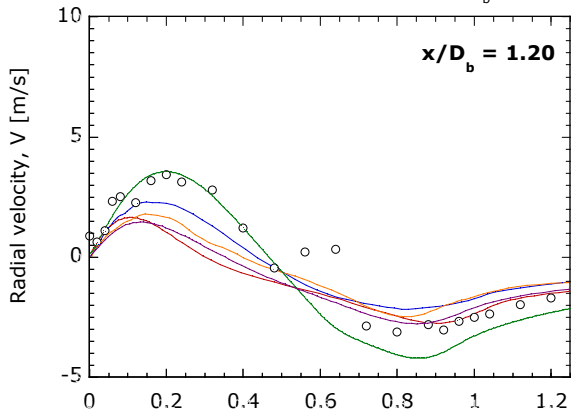
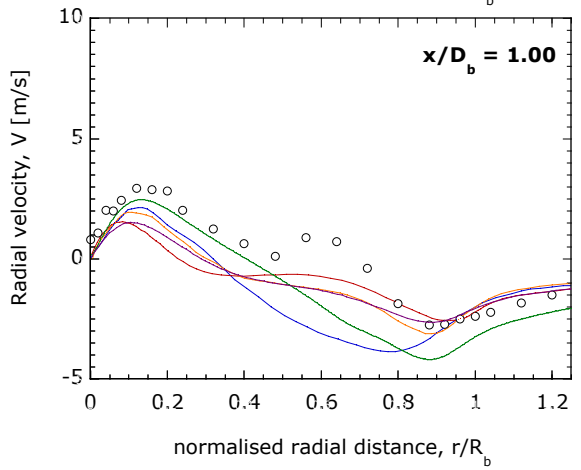
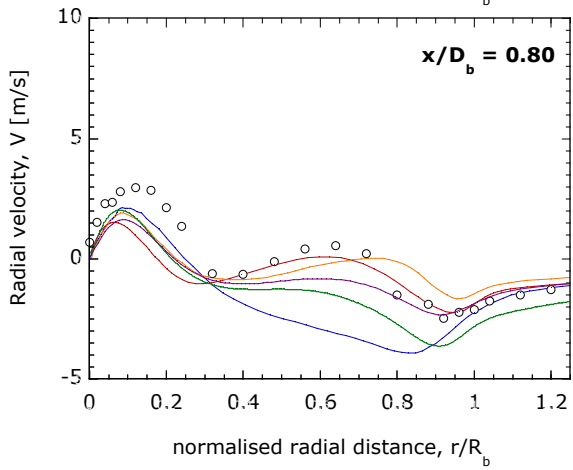
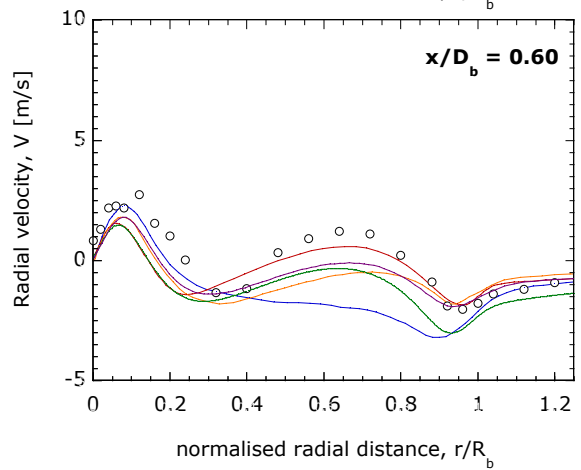
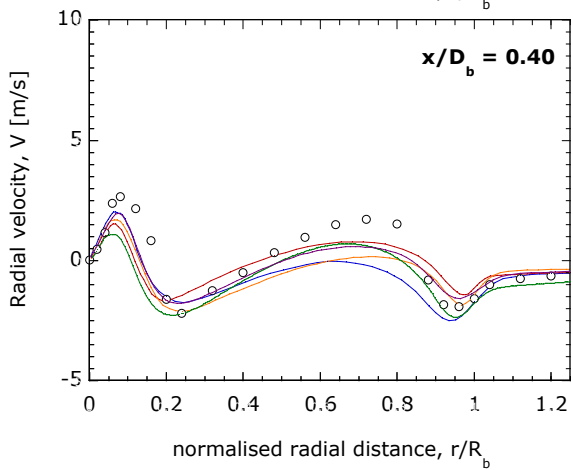
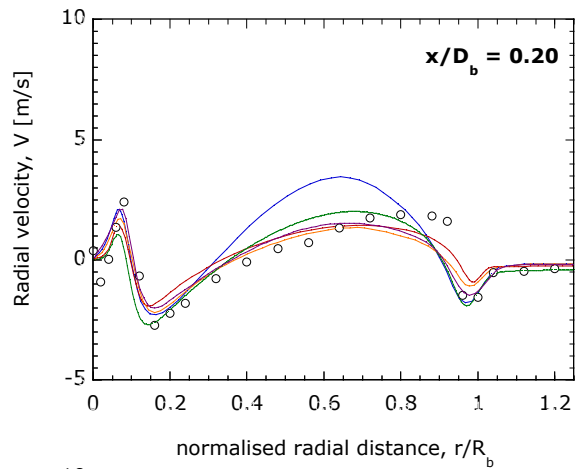
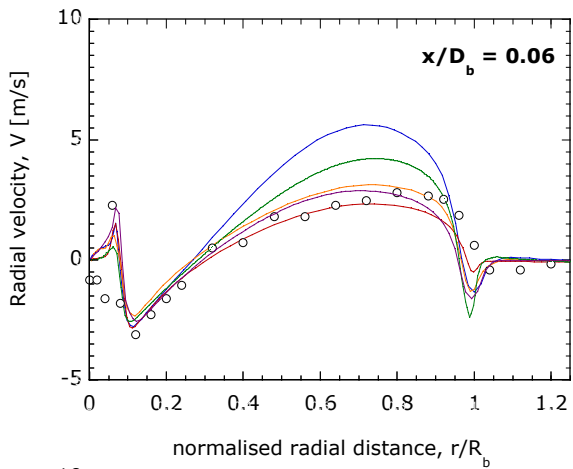


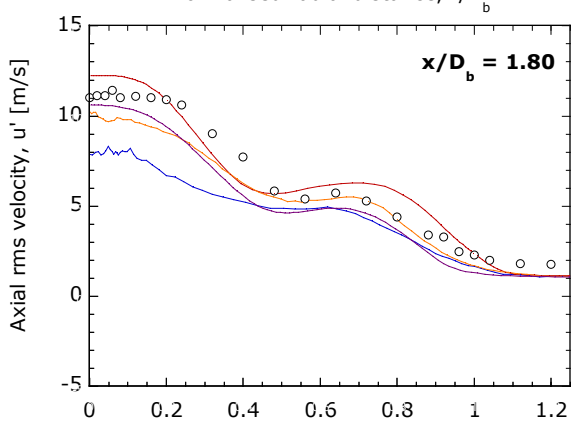
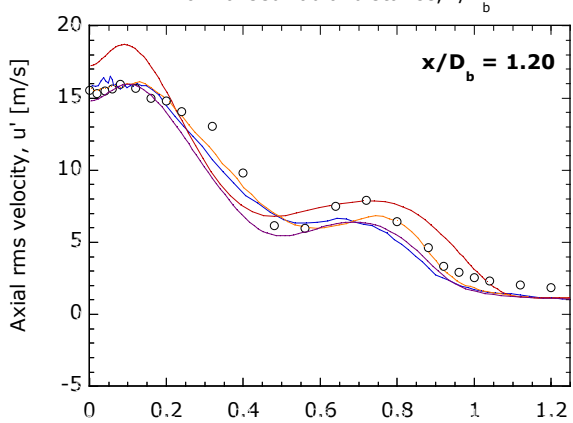
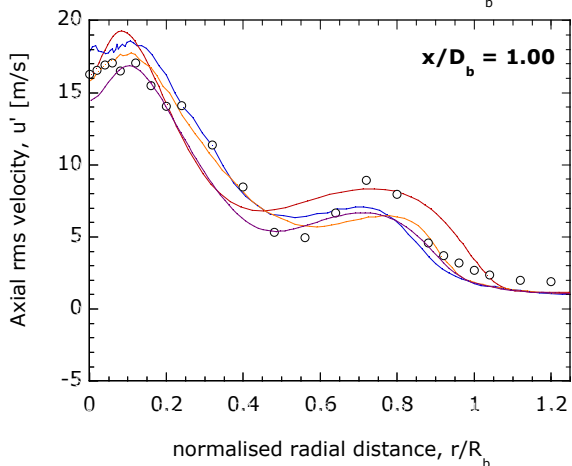
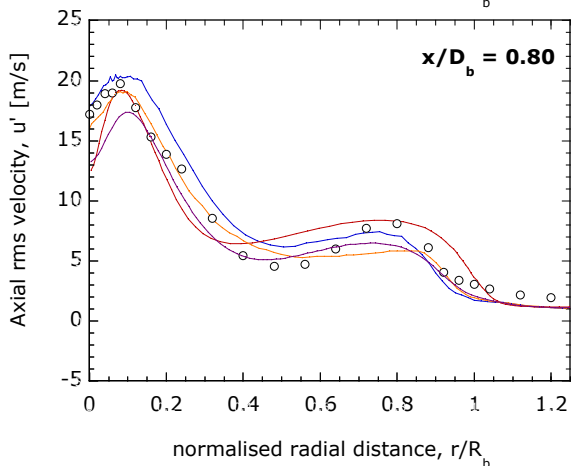
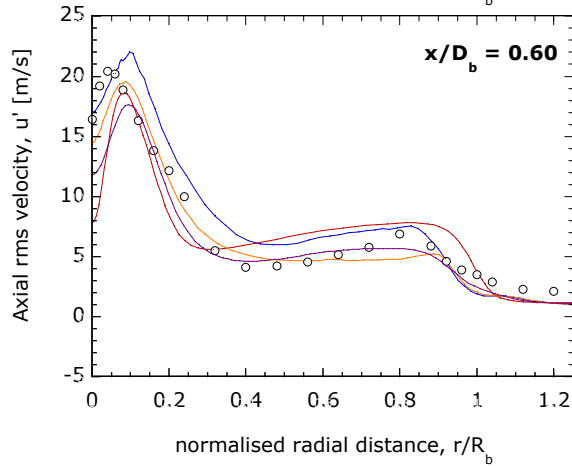
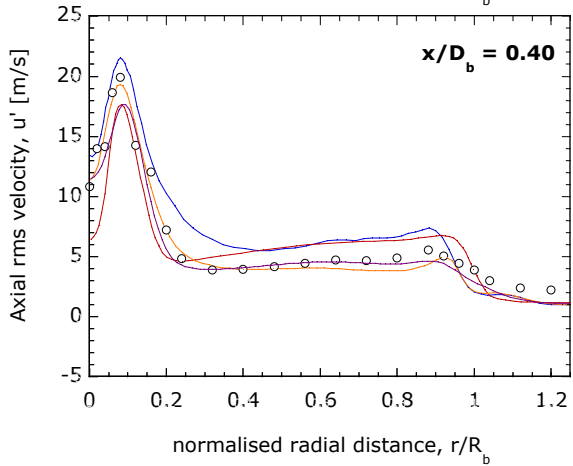
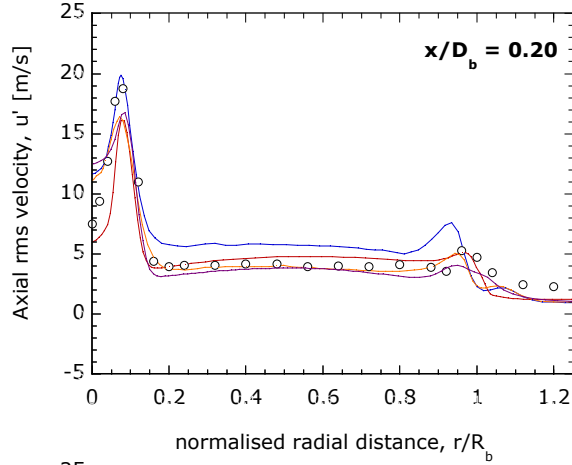
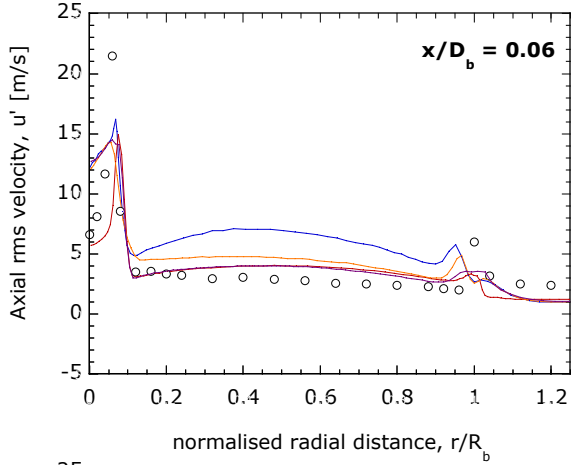


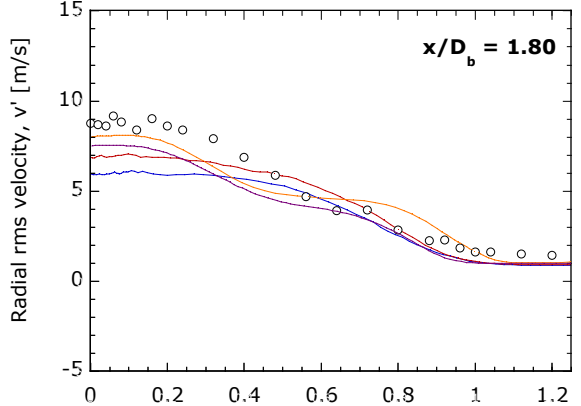
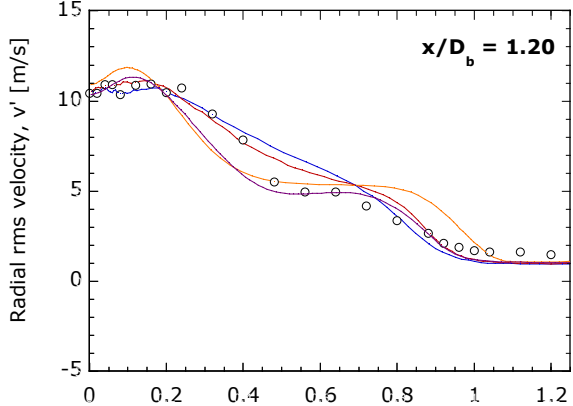
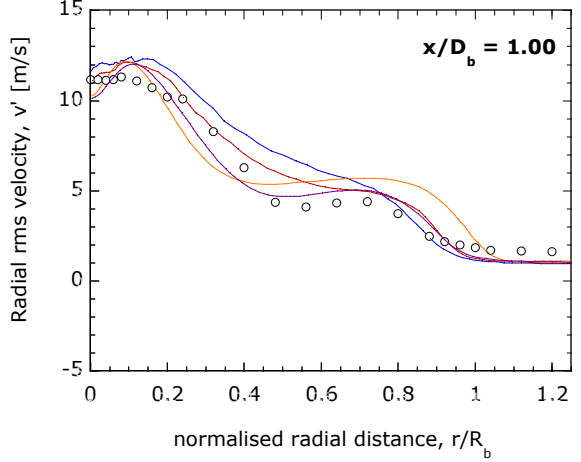
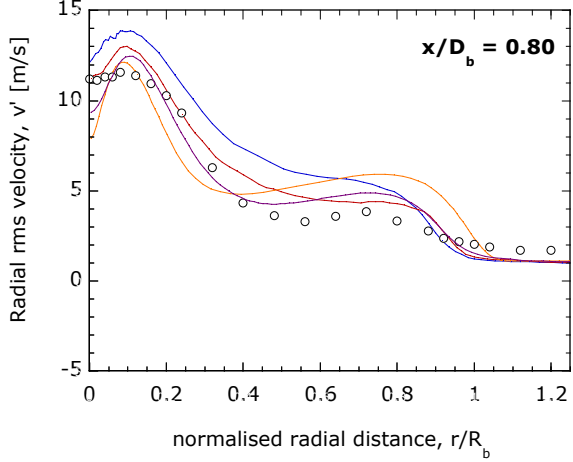
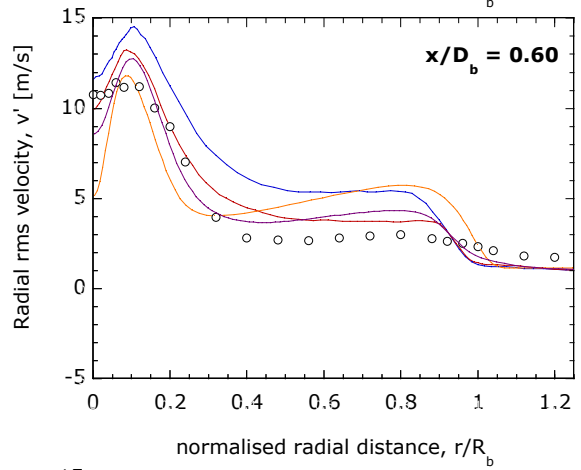
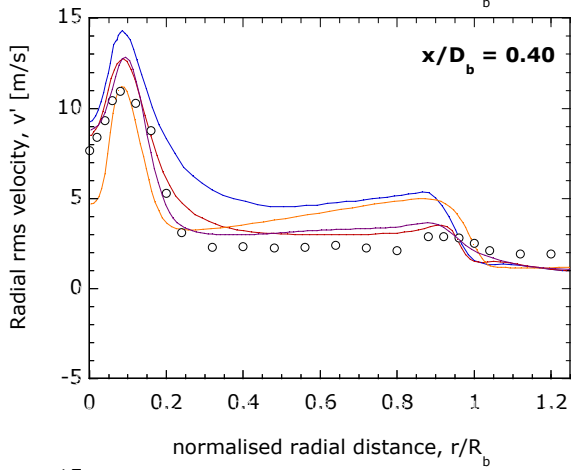
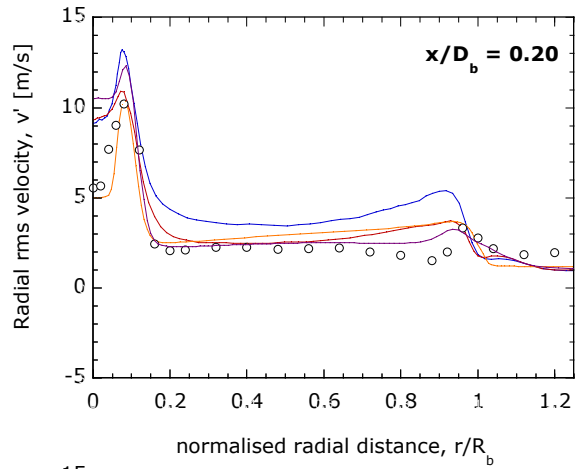
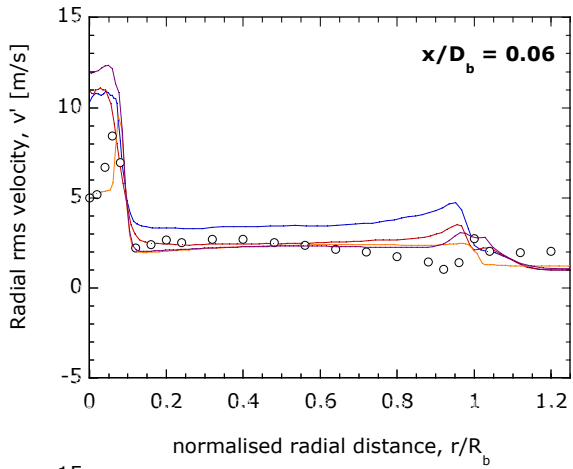


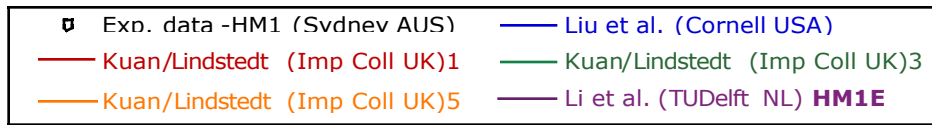
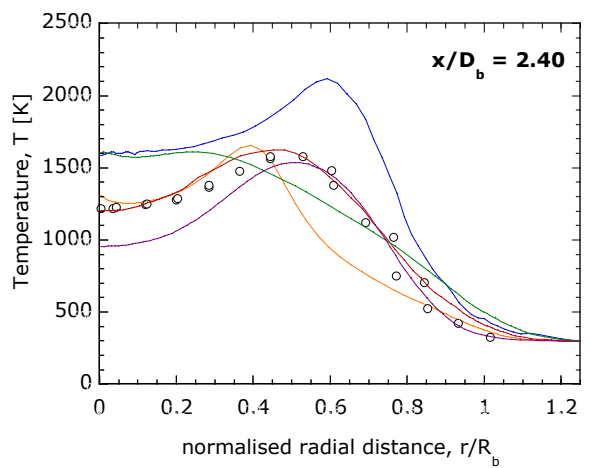
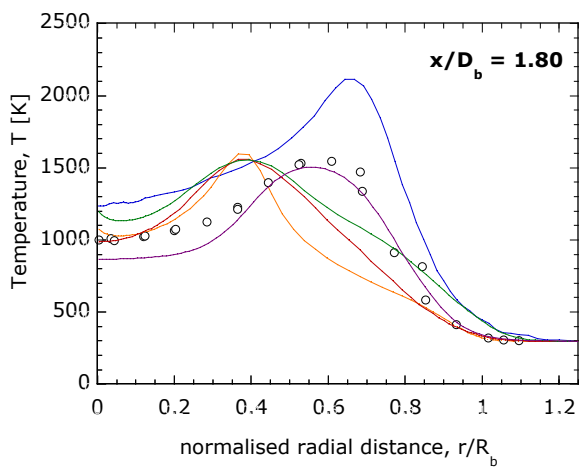
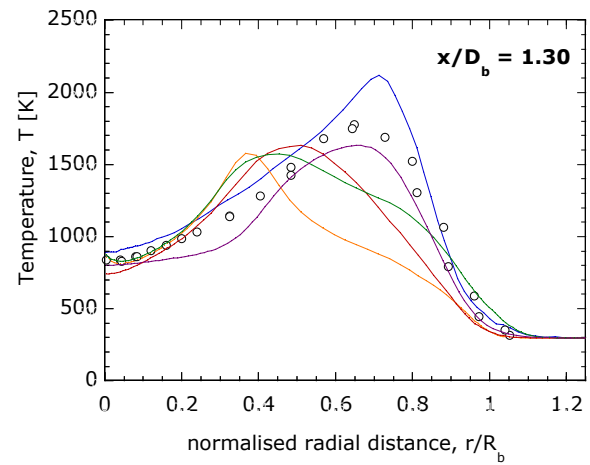
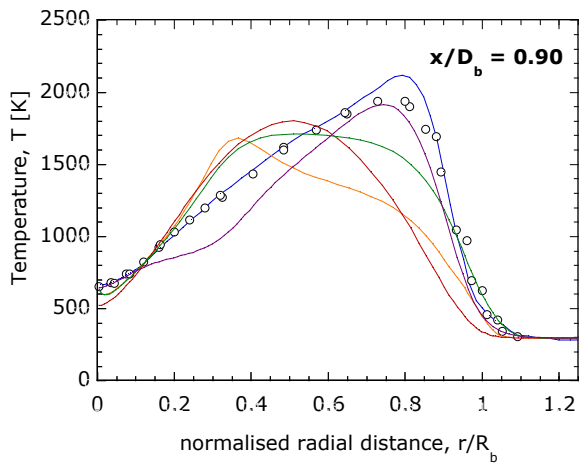
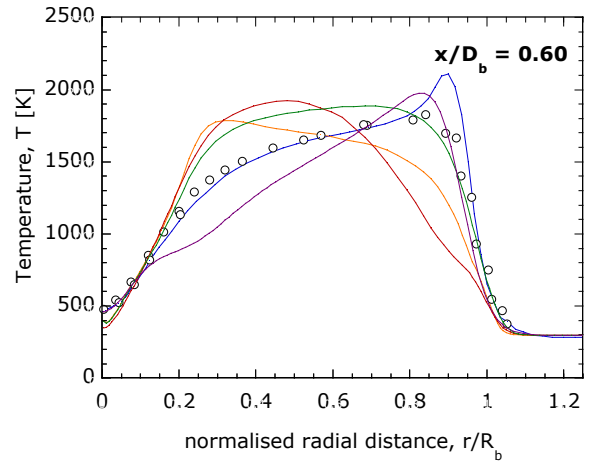
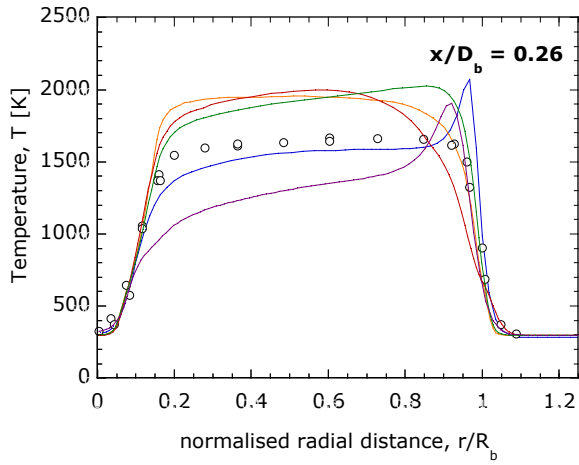


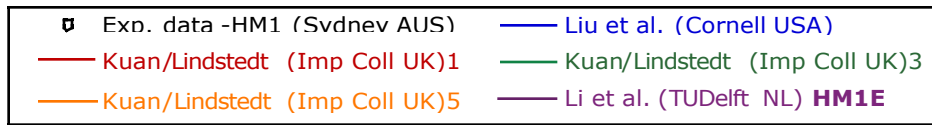
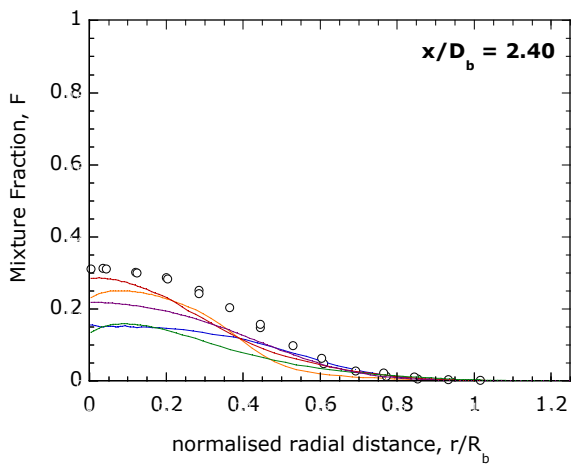
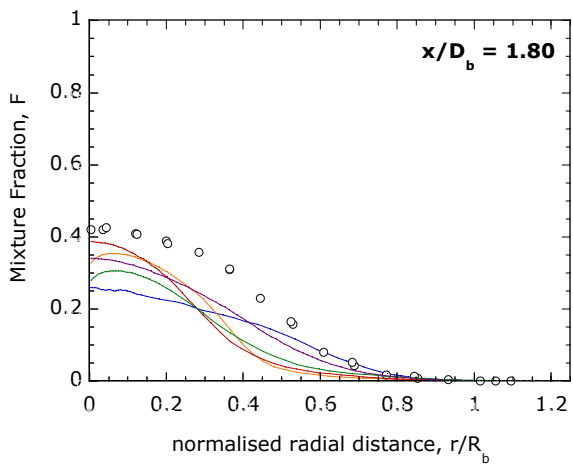
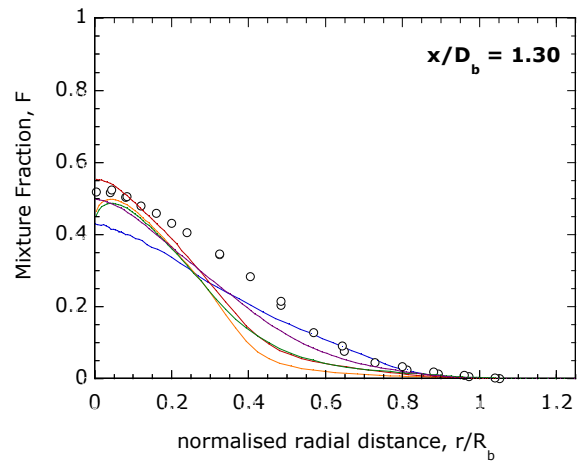
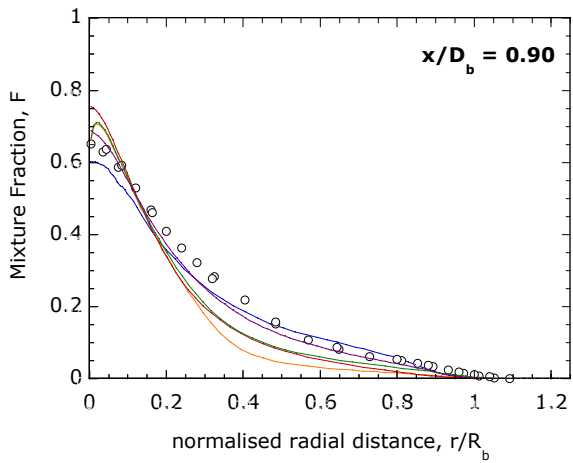
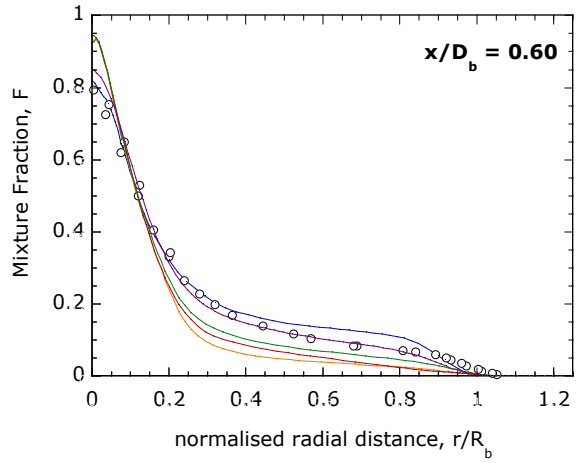
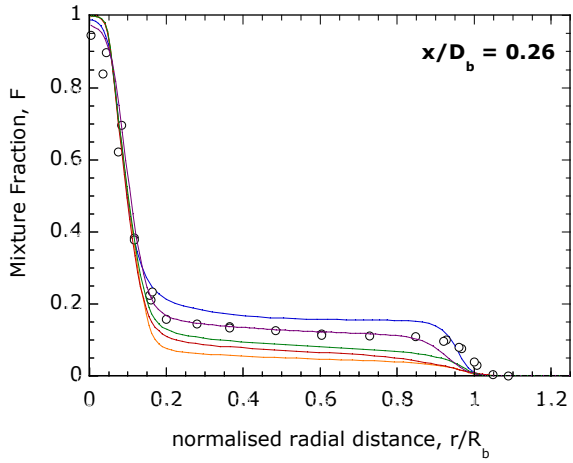


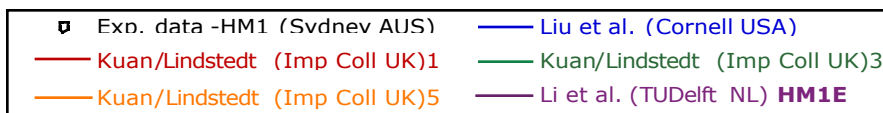
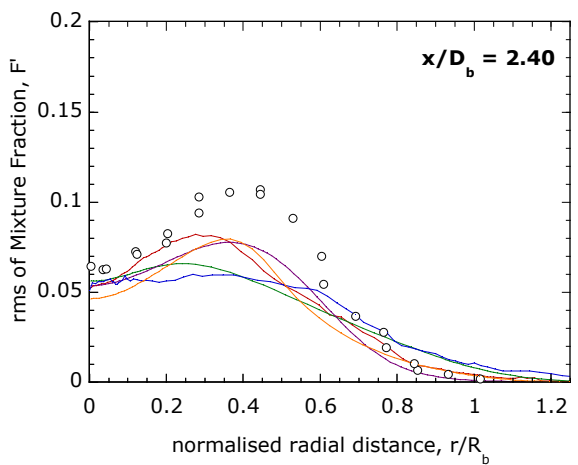
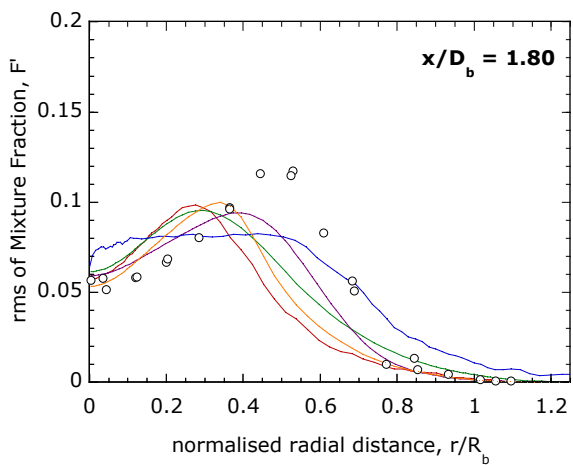
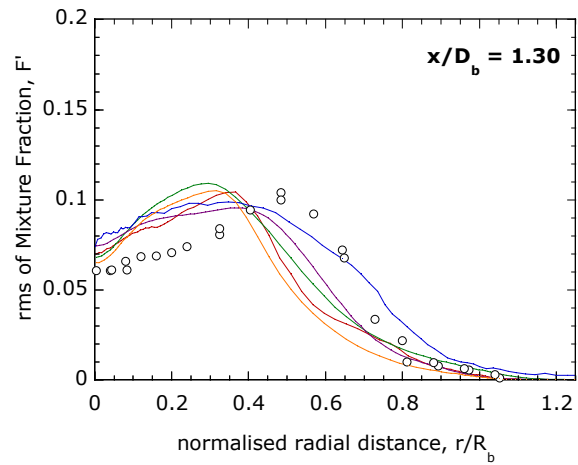
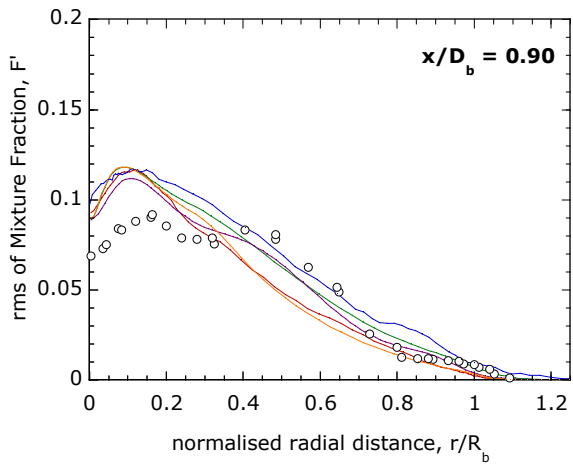
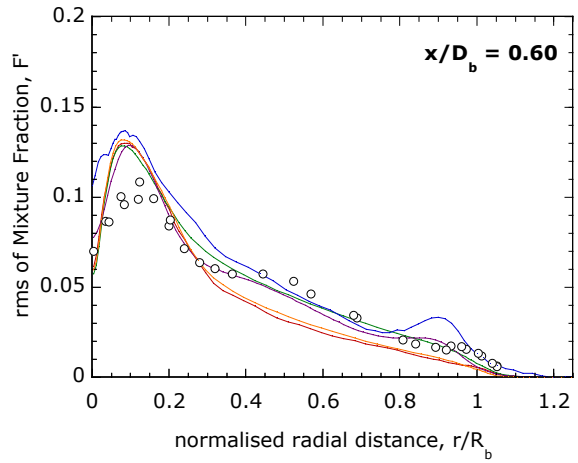
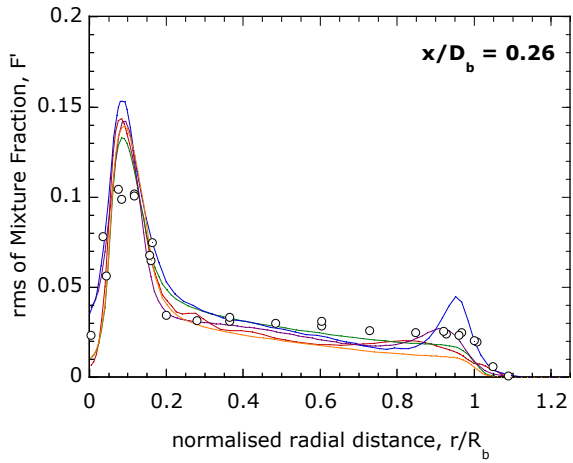


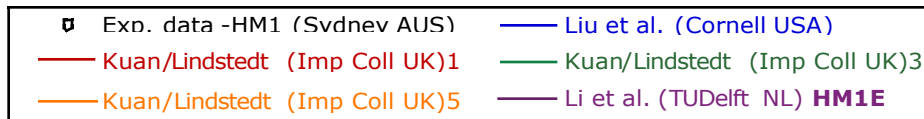
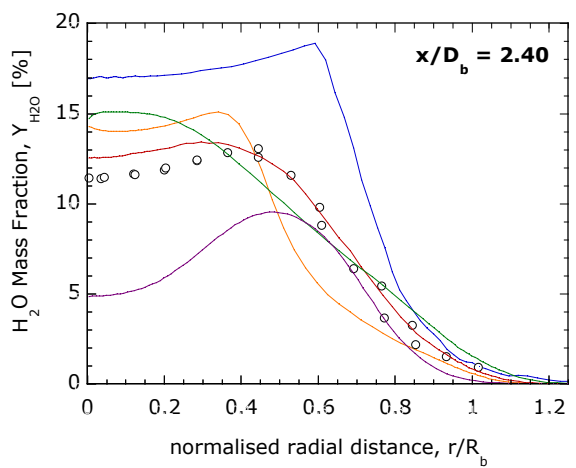
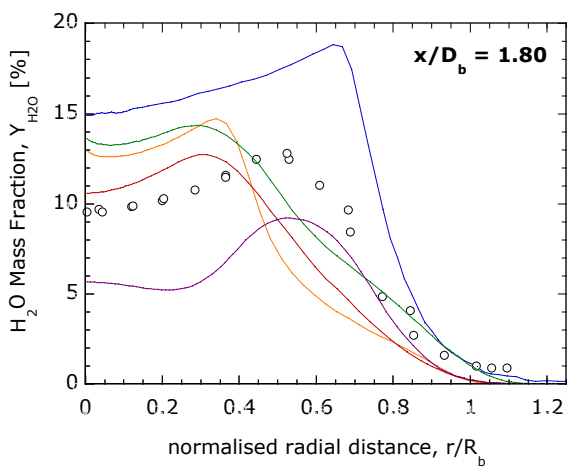
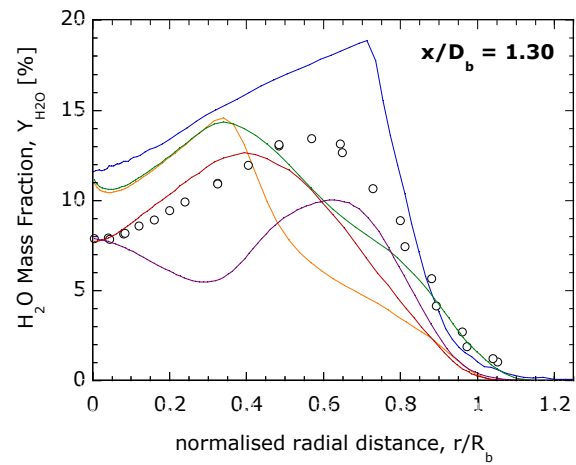
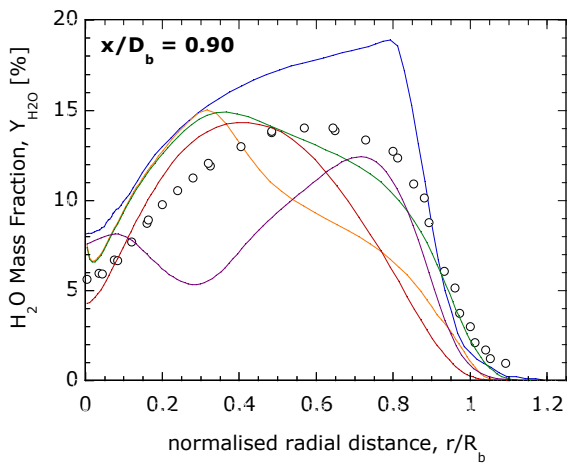
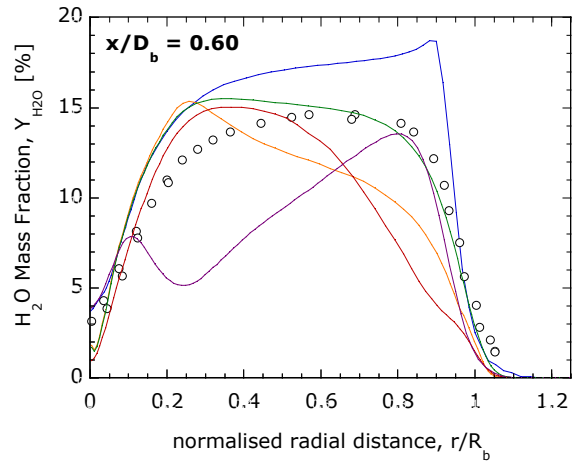
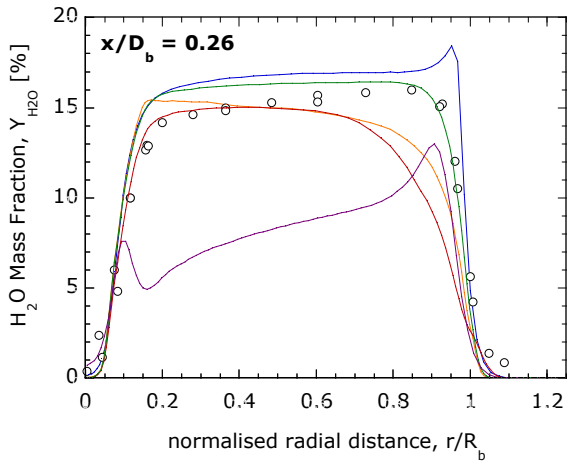


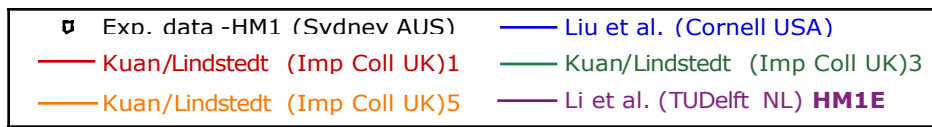
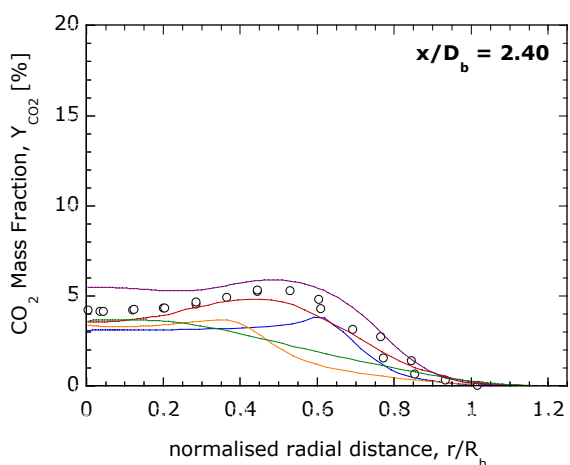
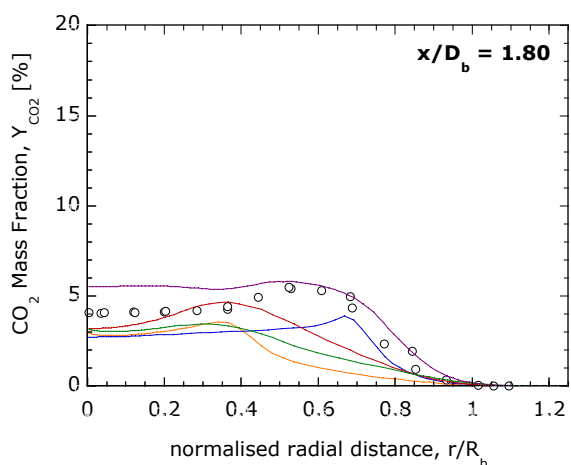
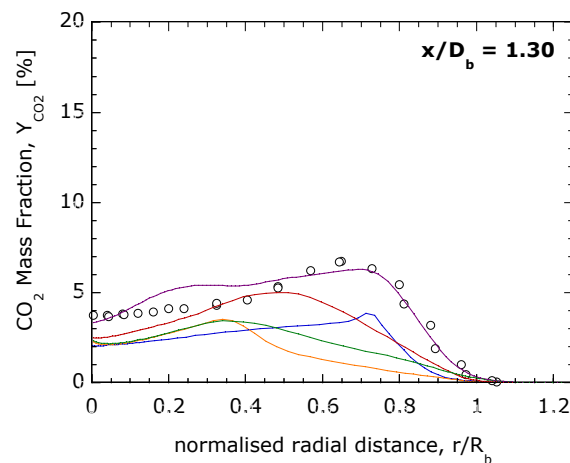
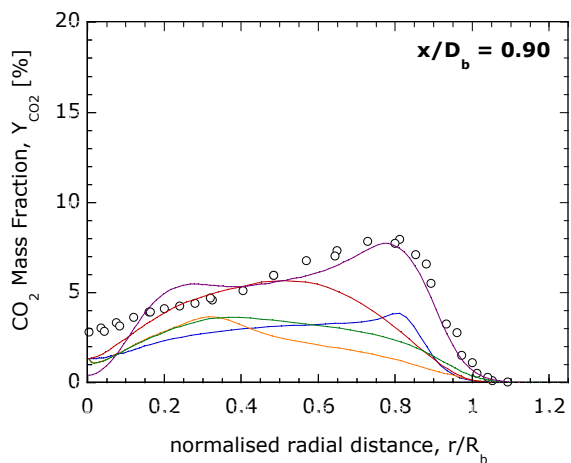
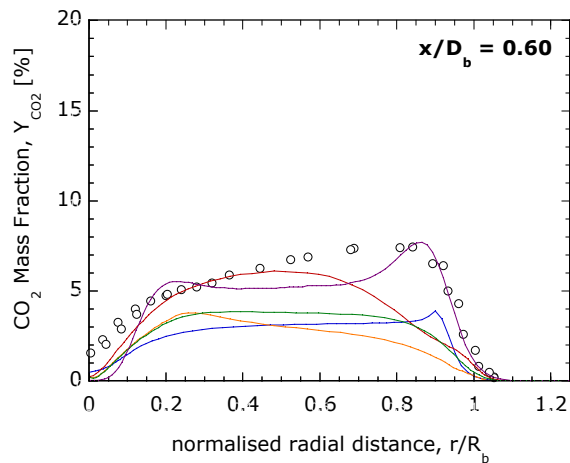
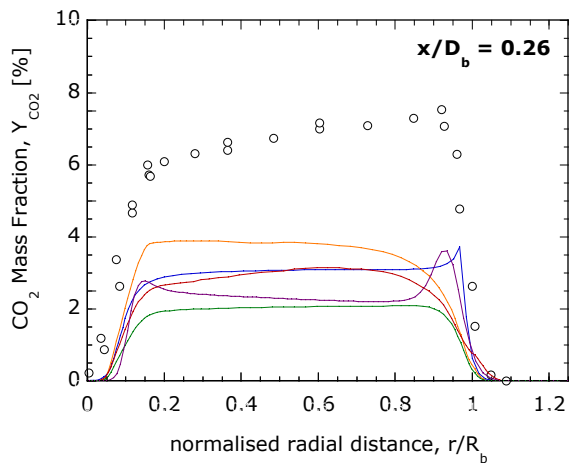


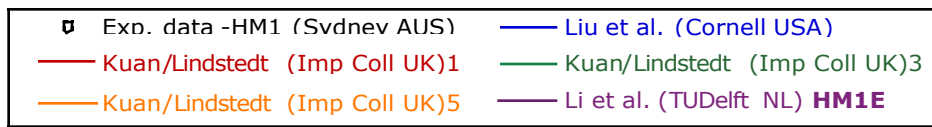
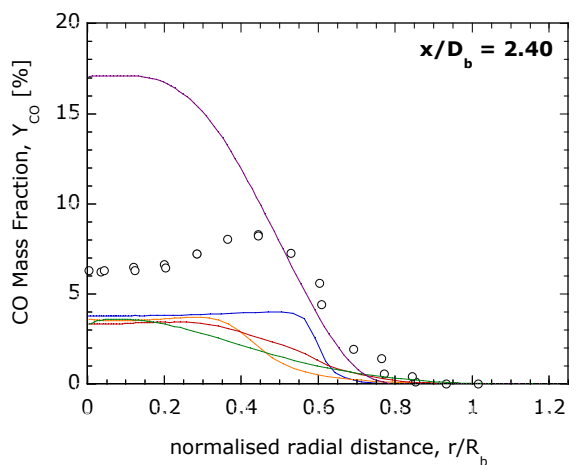
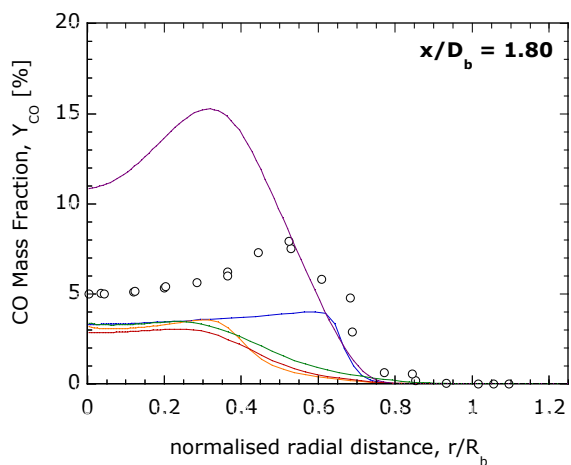
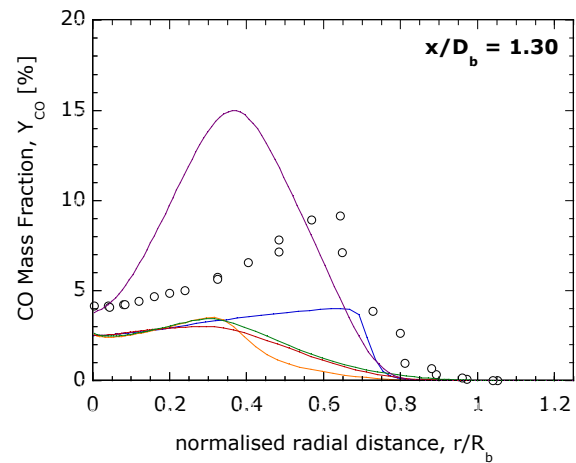
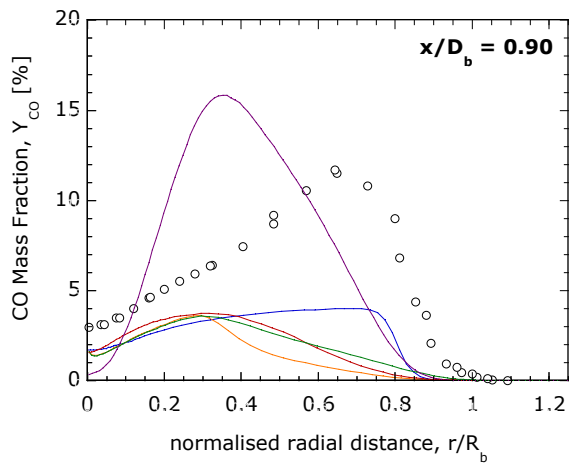
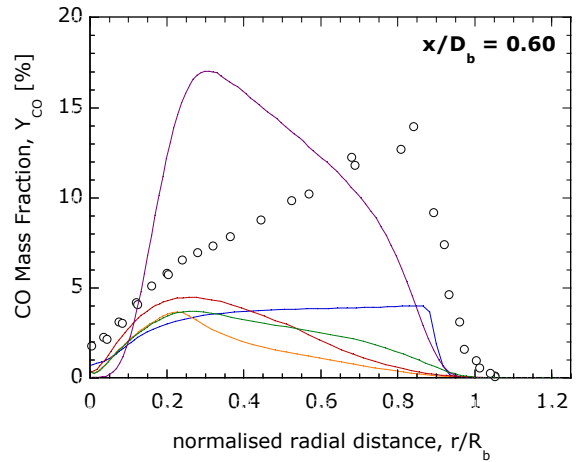
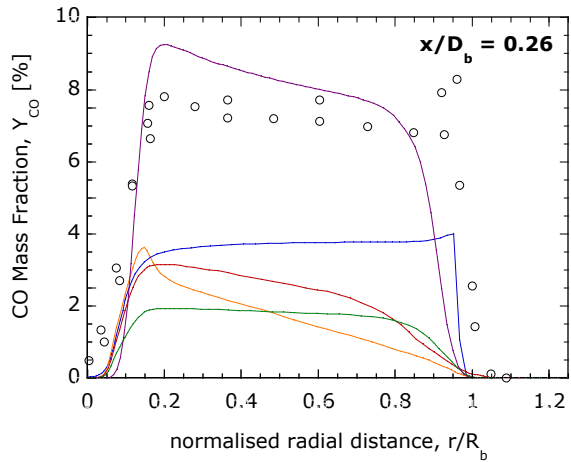


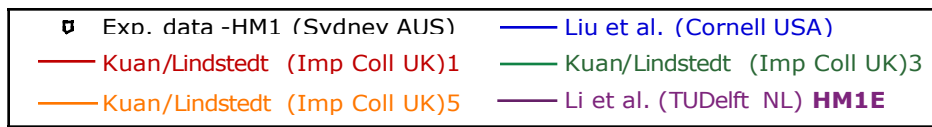
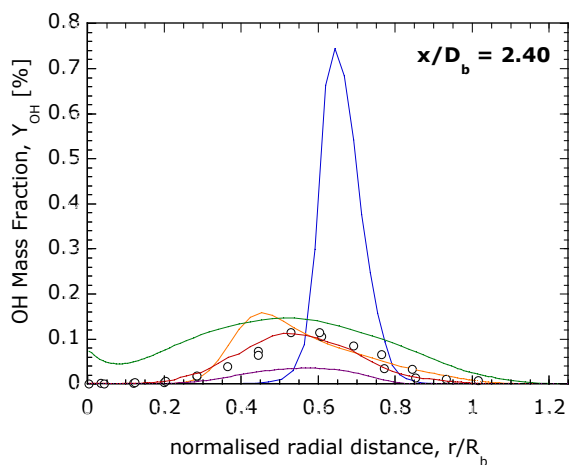
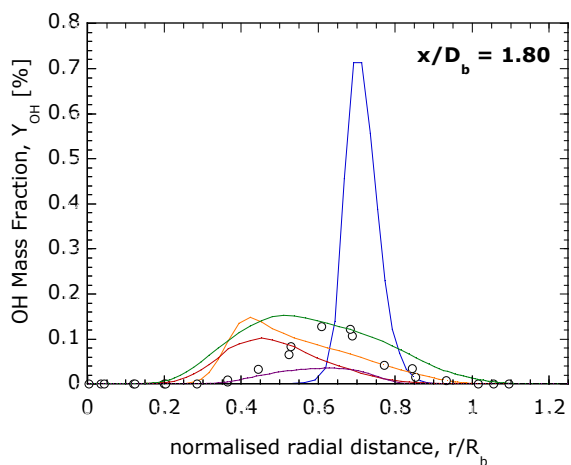
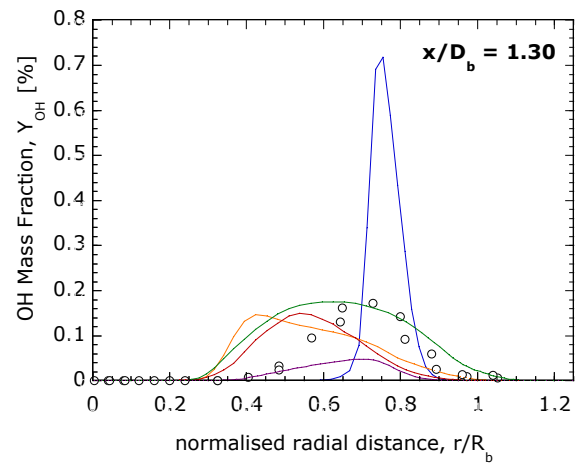
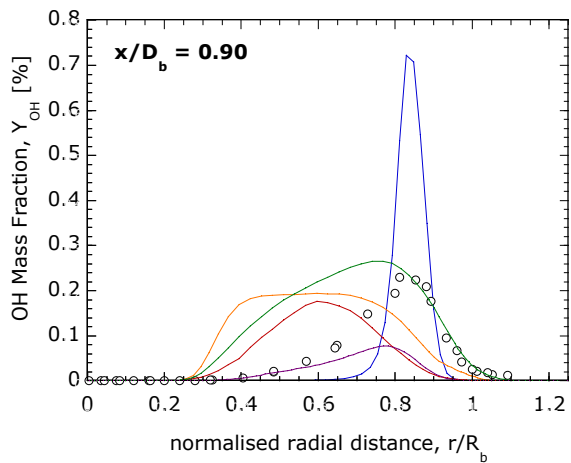
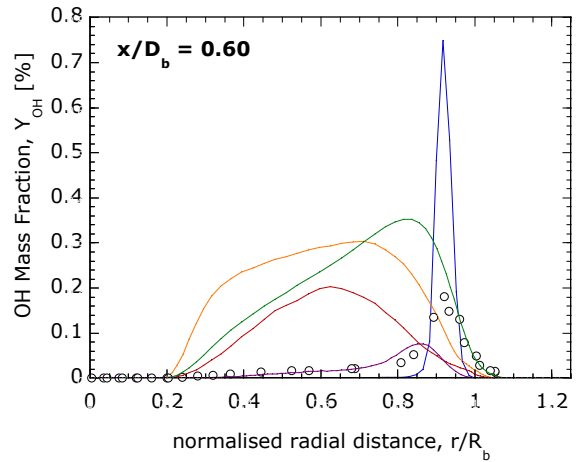
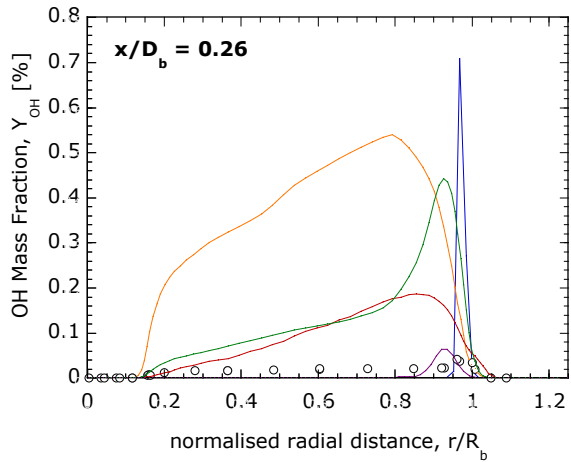


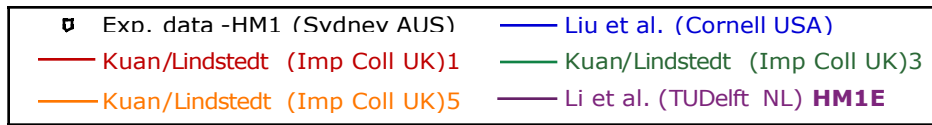
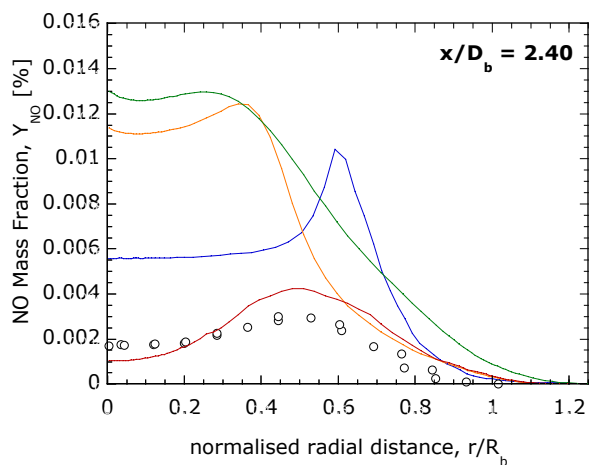
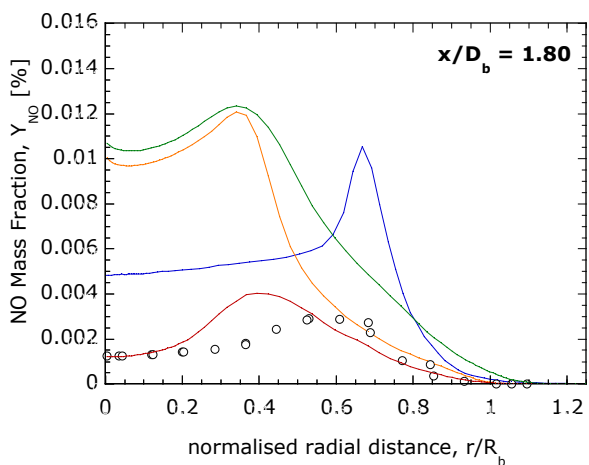
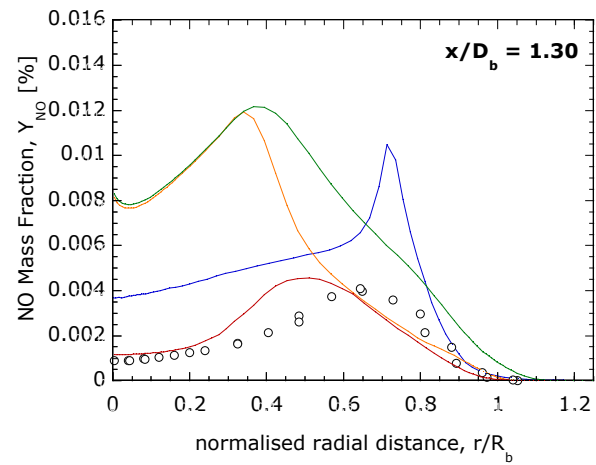
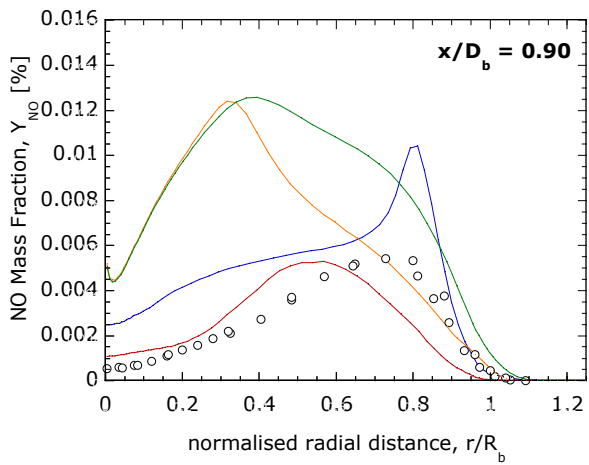
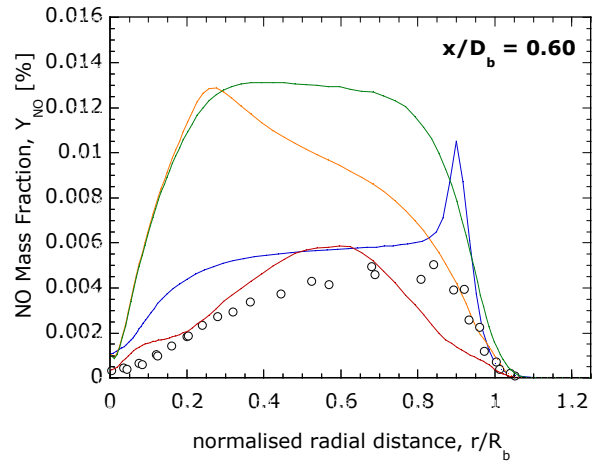
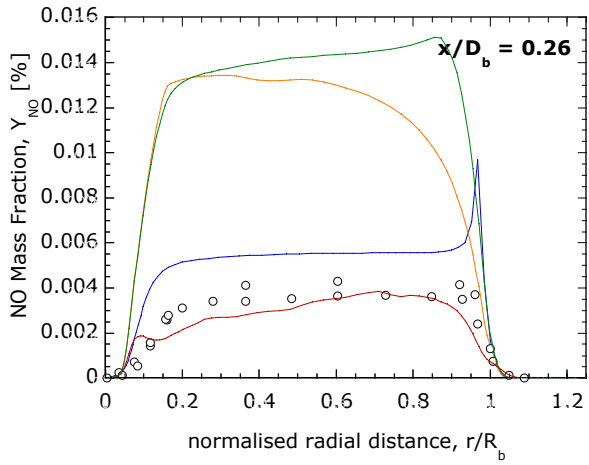












Sixth International Workshop on Measurement and Computation of Turbulent Nonpremixed Flames

Sapporo, Japan July 18-20, 2002

Swirl Stabilised Jets & Flames

Prepared by: **Assaad R. Masri and Yasir M. Al-Abdeli**
School of Aerospace, Mechanical and Mechatronic Engineering,
The University of Sydney,
NSW 2006, Australia

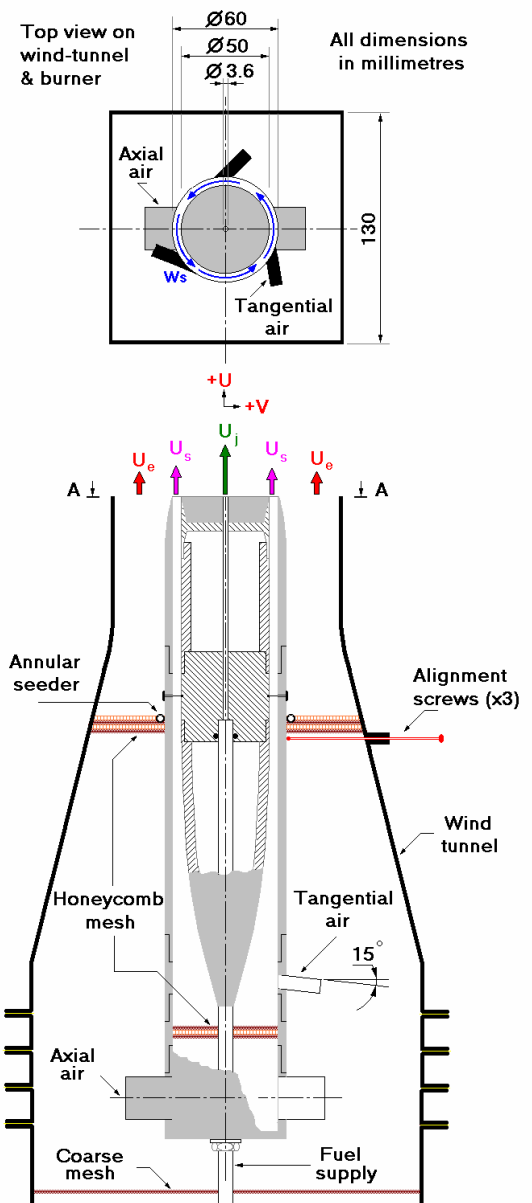
Introduction

The swirl burner described here is a simple extension of the bluff-body burner which has been adopted as a model problem for the TNF Workshop Series. It offers simple design with well-defined boundary conditions, yet it produces complex swirling flows which are not unlike those found in practical combustors. An extensive and comprehensive data bank, for selected flows on this burner configuration, was made available to TNF6 modellers through the web¹. Because, the data have not yet completely been published, this access was conditional that any publications of results based wholly or in part on the experimental data accessed will be delayed until these data appears in the literature.

Burner Geometry

The unconfined swirling flow has a 3.6 mm central jet and is surrounded by a 50mm diameter ceramic faced bluff-body. The bluff body is centered in a 60mm diameter annulus. Primary swirling air is introduced into this 5mm wide annulus using three tangential air inlets upstream of the burner exit plane. Axial air is also introduced into the primary axial stream through two upstream air ports.

The swirl number, S_g , is used for the quantitative representation of swirl strength, and is expressed as the integral of the measured mean bulk velocities (W_s/U_s), measured through LDV, above the annulus.



¹<http://www.mech.eng.usyd.edu.au/thermofluids>

The swirl number can be adjusted by varying the proportion of axial to tangential air through the annulus. The burner assembly is housed in a secondary axial (co-flow) wind tunnel. During the velocity and compositional measurements, the burner was housed in a wind-tunnel of exit cross-section 130 x 130mm and 305 x 305, respectively.

Computed Cases

The following swirling jets and flames were computed.

Non-Reacting Swirling Jets

		axial flowrate	tangential flowrate	tangential (each port)	jet flowrate	bulk jet velocity	swirl number
		Q_{ax}	Q_{tan}	$Q_{tan}/3$	$Q_{jet, AIR}$	$U_{jet, BULK}$	S_g
Flow	Gas	L/sec	L/sec	L/sec	L/sec	m/sec	(-)
N16S159	Air	0.00	14.00	4.67	0.67180	66	1.59
N29S054	Air	13.83	11.17	3.72	0.67180	66	0.54

Swirling Flames

		axial flowrate	tangential flowrate	tangential (each port)	CH4 jet flowrate	H2 diluent flowrate	total jet flowrate	bulk jet velocity	swirl number
		Q_{ax}	Q_{tan}	$Q_{tan}/3$	$Q_{jet, CH4}$	$Q_{jet, H2}$	$Q_{jet, TOTAL}$	$U_{jet, BULK}$	S_g
Flame	Fuel (vol. ratio)	L/sec	L/sec	L/sec	L/sec	L/sec	L/sec	m/sec	(-)
SMH1	CH4/H2 (1:1)	25.00	11.17	3.72	0.717	0.717	1.433	140.8	0.32

Submissions & Numerical Information

Computations for the cases above were submitted and the table below shows the pertinent numerical information.

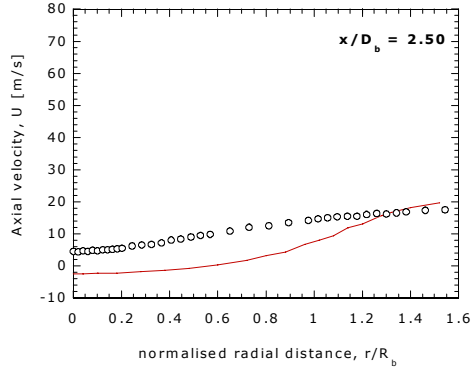
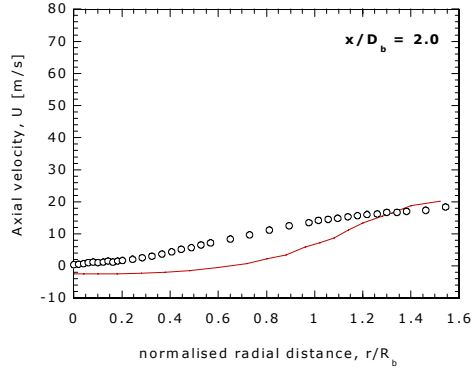
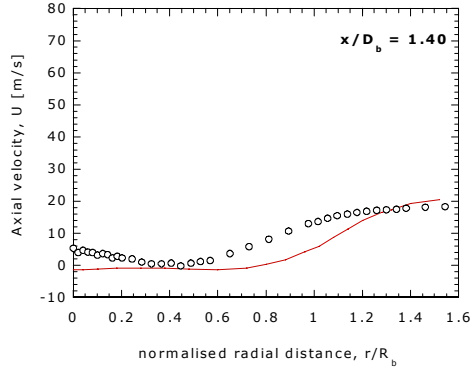
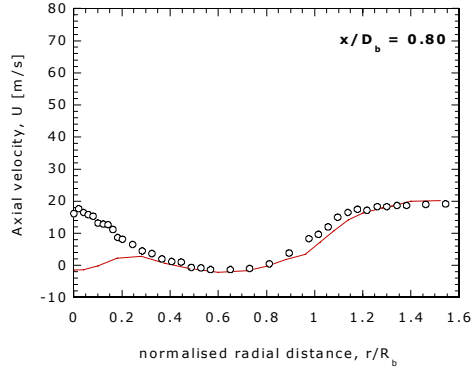
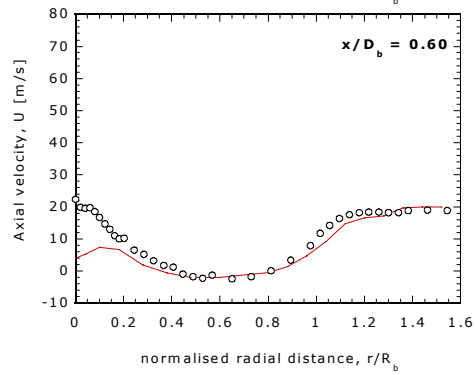
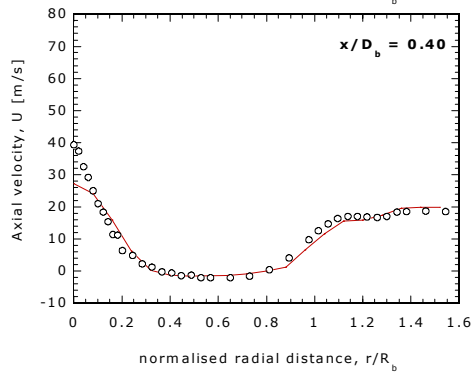
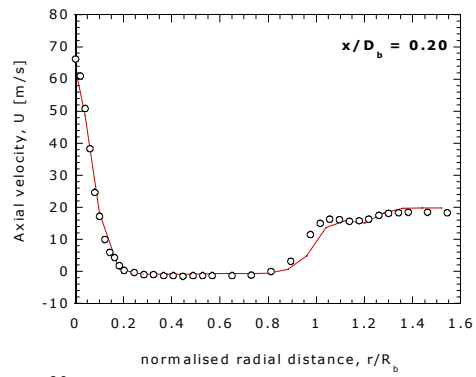
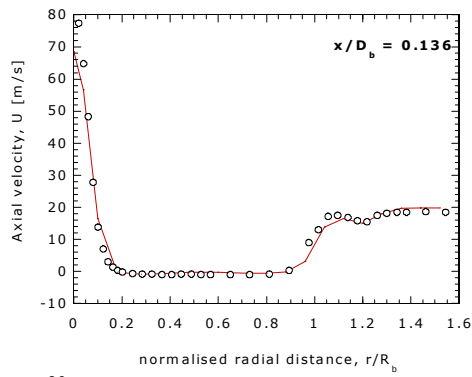
Case	<i>Non-Reacting</i>		<i>Reacting</i>
	N16S159	N29S054	SMH1
Modelers	B Guo & D Fletcher	B Guo & D Fletcher	B Guo & D Fletcher
Affiliation	Univ. of Sydney	Univ. of Sydney	Univ. of Sydney
Data Presented	<u>, <v>, <w>	<u>, <v>, <w>	<u>, <w>, T, ξ
Turbulence Model	k- ϵ	k- ϵ	RNG k- ϵ
Grid, Simulation	3D, Transient	3D, Transient	2D, Axisymmetric
Control volumes	367920	367920	11815
Domain/Axial (x_{min}, x_{max}) [mm]	-100, 450	-100, 450	-100, 450
Domain/Radial (y_{min}, y_{max}) [mm]	0, 150	0, 150	0, 150
Start of computations [mm]	x= -100	x= -100	x= -100
Model constants	c(mu)=0.09 c(epsilon1)=1.6 c(epsilon2)=1.92 sigma(k)=1.0 sigma(epsilon)=1.83	c(nu)=0.09 c(epsilon1)=1.6 c(epsilon2)=1.92 sigma(k)=1.0 sigma(epsilon)=1.83	c(mu)=0.085 c(epsilon1)=1.42 c(epsilon2)=1.68 sigma(k)=0.7179 sigma(epsilon)=0.7179
Notes	* regular jet precession predicted	* regular jet precession predicted	* chemistry: mixed-is-burnt

Acknowledgement

Thanks to B. Guo and D. Fletcher for their contributed computations.

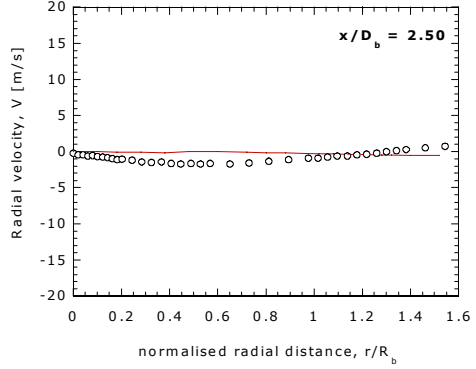
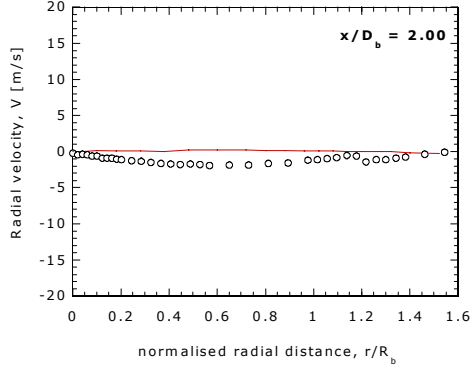
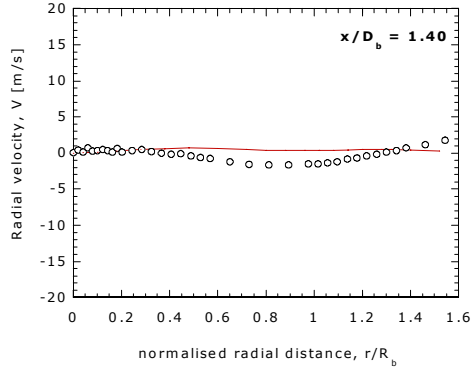
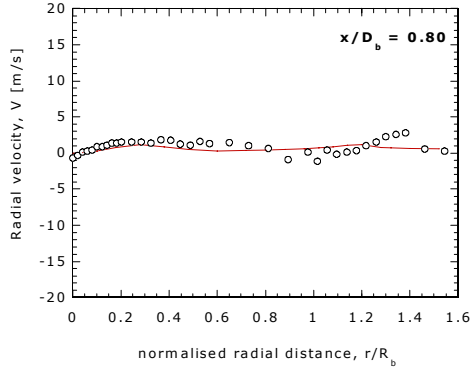
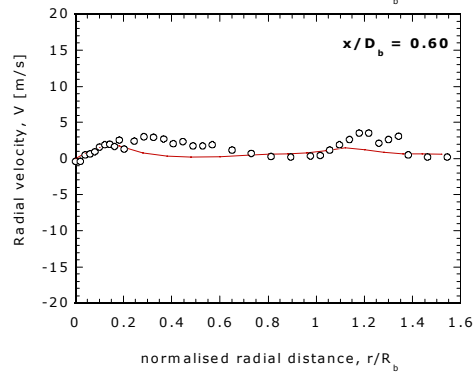
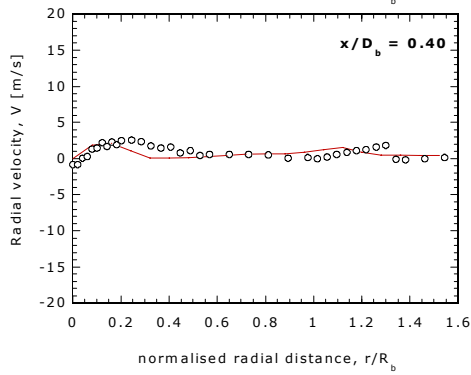
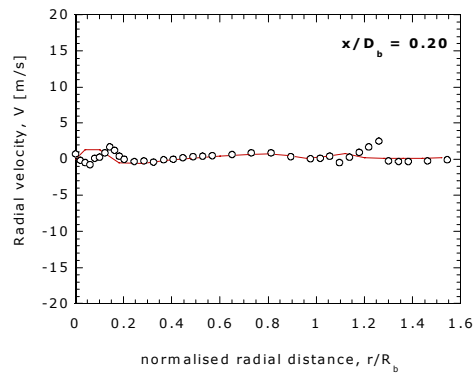
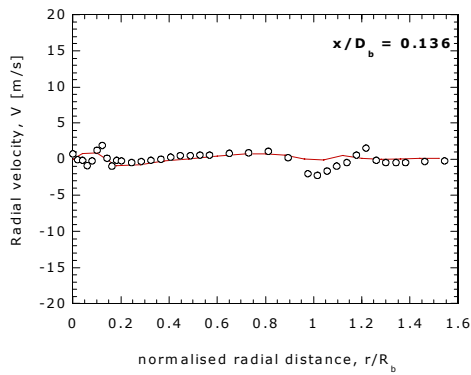
○ Exp. data - N16S159 (Sydney)

— Guo & Fletcher - KE (Sydney)



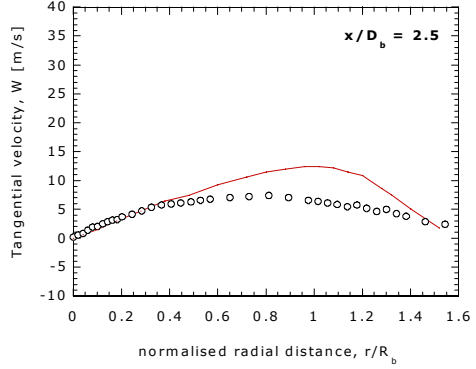
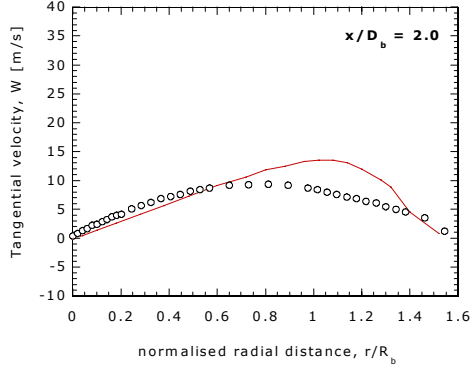
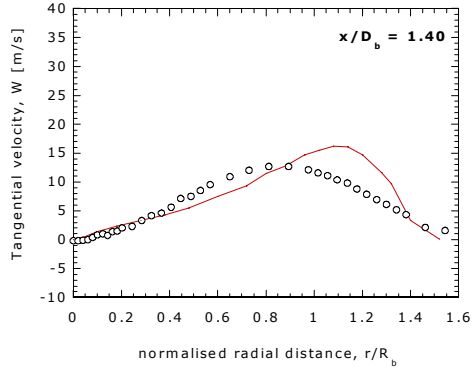
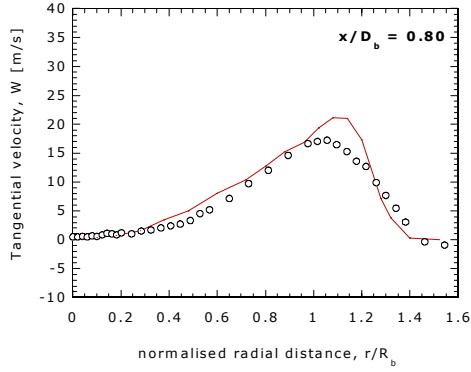
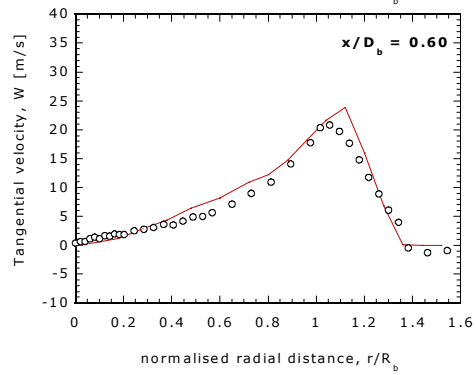
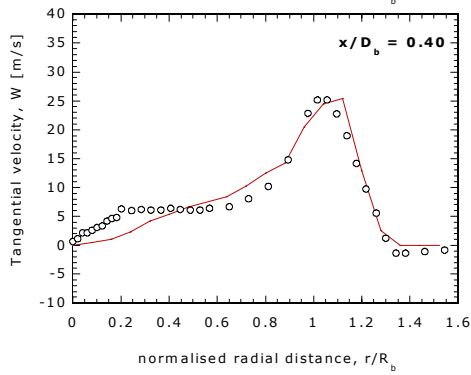
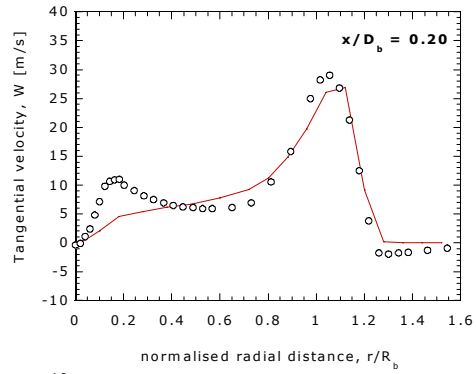
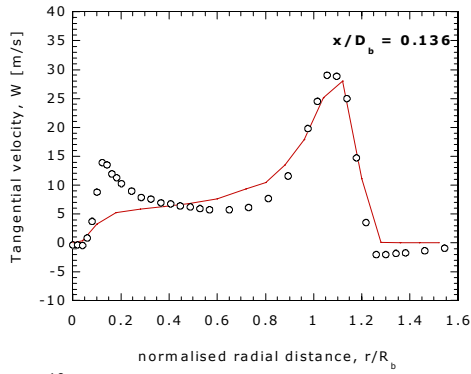
○ Exp. data - N16S159 (Sydney)

— Guo & Fletcher - KE (Sydney)



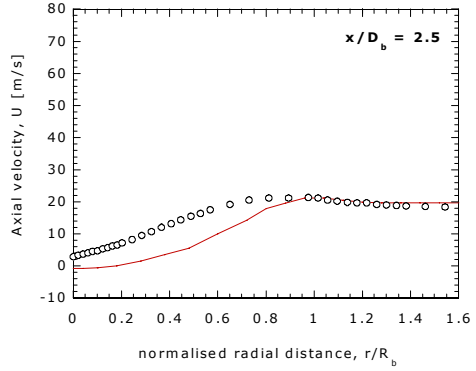
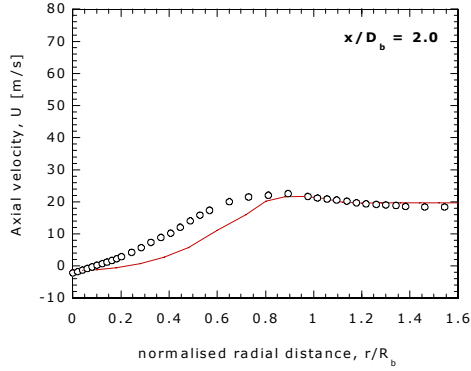
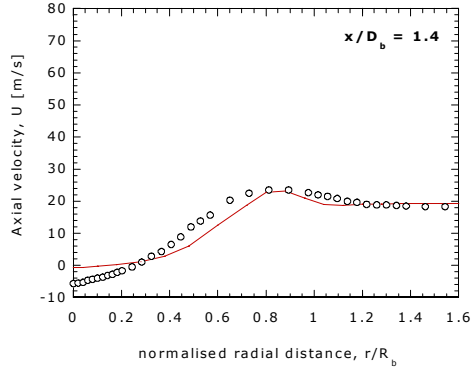
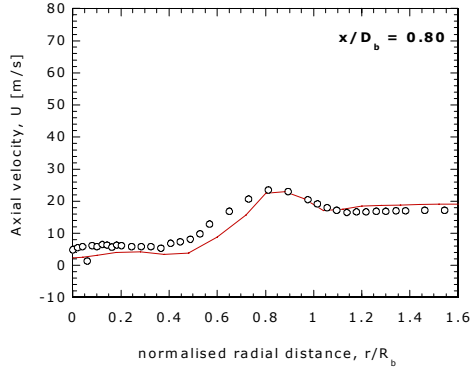
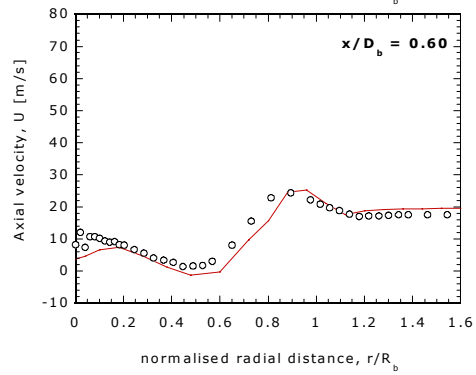
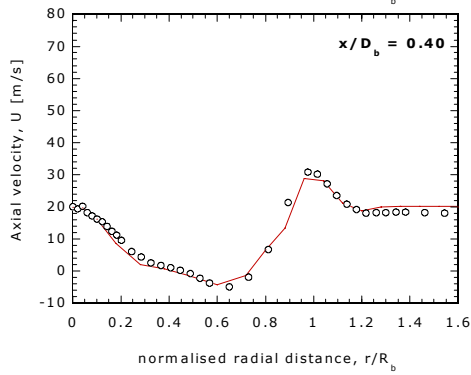
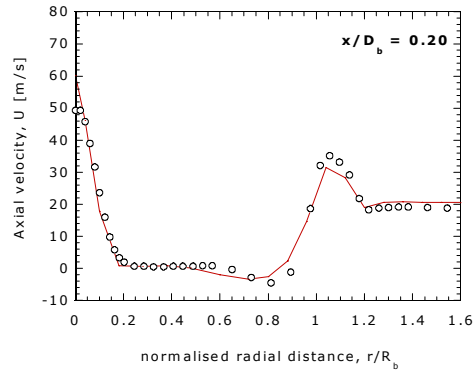
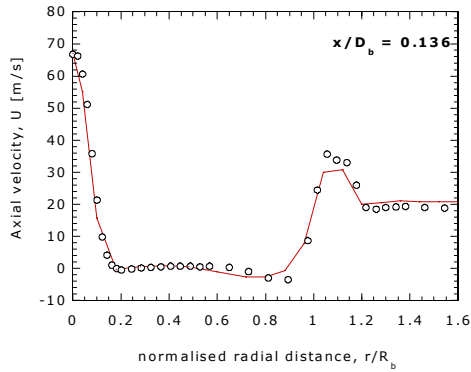
○ Exp. data - N16S159 (Sydney)

— Guo & Fletcher - KE (Sydney)



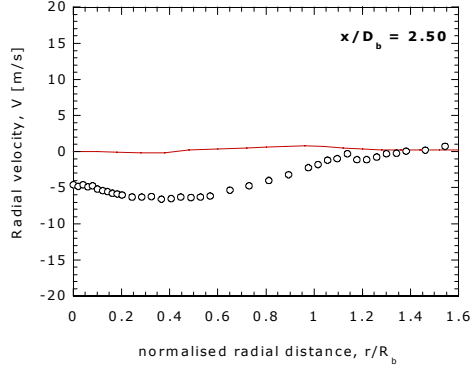
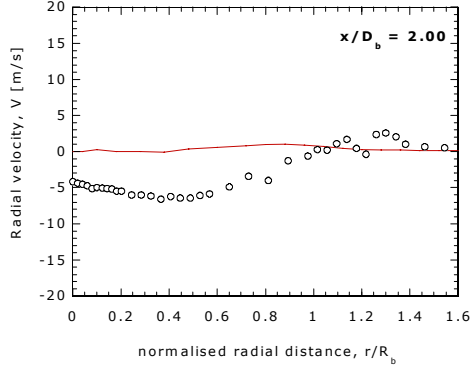
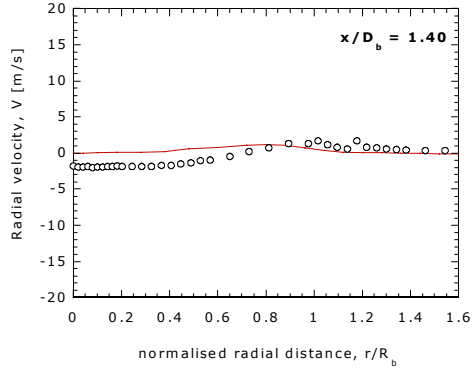
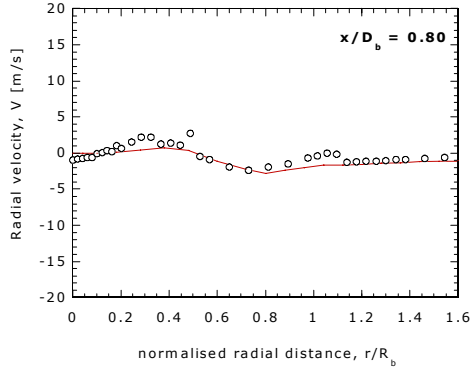
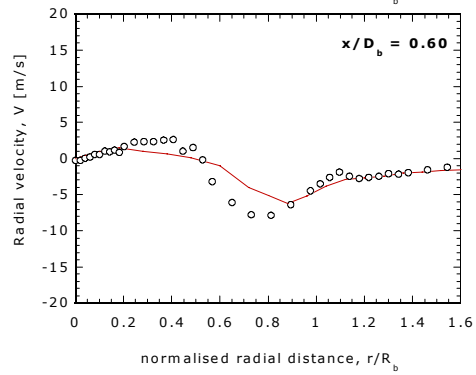
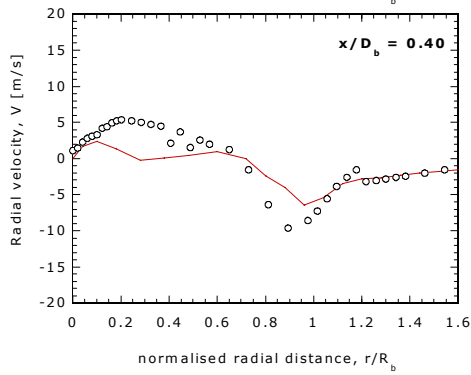
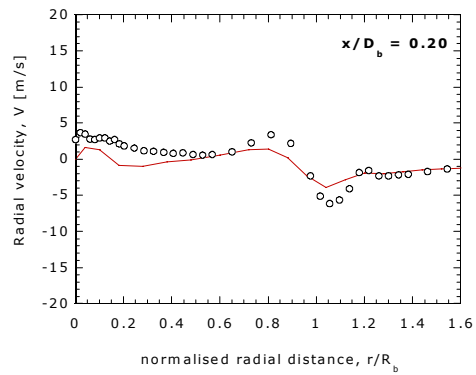
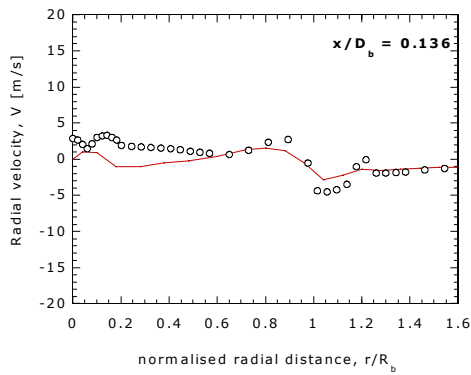
○ Exp. data - N29S054 (Sydney)

— Guo & Fletcher - KE (Sydney)



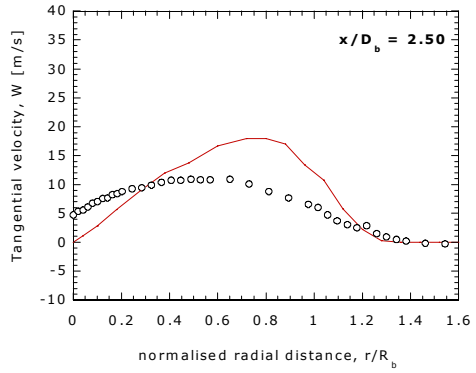
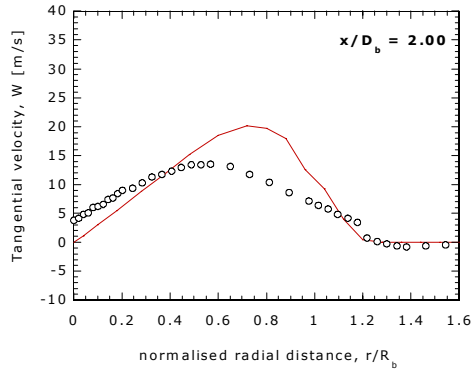
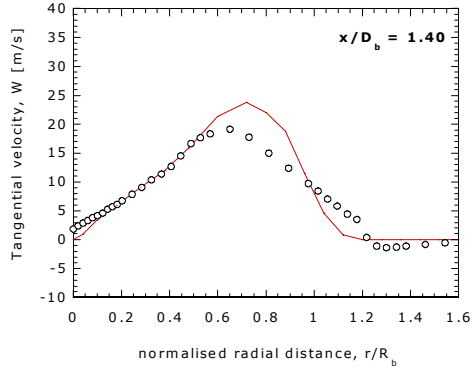
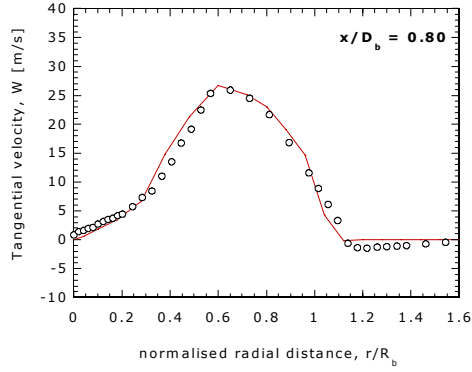
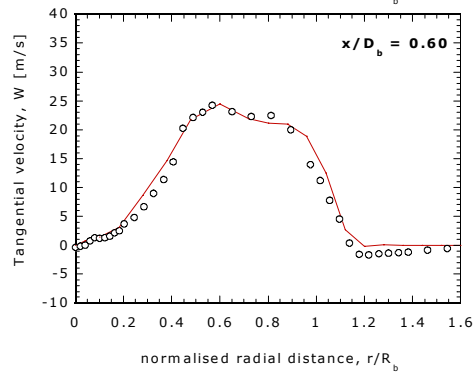
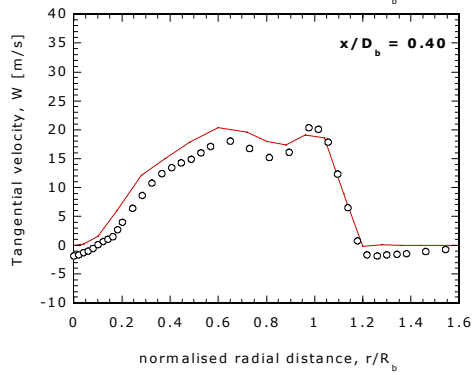
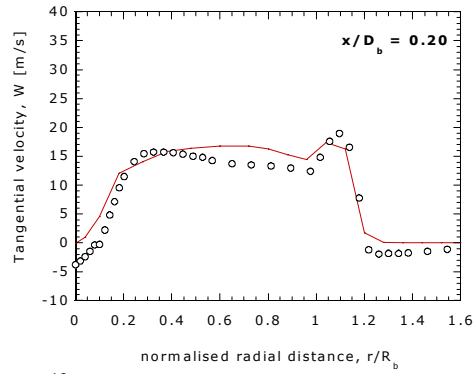
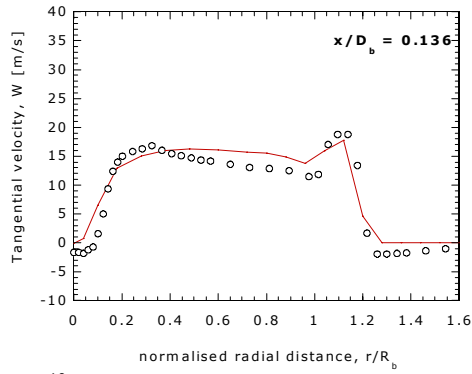
○ Exp. data - N29S054 (Sydney)

— Guo & Fletcher - KE (Sydney)



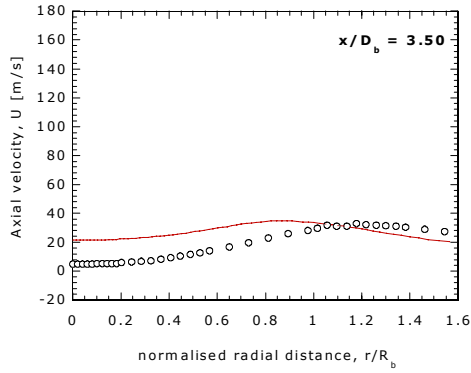
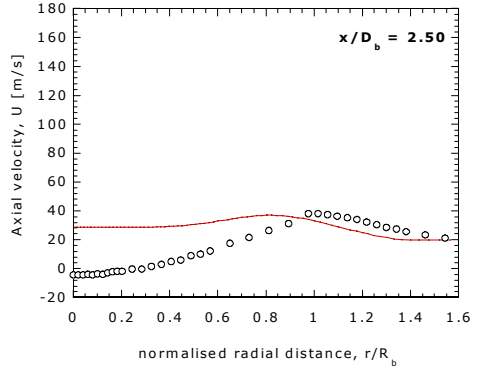
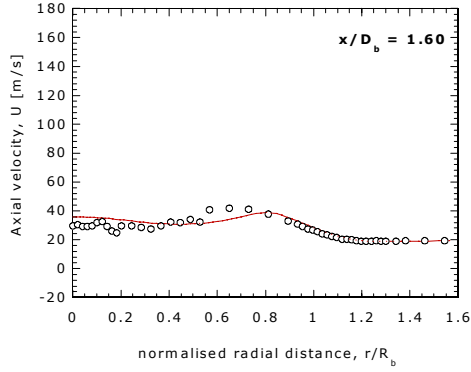
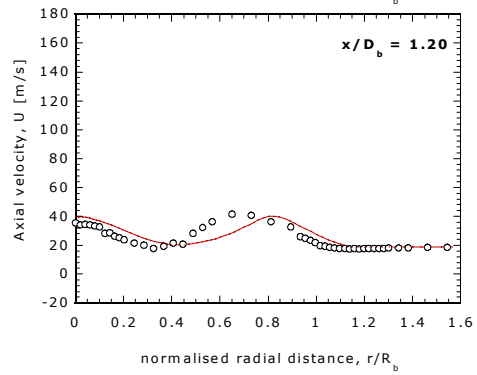
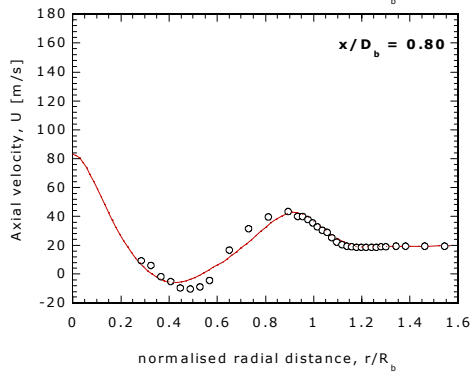
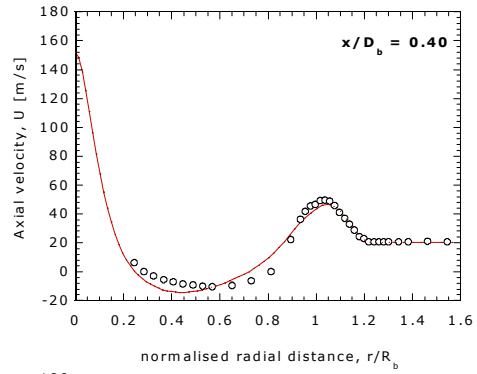
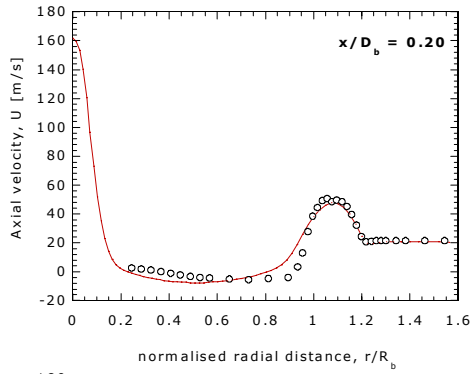
○ Exp. data - N29S054 (Sydney)

— Guo & Fletcher - KE (Sydney)



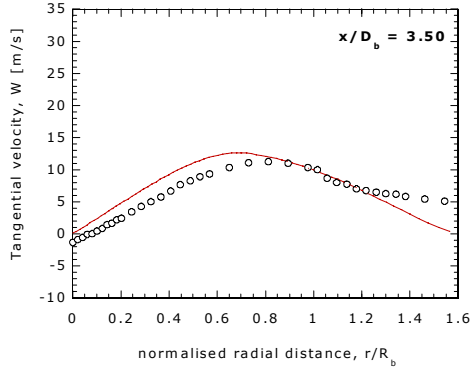
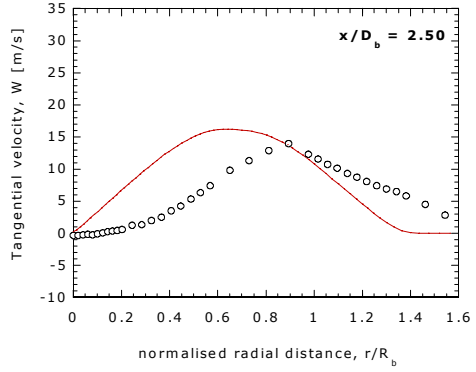
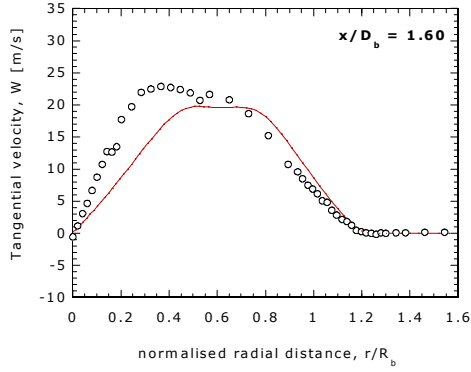
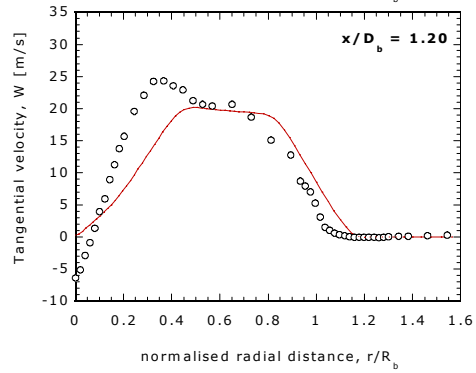
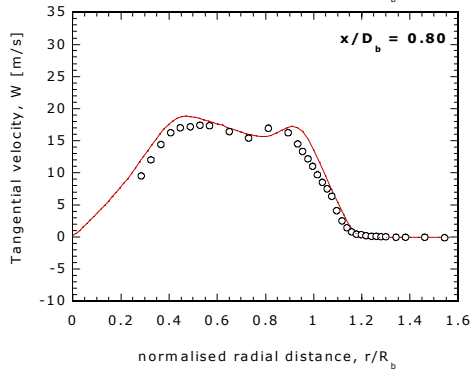
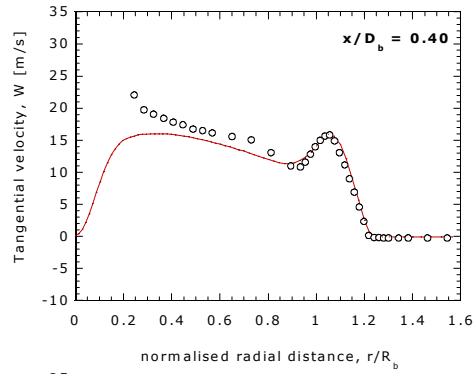
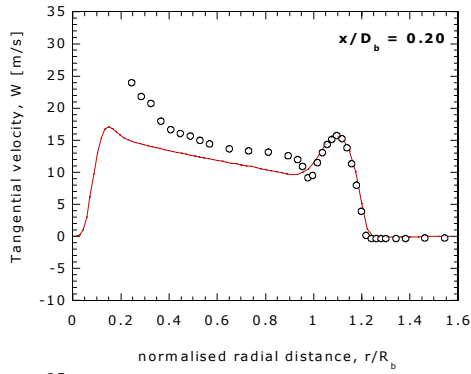
○ Exp. data - SMH1 (Sydney)

— Guo & Fletcher - KE (Sydney)



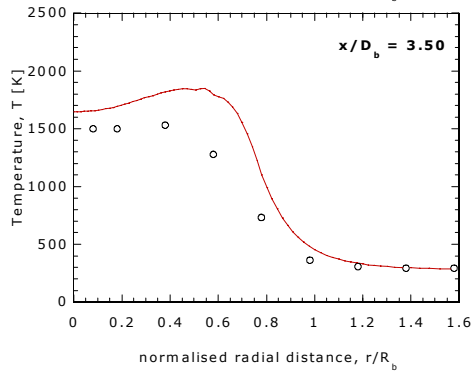
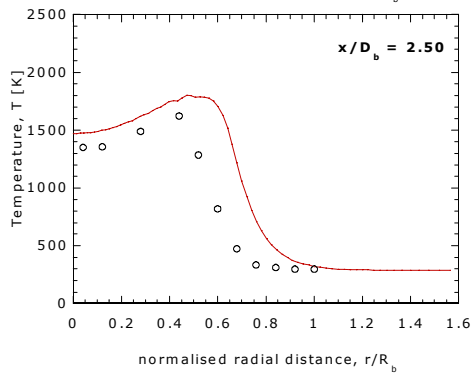
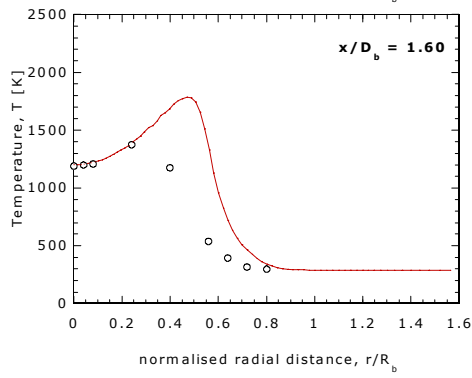
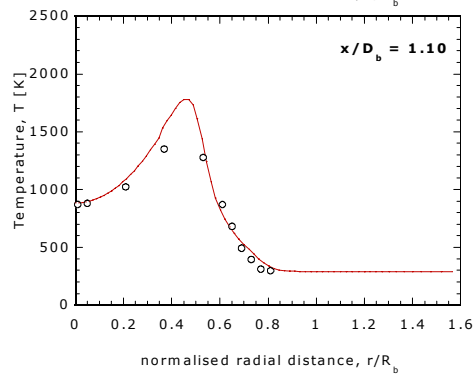
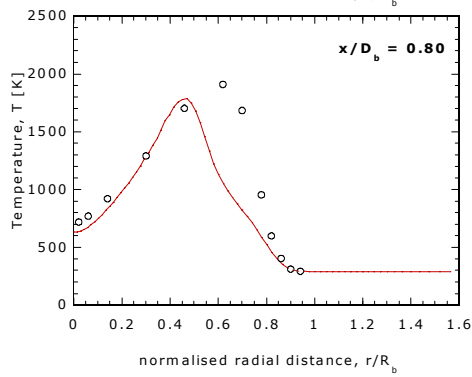
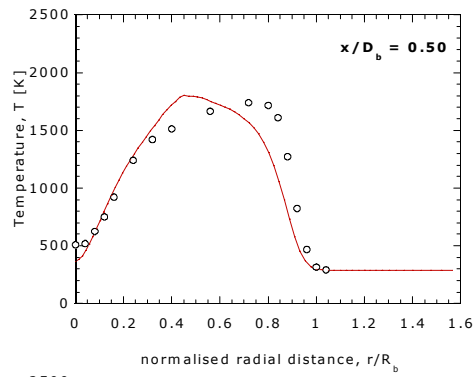
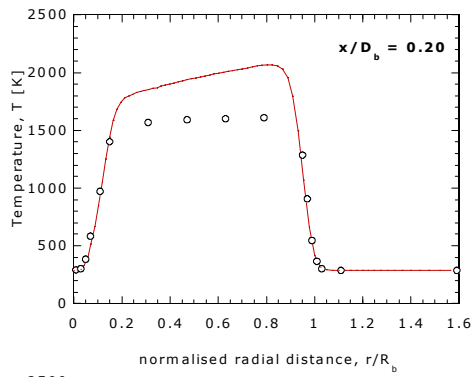
○ Exp. data - SMH1 (Sydney)

— Guo & Fletcher - KE (Sydney)



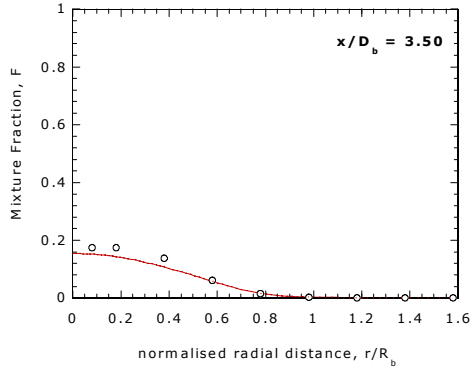
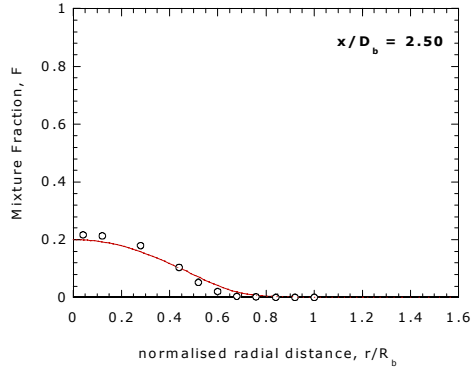
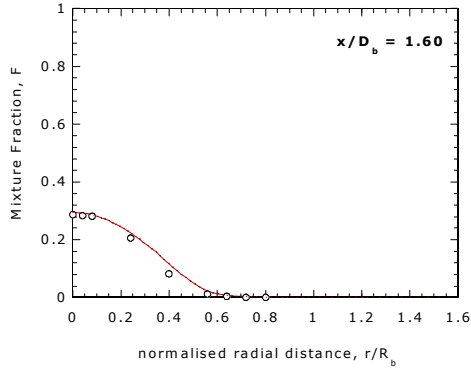
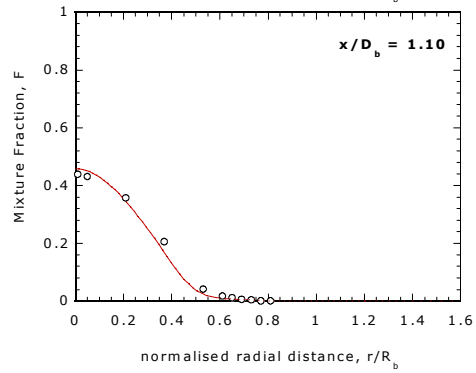
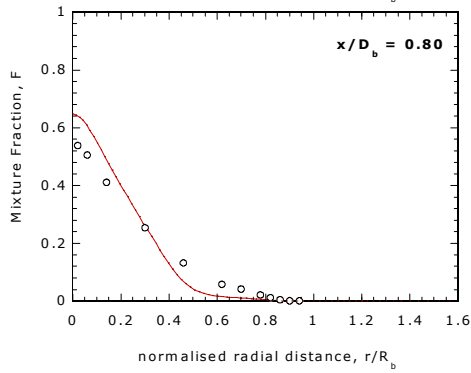
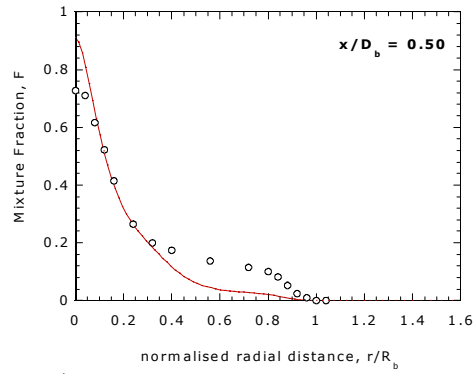
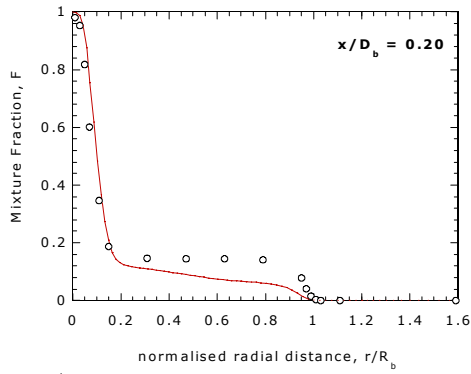
○ Exp. data - SMH1 (Sydney)

— Guo & Fletcher - KE (Sydney)



○ Exp. data - SMH1 (Sydney)

— Guo & Fletcher - KE (Sydney)

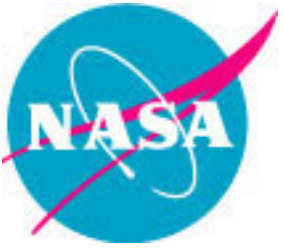


LES of the Masri Swirl Burner

Heinz Pitsch

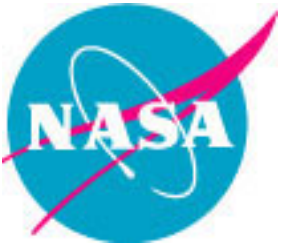
Center for Turbulence Research
Stanford University

Presently, we have performed simulations for the cold flow case only. These have been done using the CTR structured LES code by Pierce and Moin. This code employs dynamic models for all sub-grid quantities. The computational domain extends to $76 D$ in axial direction and $41 D$ in radial direction. The mesh consists of $320 \times 256 \times 64$ cells in axial, radial, and circumferential direction, respectively, resulting in approximately five million cells. This will be reduced in future simulations to approximately 2.5 million. The current mesh has been used to assess the influence of the lateral boundary conditions. Turbulent inflow conditions have been generated by performing a separate LES of a periodic turbulent pipe flow for the investigated nozzle geometry and the appropriate Reynolds number assuming fully developed turbulent flow.

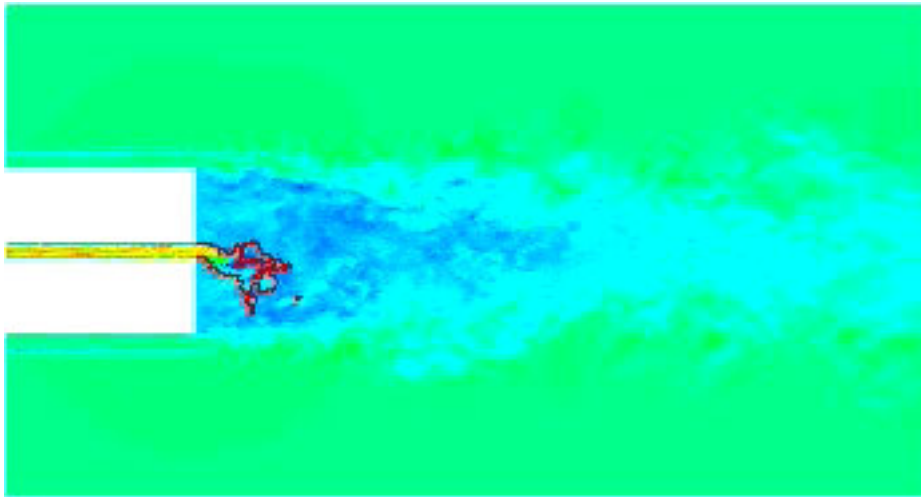


Large-Eddy Simulation of the Masri Swirl Burner

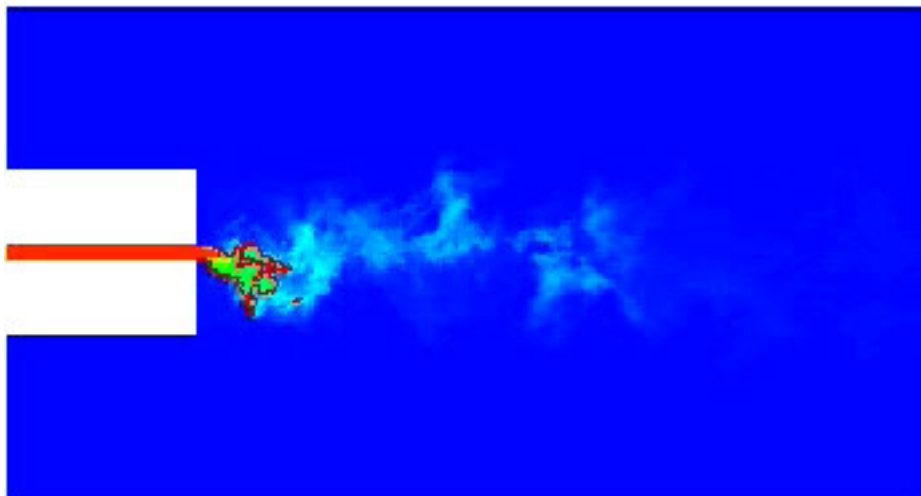
Heinz Pitsch



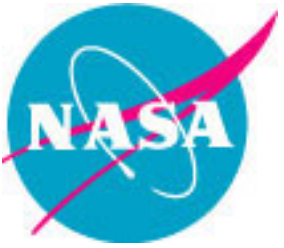
Masri Swirl Burner Cold Flow Simulation



Axial Velocity



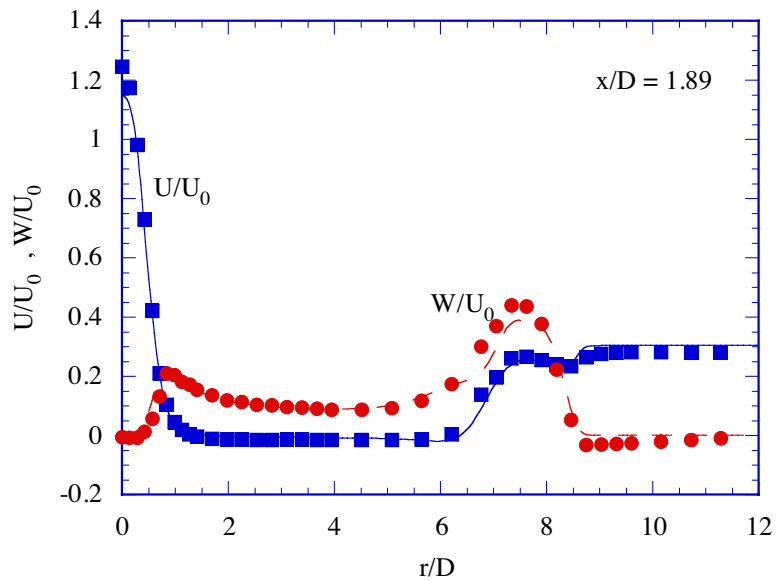
Mixture Fraction



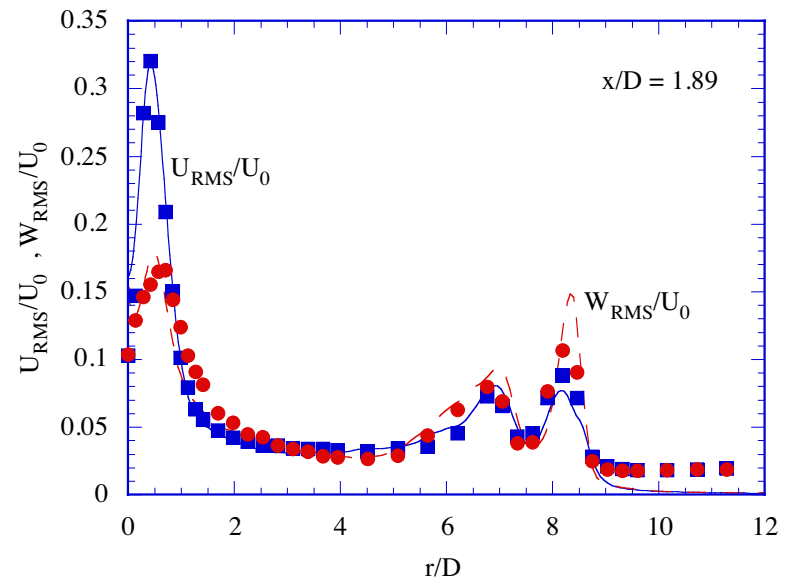
Masri Swirl Burner Cold Flow: Radial Profiles at $x/R = 1.89$

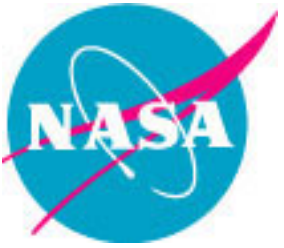


Mean Velocities



RMS Velocities

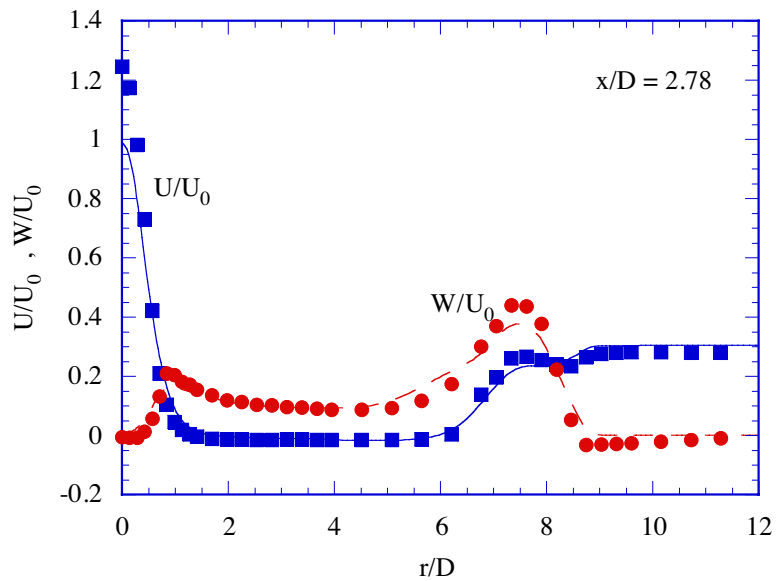




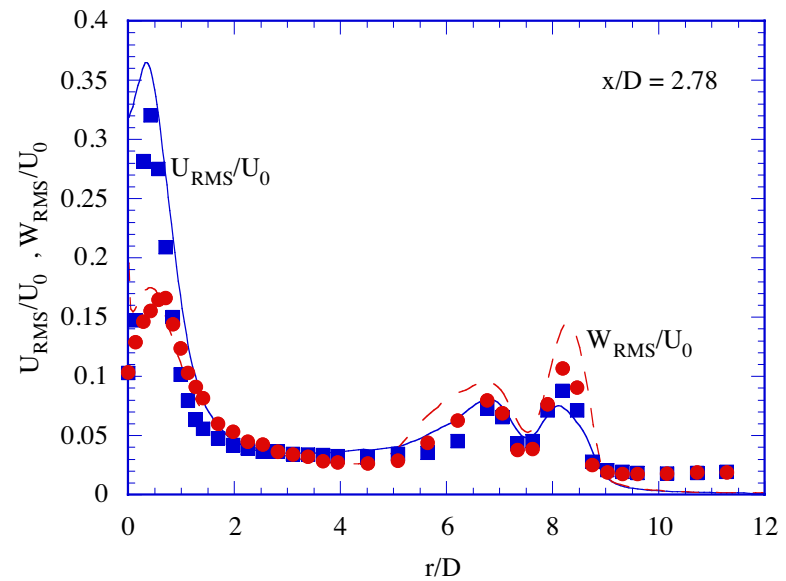
Masri Swirl Burner Cold Flow: Radial Profiles at $x/R = 2.78$

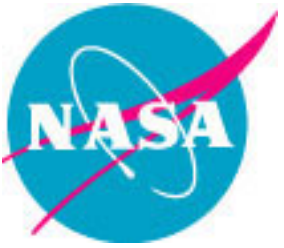


Mean Velocities



RMS Velocities

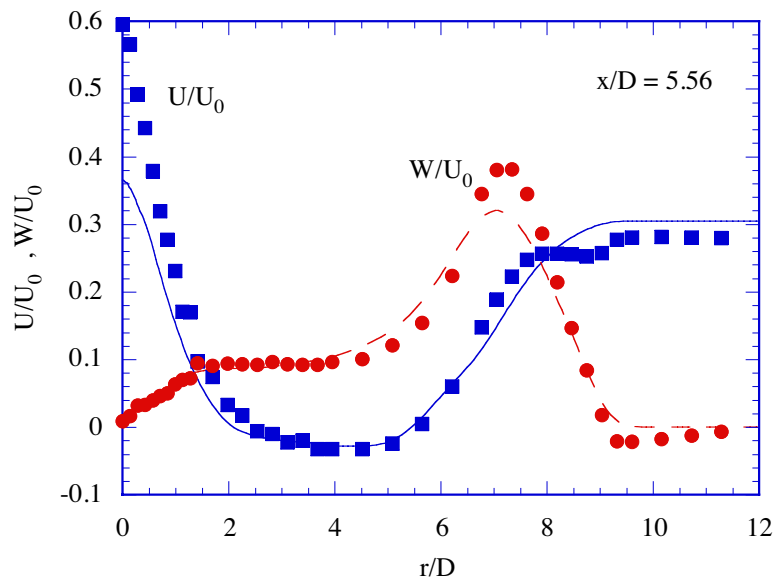




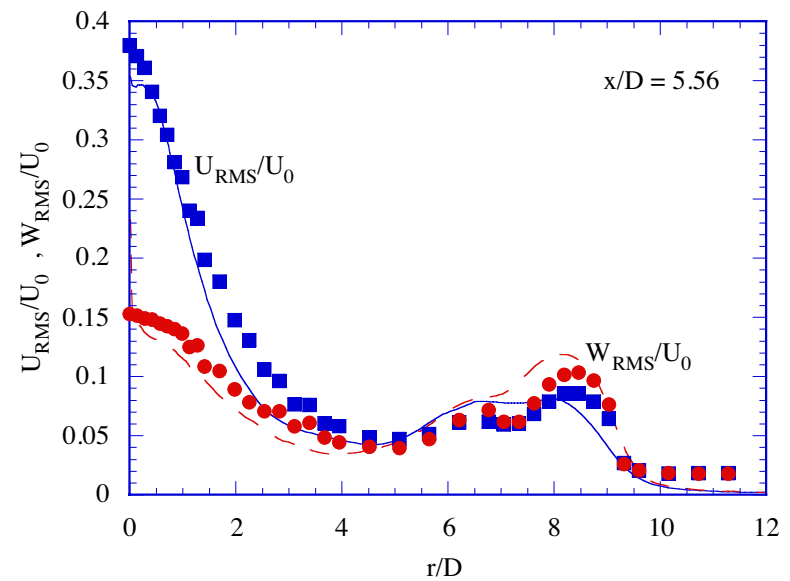
Masri Swirl Burner Cold Flow: Radial Profiles at $x/R = 5.56$

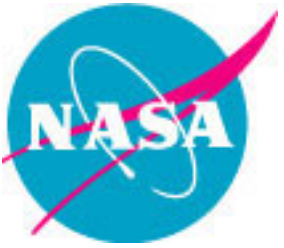


Mean Velocities



RMS Velocities

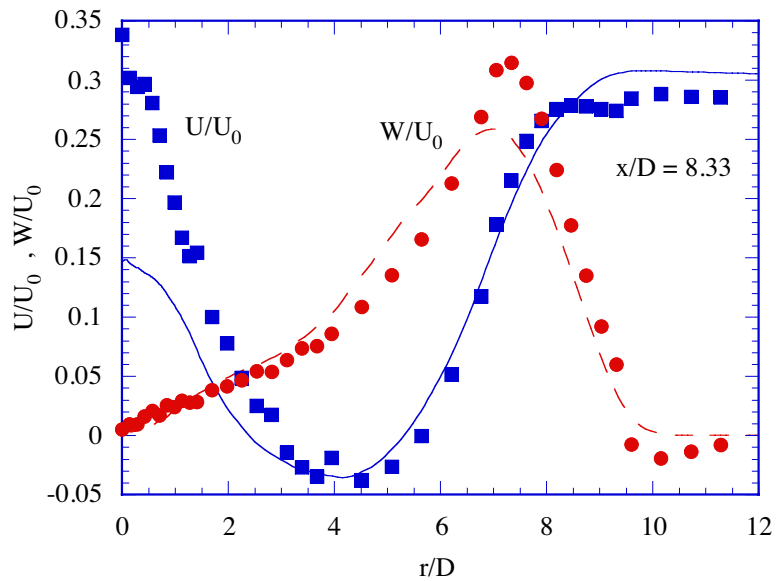




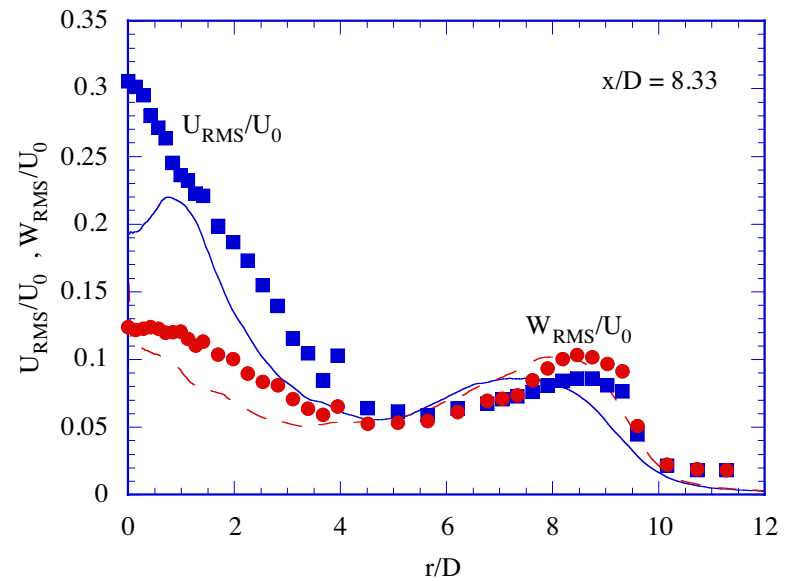
Masri Swirl Burner Cold Flow: Radial Profiles at $x/R = 8.33$

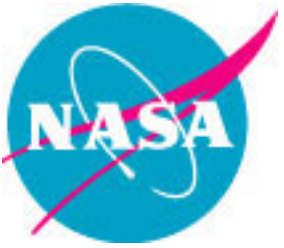


Mean Velocities

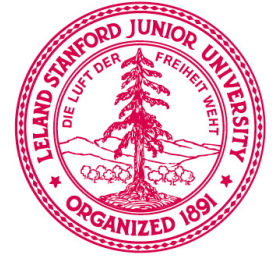


RMS Velocities

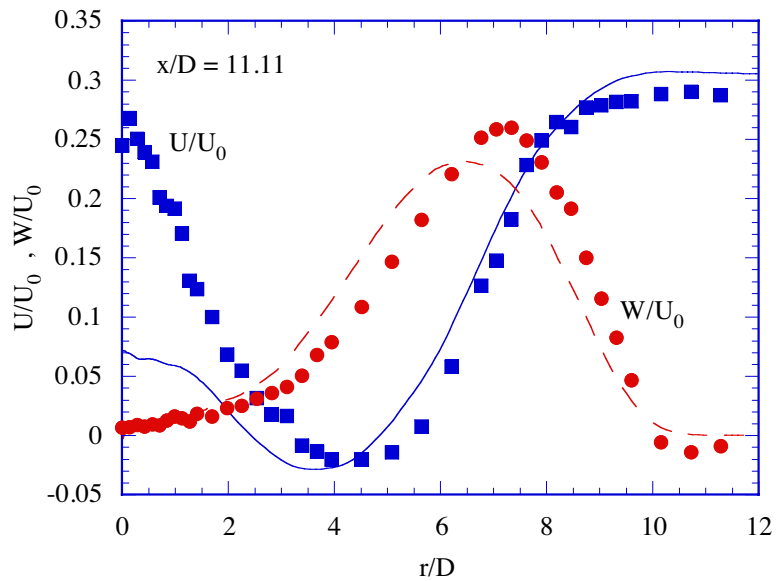




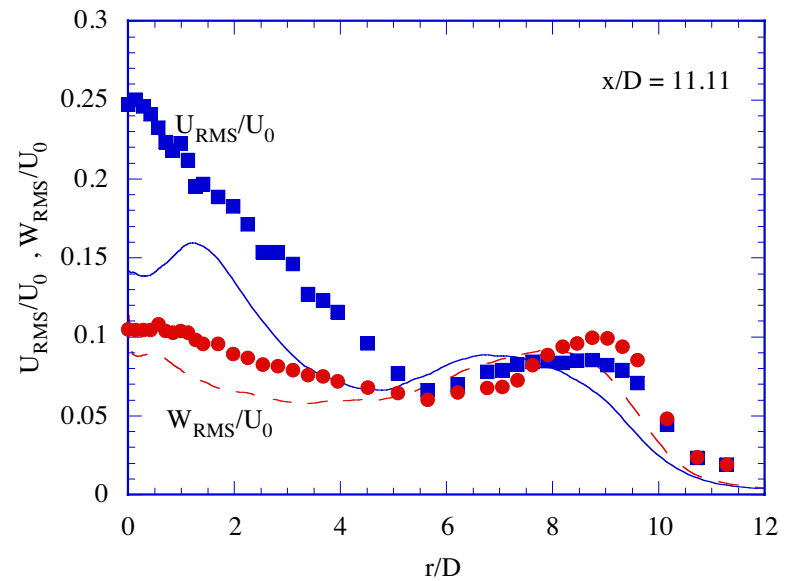
Masri Swirl Burner Cold Flow: Radial Profiles at $x/R = 11.11$

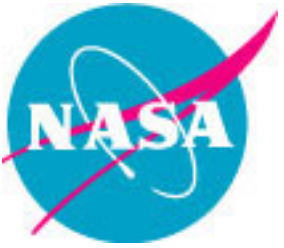


Mean Velocities



RMS Velocities

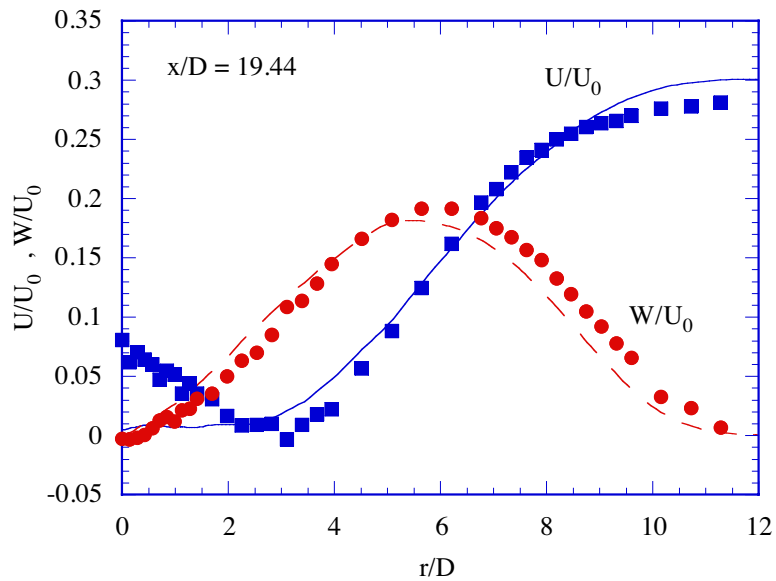




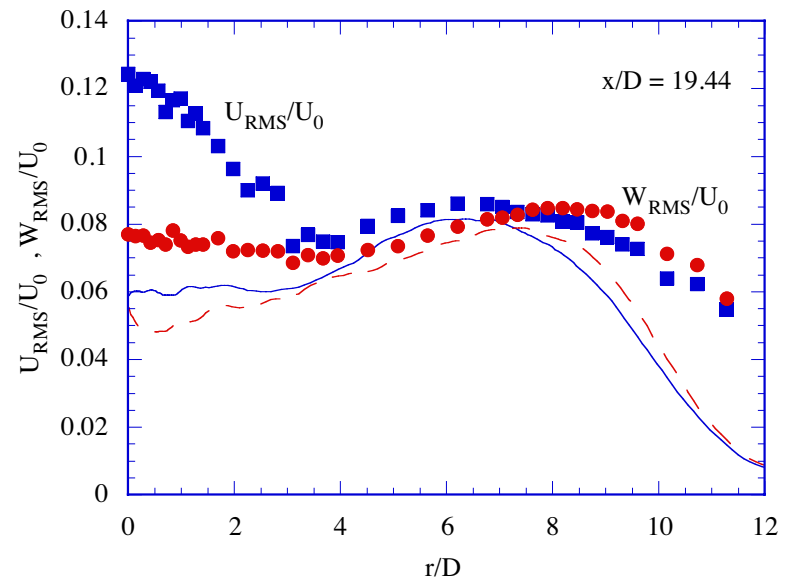
Masri Swirl Burner Cold Flow: Radial Profiles at $x/R = 19.44$

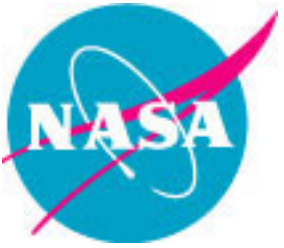


Mean Velocities



RMS Velocities

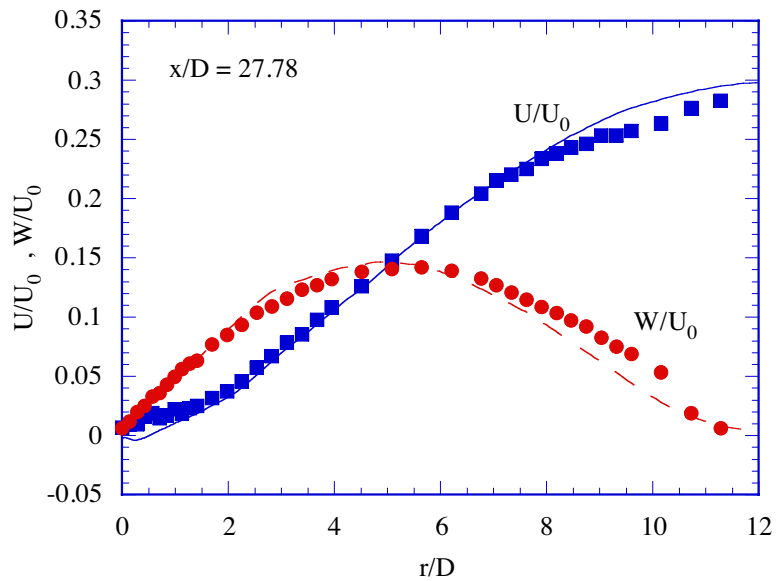




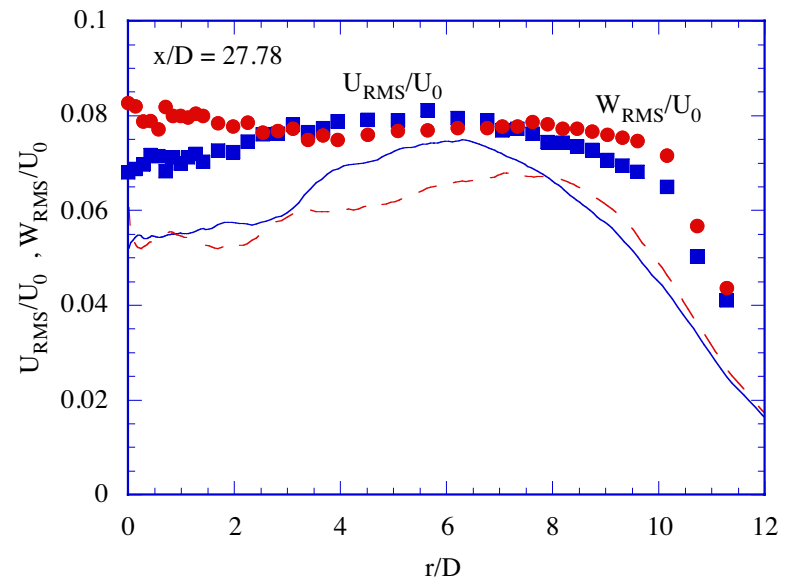
Masri Swirl Burner Cold Flow: Radial Profiles at $x/R = 27.78$

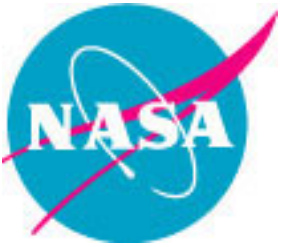


Mean Velocities



RMS Velocities

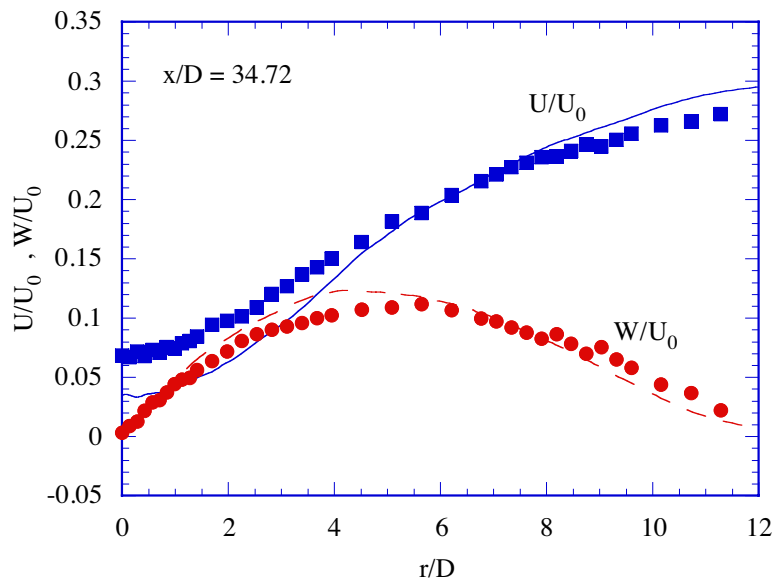




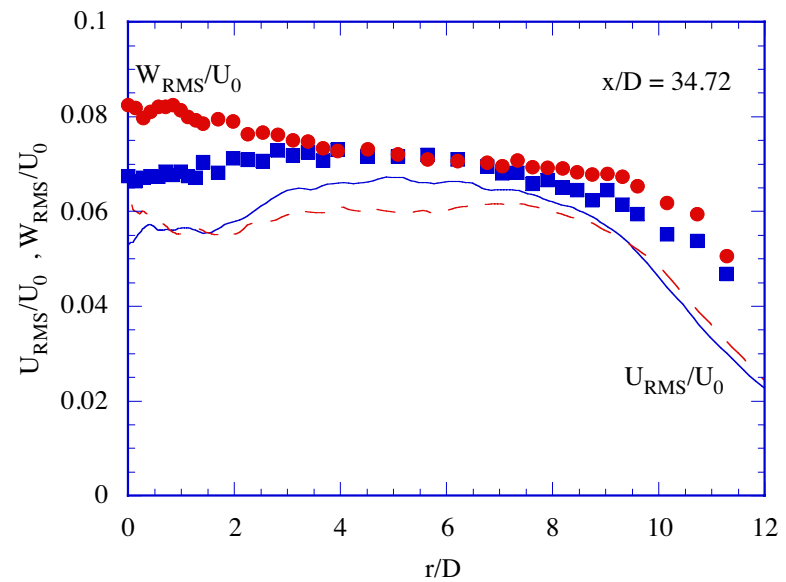
Masri Swirl Burner Cold Flow: Radial Profiles at $x/R = 34.72$

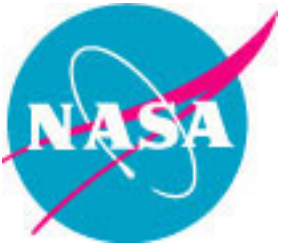


Mean Velocities



RMS Velocities





Conclusions



- Cold flow simulation for the Masri swirl burner
- Generally good agreement for axial and swirl mean velocities and velocity fluctuations
- Underprediction of fuel jet axial velocity

Modelling Scalar Dissipation

R W Bilger

School of Aerospace, Mechanical and
Mechatronic Engineering
The University of Sydney

TNF6 Sapporo

July 2002

Outline

- Motivation
- Some commonly used models for $\langle \chi | \eta \rangle$
 - Descriptions
 - Advantages and disadvantages
- Consistency with pdf transport equation
- Other models for $\langle \chi | \eta \rangle$
- $\langle \chi | \eta \rangle$ as a source of error
- Modelling scalar dissipation fluctuations
- Relationship to mixing models
- Relationship to dissipation of reactive scalars

Motivation

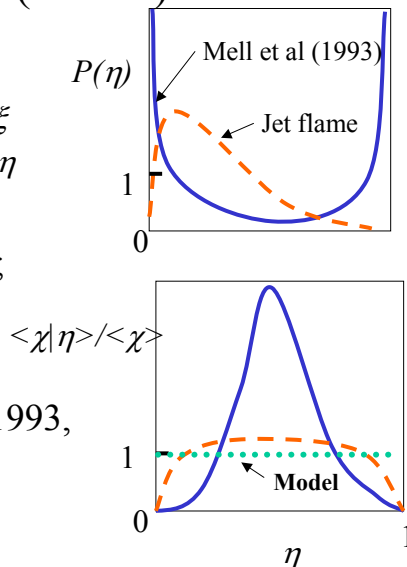
- Definitions: $\chi \equiv 2D \nabla \xi \cdot \nabla \xi$; $N \equiv \chi/2$;
 ξ is mixture fraction and η its sample space value
- Flamelet codes employ $\chi(\xi)$ and its fluctuations
- CMC requires $\langle \chi | \eta \rangle$ for first order closure and info on $\langle \chi^2 | \eta \rangle$ for second order closure
- Flamelet and CMC results for Flames D E and F appear to be sensitive to scalar dissipation modelling
- What is relationship to mixing models used in pdf calculations?

Some Commonly Used Models for $\langle \chi | \eta \rangle$, $\chi(\xi)$

- Counterflow laminar flamelet
 - $\chi(\xi) = \frac{2a}{\pi} \exp \left(-2 \left[\text{erfc}^{-1}(2\xi) \right]^2 \right)$ (1)
- Amplitude Mapping Closure
 - $\langle \chi | \eta \rangle = \langle \chi \rangle \exp \left(-2 \left[\text{erfc}^{-1}(2\eta) \right]^2 \right) / I_p$ (2)
- Advantages:
 - Some physical basis; literature pedigree
- Disadvantages:
 - Physically unrealistic; cumbersome to use

Some Commonly Used Models for $\langle \chi | \eta \rangle, \chi(\xi)$ (cont'd)

- Independent
 - $\chi(\xi)$ does not vary with ξ
 - $\langle \chi | \eta \rangle$ does not vary with η
- Advantages:
 - Simplicity; ease of use;
 - often may be okay
- Disadvantages:
 - Disrepute (Mell et al (1993, 1994) - rare problem?



Some Commonly Used Models for $\langle \chi | \eta \rangle, \chi(\xi)$

- Girimaji's model
 - $$\langle \chi | \eta \rangle = 2 \frac{\varepsilon \langle \xi \rangle (1 - \langle \xi \rangle)}{k \langle \xi'^2 \rangle} \frac{I(\eta)}{P(\eta)} \quad (3)$$
 - Homogeneous turbulence
 - Beta function pdf – integrate pdf transport eq
- Advantages:
 - Some physical basis; literature pedigree; robust
- Disadvantages:
 - Physically unrealistic in inhomogeneous flows
 - Cumbersome to use

Pdf Transport Eqn

$$\frac{\partial \rho_\eta P(\eta)}{\partial t} + \nabla \cdot (\rho_\eta P(\eta) \langle \mathbf{v} | \eta \rangle) = - \frac{\partial^2 \rho_\eta P(\eta) \langle N | \eta \rangle}{\partial \eta^2} \quad (4)$$

- Model for conditional velocity

$$\langle \mathbf{v} | \eta \rangle = \langle \mathbf{v} \rangle + \frac{\langle \mathbf{v}' \xi' \rangle}{\langle \xi'^2 \rangle} (\eta - \langle \xi \rangle) \quad (5)$$

- Integrate pdf transport eqn by parts to get

Klimenko and Bilger (1999)

- ... the result

$$\langle N | \eta \rangle P(\eta) = \frac{\partial I_1(\eta)}{\partial t} + \langle \mathbf{v} \rangle \cdot \nabla I_1(\eta) + \nabla \cdot (\langle \rho \rangle \langle \mathbf{v}' \xi' \rangle I_2(\eta) / \langle \xi'^2 \rangle) / \langle \rho \rangle \quad (6)$$

- where

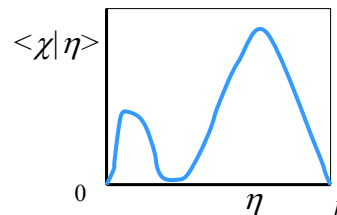
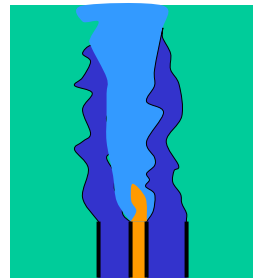
$$I_n(\eta) \equiv \int_0^1 (\eta^o - \eta)^n P(\eta^o) d\eta^o \quad (7)$$

Other Models

- **Kronenburg, et al (2000)**: "Computation of Conditional Average Scalar Dissipation in Turbulent Jet Diffusion Flames", Flow, Turbulence and Combustion, **64**, 145-159.
 - Solves Eqn (6) assuming pdfs are locally self-similar
 - Occasionally negative values obtained
- **Smith, et al (1992)**: 24th Symposium:
 - $\langle \chi | \eta \rangle = \langle \chi(r^*) \rangle$ where $\langle \xi(r^*) \rangle = \eta$
 - Roomina PhD thesis shows good agreement with Girimaji method

Piloted Jet Flames

- $\langle \chi | \eta \rangle$ has bimodal shape in near field
- How to formulate a simple model?
- More work needed



$\langle \chi | \eta \rangle$ As a Source of Error

- Klimenko and Bilger (1999) show error to be equivalent to a false chemical reaction rate of

$$\rho_{\eta} \left(N_{\eta}^{\text{model}} - N_{\eta}^{\text{true}} \right) \frac{\partial^2 Q_i}{\partial \eta^2}$$

- Error depends on relative size of advectn/diffusn/reactn terms
- More work is needed

Modelling Scalar Dissipation Fluctuations

- Log-normal distribution?
- $\chi' / \langle \chi \rangle$ increases with Re due to intermittency of dissipation?
- More work needed

Relationship to Mixing Models

- Pdf methods use various mixing models
- What do these models imply for $\langle \chi | \eta \rangle$?
 - $\langle \chi | \eta \rangle$ can be obtained from Eq (6) and (7) given above assuming Eq (6) is okay
- What do these models imply for $\chi' / \langle \chi \rangle$ and distribution of χ ?
 - How can this be determined?
- More work is needed

Relationship to Dissipation of Reactive Scalars

- Swaminathan, N. and Bilger, R.W. (1999), Physics of Fluids, **11**, 2679-2695.
 - Flamelet closure shows good agreement with DNS
- Implications for experiments
 - Difficulties near $dT/d\eta = 0$
- More work is needed

Measurement of Scalar Dissipation



Robert Barlow, Adonios Karpetsis, Jonathan Frank
Sandia National Laboratories
Livermore, CA 94550

TNF6 Workshop, 18-20 July 2002, Sapporo, Japan

- Why Scalar Dissipation is Hard to Measure
- Overview of Selected Experiments and Results
- Flame D Comparison and Cautionary Notes
- Some Issues for Discussion

Sandia National Laboratories
Combustion Research Facility



Why Scalar Dissipation is Hard to Measure



- Scalar dissipation: $\chi = 2D_\xi(\nabla\xi \cdot \nabla\xi) = 2D_\xi \left[\left(\frac{\partial\xi}{\partial x}\right)^2 + \left(\frac{\partial\xi}{\partial y}\right)^2 + \left(\frac{\partial\xi}{\partial z}\right)^2 \right]$

- Mixture fraction:
$$\xi = \frac{\frac{2(Y_c - Y_{c,O})}{W_c} + \frac{(Y_h - Y_{h,O})}{2W_h} - \frac{(Y_o - Y_{o,O})}{W_o}}{\frac{2(Y_{c,F} - Y_{c,O})}{W_c} + \frac{(Y_{h,F} - Y_{h,O})}{2W_h} - \frac{(Y_{o,F} - Y_{o,O})}{W_o}}$$

- 3D measurement not currently possible in flames
- Need accurate measure of mixture fraction from multiple scalars
- Need single-shot 1D or 2D measurements of mixture fraction with precision good enough for differentiation and spatial resolution good enough to capture the small scales
- Difficult to quantify absolute accuracy of scalar dissipation measurement or to know when resolution is good enough

Sandia National Laboratories
Combustion Research Facility



Some Scalar Dissipation Experiments in Flames



- Line-Raman/Rayleigh in H₂ jet flames:
 - Nandula et al., C&F 99:775 (1994) -- $\xi_{st}=0.0283$; Re=5000,10000; 0.02(r)x0.3x0.8mm
 - Brockhinke et al., Proc. Comb. Inst. 26:153 (1996) -- lifted flame; 0.2(r)x0.3x0.3mm
 - Chen & Mansour, CST 126:291 (1997) -- 0.7(r)x0.2x0.7mm
 - Brockhinke et al., C&F 121:367 (2000) -- lifted flames
- Line-Raman/Rayleigh in methane flames:
 - Karpets & Barlow, Proc. Comb. Inst. 29 (2002) -- flame D; 0.3x0.3x0.3mm
 - Geyer et al., TNF6 poster (2002) -- opp. jet flames; 0.35x0.38x0.11mm
- 2D imaging experiments in jet flames:
 - Stamer et al., CST 129:141 (1997) -- 2-scalar
 - Kelman & Masri, CST 129:17 (1997) -- 2-scalar + OH; 0.16x0.16x0.7mm
 - Fielding et al., Proc. Comb. Inst. 27 (1998) -- 3-scalar (N₂, CH₄, T)
 - Frank et al., Proc. Comb. Inst. 29 (2002) -- piloted flames (CO, fuel, T)
 - Sutton & Driscoll, Proc. Comb. Inst. 29 (2002) -- NO PLIF to mark fuel

Sandia National Laboratories
Combustion Research Facility



Considerations of Spatial Resolution



- W. Pitz et al. (NISTIR 6393 and TNF3 poster abstract)
 - Review of experiments in nonreacting flows indicates that required resolution is close to the Batchelor scale, $\eta_B = \eta_v Sc^{-1/2}$, rather than several times larger.
 - Recommended resolution estimate for nonreacting jets:

$$\lambda_r = C \left(\frac{v}{U'_m} \right)^{3/4} \ell^{1/4} Sc^{-1/2}, \quad 1 \leq C \leq 2$$

where $\ell = (r_{1/2})_u$ is the velocity half radius,

and U'_m is the measured fluctuation on centerline.

- Estimates of length scales in turbulent flames may be of limited utility:
 - Strong dependence of viscosity on T
 - Can generate wide range of estimates for η_B from equations used by various authors
 - Karpets note considers measured scalar length scales in the flame D reaction zone
- Typically, quoted resolution is the projection of a pixel into the measurement plane, while actual resolution is degraded by optics, image intensifier, laser thickness, and spatial filtering effect of taking derivative.
- Very useful to have high-resolution, high-SNR measurement (Rayleigh scattering) as part of scalar dissipation experiment.

Sandia National Laboratories
Combustion Research Facility



Uncertainty Contributions in Line Measurements



- From Barlow & Miles (Proc. Comb. Inst. 28, 2000) for central differencing along a radial segment the expected standard deviation in the gradient is:

$$\left\langle \left(\frac{d\xi}{dr} \right)^2 \right\rangle^{1/2} = \left(\frac{\langle \xi_{i+1}^2 \rangle + \langle \xi_{i-1}^2 \rangle}{r_{i+1} - r_{i-1}} \right)^{1/2} \approx \frac{\sqrt{2} \langle \xi'^2 \rangle^{1/2}}{2\Delta r}$$

where Δr is the superpixel resolution.

- If shot noise is the main error and $(d\xi/dr)' \ll (d\xi/dr)$ then:

$$\frac{\langle \chi_r'^2 \rangle^{1/2}}{\langle \chi_r \rangle} \approx 2 \frac{\left\langle \left(\frac{d\xi}{dr} \right)^2 \right\rangle^{1/2}}{\left\langle \frac{d\xi}{dr} \right\rangle}$$

- Relative error in χ improves as $(d\xi/dr)$ increases, provided spatial resolution is OK

Effect of Degrading Spatial Resolution



- From Stamer et al., CST 129:141 (1997)
- 0.0625 to 0.125 decrease attributed partly to reduction in noise
- Further effects attributed to spatial averaging
- Laser sheet thickness ~ 0.56 mm

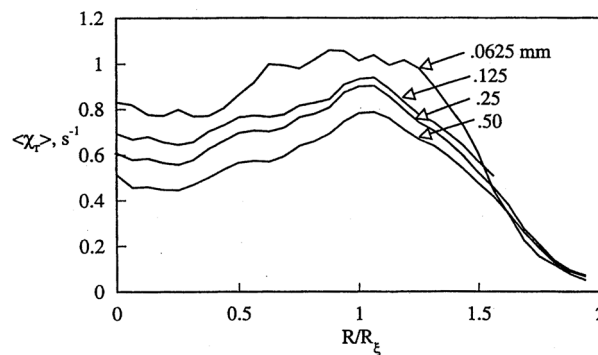
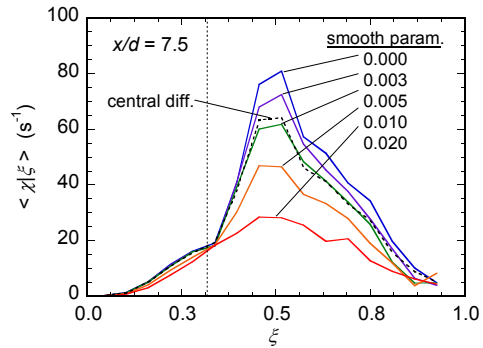


FIGURE 2 Effect of resolution (pixel size in the object plane) on computed radial component of mean scalar dissipation, $\langle \chi_r \rangle$ in the H_2 flame. The radius R is normalised by the mixture fraction half-radius, R_ξ . Average over 25 images.

Spline Smoothing vs. Central Differencing



- Smoothing parameter set to $0.005\xi + 0.005$ in Karpets & Barlow (29th Symposium 5A08) gives results similar to central differencing
- Max $\langle \chi | \xi \rangle$ is reduced by ~25%
- Conditional mean χ and pdf shapes are relatively insensitive to smoothing for values ≤ 0.005
- Can afford to push to higher 1D image resolution (200 μm for Raman, 60 μm for Rayleigh) -- most useful when gradient is aligned with laser beam



Effect of Temperature on D_{ξ}, χ



- Several studies have used $D = D_{0,\text{eff}}(T/T_0)^{1.67}$, where $D_{0,\text{eff}}$ is weighted by species mole fractions
- Karpets & Barlow used fit to results from laminar flame calculation by J-Y Chen (Chemkin)
- Big effect of T on χ (Geyer et al., TNF6, Fig. 2)
- Not a big contribution to uncertainty in χ

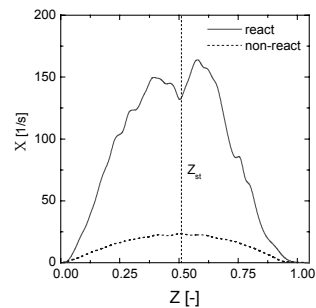
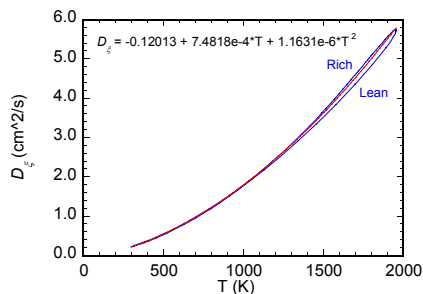


Figure 2 : Scalar dissipation rate in centerline direction non-reacting and reacting case for same configuration



Results Can Be Sensitive to Definition of ξ



- 2-scalar and 3-scalar methods use approximations and corrections to get ξ (i.e., Fielding et al., Proc. Comb. Inst. 27, 1998)
- Karpets & Barlow drop the oxygen term in the Bilger definition of ξ to reduce noise
- Calculations and experiments use various definitions of mixture fraction, making direct quantitative comparisons more difficult
- Collaboration needed to define appropriate basis for apples v. apples comparison of scalar dissipation results
- Useful to apply different techniques to the same flames and compare results

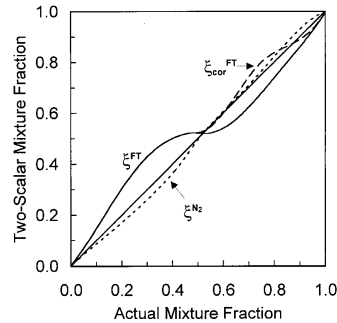
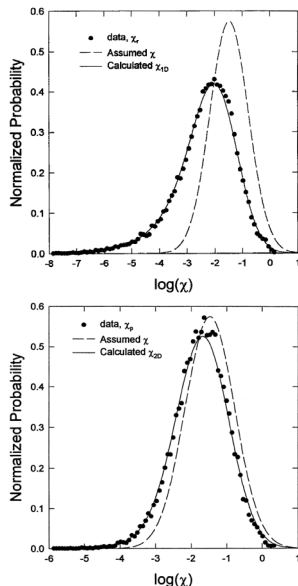


Fig. 4. Mixture fraction calculated from strained laminar flame calculations (100 s^{-1}) using the fuel-temperature (solid line) and nitrogen-temperature (short dashed) two-scalar approaches plotted against mixture fraction calculated using the formula proposed by Bilger [22]. The effect of fuel correction on ξ^{FT} is also shown (long dashed).

Sandia National Laboratories
Combustion Research Facility



1D and 2D Projections of 3D PDF of χ



- 3D scalar dissipation PDF is approx. log-normal in nonreacting turbulent jet (Dahm et al., Phys. Fluids A, 1991) and is generally assumed to be log-normal in turbulent flames
- PDF's of 1D and 2D measurements have different shape and are biased toward lower χ
- For log-normal χ_{3D} and isotropic orientation of $\nabla \xi$, the 3D PDF of χ can be constructed or estimated from 1D or 2D measurements (Dahm & Buch, Phys. Fluids A, 1989; Pitts et al., NISTIR 6369, 1999) Figures from Pitts et al.
- Jet flames are not isotropic, mean inward $\nabla \xi$

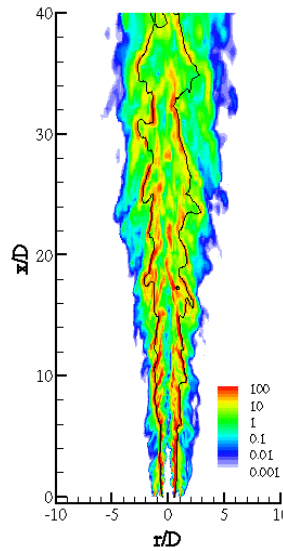
Sandia National Laboratories
Combustion Research Facility



Is High χ Coupled to Large Scales?



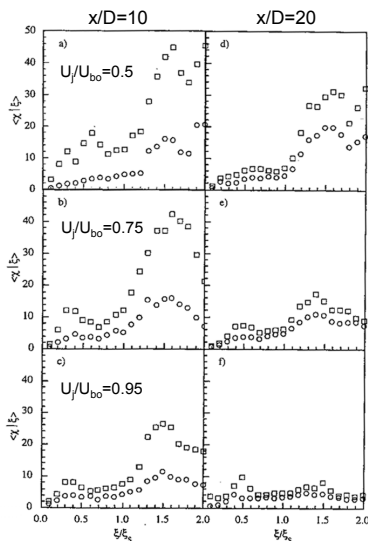
- Resolved scalar dissipation in LES of Flame D shows extended regions of high χ that are inclined to the flow (Pitsch & Steiner, Proc. Comb. Inst. 28)
- PIV/PLIF measurements have shown similar structures for high strain regions in jet flames
- Extended discussion by Pitts et al. for nonreacting jets
- Length scale of χ_r fluctuations in 1D measurements is small (Karpets & Barlow 2002), but radial measurement is nearly normal to these structures.
- Useful to have 3D info on instantaneous flame structure together with χ measurement



Sandia National Laboratories
Combustion Research Facility

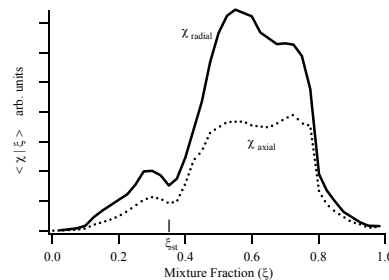


Relative Magnitudes of Dissipation Components



Kelman & Masri, CST 129:17 (1997)

$$\chi = 2D\xi \left[\left(\frac{\partial \xi}{\partial x} \right)^2 + \left(\frac{\partial \xi}{\partial y} \right)^2 + \left(\frac{\partial \xi}{\partial z} \right)^2 \right]$$



Frank et al. (TNF6 poster and Symposium paper) flame D at $x/d=?$

Sandia National Laboratories
Combustion Research Facility



Piloted Flames Approaching Blowoff

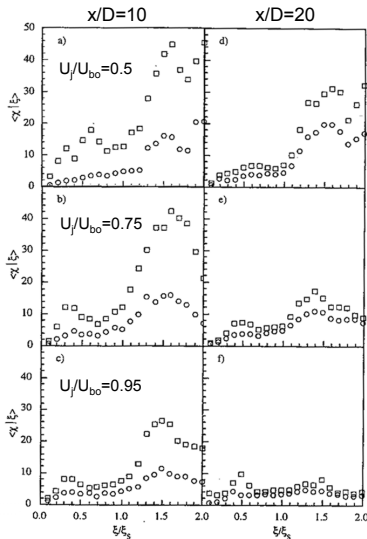


FIGURE 20 Conditional mean scalar dissipation rates (1/s) in a turbulent methane-air diffusion flame at $x/D=10$: a) $U_j/U_{bo}=50\%$, b) $U_j/U_{bo}=75\%$, c) $U_j/U_{bo}=95\%$ and at $x/D=20$: d) $U_j/U_{bo}=50\%$, e) $U_j/U_{bo}=75\%$ and f) $U_j/U_{bo}=95\%$.

- Kelman & Masri, CST 129:17, 1997
- Piloted burner with CH_4/air , CO/H_2
- $\langle \chi | \xi \rangle$ decreases for $U_j/U_{bo} = 0.5, 0.75, 0.95$
- May be due to decreased T , $D_\xi(T)$

Sandia National Laboratories
Combustion Research Facility



More Piloted Flames with Local Extinction



$$\int_0^\infty \langle \chi | \eta \rangle p_\eta(\eta) r dr / \int_0^\infty p_\eta(\eta) r dr \quad (3)$$

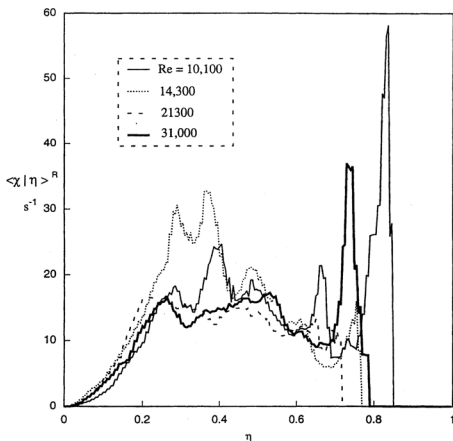


FIGURE 19 CH_4 flames: Scalar dissipation, integrated across the flow, and weighted by the pdf of the mixture fraction (Eq. 3).

- Starner et al., CST 129:141, 1997
Figure 19
- Piloted burner with CH_4/air , $\xi_{st}=0.29$
- $\langle \chi | \xi \rangle^*$ increases between $\text{Re}=10000$ and $\text{Re}=14300$, then decreases at higher Re
- May be due to decreased T , $D_\xi(T)$

Sandia National Laboratories
Combustion Research Facility

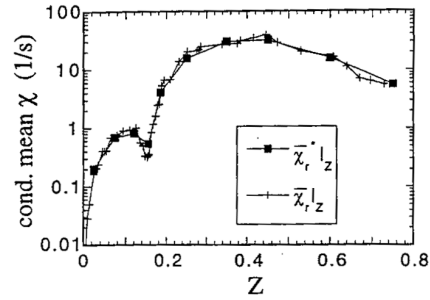
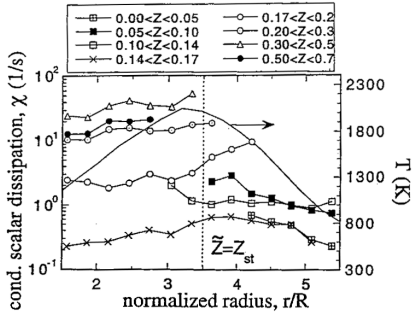


Radial Independence (?) of Conditional Mean



From Chen & Mansour, CST 126:291 (1997)

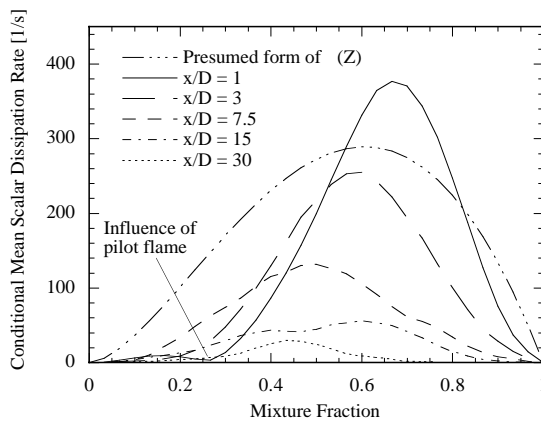
$$\langle \chi | \xi \rangle^* = \frac{\int_0^\infty \langle \chi | \xi \rangle P(\xi) r dr}{\int_0^\infty P(\xi) r dr}$$



Sandia National Laboratories
Combustion Research Facility



Dependence of $\langle \chi | \xi \rangle$ on Position in Flame D

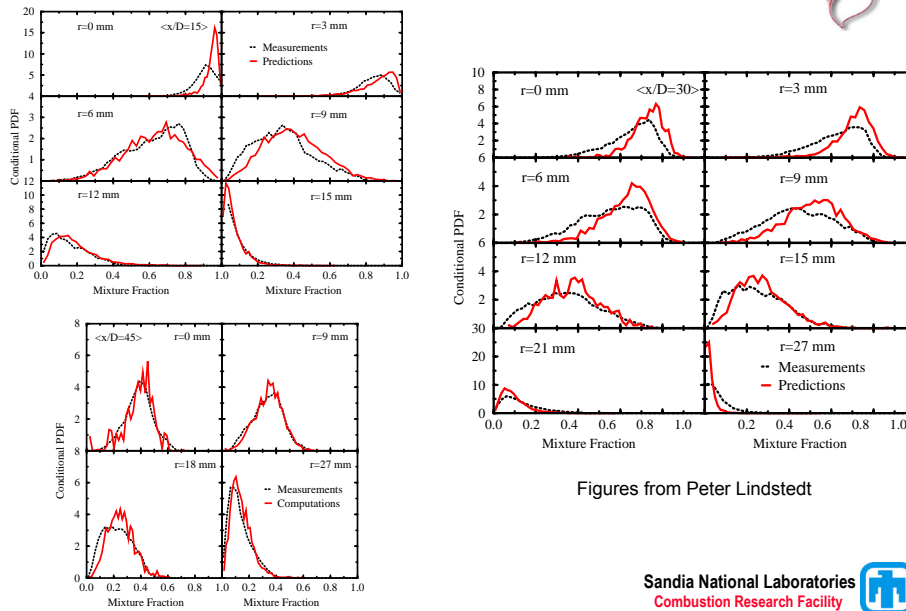


From Pitsch and Steiner, Proc. Comb. Inst 28 (2000)

Sandia National Laboratories
Combustion Research Facility

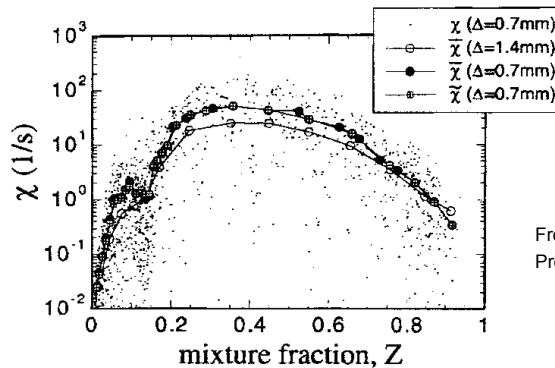


Mixture Fraction PDF's in Flame D



Sandia National Laboratories
Combustion Research Facility 

Favre vs Ensemble Averaging

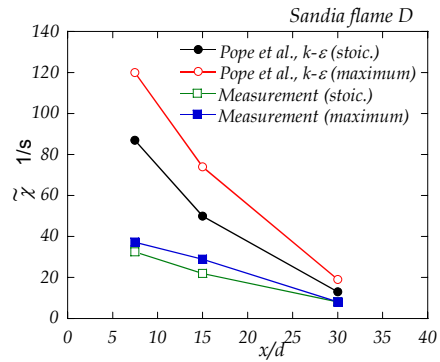
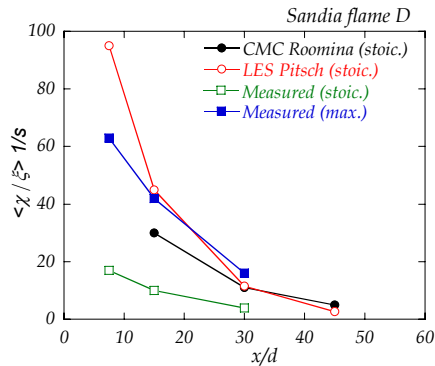


From Chen & Mansour,
Proc. Comb. Inst 26:97 (1996)

- Results from H_2/Ar jet flame show no significant of density weighting on conditional mean scalar dissipation
- Result may be different in flames with strong turbulence-chemistry interaction

Sandia National Laboratories
Combustion Research Facility 

Streamwise Decay of χ in Flame D



Some Issues for Discussion



- Spatial resolution requirements and tests
- What are the most appropriate quantities to compare with models?
- 1D and 2D measurements vs models for 3D dissipation
- Does $\langle \chi | \xi \rangle$ decrease when probability of localized extinction increases?
- Scalar dissipation in lifted flames: what does it mean when the fuel side boundary condition changes due to mixing below the flame?
- Is dissipation of the temperature field a useful thing to measure?
- ...???

Predictions of the Mean Scalar Dissipation Rate in the Barlow & Frank Flame D

by

Stephen B. Pope

Cornell University
Ithaca NY 14853

Graham M. Goldin

Fluent Inc.
Lebanon, NH

July 2002

In this note we present calculations of the mean scalar dissipation rate $\tilde{\chi}$ for the Barlow & Frank (1998) Flame D. The calculations are performed using the composition PDF method incorporated in the Fluent CFD code. The details of the calculations are as follows.

1. The flow is calculated using the standard k - ε turbulence model with the standard values of the constants, except for $C_{\varepsilon 1} = 1.52$.
2. The standard modelled composition PDF transport equation is solved by the distributed-particle method.
3. PDF transport is modelled by gradient diffusion, with $\sigma_{\phi} = 1.0$.
4. The IEM mixing model is used with the standard value $C_{\phi} = 2.0$.
5. A 16-species C_1 mechanism for methane is used, implemented via ISAT.
6. To ensure numerical accuracy, convergence tests were performed with respect to grid size, number of particles, and the ISAT error tolerance.

For reference, Fig. 1 shows radial profiles of the Favre mean mixture fraction at the first 6 axial measurement locations, i.e., $x/d = 1, 2, 3, 7.5, 15$ and 30 ; and Fig. 2 shows the locus in the x - y plane of the mean stoichiometric contour, $\tilde{\xi}(x, y) = \xi_{stoich} = 0.35$. (The radial coordinate is denoted by both r and, equivalently, y .)

The mean scalar dissipation implied by the composition PDF equation and the IEM mixing model is:

$$\tilde{\chi} \equiv C_\phi \frac{\varepsilon}{k} \widetilde{\xi''^2}. \quad (1)$$

Figures 3 and 4 show the radial profiles of the Favre mean scalar dissipation at the first three, and subsequent three, measurement locations, respectively. Figure 5 shows the Favre mean scalar dissipation against x/d along the mean stoichiometric contour.

By definition, the scalar dissipation is:

$$\chi \equiv 2D \nabla \xi \cdot \nabla \xi, \quad (2)$$

where D is the molecular diffusivity. In polar-cylindrical coordinates there are three contributions, corresponding to the three components of $\nabla \xi$. Karpetis & Barlow report measurements of the radial component, which we denote by χ_r :

$$\chi_r \equiv 2D \left(\frac{\partial \xi}{\partial r} \right)^2. \quad (3)$$

Specifically, Karpetis & Barlow report the values of the conditional means $\langle \chi_r | \xi \rangle$ at $x/d = 7.5, 15$ and 30 , around the radial location of the mean stoichiometric contour. If local isotropy prevailed, then $\tilde{\chi}$ would be three times $\tilde{\chi}_r$. It may be, however, that the gradient of ξ is predominantly in the r direction, and so $\tilde{\chi}$ may exceed $\tilde{\chi}_r$ by a factor closer to 1 than to 3.

Table 1 compares different predicted and measured statistics. The columns show: the axial location; the predicted maximum value of $\tilde{\chi}$ anywhere in the radial profile; the predicted value of $\tilde{\chi}$ on the mean stoichiometric contour; the measured value of $\langle \chi_r | \xi \rangle$ at its local minimum (which is around $\xi \approx 0.35$); and the measured value of $\langle \chi_r | \xi \rangle$ at its maximum (which is around $\xi \approx 0.5$). It may be seen that the predicted values on the stoichiometric contour are similar to the measured maximum conditional values. Recalling that $\tilde{\chi}$ exceeds $\tilde{\chi}_r$ by a factor between 1 and 3, we conclude that the predictions are not inconsistent with the measurements. Obviously it is desirable to have a more direct comparison between measurements and calculations.

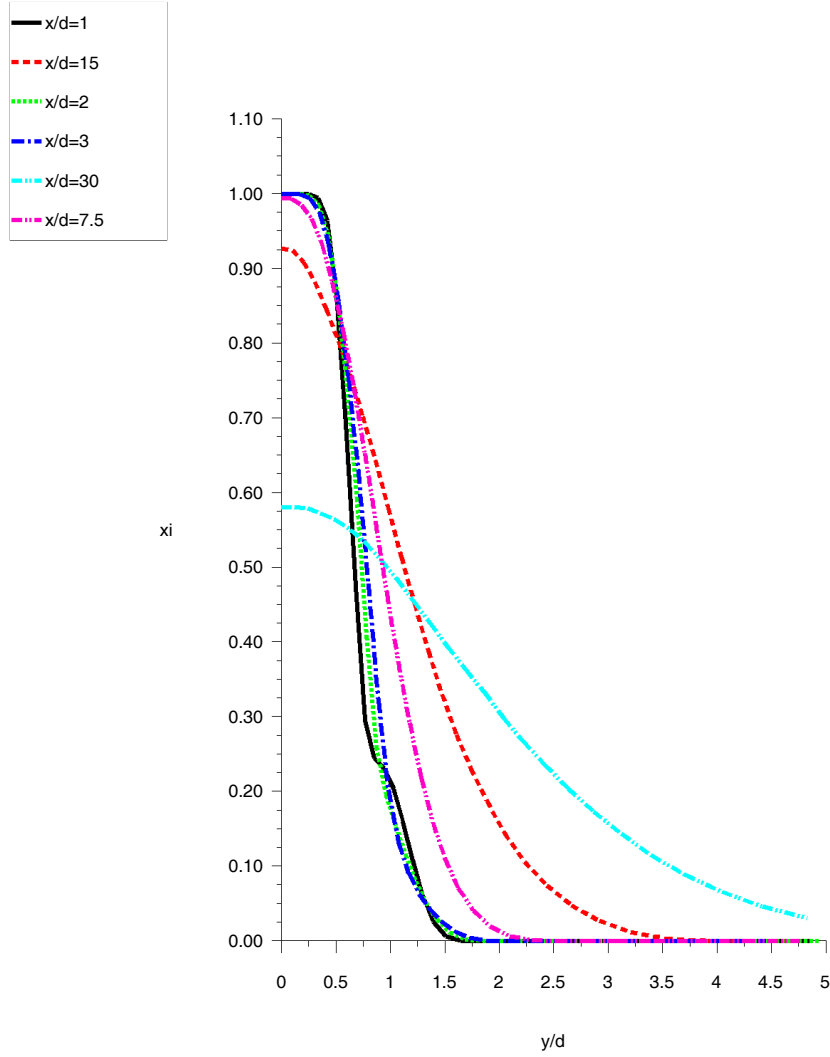


Figure 1: Favre mean mixture fraction against radial distance at different axial locations.

Table 1: Comparison of predicted and measured scalar dissipation statistics (s^{-1}).

x/d	Prediction $\tilde{\chi}_{\max}$	Prediction $\tilde{\chi}_{\xi=0.35}$	Measurement $\langle \chi_r \xi \approx 0.35 \rangle$	Measurement $\langle \chi_r \xi \approx 0.5 \rangle$
7.5	120	87	17	63
15	74	50	10	42
30	19	13	4	16

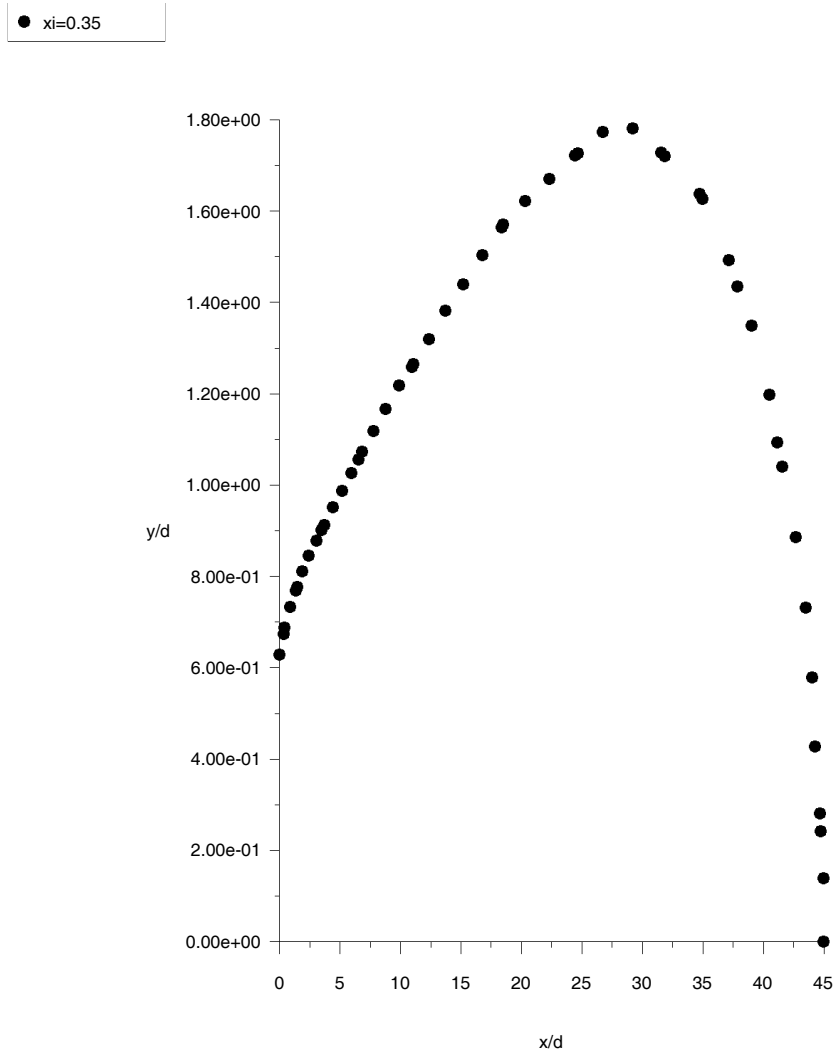


Figure 2: Locus of the mean stoichiometric contour: y/d vs. x/d such that $\tilde{\xi}(x, y) = \xi_{stoich} = 0.35$

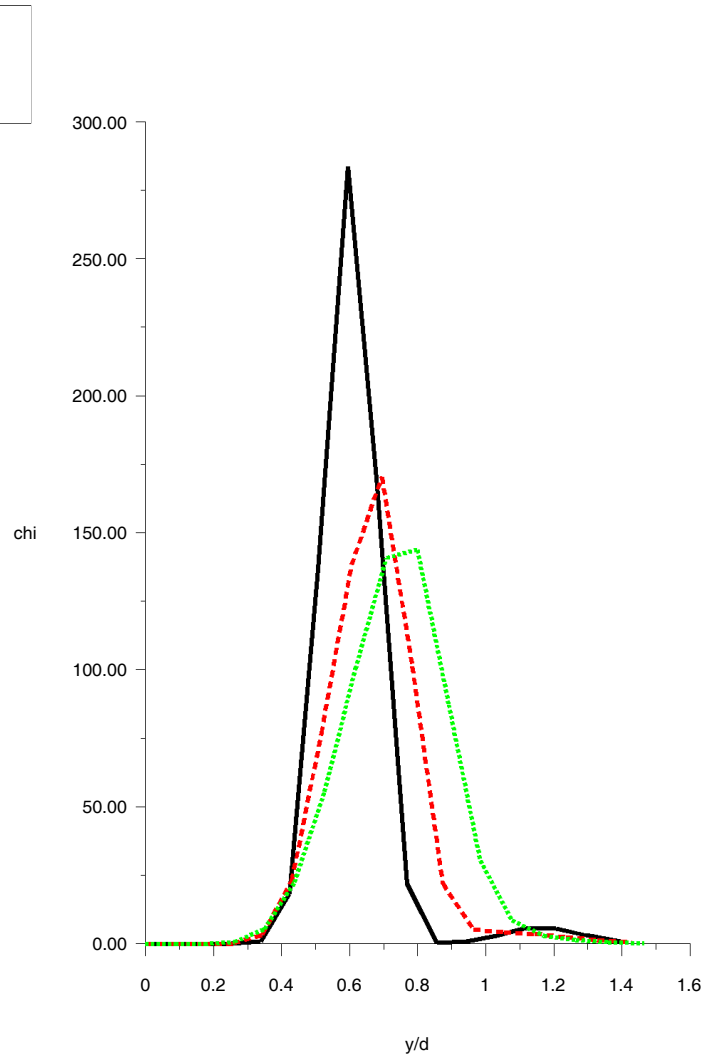


Figure 3: Favre mean scalar dissipation (s^{-1}) against radial distance at different (upstream) axial locations.

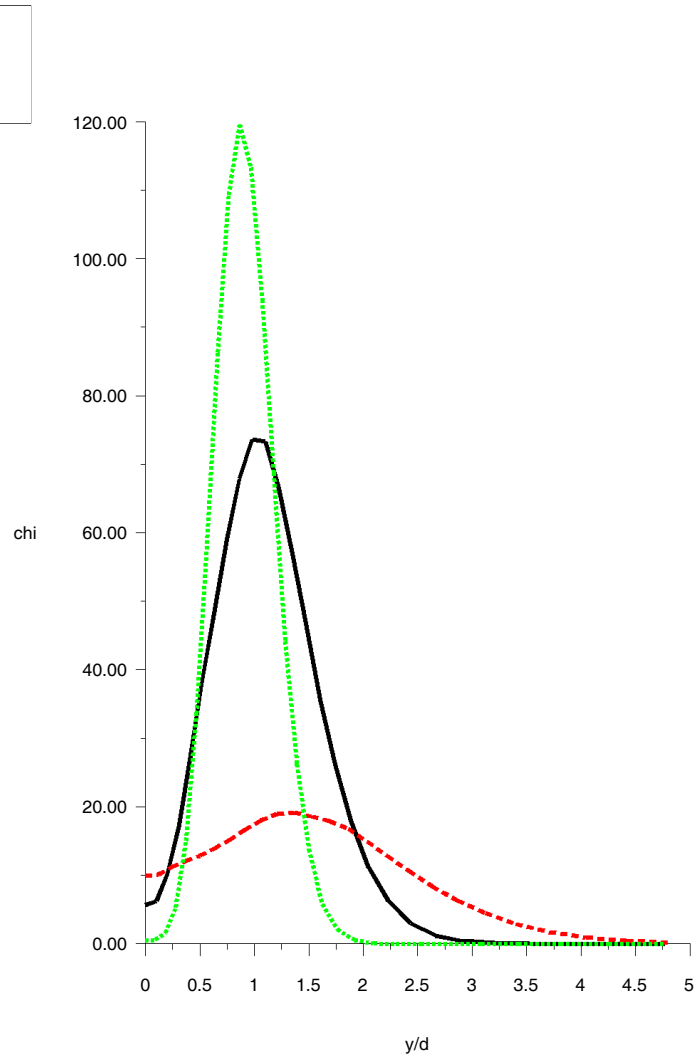


Figure 4: Favre mean scalar dissipation (s^{-1}) against radial distance at different (downstream) axial locations.

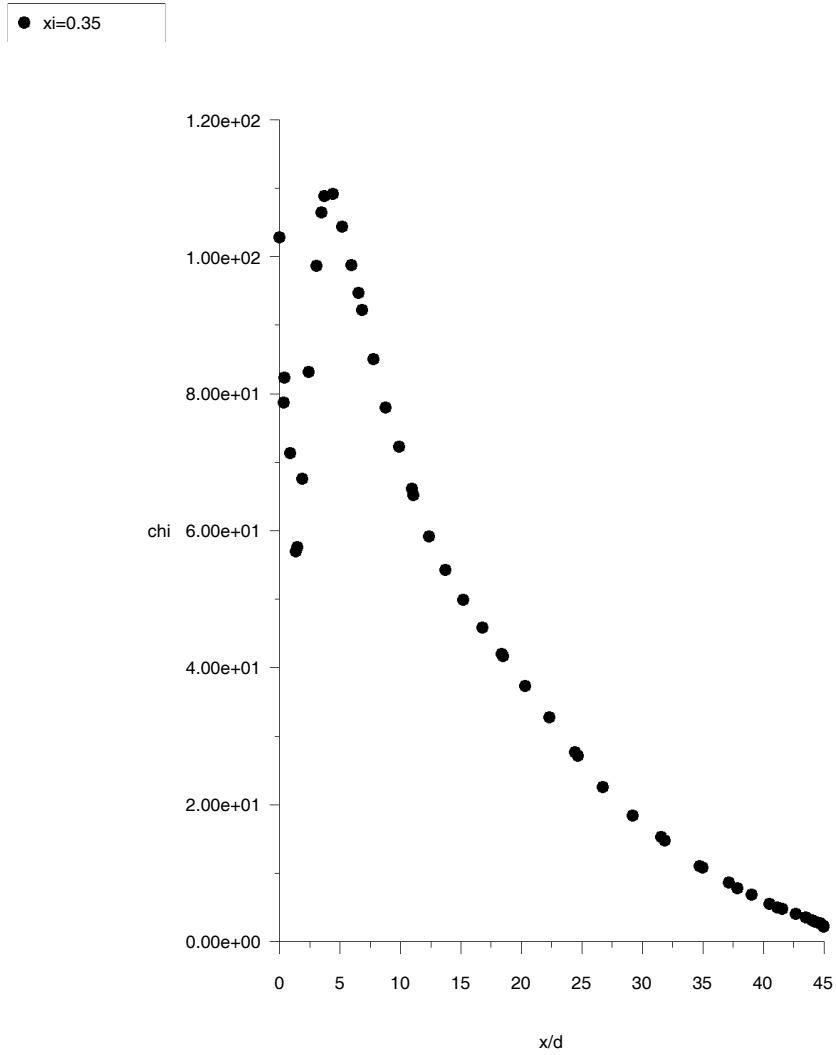


Figure 5: Favre mean scalar dissipation (s^{-1}) against axial distance along the mean stoichiometric contour.

SPATIAL STRUCTURE IN SANDIA FLAME D

A. N. Karpetis & R. S. Barlow
 Sandia National Laboratories
 Livermore, CA 94551, USA

The following describes the length-scales and the conditions of interest of the piloted (partially) premixed flame D. U_{co} is the exit bulk velocity

d	U_{co}	Re_{cold}	Composition (volume)
7.2 (mm)	50 (m/s)	22,400	25% CH ₄ , 75% Air

Table 1: Flame D data.

(STP) and Re_{cold} the equivalent cold Reynolds number

$$Re_{cold} = \frac{U_{co}d}{\nu_o}$$

The main pipe where the premixture flows through is surrounded by a pilot (18.2 mm in diameter). The pilot flame consists of equal stoichiometry and enthalpy hot products of premixed reaction. The detail of the flame holding is shown in figure 1.

Line measurements were performed at $x/d = 7.5, 15, 30$. The flame has a definite transitional/turbulent appearance at the centerline, close to the exit. This is also shown by the measurements of velocity and its fluctuation, plotted in figure 2. The local velocities (u, u') are shown in table 1. Also tabulated is the centerline value of the axial velocity fluctuation u'_c . The

x/d	r/d	u (m/s)	u' (m/s)	u'_c (m/s)
7.5	1.25	6.15	8.05	2.79
15	1.67	4.65	3.64	4.0
30	2.92	8.15	4.85	5.83

Table 2: Local parameters of turbulence.

multi-scalar line measurements were used to extract local length-scale information. The center of the line probe was positioned at the approximate

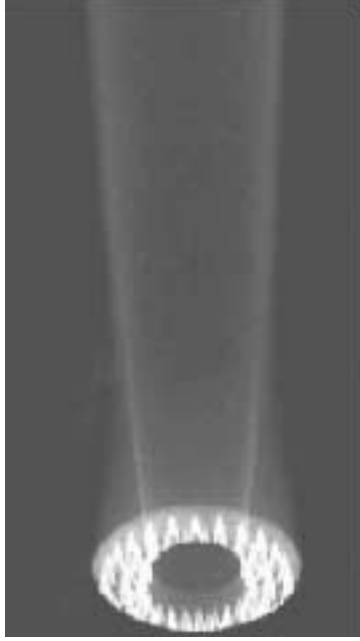


Figure 1: Flame holding.

stoichiometric position along the flame radius. The autocorrelation

$$R_{\alpha\alpha}(x, r, \Delta r) \equiv \frac{\langle \alpha'(x, r) \alpha'(x, r + \Delta r) \rangle}{\langle \alpha'^2(x, r) \rangle^{1/2} \langle \alpha'^2(x, r + \Delta r) \rangle^{1/2}}$$

with α being either scalar (ξ) or scalar dissipation (χ). Figure 3 shows the results for $R_{\xi\xi}(x, \Delta r)$. The radial dependence has been tacitly suppressed, and the autocorrelation is considered representative at each axial position (x/d). The dependence of $R_{\xi\xi}$ on Δr can be eliminated by integration, which also produces the length-scales $l_{\xi\xi}$ and $l_{\chi\chi}$.

$$l_{\xi\xi}(x) \equiv \int d\Delta r R_{\xi\xi}(x, \Delta r)$$

$$l_{\chi\chi}(x) \equiv \int d\Delta r R_{\chi\chi}(x, \Delta r)$$

The two length-scales are plotted in figure 4 and tabulated in table 3. The length-scale $l_{\chi\chi}$ may correspond to the Taylor (meso) scale or the Batchelor (micro) scale (the matter is still under debate). Either way, it is an experimental determination of the scale where most of the scalar dissipation is occurring. At the same time the length-scale $l_{\xi\xi}$ is unequivocally the macroscopic scale based on scalar fluctuations. The dynamic range is

x/d	$l_{\xi\xi}$ (mm)	$l_{\chi\chi}$ (mm)	Re_{hot}	η/Λ
7.5	1.57	0.68	12	0.25
15	2.25	0.59	24	0.21
30	3.28	0.45	51	0.17

Table 3: Macroscopic and microscopic length-scales in flame D.

minimal, a fact that correlates with the suppressed intensities shown in figure 2. Another way to gain some confidence in the measurement is the following: calculate a hot Reynolds number based on measured high temperatures (2,000 K) that apply at the measurement location. Using the values of $l_{\xi\xi}$, the centerline u'_c and a Sutherland model for diffusivity, we get the Re_{hot} values tabulated in table 3.

$$\text{Re}_{\text{hot}} = \frac{u'_c l_{\chi\chi}}{\nu_{\text{hot}}}$$

The rationale for using the centerline values of the fluctuation u'_c and not the local (higher) values of u' is the following: the higher values at the flame location are due to two reasons (a) the inherent inhomogeneity of the jet flow, which is also increased by the local heat release of the flame and (b) the intermittent nature of the turbulent flame and subsequent heat release. To apply arguments based on homogeneous (and isotropic) turbulence to such locations would be unjustified. In fact, the two locations in a jet flame where such zero dimensional arguments can be applied are either far from the flame in the cold co-flow, or at the centerline, where the gradients of quantities are zero by symmetry.

By assuming a unity Schmidt number we may evaluate the Kolmogorov (Batchelor) scale η , as

$$\eta \equiv \Lambda Sc^{-1/2} \text{Re}_{\text{hot}}^{-3/4} l_{\xi\xi}$$

tabulated in table 3. The value of Λ is meant to be calculated experimentally, and in the literature one may find values in the range 2–12. We may plot the experimentally measured values of $l_{\chi\chi}$ values against the construct $\text{Re}_{\text{hot}}^{-3/4} l_{\xi\xi}$, as shown in figure 5. It is worth noting that the values of $\text{Re}_{\text{hot}}^{-3/4} l_{\xi\xi}$ decrease monotonically with axial distance (x/d), consistent with evidence from measurements of turbulence intensity and $l_{\chi\chi}$. A value of $\Lambda \approx 3$ can also be calculated.

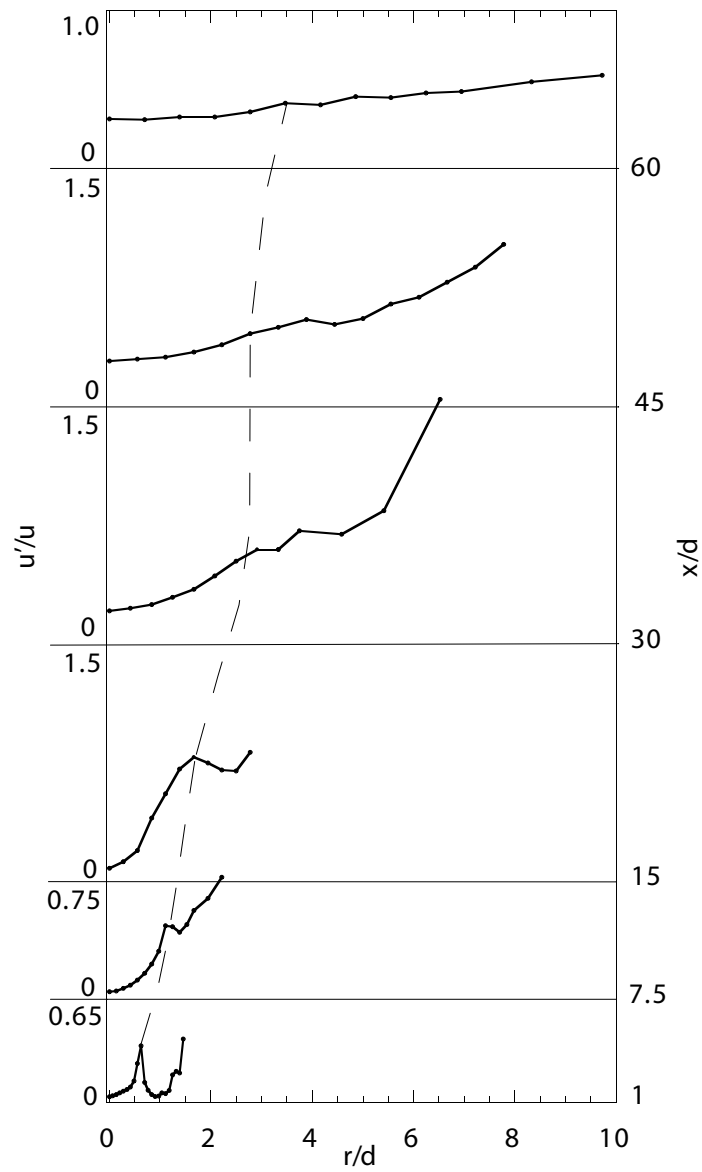


Figure 2: Axial velocity turbulence intensity within flame D. Dashed line goes through local maxima of u'/u . Velocimetry from TU Darmstadt.

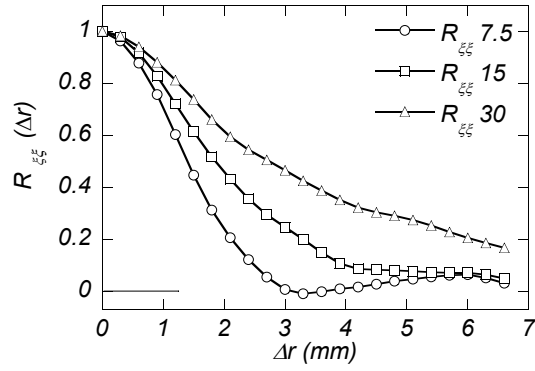


Figure 3: Local scalar autocorrelation.

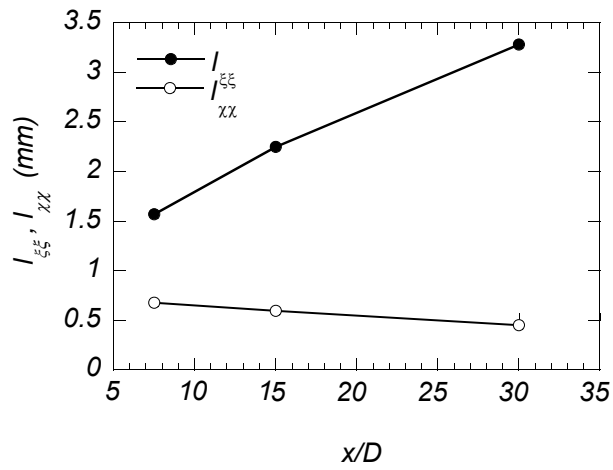


Figure 4: Macroscopic and microscopic length-scales in flame D.

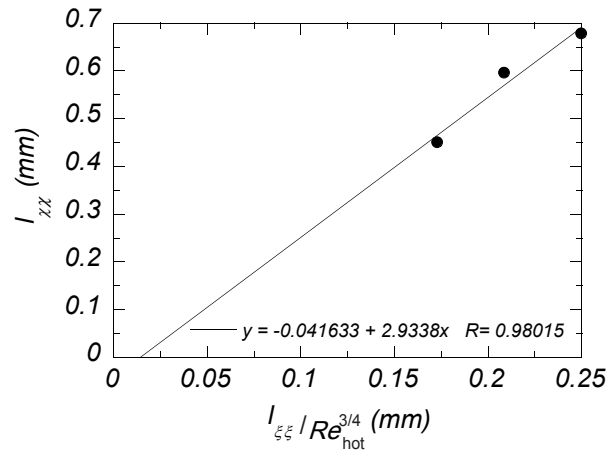


Figure 5: Comparison of measured and calculated micro-scales.

New experiments on TNF flames

Coordinator: A. Dreizler

FG Energie- und Kraftwerkstechnik, TU Darmstadt, Petersenstrasse 30, Germany

dreizler@ekt.tu-darmstadt.de

Introduction

In recent years, a large number of laser-based diagnostics have been developed to non-intrusively measure species concentration, temperature and gas velocities in turbulent flames. Despite of this large number of linear as well as non-linear methods, for the purpose of validation of numerical simulations only a very limited number of techniques have been used, such as spontaneous Raman scattering, Rayleigh scattering, laser-induced fluorescence and laser Doppler velocimetry. In most cases these techniques have been used in point-wise manner to record data on a rather low repetition rate (statistically uncorrelated events). From this fact the question rises, if these or additional techniques – extended to more spatial dimensions, applied at higher repetition rates to gain information on statistical correlations, or combined to simultaneously measure scalar- and velocity-fields – should be applied on TNF flames where already reliable data base exist. This additional information might be of very high interest to check model performance from a different view point. In recent years, especially planar techniques emerged as very useful in obtaining a more qualitative – and in some cases even quantitative – view on issues such as flame – vortex interaction. In future, these resources should be used in the TNF - context more intensely.

Aim of this session is to present examples of new or extended experimental techniques that have been applied recently on TNF flames. In addition, the session is intended to trigger the dialogue between people doing experiments and numerical simulations.

The session should inform on the following topics:

- What are the insights into physical-chemical characteristics of combustion gained by the respective technique?
- What are the main quantities potentially interesting to modellers?
- What are the limitations, error sources, accuracy,... of the method?
- What additional information has been gained on TNF flames and what experiments are planned?

The tentative agenda is as following.

- D. Geyer and A. Dreizler: 1D Raman/Rayleigh, OH PLIF and 2D LDV measurements on the TUD turbulent opposed jet burner
- A. Karpetis and R. Barlow: New measurements on piloted flames and simultaneous line Raman and crossed PLIF measurements
- J. Frank and M. Long: New developments on planar techniques
- C. Kaminski et al.: Temporally resolved PLIF – PIV experiments on the DLR jet flame
- Y. Ikeda: Local chemiluminescence measurement for flame front structure
- J. Gore: Radiation measurements as relevant to turbulence



New experiments on TNF flames

**Coordinator:
Andreas Dreizler**

**Energy- and Powerplant Technology
Technical University Darmstadt**



Outline

- **Introduction and general remarks**
- **Contributions from the TNF community**
 - **D. Geyer and A. Dreizler: New data on turbulent opposed jet flame**
 - **A. Karpetis and R. Barlow: New measurements on piloted flames and simultaneous line Raman and cross PLIF**
 - **J. Frank and M. Long: Planar techniques, reaction rate imaging and CO-imaging measurements**
 - **C. Kaminski et al.: Temporally resolved PLIF – PIV experiments on DLR jet flame**
 - **Y. Ikeda: Local chemiluminescence measurement for flame front structure**
 - **J. Gore: Radiation measurements**



Aim of the session

- **Identify and inform about new experiments**
 - What are the new insights into physical-chemical characteristics of combustion?
 - What are the main quantities potentially interesting to modellers?
 - What are the limitations, error sources, accuracy,... of the method?
 - What additional information has been gained on TNF flames and what experiments are planned?

→ Trigger new collaborations



Turbulent opposed jet

- **Investigation of turbulence-chemistry interaction**
 - Simple flow field, no walls
 - Good optical access
 - Localized reaction zone
 - Adjustable strain and mixtures
 - Short residence times result in Raman “friendly” flames
 - ⇒ Challenge for mixing-models in a simple flow field different from jet-flames

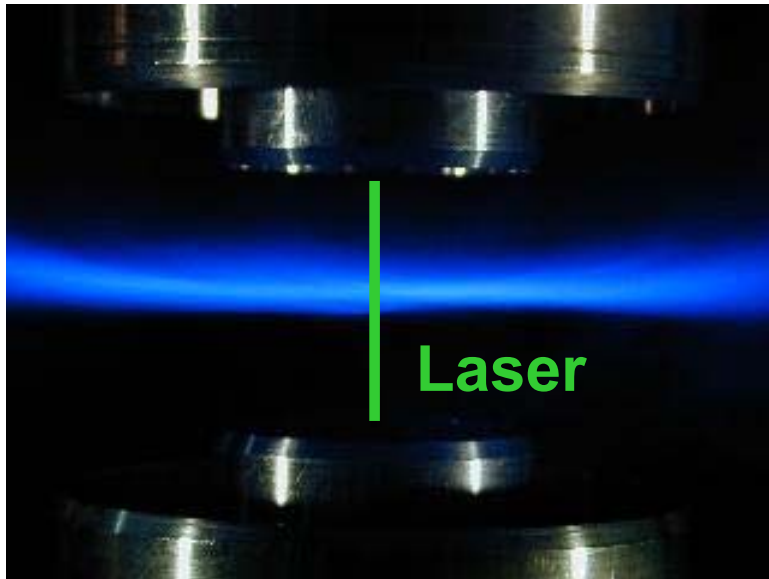
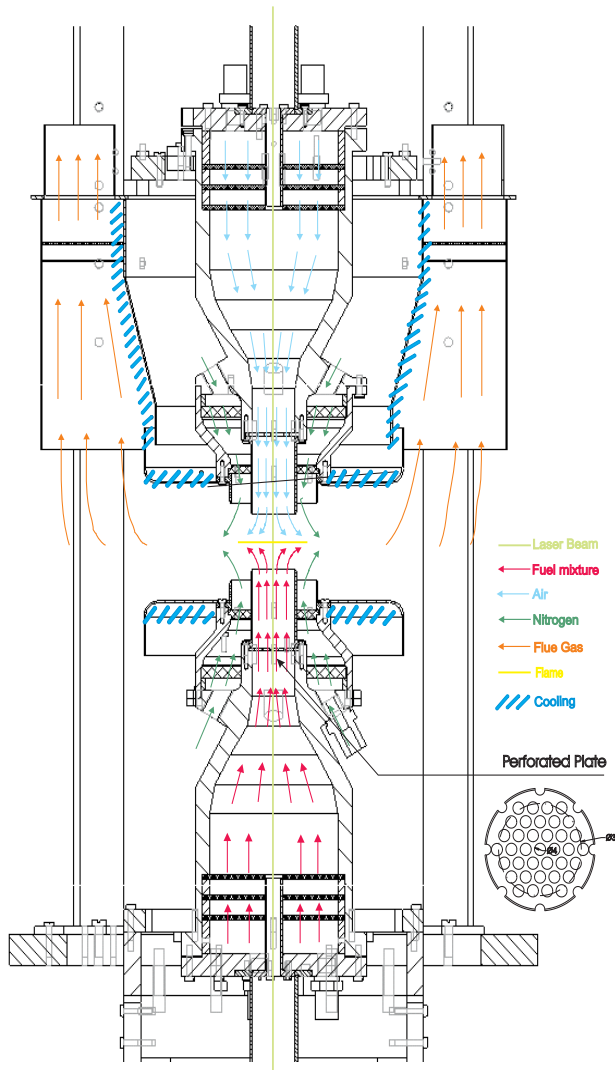


Figure: Image of turbulent opposed jet flame



Turbulent opposed jet burner: design



- Two identical opposed nozzles, aligned on-axis
- Nozzle exit diameter 30 mm, contraction 9:1
- Turbulence generated by perforated plates (TGP)
- Access for focused laser beam along centerline
⇒ beam steering avoided
- Horizontal stagnation plane, symmetric gravity influence
- Co-flow of N_2 prevents mixing with ambient air
- Water cooling for stable long term operation



TOJ: target flames

- Upper nozzle: air
- Lower nozzle: CH₄ - air mixture
- Co-flow: nitrogen
- Highest Re numbers: extinction limit ($\Phi \geq 2.0$)

Re _{Air}	a _m (1/s)	$\phi = 3.18$	$\phi = 2.0$	$\phi = 2.0$	$\phi = 1.6$	$\phi = 1.2$
3300	115	TOJ1A				
4500	158	TOJ1B	TOJ2B	TOJ2Bn	TOJ3B	TOJ4B
5000	175	TOJ1C	TOJ2C	TOJ2Cn		
6650	235	TOJ1D	TOJ2D	TOJ2Dn		
7200	255		TOJ2E	TOJ2En		

Green : measurements in TDF Lab, Sandia, also of-centerline for $\Phi=2.0$

Black : measurements at TU Darmstadt

TOJxxn : non-reacting cases

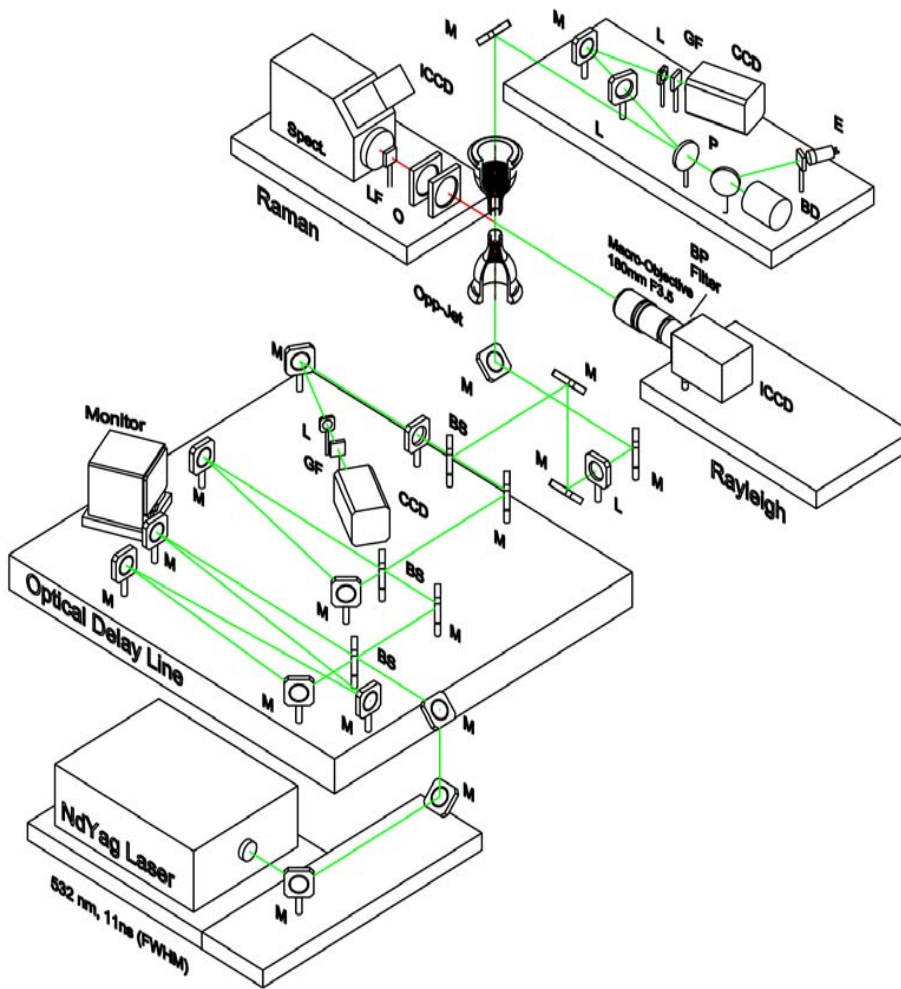


Techniques applied

- **Done**
 - 1D Raman/Rayleigh
 - Point Raman/Rayleigh/LIF (Sandia)
 - 2D LDV (including time-series)
 - Qualitative OH PLIF
- **Planned**
 - OH and CH time-series (M. Renfro)
 - (3D?)PIV&PLIF
 - Line Raman and crossed PLIF (R. Barlow)
- **Simulations**
 - Combusting LES (A. Kempf, J. Janicka)
 - Isothermal LES (B. Wegner, J. Janicka)
 - PDF simulation (J.-Y. Chen)



Spatially resolved 1D Raman/Rayleigh: setup

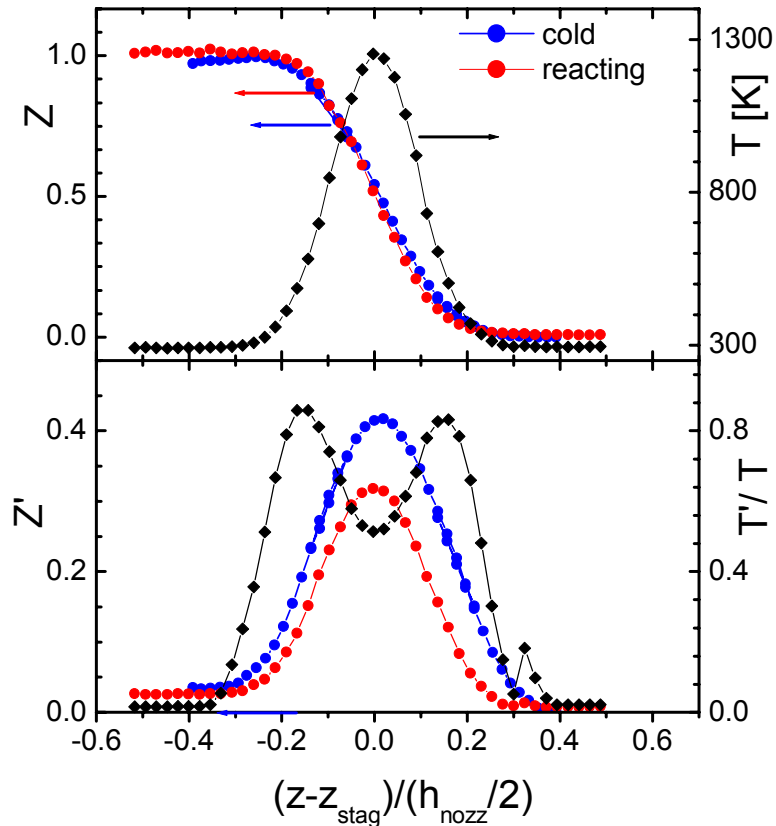


- 2ω Nd:YAG laser, 900 mJ/pulse, 11 ns FWHM
- Two delay lines
- 1D length 3.5 mm
- 10 probe volumes each $0.35 \times 0.38 \times 0.11 \text{ mm}^3$
- Raman:
 - Achromatic lens, $f_{\#} = 1.9$, $f = 270 \text{ mm}$
 - Imaging spectrograph ($f_{\#} = 4.1$) & GEN IV ICCD
- Rayleigh:
 - Lens, band-pass filter and ICCD



Mixture fraction along centerline

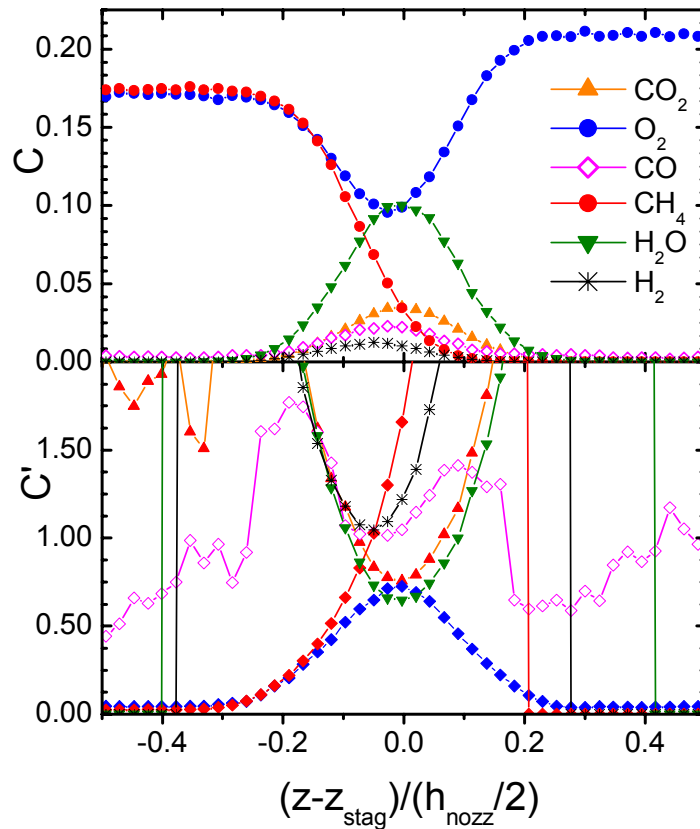
Reacting versus non-reacting case



- $Re = 6650, \phi=2.0$
- Profiles of mean mixture fraction are almost not altered by reaction
- Fluctuations are extremely high fore pure mixing
- Maximum temperature close to stagnation point - $Z_{st}=0.51$
- Flame oscillations bring maximal temperatures down



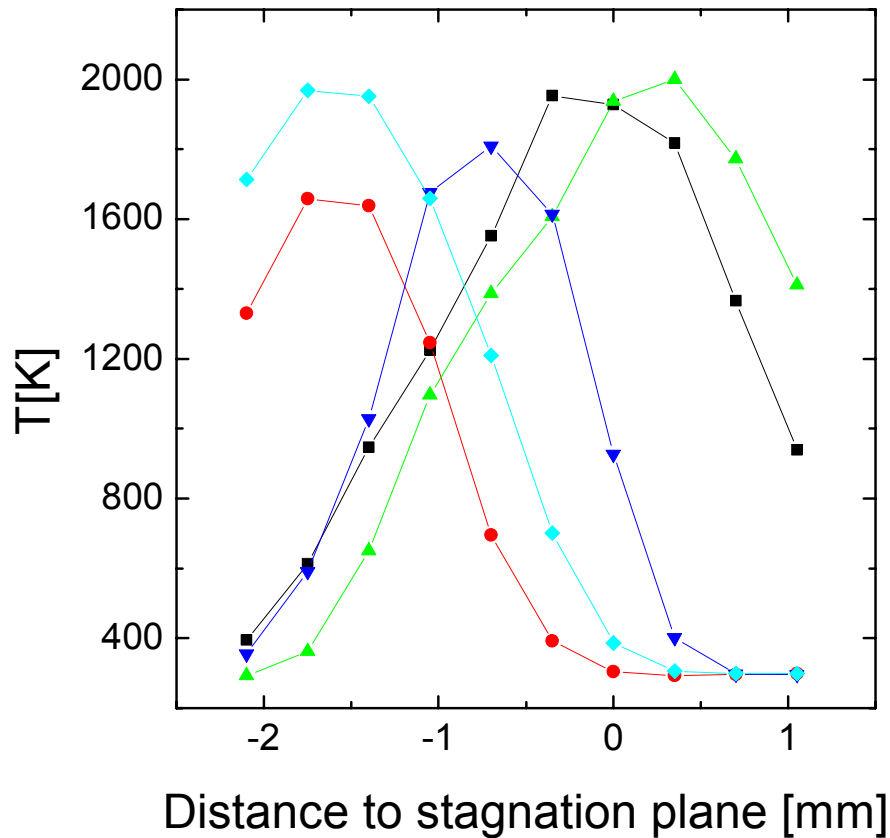
Mol Concentrations



- $\text{Re} = 6650, \phi = 2.0$
- Fast fuel consumption
- Non-premixed flame characteristics
- CO and H_2 detectable



Single-shot T-profiles

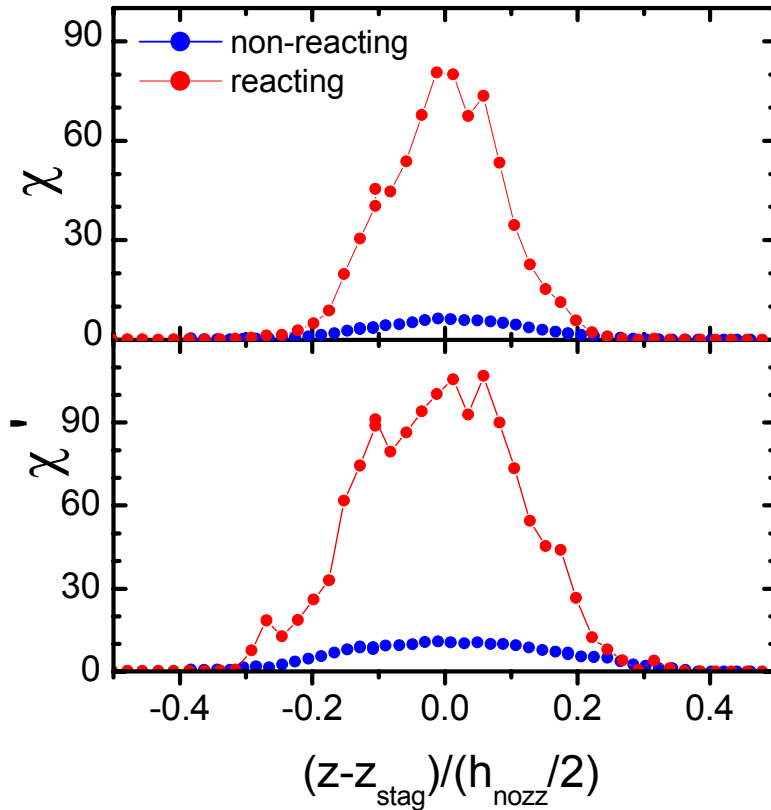


- T-profiles similar for most shots
- Flame staggers



TOJ - scalar dissipation rate

$Re = 6650, \phi = 2.0$



- **Scalar dissipation rate in centerline direction**

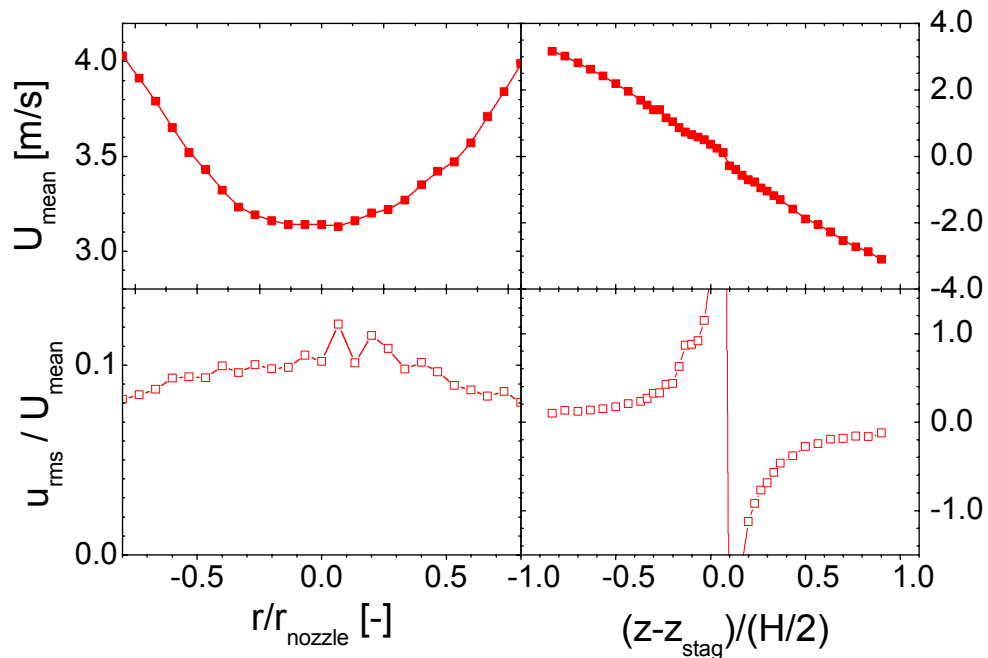
$$\chi = 2D \left(\frac{\partial Z}{\partial z} \right)^2$$

- **Highest scalar dissipation rates around stagnation plane**
- **Reacting \Leftrightarrow iso-thermal : increase by more than a magnitude**
- **High fluctuations (that are followed by extinction?)**



LDV measurements

**Axial velocities at:
nozzle exit centerline**

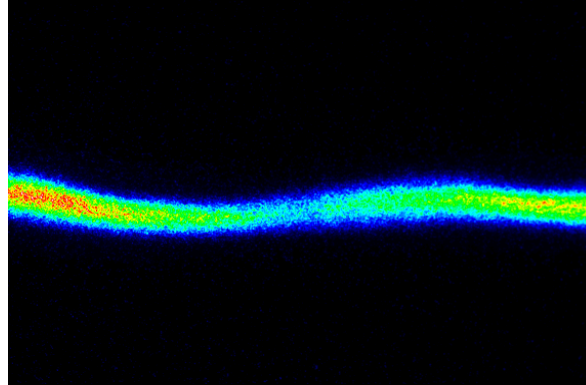


- Velocity data measured at 6 radial planes (1mm, 7.5mm and 13mm from each nozzle) and along centerline
- $Re = 6650$, $\phi=2.0$
- Symmetric exit profiles
- Turbulence intensity ca.10%
- Almost linear decrease of centerline velocity
- Relative and absolute turbulence intensity increase in stagnation plane.

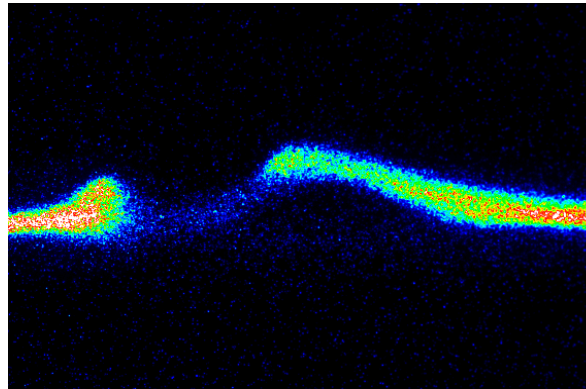


OH PLIF measurements – single-shots

- **stable**



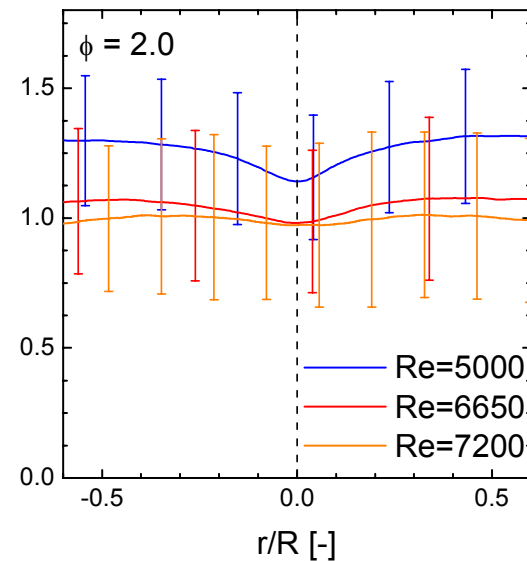
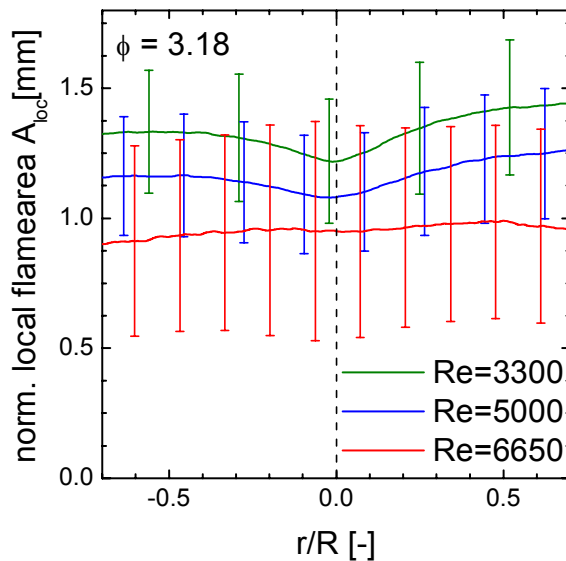
- **extinguishing**





Statistical analysis of OH-distribution

- Almost no influence of premixing on flame thickness
- Rising the Reynolds number is combined with increasing strain – OH distribution gets thinner





Conclusions

- In addition to pointwise concentrations and temperature information on gradients (scalar dissipation rate in one dimension)
- In addition to pointwise flow field information on integral time scales via time-series
- From OH PLIF information on flame areas



***New measurements on piloted flames and
simultaneous line Raman and crossed PLIF***

A.N. Karpetis and R.S. Barlow

*Combustion Research Facility, Sandia National Laboratories,
Livermore, CA 94551, USA*

*Sixth Workshop on Turbulent Non-premixed Flames
Sapporo, Japan
18 – 19 July 2002*

Supported by DOE, Basic Energy Sciences

We have developed a line Raman/Rayleigh/ CO LIF system (Turbulent Combustion Laboratory) that can provide single-shot measurements of scalar (ξ) and scalar dissipation rate (χ) in a turbulent hydrocarbon flame.

New capabilities:

Doubly conditioned statistics of many reactive scalars can be formed, providing information on turbulence-chemistry interaction.

The spatial structure of the flames can be quantified (both macroscopic and microscopic)

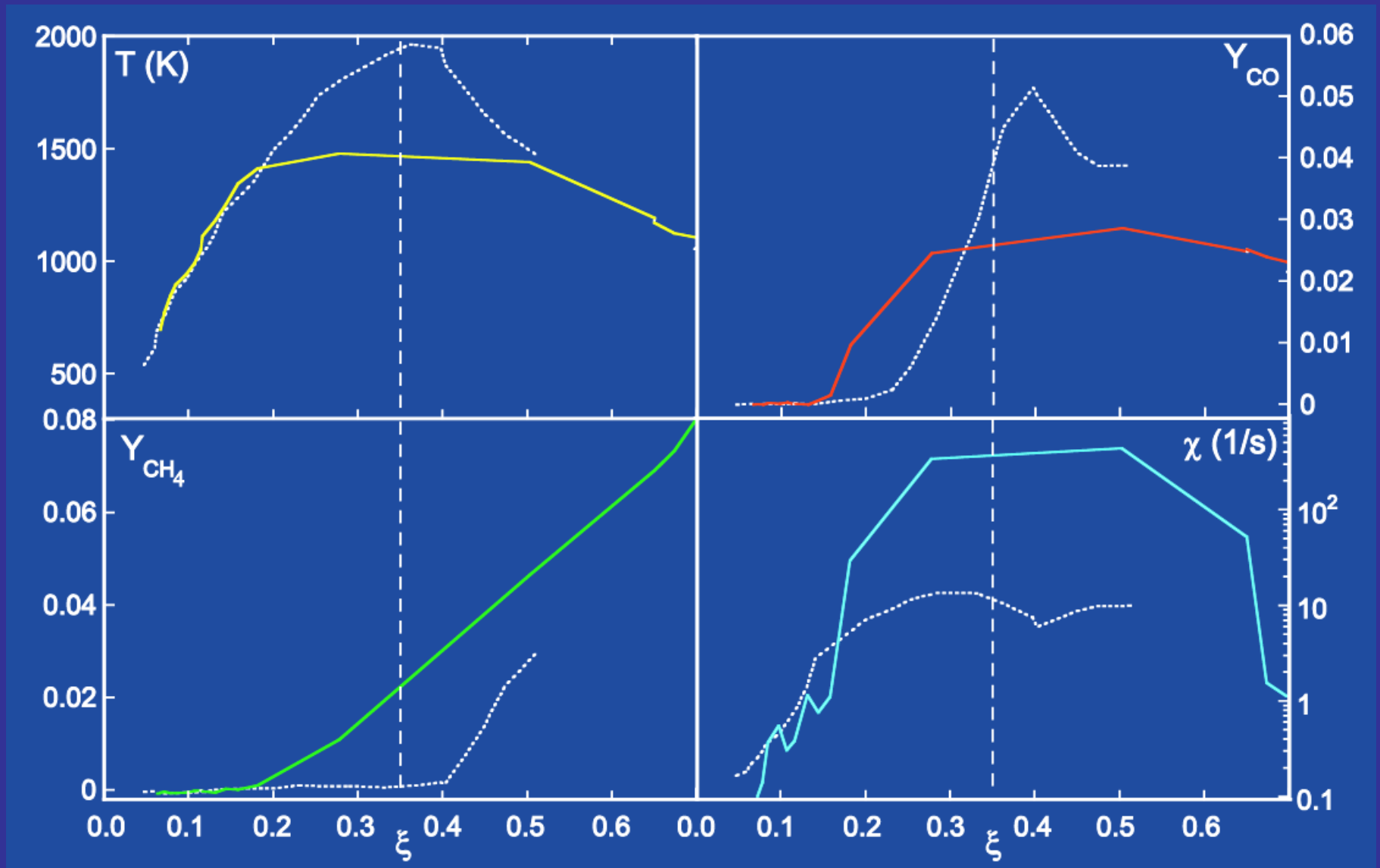
Problems:

1-D measurement of χ is biased. A scheme to obtain a 3-D measurement is presented.

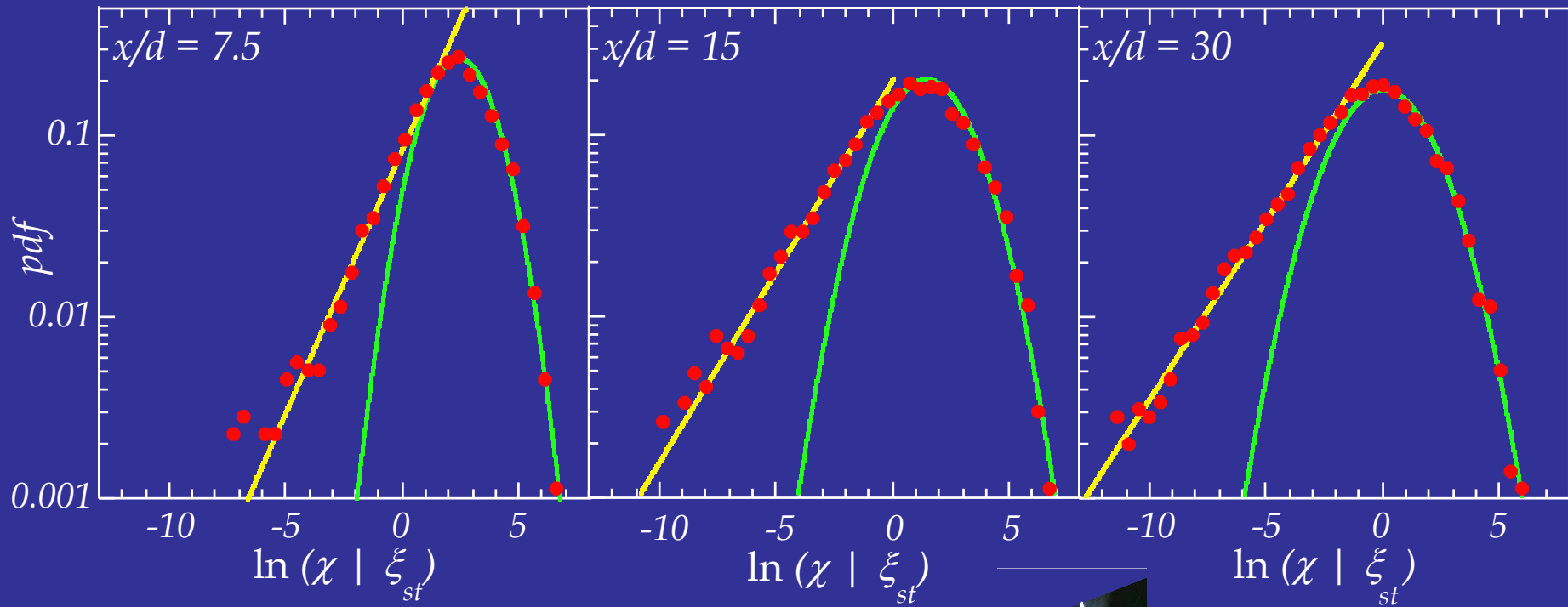
Resolution of the system needs to increase further (from 300 μm to 200 μm and possibly 60 μm)



Conditioning on χ measured in 1-D

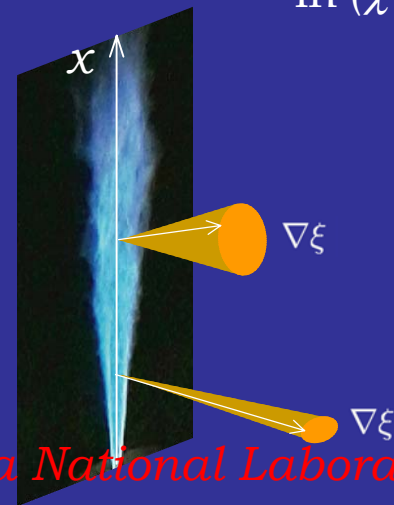


Conditional pdf of scalar dissipation at stoichiometry (bias of 1-D technique)

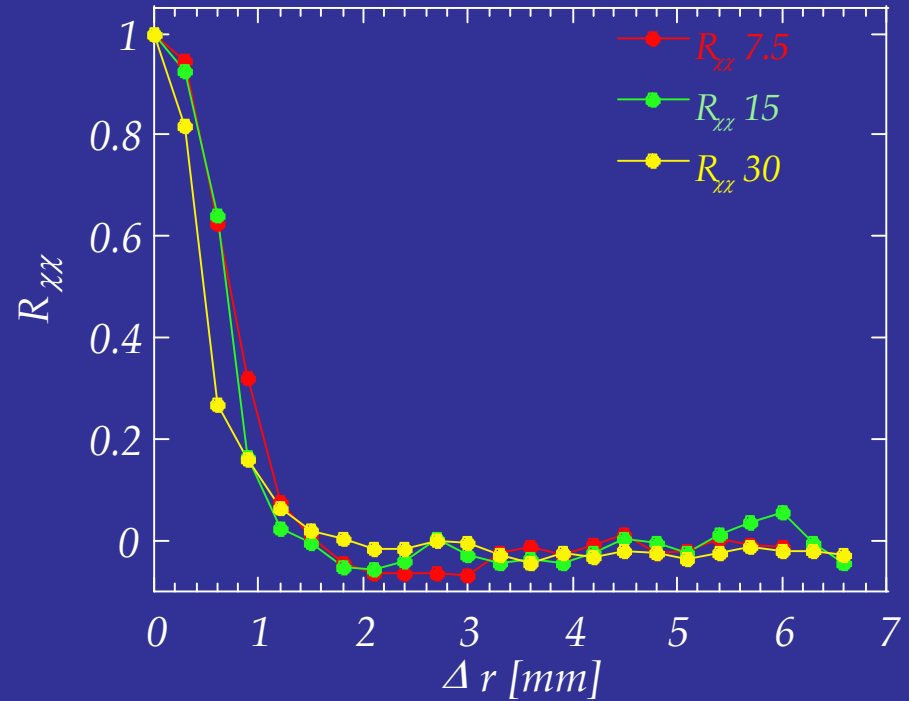
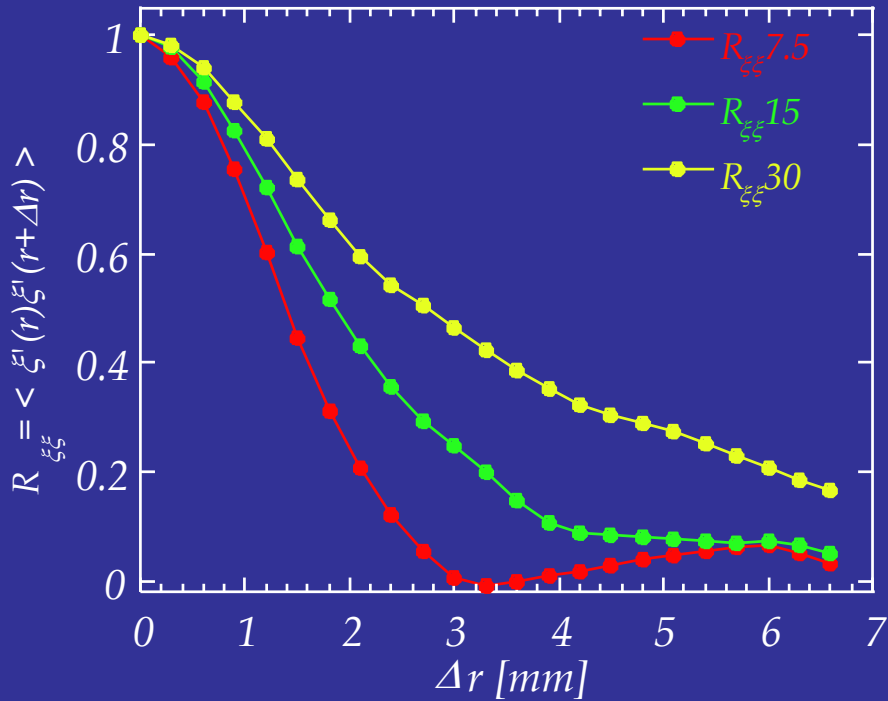


$$\text{pdf}(\chi | \xi_{st})$$

Log-normal pdf at high dissipation,
Stretched-exponential pdf at small dissipation .
Artifact of 1D measurement (Dahm 1989)



Spatial flame structure / length-scales (new information on old flames)



Spatial covariance (structure function) as a function of (x, r)

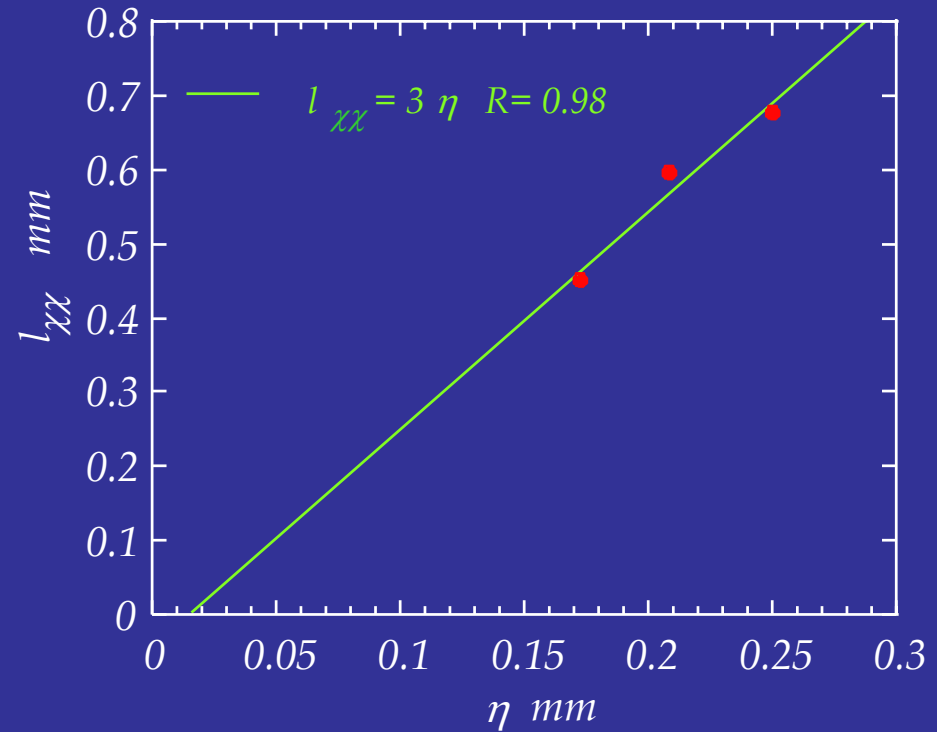
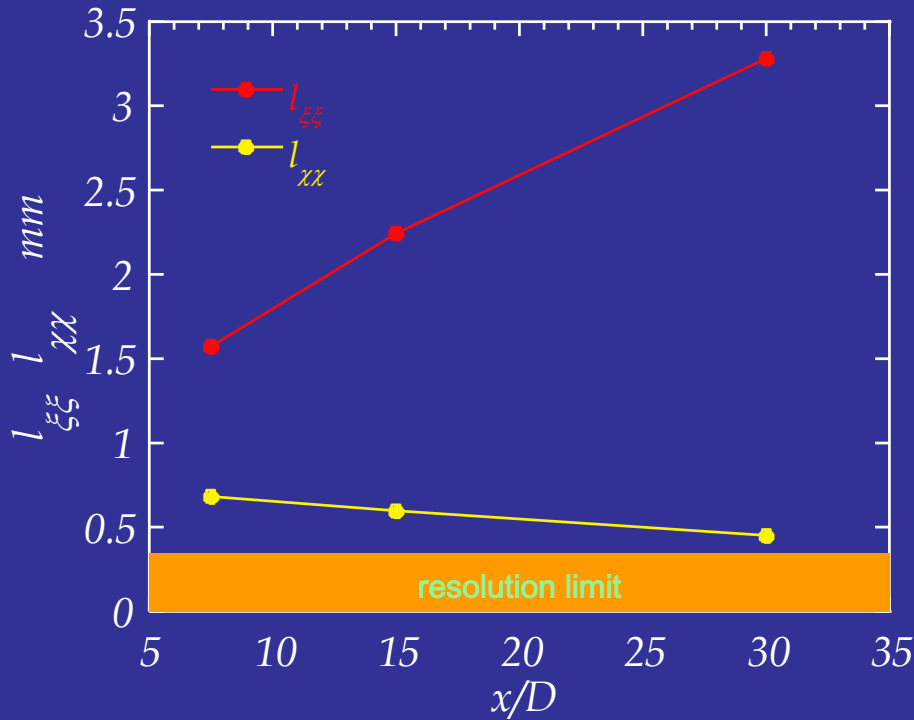
$$R_{\xi\xi}(x, r, \Delta r) = \frac{\langle \xi'(x, r) \xi'(x, r + \Delta r) \rangle}{\sqrt{\langle \xi'^2(x, r) \rangle} \sqrt{\langle \xi'^2(x, r + \Delta r) \rangle}}$$

$$R_{\chi\chi}(x, r, \Delta r) = \frac{\langle \chi'(x, r) \chi'(x, r + \Delta r) \rangle}{\sqrt{\langle \chi'^2(x, r) \rangle} \sqrt{\langle \chi'^2(x, r + \Delta r) \rangle}}$$



Combustion Research Facility, Sandia National Laboratories

Macroscopic and microscopic length-scales (problems at small scales)



$$l_{\xi\xi}(x, r) = \int d\Delta r R_{\xi\xi}(x, r, \Delta r)$$

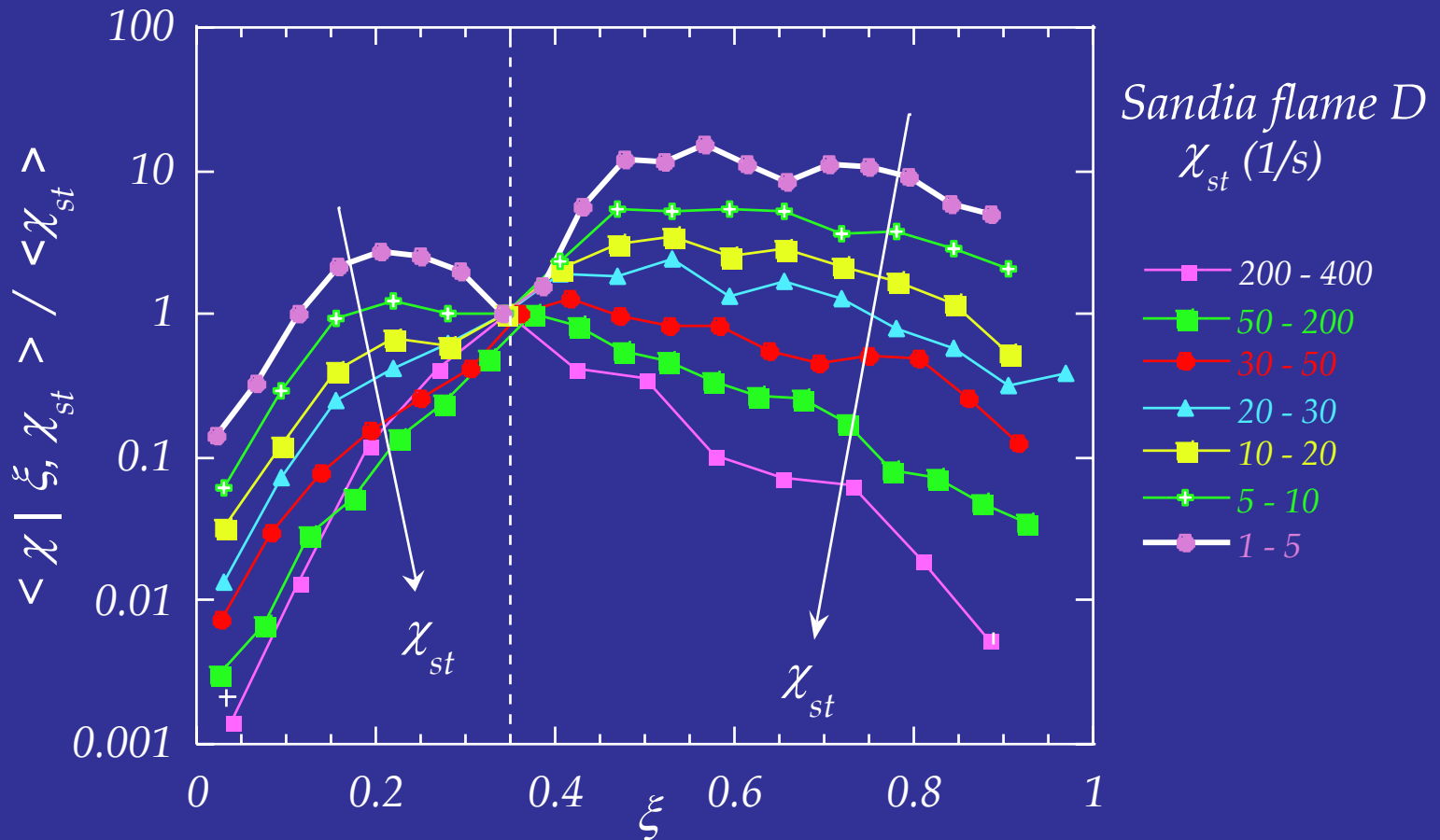
$$Re_\delta = \frac{\delta u'}{\nu} \quad \delta \equiv r_{st} \quad \nu = \nu(T_{max})$$

$$l_{\chi\chi}(x, r) = \int d\Delta r R_{\chi\chi}(x, r, \Delta r) \quad \text{Batchelor (Kolmogorov) scale} \quad \frac{\eta_B}{\delta} = \frac{\eta}{\delta} = \Lambda Re_\delta^{-\frac{3}{4}} Sc^{-\frac{1}{2}}$$

$$Sc \simeq 1 \implies \Lambda \simeq 3$$



Doubly conditional moment closure (an example of strange statistics)



Usual assumption in CMC (e.g. Cha, Kosály and Pitsch) :

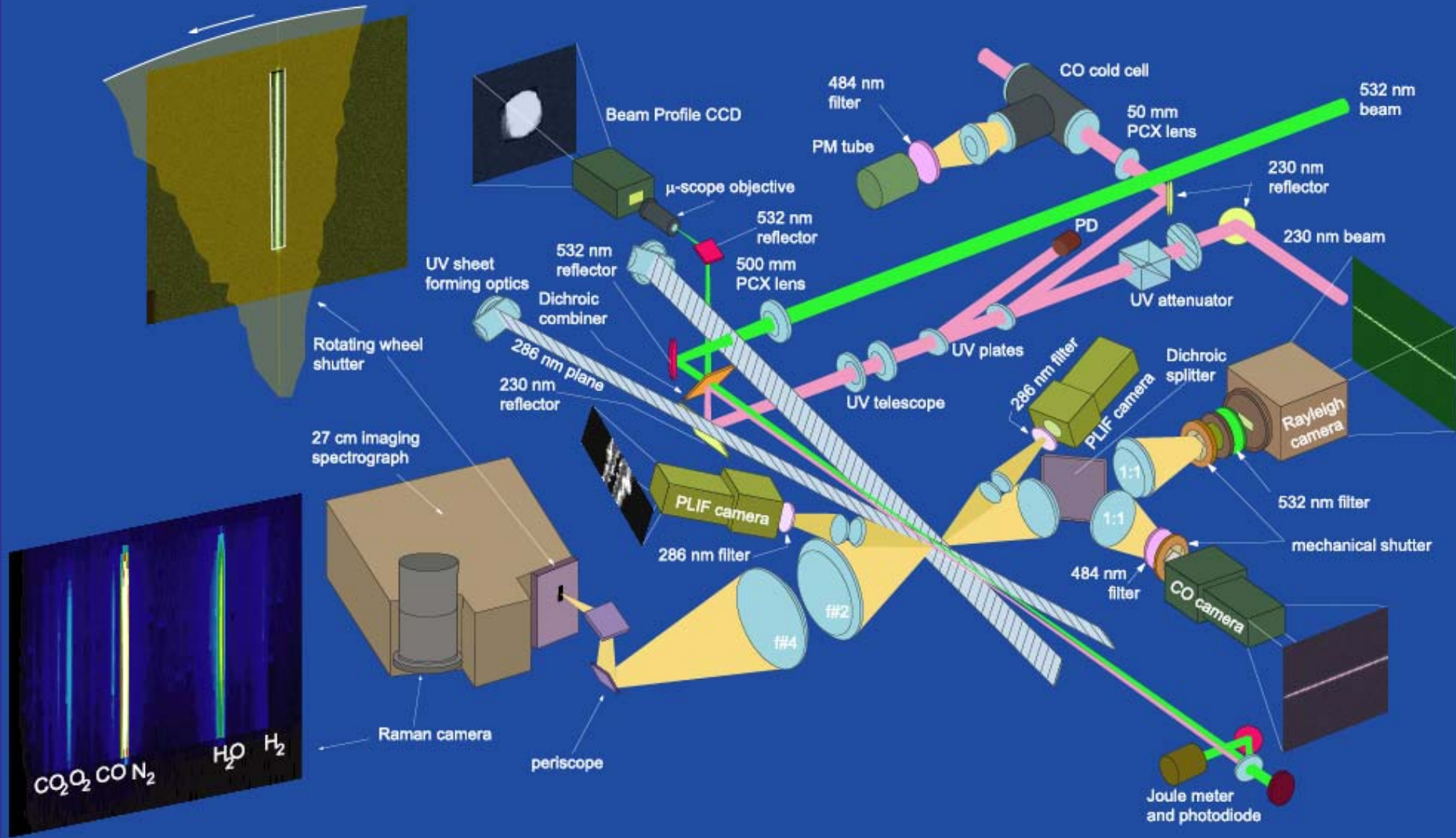
χ and ξ are statistically independent. Are they ? How high must Re be for that to hold?

Measurements can provide function

$$F(\xi, \chi) = \chi / \chi_{st}$$

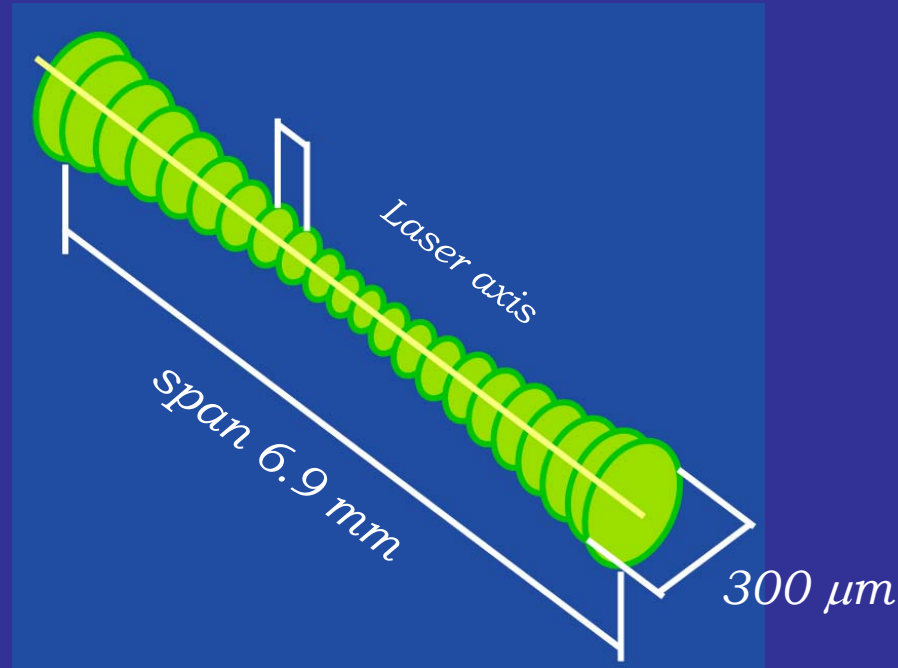


3-D measurement of scalar dissipation: 2 crossed PLIF techniques (the future)



Spatial resolution (current capabilities)

*Variable resolution: 300 μm - 200 μm (real optical)
200 μm - 60 μm (super-resolution)*

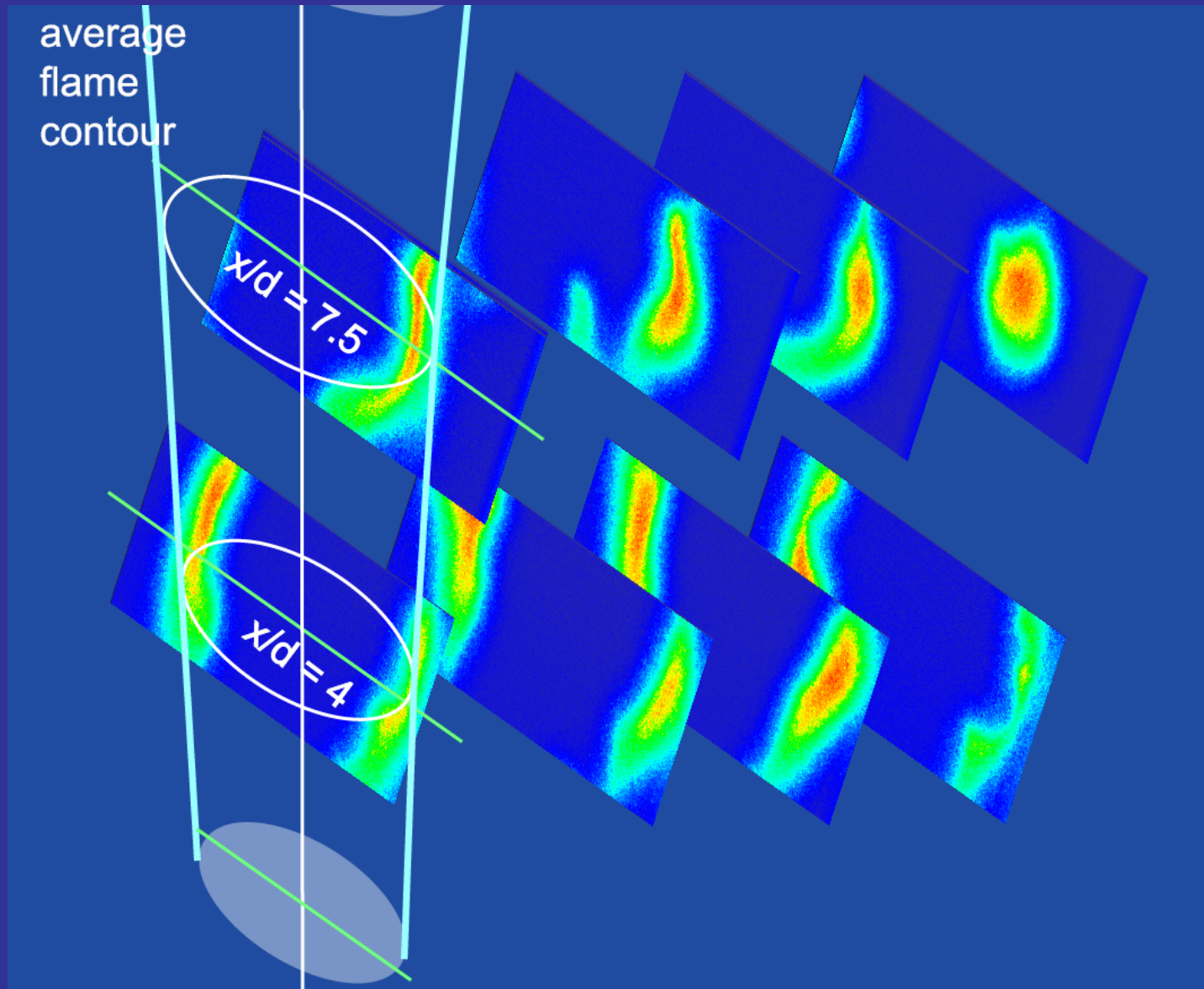


Reported measurements with 300 μm resolution: spatial averaging evident when compared with 2D measurement (Frank, Sandia & Long, Yale)



Combustion Research Facility, Sandia National Laboratories

A scheme to obtain a 3-D measurement of χ : use the crossed PLIF planes

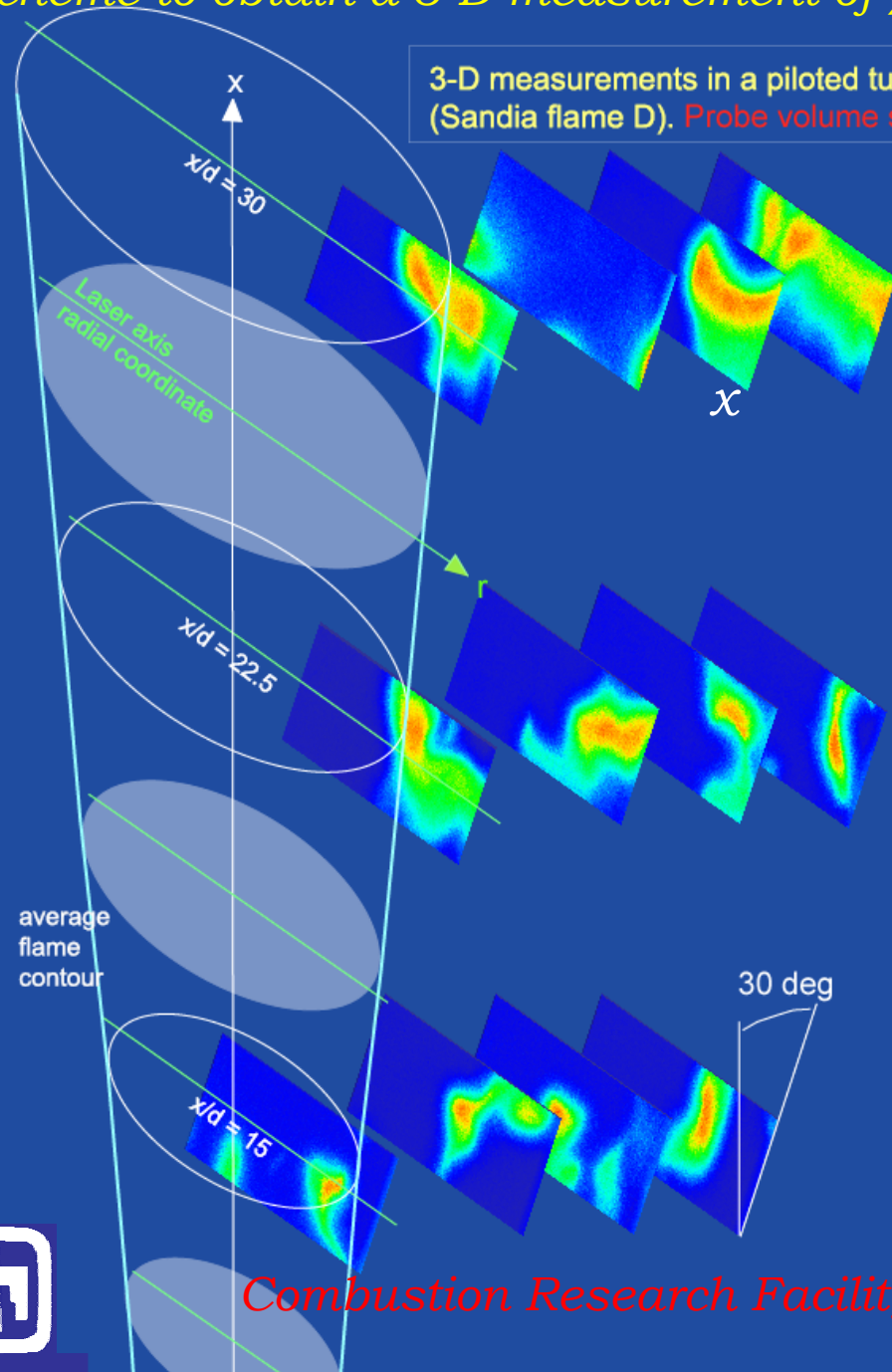


Combustion Research Facility, Sandia National Laboratories



A scheme to obtain a 3-D measurement of χ

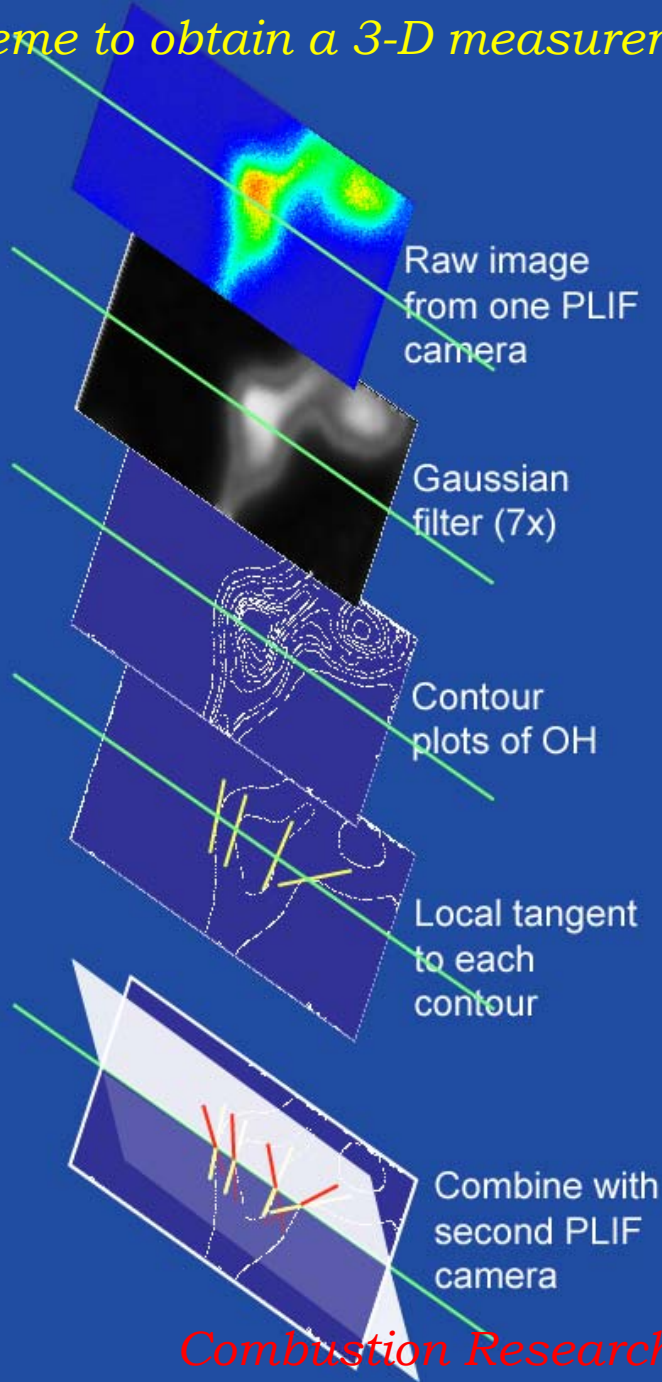
3-D measurements in a piloted turbulent flame (Sandia flame D). Probe volume size 60 μm .



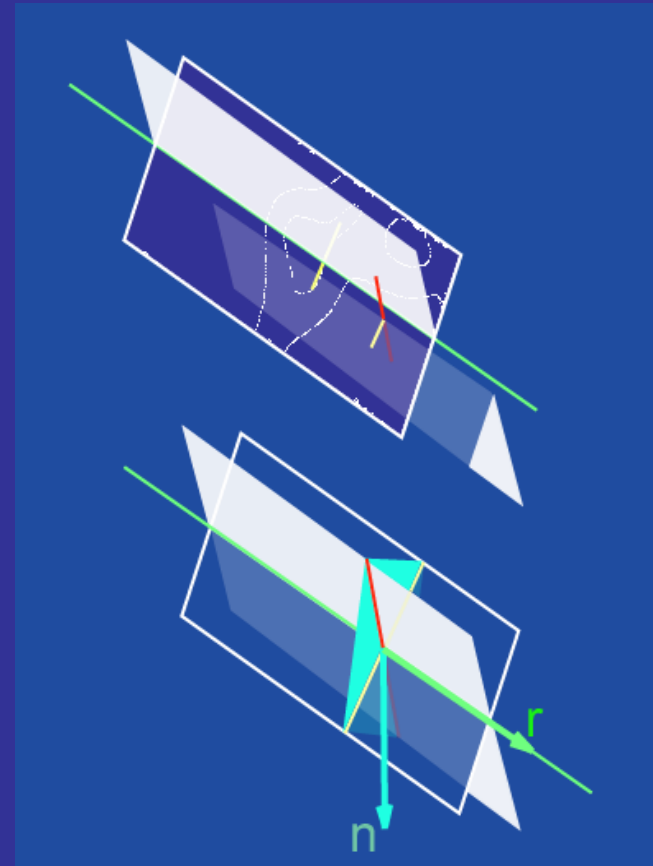
As axial distance increases, so does the corrugation of the flame front. One example (x) shows a case where the flame is parallel to the laser axis. The 1-D technique would register a very small (unrealistic) value of χ . This measurement would be eliminated, while less severe cases would be corrected.



A scheme to obtain a 3-D measurement of χ



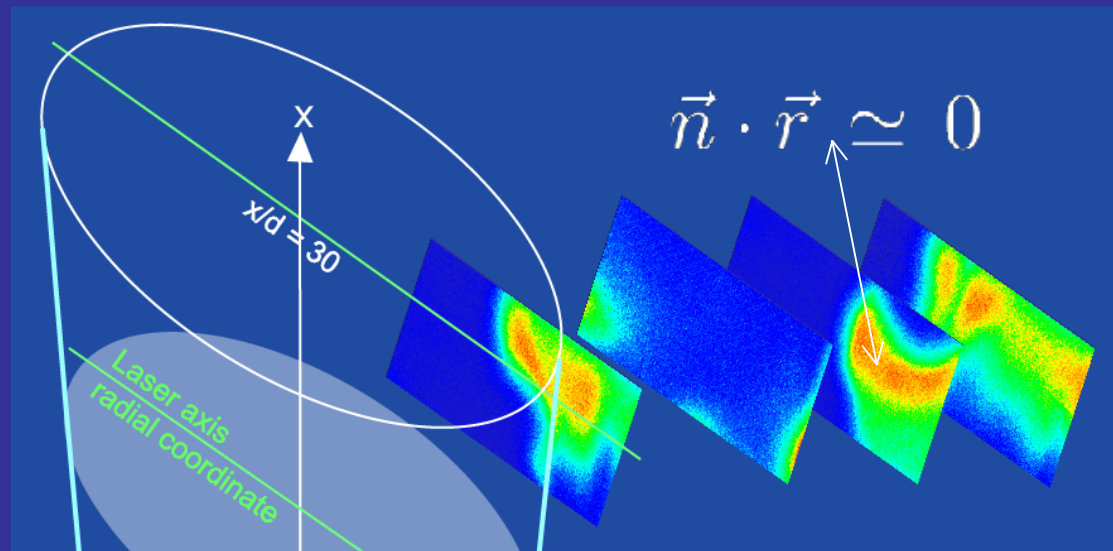
The two local tangents define a plane tangential to the flame surface. The unit vector normal to the plane (n) can be calculated for every OH contour level



3-D correction to the 1-D scalar dissipation measurement

$$\chi_{3D} = \frac{\chi_{1D}}{(\vec{n} \cdot \vec{r})^2}$$

Can be used to eliminate extremes



Improve conditioning on χ

Lead to a real measurement of χ in 3D





TWO-DIMENSIONAL REACTION-RATE, MIXTURE FRACTION, AND TEMPERATURE IMAGING IN TURBULENT METHANE/AIR JET FLAMES

JONATHAN H. FRANK

Combustion Research Facility

Sandia National Laboratories

Livermore, CA

SEBASTIAN A. KAISER and MARSHALL B. LONG

Dept. of Mechanical Engineering

Yale University

New Haven, CT



**Sandia National Laboratories
Combustion Research Facility**

**Yale Center for
Laser Diagnostics**



For More Details



- Frank, J. H., Kaiser, S. A., and Long, M. B., “Reaction-Rate, Mixture Fraction, and Temperature Imaging in Turbulent Methane/Air Jet Flames ,” *29th Combustion Symposium*, Combustion Diagnostics Session Paper 5C04
- Fielding, J., Frank, J. H., Kaiser, S. A., and Long, M. B., “Polarized/Depolarized Rayleigh Scattering for Determining Fuel Concentrations in Flames,” *29th Combustion Symposium*, Combustion Diagnostics Session Paper 4C09

Outline



- Motivation
- CO+OH Reaction-rate Imaging
- Mixture Fraction Imaging
- Results From Sandia Flame D
- Summary & Future Work

Motivation



- Develop techniques to measure fundamental quantities of interest in turbulent partially premixed flames
- Demonstrate feasibility of simultaneous 2-D measurements of mixture fraction and reaction–rate in turbulent flames
- Determine two components of scalar dissipation rate from 2-D mixture fraction measurements
- Focus on flames that are currently the subject of modeling efforts

Reaction-Rate Imaging with CO & OH PLIF



Objective:

Obtain a signal that is proportional to the forward reaction rate of $\text{CO} + \text{OH} \rightarrow \text{CO}_2 + \text{H}$ using the pixel-by-pixel product of simultaneous OH and CO PLIF measurements.

Basic Concept:

$$\text{Reaction Rate} = k(T)[\text{CO}][\text{OH}]$$

$$(\text{CO LIF}) \times (\text{OH LIF}) \propto f_{\text{CO}}(T, \xi) f_{\text{OH}}(T, \xi) [\text{CO}][\text{OH}],$$

$f(T, \xi)$ represents the temperature (T) and mixture fraction (ξ) dependence of LIF signals that results from variations in Boltzmann fraction and quenching rate

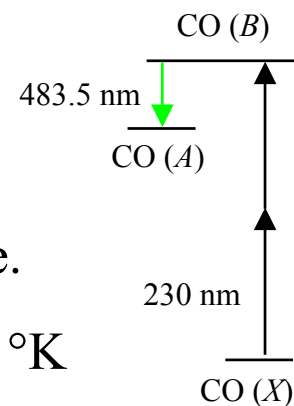
Select pump/detection schemes such that $f_{\text{CO}}(T, \xi) f_{\text{OH}}(T, \xi) \propto k(T)$ over the relevant range of mixture fraction

$$\text{Result: } (\text{CO LIF}) \times (\text{OH LIF}) \propto k(T)[\text{CO}][\text{OH}]$$

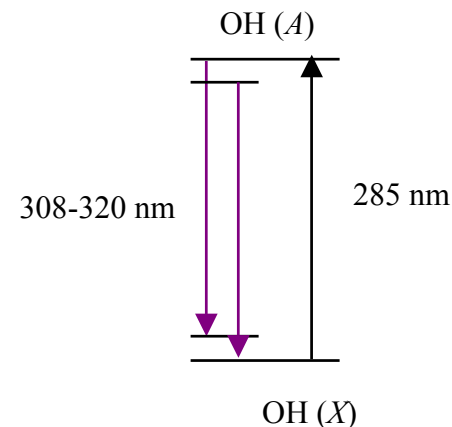
CO & OH Planar Laser-induced Fluorescence



- Two-photon CO LIF excitation B-X(0,0) at 230.1 nm
- Detection of B-A(0,1) band at 483.5 nm
- C₂ interference is avoided by narrow band detection allowing single-shot measurements without need to correct for interference.
- Temperature dependent quenching cross-sections from 300-1000 °K with extrapolation to flame temperatures*



- Single photon OH LIF excitation A-X(1,0) at 285 nm
- Detection of A-X(0,0) and A-X(1,1) bands at 308-320 nm



* Settersten, Dreizler, & Farrow, *J. Chem. Phys.* 117:7 (2002)

Measurement of Mixture Fraction



- Mixture fraction can be determined from measurements of major species at a point or along a line using linear combination of hydrogen (Y_H) and carbon (Y_C) mass fractions:

$$\xi = \frac{2(Y_C - Y_{C,2})/w_C + (Y_H - Y_{H,2})/2w_H}{2(Y_{C,1} - Y_{C,2})/w_C + (Y_{H,1} - Y_{H,2})/2w_H}$$

- Ideally want 3-D measurement of mixture fraction for determining full scalar dissipation rate. However, measuring all major species is not feasible in 2-D or 3-D.
- Can mixture fraction measurements be extended at least to 2-D by measuring a subset of scalar measurements?

2-D Mixture Fraction Measurement Techniques



- Two-scalar approach: Rayleigh scattering + fuel concentration (Raman or LIF)
 - Construct conserved scalar from enthalpy + fuel mass fraction
 - Assumes one-step chemistry

[Long *et al.*(1993), Frank *et al.* (1994), Stårner, *et al.* (1994), Kelman and Masri (1997), Sutton and Driscoll (2002)]
- Previous three-scalar approach: Rayleigh scattering + fuel + N₂ concentration (Raman)
 - Augment two-scalar method with N₂ Raman
 - Assumes one-step chemistry
 - Substitute Ar for N₂ in partially premixed fuel/air mixtures

[Fielding *et al.*(1998)]
- **Present three-scalar approach: Polarized/Depolarized Rayleigh scattering + CO LIF**
 - Inclusion of CO to improve on one-step chemistry assumption
 - Use results from point measurements to predict most probable value of mixture fraction from three measured quantities

Fuel Measurements Techniques



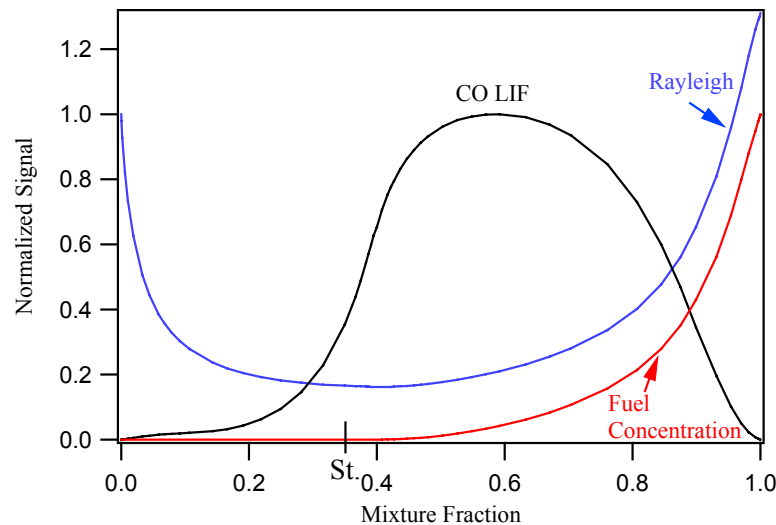
- Laser-induced fluorescence of fuel or fuel tracer
 - Breakdown of fuel well on rich side of stoichiometric contour
 - Relatively large quantities of tracer required
- Fuel Raman
 - Weak signal
- Polarized/Depolarized Rayleigh*
 - Depolarized Rayleigh signal order of magnitude greater than fuel Raman

* See “Polarized/Depolarized Rayleigh Scattering for Determining Fuel Concentrations in Flames,” Fielding, Frank, Kaiser, Smooke, and Long, *29th Combustion Symposium*, Paper 4C09

Choice of Scalars for Determining Mixture Fraction



- Use laminar flame calculations and multiscalar point measurements to guide the diagnostic development.
- Need a strong scattering process with a signal that varies monotonically with mixture fraction.
- Rayleigh scattering has high signal-to-noise ratio but is not monotonic.
- Need additional measurement(s)
 - Distinguish rich and lean sides: Fuel concentration
 - Have sensitivity near stoichiometric: CO LIF



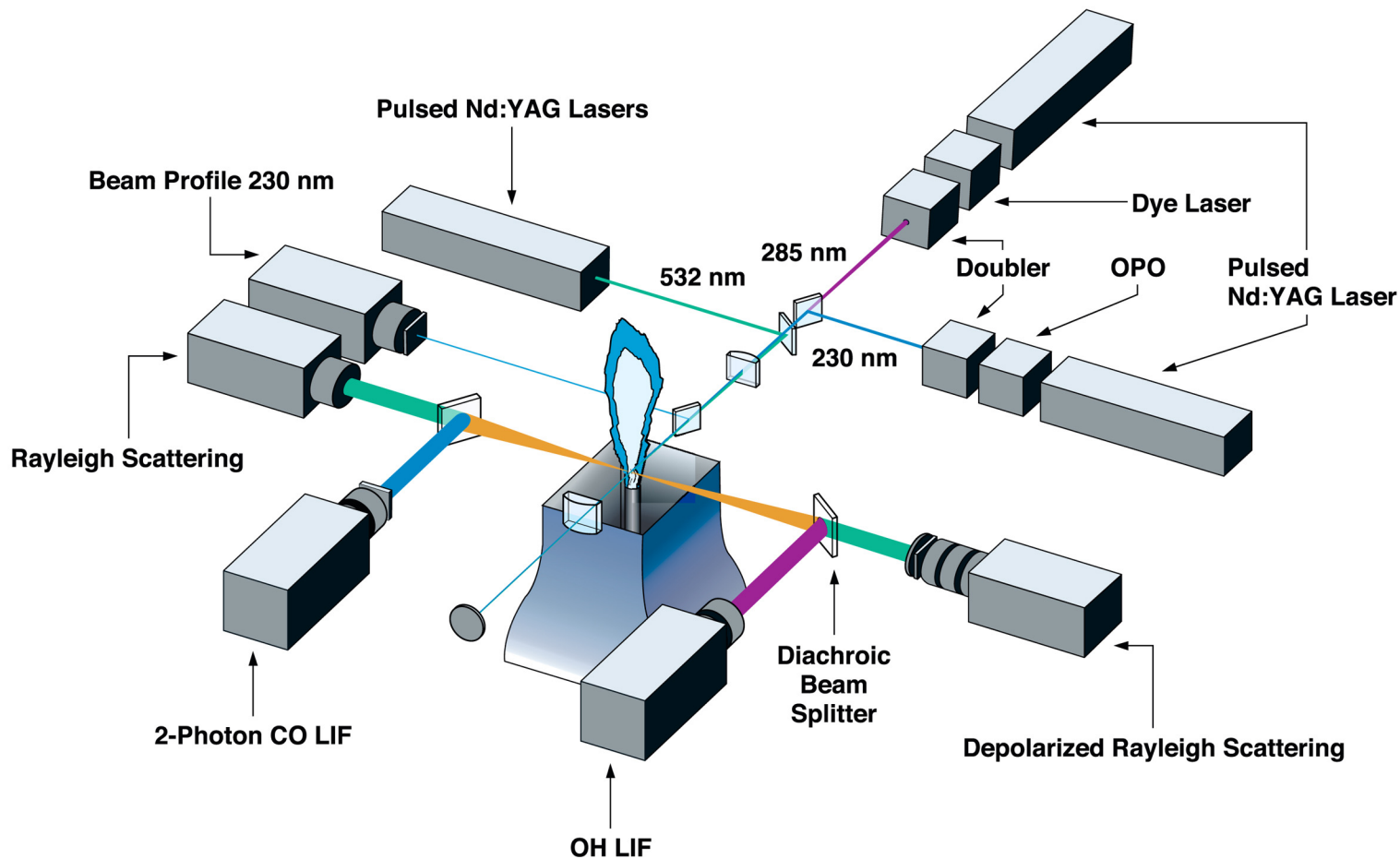
Turbulent CH₄/Air Jet Flame with Piloted Burner



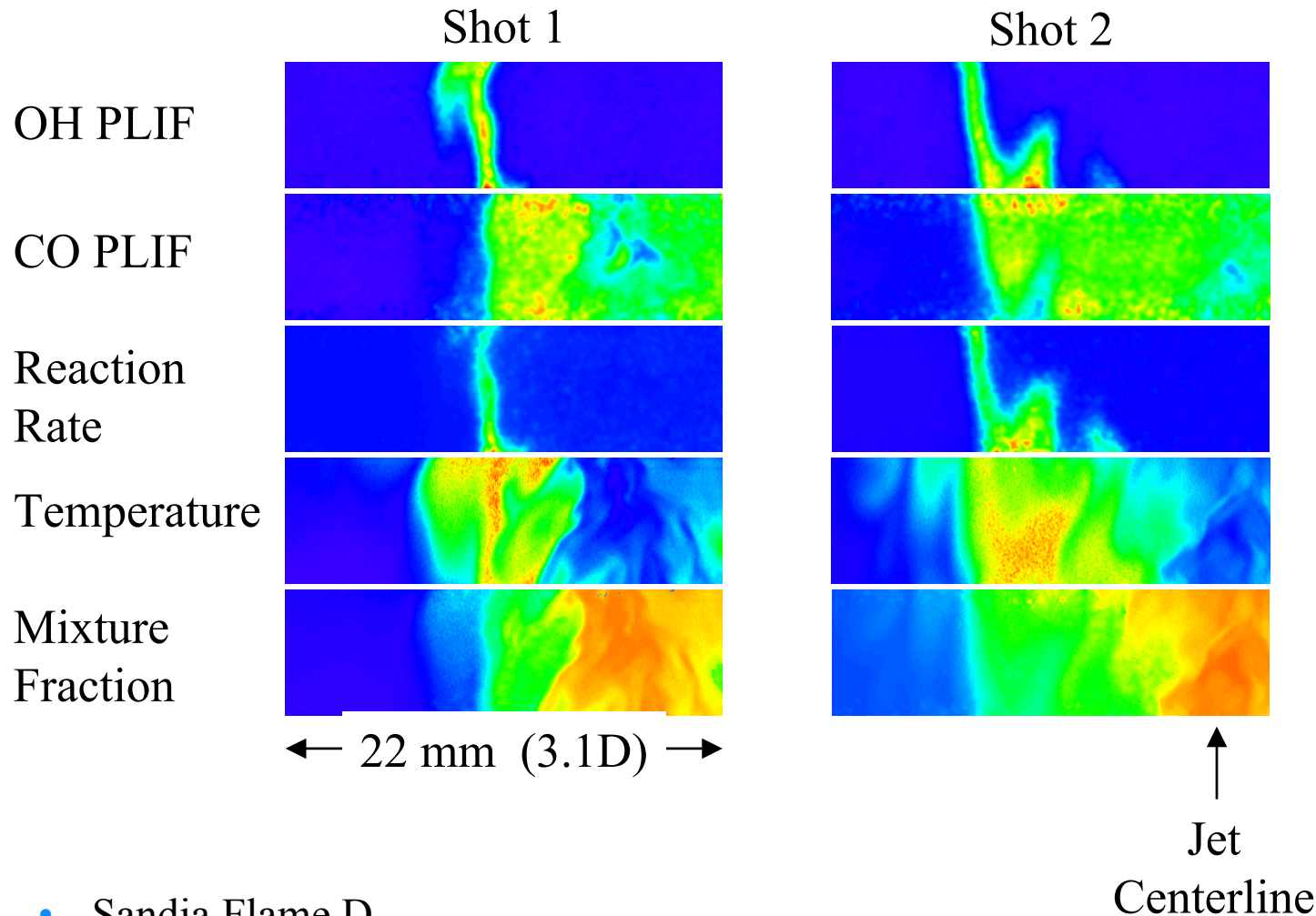
- Dimensions: Nozzle Diameter = 7.2 mm
Pilot Diameter = 18.2 mm
- Main Jet: CH₄/Air (1/3 by volume)
Re = 22,400 (Flame D in TNF Workshop)
- Pilot: Premixed C₂H₂, H₂, Air, CO₂, N₂



Experimental Apparatus for Simultaneous Reaction-Rate, Mixture-Fraction, and Temperature Measurements

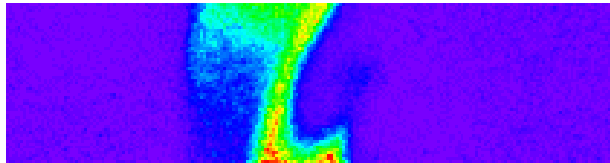


Instantaneous 2-D Measurements of Reaction Rate, Temperature, Mixture Fraction in a Turbulent Jet Flame

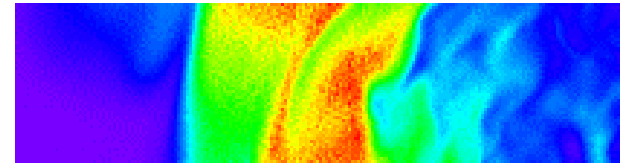


- Sandia Flame D
- Imaged region centered at $x/d = 15$

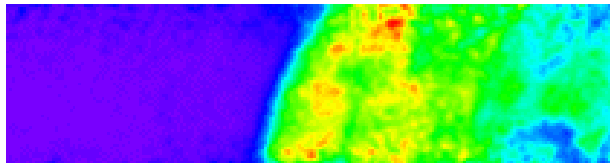
2-D Measurements of Reaction Rate, Temperature, Mixture Fraction, and Scalar Dissipation in a Turbulent Jet Flame



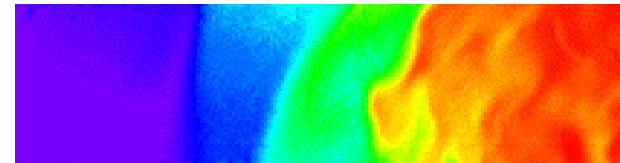
OH



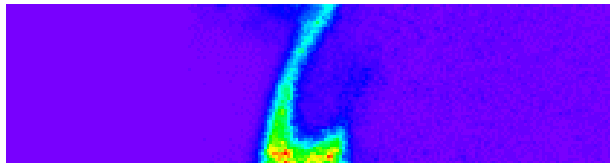
T



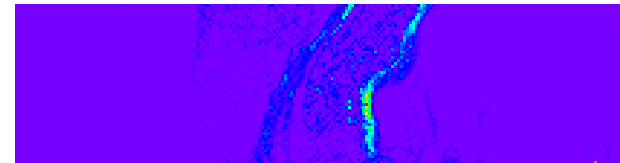
CO



Mixture
Fraction



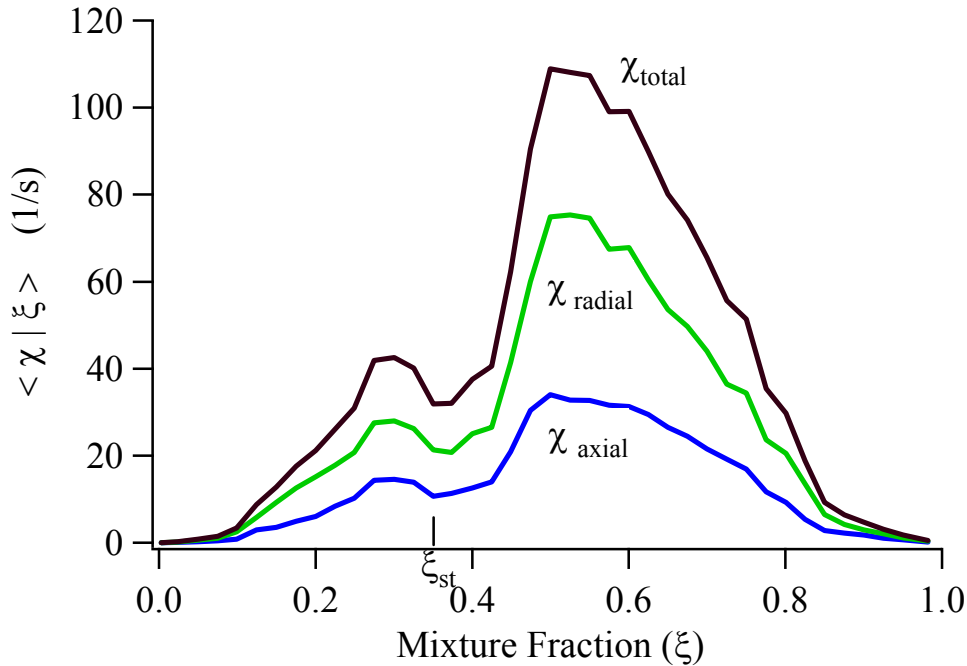
Reaction
Rate



Scalar
Dissipation

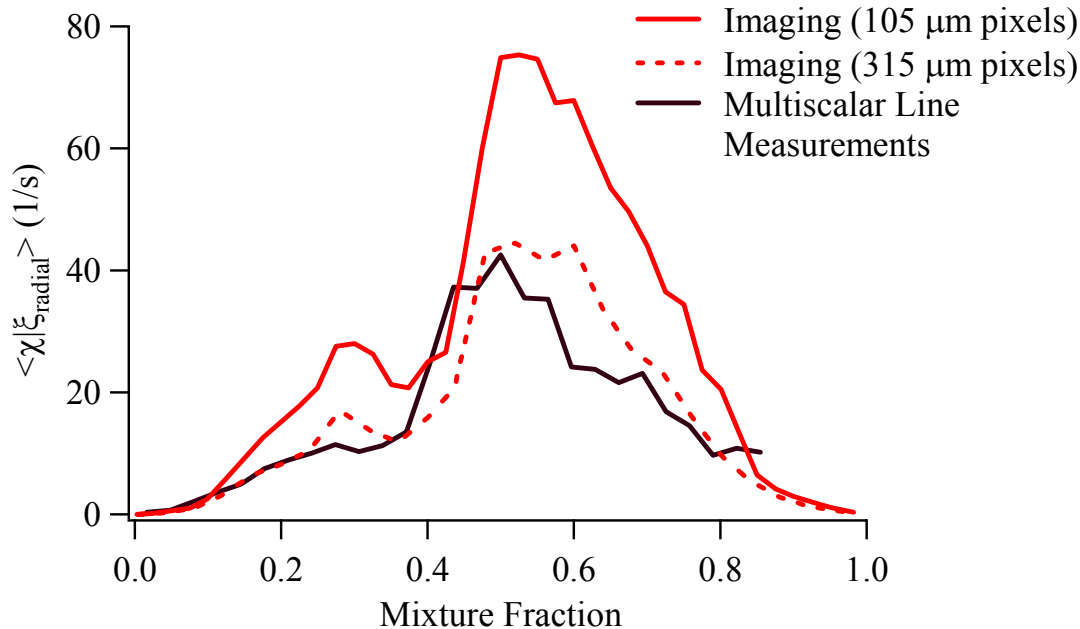
↑
Jet
Centerline

Two Components of Conditional Scalar Dissipation in Turbulent Jet Flame



- Conditional mean values of ξ determined from 70 images centered at $x/d = 15$
- Ratio of lean and rich peaks for $\langle \chi_{\text{radial}} | \xi \rangle$ consistent with line measurements
- χ_{axial} contributes significantly to total scalar dissipation
- Correlation coefficient: $R_{\chi_{\text{radial}}\chi_{\text{axial}}} = 0.2 - 0.4$ depending on ξ
- 2-D measurements of scalar dissipation necessary

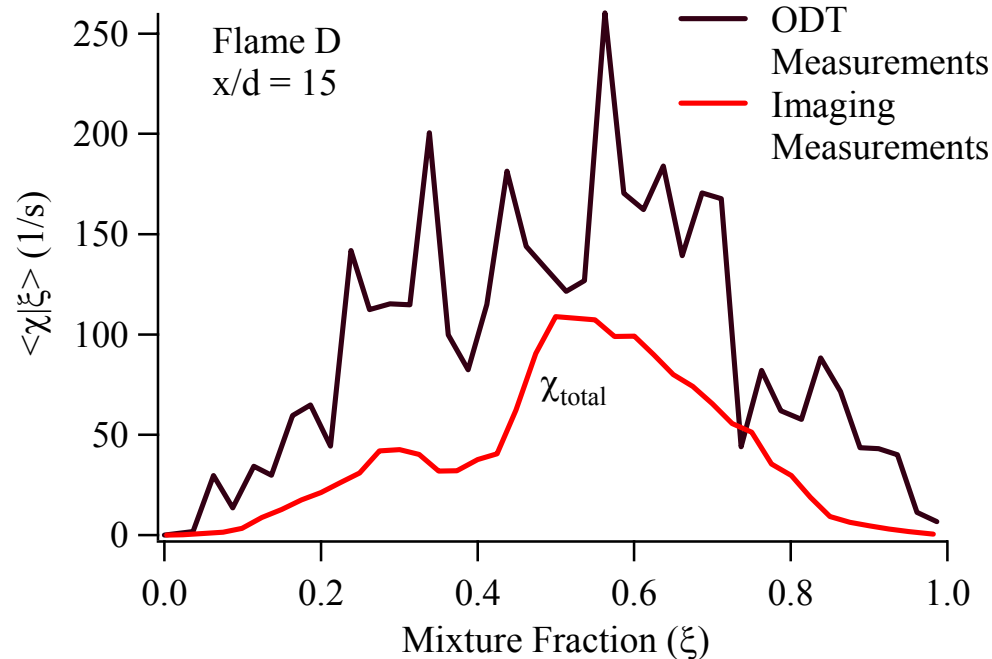
Comparison of Imaging and Multiscalar Line Measurements in Flame D ($x/d = 15$)



- $\langle \chi_{\text{radial}} | \xi \rangle$ from images compared with multiscalar line measurements*
- Line measurements of major species allow more complete formulation for mixture fraction but only yield one component of scalar dissipation rate
- Line and imaging measurements show good agreement when images are binned to give a comparable pixel size

*Karpetsis and Barlow, 29th *Combustion Symposium*, Paper 5A08

Comparison of Scalar Dissipation Rates Imaging Measurements and ODT Model



Imaging measurements by J. H. Frank (Sandia), S. A. Kaiser (Yale), & M. B. Long (Yale)

One-Dimensional Turbulence (ODT) results by T. Echehki (N.C. State), A. R. Kerstein (Sandia), J.-Y. Chen (U.C. Berkeley)

Summary



- Feasibility of 2-D joint mixture fraction, temperature, and CO/OH reaction-rate measurements demonstrated in turbulent CH₄/air jet flame
- Demonstrated 3-scalar approach to measuring mixture fraction using polarized/depolarized Rayleigh scattering and two-photon CO PLIF
- Previous multiscalar single-point measurements provided guidance for mixture fraction measurement technique
- Polarized/depolarized Rayleigh scattering used for temperature and fuel measurements. Technique offers advantages over fuel Raman and LIF
- Correlation of axial and radial components of scalar dissipation rate shows need for multi-dimensional mixture fraction measurements

Future Work



- Extend technique to flames with significant extinction
- Investigate joint statistics of mixture fraction, scalar dissipation, and reaction rate for comparison with models
- Study effects of spatial resolution on scalar dissipation measurements
- Use 2-D measurements to complement multiscalar line and single-point data



UNIVERSITY OF
CAMBRIDGE

Time domain imaging

Clemens Kaminski group

Department of Chemical Engineering

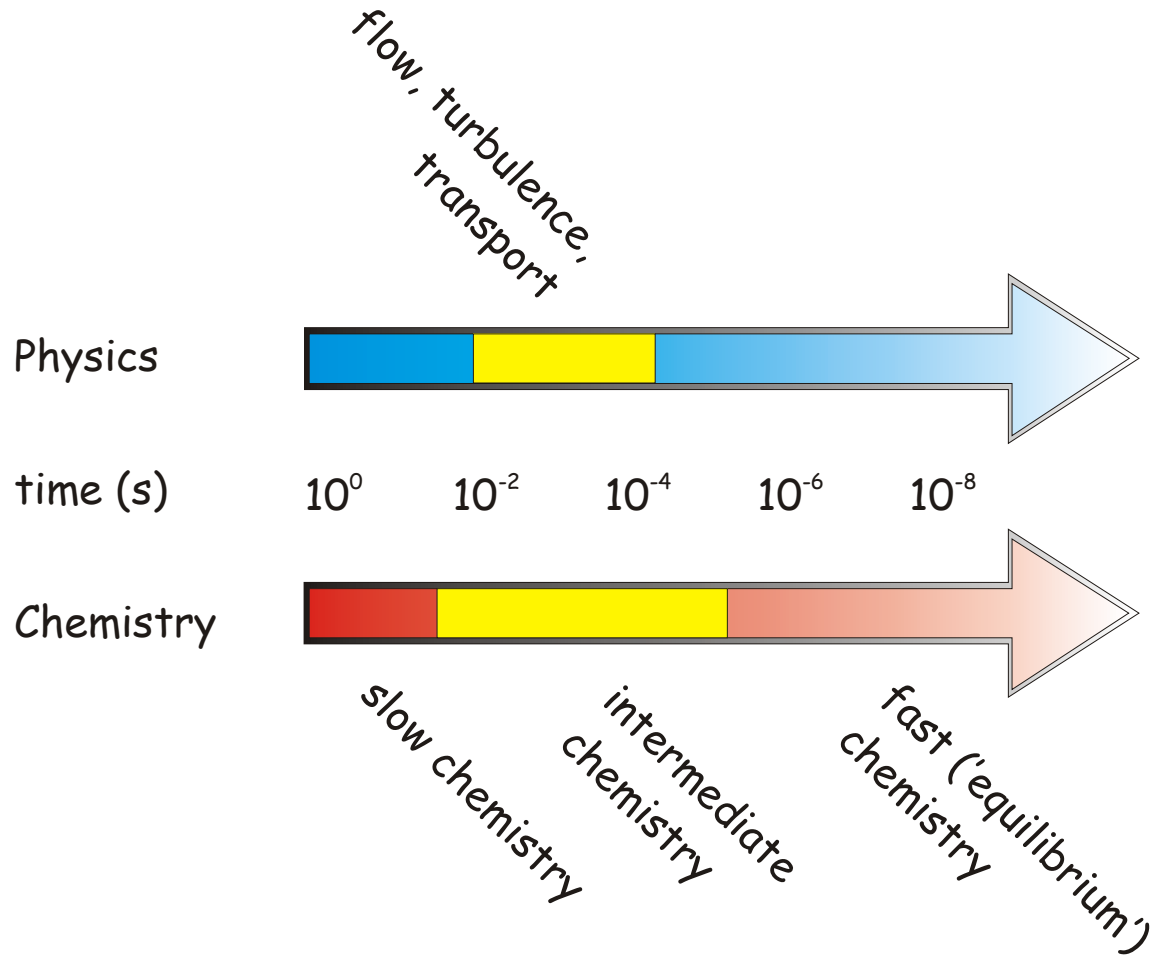
University of Cambridge

Clemens_kaminski@cheng.cam.ac.uk

<http://www.cheng.cam.ac.uk/kaminski.html>

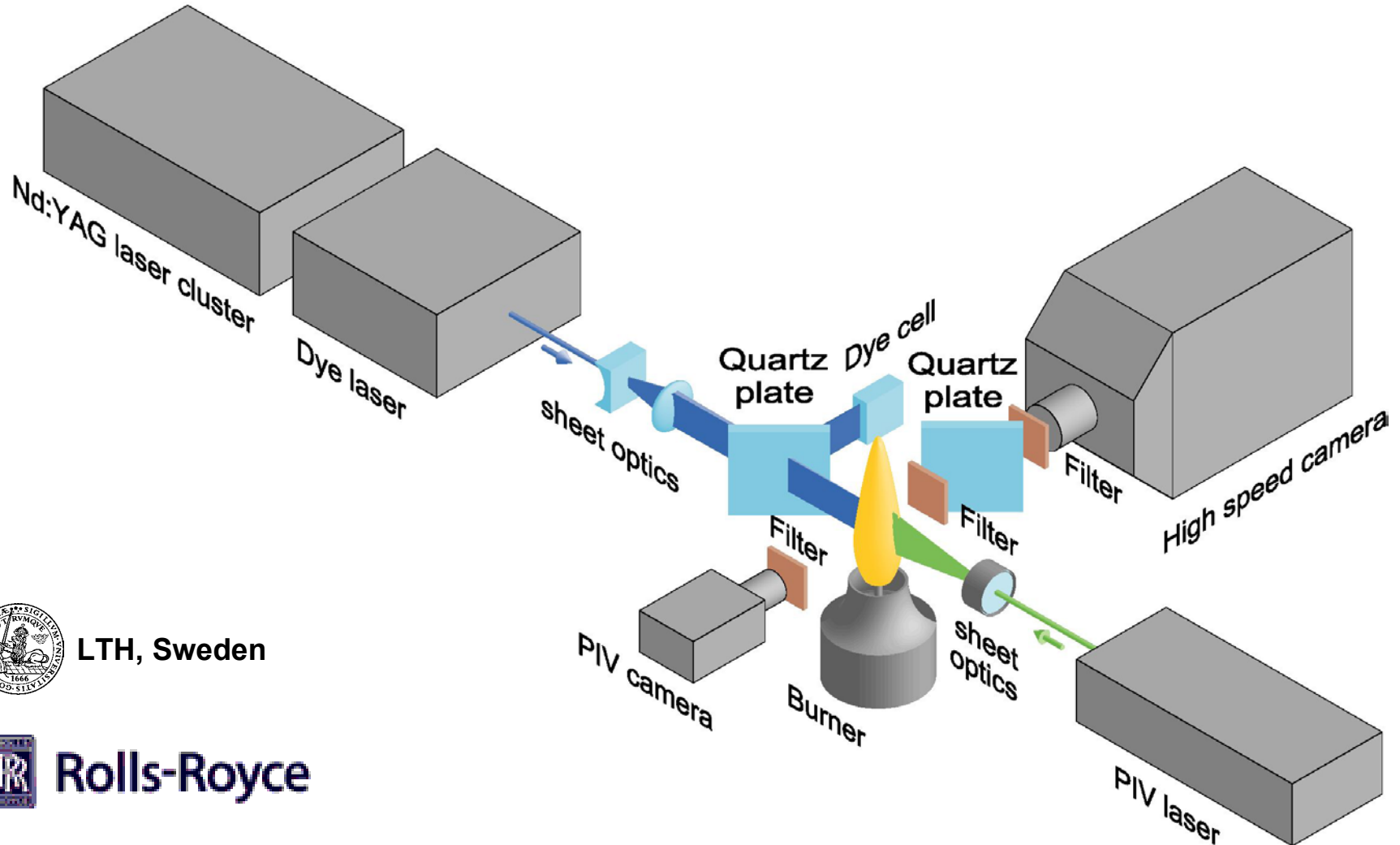


Turbulence-Chemistry interactions





The high speed imaging facility



LTH, Sweden



Rolls-Royce

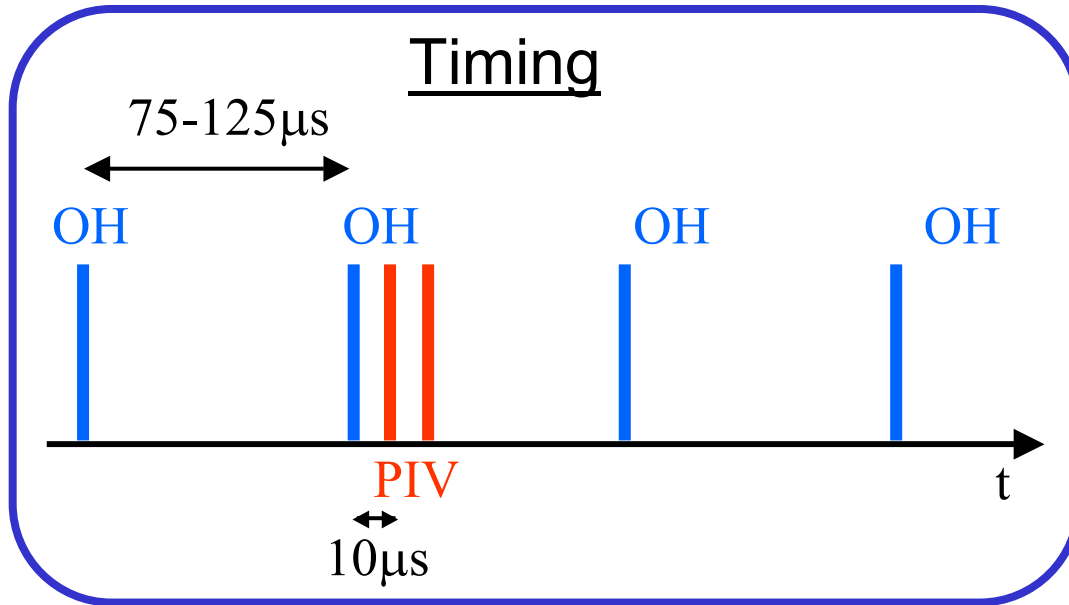


DEPARTMENT OF
ENGINEERING

Clemens Kaminski



Experimental details



- OH excitation: 283 nm
- OH detection: 309 nm
- PIV: 532 nm

PIV processing

- Dantec PIV2000 processor and FlowManager software
- FFT cross-correlation
- Validation steps: velocity range, peak, manual, moving average
- Mean velocity subtracted



Local extinction

Turbulence/chemistry interactions

- Local extinction?
- Re-ignition?
- Time scales?

Multiple visualization

- Flame front: 4xOH PLIF
- Flow: PIV

Turbulent non-premixed flame

(target flame - TNF workshop)

Fuel: 33% H₂, 22% CH₄, 45% N₂

Reynolds number: 20000

Seeding: TiO₂ (d=1 μm)



DLR flame

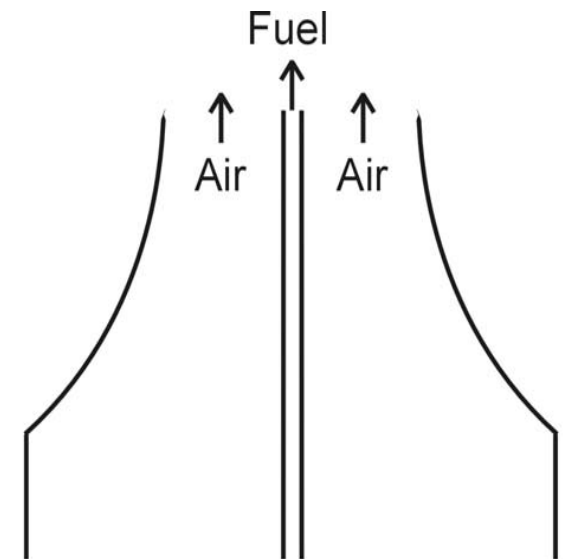
Well characterised turbulent non-premixed flame
(target flame of the TNF workshop)

Fuel mixture: 33% H₂, 22% CH₄, 45% N₂

Coflow: air

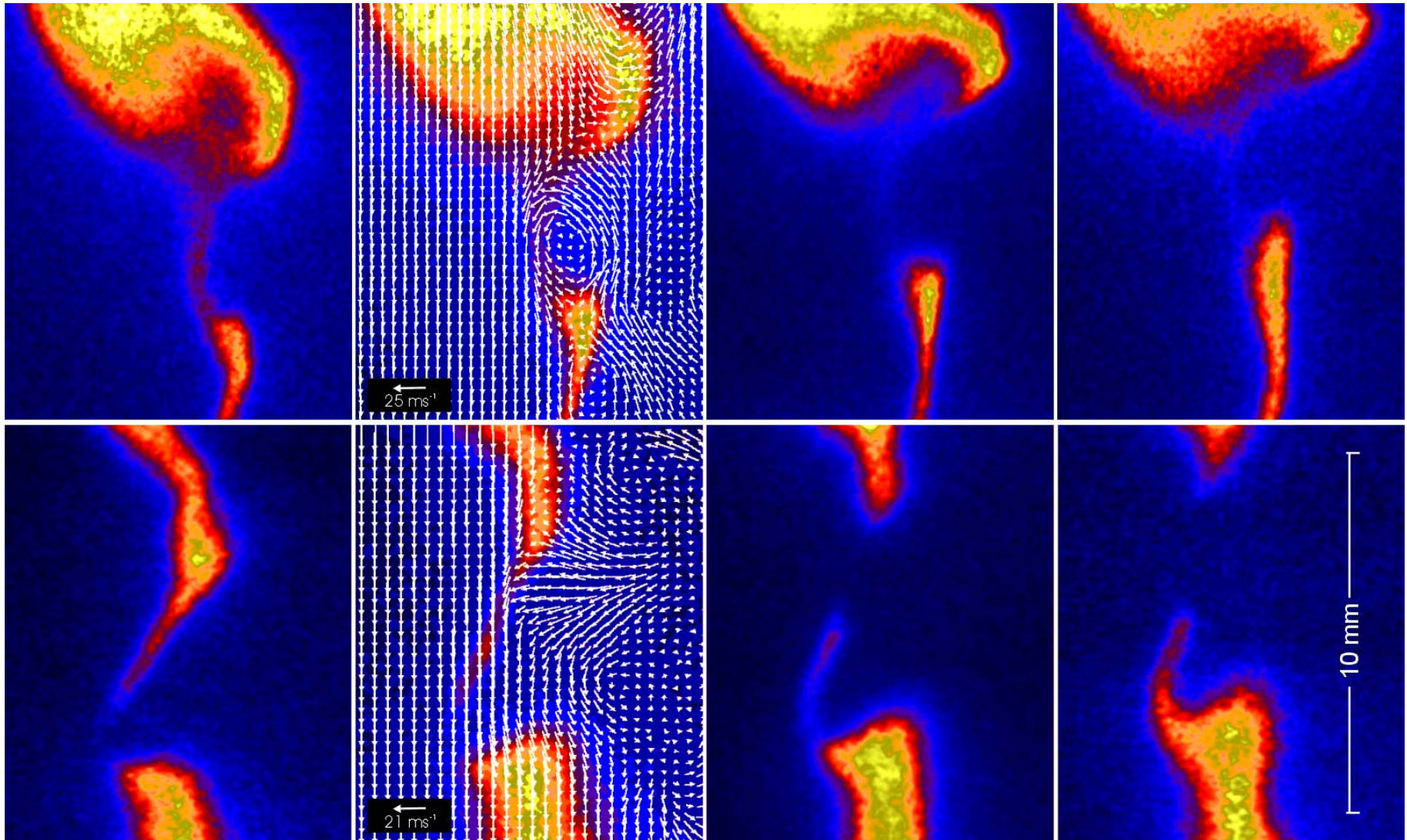
Re=20000

Both flows seeded with 1 μm TiO₂ particles





Turbulence-Chemistry interactions



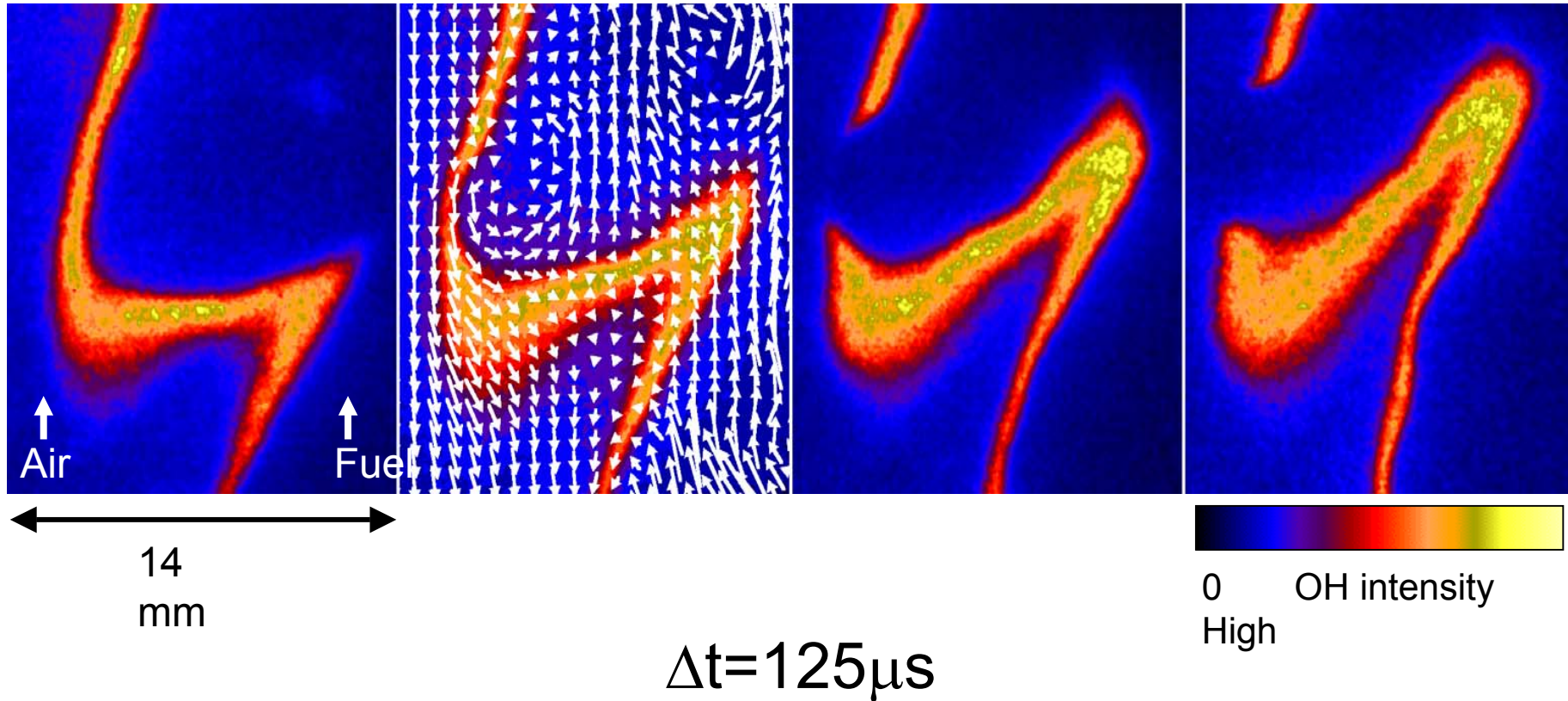
J. Hult, G. Josefsson, M. Aldén, and C.F. Kaminski.

Proc. 10th Int. Symp. on Application of Laser Techniques to Fluid mechanics, Lisbon (2000)

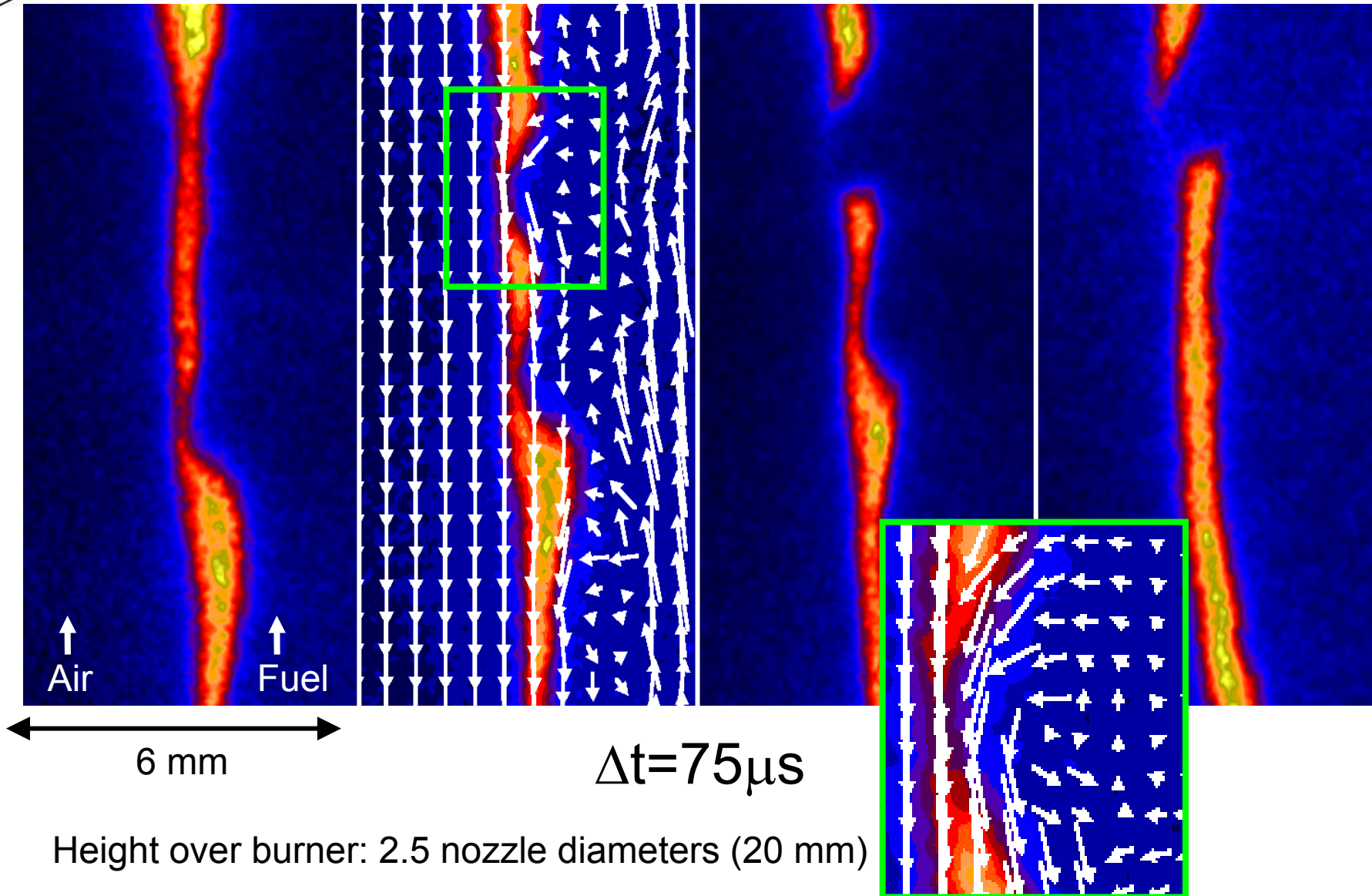
Clemens Kaminski



Quenching by fuel vortex



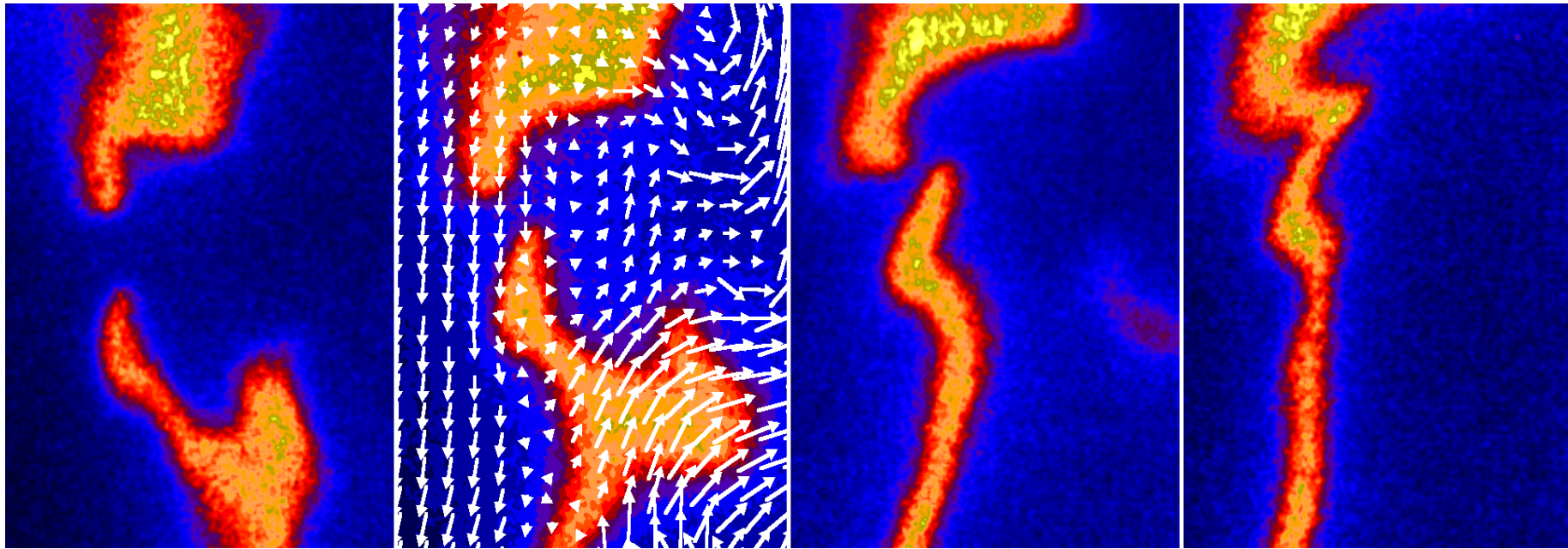
Height over burner: 19 nozzle diameters (150 mm)



Height over burner: 2.5 nozzle diameters (20 mm)



Re-ignition: homogeneous velocity field



11 mm

$\Delta t = 125 \mu s$



0 OH intensity
High

Height over burner: 16 nozzle diameters (130 mm)



Conclusions

- Simultaneous time resolved OH PLIF and PIV performed
- Extinction caused by fuel vortices
- Extinction time scale: $< 100 \mu\text{s}$

Current work

- Separate flow and chemistry effects on flame front structure
- Combine time resolved OH PLIF with other techniques

Measurements and Calculations of Mean Spectral Radiation Intensities Leaving Turbulent Non-Premixed and Partially Premixed Flames

Yuan Zheng, R. S. Barlow⁺ and J. P. Gore

School of Mechanical Engineering
Purdue University
W. Lafayette, IN 47907 – 1003, USA

⁺ Combustion Research Facility
Sandia National Laboratories
Livermore, CA 94551-0969, USA

Corresponding Author: Jay P. Gore
1003, Chaffee Hall
School of Mechanical Engineering
Purdue University
West Lafayette, IN 47907-1003, USA
Phone: 765 494 1452
Fax: 765 494 0530
Email: gore@ecn.purdue.edu

Abstract: Instantaneous line of sight spectral radiation intensities for diametric and chord-like paths in six non-sooting flames were measured using a fast IR array spectrometer. Using well-documented scalar data from the TNF workshop, the mean spectral intensities were also computed using the mean property approach and using a stochastic time and space series (STAS) simulation based method. The impact of turbulence/radiation interaction (TRI) for these flames was studied by comparing the two sets of computations with the experimental data. In most of these flames, it is found that the effect of TRI is significant only for regions away from the flame axis. For flames with identical fuel streams and burners, the mean intensities do not increase significantly with increases in flow rate (and therefore the Reynolds numbers) because of relatively small increases in radiation path lengths as well as self absorption of radiation. Local extinction effects may also contribute to the lack of significant increase in radiation intensities. The radiation data and the above findings are of value in the evaluation of radiation sub-models increasingly used in turbulent combustion calculations.

Nomenclature

D	diameter of the burner
Q	radiation heat loss
x	height above the burner exit
r	radius

Subscripts

a	absorption
e	emission
r	radiation

Introduction

Radiation heat loss has significant effects on the nitric oxide (NO) formation and emissions from non-luminous turbulent flames [1-3]. For a small volume in the flame, the time averaged net volumetric radiation heat loss ($\overline{Q_r}$) consists of emitted energy ($\overline{Q_e}$) by the participating gaseous media within that volume minus the absorbed energy ($\overline{Q_a}$) by the media from the incident radiation field [4]. Emission and absorption are determined by temperature and species concentrations through highly non-linear relations. The scalar fields in turbulent flames, however, vary in both temporal and spatial domains. Therefore, radiation and turbulence cannot be treated separately from each other. This effect is known as turbulence/radiation interaction (TRI). Accurate evaluation of $\overline{Q_e}$ requires single-point realizations of the turbulent scalar properties, while the evaluation of $\overline{Q_a}$ requires multi-point scalar realizations of the entire field. If the emitted energy dominates the absorbed energy then the absorption term can be neglected simplifying the computations to those of single point scalar realizations rather than those of the entire field [5-7].

Turbulence radiation interactions (TRI) are important in some non-premixed flames. Gore, *et al.* [8] observed significant effects of TRI in hydrogen flames, with stochastically predicted line-of-sight (LOS) spectral radiation intensities being as much as twice those based on the mean property predictions. Kounalakis, *et al.* [9] used time series simulation method in CO/H₂ flames and also found that TRI enhanced LOS spectral radiation intensities for diametric paths at different axial locations by 10-100 % at $\lambda = 2.7 \mu\text{m}$. For a CH₄/H₂ flame, 20-30 % TRI enhanced LOS radiation in the water vapor bands were reported by Hall and Vranos [10]. By solving the transport equations for the probability density functions (PDF) in non-sooting methane flames, recent studies [6] found that the flame temperatures decreased by approximately 100 K when TRI were considered

For dilute hydrogen flames, a simplified radiation sub-model, adopting the consideration of only the emitted energy and the mean-property approach was found to be appropriate [1]. These simplifications, however, may not be applicable to hydrocarbon flames because of the stronger bands of the CO₂ molecule. Previous computational studies [2] on a dilute carbon monoxide flame, which is one of the turbulent non-premixed flame (TNF) workshop flames [11], demonstrated that the neglect of absorbed energy was not appropriate. This work also indicated the importance of considering the effects of TRI, although the total radiant fractions of the flames under investigation were less than 10%. Well-documented experimental data on velocity and scalar fields of the TNF flames are available in the literature [11-14], but spectral radiation

intensity data are not available. This has motivated the present measurements. The experimental data are also very useful for the evaluation of the radiation sub-models being incorporated in current and future computational tools.

In evaluating the impact of the TRI, the difference between the experimental data and the calculated results by using mean properties approach can be an indicator. The stronger the TRI, the greater is the difference between the measurements and the mean property calculations. Recent research has also disclosed that the investigations on LOS flame radiation from both diametric and other chord-like paths are important for understanding TRI [15].

Motivated by this, our present work consisted of the following:

- (1) Instantaneous LOS spectral radiation intensities for diametric and various chord-like paths at three heights were measured using a fast IR array spectrometer (FIAS) [16]. Spectra for mean intensities were extracted by averaging the experimental data. Six TNF workshop turbulent jet flames were studied, including one H₂/N₂ flame, two CH₄/H₂/N₂ flames and three pilot CH₄/air flames [11-13].
- (2) The mean spectral radiation intensities were calculated by integration of the radiation transfer equation (RTE) for non-homogenous paths with arbitrary optical thickness in conjunction with the mean values of the species concentrations and temperatures.
- (3) The mean spectral radiation intensities were also calculated by using the stochastic time and space series (STAS) based stochastic simulation. Taking into account the effects of TRI, this stochastic approach can give improved estimates of the LOS radiation intensities illustrating the importance of TRI [15].

In the above calculations, experimental results for the mean scalar values and the scalar statistics from the TNF workshop literature [11-14] were adopted to avoid uncertainties of specific combustion models.

Experimental Method

The operating conditions for the flames under investigation are listed in Table 1, where L_{stoich} is the height above the burner at which the Favre averaged mixture fraction reaches the stoichiometric value based on the measurements [2]. The radiation measurements were conducted at the Turbulent Diffusion Flame (TDF) Laboratory and the Turbulent Combustion Laboratory (TCL) at Sandia National Laboratories. The flow facilities for the simple jet flames (DLR_A & B, H3) and the piloted flames (C, D, E) have been discussed elsewhere [1, 13, 14,17] and will only be briefly described here.

The simple jet burner is a long tube with an inner diameter of 8 mm tapered to a thin edge. The piloted burner has a main jet diameter of 7.2 mm and a pilot diameter of 18.2 mm. The main CH₄/air jet is partially premixed with an equivalence ratio of 3.17 (25% CH₄ by volume). The pilot flame burns a pre-mixture of C₂H₂, H₂, CO₂, N₂ and air, having the same enthalpy and equilibrium composition as a CH₄/air flame with an equivalence ratio of 0.77. Both burners can be moved in three dimensions for positioning. Air co-flows were fed to all six flames through wind tunnels, with velocities of 0.3 m/s for the simple jet flames and 0.9 m/s for the piloted flames.

For each flame, the instantaneous LOS spectral radiation intensities for the diametric and between 6 to 13 chord-like paths at three heights were measured using a fast infrared array spectrometer (FIAS) [16]. The spectral range of the FIAS is from 1.4 to 4.8 μm with 20 nm resolution, covering the important molecular radiation bands of H₂O and CO₂. The sampling rate for the individual wavelengths is 6250 Hz. The spatial resolution of the present measurements is

2 mm based on the FIAS optics. For each radiation path, 6000 samples were collected. Experimental uncertainties based on repeated measurements were less than 10%.

Computational Method

For all six flames, the mean LOS spectral radiation intensities were computed by adopting the mean property distributions along the radiation paths ignoring TRI. The RTE was solved for various non-homogeneous paths through the flames by the RADCAL program with a narrow band radiation model [18, 19]. The mean properties needed for the computations were taken directly from the experimental data available in the literature [11-14].

Time and space series analysis computations that account for TRI were considered for these six flames. The instantaneous realizations of the scalar properties along a non-homogeneous radiation path were simulated first by using the TASS analysis. Then, the instantaneous LOS spectral radiation intensities for that path were calculated by using RADCAL. Finally the mean intensities were extracted from the 6000 simulated realizations for each radiation path. The TASS based computation, involving a tomography-like procedure to determine the integral lengths along the radiation paths, has been discussed in detail in Refs. [15, 20]. This approach can simulate the two-time/two-point statistics by using the measured single-point PDFs of scalar properties [11] in conjunction with prescriptions of the integral length and time scales for scalar fluctuations.

Results and Discussions

The measured and calculated mean radiation spectra for nine paths in each of the six flames are illustrated in Figs 1-18. For each of the three axial locations in the flames, the spectral radiation intensities for the diametric path ($r = 0$ mm) and one of the chord-like paths are selected as representative. At a fixed axial location, the LOS intensities for the diametric radiation path are higher than those for most of the chord-like paths, which are shorter. The intensities for some chord-like paths that are near the flame sheet location are higher than those for the diametric path. However, the chord-like paths selected here are always farther out on the lean side of the flame sheet and have intensities that are much lower than those for the diametric path.

Measurements and calculations of spectral radiation intensities for $x/D = 20, 30$ and 40 in flame H3 (H_2/N_2) are illustrated in Figs. 1-3. The spectral radiation intensities for this dilute hydrogen flame are relatively low. The spectra are dominated by the 1.87 and 2.7 μm bands of water vapor. In this flame, the combustion process is complete at approximately $L_{\text{stoich}}/D = 36$. Therefore, the measured mean spectral radiation intensities at $x/D = 30$ and 40 are almost identical and are 50 % larger than those at $x/D = 20$. Except for the radiation intensities for the path at $r = 15$ mm at $x/D = 20$, the calculations ignoring TRI agree with the measurements quite well. Although improvement can be achieved when the TASS approach is used, the effects of TRI in this flame are not significant. This explains the reason for the reasonably good predictions of NO formation in similar H_2 jet flames without considering TRI [1].

Measurements and calculations of spectral radiation intensities for $x/D = 20, 40$ and 60 in the DLR_A flame ($CH_4/H_2/N_2$) are illustrated in Figs. 4-5. The results of the TASS based computations are presented together with the mean property calculations and experimental data. In this flame, the spectra are dominated by radiation from water vapor and CO_2 . The measured radiation intensities increase dramatically from $x/D = 20$ to 40 and then increase slightly at $x/D = 60$, which is near the stoichiometric flame height ($L_{\text{stoich}}/D = 64$). For the diametric paths at three axial locations, both the mean property and the TASS based calculations agree with the data.

Thus, the effects of TRI are weak for the diametric paths. For chord-like paths, where the LOS spectral radiation intensities are a half to a third of those for the diametric paths, the mean property method significantly under-predicted the spectral radiation intensities for the 2.7- μm H₂O/CO₂ band and the long wavelength wing of the 4.3- μm CO₂ band. In evaluating the impact of TRI, the 2.7- μm band and the long wavelength wing of the of the 4.3- μm band are much more suitable than the peak of the 4.3- μm band due to re-absorption effects caused by CO₂ in the path between the flame and the FIAS [21]. As illustrated in the figures, TRI are significant for regions away from the axis for this flame, where the turbulence intensities ($T_{\text{rms}} / T_{\text{mean}}$ shown later in Fig. 19) are higher.

Figures 7-9 demonstrate the spectra for the flame DLR_B, which has a 50% higher Reynolds number than the DLR_A flame. The measured radiation intensities remain almost constant in spite of a 50 % increase in the fuel input. This is a result of similar flame structure as indicated by Fig. 19 [11]. In addition, it is noted that the stoichiometric flame height does not change significantly ($L_{\text{stoich}}/D = 64$) due to the momentum controlled nature of these flames. For the diametric paths, the calculated spectral radiation intensities ignoring TRI agree with the measurements quite well. For paths away from the flame axis, however, more than 50 % under-prediction by the mean property method can be observed indicating very strong effects of TRI. Especially, the calculated radiation intensities based on the mean property method from the 2.7- μm H₂O/CO₂ band are almost negligible for the path at $r = 60$ mm at $x/D = 60$.

Measurements and calculations of spectral radiation intensities for $x/D = 30, 45$ and 60 in flame D (piloted CH₄/air) are illustrated in Figs. 10-12. These spectra are also dominated by the radiation from water vapor and CO₂. Being close to the stoichiometric flame height ($L_{\text{stoich}}/D = 47$), the measured intensities are highest at $x/D = 45$ and decrease on the upstream ($x/D = 30$) and the downstream ($x/D = 60$) sides. For the diametric paths, the calculations based on mean properties under-predict the radiation intensities by 5 to 20 %. Up to 50 % under-prediction is observed for paths away from the flame center at all three heights. The calculations considering TRI (TASS), however, match the experimental data very well for all radiation paths. Thus, the effect of TRI is significant in this flame. Using the mean property approach for the same flame, Frank, *et al.* [2] also calculated the LOS spectral radiation intensities for the diametric path at $x/D = 45$ using emission-only and emission/absorption formulations. Intensities in the 4.3 μm CO₂ band from the emission-only calculations were as much as twice those from the emission/absorption calculations.

Figures 13-15 and 16-18 present the spectra for two additional piloted CH₄/air flames with lower and higher Reynolds numbers. There is no significant change in the measured stoichiometric flame height showing a momentum control of this quantity. For chord-like paths at identical radial locations and height above the burner, the measured radiation intensities are greater for flame E than for flame D, which are greater than those for flame C. This is a result of the increasing extent of the hot gas region with increasing Re number as indicated by Fig. 20 [11]. The changes in spectral intensities for the diametric paths, however, are small compared to the significant increases in the fuel flow rate especially for the flames D and E. This is a result of self-absorption of radiation over a longer path and the effects of increases in volumetric combustion rates by turbulence. The spectral radiation intensities for the diametric paths were slightly under-predicted by the mean property method for these flames also. In addition, significant under-predictions (50%) occurred for paths away from the flame axis in both flames.

Summary and Conclusions

In order to evaluate the impact of turbulence/radiation interaction (TRI), mean line-of-sight (LOS) spectral radiation intensities for six well-documented flames burning various fuels and with different Reynolds numbers were investigated experimentally and computationally. The specific conclusions are as follows,

- (1) The agreement between the measurements and the STAS predictions supports the fidelity of the present scalar measurements. In addition, the present treatment of TRI is supported by the results.
- (2) For all the flames studied, the mean LOS spectral radiation intensities for the diametric paths reach maximum closest to the axial location corresponding to the stoichiometric flame height.
- (3) In the range of this study, the effect of Reynolds number on the mean radiation intensities is not strong. This observation is consistent with the scalar measurements.
- (4) In the dilute hydrogen flame, the TRI have only a weak impact on the already low radiation levels.
- (5) In the dilute and partially premixed methane flames, the impact of TRI is not significant for regions near the flame axis. Therefore, mean property approach for radiation heat loss calculations is adequate for these paths.
- (6) In the dilute and partially premixed methane flames, the effects of TRI are significant for regions away from the flame axis where the turbulent intensities are higher.

Acknowledgement

The Indiana 21st Century Research and Technology Fund supported this work with a grant to the Mid Infrared Sensing Diagnostics and Control Consortium with additional support provided by the Air Force Office of Scientific Research. Experiments at Sandia were supported by the Department of Energy, office of Basic Energy Sciences. Dr. Andreas Dreizler, from TU Darmstadt, Germany, provided the velocity data used in this work. His kind help is highly appreciated.

References

- [1] Barlow, R. S., Smith, N. S. A., Chen, J. -Y., and Bilger, R. W., 1999, "Nitric Oxide Formation in Dilute Hydrogen Jet Flames: Isolation of the Effects of Radiation and Turbulence-Chemistry Submodels," *Combustion and Flame*, 117: 4-31.
- [2] Frank, J. H., Barlow, R. S., and Lundquist, C., 2000, "Radiation and Nitric Oxide Formation in Turbulent Non-premixed Jet Flames," *Proceedings of the Combustion Institute*, 28: 447-454.
- [3] Vranos, A., Knight, B. A., Proscia, W. M., Chiappetta, L., and Smooke, M. D., 1992, "Nitric Oxide Formation and Differential Diffusion in a Turbulent Methane-hydrogen Diffusion Flame," *Proceedings of the Combustion Institute*, 24: 377-384.
- [4] Gore, J. P., Ip, U. -S., and Sivathanu, Y. R., 1992, "Coupled Structure and Radiation Analysis of Acetylene/Air Flames," *Journal of Heat Transfer*, 114: 487-493.
- [5] Hartick, J. W., Tacke, M., Fruchtel, G., Hassel, E. P., and Janicka, J., 1996, "Interaction of Turbulence and Radiation in Confined Diffusion Flames," *Proceedings of the Combustion Institute*, 26: 75-82.

- [6] Mazumder, S. and Modest, M. F., 1999, "A Probability Density Function Approach to Modeling Turbulence-radiation Interaction in Non-luminous Flames," *International Journal of Heat and Mass Transfer*, 42: 971-991.
- [7] Brookes, S. J. and Moss, J. B., 1999, "Predictions of Soot and Thermal Radiation Properties in Confined Turbulent Jet Diffusion Flames," *Combustion and Flame*, 116: 486-503.
- [8] Gore, J. P., Jeng, S. -M, and Faeth, G. M., 1987, "Spectral and Total Radiation Properties of Turbulent Hydrogen/Air Diffusion Flames," *Journal of Heat Transfer*, 109: 165-171.
- [9] Kounalakis, M. E., Gore, J. P., and Faeth, G. M., 1989, "Mean and Fluctuating Radiation Properties of Nonpremixed Turbulent Carbon Monoxide/Air Flames," *Journal of Heat Transfer*, 111: 1021-1030.
- [10] Hall, R. J. and Vranos, A., 1994, "Efficient Calculation of Gas Radiation from Turbulent Flames," *International Journal of Heat and Mass Transfer*, 37: 2745-2750.
- [11] Sandia National Laboratories, www.ca.sandia.gov/tdf/Workshop.html.
- [12] Meier, W., Prucker, S., Cao, M. -H., and Stricker, W., 1996, "Characterization of Turbulent H₂/N₂/Air Jet Diffusion Flames by Single-Pulse Spontaneous Raman Scattering," *Combustion Science and Technology*, 118: 293-321.
- [13] Meier, W., Barlow, R. S., Chen, Y. -L., and Chen, J. -Y., 2000, "Raman/Rayleigh/LIF Measurements in a Turbulent CH₄/H₂/N₂ Jet Diffusion Flame: Experimental Techniques and Turbulence-Chemistry Interaction," *Combustion and Flame*, 123: 326-343.
- [14] Barlow, R. S. and Frank, J. H., 1998, "Effects of Turbulence on Species Mass Fractions in Methane/Air Jet Flames," *Proceedings of the Combustion Institute*, 28: 1087-1095.
- [15] Zheng, Y., Sivathanu, Y. R., and Gore, J. P., 2002, "Measurement and Stochastic Time and Space Series Simulations of Spectral Radiation in a Turbulent Non-premixed Flame," *Proceedings of the Combustion Institute*, 29: accepted.
- [16] Ji, J., Gore, J. P., Sivathanu, Y. R., and Lim, J., 2000, "Fast Infrared Array Spectrometer used for Radiation Measurements of Lean Premixed Flames," *Proceeding of the 34th National Heat Transfer Conference*, ASME, Pittsburg, PA.
- [17] Masri, A. R., Dibble, R. W. and Barlow, R. S., 1996, "The Structure of Turbulent Nonpremixed Flames Revealed by Raman-Rayleigh-LIF Measurements," *Progress in Energy and Combustion Science*, 22: 307-362.
- [18] Grosshandler, W. L., 1993, "RADCAL: a Narrow-band Model for Radiation Calculations in a Combustion Environment," *NIST Technical Note 1402*.
- [19] Grosshandler, W. L., 1980, "Radiation Heat Transfer in Nonhomogenous Gases: a Simplified Approach," *International Journal of Heat and Mass Transfer*, 23: 1447-1459.
- [20] Zheng, Y., Barlow, R. and Gore, J. P., "Reconstruction of Local Integral Scales in Turbulent Non-premixed Flames," *in preparation*.
- [21] Krebs, W., Koch, R., Ganz, B., Eigenmann, L. and Swittig, S., 1996, "Effect of Temperature and Concentration Fluctuations on Radiation Heat Transfer in Turbulent Flames," *Proceedings of the Combustion Institute*, 26: 2763-2770.

Table 1: Flame Conditions [2]

Flame	Fuel mixture (by volume)	D (burner diameter), mm	Re	Normalized Stoichiometric Flame Height L_{stoich} / D
DLR A	22% CH ₄ , 33% H ₂ , 45% N ₂	8	15200	64
DLR B	22% CH ₄ , 33% H ₂ , 45% N ₂	8	22800	68
C	25% CH ₄ , 75% air	7.2	13400	47
D	25% CH ₄ , 75% air	7.2	22400	47
E	25% CH ₄ , 75% air	7.2	33600	47
H3	50% H ₂ , 50% N ₂	8	10000	36 [11]

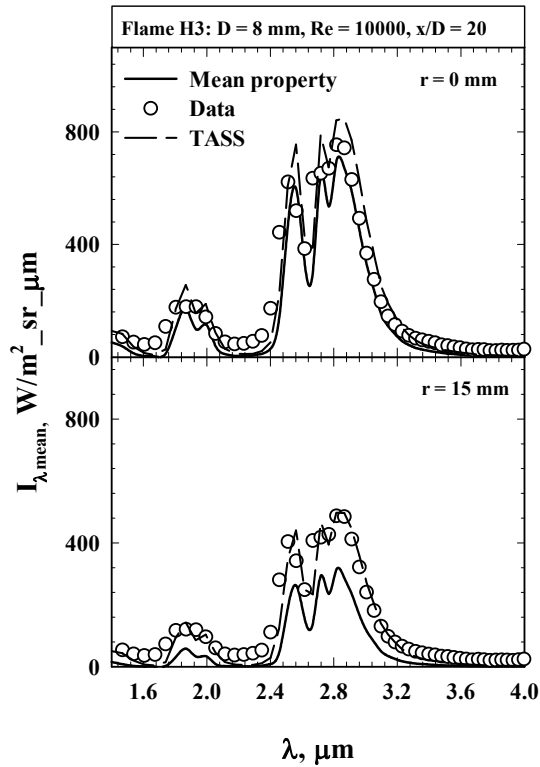


Figure 1: Spectral radiation intensities in flame H3 ($x/D = 20$).

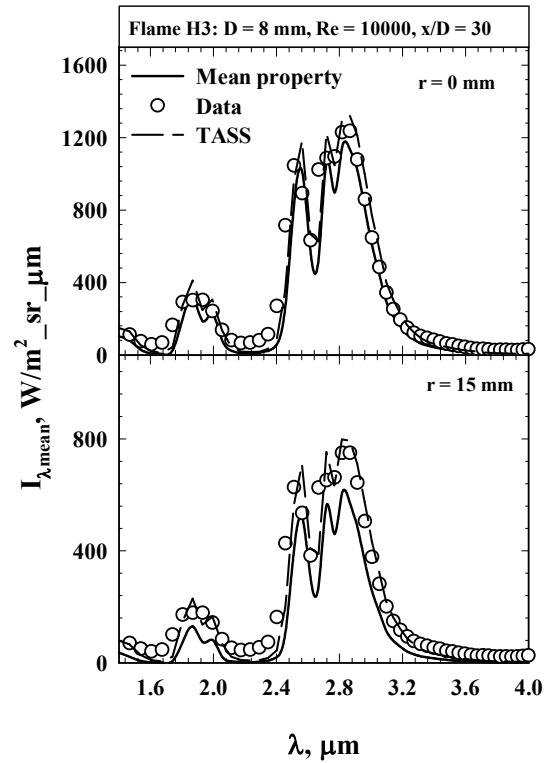


Figure 2: Spectral radiation intensities in flame H3 ($x/D = 30$).

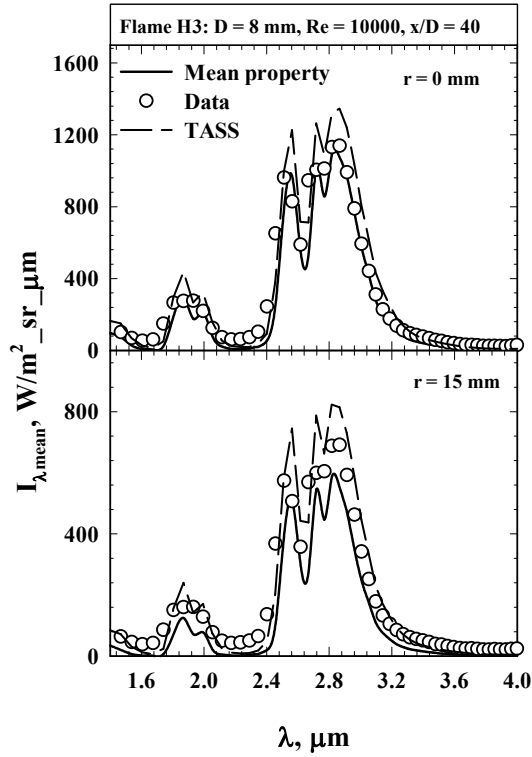


Figure 3: Spectral radiation intensities in flame H3 ($x/D = 40$).

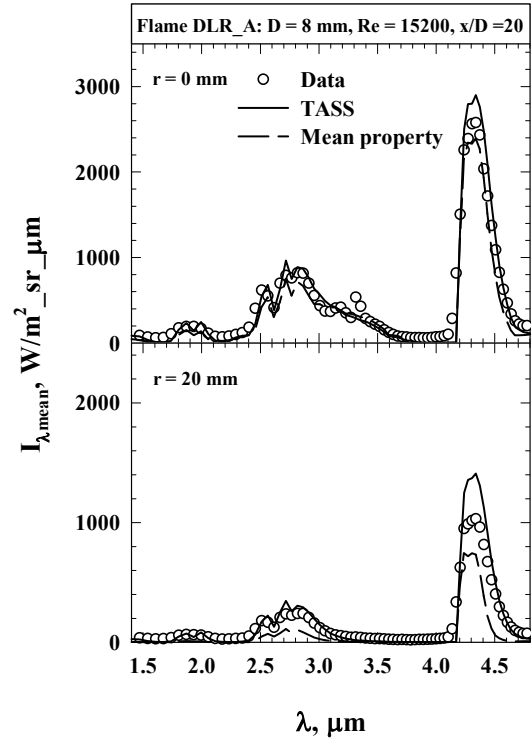


Figure 4: Spectral radiation intensities in flame DLR_A ($x/D = 20$).

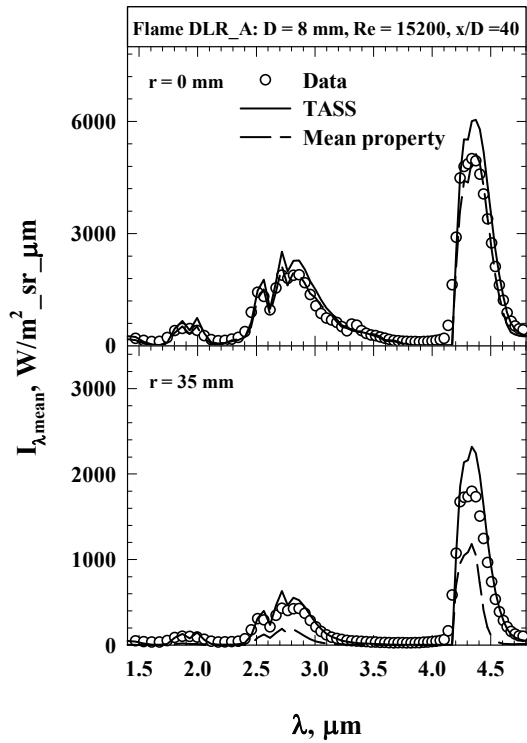


Figure 5: Spectral radiation intensities in flame DLR_A ($x/D = 40$).

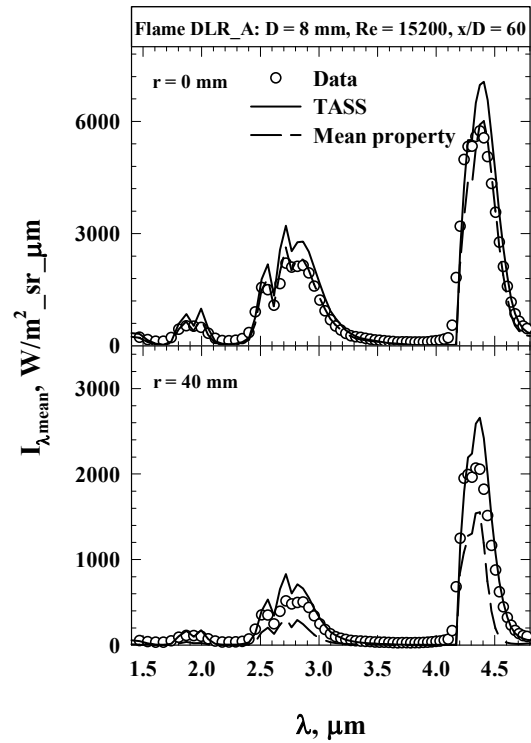


Figure 6: Spectral radiation intensities in flame DLR_A ($x/D = 60$).

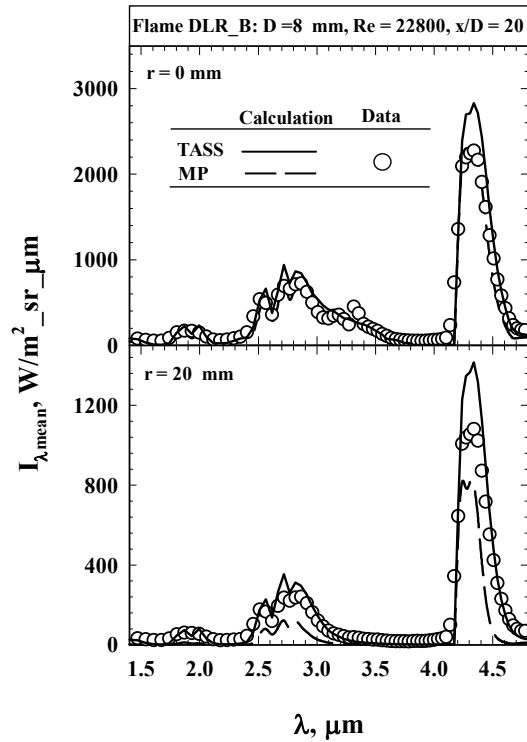


Figure 7: Spectral radiation intensities in flame DLR_B ($x/D = 20$).

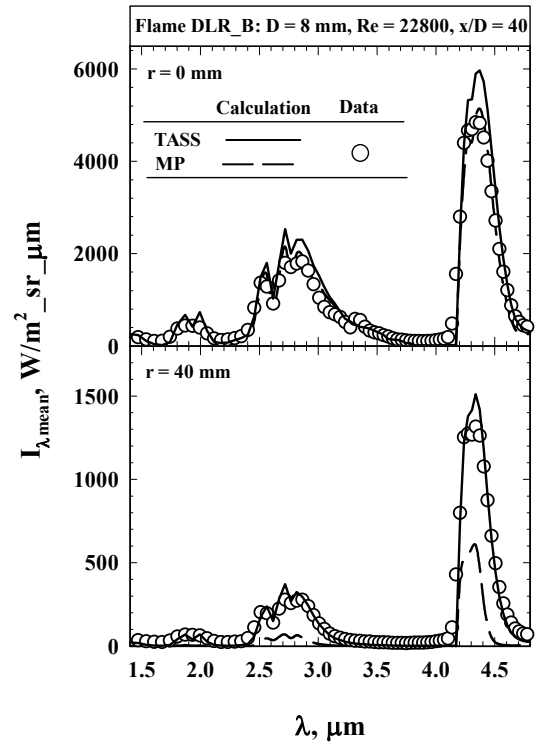


Figure 8: Spectral radiation intensities in flame DLR_B ($x/D = 40$).

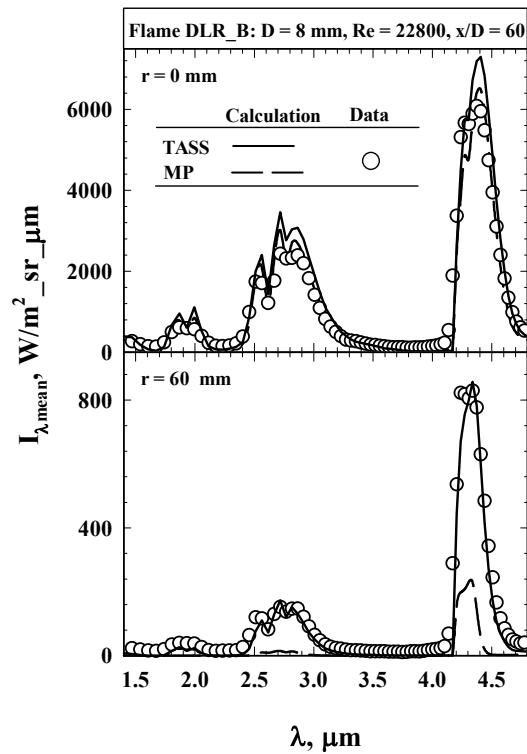


Figure 9: Spectral radiation intensities in flame DLR_B ($x/D = 60$).

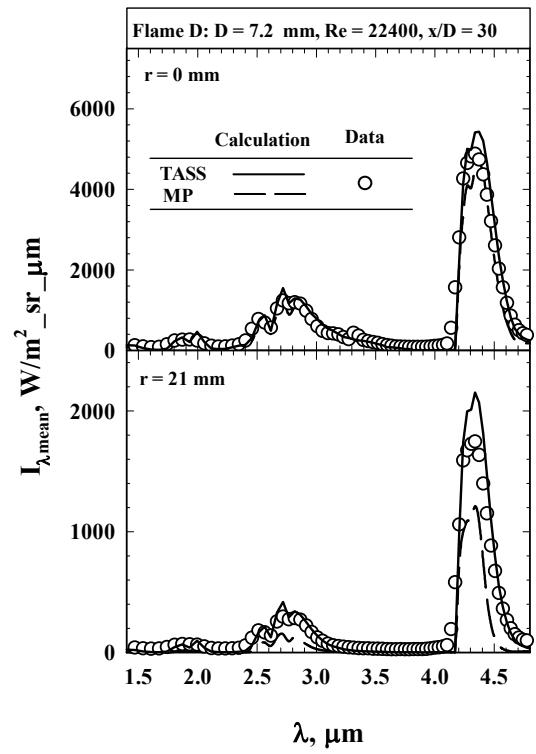


Figure 10: Spectral radiation intensities in flame D ($x/D = 30$).

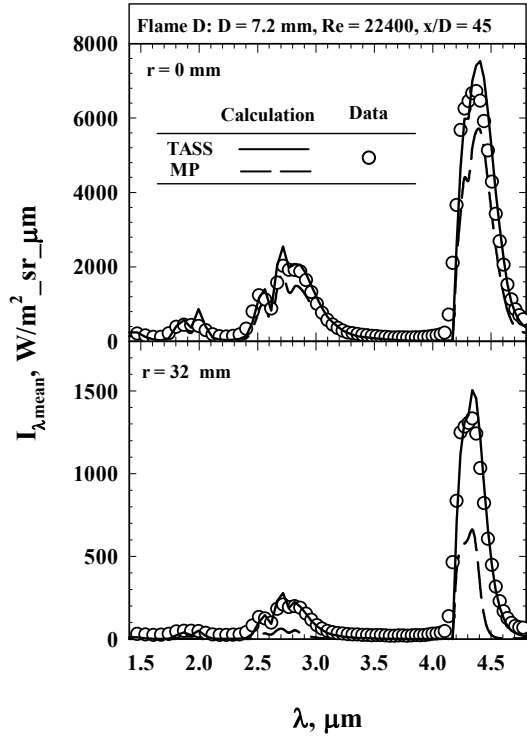


Figure 11: Spectral radiation intensities in flame D ($x/D = 45$).

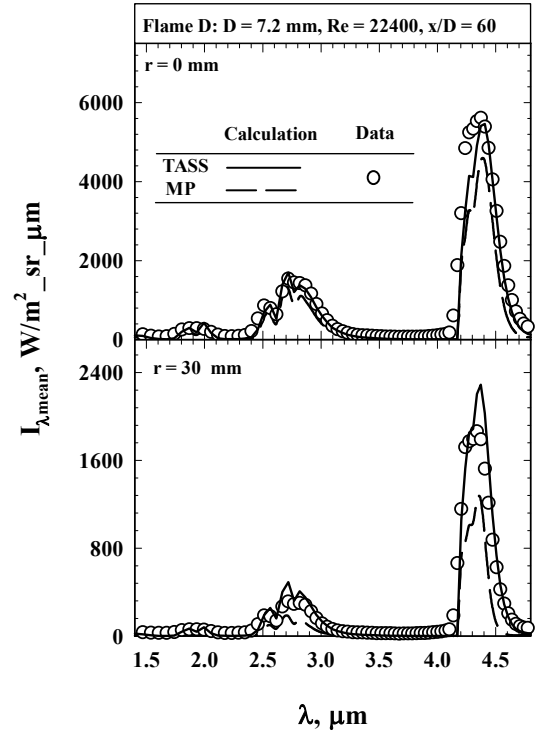


Figure 12: Spectral radiation intensities in flame D ($x/D = 60$).

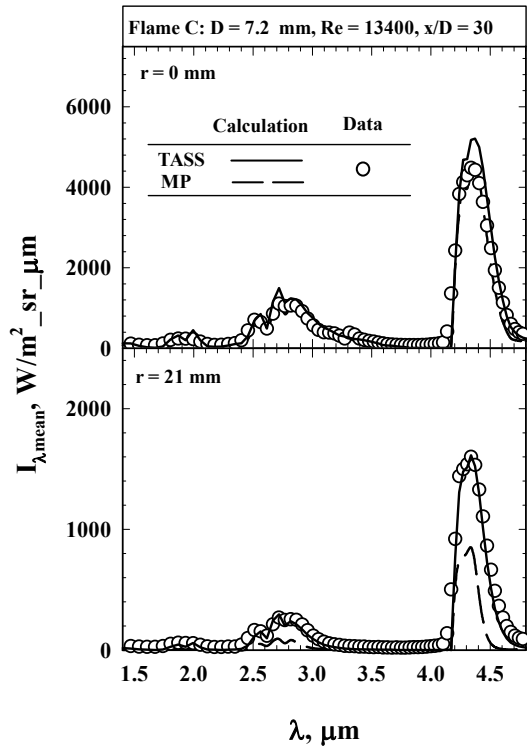


Figure 13: Spectral radiation intensities in flame C ($x/D = 30$).

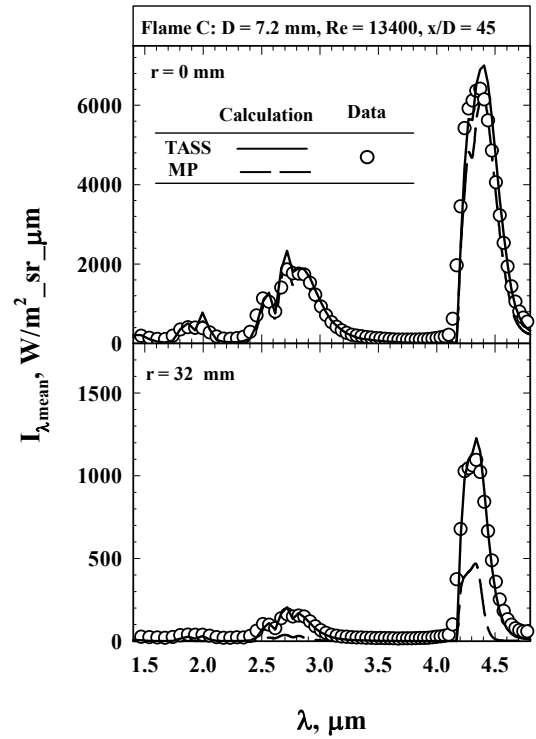


Figure 14: Spectral radiation intensities in flame C ($x/D = 45$).

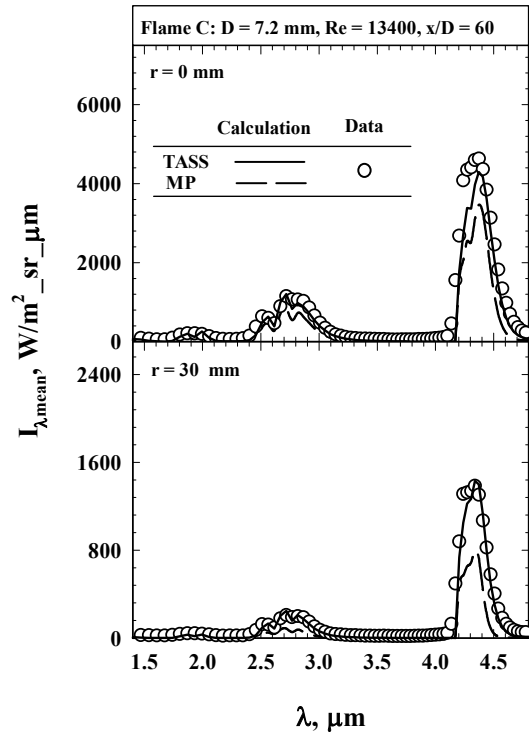


Figure 15: Spectral radiation intensities in flame C ($x/D = 60$).

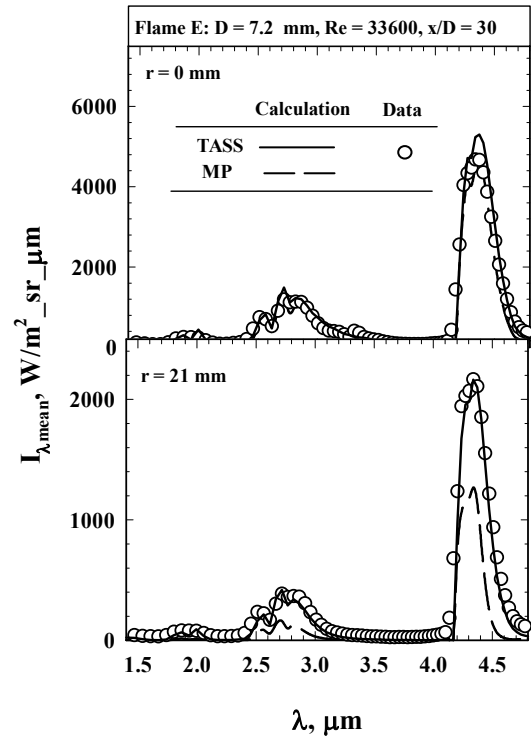


Figure 16: Spectral radiation intensities in flame E ($x/D = 30$).

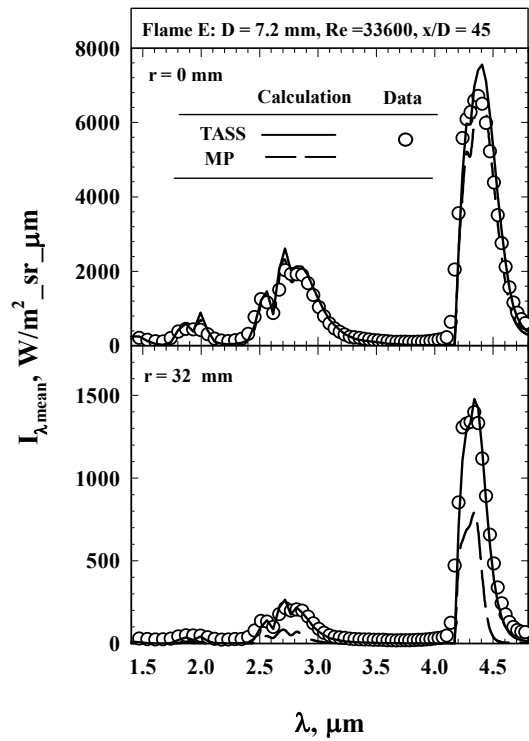


Figure 17: Spectral radiation intensities in flame E ($x/D = 45$).

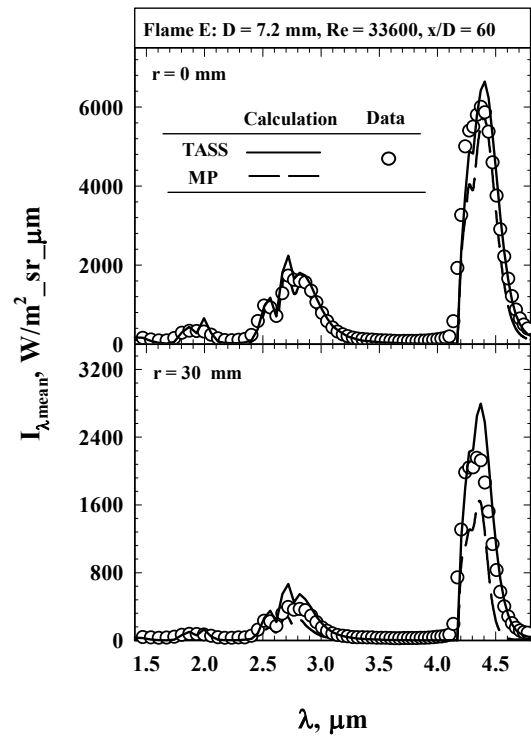


Figure 18: Spectral radiation intensities in flame E ($x/D = 60$).

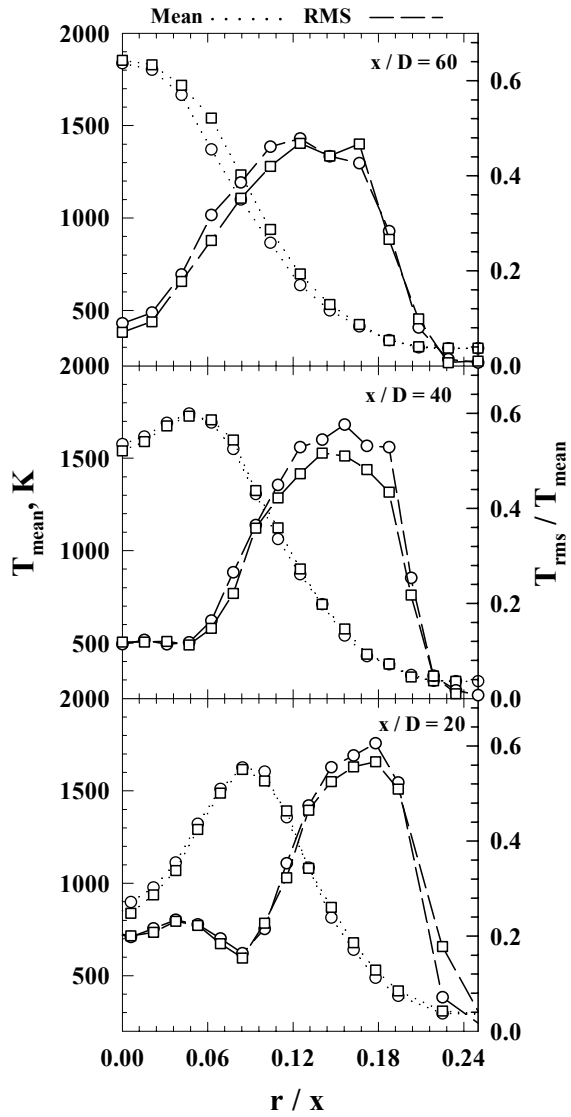


Figure 19: Temperature distributions in flames DLR_A (circle) and B (square).

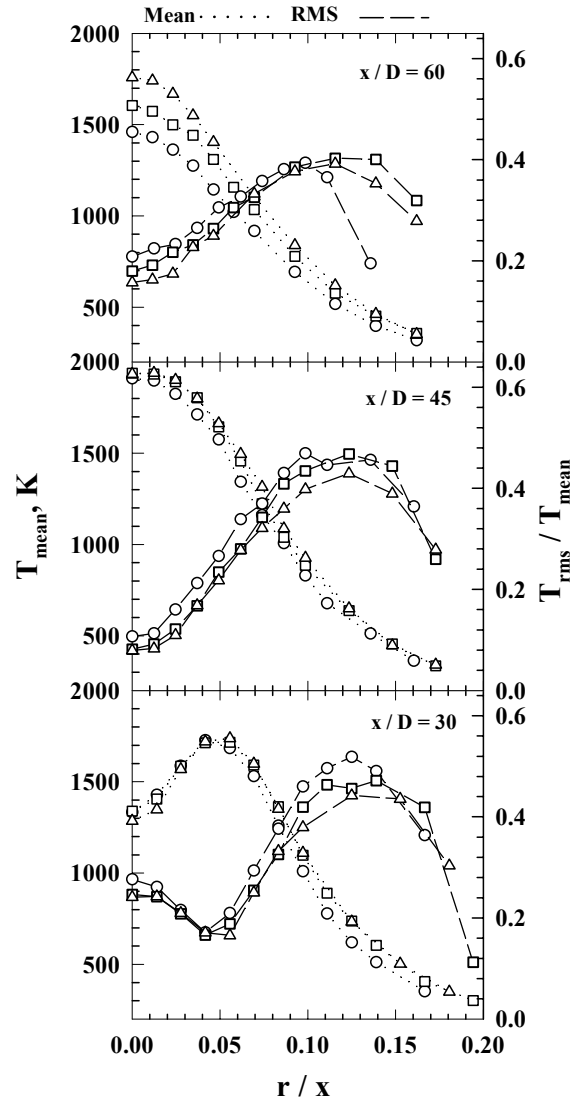


Figure 20: Temperature distributions in flames C (circle), D (square) and E (triangular).

Measurements directed at LES validation

A. Dreizler, J. Janicka

FG Energie- und Kraftwerkstechnik, TU Darmstadt, Petersenstrasse 30, Germany

dreizler@ekt.tu-darmstadt.de

Introduction

Recently, large eddy simulation (LES) has emerged to be a very promising technique to predict turbulent reacting flows. Within the LES approach, turbulent motion is separated into small and large scales. This separation is achieved by spatially filtering the conservation equations. The filter size is larger than the Kolmogorov scale and therefore sub-filter scales have to be modeled. As a consequence, experimental data is required to assist the development and validation of LES models.

In contrast to the traditional Reynolds averaged Navier Stokes (RANS) assumption, LES has the potential to describe transient flows. Accordingly, the experimental requirements rise. While single-point statistics (mean values and higher moments) of the velocity vector, species concentrations, and temperature are sufficient to test the RANS simulation performance, for LES validation, in addition, spatially and temporally correlated information is essential.

In a first step, the task “LES validation” can be split into two subtasks: (1) *a priori* test of sub-model assumptions, and (2) *a posteriori* analysis of the simulation. The first subtask is addressed to measure quantities determined by a sub-model that are not resolved by the spatial filter. Inherently, this requires experimental approaches using spatially a high resolution much finer than the LES filter size. At the current stage, however, it is under debate if a priori testing is of significance. The second subtask is to measure quantities that are predicted by LES. In this way models are evaluated after their implementation in a simulation. To be useful, this second task needs very detailed information on the inflow boundaries.

Similar to a discussion forum for non-reactive LES ¹, this contribution is intended to trigger a discussion identifying the most promising diagnostics and experiments for combusting LES. Exemplary, some experimental approaches are discussed.

General aspects

As stated before, LES needs the same experimental data as necessary for RANS validation but in addition spatially and temporally correlated information. It is essential that temporal and especially spatial resolution applied in the experiments are well documented. It is desirable to experimentally achieve a spatial resolution as high as possible. Taking laser Doppler velocimetry (LDV) as an example, this technique – as a commonly used laser diagnostic method – exhibits an extension of the measurement volume in beam direction in the order of 0.5 to 1 mm – a range similar to most recent and future LES approaches. Consequently, efforts to reduce measurement volumes in laser diagnostics are of high importance. In addition, an increase of repetition rates is desirable for some common laser diagnostics to deduce reliable temporal gradients and auto-correlations from highly resolved time series.

Inflow boundaries

In addition to single-point statistics regarding the inflow velocity vector and – for more complex geometries than jets – parameters such as unmixedness of fuel and oxidizer, temporally resolved information at a single-point (time series) as well as multi-point velocity measurements are important. From single-point time-series measurements, a temporal auto-correlation can be deduced. Subsequently, temporal time scale and power spectrum can be obtained by integration and Fourier transformation, respectively. In the spatial domain, similar information can be obtained by two- or multi-point correlation measurements. For these tasks, in general, highly repetitive techniques with small measurement volumes are needed. On the poster an example will be given using two-point LDV to measure both temporal auto- and spatial cross-correlations.

As LES requires temporally resolved inflow boundaries, in principal time series recorded simultaneously at various locations might be used to feed the simulation directly. However, it seems to be more practical to deduce these temporally and spatially resolved inflow boundaries from correlation information such as integral length scales using an inflow generator ². Alternatively, the LES inflow boundary can be set upstream of the burner mouth, but for model validation purposes this approach is, in general, computationally expensive.

A posteriori analysis

As for the inflow boundaries, time series of single-point measurements and spatial multi-point investigations are valuable. Most important, these techniques should be developed and applied on the flow field and on the mixture fraction as the most important scalar in non-premixed flames. Applying random mode sampling and a slot correlation technique on LDV, for the flow field already a promising technique exists. For scalars, however, high repetitive LIF for radical-time series measurement has been developed³ but might be extended to high repetitive mixture fraction determination. Alternatively, *cw* Rayleigh scattering could be used to temporally track the density. From time series of velocities, in addition to temporal auto-correlation, time scales, and power spectra as mentioned before, time derivatives applied on velocity measurements can be used to deduce acceleration as exemplified in⁴.

Supplementary to these quantities, the measurements of cross-correlations are important. While using LDV cross-correlations of the form $u'_i u'_j$ can be measured, but only some approaches exist to determine $u'_i f'$ that requires the simultaneous measurement of a mixture fraction (or a different scalar) and at least one velocity component⁵.

Similar to the time domain, spatial correlation measurements are of high importance for LES validation to achieve, i.e., integral length scales. This is especially important when Taylor's hypothesis is not valid. In analogy to time derivatives, space derivatives are especially valuable. Taking the mixture fraction as an example, its space derivative can be used to determine the scalar dissipation rate. For this purpose 1D line Raman measurements⁶ show very promising potential.

A priori tests of sub-models

For low Reynolds-numbers direct numerical simulation (DNS) is most commonly used to develop and test sub-models. In general, it is difficult to achieve representative boundary conditions and computational prohibitive to apply high Re-numbers important for technical combustion. Therefore, effort is needed to experimentally perform a priori tests of sub-models. This task is difficult due to the high spatial resolution required. If, for example, the sub-grid variance of the mixture fraction determined by a sub-model is to be tested, at a single time the mixture fraction has to be measured at various spatial locations. Most promising for this kind of task are 2D techniques such as particle imaging velocimetry (PIV), planar Rayleigh or planar laser-induced fluorescence (PLIF) to measure flow- and scalar-field properties, respectively. Compared to approaches commonly used, the spatial resolution has to be improved by an order of magnitude. No principal difficulties are expected but problems might occur with respect to appropriate particle densities seeded to the flow for PIV or a relatively low signal-to-noise ratio for PLIF applications.

Conclusions

For LES sub-model development few selected but very detailed measurements are required. It might be useful to evaluate a test case by DNS and experimental methods for a variety of Re-numbers. By this means the reliability of extrapolation of model assumptions obtained by DNS to high Re-numbers might be checked. For a posteriori analysis, more and different configurations have to be characterised, including a detailed investigation of the inflow boundaries of each test case. In total, this approach should help to identify and characterise the applicability of LES models and to build up confidence what type of turbulent flame can be predicted by the respective set of models.

Generally speaking, dedicated laser based methods exist to determine the information required but efforts are needed to improve the spatial resolution of multi-point techniques and the repetition rate of single-point techniques to obtain correlated information both in space and time. In addition, combination of methods is essential to simultaneously measure properties of the flow- and scalar field.

¹ Adrian, R. J., Meneveau, C., Moser, R. D., Riley, J.: "Final Report on "Turbulence Measurements for LES" Workshop." (1999).

² Klein, M., Sadiki, A., Janicka, J.: "A Digital Filter Based Generation of Inflow Data for Spatially Developing Direct Numerical or Large Eddy Simulations." submitted for publication (2002).

³ Renfro, M., Guttenfelder, W. A., King, G. B., Laurendeau, N. M.: "Scalar Time-Series Measurements in Turbulent CH₄/H₂/N₂ Nonpremixed Flames: OH.", *Combust. Flame* 123, 389 (2000).

⁴ Nobach, H., Schneider, C., Dreizler, A., Janicka, J., Tropea, C.: "Laser-Doppler-Messungen von Teilchenbeschleunigungen und der Dissipationsrate in einem runden Freistrah." to be presented at GALA (2002).

⁵ Dibble, R. W., Hartmann, V., Schefer, R. W., Kollmann, W.: "Conditional sampling of velocity and scalars in turbulent flames using simultaneous LDV-Raman scattering." *Exp. in Fluids* 5, 103 – 113 (1987).

⁶ Geyer, D., Dreizler, A., Janicka, J.: "A Comprehensive Characterization of a Turbulent Opposed Jet Burner by 1D-Raman/Rayleigh, 2D-LIF and LDV." *TNF* 6 (2002).



Measurements directed at LES validation

**Coordinator:
Andreas Dreizler**

Energy- and Powerplant Technology
Technical University Darmstadt



TNF 6



Outline

- Introduction and general remarks
- Survey of potential techniques
- Contributions from the TNF community





State-of-the-art

- **Single-point techniques**
 - Low repetition rate, statistical independent single-shot information
 - Well documented accuracy
 - Examples: Raman/Rayleigh/LIF
LDV
- **Very successful to validate models within the RANS approach**
- **Basis for model validation for LES and transient RANS approach**



Additional requirements for LES validation

- **LES has the potential to determine**
 - Single-point statistics
 - Temporal correlations
 - Spatial correlations
 - Coherent structures
 - ...
- **Need for additional experimental data for comparison purposes**





General issues (1)

- **LES delivers filtered quantities**
 - Common practice: comparison of these filtered data to experimental values obtained in a certain probe volume
 - systematic error, quantification of this error?
- **Is there a need for smaller probe volumes?**
- **What are the most important quantities to be validated experimentally?**
 - Flow field
 - Spatial and temporal auto-correlation functions
 - Spatial and temporal (acceleration) gradient
 - Coherent structures
 - ...?



General issues (2)

- Scalar field
 - Spatial and temporal auto-correlation functions
 - Spatial (→scalar dissipation rate) and temporal gradient
 - ...?
- Combinative techniques (flow and scalar field characterization)
 - PIV&PLIF
 - LDV&Raman
 - ...
- Conditioned measurements
 - Scalar and stabilization point (lifted flames)
 - ...





General issues (3)

- What techniques are capable to resolve sub-grid structure and is there a need for such measurements?
- Do we need more information regarding inflow boundary compared to RANS validation purposes?
- Aside of validation purposes: what do we learn about physics of combustion processes from these additional experiments?



Overview techniques

	Single-point techniques : Time series			Two-point techniques		1D techniques		2D techniques		
	Velocity	Scalar		Velocity	Scalar	Velocity	Scalar	Velocity	Scalar	
Method	LDV	Ray	PITLIF	LDV	Ray?		1D Ram/Ray	PIV	PLIF	Ray, Ram
Additional information	Templ. AC of v, acceleration	Templ. AC of ρ	Templ. AC of OH, CH, and of f ?	Templ. AC+spat. cross-corr. of v			grad c, grad f, χ	Spatial cross-corr. of v, grad v	Structural quantities, spatial corr., grad c, reaction rate imaging	2D distribution of f and χ .
	Time scale	Time scale	Time scale	Length and time scales			Length scale	Length scale, coherent structures?	Length scale	
Reliability	established			established			χ ~20-30%	established		
Suited for inflow boundaries	yes	Limited from scattering of surfaces		yes			yes	yes		
In work/done exemplary	Schneider & Dreizler Roekaerts et al.		Renfro & Laurendeau	Schneider & Dreizler			Karpentis & Barlow Geyer & Dreizler	Gore	Long, Frank	Long
Planned							Meier			





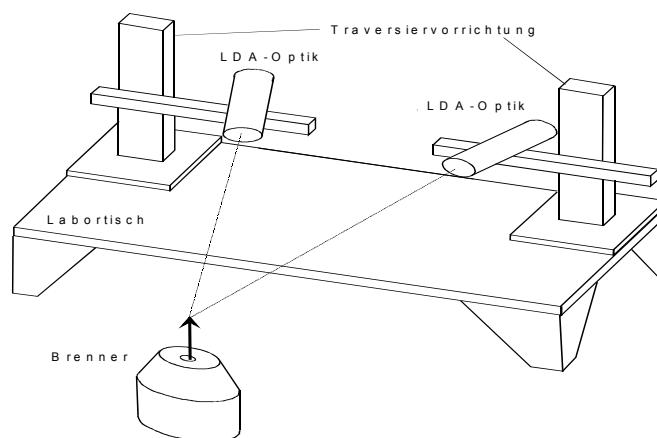
Inflow boundaries

- From numerical studies

LES
Inflow generator
Based on measured spat. length scales
Klein&Janicka

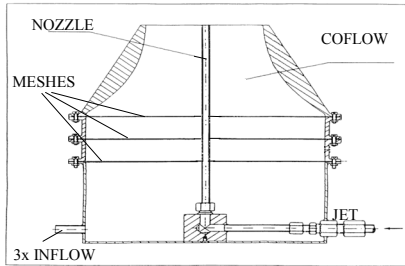


Two-point LDV, time-series





Isothermal jet



Inner diameter	[mm]	8
Diameter coflow	[mm]	140
u_0 jet	[m/s]	35.9
u_0 coflow	[m/s]	0.5
Flow rate jet	[m ³ /h]	6.5
Flow rate coflow	[m ³ /h]	27.6
Reynolds number	[-]	20.000



Correlation measurements

Correlation R

$$R_{ij}(\bar{x}, t, \bar{x}_1, t_1) = \frac{u_i'(\bar{x}, t)u_j'(\bar{x}_1, t_1)}{\sqrt{u_i'^2(\bar{x}, t)}\sqrt{u_j'^2(\bar{x}_1, t_1)}}$$

Turbulent length scale L

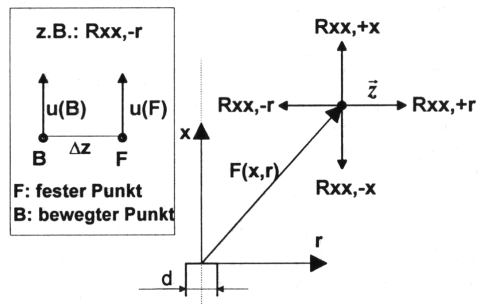
$$L_{ij,k}(\bar{x}, t) = \frac{1}{2} \int_{-\infty}^{\infty} R_{ij}(\bar{x}, t, z_k, 0) dz_k$$

$$\bar{z} = \bar{x} - \bar{x}_1$$

Turbulent time scale T

$$T_{ij}(\bar{x}, t) = \frac{1}{2} \int_{-\infty}^{\infty} R_{ij}(\bar{x}, t, 0, \tau) d\tau$$

$$\tau = t_1 - t$$



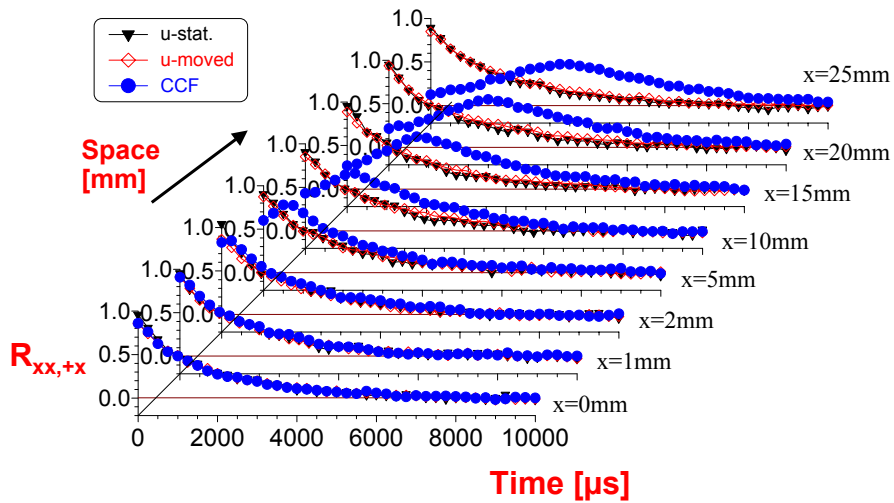
Rxx,x: longitudinal correlation

Rxx,r: lateral correlation

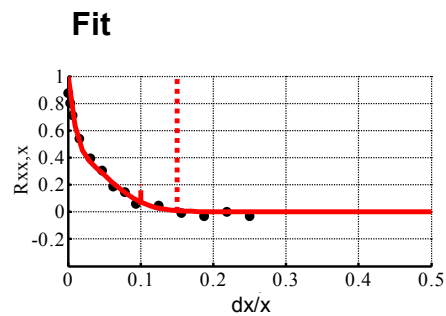
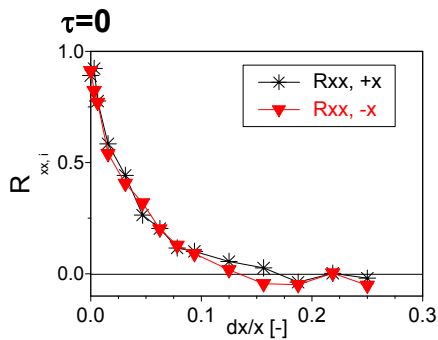




Turbulent jet, isothermal $x/D=40, R_{xx,+x}$



Spatial correlation, isothermal jet

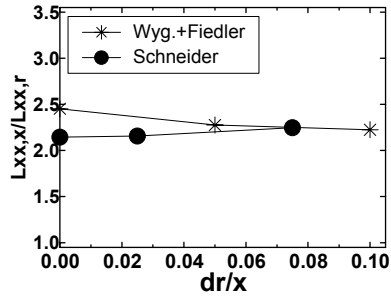
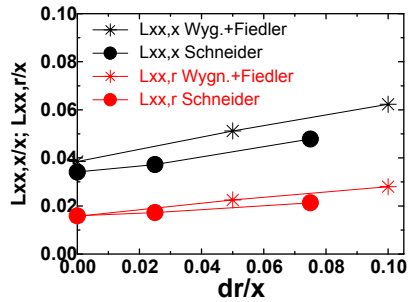




Comparison length scales

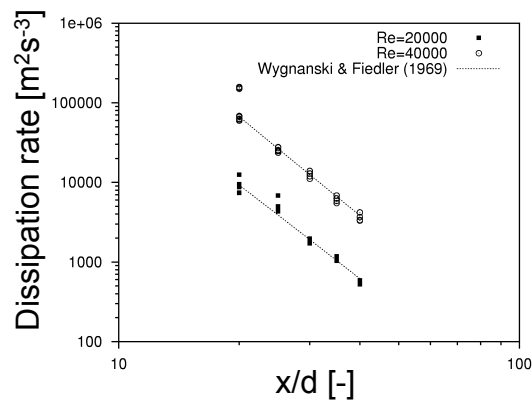
$x/D = 40$

ratio



Dissipation rate

- Isotropic conditions



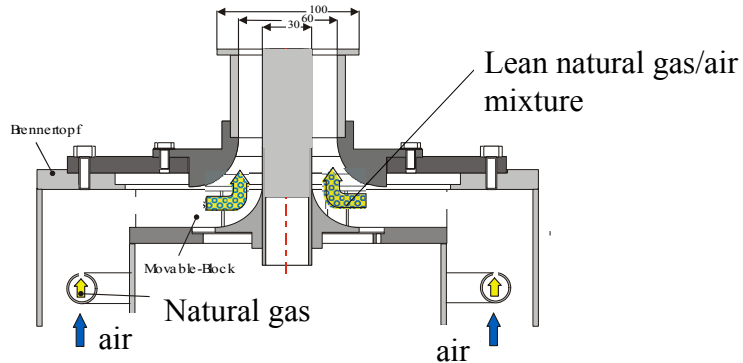
- Best way to determine dissipation rate is via integral length or time scale, not via Taylor scales





Premixed sirl burner

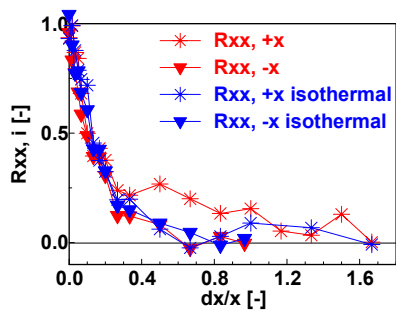
- Based on non-premixed TECFLAM burner
- Prior to movable block: mixing of natural gas and air



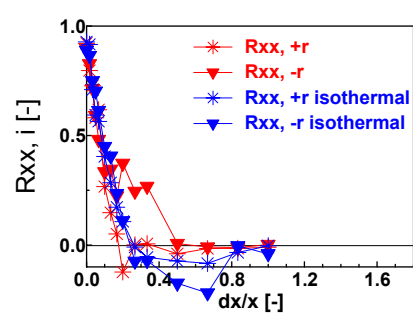
Premixed swirl flame

Measurement position: $x=30$ mm, $r=30$ mm

Longitudinal corr. $R_{xx,x}$



Lateral corr. $R_{xx,r}$



- Flame enlarges length scale
- Asymmetric correlation functions



Comparison of measured and predicted scalar time scales in flame H3

Sixth International Workshop on Measurement and Computation of Turbulent Nonpremixed Flames

July 18-20, Sapporo, Japan

Michael W. Renfro¹

Mechanical Engineering Department, University of Connecticut

Storrs, CT 06269-3139, USA

Amit Chaturvedy, Galen B. King, Normand M. Laurendeau²

School of Mechanical Engineering, Purdue University

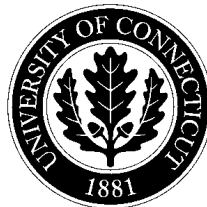
West Lafayette, IN 47907, USA

Andreas Kempf, Andreas Dreizler³, Amsini Sadiki, Johannes Janicka

Technische Universität Darmstadt

Petersenstraße 30, 64287 Darmstadt, Germany

¹renfro@engr.uconn.edu, ²laurende@ecn.purdue.edu, ³dreizler@ekt.tu-darmstadt.de



TECHNISCHE
UNIVERSITÄT
DARMSTADT

Temporal Correlations Available for LES Validation

- Single-point, two-time statistics (time-series measurements):
 - velocity by point-LDV (Gokalp *et al.*)
 - temperature/density by Rayleigh scattering (Dibble *et al.*)
 - chemiluminescence (Ikeda *et al.*)
 - radiation (Gore *et al.*)
 - minor-species by high-bandwidth LIF (Renfro *et al.*)
- Two-point, two-time statistics (two-shot imaging)
 - multiple-shot PIV for velocity (Driscoll *et al.*)
 - two-shot PLIF techniques for minor-species (e.g. Kaminski *et al.*)
- Missing statistics: Z time scales in reacting flows
- Potential experiments:
 - 2-shot multi-species Raman (~1 hr of measurements per point)
 - tracer LIF (needs to survive flame and be accessible above 280 nm)
 - particle scattering (Sc# differences cause problems)

Utility of Time-Series Measurements

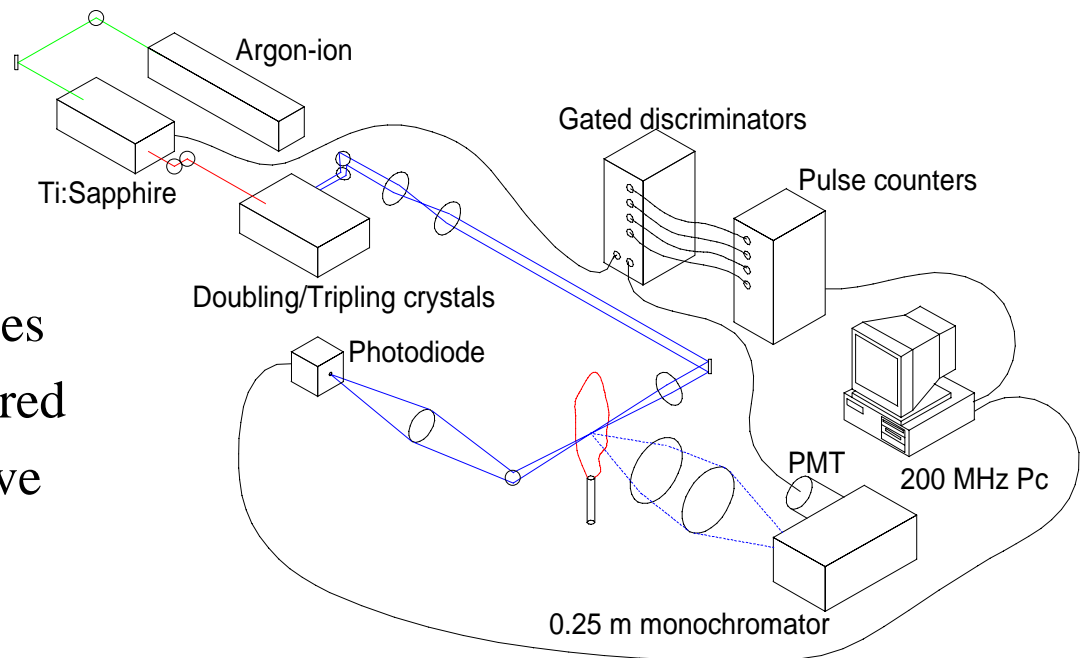
- 2-time statistics:
 - PSD/autocorrelation function shape (scale distribution)
 - Integral time scales (mixing rates, intermittency)
- Higher-order temporal statistics:
 - 3-time, 4-time, etc. (pattern matching)
 - Time-symmetry (burst/flame shape)
- Minor-species concentration time series:
 - spatial resolution $\sim 100 \mu\text{m}$, temporal resolution up to $25 \mu\text{s}$, time-scale accuracy $\sim 20\%$
 - typical LIF problems for accurate mean measurements do not affect time scale measurements: surface scattering, quenching, calibration
 - shot-noise limits temporal resolution, shot-noise and chemiluminescence limit weaker signals (CH)
 - measurement at a point completed in $\sim 1 \text{ min}$
 - integral time-scales dominated by large-scale fluctuations – may not test SGS models directly

LES - Numerical Details

- LES results computed by mixture fraction formulation and flamelet assumption
- Governing equations solved by 3d finite volume code (low-Ma assumption): time-step limited by convection
- Time integration by 3rd order low-storage Runge Kutta scheme
- Momentum fluxes modeled by 2nd order central schemes
- Species transport modeled by 2nd order TVD scheme (Charm) to avoid numerical oscillations.
- Space-variable scalar dissipation rates considered
- Subgrid-variance of mixture-fraction modeled using resolved variance in test-filter cell
- Subgrid-fluctuation of the scalar dissipation rate modeled by a Dirac-peak, and dissipation itself computed by approach of Girimaji & Zhou (1996) and de Bruyn Kops *et al.* (1997)

PITLIF - Experimental Details

- 80-MHz repetition rate,
Ti:Sapphire laser pumped at 20 W
- 2 or 18-ps mode-locked pulse widths
- Fluorescence detected by gated photon counting
- Spatial resolution $\sim 110 \mu\text{m}$
- Photon counts up to 24 million/second
- 4096 time-series points per series
- Fluorescence quenching measured at each time yielding quantitative concentrations

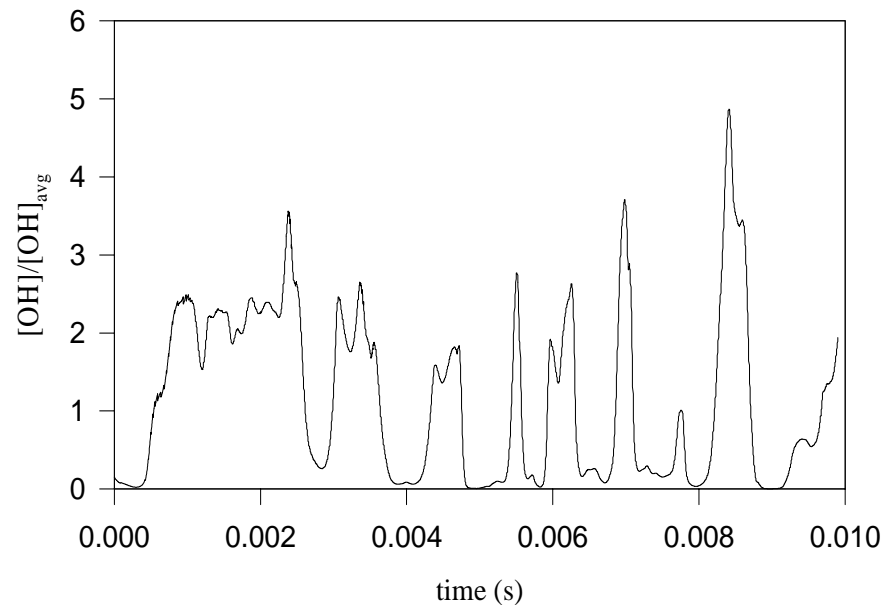


Time-Series Processing

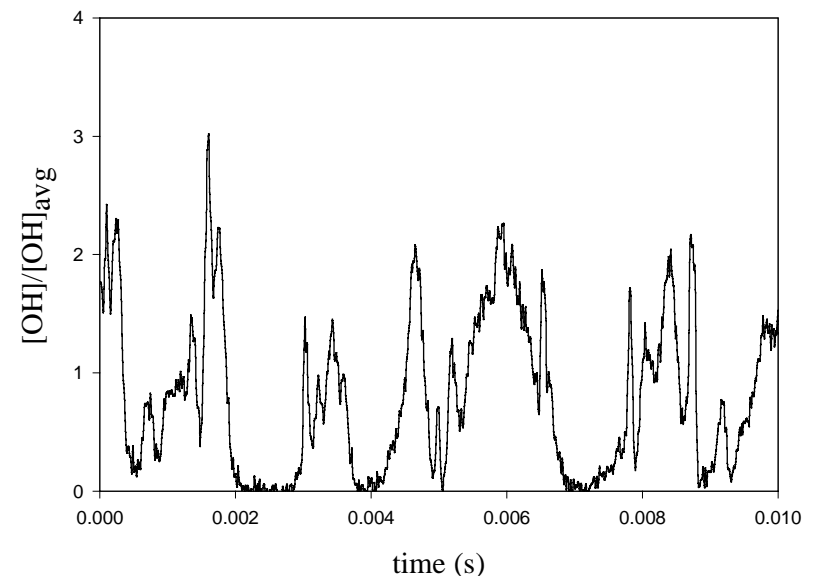
- LES
 - Yields time series with unequal time steps
 - Output re-sampled at constant 10 μ s step size
 - First 0.1 s ignored to allow for development of turbulence
 - One time series sampled for 140 ms
- PITLIF
 - Time series measured with 12 kHz sampling rate
 - 50 independent 340-ms time series measured at each point
 - Statistics corrected for shot noise and averaged over 50 series (17 s total)
- Statistics computed: mean, rms, PDF, PSD, autocorrelation function, integral time scale, triple correlation
- Integral time scale computed by exponential fit to autocorrelation function over $\Delta t = 0 - 1$ ms
- PSDs smoothed by 5-point moving average

Typical OH Time-Series

- Comparison of OH time series in H3 flame (Re=10,000)
- LES and PITLIF show similar intermittent structure for OH time series



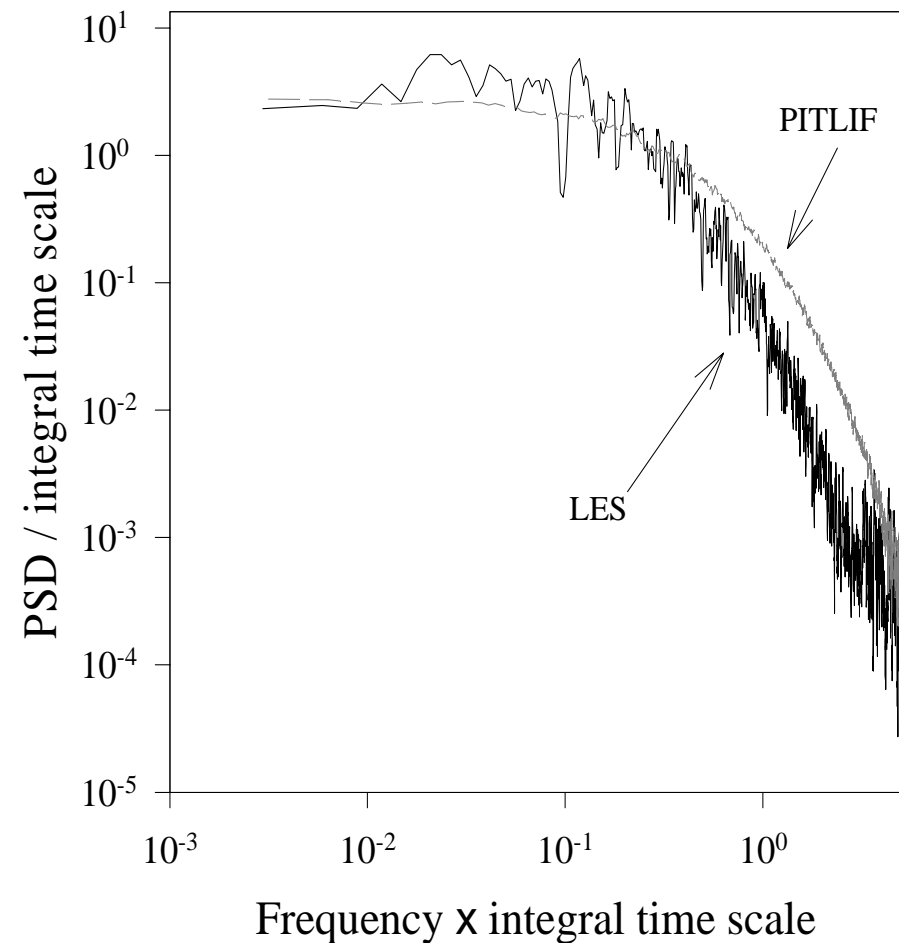
OH time-series predicted by LES



OH time-series measured by PITLIF

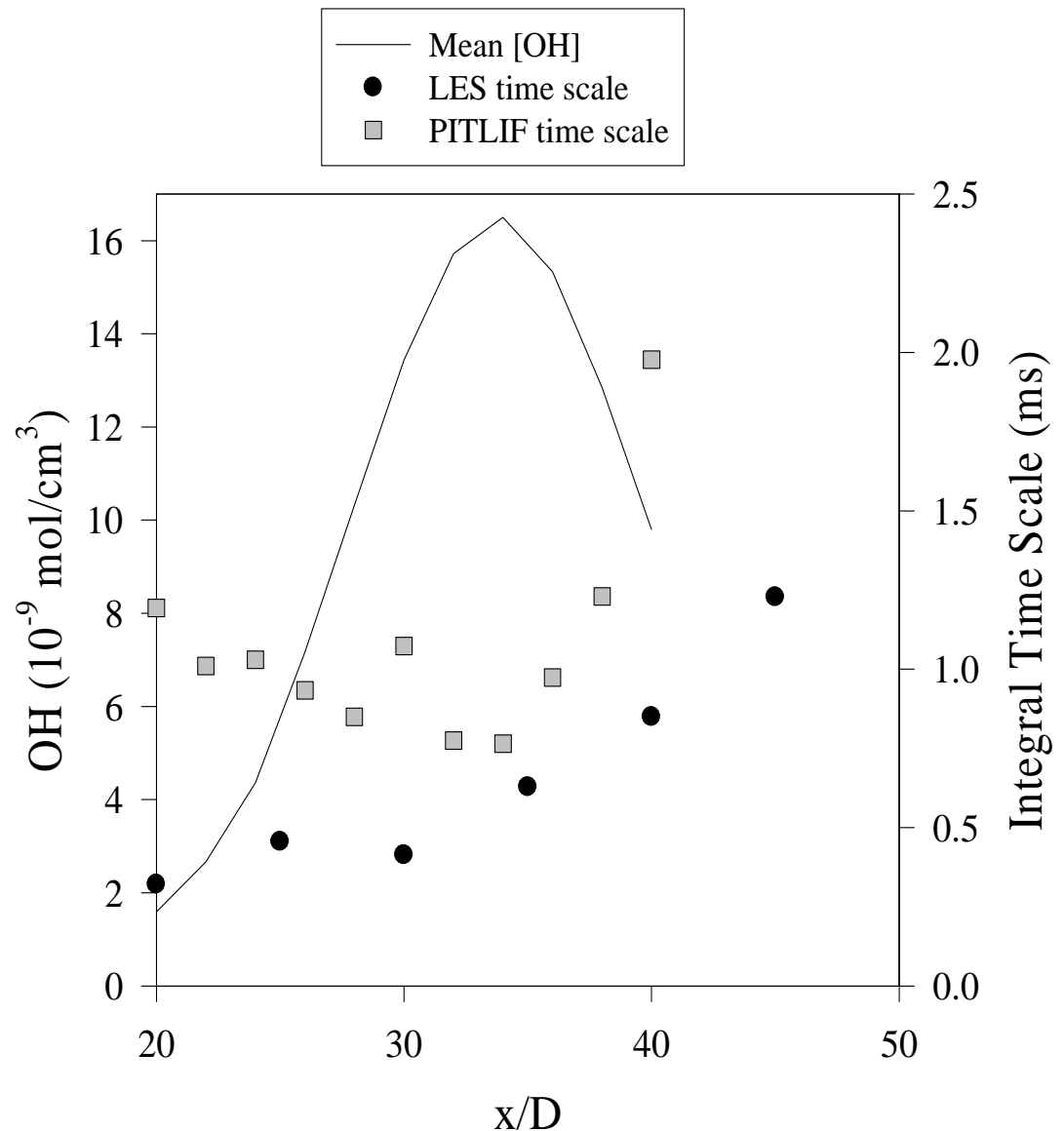
OH Power Spectra Comparison

- Comparison shown for $x/D=30$ (just below flame tip)
- LES displays more scatter due to smaller time series for calculation of statistics (0.14 s for LES, 17 s for measurements)
- **Good comparison for measured and predicted PSD shape**: similar roll-off at high frequencies



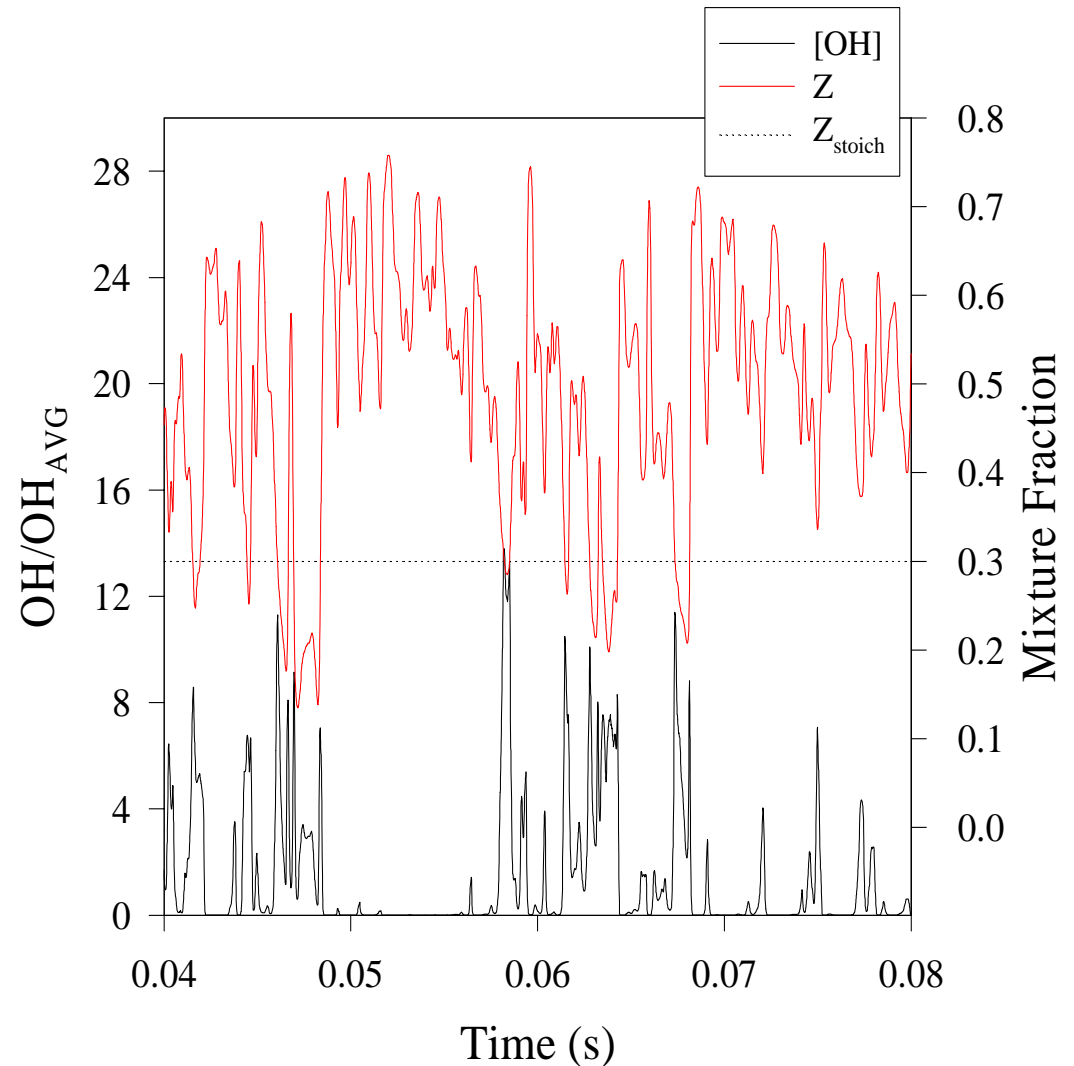
Time-Scale Comparison

- Measured time scales along centerline are nearly constant below flame tip, show minimum at flame tip, followed by rapid increase downstream
- LES time scales are nearly constant from $x/D=5-20$ then increase gradually – available points are slightly off center ($r/D=0.9$)
- **LES time scales are ~2-3 times lower than measured time scales**



OH and Z Time-Series - LES

- $x/D=10$: locations below flame tip
- $Z_{stoich} = 0.30$
- OH and Z time series are dissimilar due to scalar intermittency
- Small fluctuations in Z amplified in OH time series
- Many Z fluctuations missing in OH time series



Time-scale Targets for LES

- Radial dependence of scalar time scales has characteristic shape
- Reynolds number dependence departs from non-reacting jet theory

